

UCC Library and UCC researchers have made this item openly available.  
 Please [let us know](#) how this has helped you. Thanks!

<b>Title</b>	Atomic layer deposition of metals: Precursors and film growth
<b>Author(s)</b>	Hagen, D. J.; Pemble, Martyn E.; Karppinen, M.
<b>Publication date</b>	2019-11-05
<b>Original citation</b>	Hagen, D. J., Pemble, M. E. and Karppinen, M. (2019) 'Atomic layer deposition of metals: Precursors and film growth', Applied Physics Reviews, 6(4), 041309. doi: 10.1063/1.5087759
<b>Type of publication</b>	Article (peer-reviewed)
<b>Link to publisher's version</b>	<a href="https://aip.scitation.org/doi/abs/10.1063/1.5087759">https://aip.scitation.org/doi/abs/10.1063/1.5087759</a> <a href="http://dx.doi.org/10.1063/1.5087759">http://dx.doi.org/10.1063/1.5087759</a> Access to the full text of the published version may require a subscription.
<b>Rights</b>	© 2019, the Authors. Published by AIP Publishing. This article may be downloaded for personal use only. Any other use requires prior permission of the author and AIP Publishing. This article appeared as Hagen, D. J., Pemble, M. E. and Karppinen, M. (2019) 'Atomic layer deposition of metals: Precursors and film growth', Applied Physics Reviews, 6(4), 041309. doi: 10.1063/1.5087759, and may be found at <a href="https://doi.org/10.1063/1.5087759">https://doi.org/10.1063/1.5087759</a>
<b>Item downloaded from</b>	<a href="http://hdl.handle.net/10468/9285">http://hdl.handle.net/10468/9285</a>

Downloaded on 2020-06-06T01:42:02Z

## Atomic Layer Deposition of Metals: Precursors and Film Growth

D. J. Hagen<sup>a,\*</sup> M. E. Pemble<sup>b</sup> and M. Karppinen<sup>a,\*</sup>

<sup>a</sup> *Department of Chemistry and Materials Science, Aalto University, 02150, Espoo, Finland*

<sup>b</sup> *School of Chemistry and Tyndall National Institute, University College Cork, Cork, Ireland*

The coating of complex three-dimensional structures with ultra-thin metal films is of great interest for current technical applications, particularly in microelectronics, as well as for basic research on, for example, photonics or spintronics. While atomic layer deposition (ALD) has become a well-established fabrication method for thin oxide films on such geometries, attempts to develop ALD processes for elemental metal films has met with only mixed success. This can be understood by the lack of suitable precursors for many metals, the difficulty of reducing the metal cations to the metallic state, and the nature of metals as such, in particular their tendency to agglomerate to isolated islands. In this review, we will discuss these three challenges in detail for the example of Cu, for which ALD has been studied extensively due to its importance for microelectronic fabrication processes. Moreover, we give a comprehensive overview over metal ALD, ranging from a short summary of the early research on the ALD of the platinoid metals, which has meanwhile become an established technology, to very recent developments that target the ALD of electropositive metals. Finally, we discuss the most important applications of metal ALD.

## 1. Introduction

The increase of interest in the development of atomic layer deposition (ALD) processes during the last decade was to a large extent caused by the needs of the microelectronics industry. Here, ALD is regarded as an economical fabrication method as it allows one to deposit films with thickness control in the monolayer range across the whole wafer and provides conformal coating on complex topographies. These advantages outweigh the perceived disadvantage of low growth rate for an increasing number of applications, as the critical dimensions of CMOS devices keep shrinking. Arguably, the most prominent application at the present time is the deposition of high-k oxides for CMOS gate stacks which has become well-established in industrial production. Associated with this, there is a strong desire for reliable ALD processes for the deposition of pure metal films in all levels of the CMOS fabrication process. In the front-end-of-line (FEOL) process, in which the active structures such as transistors are fabricated, poly-Si, highly doped, polycrystalline Si, has been replaced by metals as material of choice for the gate electrode. Here, critical structures not only decrease in size but also increase in complexity as multi-gate structures are introduced. A further application of metals in the FEOL process is the deposition of metal films for the silicide formation at the contacts. In the middle-of-line (MOL) process, W contacts are fabricated by chemical vapor deposition (CVD). As contact holes have a large aspect-ratio the use of ALD has also been introduced. However, the application in which most research effort for the development of a metal ALD process has been applied thus far is in the fabrication of Cu interconnects in the back-end-of line (BEOL) process. Here, thin Cu seed layers need to be deposited to enable the electrochemical filling of trenches and vias. This review starts with an introduction on the basics of the ALD method highlighting the differences of the growth of metals and that of oxides. The ALD of Cu is discussed in detail taking into account the different aspects of the problem: precursor

chemistry, reducing agents, influence of the substrate material. Next, ALD processes for other metals are discussed and finally the most important applications of metal ALD are described. This review is specifically limited to elemental metals, and does not consider metallic nitrides such as TiN and TaN or metallic oxides.

## 2. Basics of ALD

In most thin-film deposition techniques, film growth depends on the rate and type of precursor transport as well as on the chemical reaction kinetics. Thus, films grow faster at places to which the precursor is transported more rapidly. Atomic layer deposition (ALD) is a thin film deposition technique, which is characterized by film growth which is independent of transport. This is achieved by splitting the process into saturated half-reactions. As described in Figure 1 the first precursor A is pulsed onto a substrate where it chemisorbs by reacting with available surface groups. This process is saturated in the sense that the adsorbates inhibit further precursor from reacting with the surface and no desorption takes place on relevant time scales. After the remaining molecules are purged out of the chamber a second reactant B is delivered to the substrate and reacts with the surface groups provided by the adsorbate A\*. This half-reaction is in the same way saturated as the first and provides surface groups for A to react within the next deposition cycle. As the two precursors are never present at the same time in the reaction chamber, no gas-phase reaction can occur. ALD is often described as a variant of chemical vapor deposition (CVD) but this is not a definitive description as ALD processes exist which are based on other technologies. A prominent example is the early work of Suntola et al. already aiming at industrial application on the growth of compound thin films that resulted in the first patent<sup>1</sup> and a subsequent paper<sup>2</sup> on ALD. They used a molecular beam epitaxy (MBE) reactor in order to ‘pulse’ the components in elemental form separately.



Saturation was achieved because the vapor pressure of both elements was much higher than that of the compound formed. They demonstrated the saturated deposition of ZnS, SnO<sub>2</sub>, GaP and ZnTe, and named the process atomic layer epitaxy (ALE) when epitaxial growth was carried out on single-crystalline substrates.<sup>1</sup>

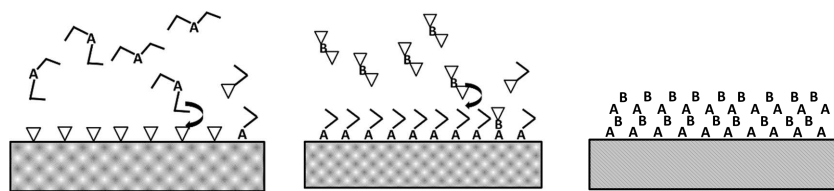
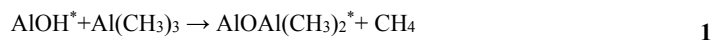


Figure 1: Growth of a film by ALD: (a) first pulse, (b) second pulse, (c) film of structure ABAB.

For the case of non-epitaxial growth, Suntola et al.<sup>2</sup> used the term atomic layer evaporation with the same abbreviation ALE. Atomic layer epitaxy remained the term used for ALD processes for a long time,<sup>3-9</sup> and was also used to describe non-epitaxial growth. As epitaxial growth is rather the exception than the normal case, ALD has been established as the term of choice. For example, CMOS gate oxides, which are among the most successful examples for the application of ALD, are usually amorphous. It is important to note that the term ALE has meanwhile become more commonly used for atomic layer etching than for epitaxy.<sup>10-12</sup> The growth of the high-k dielectric Al<sub>2</sub>O<sub>3</sub> with trimethylaluminum (TMA) and H<sub>2</sub>O is regarded as a model for ALD processes:<sup>13-15</sup>



Here, the asterisks describe adsorbed species. Other important oxides of interest include HfO<sub>2</sub>,<sup>16-19</sup> which is also a high-k gate oxide, TiO<sub>2</sub>,<sup>20,21</sup> which is used in its amorphous form as passivation layer and in the

polymorph anatase as photocatalyst, and ZnO,<sup>22</sup> which is a transparent conductor. The ALD of nitrides such as TiN,<sup>23-33</sup> TaN<sub>x</sub>,<sup>32,34-41</sup> NbN<sub>x</sub>,<sup>42,43</sup> WN<sub>x</sub>,<sup>28,44-48</sup> SiN<sub>x</sub>,<sup>49,50</sup> or BN<sub>x</sub><sup>51,52</sup> have been reported. In most of these deposition experiments molecular NH<sub>3</sub> was the reactant. However, in many cases it was challenging to obtain the desired stoichiometry and the use of additional reducing agents or plasma was necessary. Many nitrides are refractory solids and their use as diffusion barriers is an important application for example in the microelectronic industry.

The ALD of elemental metals distinguishes itself from that of oxides and nitrides since the metal cations in the precursor complexes need to be reduced to the metallic state. Therefore, it is not surprising that the noble metals, in particular the platinoids, can be regarded as the group of metals for which ALD has been the most successful. The ALD of platinoid metals has already been comprehensively reviewed by Hämäläinen,<sup>53</sup> and will be discussed only briefly in this review. Further reviews on metal ALD include an article by George et al.<sup>54</sup> on the subject of the precursors available for Cu ALD and an article by Knisley et al.<sup>55</sup> regarding precursors for the ALD of first-row transition metals.

This present work will provide a comprehensive overview on the ALD of metals discussing different approaches for precursors and co-reagents. A special focus will be put on the growth mechanisms and the influence the substrate material can have on these.

### 3. The ALD of Cu Films

The ALD of Cu has been intensively researched due to its importance for the fabrication of microelectronic devices. Furthermore, Cu can be regarded as sharing some of the properties of noble and non-noble metals as can be seen from its low positive redox potential of 0.35 V (with  $\text{Cu}^{2+}$ ). This makes it suitable as an example to discuss the various aspects of metal ALD. The research effort on Cu has remained quite constant during the last decade with close to 10 publications appearing every year (Figure 2, according to Web of Science). The most important Cu-containing materials have been its oxides and sulfides.

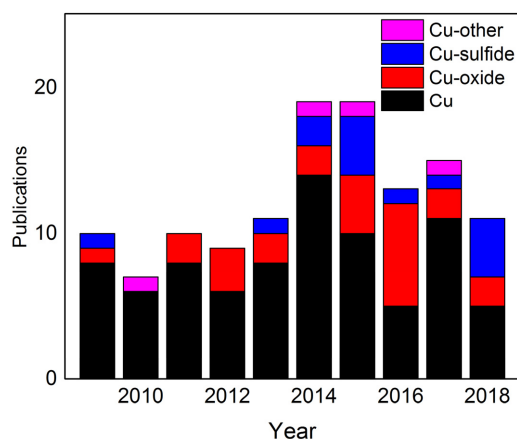


Figure 2: Scientific publications on the ALD of Cu and Cu compound per year as obtained with Web of Science.

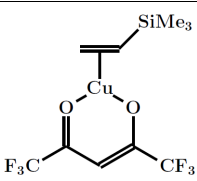
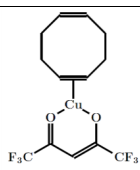
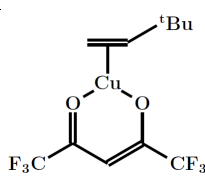
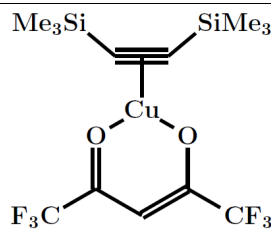
#### 3.1 Precursors

Although Cu ALD with  $\text{CuCl}$  has been reported,<sup>7,9,56,57</sup> Cu-halides are usually not regarded as a suitable choice for the growth of Cu by ALD because their low vapor pressures require the use of high

temperatures. Therefore, numerous metalorganic Cu precursor systems have been developed. Complexes are formed from Cu(I) ions as well as Cu(II) ions and both have been used for ALD experiments.

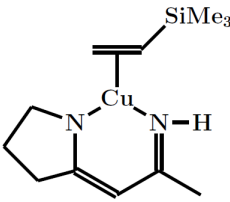
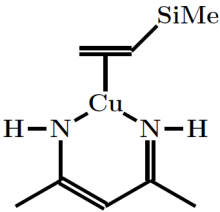
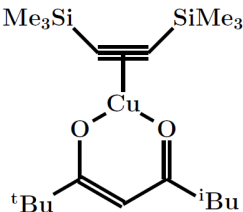
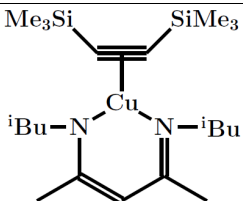
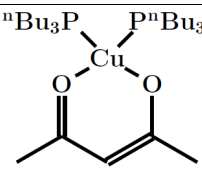
### 3.1.1 Cu(I)-Metalorganics

Table 1: Summary of Cu(I) metalorganics evaluated as precursors for the ALD or CVD of Cu

Name	Structure	References
Trimethylvinylsilyl- Cu(1,1,1,5,5,5-hexafluoroacetylacetonate), TMVS-Cu(hfac), Cupraselect		58,59
1,5-cyclooctadiene-Cu(1,1,1,5,5,5-hexafluoroacetylacetonate), COD-Cu(hfac)		60
3,3-dimethyl-1-butene-Cu(1,1,1,5,5,5-hexafluoroacetylacetonate), DMB-Cu(hfac)		61
bis(trimethylsilyl)acetylene-Cu(1,1,1,5,5,5-hexafluoroacetylacetonate), BTMSA-Cu(hfac)		62

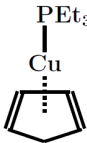
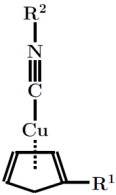
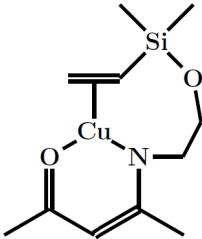
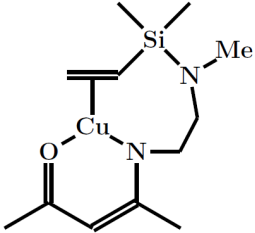
This is the author's peer reviewed, accepted manuscript. However, the online version of record will be different from this version once it has been copyedited and typeset.

PLEASE CITE THIS ARTICLE AS DOI: 10.1063/1.5087759

TMVS-Cu(1-pyrrolidine- 2-N-amino-1-propen)		63-67
TMVS-Cu(2,4-di- N-amino-3-penten)		65,68
Cu(I)-2,2,7-trimethyloctane- 3,5-dionate		69
bis-trimethylsilylacetylene-Cu-2,4-di-N- isobutylamino-hepta-3,4-diene		69
bis[tri-n-butylphosphine]-Cu(acetylacetonate), [ <sup>n</sup> Bu <sub>3</sub> P] <sub>2</sub> -Cu(acac)		70,71

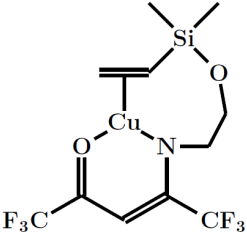
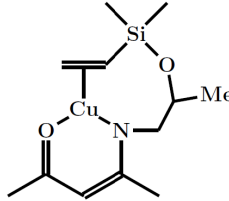
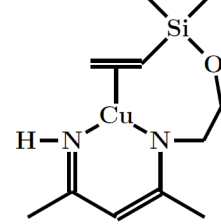
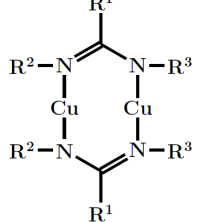
This is the author's peer reviewed, accepted manuscript. However, the online version of record will be different from this version once it has been copyedited and typeset.

PLEASE CITE THIS ARTICLE AS DOI: 10.1063/1.5087759

triethylphosphine-Cu-cyclopentadienyl,  PEt <sub>3</sub> -CuCp		72
Isocyanide-CuRCp	  R <sup>1</sup> = H, Me, Et, <sup>i</sup> Pr;  R <sup>2</sup> = <sup>i</sup> Pr, <sup>t</sup> Bu, Cy, Ph, Xyl, Mes	73
Cu-4N-ethyl(dimethylethenesilyl)ether-amino-pent-3-ene-2-onate, KI-1		74
Cu-4N-ethyl(dimethylethenesilyl)methylamine-amino-pent-3-ene-2-onate, KI-2		74

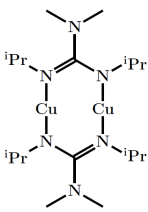
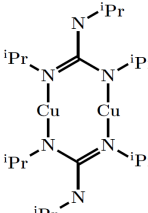
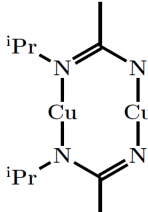
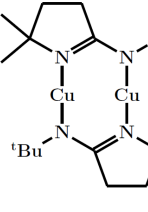
This is the author's peer reviewed, accepted manuscript. However, the online version of record will be different from this version once it has been copyedited and typeset.

PLEASE CITE THIS ARTICLE AS DOI: 10.1063/1.5087759

<p>Cu-1,1,1,5,5,5hexafluoro-4N-ethyl(dimethylethenesilyl)ether-amino-pent-3-ene-2-onate, KI-3</p>		<p>75</p>
<p>Cu-4N-sec-butyl(dimethylethenesilyl)ether-amino-pent-3-ene-2-onate, KI-5</p>		<p>75,76</p>
<p>Cu-4N-ethyl(dimethylethenesilyl)ether-amino-pent-3-ene-2-imide, DI-1</p>		<p>74</p>
<p>Bis-[Cu-amidines]</p>	 <p>1: R<sup>1</sup>=Me, R<sup>2</sup>=<sup>n</sup>Pr, 6: R<sup>1</sup>=<sup>n</sup>Bu, R<sup>2</sup>=<sup>n</sup>Bu, 7: R<sup>1</sup>=Me, R<sup>2</sup>=<sup>i</sup>Bu, 8: R<sup>1</sup>=<sup>n</sup>Bu, R<sup>2</sup>=<sup>i</sup>Bu, 9: R<sup>1</sup>=Me, R<sup>2</sup>=R<sup>3</sup>=<sup>s</sup>Bu, 10: R<sup>1</sup>=<sup>n</sup>Bu, R<sup>2</sup>=<sup>s</sup>Bu (for</p>	<p>77-83</p>

This is the author's peer reviewed, accepted manuscript. However, the online version of record will be different from this version once it has been copyedited and typeset.

PLEASE CITE THIS ARTICLE AS DOI: 10.1063/1.5087759

	1-10 $R^2=R^3$ ), 12: $R^1=Me$ , $R^2=iBu$ , $R^3=iBu$ ;	
$[Me_2NC(iPrN)_2Cu]_2$		84,85
$[iPrN(H)C(iPrN)_2Cu]_2$		84
$[MeC(iPrN)_2Cu]_2$		84,86
Bis[Cu(tert-butyl-imino-2,2-dimethylpyrrolidinate)], Bis(Cu-pyrrolidinate)		87

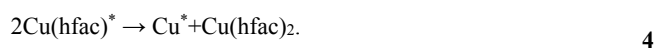
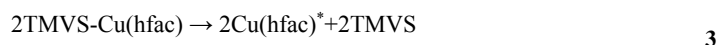


This is the author's peer reviewed, accepted manuscript. However, the online version of record will be different from this version once it has been copyedited and typeset.

PLEASE CITE THIS ARTICLE AS DOI: 10.1063/1.5087759

Unsaturated N-heterocyclic-carbene-Cu(bis-trimethylsilyl-amide),  Unsaturated NHC-Cu(hmds)	<p>1: R<sup>1</sup>=<sup>i</sup>Pr, R<sup>2</sup>=H, 2: R<sup>1</sup>=<sup>t</sup>Bu, R<sup>2</sup>=H, 3: R<sup>1</sup>=<sup>i</sup>Pr, R<sup>2</sup>=CH<sub>3</sub></p>	88,89, 90
Saturated N-heterocyclic-carbene-Cu(bis-trimethylsilyl-amide),  Saturated NHC-Cu(hmds)	<p>4: R<sup>1</sup>=Et, R<sup>2</sup>=H, 5: R<sup>1</sup>=<sup>i</sup>Pr, R<sup>2</sup>=H, 6: R<sup>1</sup>=<sup>t</sup>Bu, R<sup>2</sup>=H, 7: R<sup>1</sup>=<sup>t</sup>Bu, R<sup>2</sup>=CH<sub>3</sub></p>	88,89,91, 90
Acyclic-diamino-carbene-Cu(bis-trimethylsilyl-amide),  Acyclic-diamino-carbene-Cu(hmds)	<p>8: R=Me, 9: R=Et, 10: R=<sup>i</sup>Pr</p>	90
Tetra-[Cu-bis-trimethylsilyl-amide]  [Cu(hmds)] <sub>4</sub>		92

Cu(I) complexes are relatively unstable and many disproportionate forming metallic Cu and a Cu(II) complex. These properties have been exploited for the CVD of Cu. One such example is the Cu(I)-diketonate trimethylvinylsilyl-Cu(hexafluoroacetylacetonate) (TMVS-Cu(hfac)), which is also known by the trade-name Cupraselect.<sup>58</sup> When the complex adsorbs on a substrate the dative ligand TMVS is released and the Cu(hfac)\* surface species react by disproportionation:<sup>58</sup>



As this process is not saturated, it is not regarded as suitable chemistry for ALD. Furthermore, later studies indicated that disproportionation was already taking place during the evaporation process giving rise to a lack of stability. This can be mitigated when the precursor container contains an excess of TMVS. For this reason, Air Products currently sells Cupraselect with TMVS and Hhfac as additives.<sup>59</sup> Unfortunately, this prevents the use of a simple precursor transport technique such as direct draw from a cylinder or with carrier gas from a bubbler. Instead, a more sophisticated vaporization method such as direct liquid injection is required. Cohen et al.<sup>60</sup> demonstrated the same disproportionation reaction for a similar molecule where the TMVS ligand was replaced by 1,5-cyclooctadiene (COD), COD-Cu(hfac). They reported that the COD ligand is already released at 30 °C on metallic surfaces. Choi and Rhee<sup>61</sup> carried out CVD experiments with 3,3-dimethyl-1-butene-Cu(hfac) (DMB-Cu(hfac)), and reported an increase of the deposition rate when H<sub>2</sub> was used as a carrier gas. Using this reducing agent also improved the purity of the Cu films. This indicates that the reaction of Cu(I)-diketonates by disproportionation alone can be incomplete. Norman<sup>62</sup> synthesized alkyne-Cu(hfac) complexes, where alkynes included trimethylsilylpropyne (TMSP) and bis(trimethylsilyl)acetylene (BTMSA), and reported CVD growth with

the latter. He claimed improved stability as compared to alkene-Cu(hfac) complexes due to the saturation of the Cu center.

There is a preference by the microelectronic industry for precursors which do not contain oxygen or halogens because both are seen as problematic contaminants. Researchers at DuPont, Wilmington, Delaware, synthesized a range of Cu(I)diketiminates<sup>63-66</sup> and carried out ALD experiments with TMVS-Cu(1-pyrrolidine-2-N-amino-1-propen)<sup>67</sup> and TMVS-Cu(2,4-di-N-amino-3-penten).<sup>68</sup> Although a lack of saturation was still observed, thin, conformal Cu films could be deposited. Differences in the stability of Cu(I)-diketonates and these Cu(I)-diketiminates were observed and attributed to the impact of the anionic ligands on the bond strength between the Cu center and the dative ligand. Thompson et al.<sup>69</sup> investigated the differences of the bonding of the trimethylsilylacetylene ligands in the Cu(I)-diketonate bis-trimethylsilylacetylene-Cu-2,2,7-trimethyloctane-3,5-dionate and the Cu(I)-diketimate bis-trimethylsilylacetylene-Cu-2,4-di-N-isobutylamino-hepta-3,4-diene. They observed a stronger  $\pi$ -backbonding between the Cu(I) ion and trimethylsilylacetylene for the diketimate complex. This can be explained with its stronger Lewis base character, which provides a larger electron density around the Cu(I) ion.

Waechtler et al.<sup>70,71</sup> carried out ALD experiments with bis[tri-n-butylphosphine]-Cu(acetylacetonate) ( $[\text{nBu}_3\text{P}]_2\text{-Cu(acac)}$ ) and reported stable ALD growth. Phosphines have a stronger Lewis base character than alkenes or alkynes and thus bond more strongly to the Cu(I) ion and prevent disproportionation during the evaporation process. The stabilizing Lewis base character of phosphines was also exploited by Senocq et al.<sup>72</sup> who used triethylphosphine-Cu-cyclopentadienyl ( $\text{PEt}_3\text{-CuCp}$ ) for Cu CVD. They reported stable and repeatable evaporation and an onset of decomposition at 150 °C. Thus, the use of this precursor for ALD would be limited to low temperatures. The researchers obtained films of good quality and observed no P contamination, which would have a strong impact on the resistivity, when analyzing the films with

EDX. Driven by the potential problems associated with of P contamination, Willcocks et al.<sup>73</sup> synthesized a number of isocyanide Cu-Cp complexes. Although the complexes <sup>1</sup>PrCN-CuCp and <sup>1</sup>BuCN-CuCp suffered from limited stability with decomposition temperatures around 100 °C, by substituting the Cp anion with MeCp or EtCp, the authors were able to obtain complexes with increased volatility. However, the stabilities of those molecules were inferior.

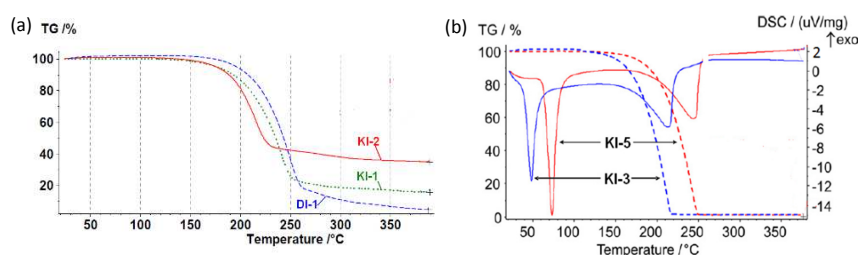


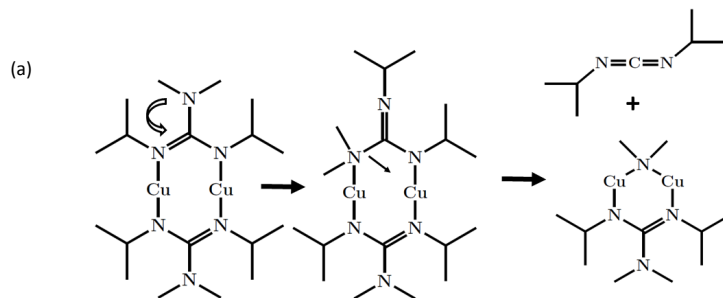
Figure 3: TGA characteristics for: (a) KI-1, KI-2 and DI-1,<sup>74</sup> and (b) KI-3 and KI-5<sup>75</sup> (including DSC); for the structures see table 1. Adapted with permission from J. A. T. Norman et al., *ECS Trans.* 3, 161-170 (2007); Copyright 2007 The Electrochemical Society, and Norman et al., *Microelectron. Eng.* 85, 2159-2163 (2008); Copyright 2008 Elsevier, respectively.

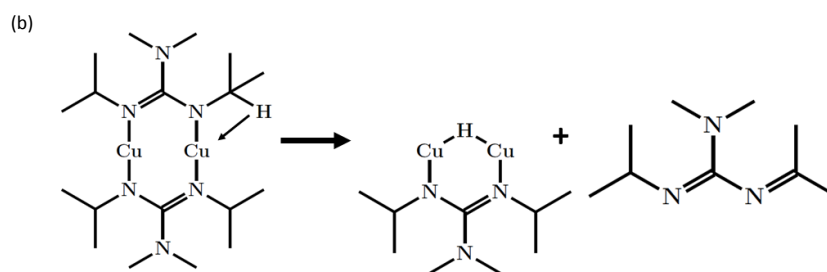
An interesting approach designed to stabilize the ligand bond was developed by the Norman group at Air Products.<sup>74,75,93</sup> They linked the dative and the ionic ligand, with a molecular bridge, **an ether or an amine**. The researchers evaluated **four Cu(I)-ketoiminates and one Cu(I)-diketiminat** as precursors for ALD or CVD. Norman et al.<sup>74</sup> compared the thermodynamics of the reaction of **Cu-4N-ethyl(dimethylethenesilyl)ether-amino-pent-3-ene-2-onate** (KI-5, see table 1) and **Cu-4N-ethyl(dimethylethenesilyl)ether-amino-pent-3-ene-2-imide** (DI-5, see table 1), which only differ in the O being replaced with NH in the imide, with H<sub>2</sub> to form metallic Cu. Using DFT based simulations they obtained a reaction energy of  $\Delta E = -83.60$  kJ/mol for KI-1 and  $\Delta E = -56.15$  kJ/mol for DI-1. They concluded that the Cu-N bond is stronger than the Cu-O bond for these kinds of precursors. The stability

of a range of these compounds was evaluated with thermo-gravimetric analysis (TGA) (Figure 3). Mass loss was observed to start between 150 and 200 °C for all compounds. The residual mass is relatively large for KI-2 and low for KI-3 and KI-5. Furthermore, the endothermic peak in the differential scanning calorimetry (DSC) curves for KI-3 and KI-5 indicate that the mass loss was caused by evaporation and not by decomposition for both molecules. The peak is at a lower temperature for KI-3 which indicates a higher vapor pressure for the fluorinated complex. This was confirmed by vapor pressure measurements. The vapor pressure of KI-1, KI-2, and DI-1 is relatively low (~0.1 Torr at 100 °C). Although they demonstrated good stability and the deposition of Cu films, when ALD experiments were carried out with KI-2 and DI-1,<sup>74</sup> saturated growth was not proven with either of these molecules. KI-3 and KI-5 were evaluated for CVD growth and the results were strongly dependent on the reducing agent<sup>94</sup> as will be discussed below in section 3.3. Norman et al.<sup>74,94</sup> proposed that all compounds adsorb as complete molecules but did not provide any experimental data by way of proof.

The Gordon group at Harvard University obtained some remarkable results when they synthesized Cu(I)amidinate-dimers.<sup>77,78</sup> Cu(I)-amidinates can be obtained from the corresponding amidine via the formation of Li-amidinate and its reaction with CuCl. An interesting detail is that the same Cu(I) dimer was obtained when CuCl<sub>2</sub> was used instead of CuCl.<sup>77</sup> In TGA measurements, the weight loss of most of those complexes started between 150 and 200 °C. Among those Cu-amidinates, bis[Cu-N,N-Di-sec-butylacetamidinate] ([Cu(<sup>s</sup>Bu-Me-amd)]<sub>2</sub>) combines a low residual mass, thus indicating nearly complete evaporation, with a low melting point of 77 °C, which allows its evaporation as a liquid. Furthermore, this compound has a relatively high vapor pressure of 0.1 Torr at 85 °C. Therefore, it has been the most intensively studied Cu-amidinate in ALD, and also CVD, experiments.<sup>79-81</sup> ALD resulted in the deposition of very thin films (2 nm)<sup>80</sup> and the conformal coating of high aspect-ratio structures.<sup>79</sup>

Guanidines are very similar to amidines, and are distinguished from these by having an amido group as exocyclic moiety. Coyle et al.<sup>84</sup> synthesized the Cu(I) guanidines  $[\text{Me}_2\text{NC}(\text{iPrN})_2\text{Cu}]_2$  and  $[\text{iPrN}(\text{H})\text{C}(\text{iPrN})_2\text{Cu}]_2$  and compared their thermochemistry with that of the Cu(I) amidine  $[\text{Me}_2\text{C}(\text{iPrN})_2\text{Cu}]_2$ . Using sealed NMR tube thermolysis, they observed an onset of carbodiimide deinsertion (Scheme 1 (a)) at 135 °C for the both guanidines but no such mechanism was observed for the amidine in the investigated temperature range until 235 °C. In gas-phase investigations involving mass spectroscopy the deinsertion temperatures were higher (225 and 250 °C, respectively), which Coyle et al.<sup>84</sup> then attributed to kinetic effects. However, a later experimental investigation along with DFT calculations also by Coyle et al.<sup>85</sup> showed that carbodiimide de-insertion is an unlikely process at these higher temperatures and the decomposition proceeds via  $\beta$ -hydride elimination (Scheme 1 (b)). Both guanidines were tested as single source precursors for CVD<sup>84</sup> and films were obtained at a substrate temperature of 225 °C.





Scheme 1: Decomposition of Cu(I)-guanidates: (a) carbodiimide de-insertion. (B)  $\beta$ -hydride elimination.<sup>85</sup>

While clean decomposition processes are favored for CVD, they inhibit the self-limiting half reactions essential for ALD. Coyle et al.<sup>87</sup> therefore synthesized the Cu(I)-amidinate bis[Cu(tert-butyl-imino-2,2-dimethylpyrrolidinate) (Cu-pyrrolidinate) which does not easily undergo carbodiimide de-insertion and  $\beta$ -hydride elimination. TGA measurements of Cu-pyrrolidinate and  $[\text{MeC}(\text{tPrN})_2\text{Cu}]_2$  clearly showed a higher stability of the first. Furthermore, the residual mass of  $[\text{MeC}(\text{tPrN})_2\text{Cu}]_2$  varied significantly with the sample size, which can be understood from a kinetics perspective. The small samples evaporated rapidly and as such no decomposition was observed.

Coyle et al.<sup>88</sup> reported that the Cu-amidinate dimers can be broken by N-heterocyclic carbenes (NHCs) but not by phosphines or alkenes. This can be explained with N-heterocyclic carbenes being very strong  $\sigma$ -electron donors. Having recognized the potential of N-heterocyclic carbenes as ligands for the synthesis of stable and volatile Cu(I) complexes, Coyle et al.<sup>88</sup> synthesized NHC-Cu-bis(trimethylsilyl)amides (NHC-Cu(hmds)). These NHC-Cu(hmds)s were first obtained from the reaction of NHC-CuCl with K guanidates via de-insertion of a carbodiimide in attempts to obtain monomeric Cu guanidates.

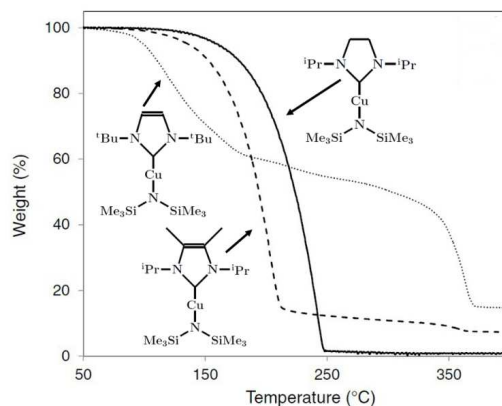


Figure 4: TGA of NHC-Cu(hmnds) compounds.<sup>88</sup> Adapted with permission from S. T. Barry.

NHC-Cu(hmnds) can also be more directly synthesized via salt metathesis from alkali-silylamides.<sup>88,89</sup> As can be seen from the TGAs in Figure 4 the compound with the saturated NHC 1,3-Diisopropyl-imidazolin-2-ylidene is more stable than the molecules with unsaturated NHCs and can be readily evaporated. The NHC-Cu(hmnds) compound has a vapor pressure of 1 Torr at 131 °C as was calculated from a Clausius-Clapeyron curve using "stepped isothermal TGA" and a melting point of 51 °C which means that it can be evaporated as a liquid.<sup>89</sup> At a typical evaporation temperature of 90 °C where the vapor pressure is about 140 mTorr, long time stability has been shown by Coyle et al.<sup>88</sup> by storing it for two weeks at this temperature and was confirmed by Hagen et al.<sup>91</sup> during a series of ALD experiments. This can be explained by the strong bond between the NHC ligand and the Cu center, which mitigates a reaction according to equation 5 below which is believed to occur under evaporation conditions.



Coyle et al.<sup>89</sup> calculated a Cu-NHC bond strength of 293 kJ/mol using DFT simulation. Furthermore, it is not believed that the corresponding Cu(II) compound, Cu(hmnds)<sub>2</sub>, is stable since linear Cu(II) complexes



are very rare.<sup>95</sup> Therefore, disproportionation similarly as described in equations 3 and 4 is not expected to occur. Instead the Cu(I) tetramer [Cu(hmde)]<sub>4</sub> is known as the stable solid form.<sup>92</sup> Although its application as CVD precursor was reported,<sup>92</sup> its vapor pressure is quite low which limits its suitability for ALD processes. However, the results obtained by Coyle et al.<sup>88,89</sup> and Hagen et al.<sup>91</sup> clearly demonstrated that the inhibition of the reaction described by equation 5 prevents the formation of tetramers under evaporation condition, and permits ALD growth to occur with this precursor.

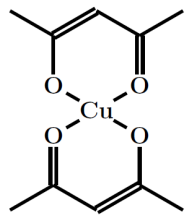
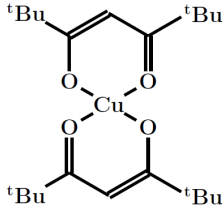
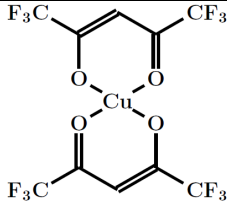
Table 2: Thermal properties of carbene-Cu(hmde) complexes.<sup>90</sup>

R <sup>1</sup>	R <sup>2</sup>	TGA res (%)	mp (°C)	1 Torr (°C)
<b>Unsaturated NHCs</b>				
<sup>i</sup> Pr	H			
<sup>t</sup> Bu	H	14.7	119	
<sup>i</sup> Pr	CH <sub>3</sub>	4.4	115	158
<b>Saturated NHCs</b>				
Et	H	1.5	Liquid	153
<sup>i</sup> Pr	H	1.1	51	149
<sup>t</sup> Bu	H	0.7	98	172
<sup>t</sup> Bu	CH <sub>3</sub>	1	118	162
<b>ADCs</b>				
Me		1.6	45	143
Et		0.6	Liquid	145
<sup>i</sup> Pr		1.1	184	169

One intriguing feature of the TGA curves in Figure 4 is the huge difference in stability between these very similar molecules. Coyle et al.<sup>90</sup> investigated the stability of Cu(hmds) complexes with different carbene ligands more closely in a recent study. Supporting their earlier results, they observed that saturated NHCs are more stable than unsaturated, and methyl groups can increase the stability of unsaturated carbenes. The decomposition occurs within the carbene groups, for example by hydrogen abstraction and through the breaking of the Cu-carbene bond. Furthermore, they observed that acyclic diamino carbenes can have similar stability as NHCs.

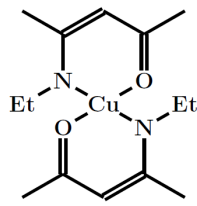
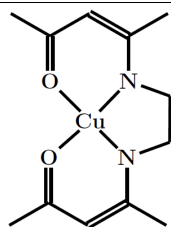
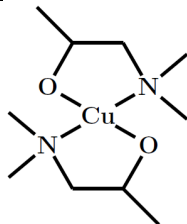
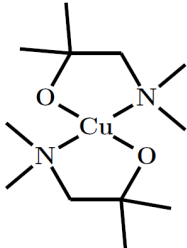
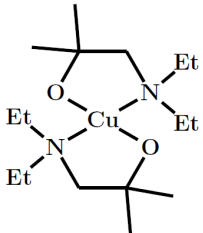
### 3.1.2 Cu(II)-Metalorganics

Table 3: Summary of Cu(II) metalorganics evaluates as precursors for the ALD or CVD of Cu

Name	Structure	References
Cu-bis(acetylacetonate),  Cu(acac) <sub>2</sub>		96
Cu-bis(2,2,6,6-methylheptane-3,5-dionate),  Cu(tmhd) <sub>2</sub>		97-99
Cu-bis(1,1,1,5,5,5-hexafluoroacetylacetonate),  Cu(hfac) <sub>2</sub>		100-103

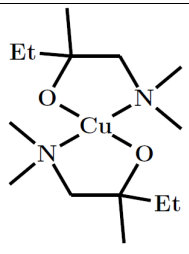
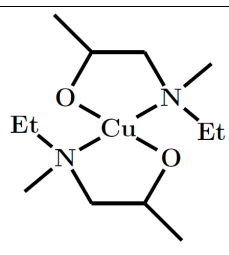
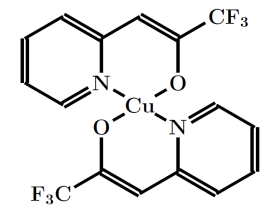
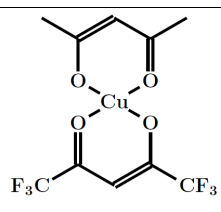
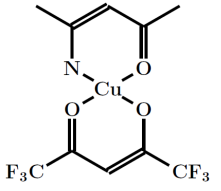
This is the author's peer reviewed, accepted manuscript. However, the online version of record will be different from this version once it has been copyedited and typeset.

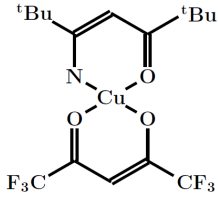
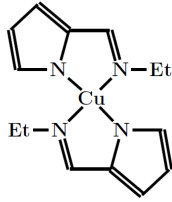
PLEASE CITE THIS ARTICLE AS DOI: 10.1063/1.5087759

Cu-bis(4N-ethylamino-pent-3-ene-2-onate)		104-109
Cu-(4,4'-N,N'-ethylene-bis(pentonate))		110
Cu-bis(dimethylamino-2-propoxide), Cu(dmap) <sub>2</sub>		111-118
Cu-bis(dimethylamino-2-methyl-2-propoxide), Cu(dmamp) <sub>2</sub>		119
Cu-bis(diethylamino-2-methyl-2-propoxide), Cu(deamp) <sub>2</sub>		119

This is the author's peer reviewed, accepted manuscript. However, the online version of record will be different from this version once it has been copyedited and typeset.

PLEASE CITE THIS ARTICLE AS DOI: 10.1063/1.5087759

<p>Cu-bis(dimethylamino-2-methyl-2-butoxide),</p> <p><math>\text{Cu}(\text{dmamb})_2</math></p>		119-121
<p>Cu-bis(ethylmethylamino-2-propoxide)</p>		122
<p>Cu-bis(N-heteroarylalkenolate)</p>		123,124
<p>Cu-(acetylacetonato)-(1,1,1,5,5,- hexafluoroacetylacetonate),</p> <p><math>\text{Cu}(\text{acac})(\text{hfac})</math></p>		125,126
<p>Cu-(pentane-2-imino-4-onato)-(1,1,1,5,5,- hexafluoroacetylacetonate),</p> <p><math>\text{Cu}(\text{ki})(\text{hfac})</math></p>		125,126

<p>Cu-(2,2,6,6-tetramethyl-3-iminoheptane-5-onato)- (1,1,1,5,5,-hexafluoroacetylacetonate),  Cu(dpk)(hfac)</p>		<p>125,126</p>
<p>Cu-bis(N-ethyl-2-pyrrolylaldimine)</p>		<p>127</p>

Cu(II)-metalorganics are usually more stable than their Cu(I) counterparts. The most intensively studied class of Cu(II) precursors are the bisdiketonates, namely Cu(acac)<sub>2</sub> and its derivatives. Cu(acac)<sub>2</sub> has a relatively low vapor pressure and usually needs to be evaporated at temperatures as high as 138 °C.<sup>96</sup> Cu(tmhd)<sub>2</sub> has a slightly larger vapor pressure but still requires high evaporation temperatures.<sup>97</sup> Both precursors are relatively inert and plasma processes are used to obtain growth at reasonable temperatures.<sup>96,97</sup> The high evaporation temperatures are problematic as they limit the minimum substrate temperature due to condensation effects. The fluorinated derivative Cu(hfac)<sub>2</sub> has a higher vapor pressure than the non-fluorinated compounds because the fluorine atoms attract electrons and decrease the van-der-Waals interaction.<sup>100,128</sup> Unfortunately, Cu(hfac)<sub>2</sub> is most stable as a monohydrate and the loss of H<sub>2</sub>O during evaporation is problematic for achieving a reliable precursor transport. Obtaining anhydrous Cu(hfac)<sub>2</sub> is known to be relatively difficult. Furthermore, precursors containing halogens are not preferred due to concerns about possible contamination of the Cu film and its interface with the substrate.

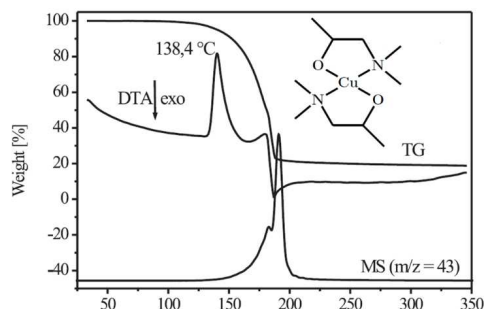


Figure 5: Thermogravimetric Analysis of  $\text{Cu}(\text{dmap})_2$ .<sup>111</sup> Adapted with permission from R. Becker et al., *Chem. Vap. Dep.* 9, 149 - 156 (2003). Copyright 2003 WILEY VCH Verlag GmbH and Co. KGaA.

Han et al.<sup>104</sup> and Park et al.<sup>105</sup> presented Cu films deposited with a Cu(II)ethylketoiminate, which is a liquid at room temperature and has a higher vapor pressure than non-fluorinated Cu(II)diketonates. Gerfin et al.<sup>110</sup> used a similar Cu-bisketoiminate, Cu-(4,4'-N,N'-ethylene-bis(pentonate)), for CVD in earlier work. This compound has a low vapor pressure (comparable to  $\text{Cu}(\text{acac})_2$ ) and high evaporation temperatures of 150-185 °C were therefore needed.



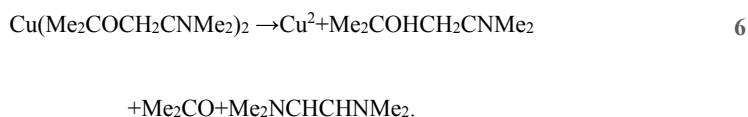
Scheme 2: Decomposition process of  $\text{Cu}(\text{dmap})_2$  as suggested by Young and coworkers.<sup>129</sup>

Another interesting class of Cu(II) compounds are the aliphatic alkoxides. Cu alkoxides are usually not very stable<sup>130</sup> but can be stabilized by interaction of electron donating groups, e.g. amino groups, with the metal center. Becker et al. tested Cu(II)aminoalkoxides for their suitability as CVD precursors.<sup>111-113</sup> Cu-bis(dimethylamino-2-propoxide) ( $\text{Cu}(\text{dmap})_2$ ) was shown to have very good thermal properties as it can be evaporated cleanly at moderate temperatures as indicated by the thermo-gravimetric analysis (TGA)

curve in Figure 5. A single mass loss step was observed at about 150 °C. The remaining mass was slightly less than 20%, which is consistent with a complete pyrolysis of the molecule. The differential thermal analysis (DTA) curve shows an endothermic peak at 139 °C indicating the melting point and an exothermic peak at 185.4 °C indicating pyrolysis. Furthermore, they demonstrated in isothermal TGA that the precursor can be transported readily when it is evaporated at low temperatures. Therefore, the precursor is suitable for low temperature ALD as well as for CVD by pyrolysis. ALD processes were reported by Lee et al.<sup>114</sup> and Knisley et al.<sup>115</sup> at temperatures as low as 100 °C. CVD by pyrolysis was reported by R.Becker et al.<sup>111,112,116</sup> and M.Becker et al.<sup>117</sup> typically around 260 °C. Young et al.<sup>129</sup> investigated the decomposition process of Cu(II)-aminoalkoxides on surfaces by IR-spectroscopy and suggested the mechanism depicted in Scheme 2. In this scheme one of the ligands loses an H-atom to the surface by  $\beta$ -hydride elimination resulting in an aldehyde. The hydrogen surface species formed are then available for reaction with adsorbed ligands to form an alcohol.

Further Cu(II)-aminoalkoxides have been reported as precursors for Cu CVD, mainly in the patent literature.<sup>131,132,119</sup> Here, Kim et al.<sup>119</sup> reported Cu(II)-aminoalkoxides which do not contain  $\beta$ -hydrogens at the alkoxy group. They evaluated Cu-bis(dimethylamino-2-methyl-2-propoxide) (Cu(dmamp)<sub>2</sub>), Cu-bis(diethylamino-2-methyl-2-propoxide) (Cu(deamp)<sub>2</sub>) and Cu-bis(dimethylamino-2-methyl-2-butoxide) (Cu(dmamb)<sub>2</sub>) as CVD precursors. All three compounds could be evaporated at moderate temperatures (38 - 70 °C). With Cu(dmamp)<sub>2</sub> metallic Cu films, as identified using X-ray diffraction (XRD), were obtained at substrate temperatures of 250 and 300 °C. However, the resistivity of the films was quite high, at 50  $\Omega$ cm for a film grown at 250 °C and 80  $\Omega$ cm for a film grown at 300 °C (no information on the thickness was given). Using Cu(deamp)<sub>2</sub> metallic Cu was also obtained when growth was carried out at 250 °C, but an amorphous deposit, probably consisting of decomposed precursor, was grown at 300 °C. With Cu(dmamb)<sub>2</sub>, lower growth temperatures could be applied and a film with a low resistivity of 2.3  $\mu\Omega$ cm was grown at 200 °C. TGA of Cu(dmamp)<sub>2</sub> showed a single step mass loss at about 200 °C and the

decomposition product formed for a sample heated for 3 hours at 200 °C was metallic Cu as shown by XRD. From the analysis of the byproducts it was concluded that the decomposition proceeds via  $\beta$ -hydride elimination, which involves the hydrogen atoms at the carbon bound to the amino group, and hydrogenation according to:



Adeka Corp., from Japan described a large number of Cu(II) aminoalkoxides in a patent<sup>122</sup> including such with different R-moieties at the amino group. One example is Cu-bis(ethylmethylamino-2-propoxide) ( $\text{Cu}(\text{emap})_2$ ) which has a melting point of 38 °C, and can therefore be evaporated as a liquid. The researchers tested this compound, as well as Cu-bis(isopropylmethylamino-2-propoxide) and Cu-bis(isopropylethylamino-2-propoxide), for ALD at 60 °C, and observed GPC values of 0.2-0.3 Å/cycle.

Giebelhaus et al.<sup>123</sup> synthesized a Cu alkoxide with an N-heterocyclic aryl group ( $[\text{Cu}((\text{C}_5\text{H}_4\text{N})(\text{CHCOCF}_3))_2]_2$ ), which crystallizes as dimer but sublimates as a monomer as shown with mass spectrometry. Unlike most Cu-alkoxides, this compound is stable in air. Sasinska et al.<sup>124</sup> from the same group demonstrated the ALD of metallic Cu using this molecule.

Due to the increasing commercial interest in Cu ALD, companies are now selling new precursors using only a trade name but not the structural name. An example is the AbaCus compound developed by Air Liquide.<sup>106-108</sup> The compound has a higher vapor pressure (~0.1 Torr at 110 °C) than  $\text{Cu}(\text{acac})_2$  or  $\text{Cu}(\text{tmhd})_2$  without containing any halogens. Although, only the term AbaCus has been used in scientific publications and Air Liquide advertisement thus far, the structural formula was published in a patent as Cu-bis(4-ethylamino-pent-3-ene-2-onate), which is the same name as that published by Park et al. and



This is the author's peer reviewed, accepted manuscript. However, the online version of record will be different from this version once it has been copyedited and typeset.

PLEASE CITE THIS ARTICLE AS DOI: 10.1063/1.5087759

Han and coworkers.<sup>104,105</sup> However, the data on the precursor properties provided by both groups are different. Park et al. and Han et al. reported a significantly higher vapor pressure of 2 Torr at 120 °C and a different color (dark brown). One explanation could be solvents being present within the precursor sample of one of the groups. However, TGA data published by these groups do not contradict each other.

Hagen et al.<sup>109</sup> evaluated the AbaCus compound for low temperature Cu ALD and achieved growth on several substrates at 60 and 100 °C. In the same work and in a second paper,<sup>133</sup> the researchers also tested the Cu-bis(aminoalkoxide) CTA-1 which was supplied by Adeka Corp. This compound has a relatively high vapor pressure of 0.3 Torr at 65.8 °C. This high vapor pressure facilitated the precursor transport and reproducible deposition of Cu films was achieved at temperatures as low as 30 °C.

One strategy to obtain precursors with tailored properties is the synthesis of heteroleptic complexes. Krisyuk et al.<sup>125,126</sup> synthesized the heteroleptic complexes Cu(acac)(hfac), Cu(ki)(hfac) and Cu(dpk)(hfac) (ki= pentane-2-imino-4-onate, dpk = 2,2,6,6-tetramethyl-3-iminoheptane-5-onate) through the reaction of the homoleptic compounds in toluene and vacuum sublimation. The researchers analyzed Cu(acac)(hfac) and Cu(ki)(hfac) using TGA, DTA and vapor pressure measurements. The TGA curve of Cu(acac)(hfac) shows a two-step process where the complex decomposed resulting in Cu(acac)<sub>2</sub> and Cu(hfac)<sub>2</sub> before the sublimation was complete. Cu(ki)(hfac) crystallizes in two polymorphs: a monomeric  $\alpha$ -modification and a dimeric  $\beta$ -modification, where the Cu centers are bonded to the oxygen atom of the ki ligands of each other. The  $\alpha$ -modification was obtained by slow crystallization from solution and the  $\beta$ -modification from evaporation and condensation. The TGA curves of both modifications show single-step processes with the  $\alpha$ -modification subliming more readily than the  $\beta$ -modification. The vapor pressures of Cu(acac)(hfac) and the two Cu(ki)(hfac) polymorphs are between the vapor pressures of the homoleptic compounds and the differences between the three were within the margins of error.

This is the author's peer reviewed, accepted manuscript. However, the online version of record will be different from this version once it has been copyedited and typeset.

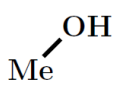
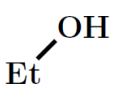
PLEASE CITE THIS ARTICLE AS DOI: 10.1063/1.5087759

Cu(dpk)(hfac) has a higher vapor pressure than Cu(acac)(hfac) and Cu(ki)(hfac) and was successfully evaluated for Cu CVD.<sup>126</sup>

### 3.2 Reducing Agents for Cu ALD

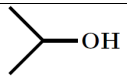
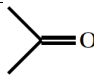
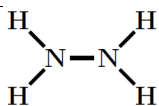
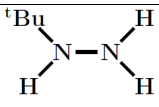
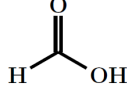
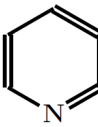
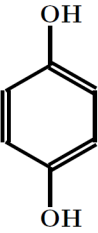
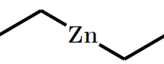

As discussed in the introduction, the requirement to reduce the cations in the precursors to the metallic state makes the deposition of elemental metals more challenging than the deposition of oxides. Molecular  $H_2$  can be regarded as the simplest reducing agent and has been widely used for the ALD of Cu. However, its limited reactivity is a major challenge, as it will be discussed in the first part of this section. Hydrogen plasma can be applied to reduce virtually all Cu-precursors to metallic Cu. A limitation here is concerns about an insufficient conformality on 3d structures. Plasma enhanced ALD (PEALD) of Cu will be discussed in the second part of this section. The problems associated with molecular  $H_2$  and H plasma have triggered intensive research on alternative reducing agents. These can be divided into two groups, organic and metal-containing reactants, which is discussed in the third and fourth part of this section. Finally, the strategy to grow films of a Cu-containing material such as a Cu-oxide or Cu-nitride and convert it to metallic Cu by subsequent annealing in reductive atmosphere is discussed.

Table 4: Summary of coreagents evaluated for the ALD of Cu

Molecule	Structure	References
$H_2$		6,74,79,91,99,105
$H^*$		86,89,97,103,108,109,120,122,133-135,121
Methanol		136
Ethanol		136

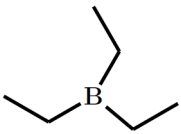
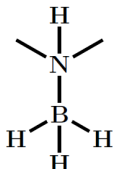
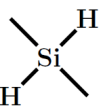
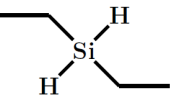
This is the author's peer reviewed, accepted manuscript. However, the online version of record will be different from this version once it has been copyedited and typeset.

PLEASE CITE THIS ARTICLE AS DOI: 10.1063/1.5087759

Isopropanol		
Formaldehyde		136
Hydrazine		115
<sup>t</sup> Bu-hydrazine		118
Formic Acid		75,115
Pyridine		101
Hydroquinone		137
Zn(C <sub>2</sub> H <sub>5</sub> ) <sub>2</sub> ,		102,114,127,138
DEZ		
Al(CH <sub>3</sub> ) <sub>3</sub> ,		127,138
TMA		

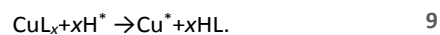
This is the author's peer reviewed, accepted manuscript. However, the online version of record will be different from this version once it has been copyedited and typeset.

PLEASE CITE THIS ARTICLE AS DOI: 10.1063/1.5087759

B(C <sub>2</sub> H <sub>5</sub> ) <sub>3</sub> ,  TEB		127,138
BH <sub>3</sub> (NHMe <sub>2</sub> )		139
SiH <sub>2</sub> (CH <sub>3</sub> ) <sub>2</sub> ,  Dimethyl-silane		68
SiH <sub>2</sub> (C <sub>2</sub> H <sub>5</sub> ) <sub>2</sub> ,  Diethyl-silane		67
Zn		56

### 3.2.1 Molecular Hydrogen

No direct reaction with molecular hydrogen in the gas phase can take place at any viable temperature. Instead, the reaction pathway is via chemisorbed hydrogen on the substrate:



Therefore, a strong dependence of the growth on the substrate material has to be expected. Martensson and Carlsson<sup>6</sup> reported that with  $\text{Cu}(\text{tmhd})_2$  Cu grows on a Pt/Pd alloy with a saturated growth per cycle (GPC) of 0.38 Å/cycle in an ALD window between 190 to 260 °C but not on air-exposed, non-noble metals or on insulators. Jezewski et al.<sup>97</sup> reported that Cu also cannot be grown on Au, which is known not to chemisorb hydrogen. Martensson and Carlsson<sup>6</sup> suggested that the reason for the lack of growth is a blocking of the transfer of electrons from the substrate to the metal center by oxygen.

Han et al.<sup>104</sup> reported the deposition of Cu with a Cu(II)ethylketoiminate on Pt and Park et al.<sup>105</sup> reported growth on Ru with the same precursor. They did not provide a GPC and indicated saturation by measuring the sheet resistance of films grown with varying pulse lengths at the same temperature. Indications for a stable growth process were observed between 160 and 200 °C on Pt<sup>104</sup> and between 140 and 200 °C on Ru.<sup>105</sup> At the low-temperature end the sheet resistance increased due to a lack of growth and increased at the high-temperature end due to island formation.

Li et al.<sup>79</sup> used molecular hydrogen in their ALD experiments with Cu(I)amidinates. They also achieved growth on glass and  $\text{Al}_2\text{O}_3$  and observed a higher GPC on those oxides than on metal films such as Ru or Co.

Norman et al.<sup>74</sup> reported the growth of metallic Cu films with molecular hydrogen on Ru coated surface when they tested the Cu(I)-ketoiminate KI-2 and the Cu(I)-diketiminatate DI-1. However, saturated growth could not be demonstrated.

Hagen et al.<sup>91</sup> carried out Cu growth with NHC-Cu(hmde) and molecular hydrogen and achieved deposits on Pd, Pt and Ru. Strong indications for saturated growth were found at temperatures

around 220 °C with a rate of 0.4 Å/cycle. Relatively little growth was obtained at temperatures below 180 °C.

### 3.2.2 Plasma-Enhanced ALD of Cu

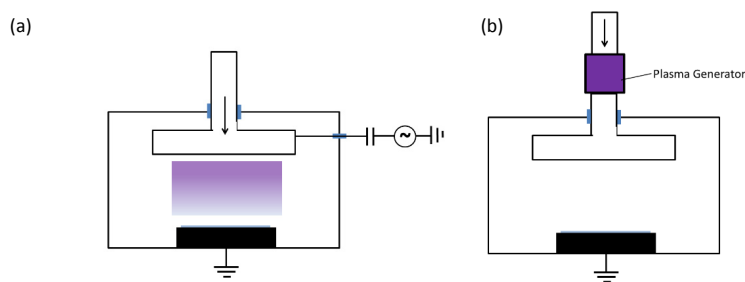


Figure 6: Plasma-enhanced ALD reactors: (a) direct plasma, (b) remote plasma.

When a plasma process is used, film growth can be obtained at lower temperatures. For plasma enhanced ALD (PEALD) direct<sup>96,140</sup> as well as indirect or remote plasmas<sup>141</sup> can be applied (Figure 6). In a direct PEALD chamber the plasma is generated directly above the substrate and ions can play an important part in the reaction process, while in a remote PEALD chamber the plasma is generated at a distance from the substrate and the major reaction species are radicals. Radicals can also be formed in hot wire reactors.<sup>142</sup> Here the molecules are broken into radicals by a hot wire in the flow path of the reactant gas. This process is often called radical enhanced ALD (REALD). This term is also used for remote plasma ALD<sup>134</sup> although PEALD is more common. A general concern is the loss of uniformity<sup>31</sup> due to the recombination of plasma species in trenches and vias. Recombination probabilities for H, O and N radicals on different materials are shown in Table 5. The effect is significantly higher for direct plasma processes as the lifetime of

radicals is usually larger than that of ions. However, direct plasma can be useful in some cases, being beneficial for surface preparation, e.g. for the removal of native surface oxides of air exposed metal substrates. Knoop et al.<sup>143</sup> developed a Monte Carlo simulation to calculate the impact of recombination on the deposition profile of trenches and demonstrated that indeed a deposition regime existed where the profile of film growth is dominated by recombination.

Table 5: Recombination probabilities of gas radicals on different surfaces.

Radical	Surface	Recombination Probability
H	Si	0.7
	SiO <sub>2</sub>	0.00004
	Al <sub>2</sub> O <sub>3</sub>	0.0018
	Cu	0.14
	Au	0.15
	Pd	0.07
	Al	0.29
O	SiO <sub>2</sub>	0.0002
	Al <sub>2</sub> O <sub>3</sub>	0.0021
	ZnO	0.0004
	Cu <sub>2</sub> O	0.043
	Si	0.0016
N	SiO <sub>2</sub>	0.0003
	Al	0.0018

They furthermore used an analytical method based on a hydrogen atom recombination model by Walraven and Silvera.<sup>144</sup> According to this the ratio  $\alpha$  of atoms which reach the bottom of a pore with an aspect ratio  $AR$  is:

$$\alpha = \frac{1}{\cosh(AR\sqrt{r})} \quad 10$$

where  $r$  is the recombination probability for a certain atom/surface pair. Using the values for hydrogen on Si, Cu and SiO<sub>2</sub> taken from Table 5, it becomes clear that recombination effects



would have significant impact on SiO<sub>2</sub> only for structures of extreme aspect ratio, while on metals or Si effects can be visible at more typical dimensions.

Wu and Eisenbraun<sup>135</sup> demonstrated the deposition of conformal Cu films on trenches in SiO<sub>2</sub> with a depth of 160 nm and an aspect-ratio of 10 using Cu(acac)<sub>2</sub> and hydrogen plasma. Niskanen et al.<sup>134</sup> also reported the conformal coating of trenches when they carried out PEALD experiments with Cu(acac)<sub>2</sub> at 140 °C. Deposition was achieved on several substrates (Si, HF cleaned Si, SiO<sub>2</sub>, glass, TaN, TiN, Cu), but the resistivity of the films was relatively large being  $1.5 \times 10^{-5} \Omega\text{cm}$  for 25 nm thick films and a significant C content was measured.

Jezewski et al.<sup>97</sup> reported an ALD window from 90 - 250 °C when they carried out PEALD experiments with Cu(tmhd)<sub>2</sub>. Below 90 °C they observed a decrease of the GPC. The most likely reason for this was condensation between the bubbler, which was at 123 °C, and the substrate. Mao et al.<sup>108</sup> performed their PEALD experiments with the AbaCus compound at temperatures as low as 30 °C, which was much lower than their evaporation temperature of 100 °C and claimed that no condensation effects were observed. They also presented conformal coating of trenches.

The impact of condensation effects depends on the vapor pressure of the precursor as well as on the design of the ALD reactor. Thus, the flow path of the precursor towards the substrate must be kept at a reasonably high temperature to secure transport while the substrate itself is at a lower temperature.

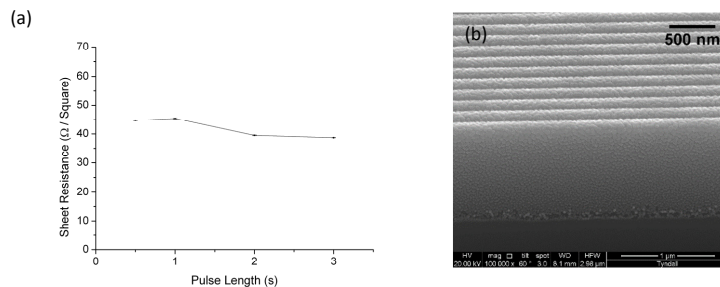


Figure 7: Cu deposits from CTA-1 and hydrogen plasma at 30 °C: (a) change of sheet resistance with precursor pulse length for film grown on Pd after 250 cycles; (b) deposit on Si trenches after 450 cycles.<sup>109</sup> Reprinted with permission from D. J. Hagen et al., *Surf. Coat. Tech.* 230, 3-12 (2013). Copyright 2013 Elsevier.

When Hagen et al.<sup>109</sup> carried out PEALD with two precursors, AbaCus and CTA-1, using a direct plasma reproducible growth was achieved at temperatures as low as 30 and 60 °C, respectively. The lower deposition temperature for CTA-1 was due to its higher vapor pressure. The films were of good quality as was confirmed by XRD and electric measurements. Although no saturation could be confirmed when the sheet resistance was measured for films deposited with varying CTA-1 pulse lengths, the parasitic CVD growth was quite small, and trenches of high aspect ratio could be coated (Figure 7). Similarly, Yoshino et al.<sup>122</sup> performed their PEALD experiments with Cu(II)-aminoalkoxides at 60 °C.

Guo et al.<sup>86</sup> investigated PEALD processes at substrate temperatures lower than the precursor sublimation temperature in detail using  $[\text{MeC}(\text{iPrN})_2\text{Cu}]_2$  and hydrogen plasma. Although the precursor was sublimated at 90 °C, the researchers found strong indications of saturated growth with a GPC of 0.7 Å/cycle. They investigated the mass change during the ALD cycles with QCM measurements and observed a significant mass loss during the purge step after the precursor exposure, and interpreted this as the removal of a physisorbed film which was about one monolayer thick. Interestingly, continuous films were obtained after moderate cycle numbers while pronounced island growth was observed for higher deposition temperatures and for higher

plasma powers. The researchers blamed the latter on an increased effective surface temperature of the samples.

Coyle et al.<sup>89</sup> deposited Cu films with NHC-Cu(hmds) and hydrogen plasma and reported saturated growth on Si. The deposition was carried out at 225 °C which is an unusually high temperature for PEALD processes indicating that the limiting mechanism is the chemisorption of this precursor as discussed above.

### 3.2.3 Organic Reducing Agents

When alcohols or formaldehyde were used as reducing agents, similar problems were observed as for the reaction with molecular H<sub>2</sub>. Solanki and Pathangey<sup>136</sup> carried out ALD experiments with Cu(hfac)<sub>2</sub> and different liquid reducing agents such as ethanol, methanol and formalin, an aqueous solution of formaldehyde, and obtained the best results with formalin. Formaldehyde is known to dissociate to H\* and CO\* surface groups on many materials.<sup>145,146</sup> Therefore one would expect similar reaction mechanisms as when H<sub>2</sub> is used, although the presence of H<sub>2</sub>O might have some impact. However, reasonable growth was only achieved above 230 °C with the best results obtained at 300 °C.

Norman et al.<sup>75</sup> reported that Cu CVD growth with the Cu(I)-ketoiminate KI-3 on Ru coated substrates resulted in metallic films when formic acid was used but in no growth or deposits of poor quality when hydrogen or isopropanol was used. They suggested that formic acid reacts via releasing H to the surface which reacts with the adsorbed ligands. However, this cannot explain the differences between the results of the use of the three reactants as all should provide H atoms to the Ru substrate. Alternative explanations would include complex formation between formic acid and the adsorbed precursor<sup>75</sup> and formation of functional surface species by formic acid with

which the precursor can react. Formic acid was also used for CVD experiments<sup>75</sup> with KI5 which resulted in the growth of metallic Cu on Ru at temperatures between 125 and 250 °C.

In a recent study, Väyrynen et al.<sup>118</sup> investigated <sup>t</sup>Bu-hydrazine as a reducing agent for Cu(dmap)<sub>2</sub>. The GPC increased throughout the entire temperature range from about 0.06 Å/cycle at 80 °C to 0.24 Å/cycle at 140 °C, and saturated growth was demonstrated for the depositions at 120 °C. Furthermore, they observed a decrease in the GPC with an increasing number of cycles, which they attributed to the changing surface during the growth process.

Knisley et al.<sup>115</sup> developed a low temperature ALD process consisting of pulses of Cu(dmap)<sub>2</sub>, formic acid and hydrazine. Here, formic acid reacts with the adsorbed Cu(dmap)<sub>2</sub> to form Cu(II)-formate:



Cu(II)-formate was readily reduced during the hydrazine pulse. Saturated growth was demonstrated and a window of saturated growth with 0.5 Å/cycle between 100 and 170 °C was identified. Above 170 °C the GPC decreases. Although this has been rarely observed for Cu ALD, it is known from other ALD processes and is usually attributed to desorption. It is important to note that it was not possible to obtain Cu films from Cu(dmap)<sub>2</sub> and hydrazine alone which is in contrast to the ALD process with Cu(dmap)<sub>2</sub> and <sup>t</sup>Bu-hydrazine reported by Väyrynen coworkers.<sup>118</sup>

A three-step process was also reported by Kang et al.,<sup>101</sup> who were able to achieve deposition of Cu down to room temperature by catalyzing the reaction of Cu(hfac)<sub>2</sub> and H<sub>2</sub> with pyridine. The

most likely reason is a weakening of the Cu-O bonds by complex formation of the adsorbed Cu(hfac)<sub>2</sub> with the Lewis base pyridine.<sup>147,148</sup>

Tripathi and Karppinen<sup>137</sup> reported an ALD process which uses an organic reducing agent, hydroquinone together with Cu(acac)<sub>2</sub> and H<sub>2</sub>O (Figure 8). Hydroquinone was exposed repeatedly after a certain number of Cu(acac)<sub>2</sub>/H<sub>2</sub>O subcycles  $n$ . The obtained GPC was very high, 2 Å/cycle, and remained constant between 200 and 250 °C. The crystalline quality increased with increasing temperature and increasing  $n$ . The electrical quality of the films was quite good as resistivity values between 2 and 5 μΩcm were measured. Moreover, Cu was also obtained when only Cu(acac)<sub>2</sub> and hydroquinone were used.

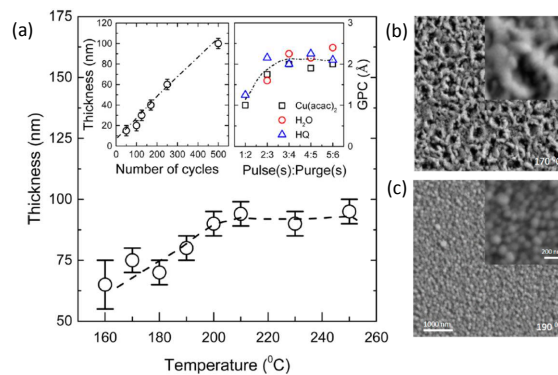


Figure 8: Cu films grown with Cu(acac)<sub>2</sub>, H<sub>2</sub>O and hydroquinone: (a) GPC vs temperature for growth with a subcycle ratio  $n$  of 1, insets thickness vs number of cycles (left) and GPC vs pulse and purge lengths (right) for growth at 210 °C; (b) SEM micrograph of film deposited at 170 °C (c) 190 °C.<sup>137</sup> Reprinted with permission from T. S. Tripathi and M. Karppinen, *Chem. Mater.* 29, 1230-1235 (2017). Copyright 2017 American Chemical Society.

### 3.2.4 Metal-Containing Reducing Agents

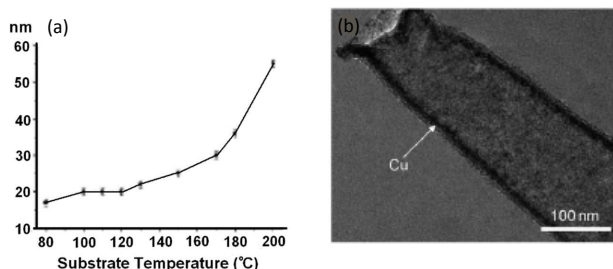
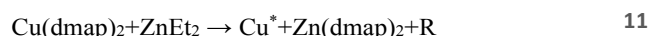


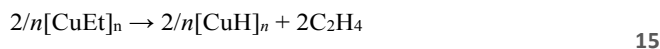
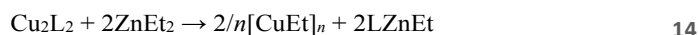
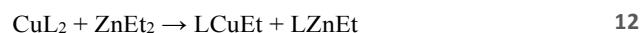
Figure 9: Results from ALD experiments with  $\text{Cu}(\text{dmap})_2$  and  $\text{ZnEt}_2$ :<sup>114</sup> (a) temperature characteristic for deposition with 1000 cycles; (b) Cu nanotube fabricated by Cu deposition into a porous membrane and subsequent removal of the membrane. Adapted with permission from B. H. Lee et al., *Angew. Chem.* 121, 4606-4609 (2009). Copyright 2009 WILEY VCH Verlag GmbH and Co. KGaA.

Lee et al.<sup>114</sup> reported a thermal Cu ALD process at temperatures as low as 100 °C when they reacted  $\text{Cu}(\text{dmap})_2$  with diethyl-zinc ( $\text{ZnEt}_2$ ):



The ALD window of this process was quite small (100 - 120 °C) as can be seen in Figure 9(a). At lower temperatures the reaction was incomplete resulting in a decrease of the GPC and incorporation of C as was confirmed by X-ray photo-electron spectroscopy (XPS). At higher temperatures the GPC increased and contamination with Zn was observed. The suitability of this reaction for coating complex structures was demonstrated by deposition onto a porous polycarbonate membrane. When they removed the membrane after Cu deposition they obtained Cu nanotubes (Figure 9(b)), which demonstrates the deposition of continuous thin films onto structures of extremely high aspect ratio.

A similar ALD mechanism was applied by Vidjayacoumar et al.<sup>127</sup> who used Cu(II)-N-ethyl-2-pyrrolylaldimine. However, they did not achieve a saturated growth regime and significant contamination of the films, especially with Zn, was observed. This was most likely due to the substrate temperatures above 120 °C, which were necessary as the vapor pressure of the compound is relatively low. They also tested AlMe<sub>3</sub> and BEt<sub>3</sub> as reducing agents but did not obtain metallic Cu films in the ALD experiments, although Cu films were obtained when the reaction was carried out in solution. Vidjayacoumar et al. investigated the reaction pathway in solution with NMR<sup>138</sup> and observed a ligand exchange mechanism:



An alternative reaction path to equation 14 is:

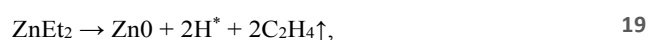


The NMR spectra clearly indicated the presence of the Cu(I) dimer intermediate although a more direct reaction path via



could not be ruled out for large  $\text{ZnEt}_2$  concentrations. Dey and Elliott<sup>149</sup> simulated the thermochemistry of the reaction mechanism using density functional theory (DFT) and concluded that Cu(I)-dimer intermediates are indeed possible for various precursors.

An important aspect of the reaction is the adsorption mechanism for  $\text{ZnEt}_2$ . It is well known that it decomposes via  $\beta$ -hydride elimination,<sup>150-153</sup>



on many surfaces at relatively low temperatures, while it is quite stable in the gas phase.<sup>154</sup> This mechanism might be a reason for the increase of the GPC and significant incorporation of Zn in the growing Cu films at relatively moderate temperatures.

A reaction of Zn with Cu complexes to form metallic Cu is possible and has been tested by Juppo et al.<sup>56</sup> who grew Cu by sequential exposure of substrates with CuCl and Zn. This process required relatively high deposition temperatures of about 400 °C as the vapor pressures of both reactants are quite low and no saturation could be observed.

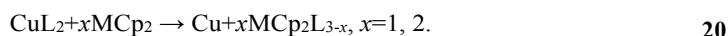
Kalutarage et al.<sup>139</sup> used  $\text{BH}_3(\text{NHMe}_2)$  as a reducing agent for  $\text{Cu}(\text{dmap})_2$ . They observed island growth and problems with nucleation. Therefore, they used long  $\text{Cu}(\text{dmap})_2$  pulses (20 s) during the first 50 pulses in order to form a nucleation layer. A temperature window from 130 – 160 °C with a GPC of 0.12 Å was observed after the initial nucleation. However, the films suffered from high impurity contents. The authors were able to improve the quality of the films by adding a formic acid pulse between the  $\text{Cu}(\text{dmap})_2$  and the  $\text{BH}_3(\text{NHMe}_2)$  pulse. The resulting films had a much lower concentration of impurities than those deposited with the two-step process and no separated nucleation cycles were required.

Thompson et al.<sup>67,68</sup> used the silane derivatives  $\text{Me}_2\text{SiH}_2$  and  $\text{Et}_2\text{SiH}_2$  for reducing adsorbed Cu-diketiminate compounds. They reported a lack of saturation even at very low deposition



temperatures. Unfortunately, they did not provide enough information to decide if this was due to disproportionation of the Cu(I) compound or to the reducing agent.

An interesting approach was presented in computational studies by Dey et al.<sup>155</sup> suggested using metallocenes as reducing agents which would be oxidized by the adsorbed Cu precursor:



VCp<sub>2</sub> turned out to be the most promising compound and solution chemistry studies showed that Cu can indeed result from this reaction depending on the solvent. However, experimental validation of the ALD process has not been presented thus far.

### 3.2.5 Reduction of Cu-Containing Films

One strategy designed to circumvent the limited reactivity between Cu precursors and molecular reducing agents is to grow a Cu-containing film by ALD, for example CuO<sub>x</sub>, and reduce it subsequently to metallic Cu. Waechtler et al.<sup>70,71</sup> first grew Cu-oxide with [<sup>n</sup>Bu<sub>3</sub>P]<sub>2</sub>-Cu(acac) and wet oxygen, a mixture of oxygen and water vapor, and then used formic acid for reduction.<sup>70</sup> They observed a saturated GPC of about 0.1 Å/cycle in a temperature window of 100 - 120 °C. A mainly Cu<sub>2</sub>O phase was detected by XPS and Auger-electron spectroscopy (AES), although Cu(II) was present too, which might partly be due to exposure to atmosphere. The success of reduction depended strongly on the substrate material. While conductive, metallic Cu films were obtained on Ru, the process was more limited on TaN.

Li and Gordon<sup>81</sup> grew Cu<sub>3</sub>N from the reaction of [Cu(sBu-Me-amd)]<sub>2</sub> with ammonia. A saturated GPC of 0.17 Å/cycle was observed for a typical substrate temperature of 160 °C. Subsequently,

they annealed the  $\text{Cu}_3\text{N}$  films at 225 °C in a forming-gas atmosphere to obtain metallic Cu. On Ru they reported indications for electrically continuous Cu films as thin as 0.8 nm. The films were smoother than films obtained from the direct reduction of the Cu precursor with  $\text{H}_2$  as the researchers demonstrated with atomic force microscopy (AFM). The approach of growing  $\text{Cu}_3\text{N}$  films by ALD for subsequent reduction was first done by Thoenndahl et al.,<sup>156</sup> who used three-pulse cycles with  $\text{Cu}(\text{hfac})_2$ ,  $\text{H}_2\text{O}$  and  $\text{NH}_3$ . However, their  $\text{Cu}_3\text{N}$  deposits were quite grainy which is partly due to the higher temperatures.

Park et al.<sup>157</sup> used  $\text{Cu}(\text{dmamb})_2$  and  $\text{NH}_3$  to deposit  $\text{Cu}_3\text{N}$  at temperatures down to 120 °C and reduced them to metallic Cu by annealing in  $\text{H}_2$  at temperatures ranging from 150 to 250 °C. As can be seen from the transmission electron microscopy (TEM) micrographs in Figure 10, very conformal and continuous films could be obtained. This is in sharp contrast to pronounced island growth these researchers reported for the growth with  $\text{H}_2$  in the same paper. The best electrical properties were obtained for a film deposited with 50 cycles at 120 °C and annealed at 200 °C (thickness 4.2 nm), for which a resistivity of 30  $\mu\Omega\text{cm}$  was measured.

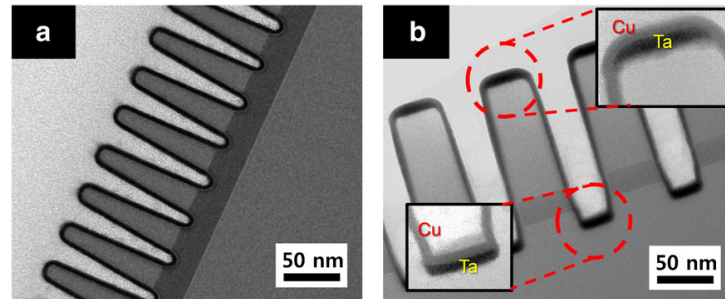
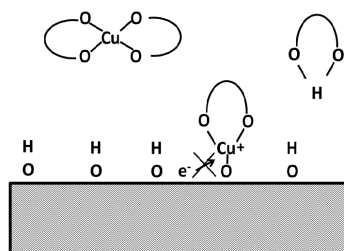


Figure 10: (a) TEM micrograph of  $\text{Cu}_3\text{N}$  film deposited with  $\text{Cu}(\text{dmamb})_2$  and  $\text{NH}_3$ ; (b) Cu film obtained by annealing of  $\text{Cu}_3\text{N}$  in  $\text{H}_2$ .<sup>157</sup> Reprinted with permission from J.-M. Park et al., *Thin Solid Films* 556, 434-439 (2014). Copyright 2014 Elsevier .

### 3.3 The Role of the Substrate Material



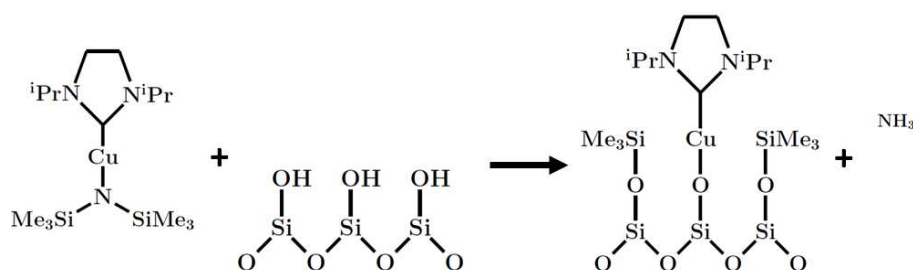
Scheme 3: Model of Martensson and Carlsson<sup>6</sup> for the lack of Cu growth on hydroxyl-terminated substrates including air-exposed metal films. Transfer of electrons across the Cu-O bond is not possible.

A general observation in experiments on Cu ALD is the strong dependence of the film growth on the substrate material. This is especially the case for the reaction of Cu(II) complexes with molecular H<sub>2</sub>. Martensson and Carlsson for example<sup>6</sup> reported growth of ALD Cu films with Cu(tmhd)<sub>2</sub> on a Pt/Pd substrate, while no growth was observed on oxides and air exposed metal films. They concluded that the reason might be lack of electron transport from the substrate to the Cu cation across the Cu-O bond (Scheme 3).

Cohen et al.<sup>60,158</sup> carried out XPS studies of Cu(hfac)<sub>2</sub> and COD-Cu(hfac) adsorbed on SiO<sub>2</sub> and Ag. While a reduction of the Cu center was observed on Ag, Cu(2+) was detected on SiO<sub>2</sub>. Furthermore, the Auger LMM peak of the Cu center of both precursors adsorbed on Ag was between that expected for Cu(0) and Cu(I) indicating interaction with the substrate electrons. Chaukulkar et al.<sup>103</sup> investigated the adsorption of Cu(hfac)<sub>2</sub> on Al<sub>2</sub>O<sub>3</sub> and its subsequent reaction with hydrogen plasma using in-situ infrared reflection absorption spectroscopy. Importantly, they observed chemisorption of Cu(hfac)<sub>2</sub> on nearly hydroxyl-free Al<sub>2</sub>O<sub>3</sub> films most-likely occurring

at Al-O-Al bridges showing that hydroxyl groups are no requirement for Cu-diketonate-based ALD processes on oxides.

Mulley et al.<sup>159</sup> undertook extensive studies on Cu(hfac)<sub>2</sub> adsorbed on rutile TiO<sub>2</sub> (110) using synchrotron radiation. They observed a reduction of the Cu center to Cu(I) in a high resolution XPS scan of the Cu 2p<sub>3/2</sub> peak. Furthermore, near edge X-ray adsorption fine structure (NEXAFS) experiments, where the adsorption by excitation of core electrons to the  $\pi$ -orbitals depends on the angle of the OCCCCO-plane of the ligand with electric field vector of the X-ray wave, revealed that the ligand is adsorbed nearly perpendicular to the surface confirming the loss of one ligand. They suggested that this ligand might also form an adsorbed species on the TiO<sub>2</sub> surface. However, these results might be very specific for the crystal system investigated by Mulley and coworkers. In a later study, Rayner et al.<sup>160</sup> investigated the development of a room-temperature deposited Cu(hfac)<sub>2</sub> film adsorbed on TiO<sub>2</sub> during annealing using XPS and STM. While XPS showed a shift of the Cu 2p from Cu(I) to lower energies indicating formation of Cu(0) species, agglomeration of Cu to islands was visible in the STM scans. With increasing temperature, the islands were growing larger while their density decreased.



Scheme 4: Proposed adsorption mechanism for 1,3-diisopropylimidazolin-2-ylidene-Cu(hmds) on SiO<sub>2</sub>.

This is the author's peer reviewed, accepted manuscript. However, the online version of record will be different from this version once it has been copyedited and typeset.

PLEASE CITE THIS ARTICLE AS DOI: 10.1063/1.5087759

Pallister and Barry<sup>161</sup> investigated the adsorption of the NHC-Cu(I)-carbenes 1,3-diisopropylimidazolin-2-ylidene-Cu(hmds) and 1,3-diethylimidazolin-Cu(hmds), as well as Hhmds, on SiO<sub>2</sub> by solid-state NMR. The samples were prepared by exposing high-surface-area SiO<sub>2</sub> powder to one very long ALD half-cycle at 150 and 250 °C. They observed that the anionic ligand reacts with hydroxyl groups forming SiMe<sub>3</sub><sup>-</sup> surface species and NH<sub>3</sub>. This behavior is very well known for Hhmds, which is widely used as primer for photoresists in microfabrication. The adsorption of the two NHCs differed very much. For 1,3-diisopropylimidazolin-2-ylidene the <sup>13</sup>C chemical shifts did not differ between the adsorbed species and the parent compound. From this, it was concluded that 1,3-diisopropylimidazolin-2-ylidene remains bonded to the Cu ion after adsorption. The amount of adsorbed 1,3-diisopropylimidazolin-2-ylidene was higher for the deposition at 250 °C than for the deposition at 150 °C. The proposed adsorption mechanism for 1,3-diisopropylimidazolin-2-ylidene-Cu(hmds) is depicted in Scheme 4. For 1,3-diethylimidazolin-Cu(hmds), very little 1,3-diethylimidazolin could be detected on the surface. From this, Pallister and Barry concluded that it is not chemisorbed but only weakly physisorbed and desorbs.

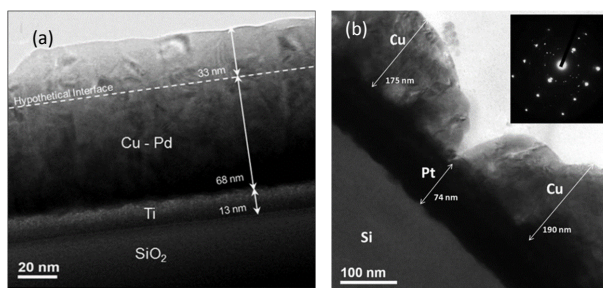


Figure 11: TEM micrographs of Cu films deposited on (a) Pd and (b) Pt using Cu(tmhd)<sub>2</sub> and H<sub>2</sub>.<sup>98</sup> Reprinted with permission from I. J. Hsu et al., *J. Vac. Sci. Technol. A* 27, 660-667 (2009). Copyright 2009 American Vacuum Society.

For ALD growth using molecular  $H_2$ , it is generally agreed that it must be adsorbed dissociatively on the substrate. For example, Jezewski et al.<sup>97</sup> reported that Cu could not be grown on Au using  $Cu(tmhd)_2$  and  $H_2$ . This means, the substrate needs to function as catalyst for the hydrogenation of the precursor. This explains why Cu growth could be obtained on Pd and Pt films.<sup>6,104,98</sup> Hsu et al. compared the growth of Cu on those two metals<sup>98</sup> and observed an intermixing of the Pd substrate and the growing Cu film resulting in no phase boundary being visible between the films in a TEM cross-section (Figure 11 (a)). On the other hand, they observed a clear phase boundary on Pt (Figure 11 (b)). Both intermetallic systems Cu/Pd and Cu/Pt are quite similar, showing complete miscibility and intermetallic phases at lower temperatures. However, from a kinetic point of view one would expect interdiffusion starting at lower temperatures for Cu on Pd. It also depends on the exact details of the substrate films such as underlayer, growth conditions or thickness. For example, Han et al.<sup>104</sup> observed interdiffusion starting at 200 °C, when they grew Cu on Pt with Cu-bis(4-ethylamino-pent-3-ene-2-onate). Park et al. demonstrated growth of Cu on Ru with this compound and obtained rather grainy films. Jiang et al.<sup>99</sup> investigated the Cu ALD process with  $Cu(tmhd)_2$  and  $H_2$  on Pd with in-situ ellipsometry. Ellipsometry is quite often used to characterize ALD growth in-situ. However, given the complexity of the structure the authors interpreted the change of the ellipsometric parameters qualitatively instead of quantifying film thicknesses for example. They analyzed the change of the parameter  $\Delta$  during each cycle, and observed a decrease of  $\Delta$  at the beginning of each  $Cu(tmhd)_2$  pulse, an increase after the pulse and little change during the  $H_2$  pulse. The researchers suggested from this observation that no adsorbed  $Cu(tmhd)_2$  remains on the surface to be reduced by the following  $H_2$  pulse, but H species on the surface remain after the  $H_2$  pulse to react with the next  $Cu(tmhd)_2$  pulse. Further adsorbed  $Cu(tmhd)_2$  desorbs during the purge following its exposure. To confirmed this model they prepared three samples for XPS measurement: normal process with 8 cycles, 8 cycles with short anneal at 320 °C after the  $H_2$  pulses, a single  $Cu(tmhd)_2$

pulse. The Cu XPS peaks for the latter two samples were very similar and much weaker than those for the first supporting their model.

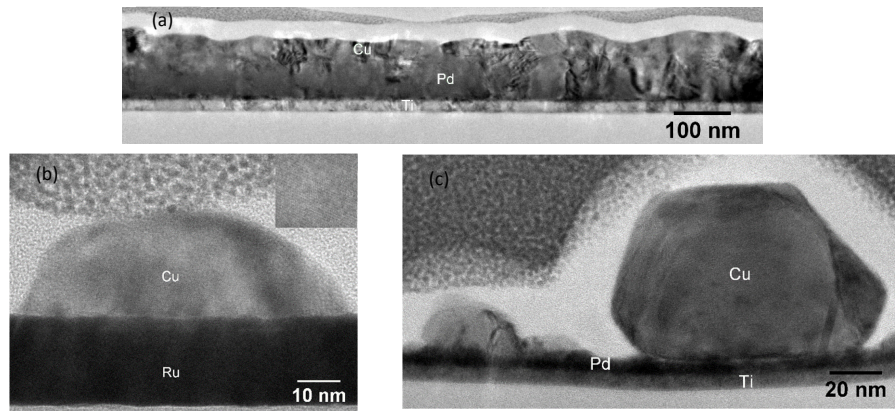


Figure 12: TEM cross-sections of Cu deposits grown after 1000 cycles at 220 °C using [NHC]Cu(hmds) and molecular H<sub>2</sub> on: (a) 70 nm thick Pd films, (b) Ru, (c) < 10 nm thick Pd films.<sup>91</sup> Reprinted with permission from D. J. Hagen et al., *J. Chem. Mater. C 2*, 9205-9214 (2014). Copyright 2014 Royal Society of Chemistry.

Hagen et al.<sup>91</sup> obtained Cu films that appeared continuous during their experiments with NHC-Cu(hmds) and molecular H<sub>2</sub> for depositions on Pd while island growth was observed on Ru. An interesting result was that island growth was also observed when ultra-thin (< 10 nm) Pd substrate films were used. These islands were less regularly distributed than those on Ru and had a larger size variation which indicates different film formation mechanisms. Furthermore, the wetting angle of Cu islands on thin Pd films was much larger than those on Ru films and had pronounced facets. They suggested<sup>91</sup> that this can be explained from classical theory. The equilibrium wetting angle  $\theta$  can be obtained from Young's equation<sup>162</sup>

$$\cos(\theta) = \frac{\gamma_{sub} - \gamma_{if}}{\gamma_{Cu}}, \quad 22$$

where  $\gamma_{sub}$ ,  $\gamma_{if}$  and  $\gamma_{Cu}$  are the substrate surface energy, the interface energy, and the surface energy of Cu, respectively. Therefore,  $\theta$  decreases with increasing  $\gamma_{sub}$ , which is phenomenologically connected with the melting point.<sup>162</sup> Furthermore,  $\theta$  increases with increasing  $\gamma_{if}$  which scales with the lattice mismatch of substrate and growing film.<sup>91,162</sup> As the melting point of Ru is higher than that of Pd and the lattice mismatch between Ru and Cu is smaller than that between Pd and Cu (0.07 Cu(111)/Pd(111), 0.04 Cu(111)/Ru(002)), a larger wetting angle can be expected for the Pd substrate. We suggested that the most likely reason for the formation of continuous Cu films on thick Pd films is the formation of a graded interlayer by interdiffusion between Pd and Cu as it was reported by Hsu and coworkers.<sup>98</sup>

Kalutarage et al.<sup>139</sup> observed a strong surface selectivity in their Cu ALD experiments with Cu(dmap)<sub>2</sub> and BH<sub>3</sub>(NHMe<sub>2</sub>) as they obtained a much higher nucleation density on Ru than on the other substrates investigated (TiN, SiO<sub>2</sub>, Si with native oxide, H-terminated Si). However, pronounced island growth was still observed. The three-step process involving formic acid resulted in very smooth films on Pt and Pd (both 15 nm with 2 nm Ti liner). An important difference between the ALD on those two films was a decrease of the GPC after a certain number of cycles for the growth on Pt. The researchers suggested that this difference is caused by a presence of Pd on the growing Cu film similar as reported by Hsu and coworkers.<sup>98</sup> They also observed surface Pd on the Cu surface by XPS although in smaller concentrations than those reported by Hsu and coworkers. In contrast to this, the lack of Pt on the surface diminishes the GPC on Pt after the Cu film reaches a certain thickness. It is worth mentioning here that in the ALD studies of Hagen et al.<sup>91</sup> with NHC-Cu(hmds) and H<sub>2</sub>, the researchers also conducted some depositions on Pt in addition to Ru and Pd, which were not published in a journal but in the Ph.D. thesis of Hagen.<sup>163</sup> The films



obtained on Pt were much thinner than those on Pd but no proof of incomplete coverage could be found in micro-characterisation (scanning electron microscopy (SEM), TEM).

Li et al.<sup>79,80</sup> obtained Cu growth with  $[\text{Cu}(\text{}^s\text{Bu-Me-Amd})]_2$  on a wide range of substrates with the best results on Ru and in-situ grown Co. The initial growth mechanism on  $\text{SiO}_2$  was investigated by Dai et al.<sup>164,165</sup> using differential infrared spectroscopy. Their data suggest the loss of one of the bidentate ligands via reaction with surface hydroxyl groups. Whether the species is adsorbed in a bridging conformation or with a single bond depends on temperature and coverage of the surface with Cu. Furthermore, the spectra indicated that the reaction product amidine re-adsorbs on the  $\text{SiO}_2$  surface being a possible cause of contamination.

Ma et al.<sup>166</sup> studied the adsorption of  $[\text{Cu}(\text{}^s\text{Bu-Me-Amd})]_2$  on Ni. They observed a reduction to metallic Cu at room temperature and reasonable CVD growth at 450 K. They also reported rapid initial decomposition of the compound in stainless steel containers. In another work, Ma et al.<sup>82</sup> investigated the adsorption and desorption of  $[\text{Cu}(\text{}^s\text{Bu-Me-Amd})]_2$  on Cu, and observed some important differences to its adsorption on Ni. The molecule adsorbs partly as dimer and monomer on Cu, while it adsorbs nearly completely as monomer on Ni. The decomposition reactions on both substrate materials were similar, for example the hydrogen elimination of the  $^s\text{Bu}$  moiety, but occur at higher temperatures on Cu. This is an important result since the reaction with Cu surfaces will be part of any Cu-ALD process after the initial nucleation. Furthermore, the authors investigated the dissociative  $\text{H}_2$  adsorption on Cu by phenomenological modeling, and demonstrated that it is not a favored process and only low coverages of less than 1% of an monolayer can be expected even at relatively high  $\text{H}_2$  pressures such as 1 mbar. Ma and Zaera<sup>167</sup> explored the surface chemistry of  $\text{Cu}(\text{acac})_2$  adsorbed on single-crystalline Ni and Cu surfaces. They observed relatively complicated adsorption and decomposition mechanisms which were stronger on Ni than on Cu. These effects appear to start below room temperature and mainly metallic Cu

is detected from 300 K for the Ni surfaces. However, significant signals of ligand atoms were visible up to very high temperatures (800 K). In another work, Ma and Zaera<sup>76</sup> performed temperature programmed desorption studies with the Cu-I precursor KI-5, and observed a removal of the silyl moiety from the Cu coordination site although it remained part of the molecule. Furthermore, their results were consistent with a dissociation reaction and decomposition starting at 280 K and 430 K, respectively.

Kim et al.<sup>168</sup> investigated the decomposition of the Cu(I)-guanidinate bis[Cu(I)-N,Ndimethyl-M',N''-diisopropylguanidate] and the Cu(I)-pyrrolydinate tetrakis[Cu(I)-N-sec-buryl-iminopyrrolidinate] on single-crystalline Ni by TPD and XPS. For the guanidinate, they observed a mechanism that distinguishes from that previously reported for amidinates as the bond between N and the alkyl moiety (here <sup>i</sup>Pr) is stronger and the hydrogen abstraction results in the release of the protonated ligand instead of the scission of the N-alkyl bond for the decomposition at lower temperatures (~290 K). Furthermore, carbodiimide deinsertion as reported for the gas phase<sup>84,85</sup> was not observed. For the pyrrolydinate, a similar hydrogen abstraction reaction, involving the H in the <sup>i</sup>Pr group, was observed. Furthermore, it became clear from the N 1s XPS peak shifts that the molecules adsorb as monomers. Yao et al.<sup>169</sup> investigated the adsorption of Cu-pyrrolidinate on SiO<sub>2</sub> using the same equipment. They observed no hydrogen abstraction showing that the compound is quite stable, and no reasonable decomposition occurs below about 550 K. These observations highlight the importance of the role that the substrate material has for the decomposition of precursors. In particular, its onset is often at relatively low temperatures for metallic surfaces. Here, we would like to highlight that in an ALD process not only the starting surface but also that of the growing film needs to be considered. Since the onset of decomposition inhibits an ALD process, the upper end of a potential ALD window can be much lower than indicated from thermochemical data of the precursor obtained by standard methods such as TGA and DSC.

Decomposition of precursors on metallic substrates can indeed be an issue as it limits the number of substrates suitable for ALD processes. A problematic substrate is Ta, as it was demonstrated for example by Machado et al.<sup>170</sup> in first principle simulations on the decomposition of metal-organic precursors. This is unfortunate because Ta is the material in use as liner for Cu interconnects on CMOS devices. Decomposition has been observed in a number of studies on the ALD and CVD of Cu on Ta coated substrates. Voss et al.<sup>94</sup> observed significant contamination and poor adhesion when they deposited Cu films on Ta by CVD using TMVS-Cu(hfac). The poor adhesion can be attributed to contamination of the Ta/Cu interface. To demonstrate this mechanism, they exposed the Ta surface to 'Cu CVD residuals'- thus mainly Hhfac -, deposited a fresh Ta layer and exposed it again to residuals repeating this sequence several times. A secondary ion mass spectrometry (SIMS) profile of this structure showed repeating high levels of C, O, and F contamination, which were due to decomposition of molecules on the Ta surfaces. Solanki and Pathangey<sup>136</sup> reported poorly wetting Cu films grown by ALD with Cu(hfac)<sub>2</sub>. However, the Ta films used were exposed to atmosphere and therefore covered by a native oxide.

Similar observations were reported by Wu and Eisenbraun<sup>135</sup> who obtained isolated Cu islands with poor adhesion on Ta while films of good quality were grown on Ru. Although Ru also contains a native surface oxide it is much more readily removed than that of Ta. Wu and Eisenbraun reported an improvement in the quality of Cu films deposited on Ru when the Ru films were subjected to pre-clean in hydrogen plasma.<sup>96</sup> The poor quality of Cu interfaces with oxidized materials is a significant experimental problem as surface oxides are difficult to remove for many metals and relatively few groups have equipment that allows samples coated with metal films to be transferred to an ALD reactor without exposure to atmosphere. Moreover, it is difficult to control the surface configuration of metal films under typical ALD conditions such as moderate vacuum and limited purity of precursors.

During experiments on Cu PEALD with AbaCus<sup>109</sup> Hagen et al. examined various plasma treatments before deposition on Ru but virtually no differences were observed. Much larger differences were observed for deposition on different Ru substrate films. On Ru with a pronounced (001) texture, quite smooth Cu films with a strong (002) texture were obtained, while the films on nanocrystalline Ru were much rougher and randomly oriented.<sup>109</sup>

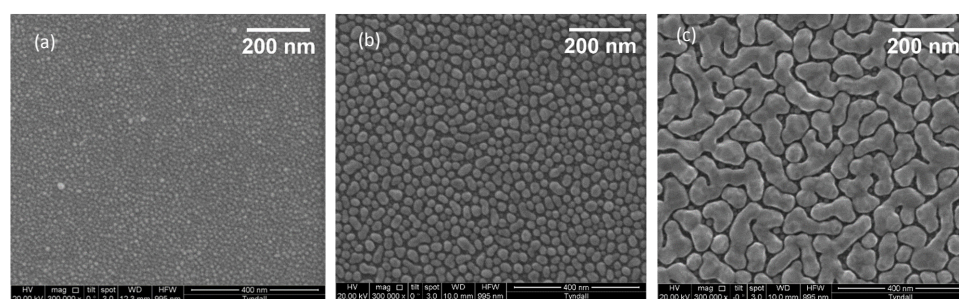


Figure 13: Cu deposits grown at 60 °C on TaN using (a) 60, (b) 150 and (c) 450 cycles.<sup>133</sup> Reprinted with permission from D. J. Hagen et al., *Adv. Mater. Interfaces*, 4, 1700274 (2017). Copyright 2017 WILEY VCH Verlag GmbH and Co. KGaA

On most other substrates studied in that work<sup>109</sup> (Si, TaN, carbon-doped oxide, Al<sub>2</sub>O<sub>3</sub>), nearly spherical isolated islands were obtained even at substrate temperatures as low as 30 °C and the shape of the deposit did not vary much in the temperature window studied (30 - 100 °C). The formation mechanism for these deposits was studied in a second work.<sup>133</sup> When the number of deposition cycles was varied for growth with CTA-1 at 60 °C, the authors observed that a very dense deposit was obtained after the initial cycles (Figure 13). When the number of cycles was increased these islands coalesced to larger, isolated islands, and a channel-like structure was formed after 450 cycles. This growth mode is caused by sintering of the islands when they touch each other during growth (static sintering). The driving force of sintering are gradients of the chemical potential due to gradients of the curvature. This means material flows from

convex to concave regions. Hagen et al.<sup>133</sup> compared their observations with Monte Carlo simulations and the well-established particle-growth model of Granqvist and Buhrman<sup>171,172</sup> which predicts a lognormal distribution of the island size:

$$f(d) = \frac{1}{\sqrt{2\pi}} \ln(\sigma) \exp \left[ -0.5 \left( \frac{\ln(d/\bar{d})}{\ln(\sigma)} \right)^2 \right], \quad 21$$

where  $d$  is the island diameter  $\sigma$  the standard deviation and  $\bar{d}$  the mean diameter. The supply of atoms from the gas phase and the loss of covered space due to coalescence under volume and shape preservation leads to the surface coverage  $P$  approaching a constant value  $P_0$ :

$$P = P_0 \left( 1 - \frac{N}{N_0} \right). \quad 22$$

Here,  $N$  is the island density and  $N_0$  the much higher initial density. This model turned out to be valid for a wide range of substrates on which Cu is wetting poorly and over a wide number of cycles. The growth stage at which the assumption of shape preservation becomes invalid depends on the deposition temperature, and according to this model it is the temperature shift of this transition and not the nucleation density which causes the often-observed deposits consisting of large isolated islands obtained at high temperatures even after many cycles.

Väyrynen et al.<sup>118</sup> observed a similar island growth regime in their experiments with Cu(dmap)<sub>2</sub> and hydroquinone as can be seen in Figure 14. Furthermore, they reported that the minimum thickness for which a continuous film can be achieved increases with the deposition temperature.

This is the author's peer reviewed, accepted manuscript. However, the online version of record will be different from this version once it has been copyedited and typeset.

PLEASE CITE THIS ARTICLE AS DOI: 10.1063/1.5087759

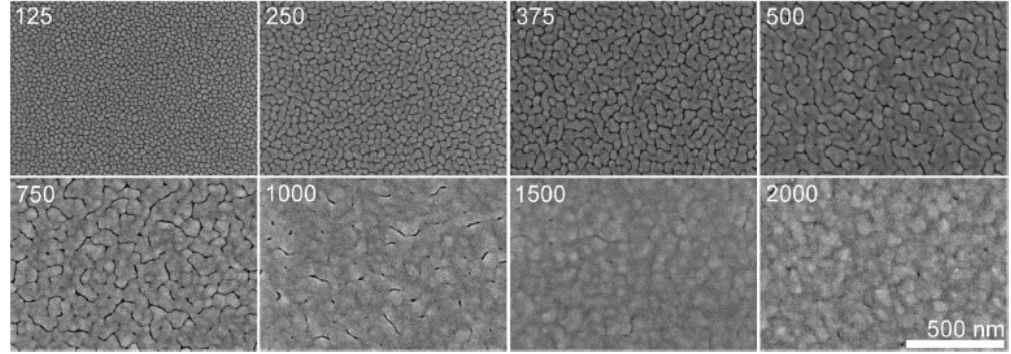


Figure 14: Cu deposited with  $\text{Cu(dmap)}_2$  and  $t\text{-Bu-hydrazine}$  at  $120^\circ\text{C}$  with different cycle numbers.<sup>118</sup> Reprinted with permission from K. Väyrynen et al., *Chem. Mater.* 29, 6502-6510 (2017). Copyright 2017 American Chemical Society

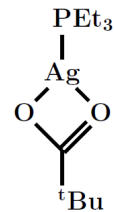
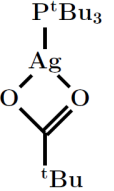
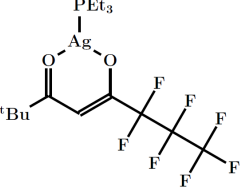
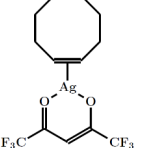
This is the author's peer reviewed, accepted manuscript. However, the online version of record will be different from this version once it has been copyedited and typeset.

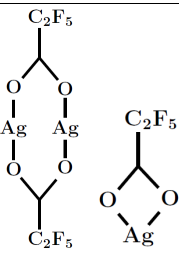
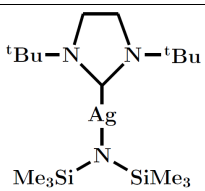
PLEASE CITE THIS ARTICLE AS DOI: 10.1063/1.5087759

## 4. ALD of Other Metal Films

### 4.1 Coinage Metals

Table 6: Ag metalaorganics explored for the ALD or CVD of Ag.

Name	Structure	References
PEt <sub>3</sub> -Ag(O <sub>2</sub> C <sup>t</sup> Bu)		173
P <sup>t</sup> Bu <sub>3</sub> -Ag(O <sub>2</sub> C <sup>t</sup> Bu)		173
2,2-dimethyl- 6,6,7,7,8,8,8-heptafluorooctane-3,5-dionate PEt <sub>3</sub> -Ag(fod)		174-176
COD-Ag(hfac)		177,178

Ag(C <sub>2</sub> F <sub>5</sub> COO)		179,180
NHC-Ag(hmds)		181

The elements of group 11 are called coinage metals. Reports of ALD of the coinage metals Ag and Au are much rarer than those of Cu. Firstly, the higher cost of these materials limits their use in commercial applications. Furthermore, Ag and Au have melting points lower than that of Cu (Cu: 1085 °C; Ag: 962 °C; Au: 1064 °C) and show a similar or even stronger tendency to agglomerate. The main difference from a chemical perspective is that they are more noble than Cu. Therefore, stable Ag(II) and Au(II) complexes are extremely rare.

Ag(I) complexes which were used for ALD or CVD are quite similar to Cu(I) precursors. However, an important difference is that they usually do not react by disproportionation due to the limited stability of Ag(II) complexes. Niskanen et al.<sup>173</sup> carried out PEALD experiments using triethylphosphine-Ag-2,2dimethylpropionate (PEt<sub>3</sub>-Ag(O<sub>2</sub>C<sup>t</sup>Bu)) and reported a relatively large saturated GPC of 1.2 Å/cycle. The Ag films were quite grainy and significant contamination levels were measured (4 % P, 10 % O), but nevertheless the films showed reasonably good electrical quality as a resistivity of 6 μΩcm was measured for a 40 nm thick film grown at 140 °C (evaporation temperature 125 °C). An interesting detail is that with a similar precursor P<sup>t</sup>Bu<sub>3</sub>-Ag(O<sub>2</sub>C<sup>t</sup>Bu) much poorer growth was observed despite both molecules



having similar TGA curves which show a single decomposition step between 200 and 280 °C leaving residues compatible with the weight share of Ag. The precursor was also used in an earlier CVD study by Piszczek et al.<sup>182</sup> who reported grainy films with a large C content and relatively low conductivity. However, these authors reported a different physical appearance of the compound than that observed by Niskanen et al.<sup>173</sup> (brownish oil vs brown powder) and used a relatively large evaporation temperature of 160 °C. Therefore, it seems likely that problems with the transport of an intact molecule might have occurred.

Kariniemi et al.<sup>174</sup> screened several precursor with TGA (Figure 15), and selected  $\text{PEt}_3\text{-Ag(fod)}$  (fod = 2,2-dimethyl- 6,6,7,7,8,8,8-heptafluorooctane-3,5-dionate), which evaporated with the lowest residual mass, for ALD experiments with hydrogen plasma, and reported saturated film growth at 120 and 140 °C with a rate of between 0.3 and 0.4 Å/cycle. Although the films were quite rough due to the island growth, they were electrically continuous and a resistivity of 6 - 8  $\mu\Omega\text{cm}$  was measured for a 23 nm thick film. The films were analyzed with time-of-flight elastic recoil detection analysis (TOF-ERDA), and a composition of about 85 at.% silver, 7 at.% hydrogen, 3 at.% carbon, 3 at.% oxygen, 0.9 at.% phosphorus, 0.5 at.% fluorine, and 0.7 at.% nitrogen was measured.

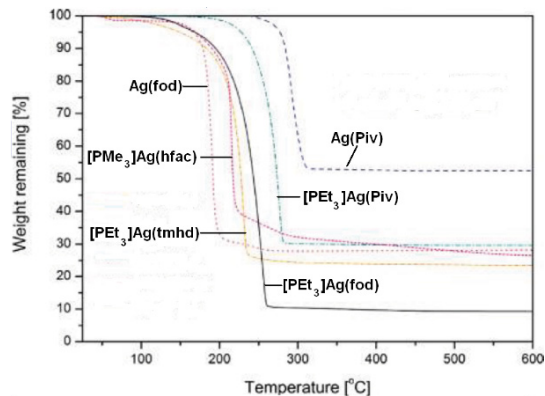


Figure 15: TGA of various Ag complexes.<sup>174</sup> Adapted with permission from M. Kariniemi et al., *Chem. Mater.* 23, 2901-2906 (2011). Copyright 2011 American Chemical Society

Mäkelä et al.<sup>175</sup> of the same group developed a thermal ALD process using  $\text{PEt}_3\text{-Ag(fod)}$  and  $\text{BH}_3(\text{NHMe}_2)$ . Films were readily obtained on Si with a GPC of about 0.3 Å/cycle in a temperature window from 110 – 120 °C. The GPC increased with the number of cycles 0.2 to about 0.35 after 1500 cycles indicating that the growing Ag film catalyzes the reaction. The films were very granular, and no continuous films could be obtained even after 2500 cycles. It is worth noting that the grain density, grain size and grain shape evolved in accordance with the model we developed for Cu ALD.<sup>133</sup> The initial grain density decreases through coalescence and the coalescence becomes less complete with increasing cycle number. The composition of the films was estimated from TOF-ERDA measurements, and the obtained values were 96.9 at.% Ag, 1.6 at.% oxygen, 0.8 at.% hydrogen and 0.7 at.% carbon. The authors assumed that the lower contamination values as compared to the PEALD process<sup>174</sup> originated from the improved post-deposition handling of the samples.

Minjauw et al.<sup>176</sup> compared the ALD of with  $\text{NH}_3$  and  $\text{H}_2$  plasma using  $\text{PEt}_3\text{-Ag(fod)}$ , and observed large differences. Firstly, the GPC, which was measured for the growth on Au at 130 °C, of the  $\text{NH}_3$  process was about 2.5 Å/cycle and therefore much higher than the GPC of the  $\text{H}_2$  process (~0.5 Å/cycle). The film

thicknesses were measured by X-ray fluorescence (XRF) with the XRF signal dependence on the Ag film thickness calibrated with films of known thickness. Secondly, the films grown with  $\text{NH}_3$  plasma consisted of small grains while those grown with  $\text{H}_2$  plasma consisted of large coalesced structures (Figure 16). The chemical composition of the films was evaluated with XPS and the measured values were:  $\text{NH}_3^*$  surface 21% C, 19% N, 6% O, 10% F, 6% P;  $\text{NH}_3^*$  bulk 4% C, 7% N, 2% O, <1% F, 4% P;  $\text{H}_2^*$  surface 11% C, 3% N, 13% O, 10% F, 3% P;  $\text{H}_2^*$  bulk <1% C, 2% N, 9% O, <1% F, <1% P. In many cases, differences between the concentration of elements on the surface and in the bulk is interpreted as resulting from environmental contamination after the deposition. However, there also exist effects that can cause such difference during the deposition, especially during island growth. For example, if an element is not solvable in a metal it can precipitate to the surface. Furthermore, the reactions on the surface of the growing film can force atoms to the surface. In this example, it appears unlikely that the high F concentration on the surfaces arose from environmental contamination and not from the precursor. The most important difference between the two films is the high N concentration in the film grown with the  $\text{NH}_3^*$  process. The researchers explored the growth mechanisms with in-situ Fourier-transform infrared spectroscopy (FTIR). Figure 16e shows differential spectra after the precursor pulses for the two processes. The main difference are the peaks between 3200 and 3500  $\text{cm}^{-1}$  in the  $\text{NH}_3^*$  process. A detailed plot of these peaks, which the authors ascribed these signals to N-H stretching vibrations, and is shown in Figure 16f. After the  $\text{NH}_3^*$  pulse, a peak was observed between 3100 and 3300  $\text{cm}^{-1}$  which was interpreted as originating from adsorbed species. After the  $\text{PEt}_3\text{-Ag(fod)}$  pulse, no negative counter-peak appeared. Instead, a positive peak shifted to a higher energy was observed. The authors concluded that the surface amide species were not completely removed, and exposed to a different chemical environment. The  $\text{PEt}_3\text{-Ag(fod) / H}_2^*$  process was also investigated by Amusan et al.<sup>183</sup> in the temperature range 70 – 200 °C. The films grew with a GPC of about 0.3 Å/cycle in the whole temperature range, contained very little contamination except those deposited at the lowest temperatures, and a resistivity of 5.7  $\mu\Omega\text{cm}$  was

measured for a film with a thickness of about 97 nm grown on SiO<sub>2</sub>. The researchers investigated different metallic substrate film. While relatively smooth Ag films were obtained on Co and Ni, the films on W were quite rough. The authors blamed this on the presence of a surface oxide that could not be removed by a H<sub>2</sub><sup>+</sup>-plasma exposure prior to deposition.

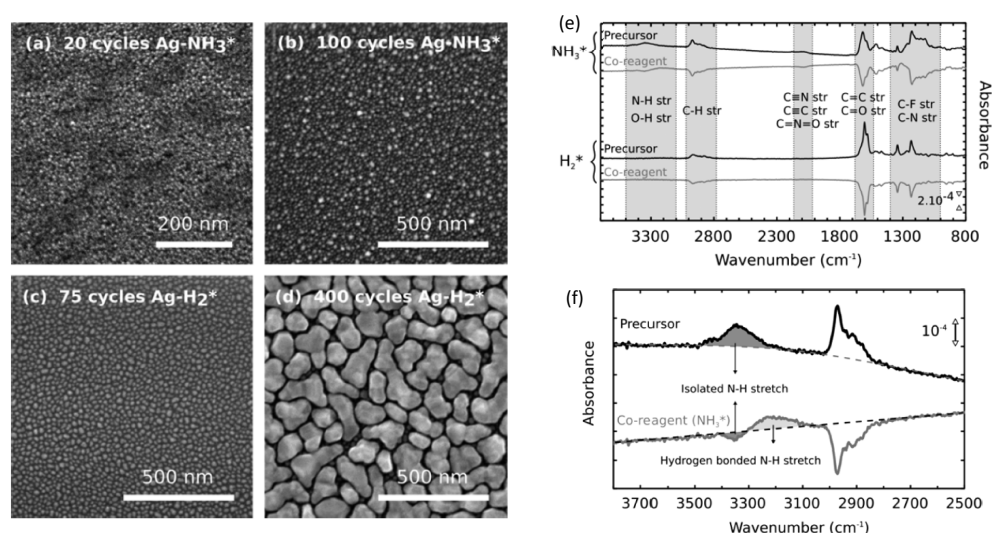


Figure 16: Ag films deposited with [PEt<sub>3</sub>]Ag(fod) and NH<sub>3</sub> or H<sub>2</sub>: (a) – (d) SEM images of films grown with (a), (b) NH<sub>3</sub> and (c), (d) H<sub>2</sub>, the samples were chosen to have similar nominal thicknesses with both reactants; (e) FTIR differential absorbance spectra of films grown with the two reactants, (f) highlighted region of FTIR spectra of film grown with NH<sub>3</sub>.<sup>176</sup>, Reprinted with permission from M.M. Minjauw et al., *Chem. Mater.* 29, 7114-7121 (2017). Copyright 2017 American Chemical Society

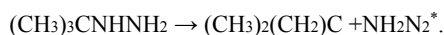
Van den Bruele et al.<sup>184</sup> demonstrated the suitability of the PEt<sub>3</sub>-Ag(fod) precursor for atmospheric-pressure spatial ALD with a H<sub>2</sub><sup>+</sup> / N<sub>2</sub><sup>+</sup> plasma. However, the authors were not able to demonstrate saturation with exposure times, and the growth rate varied even within the small temperature range of 100 – 120 °C investigated. Isolated islands were obtained even for quite large numbers of cycles such as 2250 and the morphology of the deposit varied strongly with the deposition conditions; the deposits grown at 120 °C had a larger island size and a lower island density *N* than those grown at 100 °C. The researchers described this observation in the framework of nucleation theory as described by Brune.<sup>185</sup>

$$N \propto \left(\frac{D}{F}\right)^{-\frac{i}{i+2}}.$$

23

Here,  $D$  is the diffusion coefficient,  $F$  the flux rate and  $i$  the critical island size from which the atom-capture rate becomes higher the atom-loss rate. The last value is typically small, and was assumed to be 1 in this work. This model suggests a decrease of  $N$  with increasing  $D$  and thus with increasing temperature. However, the observations are also consistent with the model of static coalescence as suggested by Hagen et al.<sup>133</sup> for Cu ALD. Here, the different morphologies can be explained by the different GPC values. Electrically continuous films were only obtained for films deposited with very large numbers of cycles such as 4500, and the resistivities were quite high ( $\sim 18 \mu\Omega\text{cm}$ ).

Chalker et al.<sup>177</sup> reported ALD growth with COD-Ag(hfac) and n-propanol. By using direct liquid injection, they were able to minimize the problems associated with the precursor transport. However, the saturated growth regime was limited to a very narrow temperature window between 122 and 127 °C. Golrokhi et al.<sup>178</sup> of the same group were able to extend the ALD window to lower temperatures (105 °C) by using <sup>t</sup>Bu-hydrazine as reducing agent. Furthermore, the GPC within the ALD window increased and a better-connected deposit was obtained. The reactivity of <sup>t</sup>Bu-hydrazine was explained with its decomposition via  $\beta$ -hydride elimination on the substrate surface:



24

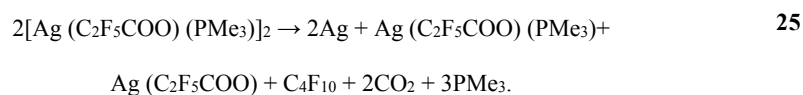
The researchers put this in contrast to the oxidative dehydrogenation of n-propanol which is catalyzed by the Ag particles, and used this difference to explain the different morphologies of the deposits obtained

with these two processes. The reason for Golrokhi et al. to use <sup>t</sup>Bu-hydrazine and not directly hydrazine was the hazards of hydrazine which is poisonous and explosive.

In a recent study, Boysen et al.<sup>181</sup> reported the synthesis of a NHC-Ag(hmde) complex (with the NHC 1,3-di-*tert*-butyl-imidazolin-2-ylidene) and its evaluation for special ALD with a reactor operated under atmospheric pressure. Similar to the NHC-Cu(I) complexes discussed above, the strong electron donor NHC was capable of stabilizing monomers, which had a nearly linear coordination. In TGA measurements, the authors observed an onset of sublimation below 150 °C and decomposition at 225 °C as evident from an exothermic DTA peak. The ALD experiments were performed at a substrate temperature of 100 °C using hydrogen plasma. The observed GPC of 0.36 Å/cycle was higher than the researchers obtained with PEt<sub>3</sub>=Ag(fod) in the same study using practically identical deposition conditions (0.14 Å/cycle).

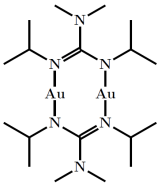
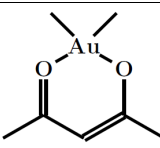
There is a number of reports about the use of Ag(I)-complexes for CVD. Gao et al.<sup>186</sup> compared COD-Ag(hfac), TEVS-Ag(hfac) (TEVS=triethylvinylsilyl) and PEt<sub>3</sub>-Ag(fod). With the first compound they could not obtain Ag films which they attributed to loss of COD during evaporation and formation of [Ag(hfac)]<sub>2</sub>, which has a vapor pressure unsuitable for CVD. With the other two compounds, conductive films were obtained with deposition starting at 180 °C for TEVS-Ag(hfac) and 230 °C for PEt<sub>3</sub>-Ag(fod). Chi et al.<sup>187</sup> reported similar results, when they carried out CVD depositions at temperatures between 160 and 280 °C using TEVS-Ag(hfac). Zanotto et al.<sup>188</sup> reported high levels of contamination when they carried out ALD experiments with 2,2-bipyridine-Ag(hfac) and N,N,N',N'-tetramethylethylenediamine-Ag(hfac) although they were using very high deposition temperatures (300 - 450 °C) and H<sub>2</sub> as reducing agent. This indicates that pyrolysis of the hfac ligand results in non-volatile contaminants which cannot be removed by reduction in H<sub>2</sub>. It is known that H<sub>2</sub> does not adsorb dissociatively on Ag. Thus, one cannot expect H atoms to be present on the film to facilitate the reduction of the contaminants.

Samoilenkov et al.<sup>179</sup> reported the use of Ag-pivalate ( $\text{Ag}((\text{CH}_3)_3\text{CCO}_2)$ ) which evaporates as dimer. Szlyk et al.<sup>180</sup> investigated the differences of  $\text{PMe}_3\text{-Ag}(\text{C}_2\text{F}_5\text{COO})$  and  $\text{Ag}(\text{C}_2\text{F}_5\text{COO})$  regarding their use as precursors and observed that the phosphine containing compound can be evaporated at lower temperatures and also reacts at lower temperatures. However, the films grown with both precursors contained significant amounts of C, O and F. They proposed that decomposition occurs via the following reaction:



Furthermore, FTIR studies indicated that  $\text{Ag}(\text{C}_2\text{F}_5\text{COO})$  evaporates partly as a bidentate monomer and partly as a dimer. In a review, Godzicki et al.<sup>189</sup> compared carboxylates of Cu, Ag and Au and their use for CVD. They highlighted the strong stabilization for  $\text{Ag(I)}$  and  $\text{Cu(I)}$  complexes that arises when using  $\pi$ -donors such as olefins as well as by  $\sigma$ -donors such as phosphines.

Table 7: Au metalorganoxides exposed as precursors for the ALD or CVD of Au.

Name	Structure	References
$[\text{Au}(\text{N}^i\text{Pr})_2\text{CNMe}_2]_2$		190
$\text{Au}(\text{acac})\text{Me}_2$		191

Similar to Cu and Ag, a range of Au(I) complexes consisting of an ionic and a dative ligand exist. They are usually linearly coordinated with coordination number 2. Organometallic complexes such as  $\text{PMe}_3\text{-AuMe}$ ,<sup>197,198</sup>  $\text{PMe}_3\text{-AuEt}$ ,<sup>197</sup>  $\text{PEt}_3\text{-AuMe}$ ,<sup>198</sup>  $\text{PEt}_3\text{-AuEt}$ ,<sup>198</sup>  $\text{PMe}_3\text{-Au}(\text{CF}_3)$ ,<sup>199</sup>  $\text{PEt}_3\text{-Au}(\text{CF}_3)$ ,<sup>199</sup>  $\text{PPh}_3\text{-AuCl}$ ,<sup>197,198</sup>

Similar to Cu and Ag, a range of Au(I) complexes consisting of an ionic and a dative ligand exist. They are usually linearly coordinated with coordination number 2. Organometallic complexes such as  $\text{PMe}_3\text{-AuMe}$ ,<sup>197,198</sup>  $\text{PMe}_3\text{-AuEt}$ ,<sup>197</sup>  $\text{PEt}_3\text{-AuMe}$ ,<sup>198</sup>  $\text{PEt}_3\text{-AuEt}$ ,<sup>198</sup>  $\text{PMe}_3\text{-Au}(\text{CF}_3)$ ,<sup>199</sup>  $\text{PEt}_3\text{-Au}(\text{CF}_3)$ ,<sup>199</sup>  $\text{PPh}_3\text{-AuCl}$ ,<sup>197,198</sup>



$\text{Au}(\text{CF}_3)^{199}$  and  $\text{MeN}=\text{C}-\text{Au}(\text{CF}_3)^{200}$  have been described and tested for CVD as well as halides such as  $\text{PF}_3-\text{AuCl}^{201}$ . All these compounds are not very stable and need to be evaporated at low temperatures. Growth can be observed at room temperature on some substrates. Evaporation at low temperatures leads to small GPC values which can be overcome by dissolving the precursor and using a liquid injection mechanism.<sup>201</sup> The decomposition of Au(I) compounds is very surface dependent and usually quite strong on bare metal surfaces and weak on insulating oxides or polymers.<sup>197</sup> Formation of a native oxide on a metal like Cr was observed to diminish the growth process significantly. Contamination of films with C, P and F was observed in many experiments. For the phosphines it was observed that  $\text{PMe}_3$  leads to better stability than phosphines with larger alkyl groups.<sup>198</sup> Au(I) fluorocarboxylates<sup>189,202</sup> with various phosphines as second ligand were also evaluated as CVD precursors. Relatively strong contamination of the grown Au films was observed which increased with the length of fluoroalkyl chain of the carboxyl ligand. For Ag fluorocarboxylates<sup>202</sup> similar observations were made.

Mandia et al.<sup>190</sup> performed Au CVD with the Au-guanidinate  $[\text{Au}(\text{N}^i\text{Pr})_2\text{CNMe}_2]_2$ . They obtained metallic Au films when they carried out depositions at 200 °C, where the precursor most probably reacted by  $\beta$ -hydride elimination. The resulting films were quite grainy, which resulted in a high resistivity of 5.73  $\Omega\text{cm}$  for a 520 nm thick film. However, the precursor was evaporated at a relatively high temperature of about 80 °C, which demonstrates its improved stability as compared to the Au(I) complexes discussed above.

In addition to Au(I) complexes, Au(III) complexes have also been investigated for CVD. The relative stability of Au(III) complexes is surprising to many people, but can be understood by relativistic effects on the energy levels. These compounds are usually four-coordinated. Examples include Au complexes with two methyl groups and a diketo-group such as acac, hfac or tfac.<sup>128,203-207</sup> CVD deposition is often

carried out with relatively exotic methods such as laser or electron beam exposure and typical deposits are matrices of Au nanoparticles in films of decomposed ligand material.

Further examples include Au complexes with a combination of three methyl (including  $\text{CF}_3$ ) and halide groups and one phosphine.<sup>199</sup> Similar problems with stability have been observed. Parkhomenko et al.<sup>191</sup> reported the coating of opals with Au nanoparticles which they grew using pulsed CVD with  $\text{Au}(\text{tmhd})\text{Me}_2$  and oxygen (which role they did not specify). They demonstrated conformal coating with SEM micrographs but did not provide details about the composition of the deposits. In the same work, Parkhomenko et al.<sup>191</sup> also reported the coating of opals with continuous Au films when they performed continuous flow CVD using  $\text{Au}(\text{OAc})\text{Me}_2$  ( $\text{OAc}$  = acetate). Moreover, they demonstrated films of relatively low contamination with XPS measurements on films deposited on flat substrates (97 % Au, C main contaminant).

Turgambaeva et al.<sup>193,194</sup> and Parhomenko et al.<sup>192</sup> synthesized several  $\text{Me}_2\text{Au}$ - complexes with S,S'-coordinated ligands. Turgambaeva et al.<sup>193</sup> compared  $\text{Me}_2\text{Au}(\text{dte})$  ( $\text{dte}$  = diethyldithiocarbamate) with the Au(III)-diketonates  $\text{Me}_2\text{Au}(\text{acac})$  and  $\text{Me}_2\text{Au}(\text{tmhd})$ . The TGA curves in Figure 17 (a) demonstrate that  $\text{Me}_2\text{Au}(\text{dte})$  can be evaporated more cleanly than the diketonates. The DTA curve of  $\text{Me}_2\text{Au}(\text{dte})$  shows an endothermic peak at 48 °C indicating its melting point. Therefore, the precursor can be evaporated as a liquid. Moreover, the vapor pressure of the compound is only slightly lower than that of the diketonates. Parhomenko et al.<sup>192</sup> carried out CVD depositions with  $\text{Me}_2\text{AuS}_2\text{P}(\text{OEt})_2$  and  $\text{Me}_2\text{AuS}_2\text{P}(\text{OMe})_2$ . Both precursors are liquids at room temperature, have a higher vapor pressure than  $\text{Me}_2\text{Au}(\text{dte})$  and decomposition was observed to start at lower temperatures (150 and 160 °C, respectively, versus 210 °C). These results indicate that these Au(III) complexes represents promising candidates for ALD processes since they can be controllably evaporated and a reasonably large energy window exists between the evaporation and the decomposition temperature, which leaves room for ALD processes to be established.

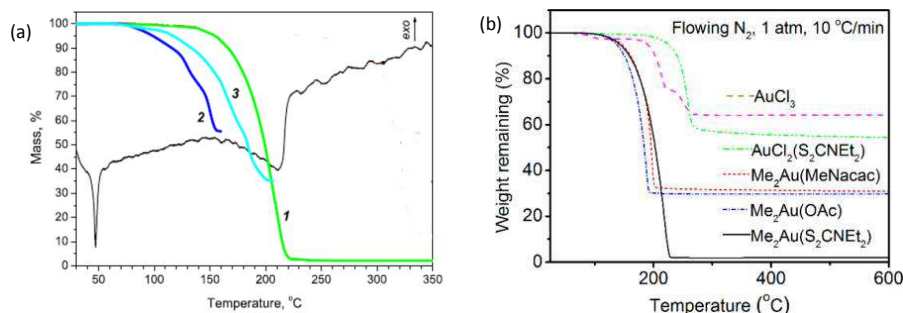
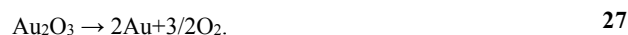


Figure 17: Thermal properties of Au-precursors: (a) TGA and DTA of 1 Me2Au(dtc), 2 Me2Au(acac) and 3 Me2Au(tmhd);<sup>193</sup> (b) TGA of various Au(III) complexes.<sup>195</sup> Reprinted with permission from A. E. Turgambaeva et al., *Gold Bull.* 29, 177-84 (2011); Copyright 2011 Springer, and M. Mäkelä et al., *Chem. Mater.* 29, 6130-6136 (2017); Copyright 2017 American Chemical Society, respectively.

The first paper on a successful Au ALD process was published as late as 2016 by Griffiths et al.,<sup>196</sup> who used PMe<sub>3</sub>-AuMe<sub>3</sub> and oxygen plasma. The depositions were carried out at 120 °C which was considered the maximum applicable temperature since the molecule starts to decompose at 130 °C. At this temperature no growth was obtained with molecular hydrogen, hydrogen plasma and molecular oxygen. The films were of poor quality and contained large O and P impurities. The authors attributed this to the formation of P<sub>2</sub>O<sub>5</sub>:



A strong indication for the presence of P<sub>2</sub>O<sub>5</sub> was the solubility of the films in water. Improved results were obtained when water was added as a third reactant which converted P<sub>2</sub>O<sub>5</sub> to volatile phosphoric acid:



The P impurities were below the detection limit of XPS and the O content small (1.8 %). The GPC was 0.5 Å/cycle, thus typical for metal ALD, and saturation was demonstrated by varying the pulse length. The adsorption mechanism of the gold complex on SiO<sub>2</sub> particles was investigated by Pallister and Barry<sup>161</sup> using solid-state NMR. From the changes of the chemical shifts of the <sup>31</sup>P and <sup>13</sup>N signals, they concluded that the Au(III) cation is partly reduced.

The first thermal Au ALD process was reported 2017 by Mäkelä et al.<sup>195</sup> in 2017 who employed O<sub>3</sub> as coreagent. They screened the thermal properties of several Au(III) complexes using TGA, obtaining the clearly most promising results with Me<sub>2</sub>Au(S<sub>2</sub>CNEt<sub>2</sub>) (Figure 17 (b)). They obtained metallic gold in the whole temperature range investigated (120 – 200 °C) with GPCs that increased with the deposition temperature from 0.4 to 1.1 Å/cycle. The saturation of the growth process was demonstrated by varying the Me<sub>2</sub>Au(S<sub>2</sub>CNEt<sub>2</sub>) pulse length for a substrate temperature of 180 °C. Furthermore, the uniformity of the films over 5 cm x 5 cm substrates was shown. The observed variation of the GPC with temperature is not in contradiction to the requirements of ALD, and is discussed in more detail later in this review for the case of Ir ALD. The temperature had also a large impact on the morphology of the films, and the grain size increased with increasing temperature as can be seen from the SEM micrographs in Figure 18. Furthermore, the films deposited at lower temperatures had more impurities than those deposited at higher temperatures, and there was a strong indication for an incomplete reduction of the Au<sub>2</sub>O<sub>3</sub> intermediate for the earlier. However, no S contamination could be detected in all of the investigated films. All studied films were conductive, and the lowest resistivity (4.5 μΩcm) was measured for a film deposited at 180 °C.

This is the author's peer reviewed, accepted manuscript. However, the online version of record will be different from this version once it has been copyedited and typeset.

PLEASE CITE THIS ARTICLE AS DOI: 10.1063/1.5087759

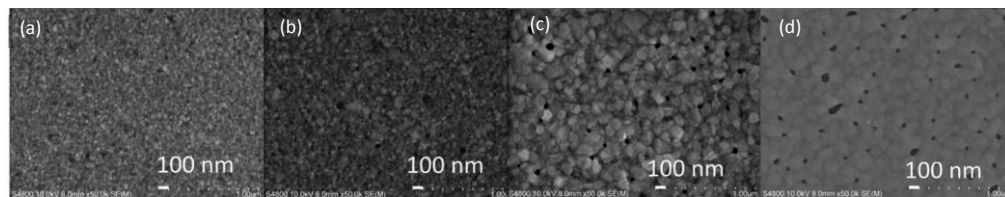
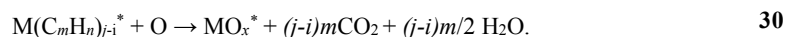


Figure 18: SEM micrographs of Au films deposited with Me<sub>2</sub>Au(S<sub>2</sub>CNet<sub>2</sub>) and O<sub>3</sub> using 500 cycles at different temperatures.<sup>195</sup> Reprinted with permission from M. Mäkelä et al., *Chem. Mater.* 29, 6130-6136 (2017). Copyright 2017 American Chemical Society.

## 4.2 Platinoid Metals

The platinoid metals  $\text{Pt}^{208-213}$ ,  $\text{Ru}^{214-221}$ ,  $\text{Os}^{222}$ ,  $\text{Rh}^{223,224}$ , and  $\text{Ir}^{225-227}$  can be deposited by combustion of adsorbed precursors in oxygen. The reaction products are proposed to be  $\text{CO}_2$  and  $\text{H}_2\text{O}$ .<sup>228</sup>



It is clear from the equations that the reaction needs to be catalyzed by the substrate as oxygen has to be split. Mackus et al.<sup>211</sup> investigated the catalytic mechanism for the reaction of (methylcyclopentadienyl)trimethyl-platinum ( $\text{MeCpPtMe}_3$ ) with oxygen and concluded that Pt catalyzes the reaction with oxygen as well as the dehydrogenation of the precursor.

At first glance, it seems rather strange that metal films are formed from the reaction with oxygen. This can be understood by the limited stability of the oxides of the platinum-group metals. However, there is a certain kinetic stability of the oxides, especially of Ru. Salaun et al.<sup>229</sup> for example obtained  $\text{RuO}_2$  from the reaction of  $\text{Ru}(\text{EtCp})_2$  with  $\text{O}_2$ . Methaapanon et al.<sup>221</sup> observed that the growth of either Ru or  $\text{RuO}_2$  strongly depends on the  $\text{O}_2$  exposure when they carried out ALD experiments with bis(2,4-dimethylpentadienyl)ruthenium and oxygen at a substrate temperature of 185 °C.  $\text{RuO}_2$  was formed for long  $\text{O}_2$  exposure times. Interestingly the impact of the  $\text{O}_2$  exposure dose was less significant than the impact of the exposure time. They proposed that subsurface oxide formation and the associated diffusion of oxygen are the rate limiting steps. A further indication for this was increased oxide formation when the deposition temperature was increased to 200 °C, which shows that oxide formation is an activated process.

Kim et al.<sup>227</sup> made different observations when they studied ALD of Ir with 1,5-cyclooctadiene-Ir(ethylcyclopentadienyl) (COD-Ir(EtCp)) and oxygen as they observed formation of IrO<sub>2</sub> was increased with increasing O<sub>2</sub> partial pressure but not when the oxygen pulse time was increased. Moreover, the researchers reported that IrO<sub>2</sub> was more readily formed at lower deposition temperatures. Chen et al.<sup>230</sup> observed a similar dependence of the IrO<sub>2</sub> formation on the oxygen pressure during CVD experiments. Hämäläinen et al.<sup>231</sup> demonstrated growth of IrO<sub>2</sub> instead of Ir from Ir(acac)<sub>3</sub> when a stronger oxidation agent such as O<sub>3</sub> was used. The same group<sup>212</sup> also observed the growth of PtO<sub>x</sub> from Pt(acac)<sub>2</sub> and ozone at 120 and 130°C. At higher temperatures metallic Pt was obtained. The PtO<sub>x</sub> films could easily be reduced to Pt. Hämäläinen et al. did not observe the formation of an Os-oxide, when they increased the O<sub>2</sub> pulse length during their studies on Os ALD with OsCp<sub>2</sub> and O<sub>2</sub>, but reported a decrease of film thickness when the substrate temperature was increased to 400 °C. They concluded that at this high temperature volatile OsO<sub>4</sub> was formed. For many ALD systems there exist more than one possibility for the molecule to adsorb. This can cause a change of GPC with temperature. This is not contradictory to an ALD mechanism as long as the growth is saturated for each temperature. For example, Aaltonen et al.<sup>225</sup> observed a temperature dependency of the GPC within an ALD window when they grew Ir with Ir(acac)<sub>3</sub> and O<sub>2</sub> (Figure 19).

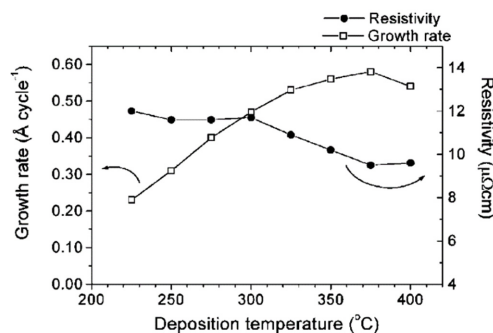


Figure 19: GPC of Ir as a function of temperature for the reaction of Ir(acac)<sub>3</sub> with O<sub>2</sub>.<sup>225</sup> Reprinted with permission from T. Aaltonen et al., *J. Electrochem. Soc.* 151, G489-G492 (2004). Copyright 2004 The Electrochemical Society.

This is the author's peer reviewed, accepted manuscript. However, the online version of record will be different from this version once it has been copyedited and typeset.

PLEASE CITE THIS ARTICLE AS DOI: 10.1063/1.5087759

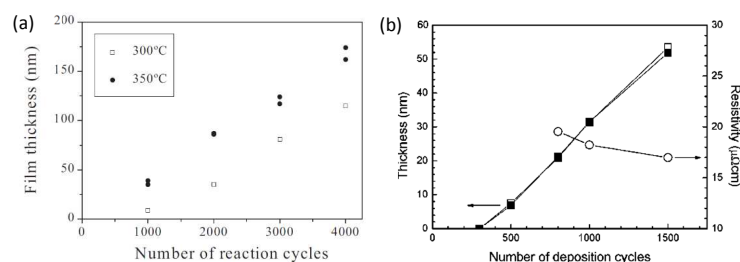


Figure 20: Initial delay during ALD growth by oxygen combustion on Al<sub>2</sub>O<sub>3</sub>: (a) Ru growth from RuCp<sub>2</sub>;<sup>232</sup> (b) Os growth from OsCp<sub>2</sub> at 350 °C.<sup>222</sup> Reprinted with permission from T. Aaltonen et al., *Chem. Vap. Depos.* 9, 45-49 (2003); Copyright 2003 WILEY VCH Verlag GmbH and Co. KGaA, and J. Hämäläinen et al., *Chem. Mater.* 24, 55-60 (2012); Copyright 2012 American Chemical Society, respectively.

Furthermore, an initial growth delay was often observed. In Figure 20 two examples are shown. Aaltonen et al.<sup>232</sup> (Figure 20 (a)) reported an initial delay during the growth of Ru from RuCp<sub>2</sub> and O<sub>2</sub> on Al<sub>2</sub>O<sub>3</sub>. They observed a strong dependence of the delay on the substrate temperature as it was much longer for growth at 300 °C than for growth at 350 °C. A long initial growth delay was observed by Hämäläinen et al.<sup>222</sup> for the growth of Os from OsCp<sub>2</sub> and O<sub>2</sub> at 350 °C on Al<sub>2</sub>O<sub>3</sub> (Figure 20 (b)). Possible reasons for the delay are lack of activation of O<sub>2</sub> on the initial substrate surface and insufficient adsorption of the metal precursor. The latter was indicated in the experiments of Kim et al.<sup>233</sup> who investigated the initial Ru growth from 2,4-(dimethylpentadienyl)(ethylcyclopentadienyl)Ru and O<sub>2</sub> on different substrates. They observed a significant incubation period on SiO<sub>2</sub>, TiN and TiO<sub>2</sub> but virtually none on Au, and Pt. They suggested that O<sub>2</sub> is not known to dissociate on Au and the catalysis of the reaction with oxygen is unlikely the reason for the different growth mechanisms. Heo et al.<sup>214</sup> observed that the adsorption of 2,4-(dimethylpentadienyl) (ethylcyclopentadienyl)Ru on carbon-doped oxide and thus the initial growth depends strongly on the surface groups present. Hydrophobic methyl groups impeded adsorption while OH groups facilitated it. Lee et al.<sup>234</sup> observed a growth delay of 21 cycles at 300 °C for Ru ALD on SiO<sub>2</sub>



when they used MeCpPtMe<sub>3</sub> and O<sub>2</sub> but no delay when they used O<sub>3</sub>. Moreover, the delay of the O<sub>2</sub> process diminished when the SiO<sub>2</sub> substrates were exposed to O<sub>3</sub> before the deposition. The researchers suggested that an oxygen-enriched surface reacted with MeCpPtMe<sub>3</sub>.

Chang et. al.<sup>235</sup> reported quite complex surface reaction mechanisms when they investigated the growth of Ru on Si with [CO]<sub>2</sub>-Ru(cyclopentadienyl)ethyl and O<sub>2</sub> using IR spectroscopy. They observed GPC values higher than one monolayer per cycle but found nevertheless strong indications for saturation. They concluded that the Cp and Et groups do not passivate the substrate. Film growth was instead controlled by CO surface groups. Terminal CO groups facilitated the adsorption of the Ru precursor, while bridged CO groups inhibited it. Park et al. detected bridged CO groups as the dominant surface species after the precursor pulse. During the O<sub>2</sub> pulse, bridged CO groups were converted to terminal CO groups and CO<sub>2</sub> resulting in a surface activated for precursor adsorption. A further observation was the presence of Ru-oxides more diverse than the simple model of surface oxide species suggests which indicated the presence of sub-surface oxides. Moreover, an initial nucleation period was observed. Leick et al.<sup>236</sup> compared growth with molecular O<sub>2</sub> and O plasma with the same precursor as was used by Park and coworkers. They obtained a shorter nucleation period with the plasma process but observed rougher films.

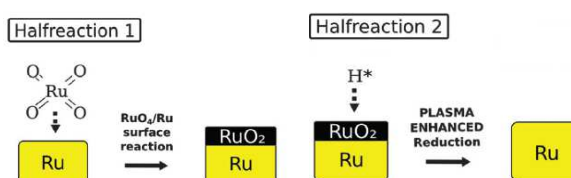


Figure 21: ALD process with RuO<sub>4</sub> and H plasma.<sup>237</sup> Reprinted with permission from M. M. Minjauw et al., *J. Mater. Chem. C* 3, 4848-4851 (2015). Copyright 2015 Royal Society of Chemistry.

Gatineau et al.<sup>238</sup> and Minjauw et al.<sup>237</sup> applied an inorganic compound RuO<sub>4</sub> for the ALD of Ru (Figure 21). RuO<sub>4</sub> has a melting point of 25.4 °C and a boiling point of 130 °C. Its vapor pressure at 25 °C is 10 Torr. To overcome stability limitations it was supplied from a solution. The researchers proposed that RuO<sub>4</sub> decomposes on the Ru surface resulting in a RuO<sub>2</sub> film, which blocks the RuO<sub>4</sub> decomposition. The RuO<sub>2</sub> film was reduced to Ru in the second half-reaction using H<sub>2</sub> or H-plasma. In the second case depositions were possible at temperatures as low as 50 °C with a GPC of 0.1 Å/cycle. The upper temperature limit was about 100 °C where RuO<sub>4</sub> started to decompose on RuO<sub>2</sub>. The authors did not explicitly discuss the initial growth and the substrate selectivity of the process. However, they obtained similar thin, dense, conductive films on Pt, H-terminated Si, and on the polymers polypropylene, polyethylene and polystyrene, and observed no nucleation delay.

A number of zero-valent precursors was also investigated for the ALD of Ru. Jung et al.<sup>239</sup> synthesized the Ru(0) complex (1,5-hexadiene)(1-isopropyl-4-methylbenzene)Ru and evaluated it for ALD with O<sub>2</sub>.

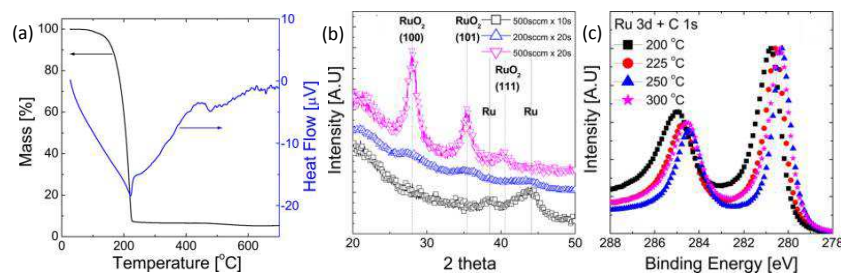


Figure 22: ALD study with zero-valent (1,5-hexadiene)(1-isopropyl-4-methylbenzene)Ru (a) TGA and DTA curves, (b) XRD patterns of films grown at 200 °C with different O<sub>2</sub> exposures, and (c) XPS Ru 3d peaks of films grown at different temperatures.<sup>239</sup> Reprinted with permission from H. J. Jung et al., *Chem. Mater.* 26, 7083-7090 (2014); Copyright 2014 American Chemical Society.

As can be seen from the TGA curve in Figure 22 (a), the compound evaporates at 200 °C at atmospheric pressure leaving fairly low residue. The nature of the resulting films depended again strongly on the

deposition conditions. Long O<sub>2</sub> exposure times and low temperatures resulted in the formation of RuO<sub>2</sub> (Figure 22 (b),(c)). Further zero-valent Ru precursors studied for ALD include (ethylbenzene)(1,3-butadiene)Ru(0),<sup>240</sup> (Isopropylmethylbenzene)(Cyclohexadiene)Ru(0),<sup>241</sup> (ethylbenzene)(cyclohexadiene)Ru(0),<sup>242</sup> (ethylbenzyl) (1-ethyl-1,4-cyclohexadienyl)Ru(0),<sup>243</sup> and (η-2,3-dimethylbutadiene)(tricarbonyl)Ru(0).<sup>244</sup> A typical observation for thermal ALD processes is a much shorter, or even negligible, nucleation delay as compared to Ru(II) and Ru(III) precursors.

Geyer et al.<sup>245</sup> studied the evolution of morphology and texture during Pt ALD with MeCpPtMe<sub>3</sub> and O<sub>2</sub> at 300 °C on Si. The islands started to coalesce after 200 cycles and a continuous film was formed after 600 cycles. The authors observed a preferred (111) orientation which became more pronounced when the islands coalesced to continuous films. Furthermore, the in-plane strain changed from comparative to tensile to reduce the surface energy of the merging islands. This was concluded from the shift of the (111) out-of-plane XRD peak to higher values for the scattering vector and of the in-plane peak to lower values. The in-plane diameter of the grains remained constant after coalescence while the out-of-plane diameter increased, thus columnar growth was observed.

Mackus et al.<sup>246</sup> compared the island growth during Pt ALD with a two-step process employing MeCpPtMe<sub>3</sub> and O<sub>2</sub> with a three-step process employing MeCpPtMe<sub>3</sub> oxygen plasma and hydrogen plasma, and observed a much broader island-size distribution for the first process. The researchers explained this with different mobilities of the Pt atoms on the substrate surface during the two processes; a lower mobility causes smaller diffusion distances and the nucleation of new islands at the later stage of the deposition process. They speculated that the lower mobility of the thermal process is due to the presence of unreacted ligands on the surface.

The initial island formation process was studied by Grillo et al.<sup>247,248</sup> based on the growth of Pt from MeCpPtMe<sub>3</sub> and O<sub>2</sub> and in phenomenological simulations. They compared different growth regimes such

as selective growth between Pt grains and substrate, particle diffusion and sintering, and Ostwald ripening and concluded from comparing the experimentally observed grain-size distribution with their simulations that grain diffusion and sintering is the most likely mechanism. An interesting feature is the difference of the size distribution for depositions at low (80 – 100 °C) and high (150 – 250 °C) temperatures. The authors observed a shift of the distribution maximum to larger islands for the low-temperature processes, and explained it with the immobility of the larger grains under these conditions and a diffusion by the smallest grains only. This leads to a consumption of the latter. From their simulations, the researchers draw two further important conclusions: the combination of island nucleation and sintering can lead to a constant grain density, which can be easily miss-interpreted as an absence of sintering, and very narrow size distributions can be achieved by the combination of the two processes under certain conditions. The low deposition temperatures used in this research, which are far below those typically defined as Pt-ALD window by other authors, can be explained by the atmospheric-pressure-ALD technique used; thus, the high partial pressure of oxygen (~0.2 bar) and the long exposure times.

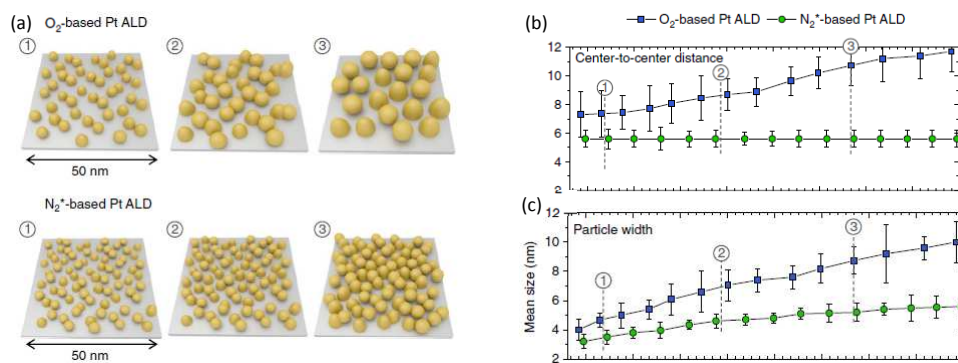


Figure 23: Island formation during Pt ALD with O<sub>2</sub> or nitrogen plasma: (a) illustration, (b) change of island distance and (c) of island width with number of cycles.<sup>249</sup> Reprinted with permission from J. Dendooven et al., *Nature Comm.* 8, 174 (2017); Creative Commons Licence.

Dendooven et al.<sup>249</sup> observed in in-situ small angle X-ray scattering (GISAXS) studies that the island growth during Pt ALD with MeCpPtMe<sub>3</sub> proceeds very differently whether O<sub>2</sub> or nitrogen plasma is employed as co-reagent (Figure 23). Strong coarsening was observed in the first case, while virtually none in the second. The mechanism responsible for this was not discussed in that paper. However, by combining the two processes the authors were able to fine-tune the deposits' morphology. In another paper, Solano et al.<sup>250</sup> of the same group used the Pt deposits grown with this process to study the coarsening phenomena in different atmospheres. In most cases they observed Ostwald ripening starting at temperatures above 500 °C. However, when Pt particles with oxidized surfaces were subjected to reductive atmosphere, ripening was observed at temperatures nearly down to room temperature. The authors suggested that the surface PtO<sub>2</sub> became reduced to PtO or Pt<sub>2</sub>O<sub>3</sub> which are very mobile species.

Although Pd shares many properties with the other platinoid metals, attempts to grow Pd layers with ALD using combustion in O<sub>2</sub> were not successful. Aaltonen et al.<sup>251,252</sup> reported the growth of metallic Pd films with Pd-bis(1,1,1,5,5,5-hexafluoro-4-n-butylamino-pent-3-ene-2-dionate), but the growth was not saturated as the GPC increased with the precursor pulse time indicating decomposition of the precursor or poor reactivity. Moreover, the quality of the films decreased when longer oxygen pulses were applied. Unfortunately, no graphical data of the Pd film growth were presented in that work. More papers report the growth of Pd films using similar reduction chemistry as is used for Cu ALD.

Senkevich et al.<sup>253</sup> demonstrated the growth of Pd with Pd(hfac)<sub>2</sub> and H<sub>2</sub> on Ir coated substrates. They observed that after an initial growth with about 0.27 Å/cycle the rate decreased to 0.094 Å/cycle when deposition was carried out at 130 °C while at a deposition temperature of 80 °C the GPC remained at 0.27 Å/cycle. They attributed this to the stronger polarisability and therefore stronger van-der-Waals interaction of Ir as compared to Pd. In an earlier study Senkevich et al.<sup>254</sup> demonstrated in XPS studies that Pd(hfac)<sub>2</sub> adsorption is inhibited on oxidized surfaces but occurs readily on Ir. By first depositing a P monolayer Pd

could be deposited on most surfaces. This was attributed to the high polarisability of P. They furthermore demonstrated with Rutherford backscattering analysis that  $\text{Pd}(\text{hfac})_2$  begins to decompose above 220 °C, which is a similar temperature to that where Jezewski et al.<sup>97</sup> observed decomposition of  $\text{Cu}(\text{hfac})_2$  on Pt and  $\text{SiO}_2$ . Senkevich et al.<sup>253</sup> prepared dielectric substrates with a self-assembled monolayer, which was grown with bis[3-(triethoxysilyl)propyl]tetrasulfide, to facilitate the adsorption of  $\text{Pd}(\text{hfac})_2$ . Chemisorption was evidenced by a shift of the S 2p XPS peak. The adsorbed  $\text{Pd}(\text{hfac})_2$  was reduced with glyoxylic acid at 210 °C, since this acid is known to decompose to formaldehyde and  $\text{CO}_2$  at high temperatures.<sup>255</sup>

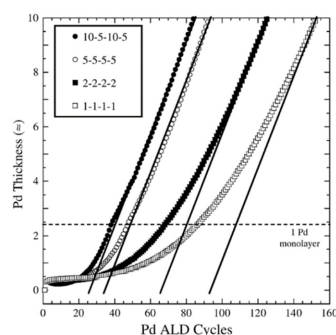
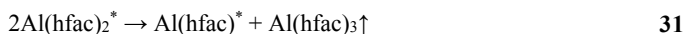


Figure 24: Pd film growth with  $\text{Pd}(\text{hfac})_2$  and formalin on  $\text{Al}_2\text{O}_3$ .<sup>256</sup> Reprinted with permission from J. Elam et al., *Thin Solid Films* 515, 1664-1673 (2006). Copyright 2006 Elsevier.

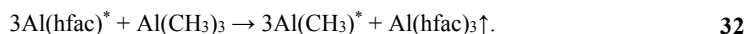
Elam et al.<sup>256</sup> reported somewhat contradictory results as they were able to grow Pd films on  $\text{Al}_2\text{O}_3$  with  $\text{Pd}(\text{hfac})_2$  and formalin. However, they reported a nucleation delay which strongly depended on the cycle times (Figure 24) and no reasonable nucleation was observed using other reducing agents such as  $\text{H}_2$ , methanol, ethanol, isopropanol, acetone or TMA, or oxidation agents such as  $\text{H}_2\text{O}$ ,  $\text{O}_2$ ,  $\text{O}_3$  or  $\text{H}_2\text{O}_2$ . After initial nucleation was achieved using formalin, growth was achieved with more reducing agents. One explanation for this involves decoration of the surface with polarizable carbonyl groups as formaldehyde is known to dissociate to hydrogen and CO. After the nucleation the GPC changed only slightly with

variation of cycle times. Elam et al.<sup>256</sup> also detected remnants of the hfac ligands remaining on the surface by XPS.

Goldstein and George<sup>257,258</sup> investigated the reaction of Pd(hfac)<sub>2</sub> and formalin on Al<sub>2</sub>O<sub>3</sub> in FTIR studies. They observed that Al(hfac)\* surface species were not removed by formalin while Pd(hfac)\* species were. Moreover, they detected a loss of Al(hfac)\* with time which was mitigated by the presence of formate groups from the adsorption of formaldehyde. The loss displayed second order kinetics<sup>258</sup> and therefore they concluded that the loss was mainly due to a desorption mechanism such as



and not to decomposition although decomposition products such as Al(tfa)\* were also detected. The mitigation of Al(hfac)\* loss when formate species were present was attributed to a hindering of surface diffusion. Goldstein and George<sup>257</sup> furthermore demonstrated that Al(hfac)\* surface species can be removed by TMA:



Eyck et al.<sup>259</sup> studied the growth of Pd with Pd(hfac)<sub>2</sub> and H<sub>2</sub> on air-exposed (thus oxidized) Ta and Si at a deposition temperature of 80 °C. While growth could be achieved on Ta, virtually no growth was obtained on Si. Although no saturation was proven as the GPC strongly depended on the H<sub>2</sub> pulse length, the results indicated that Pd growth with molecular H<sub>2</sub> is not limited to noble surfaces. They proposed that H<sub>2</sub> diffuses through the surface oxide to split on the Ta/TaO<sub>x</sub> interface. The resulting H atoms are able to migrate to the surface and react with the adsorbed precursor.

Similar to Cu growth, hydrogen plasma can be used to achieve growth on numerous substrates at moderate temperatures. Eyck et al.<sup>141,260</sup> carried out PEALD experiments with Pd(hfac)<sub>2</sub> on Si, W, and Ir and

This is the author's peer reviewed, accepted manuscript. However, the online version of record will be different from this version once it has been copyedited and typeset.

PLEASE CITE THIS ARTICLE AS DOI: 10.1063/1.5087759

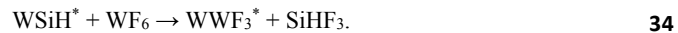
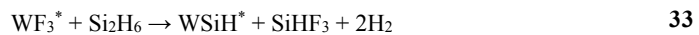
achieved purer films than could be obtained with thermal processes. The GPC was surface-dependent and largest for growth on W. Furthermore, the grain density was much larger on W while the surface roughness was larger on Si. Eyck et. al.<sup>260</sup> obtained a higher GPC on Si when they used a mixed N<sub>2</sub>/H<sub>2</sub> plasma instead of a pure H<sub>2</sub> plasma. They attributed this effect to the formation of surface nitride species which facilitate the adsorption of Pd(hfac)<sub>2</sub>. A similar effect was observed for growth on poly(p-xylylene),<sup>260</sup> where no growth could be obtained when using hydrogen plasma only but considerable growth was obtained using a mixed hydrogen/nitrogen plasma.

Hämäläinen et al.<sup>261</sup> used a mixture of the direct reduction process discussed in this section and the oxygen combustion reaction with which the other platinum group metals are typically grown. When they reacted Pd(tmhd)<sub>2</sub> at 120 °C with ozone, they were able to grow ALD PdO films on Al<sub>2</sub>O<sub>3</sub>. When molecular H<sub>2</sub> was added after the ozone pulse metallic Pd films were obtained. However, these films were not very uniform across the substrate. The same reaction mechanism was also used for the deposition of Rh from Rh(acac)<sub>3</sub> at 150 °C and Pt from Pt(acac)<sub>2</sub> at 110 °C and metallic films of good quality were obtained.

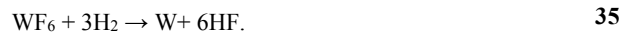


### 4.3 Tungsten and molybdenum

The CVD of W is well established in the CMOS production. It was used for the filling of vias between the metallization levels in the old Al technology and is still used for the fabrication of contacts between the transistors and the metal-1 layer. Here, contact holes are usually filled in a two-step CVD process. Firstly, a seed layer is deposited by a fluorosilane elimination reaction with  $\text{WF}_6$  and  $\text{SiH}_4$  or  $\text{Si}_2\text{H}_6$ :



Next, the contact hole is filled by reaction of  $\text{WF}_6$  with  $\text{H}_2$ :



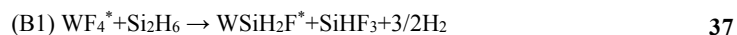
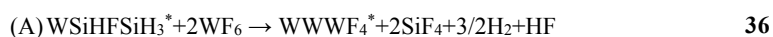
The fluorosilane-elimination process is characterized by a relatively large sticking coefficient. While this causes a lack of conformality, it provides rapid nucleation of a seed layer for the hydrogen reduction process as described by equation 37, as the contact holes can be super-conformally filled. It seems to be an obvious strategy to develop an ALD process based on the reaction described by the equations 35 and 36 to overcome the issue of limited conformality.

Klaus et al.<sup>262</sup> carried out ALD experiments on W growth with  $\text{WF}_6$  and  $\text{Si}_2\text{H}_6$  in which they monitored the thickness of the growing film in-situ with spectroscopic ellipsometry. Saturation was observed towards the  $\text{WF}_6$  and  $\text{Si}_2\text{H}_6$  exposure (the exposure was varied by carrying out multiple pulses of each precursor instead of changing the pulse length due to the technical characteristics of the ALD system) during the experiment and the GPC changed only slightly with temperature from 425 K until 600 K. The refractive

index obtained from the ellipsometry measurements was consistent with metallic W. The films were quite smooth as observed with AFM and little crystallinity could be observed with grazing incidence XRD measurements suggesting amorphous or at least nanocrystalline films. This poor crystallinity might explain the large resistivity measured ( $1.22 \times 10^{-4} \Omega\text{cm}$  for a 32 nm thick film).

Lei et al.<sup>263</sup> undertook extensive studies where they monitored the reaction in-situ by quadrupole mass spectroscopy (QMS). The  $\text{H}_2$  signal diminished during the long  $\text{SiH}_4$  pulse as does the  $\text{SiF}_4$  signal during the  $\text{WF}_6$  pulse. This indicates a saturation mechanism. However, the GPC was strongly dependent on temperature. The GPC is about 4 Å/cycle at 175 °C, while it is about 10 Å/cycle at 325 °C. Lei et al. attributed this to the activation energy of adsorption. However, GPC values higher than one monolayer per cycle strongly indicate that the adsorption mechanism is more complicated than a chemisorbed molecular monolayer as is usually proposed for ALD mechanisms. Another observation indicating this is that the GPC depended on the flow rate and reactor pressure.

The mechanism responsible for the high GPC values observed was investigated by the group of George<sup>264-266</sup> using mass spectrometry, AES, XPS and quartz-crystal microbalance (QCM). They detected a mass gain during the  $\text{Si}_2\text{H}_6$  pulse (Figure 25), and proposed a reaction according to:



where  $\text{Si}_2\text{H}_6$  is inserted into the surface Si-H bond.

This is the author's peer reviewed, accepted manuscript. However, the online version of record will be different from this version once it has been copyedited and typeset.

PLEASE CITE THIS ARTICLE AS DOI: 10.1063/1.5087759

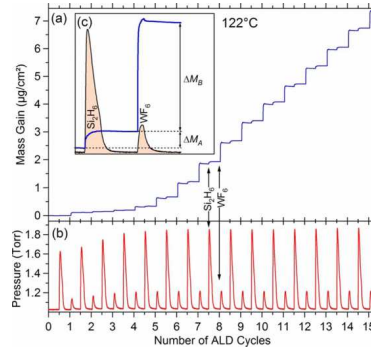


Figure 25: Tungsten ALD with  $\text{WF}_6$  and  $\text{Si}_2\text{H}_6$ : (a) Mass gain measured with QCM, (b) chamber pressure, (c) highlighted plot for the 15th cycle.<sup>265</sup> Reprinted with permission from R. W. Wind et al., *J. Appl. Phys.* 105, 074309 (2009). Copyright 2009 American Institute of Physics.

The viability of a W ALD process to coat complex structures was demonstrated by Elam et al.<sup>267</sup> who were able to coat the pores of carbon aerogels and of AAO membranes with an extremely high aspect ratio (70 000 nm : 40 nm) using  $\text{WF}_6$  and  $\text{Si}_2\text{H}_6$  at 200 °C. On a flat Si substrate, they observed a GPC of 7.2 Å/cycle after a short nucleation period. Baumann et al.<sup>268</sup> used the same method to coat alumina and germania aerogels (Figure 26).

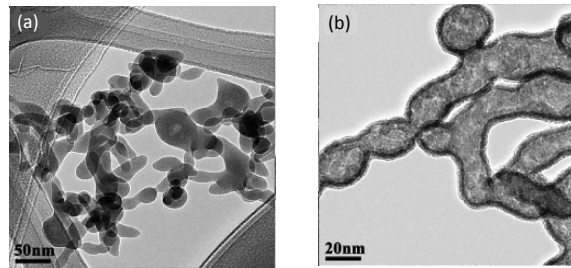
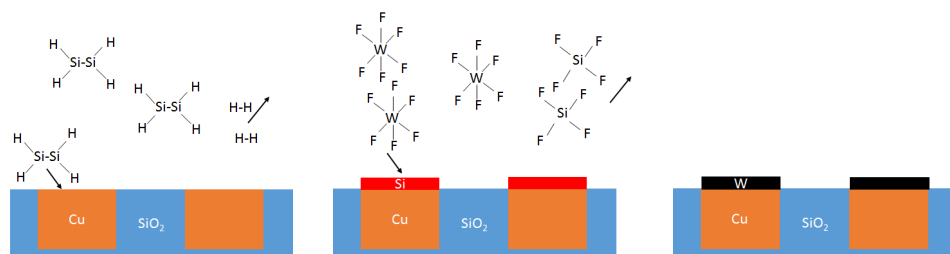


Figure 26: Germania aerogels coated with ALD W: (a) uncoated aerogels, (b) aerogels after 6 W-ALD cycles.<sup>268</sup> Reprinted with permission from T. F. Baumann et al., *Chem. Mater.* 18, 6106-6108 (2006). Copyright 2006 American Chemical Society.

As argued at the top of this section, a main driver for the development of a W ALD process is the requirements for the fabrication of CMOS contacts. Although the self-limiting nature of these processes

is still in question, W ALD is already becoming an established process in industrial CMOS manufacturing, where it is used to provide an ultra-thin seed layer for the subsequent filling of the contact holes by superconformal CVD via the  $H_2$  reduction reaction in equation 37.<sup>269</sup>

A number of researchers used the excellent properties of W ALD for further applications. Blanchard et al.<sup>270</sup> demonstrated the deposition of a conformal W gate electrode around a GaN nanowire transistor. Lee et al.<sup>271</sup> used W ALD for the deposition of interconnects for GaN nanowire LEDs as it provides conformal coating even on such high- aspect-ratio structures. Moreover, W ALD was used for the deposition of the beam of nano-electromechanical system (NEMS) transistors<sup>272,273</sup> where bending of the (source) beam by a gate voltage enables contact to a drain electrode below.



Scheme 5: Area-selective W deposition process developed by Haukka and coworkers.<sup>274</sup>

Haukka et al.<sup>274</sup> of ASM International developed a process for the selective deposition of W on metallic surfaces based on a similar chemistry (Scheme 5). The purpose of this was to deposit the tungsten film on a Cu interconnect line in a microelectronic device but not on the dielectric surrounding it. This has the advantage that electromigration is typically much lower at Cu-metal interfaces than at Cu-insulator interfaces. A structure of Cu pattern in  $SiO_2$  was exposed to disilane resulting in a selective Si deposition on Cu. Next, the sample was exposed to  $WF_6$  resulting in the formation of  $SiF_4$  and a W film. The patent also described a number of related processes and the selectivity was above 90%. Here, it is interesting to

note that among the best results were achieved on a low-k dielectric with a permittivity of 2.3 (98 %). Cleaning of the surface by etching after the deposition was proposed to remove the metal contamination from the dielectric surface.

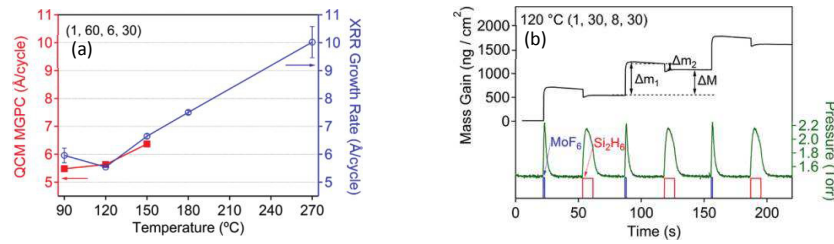
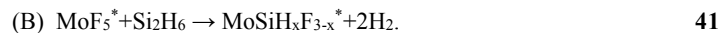
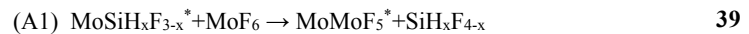


Figure 27: Growth characteristic of Mo ALD with MoF<sub>6</sub> and Si<sub>2</sub>H<sub>6</sub>: (a) GPC vs temperature measured with QCM and X-ray reflection (XRR), (b) mass gain during ALD cycles.<sup>275</sup> Reprinted with permission from D. Seghete et al., *Chem. Mater.* 23, 1668-1678 (2011). Copyright 2011 American Chemical Society.

Seghete et al.<sup>275</sup> explored a similar reaction chemistry to that used for W ALD for the deposition of Mo using MoF<sub>6</sub> and Si<sub>2</sub>H<sub>6</sub>. Similarly as for the ALD of W, GPC values exciting one monolayer per cycle were obtained (Figure 27). However, the researchers observed an important difference in QCM investigations as the sample mass did not increase but decrease during the Si<sub>2</sub>H<sub>6</sub> pulse. The researchers proposed that the high GPC is caused by the decomposition of MoF<sub>6</sub> during the MoF<sub>6</sub> pulse, and the reaction can be described by:



This is the author's peer reviewed, accepted manuscript. However, the online version of record will be different from this version once it has been copyedited and typeset.

PLEASE CITE THIS ARTICLE AS DOI: 10.1063/1.5087759

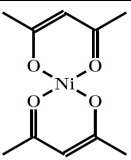
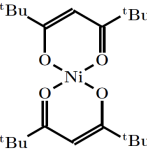
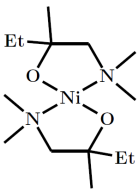
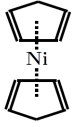
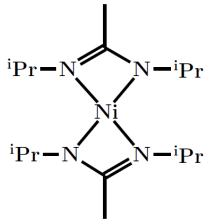
Here, the exothermic reaction A1 would enable the endothermic reaction A2. The GPC increased with temperature from about 6 Å/cycle at 90 °C to 10 Å/cycle at 270 °C. Continuous Mo films were formed after a very short number of cycles, and the analysis of XRD patterns showed very small grain sizes of about 1.5 nm. Furthermore, an average electrical resistivity of 124  $\mu\Omega\text{cm}$  was measured for 30 nm thick films deposited at 120 °C. The Si contamination of the Mo films was quite high between 15 and 30 % and decreased with decreasing temperature. When the reaction was conducted in a high vacuum reactor which allowed the dosing of  $\text{Si}_2\text{H}_6$  at very low pressures no Si contamination was detected.

This is the author's peer reviewed, accepted manuscript. However, the online version of record will be different from this version once it has been copyedited and typeset.

PLEASE CITE THIS ARTICLE AS DOI: 10.1063/1.5087759

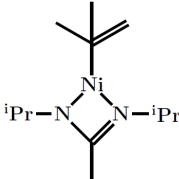
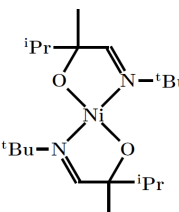
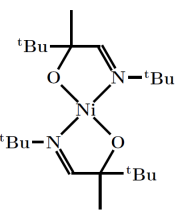
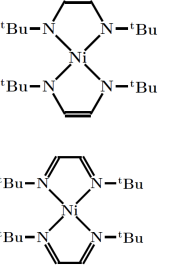
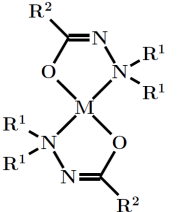
## 4.4 Magnetic Metals

Table 8: Nickel metalorganics explored for the ALD or CVD of Ni.

Name	Structure	References
Ni-bis(acetylacetonate)  Ni(acac) <sub>2</sub>		276
Ni-bis(2,2,6,6-methylheptane-3,5-dionate),  Ni(tmhd) <sub>2</sub>		277
Ni-bis(1-dimethylamino-2-methyl-2-butoxide),  Ni(dmamb) <sub>2</sub>		278-281
Ni-bis(cyclopentadienyl),  Ni(Cp) <sub>2</sub> ,  nickelocene		282,283
Ni-bis(N,N'-diisopropylacetamidinate)		284,285

This is the author's peer reviewed, accepted manuscript. However, the online version of record will be different from this version once it has been copyedited and typeset.

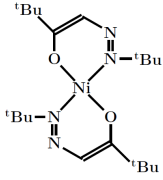
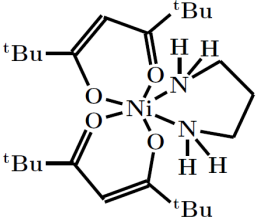
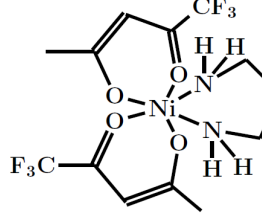
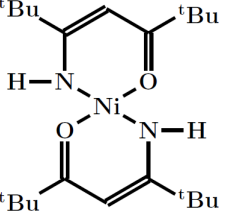
PLEASE CITE THIS ARTICLE AS DOI: 10.1063/1.5087759

Ni(2-methylallyl)(N,N'-diisopropylacetamidinate)		286
Ni( <sup>t</sup> PrMeCOCN <sup>t</sup> Bu) <sub>2</sub>		287
Ni( <sup>t</sup> BuMeCOCN <sup>t</sup> Bu) <sub>2</sub>		287
Ni-bis(diazadienyl)		288
Ni-bis(carbohydrazide)		289



This is the author's peer reviewed, accepted manuscript. However, the online version of record will be different from this version once it has been copyedited and typeset.

PLEASE CITE THIS ARTICLE AS DOI: 10.1063/1.5087759

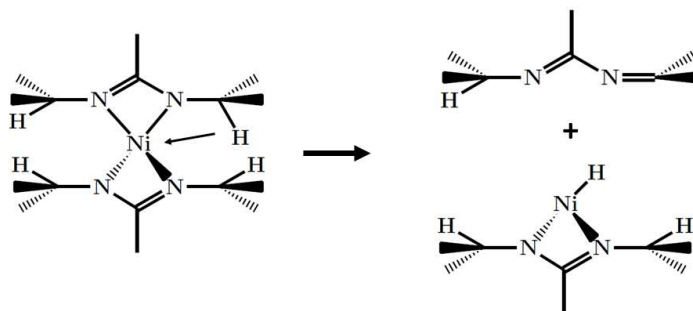
	1: R <sup>1</sup> =Me, R <sup>2</sup> = <sup>t</sup> Bu, 2: R <sup>1</sup> =Me, R <sup>2</sup> = <sup>i</sup> Pr, 3: R <sup>1</sup> =Me, R <sup>2</sup> =Me, 4: R <sup>1</sup> =(CH <sub>2</sub> ) <sub>5</sub> , R <sup>2</sup> = <sup>t</sup> Bu, 5: R <sup>1</sup> =(CH <sub>2</sub> ) <sub>5</sub> , R <sup>2</sup> = <sup>i</sup> Pr, 6: R <sup>1</sup> =(CH <sub>2</sub> ) <sub>5</sub> , R <sup>2</sup> =Me	
Ni-bis(hydrazonate)		290
1,3-diaminopropane-Ni-bis(2,2,6,6-methylheptane-3,5-dionate),  pda-Ni(tmhd) <sub>2</sub>		277
1,3-diaminopropane-Ni-bis(1,1,1-trifluoro-5,5-dimethyl-hexane-2,4-dionate),  pda-Ni(tfac) <sub>2</sub>		277
Ni-bis(2,2,6,6-tetramethyl-5-amino-hept-4-ene-3-onate),  Ni(i-tmhd) <sub>2</sub>		277

Ni and Co are used in microelectronics as contact and gate materials. Furthermore, their ferromagnetic properties can be used for many other applications including magnetic memories. Utriainen et al.<sup>276</sup>

compared the use of  $\text{Ni}(\text{acac})_2$  and  $\text{Cu}(\text{acac})_2$  for ALD with molecular  $\text{H}_2$ . A higher evaporation temperature was needed for  $\text{Ni}(\text{acac})_2$  (155 °C vs 130 °C) and the Ni compound turned out to be more stable at the deposition temperature of 250 °C. Metallic films were obtained for both precursors on Al and Ti, but no films were obtained on glass for  $\text{Ni}(\text{acac})_2$ , while non-metallic deposits were obtained for  $\text{Cu}(\text{acac})_2$  most likely due to decomposition of the precursor at the process temperature of 250 °C. This shows a similar surface selectivity for Ni ALD with molecular  $\text{H}_2$  as is observed for Cu ALD.

Do et al.<sup>278</sup> reported the growth of Ni with the Ni(II) aminoalkoxide Ni-bis(1-dimethylamino-2-methyl-2-butoxide) ( $\text{Ni}(\text{dmamb})_2$ ) and molecular  $\text{H}_2$ . They observed a relatively constant GPC of about 1.25 Å/cycle between 200 and 250 °C. The carbon content was quite large (25 %) but the sheet resistance of 18.6 Ω/sq after 200 cycles at 220 °C was relatively low and comparable to similar films grown with physical vapor deposition (PVD). They attributed the low resistance to the formation of a metastable  $\text{Ni}_3\text{C}$  phase which was also indicated by XRD measurements. Kim et al.<sup>279</sup> used ammonia as a reducing agent for an ALD process with the same precursor. They reported a lower GPC (0.64 Å/cycle) than Do et al.<sup>278</sup> although the substrate temperature of 300 °C was clearly above the ALD window reported by Do and coworkers. Growth was achieved on H-terminated Si as well as on OH-terminated  $\text{SiO}_2$  and the films had a grainy morphology, which was more pronounced on H-terminated Si. The texture of the films was very different as strong (002) preferential growth was obtained on  $\text{SiO}_2$  while a (111)/(002) peak ratio closer to that for randomly oriented Ni was obtained on H-terminated Si. The purity of the films was better than that obtained by Do et al.,<sup>278</sup> as XPS measurements indicated a significantly lower C content. Virtually no growth was obtained on a self-assembled mono-layer of octadecyltrichlorosilane (OTS), an effect that can be exploited for area selective growth. A similar selectivity was observed by Lee et al.<sup>114</sup> in their Cu ALD studies. OTS is an amphiphilic material and its hydrophilic chloro-groups react with the hydroxyl groups of the substrate surface, while the long alkane group provides a strongly hydrophobic surface that prevents adsorption of metalorganic complexes. Although the films reported by Kim et al.<sup>279</sup> were more grainy than

films obtained with methods such as PVD, they are continuous and of reasonably good quality as compared to island-like Cu deposits obtained under similar deposition conditions. Lee et al.<sup>280</sup> carried out similar ALD experiments with  $\text{Ni}(\text{dmamb})_2$  and  $\text{NH}_3$  at 300 °C on  $\text{SiO}_2$  and reported a GPC of 0.3 Å/cycle.



Scheme 6: Proposed  $\beta$ -hydride elimination mechanism for Ni-amidates.<sup>291</sup>

Lim et al.<sup>284</sup> reported ALD growth of Ni with Ni-bis( $\text{N},\text{N}'$ -diisopropylacetamidate) and hydrogen with a GPC of 0.4 Å/cycle at 250 °C in their work on transition-metal amidates but gave little details about the Ni films. These Ni-amidates were synthesized via a similar reaction chemistry as that used to synthesize Cu(amidates).<sup>77</sup> Similar to Cu-amidates, limited stability can be an issue for Ni-amidates. Wu et al.<sup>291</sup> carried out DFT based simulations that showed that  $\beta$ -hydride elimination is a likely pathway for the observed decomposition of the Ni(II)-amidates Ni-bis( $\text{N},\text{N}'$ -diisopropylacetamidate) and Ni-bis( $\text{N},\text{N}'$ -di-tert-butylacetamidate) (Scheme 6). This effect also needs to be considered for amidates of other metals such as Cu when they are adsorbed on Ni or Ni containing alloys.<sup>166</sup>

Improvement of stability was reported by Lansalot-Matras<sup>286</sup> for heteroleptic Ni-alkenyl-amidate precursors. In particular, he evaluated  $\text{Ni}(\text{2-methylallyl})(\text{N},\text{N}'\text{-diisopropylacetamidate})$  and observed significantly less residue material as compared to the corresponding homoleptic Ni-amidate in TGA. An ALD window of 200 - 350 °C for PEALD with hydrogen and ammonia plasma was claimed by the

researcher and justified with a characteristic showing saturation of the GPC at 1.4 Å/cycle when the Ni-precursor pulse length was increased for deposition at 300 °C using ammonia plasma. However, a lack of saturation with the plasma pulse time was reported. The purity of the films was better for the use of ammonia plasma than for the use of hydrogen plasma, and the contamination increased with increasing plasma pulse length. The researcher demonstrated quite pure films for growth at 300 °C using ammonia plasma with XPS measurements.

Similar to Cu deposition, H<sub>2</sub> plasma was also used as reducing agent for the growth of Ni films. Lee et al. carried out PEALD experiments<sup>292</sup> with an unspecified precursor and reported a GPC of 1.55 Å/cycle at 220 °C on deoxidized Si, a value that is slightly higher than the GPC of 1.25 Å/cycle reported by Do and coworkers.<sup>278</sup> For 31 nm thick films, a resistivity of 9.6 μΩcm was measured, and XRD indicated polycrystalline films with a nearly random texture, while AES depth profiling showed relatively low levels of contamination. The Ni films were used to grow NiSi by rapid thermal annealing (RTA) and high quality films were obtained. Guo et al.<sup>285</sup> explored an PEALD process with Ni-bis(N,N'-diisopropylacetamidinate) and hydrogen plasma, and obtained NiC<sub>x</sub> instead of Ni with a GPC of 0.4 Å/cycle between 75 and 250 °C. The authors analyzed films deposited at 95 °C in detail, and were able to identify a rhombohedral Ni<sub>3</sub>C phase by XRD and electron diffraction. Chae et al.<sup>282</sup> reported that it was not possible to grow Ni films on TiN using nickelocene (NiCp<sub>2</sub>) and hydrogen plasma but that Ni films could be grown using a three step NiCp<sub>2</sub>/H<sub>2</sub>O/H sequence (substrate temperature 165 °C). When H<sub>2</sub>O was used as sole reagent, a mixed Ni/NiO film was grown. The lack of growth using only hydrogen plasma was attributed to the lack of ability of hydrogen atoms to form a volatile compound by reaction with the Cp\* ligands. Another possible reason for the observed difference was the formation of active surface sites by the H<sub>2</sub>O pulse that facilitate the adsorption of NiCp<sub>2</sub>. In the three-step process, a GPC of 1.9 Å/cycle was observed and the films contained a significant amount of carbon impurities which were 5 % (atomic)

under the optimized plasma power of 150 W and increased when the power was lowered. This high carbon content resulted in an increased resistivity of 25 – 30  $\mu\Omega\text{cm}$  for a 15 nm thick film.

A similar three-step process using molecular  $\text{H}_2$  instead of plasma was reported by Daub et al.<sup>283</sup> to grow Ni nanotubes by deposition into porous alumina and  $\text{TiO}_2$  coated porous alumina. They observed a relatively low GPC of about 0.15 Å/cycle in spite of a high deposition temperature of 330 °C. In a second growth process Daub et al. first grew NiO by reaction of  $\text{Ni}(\text{Cp})_2$  with  $\text{O}_3$  which was subsequently reduced by annealing in  $\text{H}_2$  at 400 °C. The second method provided a much finer grain structure. A possible reason for these differences is that less agglomeration occurs during the growth of NiO than during the growth of Ni at 330 °C. The secondary grain formation during annealing would have less effect than the primary grain formation during the direct Ni growth.

The strategy of subsequent reduction of an oxide film was also investigated by Ultriainen et al.,<sup>276</sup> who were able to grow a crystalline NiO film with  $\text{Ni}(\text{acac})_2$  and  $\text{O}_3$  at 250 °C on glass while no growth was obtained under the same conditions with  $\text{H}_2$ .<sup>276</sup> The films were transformed to metallic Ni by annealing in  $\text{H}_2$  (5 % in Ar) at temperatures of between 230 and 500 °C.

Kang et al.<sup>281</sup> investigated the influence of adsorbed iodine on the ALD growth of Ni on plasma cleaned Si samples by exposing them to  $\text{CH}_3\text{CH}_2\text{I}$  vapor before deposition. Reactants were  $\text{Ni}(\text{dmamb})_2$  and molecular  $\text{H}_2$ . The use of iodine resulted in smoother films. However, those films contained significant amounts of iodine and carbon, which increased their resistivity except for the thinnest films where the effect of morphology improvement seems to dominate. The contamination had little effect on the texture as similar XRD patterns, which are typical for randomly oriented Ni films, were achieved for both types of film.

Zarkova et al.<sup>277</sup> synthesized and characterized Ni-bis(ketoiminates). The authors highlighted that these compounds have little tendency to form oligomers, which is a problem often observed for Ni-bis(diketonates). However, the vapor pressures of Ni-bis(ketoiminates) are not very high. For example, Ni-bis(2,2,6,6-tetramethyl-5-amino-hept-4-ene-3-onate) needs to be heated to 168 °C to achieve a vapor pressure of 0.1 Torr, while 143 °C is needed for the corresponding diketonate Ni-bis(tmhd)<sub>2</sub>.<sup>277</sup> The complexes can nevertheless be evaporated with little remnants in TGA. A second approach for Ni precursors evaluated by Zarkova et al. in the same work<sup>277</sup> was the addition of a dative ligand, 1,3-diaminopropane (pda), to Ni-bis(diketonates). This resulted in an increase of the vapor pressure of Ni(tmhd)<sub>2</sub> (0.1 Torr at 135 °C for pda-Ni(tmhd)). However, for other precursors, in particular Ni-bis(1,1,1-trifluoro-5,5-dimethyl-hexane-2,4-dionate) (Ni(tfac)<sub>2</sub>), the addition of pda decreased the vapor pressure. This was explained by differences of the structure of the molecular crystals, namely by the shorter intermolecular distances in the pda-Ni(pfac). This highlights again the difficulty to predict the properties of precursors. Both classes of precursor were tested for CVD with H<sub>2</sub> resulting in metallic films of relatively high contamination (C, O).

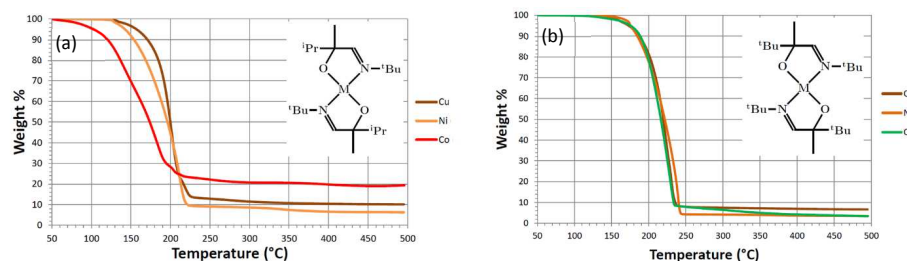


Figure 28: TGAs of metal-iminoalkoxides.<sup>287</sup> Adapted with permission from L. C. Kalutarage et al., *J. Am. Chem. Soc.* 135, 12588-12591 (2013). Copyright 2013 American Chemical Society.

Kalutarage et al.<sup>287</sup> synthesized the Ni- $\alpha$ -iminoalkoxide complexes Ni(PrMeCOCN<sup>t</sup>Bu)<sub>2</sub> and Ni(tBuMeCOCN<sup>t</sup>Bu)<sub>2</sub> (Figure 28) and tested Ni(PrMeCOCN<sup>t</sup>Bu)<sub>2</sub> for ALD with BH<sub>3</sub>(NHMe<sub>2</sub>). At a

deposition temperature of 180 °C films could only be obtained on a reactive substrate such as Ru and initial nucleation cycles with long Ni-precursor pulses (20 s) were necessary. Furthermore, the GPC declined after 1000 cycles, which was most likely due to the coverage of the catalyzing Ru substrate. However, saturated growth with a GPC of 0.09 Å/cycle was observed, and the films were metallic and contained a low level of contaminations as shown by XPS after sputtering.

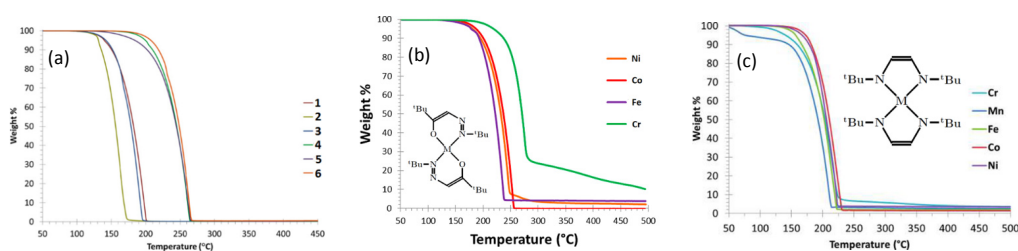
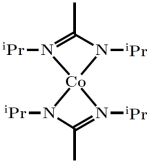


Figure 29: TGA of different precursor developed by the Winter group: (a) Ni carbohydrazides;<sup>289</sup> the structures can be found in table 8; (b) metal hydrazonates;<sup>290</sup> (c) metal diazodienyls.<sup>288</sup> Adapted with permission from M. C. Karunaratne et al., *Polyhedron* 52, 820-830 (2013); Copyright 2013 Elsevier, and L. C. Kalutarage et al., *Inorg. Chem.* 52, 5385-5394 (2013); Copyright (2013) American Chemical Society, and T. J. Knisley et al., *Organometallics* 30, 5010-5017 (2011); Copyright 2011 American Chemical Society, respectively.

Karunaratne et al.<sup>289</sup> developed several transition-metal carbohydrazides including the Ni complexes, whose TGA curves are shown in Figure 29 (a). These complexes were monomers, as were the Co and Cu complexes and could be cleanly evaporated at temperatures between 150 and 250 °C under a pressure of 0.05 Torr. Cu and Co complexes with this family of ligands behaved very similar. On the other hand, complexes with Cr, Mn and Fe could not be evaporated, and the Mn and Fe complexes were dimers. In order to avoid this dimer formation, Kalutarage et al.<sup>290</sup> of the same group synthesized bulkier ligands, hydrazonates, and tested their thermochemistry. Now, monomeric and volatile complexes were also obtained for Mn, Fe and Cr.

Knisley et al.<sup>288</sup> synthesized diazadienyl complexes of various transition metals including Ni. This class of ligands is non-innocent, which means the oxidation state of the ligand is not determined. The two limit structures are shown in Table 8. In this class of complexes, the energy required to transfer electrons between the metal ion and the ligand is small, and the molecules can decompose by separation into the metal and the neutral ligands. The decomposition temperature of these complexes decreases with the reduction potential of the  $M^{2+}/M^0$  couple from 320 °C for the Mn complex to about 230 °C for the Ni and Co compounds. It is interesting to note here that attempts of the researchers to synthesize an equivalent Cu complex failed and resulted in metallic Cu. The TGA curves in Figure 29 (c) show evaporation at temperatures between 150 and 225 °C. The Mn complex shows a first small weight loss at low temperature and a residual mass of about 4%. The residual mass for the Cr complex was about 8 % and the highest for these compounds. The authors blamed these observations on the air sensitivity of the molecules with makes their handling challenging. However, their high vapor pressures (e.g. ~0.1 Torr at 65 °C for the Ni complex) facilitate low evaporation temperatures and therefore the possibility of a suitable ALD window before the onset of decomposition.

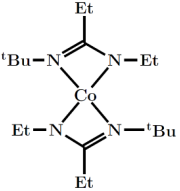
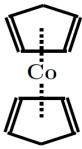
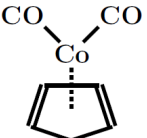
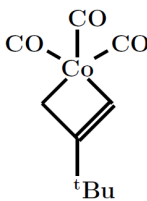
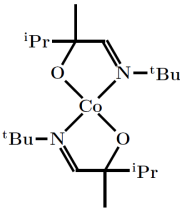
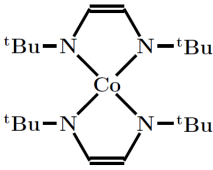
Table 9: Co metalorganics explored for the ALD or CVD of Co.

Name	Structure	References
Co-bis(N,N'-diisopropyl-acetamidinate)		284,293,294



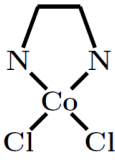
This is the author's peer reviewed, accepted manuscript. However, the online version of record will be different from this version once it has been copyedited and typeset.

PLEASE CITE THIS ARTICLE AS DOI: 10.1063/1.5087759

Co-bis(N-tert-butyl-N'-ethylpropionamidinate)		295-297
Co(Cp) <sub>2</sub>		142,298-300
[CO] <sub>2</sub> -Co(Cp)		299
[CO] <sub>3</sub> -Co( <sup>t</sup> Bu-allyl)		301
Co( <sup>i</sup> PrMeCOCN <sup>t</sup> Bu) <sub>2</sub>		287
Co-bis(1,4-di-tert-butyl-1,3-diazabutadienate), Co-bis(diazadienyl)		302,303

This is the author's peer reviewed, accepted manuscript. However, the online version of record will be different from this version once it has been copyedited and typeset.

PLEASE CITE THIS ARTICLE AS DOI: 10.1063/1.5087759

TMEDA-CoCl <sub>2</sub>		304
-------------------------	--	-----

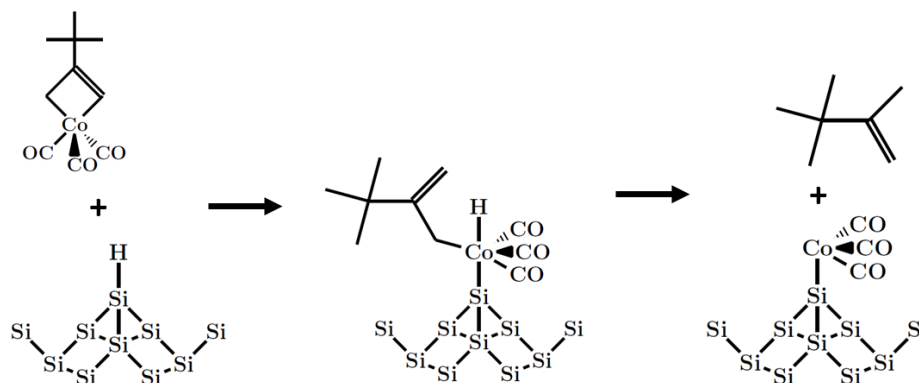
CVD of Co has become established in the fabrication of microelectronic devices in recent years and the dominant precursors are the zero-valent dicobalt-octacarbonyl ([Co(CO)<sub>4</sub>]<sub>2</sub>) and its derivatives.<sup>305-311</sup> However, Co precursors with Co in higher oxidation states have been used nearly exclusively in ALD. Co(II)-amidates are more stable than Ni(II)-amidates<sup>291</sup> as  $\beta$ -hydride elimination is energetically more costly for the former. Lim et al.<sup>284</sup> investigated ALD of Co films using Co-bis(N,N'-diisopropyl - acetamidinate) and molecular H<sub>2</sub> in the same work where they also reported a similar Ni ALD mechanism, which is discussed earlier in this review. For Co, they reported growth with a very low GPC of 0.04 Å/cycle at 300 °C, which was saturated for the variation of the pulse lengths of both reactants. However, no temperature window of constant growth could be demonstrated. Very thin films (0.8 nm) were conductive and could be used as liners for Cu ALD in the same report<sup>284</sup> and in later work by Li and coworkers.<sup>79,80</sup> Lee and Kim<sup>298</sup> were able to reproduce the results of Lim et al.<sup>284</sup> and furthermore showed that the selective deposition towards an OTS layer is possible. However, the blocking of growth was not perfect, and deposits could be observed after about 1000 cycles, possibly due to degradation of the OTS film. Lee and Kim also mentioned attempts to grow Co films with Co(Cp)<sub>2</sub> and H<sub>2</sub> in which no growth could be obtained. Lee et al.<sup>293</sup> demonstrated the deposition of Co using Co-bis(N,N'-diisopropylacetamidinate) and NH<sub>3</sub> with a GPC of about 0.3 Å/cycle at 350 °C which is higher than that observed by Lim et al.<sup>284</sup> who reported a rate of 0.12 Å/cycle at the same temperature. However, it is not clear if a real ALD process is observed at this high temperature as only saturation data for the NH<sub>3</sub> pulse were presented. Lim et al. also demonstrated selectivity between SiO<sub>2</sub> and an OTS monolayer. This selectivity was lost if they used NH<sub>3</sub> plasma. The GPC with plasma was only slightly higher than that

with molecular  $\text{NH}_3$ . In another paper, Lee et al.<sup>294</sup> compared thermal Co deposition from Co-bis(N,N'-diisopropylacetamidinate) using  $\text{H}_2$  and  $\text{NH}_3$  at 350 °C. With  $\text{H}_2$  a slightly higher GPC was observed. However, the size of the Co grains was larger and the contamination lower when  $\text{NH}_3$  was used. This resulted in a considerably lower resistivity for the films grown with  $\text{NH}_3$  ( $\sim 50 \mu\Omega \text{ cm}$  versus  $200 \mu\Omega \text{ cm}$ ). Elko-Hansen and Ekerdt<sup>295</sup> investigated the surface chemistry of the initial half-cycles of the Co ALD process with Co-bis(N-tert-butyl-N'-ethylpropionamidinate) and  $\text{H}_2$  on  $\text{SiO}_2$ , carbon-doped oxide and Cu with XPS. For the Cu substrate, they observed a reduction of the Co cation to Co(0) during the adsorption, saturated adsorption through the surface coverage by ligand fragments and an incomplete removal of the organic fragments during the  $\text{H}_2$  pulse. The results for  $\text{SiO}_2$  and carbon-doped oxide were in accordance with Co remaining in the oxidation state (II) after a reaction of the precursor with hydroxyl groups and an at least partial release of protonated ligands. Furthermore, this study indicated an ALD window for growth on Cu between 215 and 290 °C which is broader than that reported for Co-bis(N,N'-diisopropylacetamidinate). In a later article, Elko-Hansen and Ekerdt<sup>297</sup> investigated the possibility of area selective Co ALD with Co-bis(N-tert-butyl-N'-ethylpropionamidinate) and  $\text{H}_2$  the passivation of substrate materials ( $\text{SiO}_2$ , carbon-doped oxide, Cu) with Hhmds, trimethyl chlorosilane or bis(dimethylamino) chlorosilane. Moderate selectivities between Cu and the dielectric materials as well as between passivated and non-passivated substrates could be demonstrated.

Large differences between plasma and thermal ALD were reported by Lee and Kim.<sup>298,299</sup> They observed no growth with  $\text{CoCp}_2$  and  $\text{H}_2$ , while saturated growth with a rate of about 0.5 Å/cycle could be achieved with  $\text{NH}_3$  plasma. When  $[\text{CO}]_2\text{-CoCp}$  was used instead of  $\text{CoCp}_2$ ,<sup>299</sup> no saturation was observed, and the films were characterized by large resistivity and significant levels of contamination. Lee and Kim<sup>299</sup> also reported that  $\text{NH}_3$  plasma produces significantly cleaner Co films than are grown with  $\text{H}_2$  plasma, which they attributed to the role of N surface species in avoiding disproportionation of the Cp ligand.

Shimizu et al.<sup>142</sup> carried out experiments on hot-wire REALD with CoCp<sub>2</sub>, and observed that growth was achieved with NH<sub>3</sub>, but not with H<sub>2</sub> or a mixture of N<sub>2</sub> and H<sub>2</sub>. Without the hot wire no growth could be achieved at all. They concluded that the NH<sub>2</sub> radical was the species facilitating the dissociation of the precursor. The reduction of dissociation energy of CoCp<sub>2</sub> by NH<sub>2</sub> was confirmed by quantum chemical calculations. A strong indication for this effect is the dependence of the NH<sub>3</sub>-plasma pulse saturation time on the distance between the hot filament and the substrate. The mean free path of NH<sub>2</sub> radicals is much shorter than that of H radicals. Therefore, the NH<sub>2</sub> radical flux above the substrate and thus the reaction rate decreases with the distance. In a further study, Shimizu et al.<sup>300</sup> combined this Co ALD process with a W ALD process involving W(Cp)<sub>2</sub>H<sub>2</sub> to grow Co(W) alloys and observed better barrier properties to Cu migration than for pure Co films. The authors attributed this to the formation of an amorphous-like or nanocrystalline structure. Furthermore, they compared those ALD Co(W) films to Co(W) films deposited with a CVD process involving [Co<sub>2</sub>(CO)<sub>8</sub>] and [W(CO)<sub>6</sub>], and observed lower resistivities for the ALD films. The researchers attributed the high resistivities of the CVD film on the inclusion of oxygen impurities arising from the carbonyl groups.

An important question concerns the growth of metallic Co and Ni rather than nitrides when NH<sub>3</sub> or NH<sub>3</sub> plasma is used; especially, when comparing it to the growth of Cu<sub>3</sub>N with [Cu(<sup>t</sup>Bu-Me-amd)]<sub>2</sub> and NH<sub>3</sub> reported by Li and Gordon<sup>81</sup>. It is known that all three metal nitrides are thermodynamically unstable and Ni<sub>3</sub>N is assumed to be more stable than Cu<sub>3</sub>N. For example, Baiker and Mazejewski<sup>312</sup> observed the decomposition of Cu<sub>3</sub>N at 380 K in H<sub>2</sub> atmosphere and at 650 K in NH<sub>3</sub> atmosphere while Ni<sub>3</sub>N decomposed at 430 and 680 K, respectively. However, the deposition temperature for Cu<sub>3</sub>N was lower (160 °C) than the temperatures used for Ni and Co deposition.



Scheme 7: Adsorption of  $[\text{CO}]_3\text{Co}(\text{t-Bu-Allyl})$  on Si according to Kwon and coworkers.<sup>301</sup>

An interesting study on the surface chemistry of Co films was carried out by Kwon et al.<sup>301</sup> who observed that Co films grow readily on hydrogen terminated Si while little growth was observed on hydroxide terminated Si/SiO<sub>2</sub> when  $[\text{CO}]_3\text{-Co}(\text{t-Bu-Allyl})$  was used. This is surprising as hydroxyl groups are usually regarded as preferred surface species for ALD processes. By way of an explanation for this observation, they argued that  $[\text{CO}]_3\text{-Co}$  complexes are known to catalyze the hydrogenation of unsaturated functional groups in the presence of a hydrogen donor.<sup>301,313</sup> DFT calculations by Kwon et al.<sup>301</sup> suggested that H-Si species are better donors of neutral H atoms than H-O-Si species. The proposed mechanism, which has been supported by IR surface spectroscopy and DFT calculations, is depicted in Scheme 7.

Inspired by the successful three step Cu ALD process developed by their group,<sup>115</sup> Klesko et al.<sup>302</sup> attempted a similar process using the non-innocent compound Co-bis(1,4-di-tert-butyl-1,3-diazabutadienate), formic acid and 1,4-bis(trimethylsilyl)-1,4-dihydropyrazine and obtained Co films. However, the more interesting observation was that the Co complex can be directly reduced by formic acid which was in contrast to their results for Cu ALD. The growth on Ru was quite well controlled for a small temperature window between 170 and 180 °C with a relatively high GPC of  $\sim 1\text{\AA}/\text{cycle}$  although a small CVD component was identified by exposing only the Co complex (13-15 nm after 1000 cycles).

The growth process depended strongly on the substrate material, as comparable GPCs were measured on Ru, Pd, Pt and Cu while no films were visible for depositions on Si and SiO<sub>2</sub>. Furthermore, while the GPC remained constant for large cycle numbers, this was not the case for the initial growth for which a nucleation delay was observed. The electrical properties of the films deposited on the metallic substrates were quite similar as these films (after 1000 cycles, ~100 nm) had resistivities of about 20  $\mu\Omega\text{cm}$ . It is furthermore worth to notice that a similar two-step process did not work with the analogous Ni precursor, while a three-step process with 1,4-bis(trimethylsilyl)-1,4-dihydropyrazine resulted the deposition of metallic Ni with a GPC of 0.3  $\text{\AA}/\text{cycle}$ .

Kerrigan et al.<sup>303</sup> of the same group explored the amines NH<sub>2</sub><sup>t</sup>Bu, NHEt<sub>2</sub>, and NEt<sub>3</sub> as reducing agents for Co-bis(1,4-di-*tert*-butyl-1,3-diazabutadienate), and observed quite similar results as with formic acid with the first two molecules but no growth with NEt<sub>3</sub>. With NH<sub>2</sub><sup>t</sup>Bu saturated growth with a GPC of 0.98  $\text{\AA}/\text{cycle}$  in a temperature window spanning from 170 to 200 °C (Figure 30), and growth was limited to metallic substrate films (Cu, Pt, Ru). This selectivity was used for the deposition on a Pt pattern on Si. Another observation was a decrease of the GPC and an increased oxide content when N<sub>2</sub> carrier gas of low purity (<99.9% N<sub>2</sub>) was used. These researchers proposed that the amines coordinate with the Co ion of the adsorbed precursor changing its coordination from tetrahedral to planar. This would weaken the bonding and facilitate its decomposition. Here, it is important to remember the non-innocent nature of the ligands, which makes it possible to release the ligands without the transfer of a proton.

This is the author's peer reviewed, accepted manuscript. However, the online version of record will be different from this version once it has been copyedited and typeset.

PLEASE CITE THIS ARTICLE AS DOI: 10.1063/1.5087759

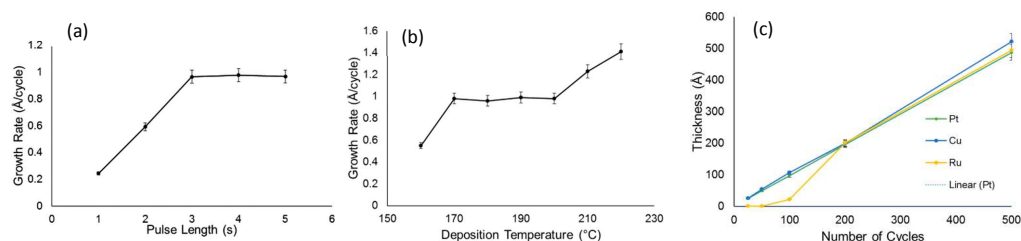


Figure 30: Growth characteristic of Co ALD with Co-bis(1,4-di-tert-butyl-1,3-diazabutadienate) and  $\text{NH}_2^t\text{Bu}$ : (a) GPC vs Co pulse length for deposition on Pt at 200 °C, (b) GPC vs temperature for deposition on Pt, and (c) thickness versus number of cycles for deposition on Pt, Cu and Ru at 200 °C.<sup>303</sup> Adapted with permission from M. M. Kerrigan et al., *Chem. Mater.* 29, 2458-2466 (2017). Copyright 2017 American Chemical Society.

Kalutarage et al.<sup>287</sup> evaluated the Co-iminoalkoxide  $\text{Co}(\text{iPrMeCOCN}^t\text{Bu})_2$  for the ALD with  $\text{BH}_3(\text{NHMe}_3)$  on Ru and obtained metallic Co with a GPC of 0.7 Å/cycle for depositions at 180 °C.

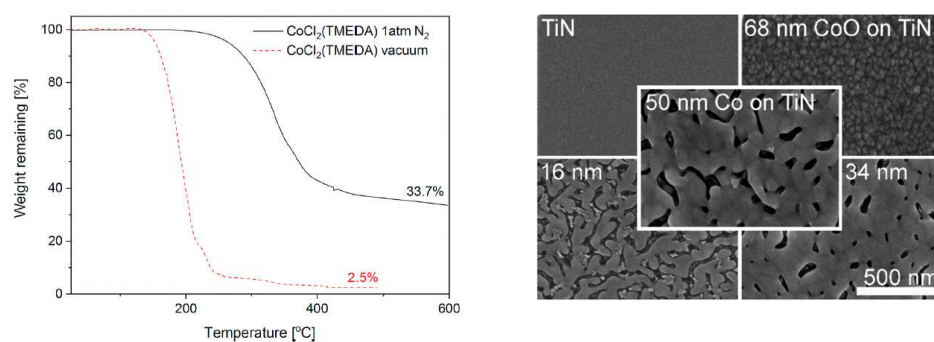


Figure 31: TMEDA-stabilized  $\text{CoCl}_2$ : (a) TGA curves under 1 atm  $\text{N}_2$  and vacuum, (b) SEM micrographs of Co films obtained from the reduction of ALD CoO grown with  $\text{H}_2\text{O}$ .<sup>304</sup> Reprinted with permission from K. Väyrynen et al., *Chem. Mater.* 30, 3499-3507 (2018). Copyright 2018 American Chemical Society.

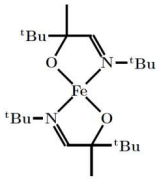
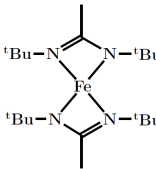
The vapor pressure of Co halides is very low due to their polymeric nature making them unsuitable as ALD precursors. However, Väyrynen et al.<sup>304</sup> demonstrated that  $\text{N,N,N',N'}$ -tetramethylethylenediamine (TMEDA) forms stable monomers with  $\text{CoCl}_2$ . As can be seen from the TGA curves in Figure 31, this compound starts to sublime below 200 °C in vacuum leaving only little amounts of residue. These researchers performed ALD experiments with  $\text{H}_2\text{O}$  and TMEDA- $\text{CoCl}_2$  using a sublimation temperature

This is the author's peer reviewed, accepted manuscript. However, the online version of record will be different from this version once it has been copyedited and typeset.

PLEASE CITE THIS ARTICLE AS DOI: 10.1063/1.5087759

of 170 °C. Crystalline CoO films with low Cl contents (~0.5-1 %), were obtained at substrate temperatures between 225 and 300 °C. The GPC values varied between 0.05 and 0.4 Å/cycle, which are quite low values for oxide ALD with chlorides. Furthermore, saturation with increasing H<sub>2</sub>O pulse duration could not be proven. An interesting observation was the presence of a hexagonal CoO phase which is not known for bulk CoO but for nano-structures<sup>314,315</sup> in addition to the typical cubic phase. The fraction of the hexagonal phase decreased with increasing film thickness. Furthermore, hexagonal CoO was only obtained on Si but not on TiN. Those different structures also had a pronounced effect on the Co films obtained after annealing at 250 °C in H<sub>2</sub> (10 % in Ar) as fairly continuous films could only be obtained on TiN (Figure 31).

Table 10: Fe metalorganics explored for the ALD of Fe.

Name	Structure	References
Fe( <sup>t</sup> BuMeCOCN <sup>t</sup> Bu) <sub>2</sub>		287
Fe-bis(N,N'-di- <sup>t</sup> Bu-acetamidinate)		284

Much fewer reports on the ALD of Fe exist than on the ALD of Ni and Co. Kalaturage et al.<sup>287</sup> used the Fe-iminoalkoxide Fe(<sup>t</sup>BuMeCOCN<sup>t</sup>Bu)<sub>2</sub> with BH<sub>3</sub>(NHMe<sub>3</sub>), and obtained metallic Fe on Ru with a GPC of 0.7 Å/cycle at 180 °C.



This is the author's peer reviewed, accepted manuscript. However, the online version of record will be different from this version once it has been copyedited and typeset.

PLEASE CITE THIS ARTICLE AS DOI: 10.1063/1.5087759

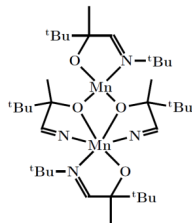
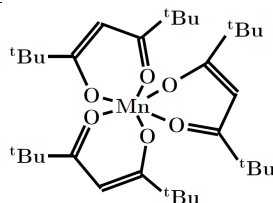
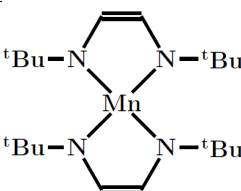
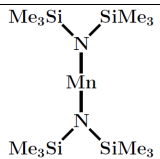
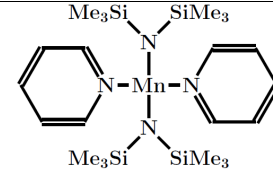
In their work on metal ALD with amidinates, Lim et al.<sup>284</sup> reported on the deposition of Fe films with a GPC of 0.08 Å/cycle but provided little details about the films obtained.

This is the author's peer reviewed, accepted manuscript. However, the online version of record will be different from this version once it has been copyedited and typeset.

PLEASE CITE THIS ARTICLE AS DOI: 10.1063/1.5087759

## 4.5 Other Metals

Table 11: Mn metalorganics explored for the ALD or CVD of Mn.

Name	Structure	References
$[\text{Mn}(\text{t}^{\text{Bu}}\text{MeCOCN}^{\text{t}^{\text{Bu}}})_2]_2$		287,316
$\text{Mn}(\text{tmhd})_3$		121
$\text{Mn-bis(1,4-di-tert-butyl-1,3-diazabutadienate)}$		288
$\text{Mn-bis(bis-trimethylsilyl-amide),}$ $\text{Mn(hmds)}_2$		317,318
$\text{Pyridine-bis(bis-trimethylsilyl-amide),}$ $\text{Pyridine-Mn(hmds)}_2$		319

This is the author's peer reviewed, accepted manuscript. However, the online version of record will be different from this version once it has been copyedited and typeset.

PLEASE CITE THIS ARTICLE AS DOI: 10.1063/1.5087759

<p>N,N,N',N'-tetramethylaminopropane-Mn-bis(bis-trimethylsilyl-amide)</p> <p>TMEDA-Mn(hmds)<sub>2</sub></p>		319
<p>Dmpe-Mn-(CH<sub>2</sub>SiMe<sub>3</sub>)<sub>2</sub></p>		320
<p>{(μ-dmpe)Mn(CH<sub>2</sub>CMe<sub>3</sub>)<sub>2</sub>}<sub>2</sub></p>		320

Kalutarage et al.<sup>287</sup> also synthesized Mn(II) complexes in their work on  $\alpha$ -imino alkoxides. Most of their complexes were dimeric in the solid state. The compound  $[\text{Mn}(\text{tBuMeCOCN}^{\text{tBu}})_2]_2$  was evaluated for ALD with  $\text{BH}_3(\text{NHMe}_3)$ , and oxide films were obtained. The researchers assumed that this was caused by subsequent oxidation after air exposure. The GPC of this process was 0.1 Å/cycle at 225 °C. In a subsequent work, Kalutarage et al.<sup>316</sup> combined this process with the Cu ALD described in<sup>139</sup> to deposit Cu/Mn alloys and Cu/Mn/Cu filmstacks. For the alloys, they combined 1400  $\text{Cu}(\text{dmap})_2/\text{BH}_3(\text{NHMe}_3)$  with 600  $[\text{Mn}(\text{tBuMeCOCN}^{\text{tBu}})_2]_2/\text{BH}_3(\text{NHMe}_3)$  cycles (using supercycles consisting of 7 and 3 subcycles, respectively) at a substrate temperature of 160 °C. Films were deposited on a large number of

This is the author's peer reviewed, accepted manuscript. However, the online version of record will be different from this version once it has been copyedited and typeset.

PLEASE CITE THIS ARTICLE AS DOI: 10.1063/1.5087759

substrates (Ru, Co, Pd, Pt, Cu, TiN, Si/SiO<sub>2</sub>, Si-H) and had compositions reasonably close to the ideal 70% Cu, 30% Mn. The deposits had a grainy structure and presence of metallic Mn was concluded from a shift of the Mn 2p XPS peaks after sputtering. Next, they attempted to deposit layered structures of Cu (1000 cycles), Mn (1000 cycles) and Cu (2000 cycles) on Ru, Pd and Pt coated substrates. For annealing experiments at 350 °C, the stacks were covered with evaporated SiO<sub>2</sub>, and the composition profile was measured by AES. In Figure 32 the results for the film on Pd are shown. Firstly, no three layer Cu/Mn/Cu structure is visible. Instead, the Mn has diffused to the interface with the SiO<sub>2</sub> capping layer already for the as-deposited film. The as-deposited Cu film is alloyed with Pd and the intermixing increases after annealing. This can also be seen from the SEM micrograph in Figure 32, where no distinct Pd and Cu films are visible and thin-grained precipitations cover the surface. The results on Pt were quite similar, while on Ru a dense coverage with Cu islands which were covered with Mn precipitates was observed. This study is a good example for the difficulty to predict structures obtained during the deposition of thin metal films as the mobility of the atoms within metals allows significant rearrangement. The ALD of Cu-Mn alloys was also investigated by Moon et al.<sup>121</sup> who combined subcycles of Cu(dmamb)<sub>2</sub>/H<sup>+</sup> and Mn(tmhd)<sub>2</sub>/H<sup>+</sup>. After annealing, they observed the precipitation of Mn to the surface and the interface with the SiO<sub>2</sub> substrate film, most likely forming a MnSi<sub>x</sub>O<sub>y</sub> layer.

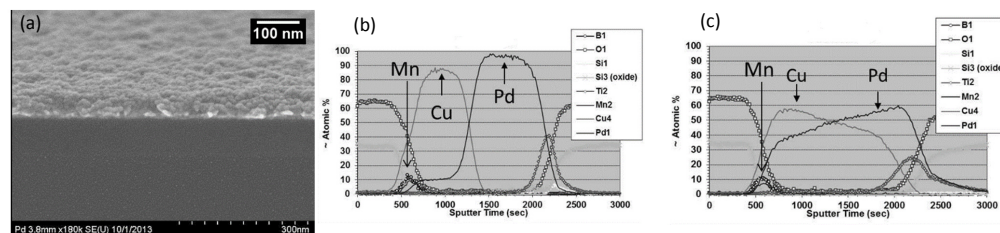


Figure 32: Cu:Mn:Cu stack on Pd: (a) SEM micrograph, (b) AES depth profile of the as-deposited film, and (c) AES depth profile after annealing at 350 °C.<sup>316</sup> K. Reprinted with permission from Kalutarage et al., *ECS Trans.* 64, 1447-157 (2014). Copyright 2014 The Electrochemical Society.

In their study using certain non-innocent diazadienyl complexes, Knisley et al.<sup>288</sup> also synthesized the Mn(II) complex Mn-bis(1,4-di-tert-butyl-1,3-diazabutadienate). This compound has a vapor pressure of 0.1 Torr at 65 °C, suggesting that it may be suitable for ALD. However, the compound is also very air sensitive, and pyrolysis in inert atmosphere resulted in  $\text{Mn}_3\text{O}_4$  powder.

$\text{Mn}(\text{hmds})_2$  is another candidate for an Mn precursor. It is quite stable as a monomer which is remarkable as transition metal complexes with such a low coordination number are very rare. It can be sublimed readily, and has been evaluated for Mn CVD<sup>317</sup> and for the ALD of  $\text{MnN}_x$ .<sup>318</sup> To increase the stability, derivatives with the dative ligands pyridine (Py) and tetramethylethylenediamine were evaluated by Knapp and Thompson.<sup>319</sup> These researcher obtained a further increased lifetime by coating the stainless-steel bubblers with inert layers such as oxides.

A limited study on the suitability of transition-metal alkyl complexes as precursors for ALD or CVD was performed by Price and coworkers.<sup>320</sup> The authors synthesized bis(trimethylsilylmethyl)- and dineopentyl-Mn(II) complexes without dative ligands and with the diphosphines 1,2-bis(dimethylphosphino)ethane (dmpe) and bis-(dimethylphosphino)methane (dmpm). Without a dative ligand  $\text{Mn}(\text{CH}_2\text{SiMe}_3)_2$  and  $\text{Mn}(\text{CH}_2\text{CMe}_3)_2$  crystallize as polymer and tetramer, respectively. Adding dmpe resulted in the monomer

dmpe-Mn(CH<sub>2</sub>SiMe<sub>3</sub>)<sub>2</sub> and the dimer {(μ-dmpe)Mn(CH<sub>2</sub>CMe<sub>3</sub>)<sub>2</sub>}<sub>2</sub>, respectively, which both were shown to be quite stable in thermal measurement and could be sublimed below 100 °C at 5 mTorr. With dmpm, dimeric Mn(II) complexes were also obtained but their volatility and thermal stability was poorer than that of the dmpe complexes. The authors investigated the reaction of the Mn(II) complexes with H<sub>2</sub> and Zn(Et)<sub>2</sub> in solution, and observed the formation of MnZn alloys with the latter. The reactivity with H<sub>2</sub> differed between the various complexes. However, the researchers highlighted that these results are not directly transferrable to ALD and CVD processes as the chemistry of adsorbed surface species will differ from that in solution.

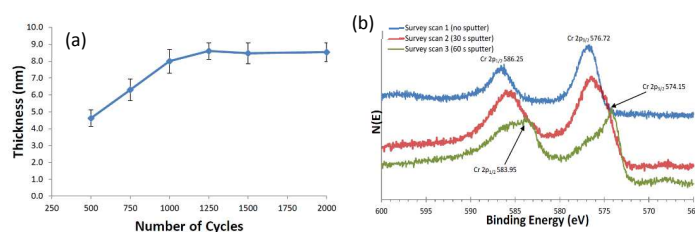


Figure 33: Cr ALD process with Cr(<sup>t</sup>BuMeCOCN<sup>t</sup>Bu)<sub>2</sub> and BH<sub>3</sub>(NHMe<sub>3</sub>)<sup>287</sup> (a) thickness vs number of cycles, (b) XPS analysis. Reprinted with permission from Kalutarage et al., *J. Am. Chem. Soc.* 135, 12588-12591 (2013). Copyright 2013 American Chemical Society.

Table 12: Cr metalorganics explored for the ALD of metallic Cr films.

Name	Structure	References
Cr( <sup>t</sup> BuMeCOCN <sup>t</sup> Bu) <sub>2</sub>		287

Among the  $\alpha$ -imino alkoxides developed by Kalutarage et al.<sup>287</sup> was also the Cr(II) complex  $\text{Cr}(\text{tBuMeCOCNtBu})_2$ . Similar to complexes with other metals the deposition with  $\text{BH}_3(\text{NHMe}_3)$  was limited to Ru substrates, initial nucleation cycles were necessary, and the GPC declined after 1000 cycles (Figure 33 (a)). The researchers observed a GPC of  $0.08 \text{ \AA/cycle}$  in an ALD window of  $170 - 185^\circ\text{C}$ . The evaporation temperature was  $140^\circ\text{C}$ . XPS depth profiling showed metallic Cr below an oxidized surface (Figure 33 (b)).

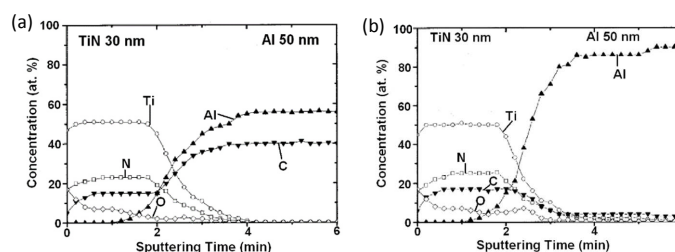


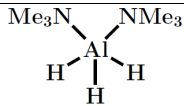
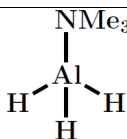
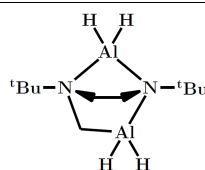
Figure 34: AES depth profiles of aluminum films grown by PEALD using TMA/ $\text{H}_2$  ratios of: (a) 1, (b) 0.1.<sup>321</sup> Reprinted with permission from Y. J. Lee and S.-W. Kang, *J. Vac. Sci. Technol. A* 20, 1983-1988 (2002). Copyright 2002 American Vacuum Society.

Table 13: A complexes explored for the ALD of metallic Al films.

Name	Structure	References
$\text{Al}(\text{CH}_3)_3$ , TMA		120,321
$[\text{AlCl}_3]_2$		322
$\text{H}_2\text{Al}(\text{tBuNCH}_2\text{CH}_2\text{NMe}_2)$		322

This is the author's peer reviewed, accepted manuscript. However, the online version of record will be different from this version once it has been copyedited and typeset.

PLEASE CITE THIS ARTICLE AS DOI: 10.1063/1.5087759

$\text{AlH}_3(\text{NMe}_3)_2$		323
$\text{AlH}_3(\text{NMe}_3)_2$		324
$\text{AlH}_2(\text{N}_2\text{C}_{11}\text{H}_{24})\text{AlH}_2$		325

Lee and Kang<sup>326</sup> reported the growth of Al with  $\text{Al}(\text{CH}_3)_3$ , which is also the reactant routinely used in  $\text{Al}_2\text{O}_3$  ALD, and  $\text{H}_2^*$  plasma at 250 °C. A saturated GPC of 1.5 Å/cycle was reported and the resistivity of the films was relatively high (10  $\mu\Omega$  cm). In a second work, Lee and Kang<sup>321</sup> pointed out that the surface reaction of TMA and H plasma causes significant contamination of the film including the formation of a highly resistive  $\text{Al}_4\text{C}_3$  phase. In order to minimize this effect, the researchers inserted a heated buffer between the reaction chamber and the precursor supply. TMA reacted in this buffer with molecular  $\text{H}_2$  to form  $\text{AlH}_3$  and volatile  $\text{CH}_4$ . The composition of the Al films strongly depended on the  $\text{H}_2$ /TMA ratio as can be seen in Figure 34. Films grown with a ratio of 1:1 contained excessive C. By increasing the  $\text{H}_2$  partial pressure, much cleaner films were grown. This can be understood from the reaction being incomplete without a large excess of  $\text{H}_2$ . Unreacted TMA remained available for surface reactions forming  $\text{Al}_4\text{C}_3$ .

Blackeney and Winter<sup>322</sup> reported a thermal ALD process using the amido-amine-stabilized Al dihydride  $\text{H}_2\text{Al}(\text{tBuNCH}_2\text{CH}_2\text{NMe}_2)$  as reducing agent for  $\text{AlCl}_3$ . Aluminum-hydrides are typically strong reducing agents for chemical synthesis with the non-volatile  $\text{LiAlH}_4$  being the most common. The volatile



This is the author's peer reviewed, accepted manuscript. However, the online version of record will be different from this version once it has been copyedited and typeset.

PLEASE CITE THIS ARTICLE AS DOI: 10.1063/1.5087759

compounds  $\text{AlH}_3(\text{NMe}_3)_2$ <sup>323</sup> and  $\text{AlH}_3(\text{NMe}_3)$ <sup>324</sup> were earlier used for the CVD of Al and Al-Ti alloy, respectively. However, their lack of stability makes them unsuitable for ALD. With the new compound, fairly well saturated growth of aluminum was observed between 100 and 160 °C. The GPC values varied between 3.5 and 4.0 Å/cycle, and therefore were clearly higher than one monolayer per cycle. The contamination of the films was quite low with C and Cl contents below the detection limit in XPS and N impurities of about 1 -2 %. Island growth was observed (Figure 35), and the islands coalesced to an electrically conductive film after about 200 cycles.

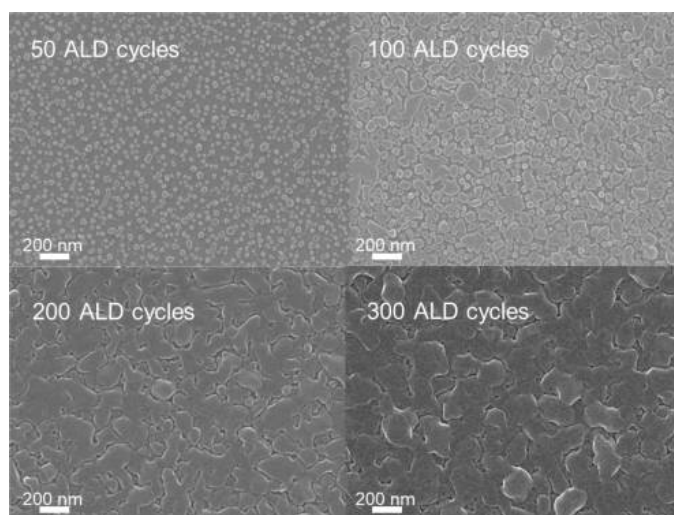
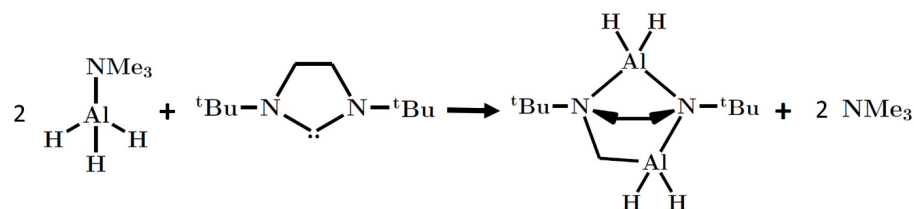


Figure 35: SEM micrographs of Al films grown with  $\text{AlCl}_3$  and  $\text{H}_2\text{Al}[(t\text{BuN})\text{CH}_2\text{CH}_2(\text{NMe}_2)]$  at 140 °C on TiN with different numbers of cycles.<sup>322</sup> Reprinted with permission from Blakeney et al., *Chem. Mater.* 30, 1844-1848 (2018). Copyright 2018 American Chemical Society.

In a recent publication, Blakeney et al.<sup>325</sup> attempted to use Al hydrides stabilized by NHCs for ALD. They synthesized Al-halides with unsaturated NHCs, which had a very low vapor pressure. Therefore, the researchers tried to synthesize Al-halides with saturated NHCs but observed a ring expansion reaction resulting in a dialane Cu-hydride complex (Scheme 8). This complex was volatile and tested for ALD with  $\text{AlCl}_3$ , and a GPC of 3.2-3-6 Å/cycle was observed in a window of 120 – 140 °C. In contrast to the

experiments with  $\text{H}_2\text{Al}[(^t\text{BuN})\text{CH}_2\text{CH}_2(\text{NMe}_2)]$ ,<sup>322</sup> the deposit consisted of isolated islands and the carbon contamination level was relatively high.



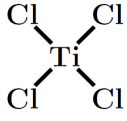
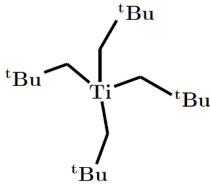
Scheme 8: Formation of Dialane-Al-hydride complex via expansion of NHC ring.<sup>325</sup>

Table 14: Ta and Ti complexes explored as precursors for the ALD of Ta and Ti films

	Structure	References
TaCl <sub>5</sub>		327-329
TaF <sub>5</sub>		330,331
Ta-tri(neopentyl)-dichloride		332,333

This is the author's peer reviewed, accepted manuscript. However, the online version of record will be different from this version once it has been copyedited and typeset.

PLEASE CITE THIS ARTICLE AS DOI: 10.1063/1.5087759

TiCl <sub>4</sub>		329,334-336
Ti-tetrakis(neopentyl)		337

Metals of high interest for the fabrication of CMOS devices are Ta and Ti as they are used for example for liner/barrier layers. Kim, Kim and Rossnagel, and Rossnagel et al.<sup>327-329</sup> reported saturated growth with about 0.8 Å/cycle for Ta from TaCl<sub>5</sub> and atomic hydrogen. However, the films were questionable in terms of quality as no formation of a dedicated cubic  $\alpha$ -Ta phase was observed in XRD measurements after annealing as is usually found for PVD Ta films. A probable reason for this is the incorporation of impurities such as Cl and H. The best measured resistivity of about  $1.8 \times 10^{-4} \Omega\text{cm}$  was very close to that measured for the tetragonal  $\beta$ -phase of Ta. A further interesting detail is an observed decrease of growth with increasing H<sub>2</sub> flux which goes hand in hand with an increase of Cl content in the Ta film. This was explained in terms of an increased recombination of H atoms under the higher process pressure, which leaves less H atoms for the reaction with TaCl<sub>5</sub>.

Lemons et al.<sup>330,331</sup> explored the possibility to obtain Ta via a fluorosilane elimination reaction which has been successfully applied for the ALD and CVD of W. However, in their ALD experiments with TaF<sub>5</sub> and Si<sub>2</sub>H<sub>6</sub>, they obtained amorphous TaSi alloys instead of pure Ta. The authors nevertheless showed with XPS measurements that the Ta(V) cation of the precursor was reduced to Ta(0). Kim et al.<sup>332</sup> and Hong et al.<sup>333</sup> investigated PEALD processes with Ta(V)-tri(neopentyl)-dichloride and hydrogen plasma.

Interestingly, they obtained crystalline TaC in the temperature range from 200 to 400 °C instead of Ta as demonstrated with XRD. The crystallinity, the resistivity and the contamination, especially with Cl, depended strongly on the process temperature and the plasma-pulse lengths with the best results for high temperatures and long exposures,

Ti films were grown by Kim and Rossnagel<sup>334</sup> and Rossnagel et al.<sup>329</sup> using TiCl<sub>4</sub> and H<sub>2</sub> plasma, and QCM measurements indicated saturation. Investigations on the reaction kinetics indicated that both TiCl<sub>4</sub> adsorption and reduction by H<sub>2</sub> plasma are first order reactions. Chlorine impurities were determined to be on the order of magnitude of a few atom-percent, while a more detailed evaluation of the films was complicated by their rapid oxidation.

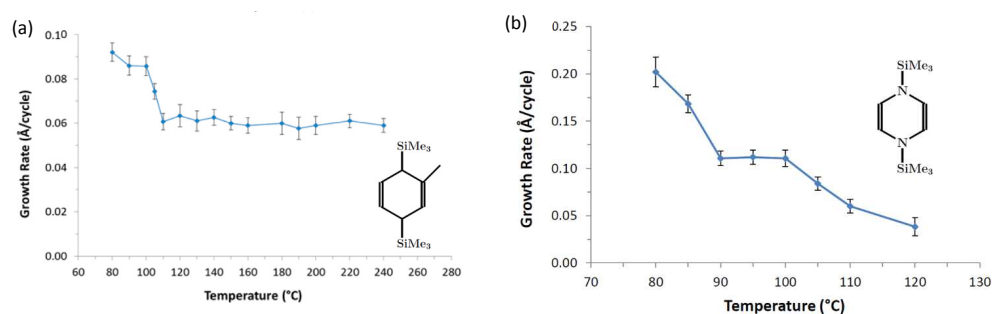
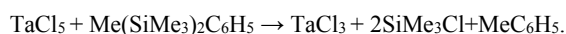


Figure 36: Temperature dependence of GPC of Ti-ALD process with (a) 2-methyl-1,4-bis(trimethylsilyl)-2,5-cyclohexadiene and (b) 1,4-bis(trimethylsilyl)-1,4-dihydropyrazine.<sup>335</sup> Adapted with permission from J. P. Klesko et al., *Chem. Mater.* 27, 4918-4921 (2015). Copyright 2015 American Chemical Society.

The first thermal ALD process for Ti was reported by Klesko et al.<sup>335</sup> who used the reductants 2-methyl-1,4-bis(trimethylsilyl)-2,5-cyclohexadiene (MBTCD) and 1,4-bis(trimethylsilyl)-1,4-dihydropyrazine with TiCl<sub>4</sub>. For the process with MBTCD, the authors observed a wide ALD window ranging from 100 to 240 °C with a relatively low GPC value of 0.06 Å/cycle (Figure 36). Again, the oxidation of the films

after air exposure complicated the analysis of the films, and metallic Ti could only be detected after a long sputtering time during XPS measurements for an 82 nm thick film. Furthermore, no crystalline phase could be detected in XRD measurements. The morphology of the films depended strongly on the deposition temperature. While very smooth films were obtained at low temperatures as confirmed by SEM and AFM micrographs, very rough films were obtained for temperatures above 200 °C. The authors did not discuss this formation of a grainy structure in detail. The selection of MBTCD as reducing agent was based on studies by Marteaga-Müller et al.<sup>338</sup> who used this compound in solution chemistry to reduce TaCl<sub>5</sub> to TaCl<sub>3</sub> and Tsurugi et al.<sup>339</sup> who reduced WCl<sub>6</sub> and WCl<sub>4</sub> to WCl<sub>2</sub> complexes. The purpose of those studies was the application of the low-valency complexes as catalysts. The solution reaction of TaCl<sub>5</sub> and MBTCD was:



42

Klesko et al.<sup>335</sup> also performed solution studies with TiCl<sub>4</sub> and MBTCD in toluene in which participates were readily formed. However, those were too reactive to confirm that they are metallic Ti.

Using the second reducing agent 1,4-bis(trimethylsilyl)-1,4-dihydropyrazine, Klesko et al.<sup>335</sup> obtained very similar results for the reaction with TiCl<sub>4</sub> in solution. However, they observed a much narrower ALD window (90 – 100 °C, Figure 36 (b)) than with MBTCD, and observed much higher levels of contamination (9-16 % C, 5-7% N, ~8 % Cl). It is furthermore worth mentioning that the usage of 1,4-bis(trimethylsilyl)-1,4-dihydropyrazine was inspired by the work of Saito et al.<sup>340</sup> who used this compound in solution chemistry to reduce TiCp<sub>2</sub>Cl<sub>2</sub> to Ti(III)Cp<sub>2</sub>Cl based coordination complexes.

Blackeney et al.<sup>336</sup> attempted to deposit Ti films using Al-hydrides inspired by their successful use as reducing agents for the ALD of Al<sup>322</sup> and for the CVD of Al-Ti alloys.<sup>324</sup> However, they obtained Ti carbonitrides instead of metallic Ti in their ALD experiments with TiCl<sub>4</sub> and AlH<sub>2</sub>(<sup>t</sup>BuNCH<sub>2</sub>CH<sub>2</sub>NMe<sub>2</sub>)

or  $\text{AlH}_2(^t\text{BuNCH}_2\text{CH}_2\text{NC}_4\text{H}_8)$ . Hong et al.<sup>337</sup> investigated PEALD processes with Ti-tetrakis(neopentyl) and hydrogen plasma, and obtained crystalline  $\text{TiC}_x$  instead of elemental Ti in a temperature range from 200 to 300 °C. Interestingly  $\text{TiC}_x$  films could also be grown with molecular  $\text{H}_2$ , but their resistivity was much higher (93 m $\Omega$  cm vs 0.60–0.93 m $\Omega$  cm).

Ramachandran et al.<sup>341</sup> deposited metallic In as part of an alloy with Pt ( $\text{In}_{1-x}\text{Pt}_x$ ). Firstly, they deposited a bi-layer of  $\text{In}_2\text{O}_3$  from  $\text{In}(\text{tmhd})_3$  and  $\text{O}_2^*$  plasma and Pt from  $(\text{MeCp})\text{PtMe}_3$  and  $\text{O}_3$ . Then, the obtained alloy particles by annealing in hydrogen. The authors were able to control the composition through the thickness-ratio of the  $\text{In}_2\text{O}_3$  films and the particle size through the combined thickness of the bi-layer. In temperature-programmed reduction studies, the reduction of  $\text{In}_2\text{O}_3$  and the formation of the Pt-In alloy started at temperatures between 300 and 330 °C resulting in different intermetallic phases:  $x = 0.67 - 0.85$   $\text{InPt}_3$ ,  $0.53 - 0.65$   $\text{In}_9\text{Pt}_{11}$ ,  $0.48 - 0.52$   $\text{In}_{48}\text{Pt}_{52}$ ,  $0.22 - 0.46$   $\text{In}_2\text{Pt}$ , and  $0.05 - 0.20$   $\text{In}_2\text{Pt}_3$ , In, respectively. In the same work, Ramachandran et al.<sup>341</sup> also fabricated  $\text{Ga}_{1-x}\text{Pt}_x$  using an analogous process. After temperature-programmed reduction the obtained  $\text{GaPt}_2$ ,  $\text{GaPt}$  and a composite of  $\text{Ga}_2\text{Pt}$  and  $\text{Ga}_3\text{Pt}_2$  were identified for films with  $x=0.66$ ,  $0.46$  and  $0.17$ , respectively. The crystallization of the  $\text{Ga}_{1-x}\text{Pt}_x$  films started at temperatures between 400 and 600 °C.

Recently, Hämäläinen et al.<sup>342</sup> reported the first ALD process for Re. Using  $\text{ReCl}_5$  and  $\text{NH}_3$ , metallic Re was obtained between 400 and 500 °C with a GPC of about 0.3 Å/cycle while the depositions at lower temperatures resulted in  $\text{ReN}_x$  with  $x$  increasing with decreasing deposition temperature. The impurity contents were moderate (low single-numbered percentages overall), and electrically continuous Re films were obtained with thicknesses as low as 3 nm. The resistivity decreased with increasing film thickness from 90  $\mu\Omega\text{cm}$  for 3 nm to about 22  $\mu\Omega\text{cm}$  for films of 500 nm or thicker.

One problem of the ALD of electropositive metals is their high reactivity towards oxidizing reagents such as  $\text{O}_2$ ,  $\text{H}_2\text{O}$  and  $\text{CO}_2$ , even at impurity levels typical for ALD processes. Niu and Cow<sup>343</sup> from the

This is the author's peer reviewed, accepted manuscript. However, the online version of record will be different from this version once it has been copyedited and typeset.

PLEASE CITE THIS ARTICLE AS DOI: 10.1063/1.5087759

equipment manufacturer SVT Associates Inc. demonstrated that with reactors operating under high vacuum and the usage of ultra-pure gases, even such an extremely electropositive metal as Mg can be deposited with Mg-bis(ethylcyclopentadienyl) and hydrogen plasma. Currently, SVT is providing ultra-high-vacuum reactors for the ALD of such reactive metals.

## 5. Potential Applications of Metal ALD

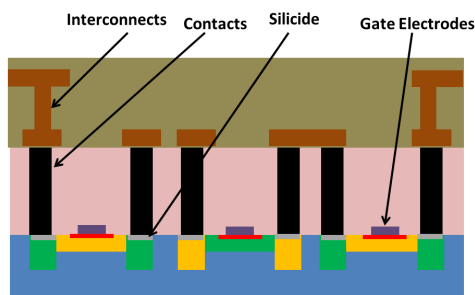


Figure 37: Potential fields of application of metal ALD for the CMOS fabrication.

The ALD of metal films has a number of potential applications in the fabrication of microelectronic devices which include transistors, DRAM capacitors and BEOL interconnects (Figure 37). The BEOL interconnects have arguably been the main driving force for the development of Cu ALD processes. These interconnect structures consist of several layers of metal wires which are hierarchically organized and connected which each other with Cu vias. Hierarchical means that the largest wires are in the highest level and connect across the whole chip (global interconnects) while the smallest wires are in the lowest layer (metal-1) and connect nearby transistors to which they are connected with W contacts. The half pitch of metal-1 wires has traditionally been used to characterize the CMOS technology nodes together with the physical gate length. It is here where ALD has been suggested to replace PVD for the deposition of conformal Cu seed layers as the metal-1 half pitch is now smaller than 30 nm and will be below 10 nm until the end of this decade (2020).<sup>344</sup> The issue of small dimensions is aggravated by the requirement for barrier and adhesion layers to avoid diffusion of Cu into the dielectric material and to provide a viable interface. Thus far, TaN and Ta have mainly been used for this purpose (Figure 38).



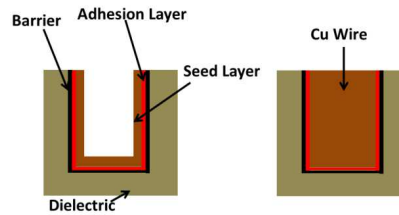


Figure 38: Schematic of Cu interconnect wire fabricated via damascene process.

The application of Cu ALD has to be regarded in comparison to alternative techniques. Thus far, it has been possible to extend the use of PVD by applying different modifications such as ionized PVD,<sup>345-348</sup> resputtering<sup>347,349-351</sup> and thermal reflow.<sup>269,350,352-355</sup> One potential alternative is the direct electro-plating of Cu on a barrier/adhesion layer such as Ru.<sup>41,356,217,357-360</sup> Taking into account these technical considerations, 2 nm may be seen as a reasonable target thickness for Cu seed layers deposited by ALD. This is relatively ambitious due to the island growth discussed in this review. Moreover, the Cu film formation strongly depends on the barrier/adhesion layers used. A particular issue is the incompatibility of Cu precursors with Ta adhesion layers.<sup>94,361</sup> More promising options are the deposition of Cu on Co and Ru layers. However, ALD of Cu seed layers is in competition with direct plating on Ru. The advantage of the latter is that no Cu seed layer is necessary. The main issue is the higher sheet resistance of Ru films as compared to Cu, which causes non-conformal growth across the wafer due to voltage drops resulting in differences in the current density. Therefore, Cu ALD needs to be seen in connection with the development of ultra-thin barrier/adhesion layers. As an alternative to the electrochemical fabrication, CVD of Cu has been investigated for the fabrication of interconnects via the so-called 'superconformal', (bottom-up) filling of structures.<sup>362-367</sup> Here, a surface catalyst, iodine from  $\text{CH}_3\text{H}_2\text{I}$ , was either added to the CVD process gases during the deposition or exposed to the structured substrate before it. The iodine accumulates at the bottom of the trenches, catalyzes the CVD reaction, and diffuses to the surface of the growing Cu film. The higher iodine density on the trench bottom as compared to the side walls leads to

the bottom up filling of the trenches. This process was demonstrated for the pyrolysis reaction with VTMS-Cu(hfac)<sup>362-366</sup> as well as for the [Cu<sup>8</sup>Bu<sub>2</sub>Meamd]<sub>2</sub> process.<sup>367</sup>

ALD has also widely been discussed for barrier/adhesion layers. While the ALD of the traditionally used nitride layers TiN<sup>23-33</sup> and TaN<sup>32,34-41</sup> is well established in industrial production, the deposition of pure metals used here such as Ta<sup>327,328</sup> and Ti<sup>334</sup> is rare due to the issues of ALD of electropositive metals. The ALD of Ru is better developed and extensively investigated for the BEOL process. Recently, Co has been introduced to the BEOL process, mainly as adhesion layer for Cu but also as the bulk conductor for the lowest interconnect levels by some manufacturers. However, it appears that the use of CVD processes has provided adequate results thus far although ALD is also investigated for this purpose. One application where metal ALD is already used in industrial production is the fabrication of W contacts between the transistors and the metallization layers.

In the transistor fabrication process, metals have replaced heavily doped silicon (polysilicon) as material for gate electrode<sup>368</sup> because polysilicon has a much higher resistivity than metals and is not compatible with high-k gate oxides due to Fermi-level pinning<sup>369</sup> and remote phonon scattering.<sup>370</sup> At the same time three-dimensional transistors are introduced to provide complete depletion and a steeper sub-threshold slope. Tri-gate fin-FETs have already been introduced to microprocessor production and nanowire gate-all-around transistors are a current research topic. For example, Colinge et al.<sup>371</sup> reported the fabrication of junctionless Si-nanowire transistors. ALD is a potential technique for the deposition of gate-all-around electrodes. The metals required for nMOS and pMOS transistors differ. From electrical considerations, metals with a low work function (e.g. Al, Ta, Ti) are needed for nMOS transistors while metals with a high work function (e.g. Pt, Ru) are needed for pMOS transistors, because the difference between the Fermi level in the semiconductor and the metal work function determines the threshold voltage. Alternatively, mid-band-gap metals such as TiN were reported as gates for both n- and pMOS. This

approach has the advantage of simpler processing but suffers from a high threshold voltage. Furthermore, the viability of the metal oxide interface, the thermal stability of the metal layer and its feasibility for further processing need to be considered. In recent years, the use of different metals for the gate electrodes to adjust the threshold voltage has become established among manufacturers. The alloy systems  $\text{TiAl}_x$  and  $\text{TiAl}_x\text{C}_y$  are attractive because they allow an adjustment of the work function required in order to optimize nMOS transistors. Moon et al.<sup>372</sup> presented an ALD process for  $\text{TiAl}_x\text{C}_y$  using  $\text{TiCl}_4$ ,  $\text{Al}(\text{CH}_3)_3$  and  $\text{H}_2^*$  plasma, and compared the threshold voltages for Si transistors with the gate dielectrics  $\text{SiO}_2$ ,  $\text{Al}_2\text{O}_3$  and  $\text{HfO}_2$ . These authors observed a significant variation of the work function and therefore of the threshold voltage with the dielectric material. From closer examination, they concluded that on  $\text{SiO}_2$  Al-rich boundary layers are formed, whose dipole concentration shifts the effective work function. For  $\text{HfO}_2$  in contrast, Fermi-level pinning appeared to be the dominant effect on the work function. This example illustrates the difficulty of predicting the properties of metal-gate transistors from the bulk properties of the metals involved.

Several research groups reported the ALD of  $\text{Ni}^{278,280,281,292,373}$  and  $\text{Co}^{280,299,373,374}$  for the formation of silicides at the transistor contacts. Although the as-deposited Ni films were relatively grainy the silicide layers formed after annealing were of good quality. Also, a possible application of metal ALD is the fabrication of capacitors for example for DRAMs or for energy storage.

An important area of application for metal ALD outside microelectronics is heterogeneous catalysis. Most solid catalysts consist of nanoparticles on a support. This support is in many cases porous to provide a huge surface area. The conformal coating of these pores is the main advantage that ALD has compared to the established and much cheaper wet chemical methods. The activity and selectivity of catalysts strongly depend on the particle loading and the particle size distribution.<sup>375,376</sup> A current research strategy is to tune ALD processes for obtaining deposit optimized morphologies. One example is the work by Dendooven et

This is the author's peer reviewed, accepted manuscript. However, the online version of record will be different from this version once it has been copyedited and typeset.

PLEASE CITE THIS ARTICLE AS DOI: 10.1063/1.5087759

al.<sup>249</sup> on Pt ALD discussed in section 3.2. The researchers compared the deposits from the O<sub>2</sub> and N<sub>2</sub><sup>\*</sup> processes and observed a higher electrocatalytic activity for hydrogen evolution from water for catalysts prepared with the second process.

Ramachandran et al.<sup>341</sup> investigated supported bimetallic InPt<sub>x</sub> particles deposited with ALD into mesoporous silica as catalysts for the dehydrogenation of propane. The bimetallic alloy is known to have a higher activity than pure Pt for this reaction, and the researchers demonstrated in initial studies similar activities for their ALD compound to commercial InPt<sub>x</sub> catalysts, highlighting the prospect for optimization due to the flexibility of their ALD process. One important issue for supported catalysts is their passivation by a carbon layers. Therefore, catalysts typically need to be regenerated by successive reduction and oxidation in H<sub>2</sub>-O<sub>2</sub> cycles. Filez et al.<sup>377</sup> investigated the stability of In<sub>9</sub>Pt<sub>13</sub> deposits prepared with this ALD process under repeated H<sub>2</sub>-O<sub>2</sub> cycles. They observed segregative oxidation of In during the O<sub>2</sub> pulse and reduction and alloy formation during the H<sub>2</sub> pulse. However, island coalescence was identified as the major issue identified.

## 6. Conclusions

A large number of metal ALD processes have already been developed, and numerous precursors evaluated, in particular for the ALD of Cu. Metalorganic precursors have been most widely investigated while halides are only very rarely employed presumably due to their very low vapor pressures. Cu(I) metalorganics are typically quite unstable which can be explained by a low bonding strength to most of the neutral ligands. Therefore, one strategy for the development of precursors has been the use of strong electron donors as ligands, and the employment of carbenes has indeed turned out to be a very promising approach for forming very stable Cu(I) complexes.<sup>89,91</sup> Among Cu(II) metalorganics, diketonates are the most studied since they are readily available. However, their limited reactivity and low vapor pressure make their application difficult. Alternative complexes include aminoalkoxides,<sup>109,114</sup> and ketoiminates.<sup>104,107-109</sup> Among these, the aminoalkoxide Cu(dmap)<sub>2</sub> has proven to be particularly promising. An important point is that molecules can decompose when they are adsorbed on surfaces at much lower temperatures than they do in the gas or in the bulk phase.

The success of using molecular H<sub>2</sub> or organic molecules as reducing agents has been shown to depend strongly on the substrate material used. The best results have been achieved on the platinoid metals. Hydrogen plasma is often regarded as a sub-optimal solution since recombination limits its use with difficult substrate topologies. However, several groups have demonstrated that sufficient conformality can be achieved on most structures relevant for microelectronic applications.<sup>109</sup> An interesting approach has been the application of ZnEt<sub>2</sub> as reducing agent as it was shown that low temperature ALD can be achieved with this.<sup>114</sup> However, contamination of the Cu films with Zn was observed to be a major issue.<sup>127</sup>

The morphology of the Cu deposits depends strongly on the substrate material, and can differ significantly for deposits on the same material, depending for example on the thickness, texture and surface oxidation

of the substrate films. Regarding the growth process, the grain size and therefore the minimum thickness of continuous films does not only depend on the initial nucleation, but also on the coalescence of islands.<sup>133</sup>

ALD processes for the other group 11 metals are reported much more rarely than for Cu. For Ag, Ag(I) metalorganics have been used exclusively. Although their limited stability remained a major problem, promising results were presented with the complex  $\text{PEt}_3\text{-Ag(fod)}$ .<sup>174,176</sup> Metallic Ag can be readily obtained applying  $\text{H}_2$  or  $\text{NH}_3$  plasma,<sup>174-176</sup> while the deposition with molecular  $\text{H}_2$  is difficult due to its inertness. However, thermal ALD of Ag was demonstrated with  $\text{PEt}_3\text{-Ag(fod)}$  and  $\text{BH}_3(\text{NHMe}_2)$ .<sup>175</sup> Similar as for Cu ALD, island growth has typically been observed.

While for the CVD of Au Au(I) and Au(III) complexes were employed, Au(III) complexes, which are typically more stable, were used in all successful Au-ALD investigations.<sup>195,196</sup> A particularly interesting observation has been the suitability of S,S'-coordinated complexes,<sup>195</sup> which has also been reported for Au CVD,<sup>192-194</sup> because this group of molecules has gained little attention for any other metal. The reactants used for Au ALD were oxygen plasma<sup>196</sup> and ozone.<sup>195</sup>

Arguably the group of metals for which ALD has been most successful is the platinumoids Pt, Ru, Ir, Os and Rh. Most studies have deposited these materials by combustion in  $\text{O}_2$ . These reactions are typically understood to be catalyzed by the growing films while the limited stability of the oxides favors the formation of the elemental metals. However, the selectivity between metal and oxide formation depends typically strongly on the growth conditions with high deposition temperatures and low  $\text{O}_2$  partial pressures favoring the metal in most cases. Within the metallic growth regime, the properties of the films, in particular their morphology and their contamination, depend strongly on the growth process. For example, Dendooven et al.<sup>249</sup> demonstrated that a higher island density and narrower size distribution can be achieved from Pt ALD with nitrogen plasma than with  $\text{O}_2$ . The most important class of precursors are derivatives of the metallocenes, but diketonates such as  $\text{Ir(acac)}_3$  have been used too. Further precursors

evaluated include  $\text{RuO}_4$ <sup>237,238</sup> and  $\text{Ru}(0)$ <sup>239</sup> complexes. Interestingly, reports about the ALD of Pd via combustion in  $\text{O}_2$  are very rare.<sup>251</sup> Instead Pd has been typically grown by direct reduction using typical reducing agents. Here, it is important to remember that the high catalytic activity of Pd supports the reaction with reactants such as  $\text{H}_2$ .

Since the CVD of W via the reaction of  $\text{WF}_6$  with  $\text{SiH}_4$  and  $\text{Si}_2\text{H}_6$  has been established in the microelectronic fabrication for a very long time, the attempt to develop an ALD process based on this chemistry appeared straightforward. However, GPC values higher than one monolayer per cycle and a strong dependency of the GPC on the process conditions caused doubt that this process is really ALD. Despite this very conformal coating was achieved on challenging topographies. The group of George<sup>264-266</sup> studied the reaction mechanisms of W ALD in detail and concluded that during the  $\text{Si}_2\text{H}_6$  pulse additional  $\text{SiH}_3^*$  groups are inserted into the formed  $\text{SiH}^*$  surface species. Mo was grown with an analogous process involving  $\text{MoF}_6$  and  $\text{Si}_2\text{H}_6$ .<sup>275</sup> Similar to the W ALD process, GPC values larger than one monolayer per cycle were observed. However, in contrast to the W process, the additional growth occurred during the  $\text{MoF}_6$  pulse through the reaction of  $\text{MoF}_6$  with  $\text{MoF}_5^*$  surface species.

The ALD of Ni and Co has been studied extensively. Similar to Cu, diketonates are readily available but suffer from a limited reactivity. Cyclopentadienyl complexes and their derivatives have been tested successfully, and they provide relatively high GPC values of above 1 Å/cycle. However, problems with obtaining metals using hydrogen plasma or radicals were reported but are not yet understood.<sup>282,142</sup> The amidinates developed by the Gordon group also include Ni and Co complexes.<sup>78,284</sup> Extensive studies delivered promising results, although problems with stability have also been reported especially for the Ni complexes.<sup>291</sup> Research on novel precursors has been very intense and classes of precursors investigated include aminoalkoxides,<sup>278,279</sup> ketoiminates,<sup>277</sup> imino-alkoxides,<sup>287</sup> carbohydrazides,<sup>289</sup> hydrazonates<sup>290</sup> and diazadienyls.<sup>288,303</sup> Most studies on Ni and Co ALD employed conventional reducing

agents such as  $H_2$ ,  $NH_3$ ,  $H_2^*$  plasma and  $NH_3$  plasma, but more exotic reactants such as  $BH_3(NHMe_2)$  have been used too.<sup>287</sup> Furthermore, it was shown that it is simpler to obtain continuous films from the reduction of a preformed oxide than from the direct ALD of the metals.<sup>283</sup>

Similar precursors as evaluated for Ni and Co have also been developed for Fe,<sup>287</sup> Mn<sup>287,288,316</sup> and Cr.<sup>287</sup> However, the number of articles on the ALD of these metals is currently has quite small.

The main challenge for the deposition of more electropositive metals is the difficulty to reduce the precursors. The deposition of Al,<sup>326</sup> Ta<sup>327-329</sup> and Ti using  $H_2^*$  plasma and precursors routinely employed for the ALD of the correspondent oxides and halides has been reported, but the films typically suffered from high contamination levels. An interesting approach for Al ALD was presented by Blackeney and Winter<sup>322</sup> who used Al-hydride-based complexes as reducing agents for  $AlCl_3$ . Attempts by Lemonds et al.<sup>330,331</sup> to develop a fluorosilane elimination reaction for Ta resulted in the deposition of AlSi alloys. For Ti, a thermal ALD process with  $TiCl_4$  and MBTCD was presented by Klesko and coworkers.<sup>335</sup> However, oxidation in atmosphere which occurred after the deposition complicated the analysis.

Arguably, the most important field of applications for metal ALD is microelectronics. For example, the research on Cu ALD has been driven by the need to develop a process for the deposition of ultra-thin seed layers for the fabrication of interconnects. Similarly, the ALD of W has been used for the deposition of seed layers for W CVD and has become an established technique in the CMOS fabrication process. Furthermore, the ALD of Ru, Co and Ta has been investigated as barrier and liner materials for interconnects. In transistors, metals are needed as contacts and as gate electrodes and the development of three-dimensional structures such as fin-FETs make the use of ALD processes attractive. The main metals investigated here include Ni, Co, Ti and Ru.



The preparation of catalysts is another important application for metal ALD, mainly explored for noble metals. Here, the possibility to coat structures with large surfaces such as porous materials is the main advantage. In contrast to electronic applications, deposits of isolated particles are needed here instead of continuous films, and the optimization of the ALD processes regarding particle-size distribution and support loading are focus points of current research.

### Acknowledgements

MEP wishes to acknowledge the support of Science Foundation Ireland via grants 07/SRC/I1172, 11/PI/1117 and 15/IA/3015.

### References

- [1] T. Suntola and J. Antson, "Method for producing compound thin films (pat no us4058430a)," 1977.
- [2] M. Ahonen, M. Pessa, and T. Suntola, "A study of znTe grown on glass substrates using an atomic layer evaporation method," *Thin Solid Films*, vol. 65, pp. 301 – 307, 1980.
- [3] J. Aarik, A. Aidla, A. Jack, M. Leskelä, and L. Niinistö, "In situ study of a strontium beta-diketonate precursor for thin film growth by atomic layer epitaxy," *J. Mater. Chem.*, vol. 4, pp. 1239 – 1244, 1994.
- [4] C. S. Chen, J. H. Lin, J. H. You, and C. R. Chen, "Properties of Cu(THD)<sub>2</sub> as a precursor to prepare Cu/SiO<sub>2</sub> catalyst using the atomic layer epitaxy technique," *J. Am. Chem. Soc.*, vol. 128, pp. 15950–15951, 2006.
- [5] E.-L. Lakomaa, "Atomic layer epitaxy (ALE) on porous substrates," *Appl. Surf. Sci.*, vol. 75, pp. 185–196, 1994.
- [6] P. Martensson and J.-O. Carlsson, "Atomic layer epitaxy of copper growth and selectivity in the Cu(II)-2,2,6,6-tetramethyl-3,5-heptanedionate/h<sub>2</sub> process," *J. Electrochem. Soc.*, vol. 145, pp. 2926–2931, 1998.

This is the author's peer reviewed, accepted manuscript. However, the online version of record will be different from this version once it has been copyedited and typeset.

PLEASE CITE THIS ARTICLE AS DOI: 10.1063/1.5087759

- [7] P. Martensson and J.-O. Carlsson, "Atomic layer epitaxy of copper on tantalum," *Chem. Vapor Depos.*, vol. 3, pp. 45–50, 1997.
- [8] M. Ritala, M. Leskelä, E. Rauhala, and J. Jokinenb, "Atomic layer epitaxy growth of tin thin films from  $\text{tin4}$  and  $\text{nh3}$ ," *J. Electrochem. Soc.*, vol. 145, pp. 2914–2920, 1998.
- [9] T. Törndahl, J. Lub, M. Ottossona, and J.-O. Carlssona, "Epitaxy of copper on  $\alpha\text{-al2o3}(0\ 0\ 1)$  by atomic layer deposition," *J. Cryst. Growth*, vol. 276, pp. 102–110, 2005.
- [10] S. M. George and Y. Lee, "Prospects for thermal atomic layer etching using sequential, self-limiting fluorination and ligand-exchange reactions," *ACS Nano*, vol. 10, pp. 4889 – 4894, 2016.
- [11] K. J. Kanarik, T. Lill, E. A. Hudson, S. Sriraman, S. Tan, J. Marks, V. Vahedi, and R. A. Gottscho, "Overview of atomic layer etching in the semiconductor industry," *J. Vac. Sci. Tech. A*, vol. 33, p. 020802, 2015.
- [12] T. Faraz, F. Roozeboom, H. C. M. Knoop, and W. M. M. Kessels, "Atomic layer etching: What can we learn from atomic layer deposition?," *ECS J. Solid State Sci. Tech.*, vol. 4, pp. N5023 – N5032, 2015.
- [13] S. M. George, "Atomic layer deposition: An overview," *Chem. Rev.*, vol. 110, pp. 111–131, 2010.
- [14] R. L. Puurunen, "Surface chemistry of atomic layer deposition: A case study for the trimethylaluminum/water process," *J. Appl. Phys.*, vol. 97, p. 121301, 2005.
- [15] S. Klejna and S. D. Elliott, "Understanding 'clean-up' of iii-v native oxides during atomic layer deposition using bulk first principles models," *J. Nanosci. Nanotechnol.*, vol. 11, pp. 8246 – 8250, 2011.
- [16] K. Kukli, M. Ritala, J. Lu, A. Harsta, and M. Leskelä, "Properties of  $\text{hfo2}$  thin films grown by ald from hafnium tetrakis(ethylmethanamide) and water," *J. Electrochem. Soc.*, vol. 151, pp. F189–F193, 2004.

- [17] R. L. Puurunen, "Analysis of hydroxyl group controlled atomic layer deposition of hafnium dioxide from hafnium tetrachloride and water," *J. Appl. Phys.*, vol. 95, p. 4777, 2004.
- [18] X. Luo, A. A. Demkov, D. Triyoso, P. Fejes, R. Gregory, and S. Zollner, "Combined experimental and theoretical study of thin hafnia films," *Phys. Rev. B*, vol. 78, p. 245314, 2008.
- [19] L. Zhong, W. L. Daniel, Z. Zhang, S. A. Campbell, and W. L. Gladfelter, "Atomic layer deposition, characterization, and dielectric properties of hfo2/sio2 nanolaminates and comparisons with their homogeneous mixtures," *Chem. Vap. Depos.*, vol. 12, pp. 143 – 150, 2006.
- [20] V. Pore, A. Rahtu, M. Leskelä, M. Ritala, D. Sajavaara, and J. Keinonen, "Atomic layer deposition of photocatalytic tio2 thin films from titanium tetramethoxide and water," *Chem. Vap. Depos.*, vol. 10, pp. 143 – 148, 2004.
- [21] J. Aarik, A. Aidla, H. Maendar, and T. Uustare, "Atomic layer deposition of titanium dioxide from ticl4 and h2o: investigation of growth mechanism," *Appl. Surf. Sci.*, vol. 172, pp. 148 – 158, 2001.
- [22] T. Tsubota, M. Ohtaki, K. Eguchi, and H. Arai, "Thermoelectric properties of al-doped zno as a promising oxide material for hightemperature thermoelectric conversion," *J. Mater. Chem.*, vol. 7, pp. 85 – 90, 1997.
- [23] J. Elam, M. Schuisky, J. Ferguson, and S. George, "Surface chemistry and film growth during tin atomic layer deposition using tdm4 and nh3," *Thin Solid Films*, vol. 436, pp. 145 – 156, 2003.
- [24] A. Satta, J. Schuhmacher, C. M. Whelan, W. Vandervorst, S. H. Brongersma, G. P. Beyer, K. Maex, A. Vantomme, M. M. Viitanen, H. H. Brongersma, and W. F. A. Besling, "Growth mechanism and continuity of atomic layer deposited tin films on thermal sio2," *J. Appl. Phys.*, vol. 92, p. 7641, 2002.
- [25] C. H. Ahn, S. G. Cho, H. J. Lee, K. H. Park, and S. H. Jeong, "Characteristics of tin thin films grown by ald using ticl4 and nh3," *Met. Mater. Int.*, vol. 7, pp. 621 – 625, 2001.

- [26] M. Juppo, P. Alen, M. Ritala, and M. Leskelä, "Trimethylaluminum as a reducing agent in the atomic layer deposition of ti(al)n thin films," *Chem. Vap. Depos.*, vol. 7, pp. 211 – 217, 2001.
- [27] J. Musschoot, Q. Xie, D. Deduytsche, S. V. den Berghe, R. V. Meirhaeghe, and C. Detavernier, "Atomic layer deposition of titanium nitride from tdm precursor," *Microelectron. Eng.*, vol. 86, pp. 72 – 77, 2009.
- [28] K.-E. Elers, V. Saanila, P. J. Soininen, W.-M. Li, J. T. Kostamo, S. Haukka, J. Juhanoja, and W. F. Besling, "Diffusion barrier deposition on a copper surface by atomic layer deposition," *Chem. Vap. Depos.*, vol. 8, pp. 149 – 153, 2002.
- [29] W. Besling, A. Satta, J. Schuhmacher, T. Abell, V. Sutcliffe, A.-M. Hoyas, G. Beyer, D. Gravesteijn, and K. Maex, "Atomic layer deposition of barriers for interconnect," in *Interconnect Technology Conference, 2002. Proceedings of the IEEE 2002 International*, vol. 288 - 291, 2002.
- [30] J. Yoon, S. Kim, and K. No, "Highly ordered and well aligned tin nanotube arrays fabricated via template-assisted atomic layer deposition," *Mat. Lett.*, vol. 87, pp. 124–126, 2013.
- [31] C. Detavernier, J. Dendooven, D. Deduytsche, and J. Musschoot, "Thermal versus plasma-enhanced ald: growth kinetics and conformality," *ECST*, vol. 16, pp. 239–246, 2008.
- [32] S. Rossnagel and H. Kim, "From pvd to cvd to ald for interconnects and related applications," in *Interconnect Technology Conference, 2001. Proceedings of the IEEE 2001 International*, pp. 3 – 5, 2001.
- [33] M. Saadaoui, H. van Zeijl, W. H. A. Wien, H. T. M. Pham, C. Kwakernaak, H. C. M. Knoop, W. M. M. E. Kessels, R. M. C. M. van de Sanden, F. C. Voogt, F. Roozeboom, and P. M. Sarro, "Enhancing the wettability of high aspect-ratio through-silicon vias lined with lpcvd silicon nitride or pe-ald titanium nitride for void-free bottom-up copper electroplating," *IEEE Trans. Compon. Packag. Manuf. Technol.*, vol. 1, pp. 1728 – 1738, 2011.

- [34] M. Ritala, P. Kalsi, D. Riihela, K. Kukli, M. Leskelä, , and J. Jokinen, "Controlled growth of tan, ta<sub>3</sub>n<sub>5</sub>, and taoxny thin films by atomic layer deposition," *Chem. Mater.*, vol. 11, pp. 1712–1718, 1999.
- [35] S. H. Kim, M. K. Song, and S. W. Rhee, "Atomic vapor deposited tantalum carbo-nitride film using tbtdet and hydrogen," *ECST*, vol. 16, pp. 355–362, 2008.
- [36] K. H. Kim, S. J. Jeong, J. S. Yoon, Y. M. Kim, and S. H. Kwon, "Plasma-enhanced atomic layer deposition of ta(c)n thin films for copper diffusion barrier," *ECST*, vol. 25, pp. 301–308, 2009.
- [37] S.-H. Kim, H. T. Kim, S.-S. Yim, D.-J. L. K.-S. Kim, H.-M. Kim, K.-B. Kim, and H. Sohn, "A bilayer diffusion barrier of ald-ru/ald-tacn for direct plating of cu," *J. Electrochem. Soc.*, vol. 155, pp. H589–H594, 2008.
- [38] W. Besling, V. Arnal, J. Guillaumond, C. Guedj, M. Broekaart, L. Chapelon, A. Farcy, L. Arnaud, and J. Tones, "Integration of ald tan barriers in porous low-k interconnect for the 45 nm node and beyond; solution to relax electron scattering effect," in *Electron Devices Meeting, 2004. IEDM Technical Digest. IEEE International*, pp. 325 – 328, 2004.
- [39] O. van der Straten, Y. Zhu, E. Eisenbraun, and A. Kaloyeros, "Thermal and electrical barrier performance testing of ultrathin atomic layer deposition tantalum-based materials for nanoscale copper metallization," in *Interconnect Technology Conference, 2002. Proceedings of the IEEE 2002 International*, pp. 188 – 190, 2002.
- [40] S.-W. Kim, S.-H. Kwon, S.-J. Jeong, and S.-W. Kang, "Improvement of copper diffusion barrier properties of tantalum nitride films by incorporating ruthenium using peald," *J. Electrochem. Soc.*, vol. 155, pp. H885–H888, 2008.
- [41] S. Kumar, D. Greenslit, T. Chakraborty, and E. T. Eisenbraun, "Atomic layer deposition growth of a novel mixed-phase barrier for seedless copper electroplating applications," *J. Vac. Sci. Technol. A*, vol. 27, pp. 572–576, 2009.

- [42] P. Alen, M. Ritala, K. Arstila, J. Keinonen, and M. Leskelä, "The growth and diffusion barrier properties of atomic layer deposited nbx thin films," *Thin Solid Films*, vol. 491, pp. 235 – 241, 2005.
- [43] M. Ziegler, L. Fritzsche, J. Day, S. Linzen, S. Anders, J. Toussaint, and H.-G. Meyer, "Superconducting niobium nitride thin films deposited by metal organic plasma-enhanced atomic layer deposition," *Supercond. Sci. Technol.*, vol. 26, p. 025008, 2013.
- [44] J. W. Klaus, S. J. Ferro, and S. M. George, "Atomic layer deposition of tungsten nitride films using sequential surface reactions," *J. Electrochem. Soc.*, vol. 147, pp. 1175 – 1181, 2000.
- [45] J. Klaus, S. Ferro, and S. George, "Atomically controlled growth of tungsten and tungsten nitride using sequential surface reactions," *Appl. Surf. Sci.*, vol. 162-163, pp. 479 – 491, 2000.
- [46] S.-H. Kim, J.-K. Kim, N. Kwak, H. Sohn, J. Kim, S.-H. Jung, M.-R. Hong, S. H. Lee, and J. Collins, "Atomic layer deposition of low-resistivity and high-density tungsten nitride thin films using b<sub>2</sub>h<sub>6</sub>, wf<sub>6</sub>, and nh<sub>3</sub>," *Electrochem. Solid State L.*, vol. 9, pp. C54 – C57, 2006.
- [47] S.-H. Kim, J.-K. Kim, J. H. Lee, N. Kwak, J. Kim, S.-H. Jung, M.-R. Hong, S. H. Lee, J. Collins, and H. Sohn, "Characteristics of ald tungsten nitride using b<sub>2</sub>h<sub>6</sub>, wf<sub>6</sub>, and nh<sub>3</sub> and application to contact barrier layer for dram," *J. Electrochem. Soc.*, vol. 154, pp. D435 – D441, 2007.
- [48] A. Rugge, J. S. Becker, R. G. Gordon, and S. H. Tolbert, "Tungsten nitride inverse opals by atomic layer deposition," *Nano Lett.*, vol. 3, pp. 1293 – 1297, 2003.
- [49] K. Park, W.-D. Yun, B.-J. Choi, H.-D. Kim, W.-J. Lee, S.-K. Rha, and C. O. Park, "Growth studies and characterization of silicon nitride thin films deposited by alternating exposures to si<sub>2</sub>cl<sub>6</sub> and nh<sub>3</sub>," *Thin Solid Films*, vol. 517, pp. 3975 – 3978, 2009.
- [50] J. Klaus, A. Ott, A. Dillon, and S. George, "Atomic layer controlled growth of si<sub>3</sub>n<sub>4</sub> films using sequential surface reactions," *Surf. Sci. Lett.*, vol. 418, pp. L14 – L19, 1998.

- [51] B. Marlid, M. Ottosson, U. Pettersson, K. Larsson, and J.-O. Carlsson, "Atomic layer deposition of bn thin films," *Thin Solid Films*, vol. 402, pp. 167 – 171, 2002.
- [52] J. Ferguson, A. Weimer, and S. George, "Atomic layer deposition of boron nitride using sequential exposures of bcl<sub>3</sub> and nh<sub>3</sub>," *Thin Solid Films*, vol. 413, pp. 16 – 25, 2002.
- [53] J. Hämäläinen, M. Ritala, and M. Leskelä, "Atomic layer deposition of noble metals and their oxides," *Chem. Mater.*, vol. 26, pp. 786 – 801, 2014.
- [54] P. G. Gordon, A. Kurek, and S. T. Barry, "Trends in copper precursor development for cvd and ald applications," *ECS J. Solid State Sci. Tech.*, vol. 4, pp. N3188 – N3197, 2015.
- [55] T. J. Knisley, L. C. Kalutarage, and C. H. Winter, "Precursors and chemistry for the atomic layer deposition of metallic first row transition metal films," *Coordin. Cem. Rev.*, vol. 257, pp. 3222 – 3231, 2014.
- [56] M. Juppo, M. Ritala, and M. Leskelä, "Deposition of copper films by an alternate supply of cucl and zn," *J. Vac. Sci. Technol. A*, vol. 15, pp. 2330–2333, 1997.
- [57] T. Törndahl, M. Ottosson, and J.-O. Carlsson, "Growth of copper metal by atomic layer deposition using copper(i) chloride, water and hydrogen as precursors," *Thin Solid Films*, vol. 458, pp. 129–136, 2004.
- [58] J. A. T. Norman, B. A. Muratore, P. N. Dyer, D. A. Roberts, and A. K. Hochberg, "New omcvd precursors for selective copper metallization," in *VLSI Multilevel Interconnection Conference, 1991, Proceedings., Eighth International IEEE*, pp. 123 – 129, 1991.
- [59] J. A. Norman, D. A. Roberts, A. K. Hochberg, P. Smith, G. A. Petersen, J. E. Parmeter, C. A. Apblett, and T. R. Omstead, "Chemical additives for improved copper chemical vapour deposition processing," *Thin Solid Films*, vol. 262, pp. 46 – 51, 1995.

- [60] S. L. Cohen, M. Liehr, and S. Kasi, "Selectivity in copper chemical vapor deposition," *Appl. Phys. Lett.*, vol. 60, pp. 1585–1587, 1992.
- [61] K.-K. Choi and S.-W. Rhee, "Effect of carrier gas on chemical vapor deposition of copper with (hexafluoroacetylacetonate)cu(i)(3,3-dimethyl-1-butene)," *J. Electrochem. Soc.*, vol. 148, pp. C473 – C478, 2001.
- [62] J. A. T. Norman, "Us patent no. 5,187,300," 1993.
- [63] K.-H. Park and W. J. Marshall, "Remarkably volatile copper(ii) complexes of n,n'-unsymmetrically substituted 1,3-diketiminates as precursors for cu metal deposition via cvd or ald," *J. Am. Chem. Soc.*, vol. 127, pp. 9330–9331, 2005.
- [64] K.-H. Park and W. J. Marshall, "Routes to n,n'-unsymmetrically substituted 1,3-diketiminates," *J. Org. Chem.*, vol. 70, pp. 2075–2081, 2005.
- [65] K.-H. Park, A. Z. Bradley, J. S. Thompson, and W. J. Marshall, "Nonfluorinated volatile copper(i) 1,3-diketiminates as precursors for cu metal deposition via atomic layer deposition," *Inorg. Chem.*, vol. 45, pp. 8480–8482, 2006.
- [66] K.-H. Park, "Us patent no. 7488435b2."
- [67] J. S. Thompson, L. Zhang, J. P. Wyre, D. J. Brill, and K. G. Lloyd, "Vapor phase deposition of copper films with a cu(i) beta-diketimate precursor," *Thin Solid Films*, vol. 517, pp. 2845–2850, 2009.
- [68] J. S. Thompson, L. Zhang, J. P. Wyre, D. Brill, and Z. Li, "Deposition of copper films with surface-activating agents," *Organometallics*, vol. 31, pp. 7884 – 7894, 2012.
- [69] J. S. Thompson, A. Z. Bradley, K.-H. Park, K. D. Dobbs, and W. Marshall, "Copper(i) complexes with bis(trimethylsilyl)acetylene: Role of ancillary ligands in determining pi back-bonding interactions," *Organometallics*, vol. 25, pp. 2712–2714, 2006.



- [70] T. Waechtler, S.-F. Ding, L. Hofmann, R. Mothes, Q. Xie, S. Oswald, C. Detavernier, S. E. Schulz, X.-P. Qu, H. Lang, and T. Gessner, "Ald-grown seed layers for electrochemical copper deposition integrated with different diffusion barrier systems," *Microelectron. Eng.*, vol. 88, pp. 684 – 689, 2011.
- [71] T. Waechtler, S. Oswald, N. Roth, A. Jakob, H. Lang, R. Ecke, S. E. Schulz, T. Gessner, A. Moskvina, S. Schulze, and M. Hietschold, "Copper oxide films grown by atomic layer deposition from bis(tri-n-butylphosphane)copper(i)acetylacetonate on ta, tan, ru, and sio<sub>2</sub>," *J. Electrochem. Soc.*, vol. 156, pp. H453–H459, 2009.
- [72] F. Senocq, A. Turgambaeva, N. Prud'homme, U. Patil, V. Krisyuk, D. Samelot, A. Gleizes, and C. Vahlas, "Thermal behaviour of cpcupet3 in gas phase and cu thin films processing," *Surf. Coat. Tech.*, vol. 201, pp. 9131 – 9134, 2007.
- [73] A. M. Willcocks, T. Pugh, S. D. Cosham, J. Hamilton, S. L. Sung, T. Heil, P. R. Chalker, P. A. Williams, G. Kociok-Koehn, and A. L. Johnson, "Tailoring precursors for deposition: Synthesis, structure, and thermal studies of cyclopentadienylcopper(i) isocyanide complexes," *Inorg. Chem.*, vol. 54, pp. 4869 – 4881, 2015.
- [74] J. A. Norman, M. Perez, X. Lei, and H. Cheng, "New precursors for the atomic layer deposition of copper," *ECS Trans.*, vol. 3, pp. 161 – 170, 2007.
- [75] J. A. Norman, M. Perez, S. E. Schulz, and T. Waechtler, "New precursors for cvd copper metallization," *Microelectron. Eng.*, vol. 85, pp. 2159–2163, 2008.
- [76] Q. Ma and F. Zaera, "Thermal chemistry of the cu-KI5 atomic layer deposition precursor on a copper surface," *J. Vac. Sci. Tech. A*, vol. 33, p. 01A108, 2015.
- [77] B. S. Lim, A. Rahtu, J.-S. Park, and R. G. Gordon, "Synthesis and characterization of volatile, thermally stable, reactive transition metal amidinates," *Inorg. Chem.*, vol. 42, pp. 7951–7958, 2003.

This is the author's peer reviewed, accepted manuscript. However, the online version of record will be different from this version once it has been copyedited and typeset.

PLEASE CITE THIS ARTICLE AS DOI: 10.1063/1.5087759

- [78] Z. Li, S. T. Barry, and R. G. Gordon, "Synthesis and characterization of copper(i) amidinates as precursors for atomic layer deposition (ald) of copper metal," *Inorg. Chem.*, vol. 44, pp. 1728–1735, 2005.
- [79] Z. Li, A. Rahtu, and R. G. Gordon, "Atomic layer deposition of ultrathin copper metal films from a liquid copper(i) amidinate precursor," *J. Electrochem. Soc.*, vol. 153, pp. C787–C794, 2006.
- [80] Z. Li, R. G. Gordon, D. B. Farmer, Y. Lin, and J. Vlassak, "Nucleation and adhesion of ald copper on cobalt adhesion layers and tungsten nitride diffusion barriers," *Electrochem. Solid-State Lett.*, vol. 8, pp. G182–G185, 2005.
- [81] Z. Li and R. G. Gordon, "Thin, continuous, and conformal copper films by reduction of atomic layer deposited copper nitride," *Chem. Vapor Depos.*, vol. 12, pp. 435–441, 2006.
- [82] Q. Ma, F. Zaera, and R. G. Gordon, "Thermal chemistry of copper(i)-n,n0.167em'-di-sec-butylacetamidinate on cu(110) single-crystal surfaces," *J. Vac. Sci. Tech. A*, vol. 30, p. 01A114, 2012.
- [83] O. Seitz, M. Dai, F. S. Aguirre-Tostado, R. M. Wallace, , and Y. J. Chabal, "Copper-metal deposition on self assembled monolayer for making top contacts in molecular electronic devices," *J. Am. Chem. Soc.*, vol. 131, pp. 18159–18167, 2009.
- [84] J. P. Coyle, W. H. Monillas, G. P. A. Yap, and S. T. Barry, "Synthesis and thermal chemistry of copper (i) guanidines," *Inorg. Chem.*, vol. 47, pp. 683 – 689, 2008.
- [85] J. P. Coyle, P. A. Johnson, G. A. DiLabio, S. T. Barry, and J. Mueller, "Gas-phase thermolysis of a guanidine precursor of copper studied by matrix isolation, time-of-flight mass spectrometry, and computational chemistry," *Inorg. Chem.*, vol. 49, pp. 2844 – 2850, 2010.
- [86] Z. Guo, H. Li, Q. Chen, L. Sang, L. Yang, Z. Liu, and X. Wang, "Low-temperature atomic layer deposition of high purity, smooth, low resistivity copper films by using amidinate precursor and hydrogen plasma," *Chem. Mat.*, vol. 27, pp. 5988–5996, 2015.

This is the author's peer reviewed, accepted manuscript. However, the online version of record will be different from this version once it has been copyedited and typeset.

PLEASE CITE THIS ARTICLE AS DOI: 10.1063/1.5087759

- [87] J. P. Coyle, A. Kurek, P. J. Pallister, E. R. Sirianni, G. P. A. Yap, and S. T. Barry, "Preventing thermolysis: precursor design for volatile copper compounds," *Chem. Commun.*, vol. 48, pp. 10440 – 10442, 2012.
- [88] J. P. Coyle, J. J. M. Hastie, J. Mueller, and S. T. Barry, "Novel monomeric copper precursors: Evaluation for low temperature thermal ald," in *ALD Conference Dresden*, 2012.
- [89] J. P. Coyle, G. Dey, E. R. Sirianni, M. L. Kemell, G. P. A. Yap, M. Ritala, M. Leskelä, S. D. Elliott, and S. T. Barry, "Deposition of copper by plasma-enhanced atomic layer deposition using a novel n-heterocyclic carbene precursor," *Chem. Mater.*, vol. 25, pp. 1232 – 1238, 2013.
- [90] J. P. Coyle, E. R. Sirianni, I. Korobkov, G. P. A. Yap, G. Dey, and S. T. Barry, "Study of monomeric copper complexes supported by n-heterocyclic and acyclic diamino carbenes," *Organometallics*, vol. 36, pp. 2800 – 2810, 2017.
- [91] D. J. Hagen, I. M. Povey, S. Rushworth, J. S. Wrench, L. Keeney, M. Schmidt, N. Petkov, S. T. Barry, J. P. Coyle, and M. E. Pemble, "Atomic layer deposition of cu with a carbene-stabilized cu(i)silylamide," *J. Chem. Mater. C*, vol. 2, pp. 9205 – 9214, 2014.
- [92] A. M. James, R. K. Laxman, F. R. Fronczek, and A. W. Maverick, "Phosphorescence and structure of a tetrameric copper(i)-amide cluster," *Inorg. Chem.*, vol. 37, pp. 3785–3791, 1998.
- [93] J. A. T. Norman, "Us patent no. 70,205,422 b2," 2007.
- [94] S. Voss, S. Gandikota, L.-Y. Chen, R. Tao, D. Cong, A. Duboust, N. Yoshida, and S. Ramaswami, "Chemical studies of cvd cu deposited on ta and tan barriers under various process conditions," *Microelectron. Eng.*, vol. 50, pp. 501–508, 2000.
- [95] C. J. Jones, *d and f block chemistry*. Wiley Interscience, 2002.

- [96] L. Wu and E. Eisenbraun, "Effects of hydrogen plasma treatments on the atomic layer deposition of copper," *Electrochem. Solid-State Lett.*, vol. 11, pp. H107–H110, 2008.
- [97] C. Jezewski, W. A. Lanford, C. J. Wiegand, J. P. Singh, P.-I. Wang, J. J. Senkevich, and T.-M. Lua, "Inductively coupled hydrogen plasma-assisted copper atomic layer deposition on metallic and dielectric surfaces," *J. Electrochem. Soc.*, vol. 152, pp. C60–C64, 2005.
- [98] I. J. Hsu, B. E. McCandless, C. Weiland, and B. G. Willis, "Characterization of atomic layer deposited copper thin films on palladium seed layers," *J. Vac. Sci. Technol. A*, vol. 27, pp. 660–667, 2009.
- [99] X. Jiang, H. Wang, J. Qi, and B. G. Willis, "In-situ spectroscopic ellipsometry study of copper selective-area atomic layer deposition on palladium," *J. Vac. Sci. Technol. A*, vol. 32, p. 041513, 2014.
- [100] P. Doppelt, "Why is coordination chemistry stretching the limits of micro-electronics technology?," *Coordination Chemistry Reviews*, vol. 178 - 180, pp. 1785 – 1809, 1998.
- [101] S.-W. Kang, J.-Y. Yun, and Y. H. Chang, "Growth of copper metal films at room temperature using catalyzed reactions," *Chem. Mater.*, vol. 22, pp. 1607–1609, 2010.
- [102] Z. Zhong, X. Wang, J. Ding, and N. Yuan, "Nanometer-thick copper films grown by thermal atomic layer deposition," *Thin Solid Films*, vol. 589, pp. 673–680, 2015.
- [103] R. P. Chaukulkar, N. F. W. Thissen, V. R. Rai, and S. Agarwal, "Low temperature hydrogen plasma-assisted atomic layer deposition of copper studied using in situ infrared reflection absorption spectroscopy," *J. Vac. Sci. Technol. A*, vol. 32, p. 01A108, 2014.
- [104] B. Han, K.-M. Park, K. Park, J.-W. Park, and W.-J. Lee, "Atomic layer deposition of copper thin film using copper(II) diacetylacetonate and  $H_2$ ," in *Interconnect Technology Conference, 2009. IITC 2009. IEEE International*, pp. 173 – 174, 2009.

- [105] K.-M. Park, J.-K. Kim, B. Han, W.-J. Lee, J. Kim, and H.-K. Shin, "Influence of the deposition temperature on the properties of copper thin films prepared by alternating injection of  $\text{Cu}(\text{ethylketoinate})_2$  and  $\text{H}_2$  on a ruthenium substrate," *Microelectron. Eng.*, vol. 89, pp. 27 – 30, 2012.
- [106] J. Mao, E. Eisenbraun, V. Omarjee, A. Korolev, and C. Dussarrat, "Scaling of copper seed layer thickness using plasma-enhanced ald and an optimized precursor," in *Advanced Semiconductor Manufacturing Conference (ASMC), 2011 22nd Annual IEEE/SEMI*, pp. 1 – 4, 2011.
- [107] J. Mao, E. Eisenbraun, V. Omarjee, A. Korolev, C. Lansalot, and C. Dussarrat, "Ultra-low temperature deposition of copper seed layers by peald," *ECST*, vol. 33, pp. 125 – 135, 2010.
- [108] J. Mao, E. Eisenbraun, V. Omarjee, A. Korolev, and C. Dussarrat, "Room temperature copper seed layer deposition by plasma-enhanced atomic layer deposition," *ECST*, vol. 35, pp. 125 – 132, 2011.
- [109] D. J. Hagen, J. Connolly, R. Nagle, I. M. Povey, S. Rushworth, P. Carolan, P. Ma, and M. E. Pemble, "Plasma enhanced atomic layer deposition of copper: A comparison of precursors," *Surf. Coat. Tech.*, vol. 230, pp. 3–12, 2013.
- [110] T. Gerfin, M. Becht, and K.-H. Dahmen, "Preparation of copper and copper oxide films by metal-organic chemical vapour deposition using  $\text{fl-ketoinato}$  complexes," *Mater. Sci. Eng.*, vol. B17, pp. 97 – 100, 1993.
- [111] R. Becker, A. Devi, J. Weiss, U. Weckenmann, M. Winter, C. Kiener, H.-W. Becker, and R. A. Fischer, "A study on the metal-organic cvd of pure copper films from low cost copper(ii) dialkylamino-2-propoxides: Tuning the thermal properties of the precursor by small variations of the ligand," *Chem. Vapor Depos.*, vol. 9, pp. 149–156, 2003.
- [112] R. Becker, H. Parala, F. Hipler, O. P. Tkachenko, K. V. Klementiev, W. Gruenert, H. Wilmer, O. Hinrichsen, M. Muhler, A. Birkner, C. Woell, S. Schaefer, and R. A. Fischer, "Mocvd-loading of

mesoporous siliceous matrices with cu/zno: Supported catalysts for methanol synthesis,” *Angew. Chem. Int. Edit.*, vol. 43, pp. 2839 – 2842, 2004.

[113] R. Becker, J. Weiß, M. Winter, K. Merz, and R. A. Fischer, “New heterometallic copper zinc alkoxides: synthesis, structure properties and pyrolysis to cu/zno composites,” *J. Organomet. Chem.*, vol. 630, pp. 253 – 262, 2001.

[114] B. H. Lee, J. K. Hwang, J. W. Nam, S. U. Lee, J. T. Kim, S.-M. Koo, A. Baunemann, R. A. Fischer, and M. M. Sung, “Low-temperature atomic layer deposition of copper metal thinfilms: Self-limiting surface reaction of copper dimethylamino-2-propoxide with diethylzinc,” *Angew. Chem. Int. Edit.*, vol. 121, pp. 4606–4609, 2009.

[115] T. J. Knisley, T. C. Ariyasena, T. Sajavaara, M. J. Saly, and C. H. Winter, “Low temperature growth of high purity, low resistivity copper films by atomic layer deposition,” *Chem. Mater.*, vol. 23, pp. 4417 – 4419, 2011.

[116] R. Becker, *Metallorganische Precursorchemie für das Cu/ZnO System*. PhD thesis, Ruhr-Universität Bochum, 2003.

[117] M. Becker, R. N. d’Alnoncourt, K. Kahler, J. Sekulic, R. A. Fischer, and M. Muhler, “The synthesis of highly loaded cu/al<sub>2</sub>o<sub>3</sub> and cu/zno/al<sub>2</sub>o<sub>3</sub> catalysts by the two-step cvd of cu(ii)diethylamino-2-propoxide in a fluidized-bed reactor,” *Chem. Vapor Depos.*, vol. 16, pp. 85–92, 2010.

[118] K. Väyrynen, K. Mizohata, J. Räisänen, D. Peeters, A. Devi, M. Ritala, and M. Leskelä, “Low-temperature atomic layer deposition of low-resistivity copper thin films using cu(dmap)<sub>2</sub> and tertiary butyl hydrazine,” *Chem. Mater.*, vol. 29, pp. 6502 – 6510, 2017.

[119] Y. Kim, C. K. Kim, T.-M. Chung, S. L. Lee, K.-S. An, T. S. Yang, and H. S. Jang, “Volatile copper aminoalkoxide complex and deposition of copper thin film using same (patent no.: Us 6,982,341 b1),” 2006.

- [120] J.-H. Park, D.-S. Han, Y.-J. Kang, S.-R. Shin, and J.-W. Park, "Self-forming al oxide barrier for nanoscale cu interconnects created by hybrid atomic layer deposition of cual alloy," *J. Vac. Sci. Tech. A*, vol. 32, p. 01A131, 2014.
- [121] D.-Y. Moon, D.-S. Han, J.-H. Park, S.-Y. Shin, J.-W. Park, B. M. Kim, and J. Y. Cho, "Plasma-enhanced atomic layer deposition of cumn films with formation of a MnSixOy barrier layer," *Thin Solid Films*, vol. 521, pp. 146–149, 2012.
- [122] T. Yoshino, M. Enzu, A. Sakurai, A. Nishida, and M. Okabe, "Copper compound, starting material for forming thin film, and method for manufacturing thin film (pat. no: Us20170044188a1)," 2017.
- [123] I. Giebelhaus, E. Varechkina, T. Fischer, M. Rumyantseva, V. Ivanov, A. Gaskov, J. R. Morante, J. Arbiol, W. Tyrre, and S. Mathur, "One-dimensional CuOSnO2 pn heterojunctions for enhanced detection of h2s," *Journal of Materials Chemistry A*, vol. 1, p. 11261, 2013.
- [124] A. Sasinska, D. Ritschel, L. Czypiel, and S. Mathur, "Metallic copper thin films grown by plasma-enhanced atomic layer deposition of air stable precursors0.167em," *Advanced Engineering Materials*, vol. 19, p. 1600593, 2016.
- [125] V. Krisyuk, I. Baidina, I. Korolkov, P. Semyannikov, P. Stabnikov, S. Trubin, and A. Turgambaeva, "New volatile heteroleptic complex of copper(ii): Comparison of two polymorphs," *Polyhedron*, vol. 49, pp. 1 – 6, 2013.
- [126] V. V. Krisyuk, S. V. Sysoev, Y. M. Rumyantsev, S. A. Prokhorova, E. V. Maximovskiy, M. L. Kosinova, and I. K. Igumenov, "New heteroleptic copper(ii) complexes as mocvd precursors," *Phys. Proc.*, vol. 46, pp. 174 – 182, 2013.

- [127] B. Vidjayacoumar, D. J. H. Emslie, S. B. Clendenning, J. M. Blackwell, J. F. Britten, and A. Rheingold, "Investigation of alme3, bet3, and znet2 as co-reagents for low-temperature copper metal ald/pulsed-cvd," *Chem. Mater.*, vol. 22, pp. 4844–4853, 2010.
- [128] T. H. Baum, "Laser chemical vapor deposition of gold: The effect of organometallic structure," *J. Electrochem. Soc.*, vol. 134, pp. 2616 – 2619, 1987.
- [129] V. L. Young, D. F. Cox, and M. E. Davis, "Metalorganic chemical vapor deposition of copper from copper(ii) dimethylamino ethoxide," *Chem. Mater.*, vol. 5, pp. 1701 – 1709, 1993.
- [130] G. M. Whitesides, J. S. Sadowski, and J. Lilburn, "Copper( i) alkoxides. synthesis, reactions, and thermal decomposition," *J. Am. Chem. Soc.*, vol. 96, pp. 2829 – 2835, 1974.
- [131] Y. Chi, P.-F. Hsu, T.-W. Lin, C.-S. Liu, and A. J. Carty, "Self-reducible cu(ii) source reagents for chemical vapor deposition of copper metal (patent no.: Us 6,369,256 b1)," 2002.
- [132] T. H. Baum, G. Bhandari, and C. Xu, "Chemical vapor deposition precursors for deposition of copper (patent no.: Us 6,822,107 b1)," 2004.
- [133] D. J. Hagen, J. Connolly, I. M. Povey, S. Rushworth, and M. E. Pemble, "Island coalescence during film growth: An underestimated limitation of cu ald," *Adv. Mater. Interfaces*, vol. 4, p. 1700274, 2017.
- [134] A. Niskanen, A. Rahtu, T. Sajavaara, K. Arstila, M. Ritala, and M. Leskeläe, "Radical-enhanced atomic layer deposition of metallic copper thin films," *J. Electrochem. Soc.*, vol. 152, pp. G25–G28, 2005.
- [135] L. Wu and E. Eisenbraun, "Integration of atomic layer deposition-grown copper seed layers for cu electroplating applications," *J. Electrochem. Soc.*, vol. 156, pp. H734–H739, 2009.
- [136] R. Solanki and B. Pathangey, "Atomic layer deposition of copper seed layers," *Electrochem. Solid-State Lett.*, vol. 3, pp. 479–480, 2000.



- [137] T. S. Tripathi and M. Karppinen, "Efficient process for direct atomic layer deposition of metallic cu thin films based on an organic reductant," *Chem. Mater.*, vol. 29, pp. 1230–1235, 2017.
- [138] B. Vidjayacoumar, D. J. H. Emslie, J. M. Blackwell, S. B. Clendenning, and J. F. Britten, "Solution reactions of a bis(pyrrolylaldimate)copper(ii) complex with peralkyl zinc, aluminum, and boron reagents: Investigation of the pathways responsible for copper metal deposition," *Chem. Mater.*, vol. 22, pp. 4854–4866, 2010.
- [139] L. C. Kalutarage, S. B. Clendenning, and C. H. Winter, "Low-temperature atomic layer deposition of copper films using borane dimethylamine as the reducing co-reagent," *Chem. Mater.*, vol. 26, pp. 3731 – 3738, 2014.
- [140] L. Wu, W. Zeng, and E. Eisenbraun, "Integration of electrochemically deposited cu on plasma enhanced atomic layer deposition-grown cu seed layers," *ECST*, vol. 11, pp. 67–78, 2007.
- [141] G. A. T. Eyck, J. J. Senkevich, F. Tang, D. Liu, S. Pimanpang, T. Karaback, G.-C. Wang, T.-M. Lu, C. Jezewski, and W. A. Lanfield, "Plasma-assisted atomic layer deposition of palladium," *Chem. Vapor Depos.*, vol. 11, pp. 60–66, 2005.
- [142] H. Shimizu, K. Sakoda, T. Momose, M. Koshi, and Y. Shimogaki, "Hot-wire-assisted atomic layer deposition of a high quality cobalt film using cobaltocene: Elementary reaction analysis on nhx radical formation," *J. Vac. Sci. Technol. A*, vol. 30, p. 01A144, 2012.
- [143] H. C. M. Knoop, E. Langereis, M. C. M. van de Sanden, and W. M. M. Kessels, "Conformality of plasma-assisted ald: Physical processes and modeling," *J. Electrochem. Soc.*, vol. 157, pp. G241–C249, 2010.
- [144] Z.-K. Tan, K. Johnson, Y. Vaynzof, A. A. Bakulin, L.-L. Chua, P. K. H. Ho, and R. H. Friend, "Suppressing recombination in polymer photovoltaic devices via energy-level cascades," *Adv. Mater.*, vol. 25, pp. 4131 – 4138, 2013.

- [145] D. Goodman, T. E. Madey, M. Ono, and J. T. Y. Jr., "Interaction of hydrogen, carbon monoxide, and formaldehyde with ruthenium," *J. Appl. Phys.*, vol. 50, pp. 279–290, 1977.
- [146] G. Ertl and J. Tornau, "The catalytic decomposition of formaldehyde on palladium," *Z. Phys. Chem. Neue Fol.*, vol. 104, pp. 301–308, 1977.
- [147] S. Delgado, A. Munoz, M. Medina, and C. Pastor, "Synthesis and structural characterization of copper(ii)bishexafluoroacetylacetonate complexes with n-donor ligands," *Inorg. Chim. Acta*, vol. 359, pp. 109 – 117, 2006.
- [148] L. L. Funcki and T. R. Ortolano, "The effects of axial ligation on the ligand field spectra of copper(ii) beta-diketonates," *Inorg. Chem.*, vol. 7, pp. 567 – 573, 1968.
- [149] G. Dey and S. D. Elliott, "Mechanism for the atomic layer deposition of copper using diethylzinc as the reducing agent: A density functional theory study using gas-phase molecules as a model," *J. Phys. Chem. A*, vol. 116, pp. 8893 – 8901, 2012.
- [150] G. Klivenyi, I. Kovacs, and F. Solymosi, "Thermal and photo-induced dissociation of (c2h5)2zn on rh(111) surface," *Surf. Sci.*, vol. 442, pp. 115–130, 1999.
- [151] I. Kovacs, N. Iost, and F. Solymosi, "Thermal and photo-induced dissociation of (c2h5)2zn to yield c2h5 on the pd(100) surface," *J. Chem. Phys.*, vol. 101, pp. 4236–4247, 1994.
- [152] M. A. Rueter and J. M. Vohs, "Adsorption and reaction of diethylzinc on gaas(100)," *J. Vac. Sci. Technol. B*, vol. 10, pp. 2163–2169, 1992.
- [153] M. Rueter and J. Vohs, "The surface reactions of ethyl groups on si( 100) formed via dissociation of adsorbed diethylzinc," *Surf. Sci.*, vol. 262, pp. 42–50, 1992.

- [154] H. Dumont, A. Marbeuf, J.-E. Bouree, and O. Gorochov, "Pyrolysis pathways and kinetics of thermal decomposition of diethylzinc and diethyltellurium studied by mass spectrometry," *J. Mater. Chem.*, vol. 3, pp. 1075–1079, 1993.
- [155] G. Dey, J. S. Wrench, D. J. Hagen, L. Keeneya, and S. D. Elliott, "Quantum chemical and solution phase evaluation of metallocenes as reducing agents for the prospective atomic layer deposition of copper," *Dalton Trans.*, vol. 44, pp. 10188 – 10199, 2015.
- [156] T. Törndahl, M. Ottosson, and J.-O. Carlsson, "Growth of copper(i) nitride by ald using copper(ii) hexafluoroacetylacetonate, water, and ammonia as precursors," *J. Electrochem. Soc.*, vol. 153, pp. C146–C151, 2006.
- [157] J.-M. Park, K. Jin, B. Han, M. J. Kim, J. Jung, J. J. Kim, and W.-J. Lee, "Atomic layer deposition of copper nitride film and its application to copper seed layer for electrodeposition," *Thin Solid Films*, vol. 556, pp. 434–439, 2014.
- [158] S. L. Cohen, M. Liehr, and S. Kasi, "Mechanisms of copper chemical vapor deposition," *Appl. Phys. Lett.*, vol. 60, pp. 50–52, 1992.
- [159] J. Mulley, R. Bennett, and V. Dhanak, "Adsorption, orientation and thermal decomposition of copper(ii) hexafluoroacetylacetonate on rutile tio2(110)," *Surf. Sci.*, vol. 602, pp. 2967 – 2974, 2008.
- [160] D. G. Rayner, J. S. Mulley, and R. A. Bennett, "Copper deposition on tio2 from copper(ii)hexafluoroacetylacetonate," *J. Vac. Sci. Technol. A*, vol. 31, p. 01A121, 2013.
- [161] P. J. Pallister and S. T. Barry, "Surface chemistry of group 11 atomic layer deposition precursors on silica using solid-state nuclear magnetic resonance spectroscopy," *J. Chem. Phys.*, vol. 146, p. 052812, 2016.

- [162] H. Kim, T. Koseki, T. Ohba, T. Ohta, Y. Kojima, H. Sato, and Y. Shimogaki, "Cu wettability and diffusion barrier property of ru thin film for cu metallization," *J. Electrochem. Soc.*, vol. 152, pp. G594 – G600, 2005.
- [163] D. J. Hagen, "Atomic layer deposition of copper for cmos interconnects," 2014.
- [164] M. Dai, J. Kwon, M. D. Halls, R. G. Gordon, and Y. J. Chabal, "Surface and interface processes during atomic layer deposition of copper on silicon oxide," *Langmuir*, vol. 26, pp. 3911 – 3917, 2010.
- [165] M. Dai, J. Kwon, E. Langereis, L. Wielunski, Y. J. Chabal, Z. Li, and R. G. Gordon, "In-situ ftir study of atomic layer deposition (ald) of copper metal films," *ECST*, vol. 11, pp. 91–101, 2007.
- [166] Q. Ma, H. Guo, R. G. Gordon, and F. Zaera, "Uptake of copper acetamidinate ald precursors on nickel surfaces," *Chem. Mater.*, vol. 22, pp. 352 – 359, 2010.
- [167] Q. Ma and F. Zaera, "Chemistry of cu(acac)<sub>2</sub> on ni(110) and cu(110) surfaces: Implications for atomic layer deposition processes," *J. Vac. Sci. Technol. A*, vol. 31, p. 01A112, 2013.
- [168] T. Kim, Y. Yao, J. P. Coyle, S. T. Barry, and F. Zaera, "Thermal chemistry of cu(i)-iminopyrrolidinate and cu(i)-guanidinate atomic layer deposition (ALD) precursors on ni(110) single-crystal surfaces," *Chem. Mater.*, vol. 25, pp. 3630 – 3639, 2013.
- [169] Y. Yao, J. P. Coyle, S. T. Barry, and F. Zaera, "Thermal decomposition of copper iminopyrrolidinate atomic layer deposition (ald) precursors on silicon oxide surfaces," *J. Phys. Chem. C*, vol. 120, pp. 14149 – 14156, 2016.
- [170] E. Machado, M. Kaczmariski, P. Ordejo, D. Garg, J. Norman, and H. Cheng, "First-principles analyses and predictions on the reactivity of barrier layers of ta and tan toward organometallic precursors for deposition of copper films," *Langmuir*, vol. 21, pp. 7608–7614, 2005.

- [171] C. G. Granqvist and R. A. Buhrman, "Statistical model for coalescence of islands in discontinuous films," *Appl. Phys. Lett.*, vol. 27, pp. 693 – 694, 1975.
- [172] C. G. Granqvist and R. A. Buhrman, "Ultrafine metal particles," *J. Appl. Phys.*, vol. 47, pp. 2200 – 2219, 1976.
- [173] A. Niskanen, T. Hatanpaa, K. Arstila, M. Leskelä, and M. Ritala, "Radical-enhanced atomic layer deposition of silver thin films using phosphine-adducted silver carboxylates," *Chem. Vapor Depos.*, vol. 13, pp. 408 – 413, 2007.
- [174] M. Kariniemi, J. Niinisto, T. Hatanpaa, M. Kemell, T. Sajavaara, M. Ritala, and M. Leskelä, "Plasma-enhanced atomic layer deposition of silver thin films," *Chem. Mater.*, vol. 23, pp. 2901 – 2907, 2011.
- [175] M. Mäkelä, T. Hatanpää, K. Mizohata, K. Meinander, J. Niinistö, J. Räisänen, M. Ritala, and M. Leskelä, "Studies on thermal atomic layer deposition of silver thin films," *Chem. Mater.*, vol. 29, pp. 2040 – 2045, 2017.
- [176] M. M. Minjauw, E. Solano, S. P. Sree, R. Asapu, M. Van Daele, R. K. Ramachandran, G. Heremans, S. W. Verbruggen, S. Lenaerts, J. A. Martens, C. Detavernier, and J. Dendooven, "Plasma-enhanced atomic layer deposition of silver using ag(fod)(PEt3) and NH3-plasma," *Chem Mater.*, vol. 29, pp. 7114 – 7121, 2017.
- [177] P. R. Chalker, S. Romani, P. A. Marshall, M. J. Rosseinsky, S. Rushworth, and P. A. Williams, "Liquid injection atomic layer deposition of silver nanoparticles," *Nanotechnology*, vol. 21, p. 405602, 2010.
- [178] Z. Golrokhi, P. A. Marshall, S. Romani, S. Rushworth, P. R. Chalker, and R. J. Potter, "The influence of tertiary butyl hydrazine as a co-reactant on the atomic layer deposition of silver," *Appl. Surf. Sci.*, vol. 399, pp. 123 – 131, 2017.

- [179] S. Samoilenkov, M. Stefan, G. Wahl, S. Paramonov, N. Kuzmina, and A. Kaul, "Low-temperature mocvd of conducting, micrometer-thick, silver films," *Chem. Vap. Depos.*, vol. 8, pp. 74 – 78, 2002.
- [180] E. Szlyk, P. Piszczek, A. Grodzicki, M. Chaberski, A. Golin'ski, J. Szatkowski, and T. Blaszczyk, "Cvd of ag(i) complexes with tertiary phosphines and perfluorinated carboxylates - a new class of silver precursors," *Chem. Vap. Depos.*, vol. 7, pp. 111 – 116, 2001.
- [181] N. Boysen, T. Hasselmann, S. Karle, D. Rogalla, D. Theirich, M. Winter, T. Riedl, and A. Devi, "An n-heterocyclic carbene based silver precursor for plasma-enhanced spatial atomic layer deposition of silver thin films at atmospheric pressure," *Angew. Chem.*, vol. 57, pp. 16224 – 16227, 2018.
- [182] P. Piszczek, E. Szlyk, M. Chaberski, C. Taeschner, A. Leonhardt, W. Bala, and K. Bartkiewicz, "Characterization of silver trimethylacetate complexes with tertiary phosphines as cvd precursors of thin silver films," *Chem. Vap. Depos.*, vol. 11, pp. 53 – 59, 2005.
- [183] A. A. Amusan, B. Kalkofen, H. Gargouri, K. Wandel, C. Pinnow, M. Lisker, and E. P. Burte, "Ag films grown by remote plasma enhanced atomic layer deposition on different substrates," *J. Vac. Sci. Tech. A*, vol. 34, p. 01A126, 2016.
- [184] F. J. van den Bruele, M. Smets, A. Illiberi, Y. Creyghton, P. Buskens, F. Roozeboom, and P. Poedt, "Atmospheric pressure plasma enhanced spatial ALD of silver," *J. Vac. Sci. Tech. A*, vol. 33, p. 01A131, 2015.
- [185] H. Brune, "Microscopic view of epitaxial metal growth: nucleation and aggregation," *Surf. Sci. Rep.*, vol. 31, pp. 125–229, 1998.
- [186] L. Gao, P. Haerter, C. Linsmeier, A. Wiltner, R. Emling, and D. Schmitt-Landsiedel, "Silver metal organic chemical vapor deposition for advanced silver metallization," *Microelectron. Eng.*, vol. 82, pp. 296 – 300, 2005.

- [187] K.-M. Chi, K.-H. Chen, S.-M. Peng, and G.-H. Lee, "Synthesis and characterization of (beta-diketonato)silver vinyltriethylsilane compounds and their application to cvd of silver thin films. crystal structure of the (2,2-dimethyl-6,6,7,7,8,8,8-heptafluoro-3,5-octanedionato)silver vinyltriethylsilane dimer," *Organometallics*, vol. 15, pp. 2575 – 2578, 1996.
- [188] L. Zanotto, F. Benetollo, M. Natali, G. Rossetto, P. Zanella, S. Kaciulis, and A. Mezzi, "Facile synthesis and characterization of new beta-diketonate silver complexes. single-crystal structures of (1,1,1,5,5,5-hexafluoro-2,4-pentanedionato)(2,2'-hipyridine)silver(I) and (1,1,1,5,5,5-hexafluoro-2,4-pentanedionato)(n,n,n',n'-tetramethylethylenediamine)silver(I) and their use as precursors in the mocvd of silver films," *Chem. Vap. Depos.*, vol. 10, pp. 207 – 213, 2004.
- [189] A. Grodzicki, I. Lakomska, P. Piszczek, I. Szymanska, and E. Szlyk, "Copper(i), silver(i) and gold(i) carboxylate complexes as precursors in chemical vapour deposition of thin metallic films," *Coordin. Cem. Rev.*, vol. 249, pp. 2239 – 2258, 2005.
- [190] D. J. Mandia, M. B. E. Griffiths, W. Zhou, P. G. Gordon, J. Albert, and S. T. Barry, "In situ monitoring by a tilted fiber bragg grating optical probe: Probing nucleation in chemical vapour deposition of gold," *Phys. Proc.*, vol. 46, pp. 12 – 20, 2013.
- [191] R. G. Parkhomenko, A. I. Plekhanov, A. Kuchyanov, S. V. Trubin, B. M. Kuchunov, and L. K. Igumenov, "Gold nanostructure formation in the photonic crystal matrix by means of mocvd technique," *Surf. Coat. Tech.*, vol. 230, pp. 279 – 283, 2013.
- [192] R. G. Parkhomenko, A. E. Turgambaeva, N. B. Morozova, S. V. Trubin, V. V. Krisyuk, and I. K. Igumenov, "New liquid precursors for the metal-organic cvd of gold films," *Chem. Vap. Depos.*, vol. 19, pp. 38 – 44, 2013.

- [193] A. E. Turgambaeva, G. Zharkova, P. Semyannikov, V. V. Krisyuk, T. Koretskaya, S. Trubin, B. Kuchumov, and I. Igumenov, "Oxygen-free precursor for chemical vapor deposition of gold films: thermal properties and decomposition mechanism," *Gold Bull*, vol. 44, pp. 177 – 184, 2011.
- [194] A. Turgambaeva, R. Parkhomenko, V. Aniskin, V. Krisyuk, and I. Igumenov, "A comparative study of a series of dimethylgold(iii) complexes with s,s chelating ligands used as mocvd precursors," *Phys. Proc.*, vol. 46, pp. 167 – 173, 2013.
- [195] M. Mäkelä, T. Hatanpää, K. Mizohata, J. Räisänen, M. Ritala, and M. Leskelä, "Thermal atomic layer deposition of continuous and highly conducting gold thin films," *Chem. Mater.*, vol. 29, pp. 6130–6136, 2017.
- [196] M. B. E. Griffiths, P. J. Pallister, D. J. Mandia, and S. T. Barry, "Atomic layer deposition of gold metal," *Chemistry of Materials*, vol. 28, pp. 44–46, jan 2016.
- [197] M. M. B. Holl, P. F. Seidler, S. P. Kowalczyk, and F. R. McFeely, "Surface reactivity of alkylgold(1) complexes: Substrate-selective chemical vapor deposition of gold from  $\text{raup}(\text{ch}_3)_3$  ( $r = \text{ch}_2\text{ch}_2$ ,  $\text{ch}_3$ ) at remarkably low temperatures," *Inorg. Chem.*, vol. 33, pp. 510 – 517, 1994.
- [198] J. L. Davidson, P. John, P. G. Roberts, M. G. Jubber, and J. I. B. Wilson, "Laser photochemical deposition of gold from trialkylphosphine alkylgold( i) complexes," *Chem. Mater.*, vol. 6, pp. 1712 – 1718, 1994.
- [199] R. D. Sanner, J. Joe H. Satcher, and M. W. Droegge, "Synthesis and characterization of (trifluoromethyl)gold complexes," *Organometallics*, vol. 8, pp. 1498 – 1506, 1989.
- [200] N. H. Dryden, J. G. Shapter, L. L. Coatsworth, P. R. Norton, and R. J. Puddephatt, "[ $\text{cf}_3\text{Au}(\text{c}=\text{nme})$ ] as a precursor for cvd of gold," *Chem. Mater.*, vol. 4, pp. 979 – 981, 1992.



- [201] P. D. Tran and P. Doppelt, "Gold cvd using trifluorophosphine gold(i) chloride precursor and its toluene solutions," *J. Electrochem. Soc.*, vol. 154, pp. D520 – D525, 2007.
- [202] E. Szlyk, P. Piszczek, I. Lakomska, A. Grodzicki, J. Szatkowski, and T. Blaszczyk, "Au(i) and ag(i) complexes with tertiary phosphines and perfluorinated carboxylates as precursors for cvd of gold and silver," *Chem. Vap. Depos.*, vol. 6, pp. 105 – 108, 2000.
- [203] S. Graells, R. Alcubilla, G. Badenes, and R. Quidant, "Growth of plasmonic gold nanostructures by electron beam induced deposition," *Appl. Phys. Lett.*, vol. 91, p. 121112, 2007.
- [204] M. Okumura, S. Nakamura, S. Tsubota, T. Nakamura, M. Azuma, and M. Haruta, "Chemical vapor deposition of gold on al<sub>2</sub>o<sub>3</sub>, sio<sub>2</sub>, and tio<sub>2</sub> for the oxidation of co and of h<sub>2</sub>," *Catal. Lett.*, vol. 51, pp. 53 – 58, 1998.
- [205] M. Tanaka, M. Shimojo, M. Han, K. Mitsuishi, and K. Furuya, "Ultimate sized nano-dots formed by electron beam-induced deposition using an ultrahigh vacuum transmission electron microscope," *Surf. Interface Anal.*, vol. 37, pp. 261 – 264, 2005.
- [206] I. Utke, B. Dwir, K. Leifer, F. Cicoira, P. Doppelt, P. Hoffmann, and E. Kapon, "Electron beam induced deposition of metallic tips and wires for microelectronics applications," *Microelectron. Eng.*, vol. 53, pp. 261 – 264, 2000.
- [207] J. D. Wnuk, J. M. Gorham, S. G. Rosenberg, W. F. van Dorp, T. E. Madey, C. W. Hagen, and D. H. Fairbrother, "Electron beam irradiation of dimethyl-(acetylacetonate) gold(iii)adsorbed onto solid substrates," *J. Appl. Phys.*, vol. 107, p. 054301, 2010.
- [208] S. T. Christensen, J. W. Elam, F. A. Rabuffetti, Q. Ma, S. J. Weigand, B. Lee, S. Seifert, P. C. Stair, K. R. Poeppelmeier, M. C. Hersam, and M. J. Bedzyk, "Controlled growth of platinum nanoparticles on strontium titanate nanocubes by atomic layer deposition," *Small*, vol. 5, pp. 750–757, 2009.

- [209] H. C. M. Knoop, A. J. M. Mackus, M. E. Donders, M. C. M. van de Sanden, P. H. L. Notten, and W. M. M. Kessels, "Remote plasma and thermal ald of platinum and platinum oxide films," *ECST*, vol. 16, pp. 209–218, 2008.
- [210] W. Zhang, T. Qiu, X.-P. Qu, and P. K. Chu, "Atomic layer deposition of platinum thin films on anodic aluminium oxide templates as surface-enhanced raman scattering substrates," *Vacuum*, vol. 89, pp. 257 – 260, 2013.
- [211] A. J. M. Mackus, N. Leick, L. Baker, and W. M. M. Kessels, "Catalytic combustion and dehydrogenation reactions during atomic layer deposition of platinum," *Chem. Mater.*, vol. 24, p. 1752–1761, 2012.
- [212] J. Hämäläinen, F. Munnik, M. Ritala, and M. Leskelä, "Atomic layer deposition of platinum oxide and metallic platinum thin films from pt(acac)<sub>2</sub> and ozone," *Chem. Mater.*, vol. 20, p. 6840–6846, 2008.
- [213] S. M. Geyer, R. Methapanon, B. Shong, P. A. Pianetta, and S. F. Bent, "In vacuo photoemission studies of platinum atomic layer deposition using synchrotron radiation," *Phys. Chem. Lett.*, vol. 4, pp. 176 – 179, 2013.
- [214] J. Heo, S.-J. Won, D. Eom, S. Y. Lee, Y. B. Ahn, C. S. Hwang, and H. J. Kim, "The role of the methyl and hydroxyl groups of low-k dielectric films on the nucleation of ruthenium by ald," *Electrochem. Solid-State Lett.*, vol. 11, pp. H210–H213, 2008.
- [215] K. J. Park, J. M. Doub, T. Gougousi, and G. N. Parsons, "Microcontact patterning of ruthenium gate electrodes by selective area atomic layer deposition," *Appl. Phys. Lett.*, vol. 86, p. 051903, 2005.
- [216] H. Wang, R. G. Gordon, R. Alvis, and R. M. Ulfig, "Atomic layer deposition of ruthenium thin films from an amidinate precursor," *Chem. Vapor Depos.*, vol. 15, pp. 312 – 319, 2009.

- [217] S.-H. Choi, T. Cheon, S.-H. Kim, D.-H. Kang, G.-S. Park, and S. Kim, "Thermal atomic layer deposition (ald) of ru films for cu direct plating," *J. Electrochem. Soc.*, vol. 158, pp. D351–D356, 2011.
- [218] I. K. Igumenov, P. P. Semyannikov, S. V. Trubin, N. B. Morozova, N. V. Gelfond, A. V. Mischenko, and J. A. Norman, "Approach to control deposition of ultra thin films from metal organic precursors: Ru deposition," *Surf. Coat. Tech.*, vol. 201, pp. 9003 – 9008, 2007.
- [219] S.-S. Yim, D.-J. Lee, K.-S. Kim, S.-H. Kim, T.-S. Yoon, and K.-B. Kim, "Nucleation kinetics of ru on silicon oxide and silicon nitride surfaces deposited by atomic layer deposition," *J. Appl. Phys.*, vol. 103, p. 113509, 2008.
- [220] T. Aaltonen, M. Ritala, K. Arstila, J. Keinonen, and M. Leskelä, "Atomic layer deposition of ruthenium thin films from ru(thd)(3) and oxygen," *Chem. Vap. Depos.*, vol. 10, pp. 215 – 219, 2004.
- [221] R. Methaapanon, S. M. Geyer, H. B. R. Lee, and S. F. Bent, "The low temperature atomic layer deposition of ruthenium and the effect of oxygen exposure," *J. Mater. Chem.*, vol. 22, p. 25154, 2012.
- [222] J. Hämäläinen, T. Sajavaara, E. Puukilainen, M. Ritala, and M. Leskelä, "Atomic layer deposition of osmium," *Chem. Mater.*, vol. 24, pp. 55 – 60, 2012.
- [223] K. J. Park and G. N. Parsons, "Selective area atomic layer deposition of rhodium and effective work function characterization in capacitor structures," *Appl. Phys. Lett.*, vol. 89, p. 043111, 2006.
- [224] T. Aaltonen, M. Ritala, and M. Leskelä, "Ald of rhodium thin films from rh(acac)3 and oxygen," *Electrochem. Solid-State Lett.*, vol. 8, pp. C99 – C101, 2005.
- [225] T. Aaltonen, M. Ritala, V. Sammelselg, and M. Leskelä, "Atomic layer deposition of iridium thin films," *J. Electrochem. Soc.*, vol. 151, pp. G489 – G492, 2004.

- [226] E. Faerm, M. Kemell, M. Ritala, and M. Leskelä, "Self-assembled octadecyltrimethoxysilane monolayers enabling selective-area atomic layer deposition of iridium," *Chem. Vapor Depos.*, vol. 12, pp. 415–417, 2006.
- [227] S.-W. Kim, S.-H. Kwon, D.-K. Kwak, and S.-W. Kang, "Phase control of iridium and iridium oxide thin films in atomic layer deposition," *J. Appl. Phys.*, vol. 103, p. 023517, 2008.
- [228] S. D. Elliott, "Mechanism, products, and growth rate of atomic layer deposition of noble metals," *Langmuir*, vol. 26, pp. 9179 – 9182, 2010.
- [229] A. Salaun, S. B. Newcomb, I. M. Povey, M. Salaun, L. Keeney, A. O'Mahony, and M. E. Pemble, "Nucleation and chemical transformation of RuO<sub>2</sub> films grown on (100) Si substrates by atomic layer deposition," *Chem. Vap. Depos.*, vol. 17, pp. 114 – 122, 2011.
- [230] Y.-L. Chen, C.-C. Hsu, Y.-H. Song, Y. Chi, A. J. Carty, S.-M. Peng, and G.-H. Lee, "Iridium metal thin films and patterned RuO<sub>2</sub> nanowires deposited using iridium(i) carbonyl precursors," *Chem. Vapor Depos.*, vol. 12, pp. 442–447, 2006.
- [231] J. Hämäläinen, E. Puukilainen, M. Kemell, L. Costelle, M. Ritala, and M. Leskelä, "Atomic layer deposition of iridium thin films by consecutive oxidation and reduction steps," *Chem. Mater.*, vol. 21, pp. 4868–4872, 2009.
- [232] T. Aaltonen, P. Alen, M. Ritala, and M. Leskelä, "Ruthenium thin films grown by atomic layer deposition," *Chem. Vap. Depos.*, vol. 9, pp. 45 – 49, 2003.
- [233] S. K. Kim, J. H. Han, G. H. Kim, and C. S. Hwang, "Investigation on the growth initiation of Ru thin films by atomic layer deposition," *Chem. Mater.*, vol. 22, p. 2850–2856, 2010.
- [234] H.-B.-R. Lee, K. L. Pickrahn, and S. F. Bent, "Effect of O<sub>3</sub> on growth of Pt by atomic layer deposition," *J. Phys. Chem. C*, vol. 118, pp. 12325 – 12332, 2014.

- [235] S. K. Park, R. Kanjolia, J. Anthis, R. Odedra, N. Boag, L. Wielunski, and Y. J. Chabal, "Atomic layer deposition of ru/ruo<sub>2</sub> thin films studied by in situ infrared spectroscopy," *Chem. Mater.*, vol. 22, pp. 4867 – 4878, 2010.
- [236] N. Leick, R. O. F. Verkuijlen, L. Lamagna, E. Langereis, S. Rushworth, F. Roozeboom, M. C. M. van de Sanden, and W. M. M. Kessels, "Atomic layer deposition of ru from cp<sub>2</sub>ru(co)<sub>2</sub> using o<sub>2</sub> gas and o<sub>2</sub> plasma," *J. Vac. Sci. Technol. A*, vol. 29, p. 021016, 2011.
- [237] M. M. Minjauw, J. Dendooven, B. Capon, M. Schaekers, and C. Detavernier, "Near room temperature plasma enhanced atomic layer deposition of ruthenium using the RuO<sub>4</sub>-precursor and h<sub>2</sub>-plasma," *J. Mater. Chem. C*, vol. 3, pp. 4848 – 4851, 2015.
- [238] J. Gatineau, K. Yanagita, and C. Dussarrat, "A new RuO<sub>4</sub> solvent solution for pure ruthenium film depositions," *Microelectron. Engin.*, vol. 83, pp. 2248 – 2252, 2006.
- [239] H. J. Jung, J. H. Han, E. A. Jung, B. K. Park, J.-H. Hwang, S. U. Son, C. G. Kim, T.-M. Chung, and K.-S. An, "Atomic layer deposition of ruthenium and ruthenium oxide thin films from a zero-valent (1,5-hexadiene)(1-isopropyl-4-methylbenzene)ruthenium complex and o<sub>2</sub>," *Chem. Mater.*, vol. 26, pp. 7083 – 7090, 2014.
- [240] S. Yeo, J.-Y. Park, S.-J. Lee, D.-J. Lee, J. H. Seo, and S.-H. Kim, "Ruthenium and ruthenium dioxide thin films deposited by atomic layer deposition using a novel zero-valent metalorganic precursor, (ethylbenzene)(1,3-butadiene)ru(0), and molecular oxygen," *Microelectron. Eng.*, vol. 137, pp. 16 – 22, 2015.
- [241] T.-K. Eom, W. Sari, K.-J. Choi, W.-C. Shin, J. H. Kim, D.-J. Lee, K.-B. Kim, H. Sohn, and S.-H. Kim, "Low temperature atomic layer deposition of ruthenium thin films using isopropylmethylbenzene-cyclohexadiene-ruthenium and o<sub>2</sub>," *Electrochem. Solid-State Lett.*, vol. 12, pp. D85 – D88, 2009.

- [242] S. Yeo, S.-H. Choi, J.-Y. Park, S.-H. Kim, T. Cheon, B.-Y. Lim, and S. Kim, "Atomic layer deposition of ruthenium (ru) thin films using ethylbenzen-cyclohexadiene ru(0) as a seed layer for copper metallization," *Thin Solid Films*, vol. 546, pp. 2 – 8, 2013.
- [243] T. Hong, S.-H. Choi, S. Yeo, J.-Y. Park, S.-H. Kim, T. Cheon, H. Kim, M.-K. Kim, and H. Kim, "Atomic layer deposition of ru thin films using a ru(0) metallorganic precursor and o2," *ECS J. Solid State Sci. Tech.*, vol. 2, pp. P47 – P53, 2013.
- [244] D. Z. Austin, M. A. Jenkins, D. Allman, S. Hose, D. Price, C. L. Dezelah, and J. F. Conley, "Atomic layer deposition of ruthenium and ruthenium oxide using a zero-oxidation state precursor," *Chem. Mater.*, vol. 29, pp. 1107 – 1115, 2017.
- [245] S. M. Geyer, R. Methaapanon, R. Johnson, S. Brennan, M. F. Toney, B. Clemens, and S. Bent, "Structural evolution of platinum thin films grown by atomic layer deposition," *J. Appl. Phys.*, vol. 116, p. 064905, 2014.
- [246] A. J. M. Mackus, M. J. Weber, N. F. W. Thissen, D. Garcia-Alonso, R. H. J. Vervuurt, S. Assali, A. A. Bol, M. A. Verheijen, and W. M. M. Kessels, "Atomic layer deposition of pd and pt nanoparticles for catalysis: on the mechanisms of nanoparticle formation," *Nanotechnology*, vol. 27, p. 034001, dec 2015.
- [247] F. Grillo, H. Van Bui, J. A. Moulijn, M. T. Kreutzer, and J. R. van Ommen, "Understanding and controlling the aggregative growth of platinum nanoparticles in atomic layer deposition: An avenue to size selection," *J. Phys. Chem. Lett.*, vol. 8, pp. 975 – 983, 2017.
- [248] F. Grillo, J. A. Moulijn, M. T. K. J., and R. van Ommen, "Nanoparticle sintering in atomic layer deposition of supported catalysts: Kinetic modeling of the size distribution," *Catal. today*, vol. tbc, p. tbc, 2018.

- [249] J. Dendooven, R. K. Ramachandran, E. Solano, M. Kurttepli, L. Geerts, G. Heremans, J. Rongé, M. M. Minjauw, T. Dobbelaere, K. Devloo-Casier, J. A. Martens, A. Vantomme, S. Bals, G. Portale, A. Coati, and C. Detavernier, “Independent tuning of size and coverage of supported pt nanoparticles using atomic layer deposition,” *Nature Comm.*, vol. 8, p. 1074, 2017.
- [250] E. Solano, J. Dendooven, R. K. Ramachandran, K. V. de Kerckhove, T. Dobbelaere, D. Hermida-Merino, and C. Detavernier, “Key role of surface oxidation and reduction processes in the coarsening of pt nanoparticles,” *Nanoscale*, vol. 9, pp. 13159–13170, 2017.
- [251] T. Aaltonen, M. Ritala, Y.-L. Tung, Y. Chi, K. Arstila, K. Meinander, and M. Leskelä, “Atomic layer deposition of noble metals: Exploration of the low limit of the deposition temperature,” *J. Mater. Res.*, vol. 19, pp. 2253 – 3358, 2004.
- [252] T. Aaltonen, *Atomic Layer Deposition of Noble Metal Thin Films*. PhD thesis, University of Helsinki, 2005.
- [253] J. J. Senkevich, F. Tang, D. Rogers, J. T. Drotar, C. Jezewski, W. A. Lanford, G.-C. Wang, and T.-M. Lu, “Substrate-independent palladium atomic layer deposition,” *Chem. Vap. Depos.*, vol. 9, pp. 258–264, 2003.
- [254] J. J. Senkevich, G.-R. Yang, T.-M. Lu, T. S. Cale, C. Jezewski, and W. A. Lanford, “Phosphorous atomic layers promoting the chemisorption of highly polarizable transition metallorganics,” *Chem. Vap. Depos.*, vol. 8, pp. 189–192, 2002.
- [255] R. A. Back and S. Yamamoto, “The gas-phase photochemistry and thermal decomposition of glyoxylic acid,” *Can. J. Chem.*, vol. 63, pp. 542 – 548, 1985.
- [256] J. Elam, A. Zinovev, C. Han, H. Wang, U. Welp, J. Hryn, and M. Pellin, “Atomic layer deposition of palladium films on al<sub>2</sub>o<sub>3</sub> surfaces,” *Thin Solid Films*, vol. 515, pp. 1664–1673, 2006.

- [257] D. N. Goldstein and S. M. George, "Enhancing the nucleation of palladium atomic layer deposition on  $\text{Al}_2\text{O}_3$  using trimethylaluminum to prevent surface poisoning by reaction products," *Appl. Phys. Lett.*, vol. 95, p. 143106, 2009.
- [258] D. Goldstein and S. George, "Surface poisoning in the nucleation and growth of palladium atomic layer deposition with  $\text{Pd}(\text{hfac})_2$  and formalin," *Thin Solid Films*, vol. 519, pp. 5339 – 5347, 2011.
- [259] G. A. T. Eyck, S. Pimanpang, H. Bakhru, T.-M. Lu, and G.-C. Wang, "Atomic layer deposition of Pd on an oxidized metal substrate," *Chem. Vapor Depos.*, vol. 12, pp. 290 – 294, 2006.
- [260] G. A. T. Eyck, S. Pimanpang, J. S. Juneja, H. Bakhru, T.-M. Lu, and Gwo-Ching Wang, "Plasma-enhanced atomic layer deposition of palladium on a polymer substrate," *Chem. Vapor Depos.*, vol. 13, pp. 307 – 311, 2007.
- [261] J. Hämäläinen, E. Puukilainen, T. Sajavaara, M. Ritala, and M. Leskelä, "Low temperature atomic layer deposition of noble metals using ozone and molecular hydrogen as reactants," *Thin Solid Films*, vol. 531, pp. 243 – 250, 2013.
- [262] J. Klaus, S. Ferro, and S. George, "Atomic layer deposition of tungsten using sequential surface chemistry with a sacrificial stripping reaction," *Thin Solid Films*, vol. 360, pp. 145–153, 2000.
- [263] W. Lei, L. Henn-Lecordier, M. Anderle, G. W. Rubloff, M. Barozzi, and M. Bersani, "Real-time observation and optimization of tungsten atomic layer deposition process cycle," *J. Vac. Sci. Technol. B*, vol. 24, pp. 780 – 789, 2006.
- [264] R. K. Grubbs, N. J. Steinmetz, and S. M. George, "Gas phase reaction products during tungsten atomic layer deposition using  $\text{WF}_6$  and  $\text{Si}_2\text{H}_6$ ," *J. Vac. Sci. Tech. B*, vol. 22, pp. 1811 – 1821, 2004.



- [265] R. W. Wind, F. H. Fabreguette, Z. A. Sechrist, and S. M. George, "Nucleation period, surface roughness, and oscillations in mass gain per cycle during w atomic layer deposition on al<sub>2</sub>o<sub>3</sub>," *J. Appl. Phys.*, vol. 105, p. 074309, 2009.
- [266] R. Grubbs, C. Nelson, N. Steinmetz, and S. George, "Nucleation and growth during the atomic layer deposition of w on al<sub>2</sub>o<sub>3</sub> and al<sub>2</sub>o<sub>3</sub> on w," *Thin Solid Films*, vol. 467, pp. 16–27, 2004.
- [267] J. W. Elam, J. A. Libera, M. J. Pellin, A. V. Zinovev, J. P. Greene, and J. A. Nolen, "Atomic layer deposition of w on nanoporous carbon aerogels," *Appl. Phys. Lett.*, vol. 89, p. 053124, 2006.
- [268] T. F. Baumann, J. Biener, Y. M. Wang, S. O. Kucheyev, E. J. Nelson, J. Joe H. Satcher, J. W. Elam, M. J. Pellin, and A. V. Hamza, "Atomic layer deposition of uniform metal coatings on highly porous aerogel substrates," *Chem. Mater.*, vol. 18, pp. 6106–6108, 2006.
- [269] [www.appliedmaterials.com](http://www.appliedmaterials.com).
- [270] P. T. Blanchard, K. A. Bertness, T. E. Harvey, A. W. Sanders, N. A. Sanford, S. M. George, and D. Seghete, "Mosfets made from gan nanowires with fully conformal cylindrical gates," *IEEE T. Nanotech.*, vol. 11, pp. 479 – 482, 2012.
- [271] M. Lee, J.-H. Cheng, Y. C. Lee, D. Seghete, S. M. George, J. B. Schlager, K. Bertness, and N. A. Sanford, "Packaging and interconnect technologies for the development of gan nanowire-based light emitting diodes," in *ECTC*, no. 843 - 847, 2009.
- [272] B. Davidson, Y. Chang, D. Seghete, S. George, and V. Bright, "Atomic layer deposition (ald) tungsten nems devices via a novel top-down approach," in *MEMS, IEEE*, pp. 120 – 123, 2009.
- [273] B. Davidson, S. George, and V. Bright, "Atomic layer deposition (ald) tungsten nano-electromechanical transistors," in *MEMS, IEEE*, pp. 424 – 427, 2010.

- [274] S. P. Haukka, A. Niskanen, and M. Tuominen, "Selective formation of metallic films on metallic surfaces (pat no us 20130189837 a1)," 2013.
- [275] D. Seghete, J. G.B. Rayner, A. Cavanagh, V. Anderson, and S. George, "Molybdenum atomic layer deposition using mof6 and si2h6 as the reactants," *Chem. Mater.*, vol. 23, pp. 1668 – 1678, 2011.
- [276] M. Utriainen, M. Kroger-Laukkanen, L.-S. Johansson, and L. Niinisto, "Studies of metallic thin film growth in an atomic layer epitaxy reactor using m(aca)2 (m=ni, cu, pt) precursors," *Appl. Surf. Sci.*, vol. 157, pp. 151–158, 2000.
- [277] G. I. Zharkova, S. I. Dorovskikh, S. V. Sysoev, I. P. Asanov, A. V. Panin, N. B. Morozova, and I. K. Igumenov, "O,n- coordinated ni(ii) beta-diketonate derivatives: Synthesis, thermal properties, mocvd applications," *Surf. Coat. Tech.*, vol. 230, pp. 290 – 296, 2013.
- [278] K.-W. Do, C.-M. Yang, I.-S. Kang, K.-M. Kim, K.-H. Back, H.-I. Cho, H.-B. Lee, S.-H. Kong, S.-H. Hahm, D.-H. Kwon, J.-H. Lee, and J.-H. Lee, "Formation of low-resistivity nickel silicide with high temperature stability from atomic-layer-deposited nickel thin film," *Japn. J. Appl. Phys.*, vol. 45, pp. 2975–2979, 2006.
- [279] W.-H. Kim, H.-B.-R. Lee, K. Heo, Y. K. Lee, T.-M. Chung, C. G. Kim, S. Hong, J. Heo, and H. Kim, "Atomic layer deposition of ni thin films and application to area-selective deposition," *J. Electrochem. Soc.*, vol. 158, pp. D1 – D5, 2011.
- [280] H.-B.-R. Lee, W.-H. Kim, Y. Park, S. Baik, and H. Kim, "Cobalt and nickel atomic layer depositions for contact applications," in *Interconnect Technology Conference, 2009. IITC 2009. IEEE International*, pp. 157 – 158, 2009.
- [281] H.-S. Kang, J.-B. Ha, J.-H. Lee, C. K. Choi, J. Y. Lee, and K.-M. Lee, "Effect of catalyst for nickel films for nisi formation with improved interface roughness," *Thin Solid Films*, vol. 519, pp. 6658 – 6661, 2011.

- [282] J. Chae, H.-S. Park, and S.-W. Kang, "Atomic layer deposition of nickel by the reduction of preformed nickel oxide," *Electrochem. Solid-State Lett.*, vol. 5, pp. C64–C66, 2002.
- [283] M. Daub, M. Knez, U. Goesele, and K. Nielsch, "Ferromagnetic nanotubes by atomic layer deposition in anodic alumina membranes," *J. Appl. Phys.*, vol. 101, p. 09J111, 2007.
- [284] B. S. Lim, A. Rahtu, and R. G. Gordon, "Atomic layer deposition of transition metals," *Nature Mater.*, vol. 2, pp. 749 – 754, 2003.
- [285] Q. Guo, Z. Guo, J. Shi, W. Xiong, H. Zhang, Q. Chen, Z. Liu, and X. Wang, "Atomic layer deposition of nickel carbide from a nickel amidinate precursor and hydrogen plasma," *ACS Appl. Mater. Interfaces*, vol. 10, pp. 8384–8390, 2018.
- [286] C. Lansalot-Matras, "Nickel allylamidinate precursors for deposition of nickel - containing films (patent no.: Us 2013/0168614 a1)," 2013.
- [287] L. C. Kalutarage, P. D. Martin, M. J. Heeg, and C. H. Winter, "Volatile and thermally stable mid to late transition metal complexes containing alpha-imino alkoxide ligands, a new strongly reducing coreagent, and thermal atomic layer deposition of ni, co, fe, and cr metal films," *J. Am. Chem. Soc.*, vol. 135, pp. 12588 – 12591, 2013.
- [288] T. J. Knisley, M. J. Saly, M. J. Heeg, J. L. Roberts, and C. H. Winter, "Volatility and high thermal stability in mid- to late-first-row transition-metal diazadienyl complexes," *Organometallics*, vol. 30, pp. 5010 – 5017, 2011.
- [289] M. C. Karunaratne, T. J. Knisley, G. S. Tunstall, M. J. Heeg, and C. H. Winter, "Exceptional thermal stability and high volatility in mid to late first row transition metal complexes containing carbohydrazide ligands," *Polyhedron*, vol. 52, pp. 820 – 830, 2013.

- [290] L. C. Kalutarage, P. D. Martin, M. J. Heeg, and C. H. Winter, "Synthesis, structure, and solution reduction reactions of volatile and thermally stable mid to late first row transition metal complexes containing hydrazonate ligands," *Inorg. Chem.*, vol. 52, pp. 5385–5394, 2013.
- [291] J. Wu, J. Li, C. Zhou, X. Lei, T. Gaffney, J. A. T. Norman, Z. Li, R. Gordon, and H. Cheng, "Computational study on the relative reactivities of cobalt and nickel amidinates via beta-h migration," *Organometallics*, vol. 26, pp. 2803 – 2805, 2007.
- [292] K.-M. Lee, C. Y. Kim, C. K. Choi, J.-B. H. Sang-Won Yun, J.-H. Lee, and J. Y. Lee, "Interface properties of nickel-silicide films deposited by using plasma-assisted atomic layer deposition," *J. Korean Phys. Soc.*, vol. 55, pp. 1153 – 1157, 2009.
- [293] H.-B.-R. Lee, J. Kim, H. Kim, W.-H. Kim, J. W. Lee, and I. Hwang, "Degradation of the deposition blocking layer during area-selective plasma-enhanced atomic layer deposition of cobalt," *J. Korean Phys. Soc.*, vol. 56, pp. 104–107, 2010.
- [294] H.-B.-R. Lee, W.-H. Kim, J. W. Lee, J.-M. Kim, K. Heo, I. C. Hwang, Y. Park, S. Hong, and H. Kim, "High quality area-selective atomic layer deposition co using ammonia gas as a reactant," *J. Electrochem. Soc.*, vol. 157, pp. D10 – D15, 2010.
- [295] T. D.-M. Elko-Hansen and J. G. Ekerdt, "XPS investigation of the atomic layer deposition half reactions of bis(n-tert-butyl-n'-ethylpropionamidinato) cobalt(II)," *Chem. Mater.*, vol. 26, pp. 2642–2646, 2014.
- [296] T. D.-M. Elko-Hansen, A. Dolocan, and J. G. Ekerdt, "Atomic interdiffusion and diffusive stabilization of cobalt by copper during atomic layer deposition from bis(n-tert-butyl-n'-ethylpropionamidinato) cobalt(II)," *J. Phys. Chem. Lett.*, vol. 5, pp. 1091–1095, 2014.
- [297] T. D.-M. Elko-Hansen and J. G. Ekerdt, "Selective atomic layer deposition of cobalt for back end of line," *ECS Trans.*, vol. 80, pp. 29–37, 2017.

- [298] H.-B.-R. Lee and H. Kim, "Area selective atomic layer deposition of cobalt thin films," *ECST*, vol. 16, pp. 219–225, 2008.
- [299] H.-B.-R. Lee and H. Kim, "High-quality cobalt thin films by plasma-enhanced atomic layer deposition," *Electrochem. Solid-State Lett.*, vol. 9, pp. G323–G325, 2006.
- [300] H. Shimizu, K. Sakoda, T. Momose, and Y. Shimogaki, "Atomic layer deposited co(w) film as a single-layered barrier/liner for next-generation cu-interconnects," *Jap. J. Appl. Phys.*, vol. 51, p. 05EB02, 2012.
- [301] J. Kwon, M. Saly, M. D. Halls, R. K. Kanjolia, and Y. J. Chabal, "Substrate selectivity of (tbutyl)co(co)<sub>3</sub> during thermal atomic layer deposition of cobalt," *Chem. Mater.*, vol. 24, pp. 1025 – 1030, 2012.
- [302] J. P. Klesko, M. M. Kerrigan, and C. H. Winter, "Low temperature thermal atomic layer deposition of cobalt metal films," *Chem. Mater.*, vol. 28, pp. 700 – 703, 2016.
- [303] M. M. Kerrigan, J. P. Klesko, and C. H. Winter, "Low temperature, selective atomic layer deposition of cobalt metal films using bis(1,4-di-tert-butyl-1,3-diazadienyl)cobalt and alkylamine precursors," *Chem. Mater.*, vol. 29, pp. 7458 – 7466, 2017.
- [304] K. Väyrynen, T. Hatanpää, M. Mattinen, M. Heikkilä, K. Mizohata, K. Meinander, J. Räisänen, M. Ritala, and M. Leskelä, "Diamine adduct of cobalt(II) chloride as a precursor for atomic layer deposition of stoichiometric cobalt(II) oxide and reduction thereof to cobalt metal thin films," *Chem. Mater.*, vol. 30, pp. 3499 – 3507, 2018.
- [305] D. X. Ye, S. Pimanpang, C. Jezewski, F. Tang, J. J. Senkevich, G. C. Wang, and T. M. Lu, "Low temperature chemical vapor deposition of co thin films from co<sub>2</sub>(CO)<sub>8</sub>," *Thin Solid Films*, vol. 485, pp. 95 – 100, 2005.

- [306] A. H. Simon, T. Bolom, C. Niu, F. H. Baumann, C. K. Hu, C. Parks, J. Nag, H. Kim, J. Y. Lee, C. C. Yang, S. Nguyen, H. K. Shobha, T. Nogami, S. Guggilla, J. Ren, D. Sabens, and J. F. AuBuchon, "Electromigration comparison of selective CVD cobalt capping with PVD ta(n) and CVD cobalt liners on 22nm-groundrule dual-damascene cu interconnects," in *2013 IEEE International Reliability Physics Symposium (IRPS)*, pp. 3F.4.1 – 3F.4.6, 2013.
- [307] C. C. Yang, P. Flaitz, P. C. Wang, F. Chen, and D. Edelstein, "Characterization of selectively deposited cobalt capping layers: Selectivity and electromigration resistance," *IEEE Electron Device Lett.*, vol. 31, pp. 728 – 730, 2010.
- [308] C. C. Yang, F. Baumann, P. C. Wang, S. Lee, P. Ma, J. AuBuchon, and D. Edelstein, "CVD co capping layers for cu/low-k interconnects: Cu EM enhancement vs. co thickness," in *2011 IEEE International Interconnect Technology Conference*, pp. 1 – 3, 2011.
- [309] H. K. Jung, H. B. Lee, M. Tsukasa, E. Jung, J. H. Yun, J. M. Lee, G. H. Choi, S. Choi, and C. Chung, "Formation of highly reliable cu/low-k interconnects by using CVD co barrier in dual damascene structures," in *2011 International Reliability Physics Symposium*, pp. 3E.2.1 – 3E.2.5, 2011.
- [310] M. He, X. Zhang, T. Nogami, X. Lin, J. Kelly, H. Kim, T. Spooner, D. Edelstein, and L. Zhao, "Mechanism of co liner as enhancement layer for cu interconnect gap-fill," *J. Electrochem. Soc.*, vol. 160, pp. D3040 – D3044, 2013.
- [311] C. Georgi, A. Hildebrandt, T. Waechtler, S. E. Schulz, T. Gessner, and H. Lang, "A cobalt layer deposition study: Dicobalttetrahydroxanes as convenient mocvd precursor systems," *J. Mater. Chem. C*, vol. 2, pp. 4676 – 4682, 2014.
- [312] A. Baiker and M. Mazeviejewski, "Formation and thermal stability of copper and nickel nitrides," *Ber. Bunsenges. Phys. Chem.*, vol. 80, pp. 2331 – 2341, 1984.

- [313] R. E. Harmon, S. Gupta, and D. J. Brown, "Hydrogenation of organic compounds using homogeneous catalysts," *Chem. Rev.*, vol. 73, pp. 21 – 52, 1973.
- [314] W. S. Seo, J. H. Shim, S. J. Oh, E. K. Lee, N. H. Hur, and J. T. Park, "Phase- and size-controlled synthesis of hexagonal and cubic CoO nanocrystals," *J. Amer. Chem. Soc.*, vol. 127, no. 17, pp. 6188 – 6189, 2005.
- [315] M. J. Redman and E. G. Steward, "Cobaltous oxide with the zinc blende/wurtzite-type crystal structure," *Nature*, vol. 193, p. 867, 1962.
- [316] L. C. Kalutarage, S. B. Clendinning, and C. H. Winter, "Manganese precursor selection and the thermal atomic layer deposition of copper/manganese alloy films," *ECS Trans.*, vol. 64, pp. 147 – 157, 2014.
- [317] D. V. Baxter, M. H. Chisholm, G. J. Gama, A. L. Hector, and I. P. Parkin, "Low pressure chemical vapor deposition of metallic films of iron, manganese, cobalt, copper, germanium and tin employing bis(trimethyl)silylamido complexes,  $m(n(\text{sime}3)_2)_n$ ," *Chem. Vap. Deposition*, vol. 1, pp. 49 – 51, 1995.
- [318] P. F. Ma, J. M. Tseng, M. Chang, A. Lakshmanan, and J. Tang, "Methods for manganese nitride integration (pat. no.: Us 2013/0292806 a1)." Patent, 2013.
- [319] D. Knapp and D. Thompson, "Metal amide deposition precursors and their stabilization with an inert ampoule liner (pat.no.: Us 20140242806 a1)." Patent, 2014.
- [320] J. S. Price, P. Chadha, and D. J. H. Emslie, "Base-free and bisphosphine ligand dialkylmanganese(II) complexes as precursors for manganese metal deposition," *Organometallics*, vol. 35, pp. 168–180, 2016.
- [321] Y. J. Lee and S.-W. Kang, "Study on the characteristics of aluminum thin films prepared by atomic layer deposition," *J. Vac. Sci. Technol. A*, vol. 20, pp. 1983 – 1988, 2002.

This is the author's peer reviewed, accepted manuscript. However, the online version of record will be different from this version once it has been copyedited and typeset.

PLEASE CITE THIS ARTICLE AS DOI: 10.1063/1.5087759

- [322] K. J. Blakeney and C. H. Winter, "Atomic layer deposition of aluminum metal films using a thermally stable aluminum hydride reducing agent," *Chem. Mater.*, vol. 30, pp. 1844 – 1848, 2018.
- [323] W. L. Gladfelter, D. C. Boyd, and K. F. Jensen, "Trimethylamine complexes of alane as precursors for the low-pressure chemical vapor deposition of aluminum," *Chem. Mater.*, vol. 1, pp. 339 – 343, 1989.
- [324] A. Ludviksson, M. Nooney, R. Bruno, A. Bailey, T. T. Kodas, and M. J. Hampden-Smith, "Low-temperature thermal cvd of ti-al metal films using a strong reducing agent," *Chem. Vap. Dep.*, vol. 4, pp. 129 – 132, 1998.
- [325] K. Blakeney, P. Martin, and C. Winter, "A volatile dialane complex from ring-expansion of an n-heterocyclic carbene and its use in atomic layer deposition of aluminum metal films," *Preprint*, vol. tbc, p. tbc, 2018.
- [326] Y. J. Lee and S.-W. Kang, "Atomic layer deposition of aluminum thin films using an alternating supply of trimethylaluminum and a hydrogen plasma," *Electrochem. Solid-State Lett.*, vol. 5, pp. C91–C93, 2002.
- [327] H. Kim and S. M. Rossnagel, "Plasma-enhanced atomic layer deposition of tantalum thin films: the growth and film properties," *Thin Solid Films*, vol. 441, pp. 311 – 316, 2003.
- [328] H. Kim, "The application of atomic layer deposition for metallization of 65 nm and beyond," *Surf. Coat. Tech.*, vol. 200, pp. 3104–3111, 2006.
- [329] S. M. Rossnagel, A. Sherman, and F. Turner, "Plasma-enhanced atomic layer deposition of ta and ti for interconnect diffusion barriers," *J. Vac. Sci. Tech. B*, vol. 18, pp. 2016 – 2020, 2000.
- [330] A. Lemonds, J. White, and J. Ekerdt, "Surface science investigations of atomic layer deposition half-reactions using taf5 and si2h6," *Surface Science*, vol. 538, pp. 191 – 203, 2003.



- [331] A. Lemonds, T. Bolom, W. Ahearn, D. Gay, J. White, and J. Ekerdt, "Atomic layer deposition of TaSi<sub>3</sub> thin films on SiO<sub>2</sub> using TaF<sub>5</sub> and Si<sub>2</sub>H<sub>6</sub>," *Thin Solid Films*, vol. 488, pp. 9 – 14, 2005.
- [332] T.-H. Kim, T.-K. Eom, S.-H. Kim, D.-H. Kang, H. Kim, S. Yu, and J. M. Lim, "Plasma-enhanced atomic layer deposition of TaC<sub>x</sub> films using tris(neopentyl) tantalum dichloride and H<sub>2</sub> plasma," *Electrochem. Solid-State Lett.*, vol. 14, p. D89, 2011.
- [333] T. E. Hong, T.-H. Kim, J.-H. Jung, S.-H. Kim, and H. Kim, "TaC<sub>x</sub> thin films prepared by atomic layer deposition as diffusion barriers for Cu metallization," *J. Am. Ceram. Soc.*, vol. 97, pp. 127–134, 2013.
- [334] H. Kim and S. M. Rossnagel, "Growth kinetics and initial stage growth during plasma-enhanced Ti atomic layer deposition," *J. Vac. Sci. Technol. A*, vol. 20, p. 802, 2002.
- [335] J. P. Klesko, C. M. Thrush, and C. H. Winter, "Thermal atomic layer deposition of titanium films using titanium tetrachloride and 2-methyl-1,4-bis(trimethylsilyl)-2,5-cyclohexadiene or 1,4-bis(trimethylsilyl)-1,4-dihydropyrazine," *Chem. Mater.*, vol. 27, pp. 4918 – 4921, 2015.
- [336] K. J. Blakeney, P. D. Martin, and C. H. Winter, "Aluminum dihydride complexes and their unexpected application in atomic layer deposition of titanium carbonitride films," *Dalton Trans.*, vol. 47, pp. 10897–10905, 2018.
- [337] T. E. Hong, S.-K. Choi, S.-H. Kim, and T. Cheon, "Growth of highly conformal TiC<sub>x</sub> films using atomic layer deposition technique," *J. Am. Ceram. Soc.*, vol. 96, pp. 1060–1062, 2013.
- [338] R. Arteaga-Muñoz, H. Tsurugi, T. Saito, M. Yanagawa, S. Oda, and K. Mashima, "New tantalum ligand-free catalyst system for highly selective trimerization of ethylene affording 1-hexene: New evidence of a metallocycle mechanism," *J. Am. Chem. Soc.*, vol. 131, pp. 5370 – 5371, 2009.

- [339] H. Tsurugi, H. Tanahashi, H. Nishiyama, W. Fegler, T. Saito, A. Sauer, J. Okuda, and K. Mashima, "Salt-free reducing reagent of bis(trimethylsilyl)cyclohexadiene mediates multielectron reduction of chloride complexes of w(VI) and w(IV)," *J. Am. Chem. Soc.*, vol. 135, pp. 5986 – 5989, 2013.
- [340] T. Saito, H. Nishiyama, H. Tanahashi, K. Kawakita, H. Tsurugi, and K. Mashima, "1,4-bis(trimethylsilyl)-1,4-diaza-2,5-cyclohexadienes as strong salt-free reductants for generating low-valent early transition metals with electron-donating ligands," *J. Am. Chem. Soc.*, vol. 136, pp. 5161 – 5170, 2014.
- [341] R. K. Ramachandran, J. Dendooven, M. Filez, V. V. Galvita, H. Poelman, E. Solano, M. M. Minjauw, K. Devloo-Casier, E. Fonda, D. Hermida-Merino, W. Bras, G. B. Marin, and C. Detavernier, "Atomic layer deposition route to tailor nanoalloys of noble and non-noble metals," *ACS Nano*, vol. 10, pp. 8770–8777, sep 2016.
- [342] J. Hämäläinen, K. Mizohata, K. Meinander, M. Mattinen, M. Vehkamäki, J. Räisänen, M. Ritala, and M. Leskelä, "Rhenium metal and rhenium nitride thin films grown by atomic layer deposition," *Angew. Chem.*, vol. 57, pp. 14538 – 14542, 2018.
- [343] F. Niu and P. Chow, "Method of forming very reactive metal layers by a high vacuum plasma enhanced atomic layer deposition system pat no: Us9828673b2)," 2017.
- [344] "Itrs 2011, interconnect," 2011.
- [345] U. Helmersson, M. Lättemann, J. Bohlmark, A. P. Ehasarian, and J. T. Gudmundsson, "Ionized physical vapor deposition (ipvd): A review of technology and applications," *Thin Solid Films*, vol. 513, pp. 1–24, 2006.
- [346] J. Hopwood, "Ionized physical vapor deposition of integrated circuit interconnects," *Phys. Plasmas*, vol. 5, pp. 1624–1631, 1998.

- [347] R. Shaviv, A. Pradhan, M. Marshall, T. Mountsier, and G. Dixit, "A comprehensive look at pvd scaling to meet the reliability requirements of advanced technology," in *Reliability Physics Symposium, 2009 IEEE International*, pp. 855 – 860, 2009.
- [348] S. Wickramanay, H. Nagahama, E. Watanabe, M. Sato, and S. Mizuno, "Using i-pvd for copper-based interconnects," *Solid State Tech.*, vol. 45, p. 67, 2002.
- [349] L. Arnaud, D. Galpin, S. Chhun, C. Monget, E. Richard, D. Roy, C. Besset, M. Vilnay, L. Doyen, P. Waltz, E. Petitprez, F. Terrier, G. Imbert, and Y. Le Fricc, "Reliability failure modes in interconnects for the 45 nm technology node and beyond," in *Interconnect Technology Conference, 2009. IITC 2009. IEEE International*, 2009.
- [350] K. Motoyama, O. van der Straten, H. Tomizawa, J. Maniscalco, and S. Chen, "Novel cu reflow seed process for cu/low-k 64nm pitch dual damascene interconnects and beyond," in *IITC*, 2012.
- [351] B. Havemann, "Cu/low k interconnect technologies for 32nm and beyond." Fudan University International Interconnect Symposium, May 2008.
- [352] L. J. Friedrich, S. K. Dew, M. J. Brett, and T. Smy, "A simulation study of copper reflow characteristics in vias," *IEEE Trans. Semicond. Manuf.*, vol. 12, pp. 353 – 365, 1999.
- [353] L. J. Friedrich, D. S. Gardner, S. K. Dew, M. J. Brett, and T. Smy, "Study of the copper reflow process using the grofilms simulator," *J. Vac. Sci. Technol. B*, vol. 15, pp. 1780 – 1787, 1997.
- [354] C.-C. Yang, F. R. McFeely, B. Li, R. Rosenberg, and D. Edelstein, "Low-temperature reflow anneals of cu on ru," *IEEE Electron Device Lett.*, vol. 32, pp. 806 – 808, 2011.
- [355] C.-C. Yang, P. Flaitz, and D. Edelstein, "Characterization of cu reflows on ru," *IEEE Electron Device Lett.*, vol. 32, pp. 1430 – 1432, 2011.

- [356] T. P. Moffat, M. Walker, P. J. Chen, J. E. Bonevich, W. F. Egelhoff, L. Richter, C. Witt, T. Aaltonen, M. Ritala, M. Leskelä, and D. Josella, "Electrodeposition of cu on ru barrier layers for damascene processing," *J. Electrochem. Soc.*, vol. 153, pp. C37–C50, 2006.
- [357] C. Bjelkevig and J. Kelber, "Stability of iodine on ruthenium during copper electrodeposition and its effects on the nucleation behavior of electrodeposited copper," *Electrochim. Acta*, vol. 54, pp. 3892 – 3898, 2009.
- [358] L. D'Urzo, S. Schaltin, A. Shkurankov, H. Plank, G. Kothleitner, C. Gspan, K. Binnemans, and J. Fransaer, "Direct-on-barrier copper electroplating on ruthenium from the ionic liquid 1-ethyl-3-methylimidazolium dicyanamide," *J. Mater. Sci.: Mater. Electron.*, vol. 23, pp. 945 – 951, 2012.
- [359] J. J. Kelly, T. Vo, O. van der Staten, Q. Huang, B. Baker, X. Shao, S. Chiang, and J. O. Dukovic, "Morphology of electrodeposited cu on 300 mm peald ru substrates," *ECST*, vol. 16, pp. 201–207, 2008.
- [360] R. Akolkar, T. Indukuri, J. Clarke, T. Ponnuswamy, J. Reid, A. J. McKerrow, and S. Varadarajan, "Direct seed electroplating of copper on ruthenium liners," in *Interconnect Technology Conference and 2011 Materials for Advanced Metallization (IITC/MAM), 2011 IEEE International*, 2011.
- [361] B. Han, J. Wu, C. Zhou, B. Chen, R. Gordon, X. Lei, D. A. Roberts, and H. Cheng, "First-principles simulations of conditions of enhanced adhesion between copper and tan(111) surfaces using a variety of metallic glue materials," *Angew. Chem. Int. Edit.*, vol. 49, pp. 148 – 152, 2010.
- [362] E. S. Hwang and J. Lee, "Surfactant-catalyzed chemical vapor deposition of copper thin films," *Chem. Mater.*, vol. 12, pp. 2076–2081, 2000.
- [363] K.-C. Shim, H.-B. Lee, O.-K. Kwon, H.-S. Park, W. Koh, and S.-W. Kang, "Bottom-up filling of submicrometer features in catalyst-enhanced chemical vapor deposition of copper," *J. Electrochem. Soc.*, vol. 149, pp. G109 – G113, 2002.

- [364] D. Josell, D. Wheeler, and T. P. Moffat, "Superconformal deposition by surfactant-catalyzed chemical vapor deposition," *Electrochem. Solid State Lett.*, vol. 5, pp. C44 – C47, 2002.
- [365] S. G. Pyo, S. Kim, D. Wheeler, T. P. Moffat, and D. Josella, "Seam-free fabrication of submicrometer copper interconnects by iodine-catalyzed chemical vapor deposition," *J. Appl. Phys.*, vol. 93, pp. 1257 – 1261, 2003.
- [366] D. Josell, S. Kim, D. Wheeler, T. P. Moffat, , and S. G. Pyo, "Interconnect fabrication by superconformal iodine-catalyzed chemical vapor deposition of copper," *J. Electrochem. Soc.*, vol. 150, pp. C368 – C373, 2003.
- [367] Y. Au, Y. Lin, and R. G. Gordon, "Filling narrow trenches by iodine-catalyzed cvd of copper and manganese on manganese nitride barrier/adhesion layers," *J. Electrochem. Soc.*, vol. 158, pp. D248 – D253, 2011.
- [368] "Itrs 2011, front end processes," 2011.
- [369] C. C. Hobbs, L. R. C. Fonseca, A. Knizhnik, V. Dhandapani, S. B. Samavedam, W. J. Taylor, J. M. Grant, L. G. Dip, D. H. Triyoso, R. I. Hegde, D. C. Gilmer, R. Garcia, D. Roan, M. L. Lovejoy, R. S. Rai, E. A. Hebert, H.-H. Tseng, S. G. H. Anderson, B. E. White, and P. J. Tobin, "Fermi-level pinning at the polysilicon/metal oxide interface-part i," *IEEE T. Electron. Dev.*, vol. 51, pp. 971 – 977, 2004.
- [370] M. V. Fischetti, D. A. Neumayer, and E. A. Cartier, "Effective electron mobility in si inversion layers in metal-oxide-semiconductor systems with a high-k insulator: The role of remote phonon scattering," *J. Appl. Phys.*, vol. 90, pp. 4587 – 4608, 2001.
- [371] J.-P. Colinge, C.-W. Lee, A. Afzalian, N. D. Akhavan, R. Yan, I. Ferain, P. Razavi, B. O'Neill, A. Blake, M. White, A.-M. Kelleher, B. McCarthy, and R. Murphy, "Nanowire transistors without junctions," *Nature Nanotech.*, vol. 5, pp. 225 – 229, 2010.

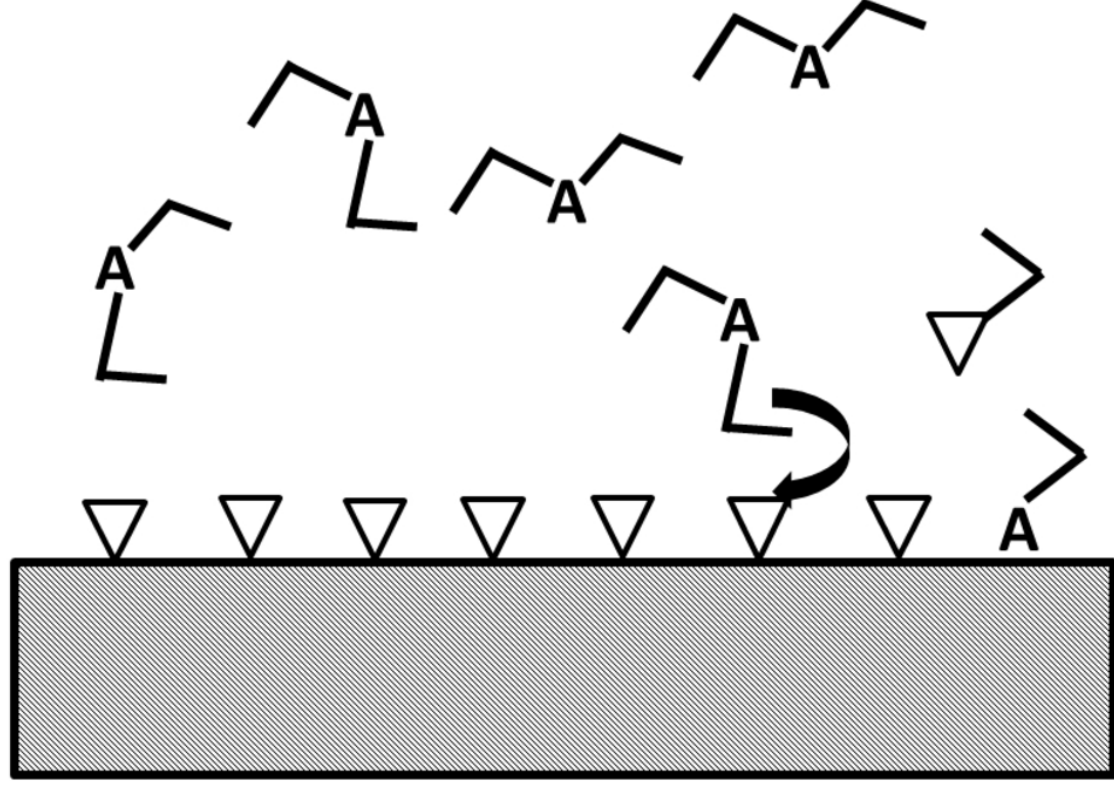
This is the author's peer reviewed, accepted manuscript. However, the online version of record will be different from this version once it has been copyedited and typeset.

PLEASE CITE THIS ARTICLE AS DOI: 10.1063/1.5087759

- [372] J. Moon, H. J. Ahn, Y. Seo, T. I. Lee, C.-K. Kim, I. C. Rho, C. H. Kim, W. S. Hwang, and B. J. Cho, "The work function behavior of aluminum-doped titanium carbide grown by atomic layer deposition," *IEEE Transactions on Electron Devices*, vol. 63, pp. 1423–1427, 2016.
- [373] H. Kim, J. Yoon, and H.-B.-R. Lee, "Atomic layer deposition for nanoscale contact applications," in *Interconnect Technology Conference and 2011 Materials for Advanced Metallization (IITC/MAM), 2011 IEEE International*, 2011.
- [374] H.-B.-R. Lee, J. Y. Son, and H. Kim, "Nitride mediated epitaxy of  $\text{CoSi}_2$  through self-interlayer-formation of plasma-enhanced atomic layer deposition co," *Appl. Phys. Lett.*, vol. 90, p. 213509, 2007.
- [375] H. Mistry, F. Behafarid, R. Reske, A. S. Varela, P. Strasser, and B. R. Cuenya, "Tuning catalytic selectivity at the mesoscale via interparticle interactions," *ACS Catalysis*, vol. 6, pp. 1075–1080, 2016.
- [376] M. Nesselberger, M. Roefzaad, R. F. Hamou, P. U. Biedermann, F. F. Schweinberger, S. Kunz, K. Schloegl, G. K. H. Wiberg, S. Ashton, U. Heiz, K. J. J. Mayrhofer, and M. Arenz, "The effect of particle proximity on the oxygen reduction rate of size-selected platinum clusters," *Nature Materials*, vol. 12, pp. 919–924, 2013.
- [377] M. Filez, H. Poelman, E. A. Redekop, V. V. Galvita, K. Alexopoulos, M. Meledina, R. K. Ramachandran, J. Dendooven, C. Detavernier, G. V. Tendeloo, O. V. Safonova, M. Nachtegaal, B. M. Weckhuysen, and G. B. Marin, "Kinetics of lifetime changes in bimetallic nanocatalysts revealed by quick x-ray absorption spectroscopy," *Angew. Chem.*, vol. 57, pp. 12430 – 12434, 2018.

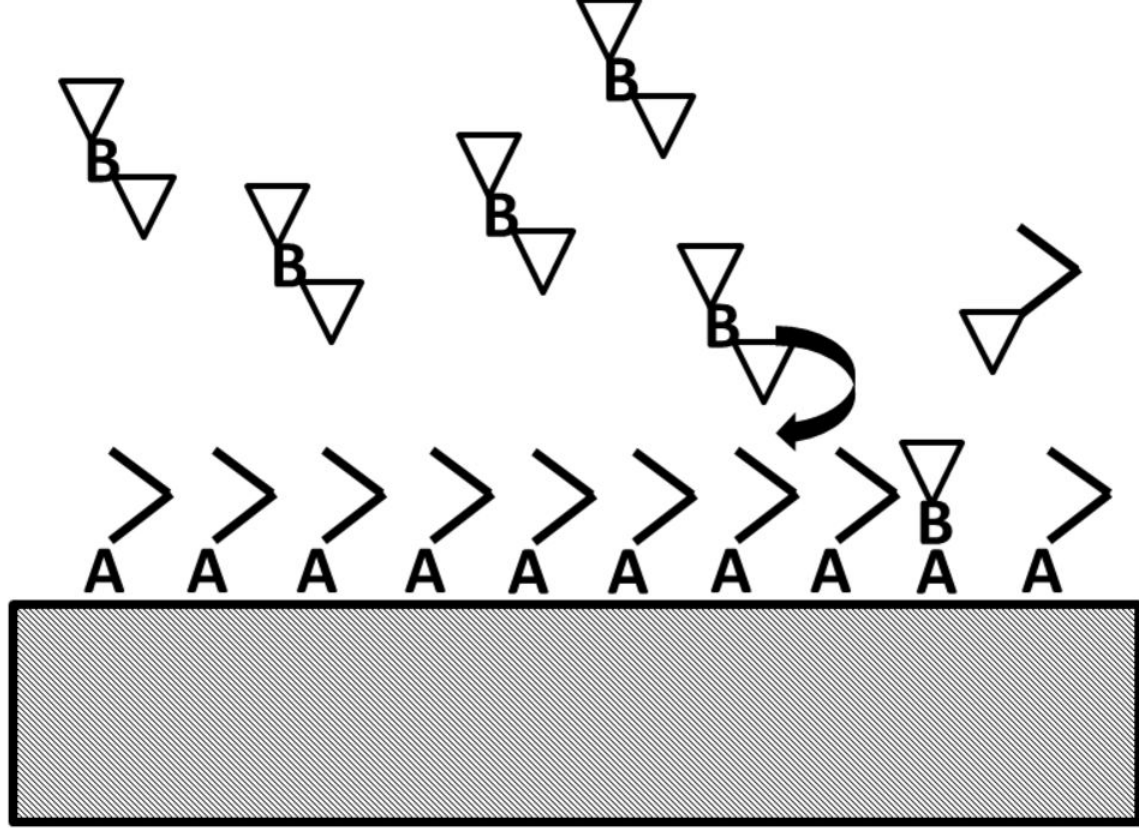
This is the author's peer reviewed, accepted manuscript. However, the online version of record will be different from this version once it has been copyedited and typeset.

PLEASE CITE THIS ARTICLE AS DOI: 10.1063/1.5087759



This is the author's peer reviewed, accepted manuscript. However, the online version of record will be different from this version once it has been copyedited and typeset.

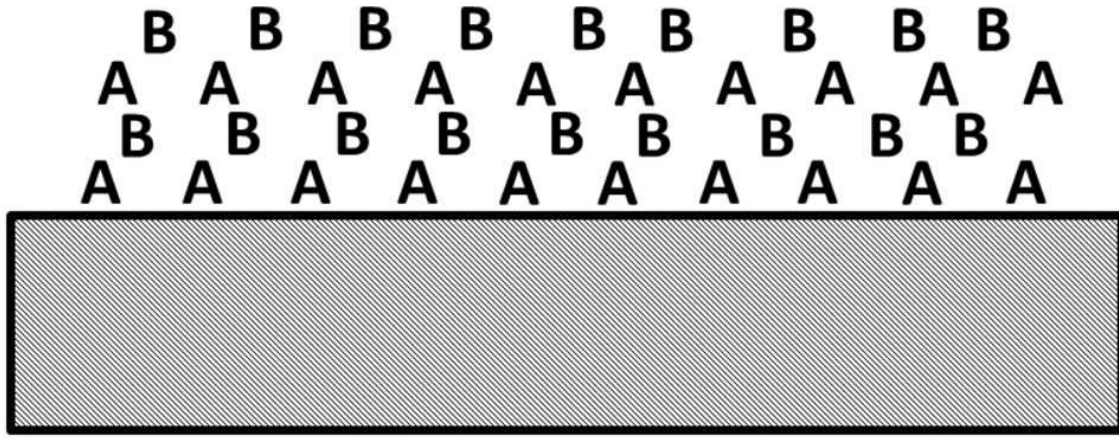
PLEASE CITE THIS ARTICLE AS DOI: 10.1063/1.5087759





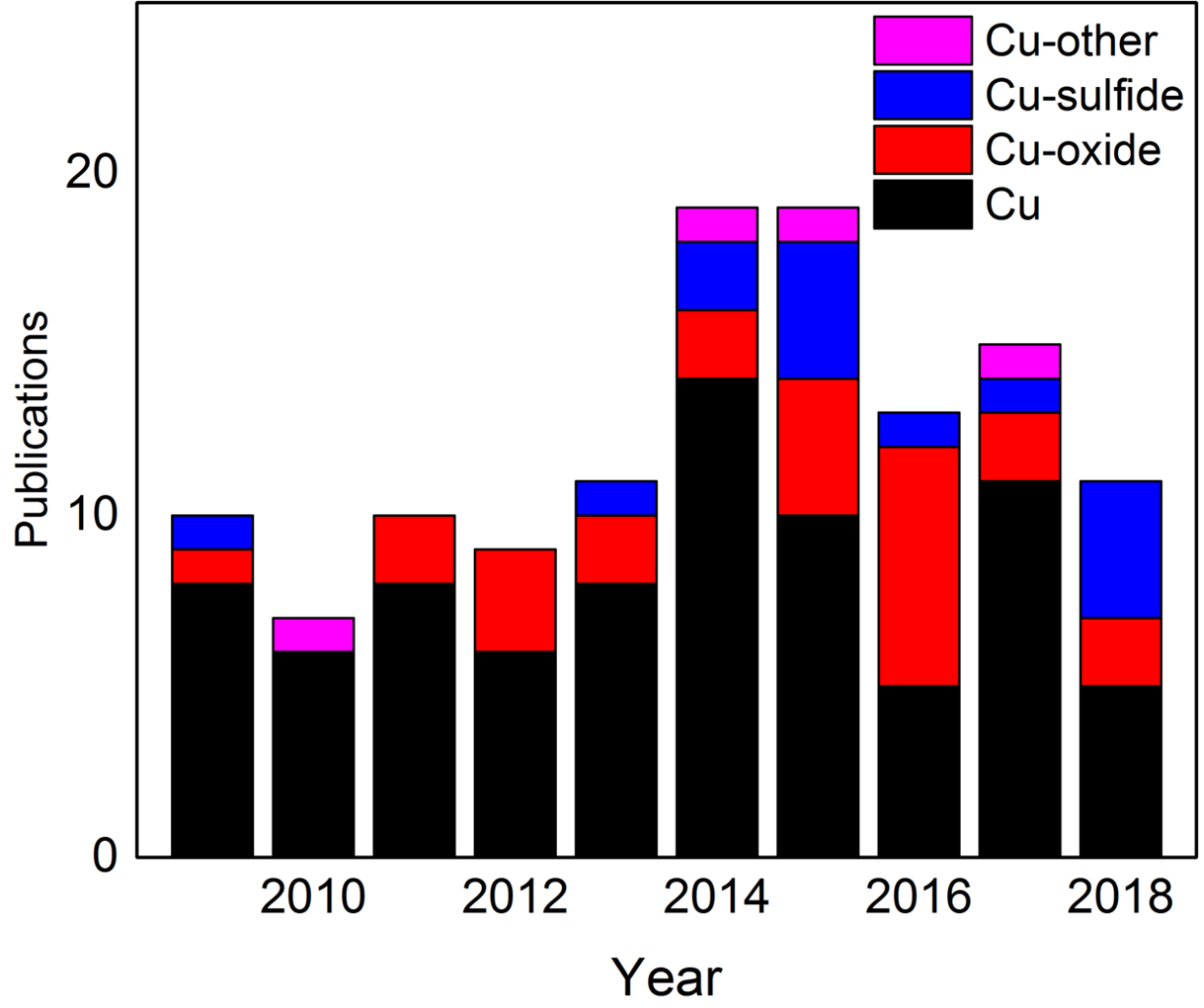
This is the author's peer reviewed, accepted manuscript. However, the online version of record will be different from this version once it has been copyedited and typeset.

PLEASE CITE THIS ARTICLE AS DOI: 10.1063/1.5087759



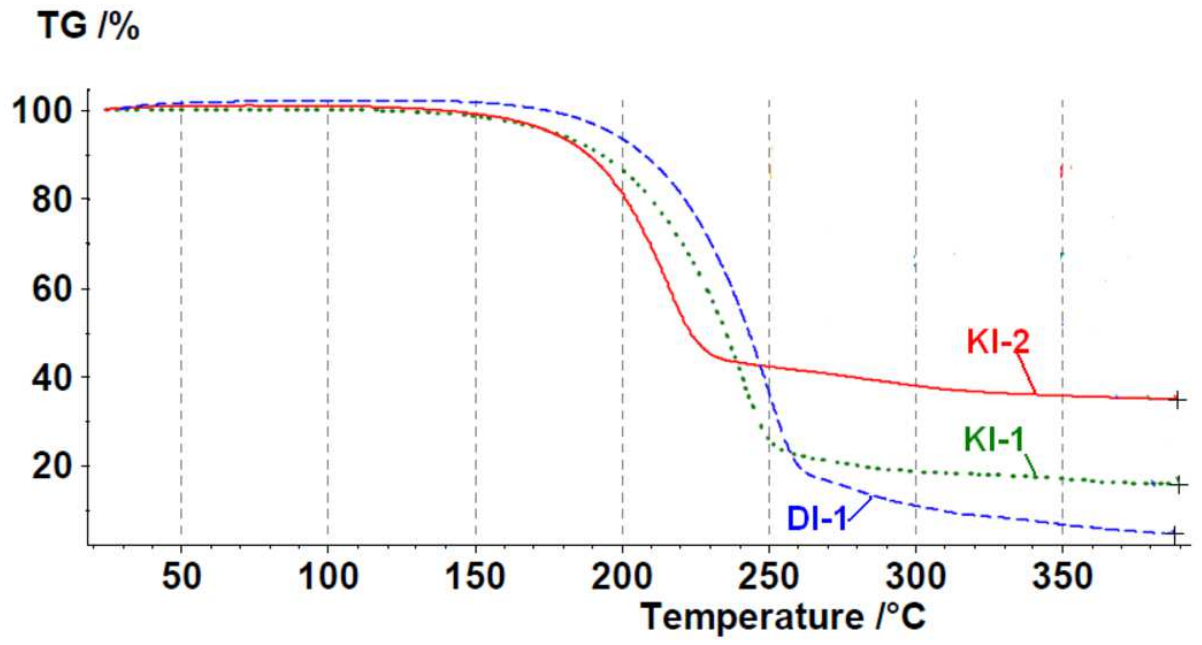
This is the author's peer reviewed, accepted manuscript. However, the online version of record will be different from this version once it has been copyedited and typeset.

PLEASE CITE THIS ARTICLE AS DOI: 10.1063/1.5087759



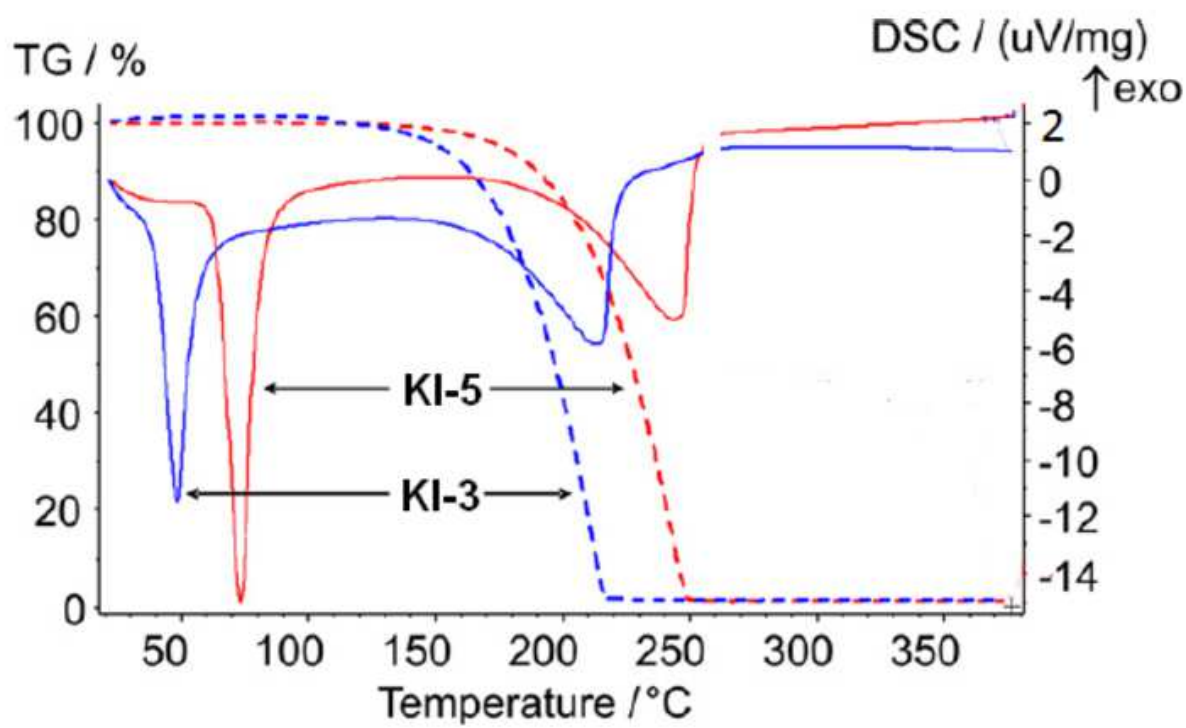
This is the author's peer reviewed, accepted manuscript. However, the online version of record will be different from this version once it has been copyedited and typeset.

PLEASE CITE THIS ARTICLE AS DOI: 10.1063/1.5087759



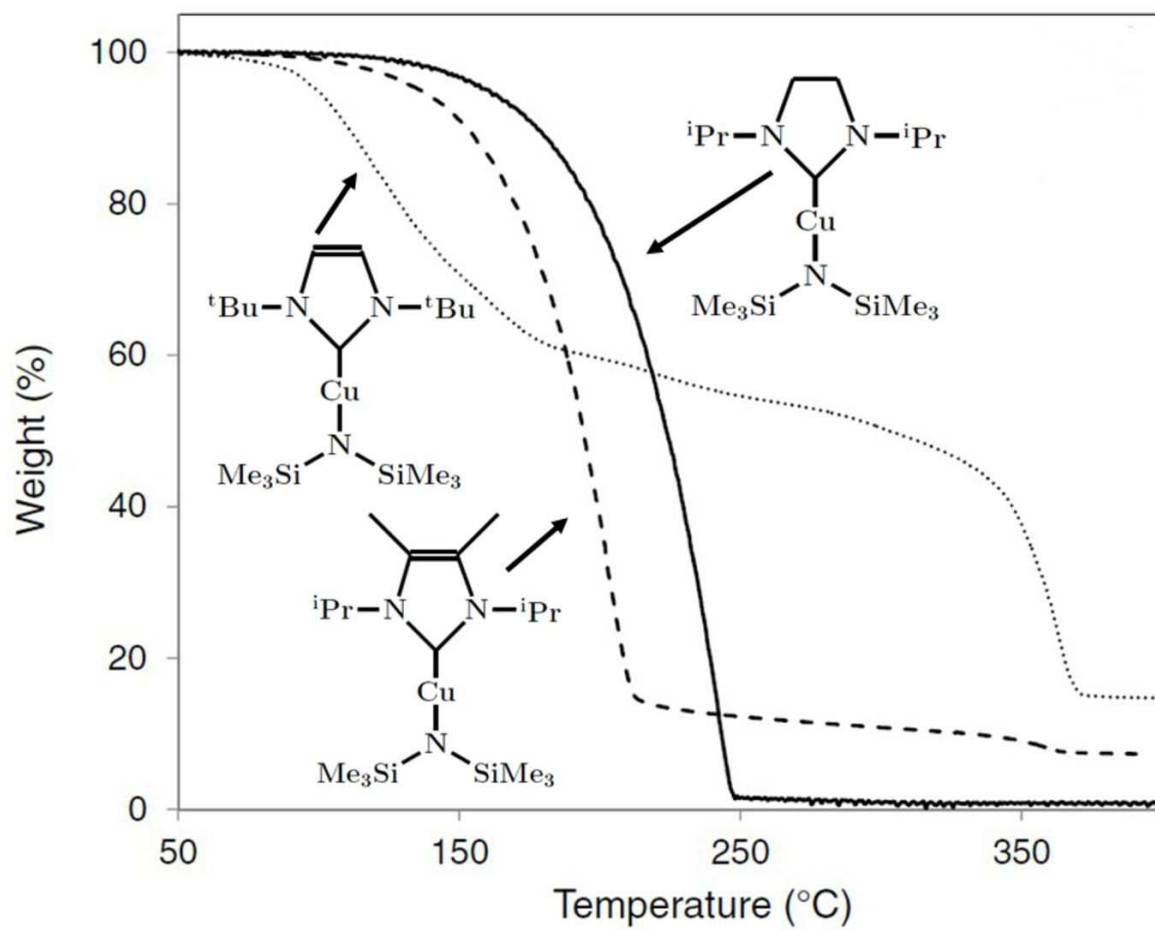
This is the author's peer reviewed, accepted manuscript. However, the online version of record will be different from this version once it has been copyedited and typeset.

PLEASE CITE THIS ARTICLE AS DOI: 10.1063/1.5087759



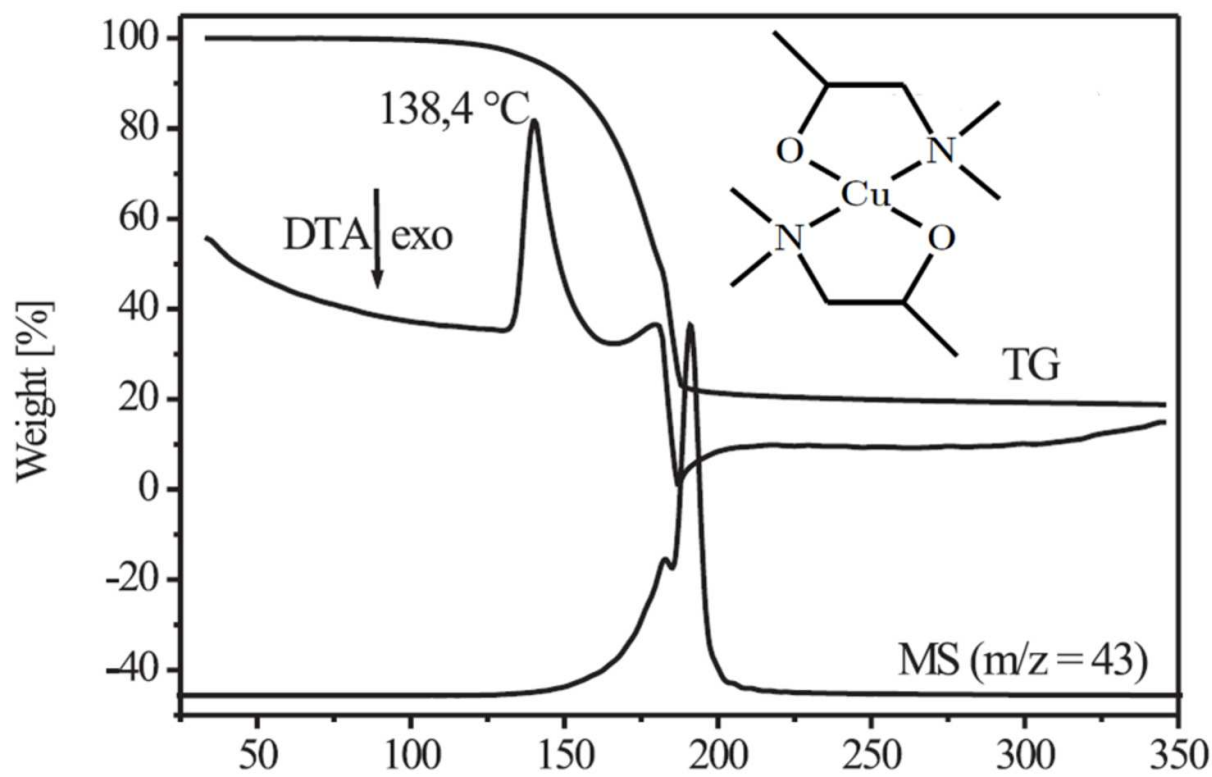
This is the author's peer reviewed, accepted manuscript. However, the online version of record will be different from this version once it has been copyedited and typeset.

PLEASE CITE THIS ARTICLE AS DOI: 10.1063/1.5087759



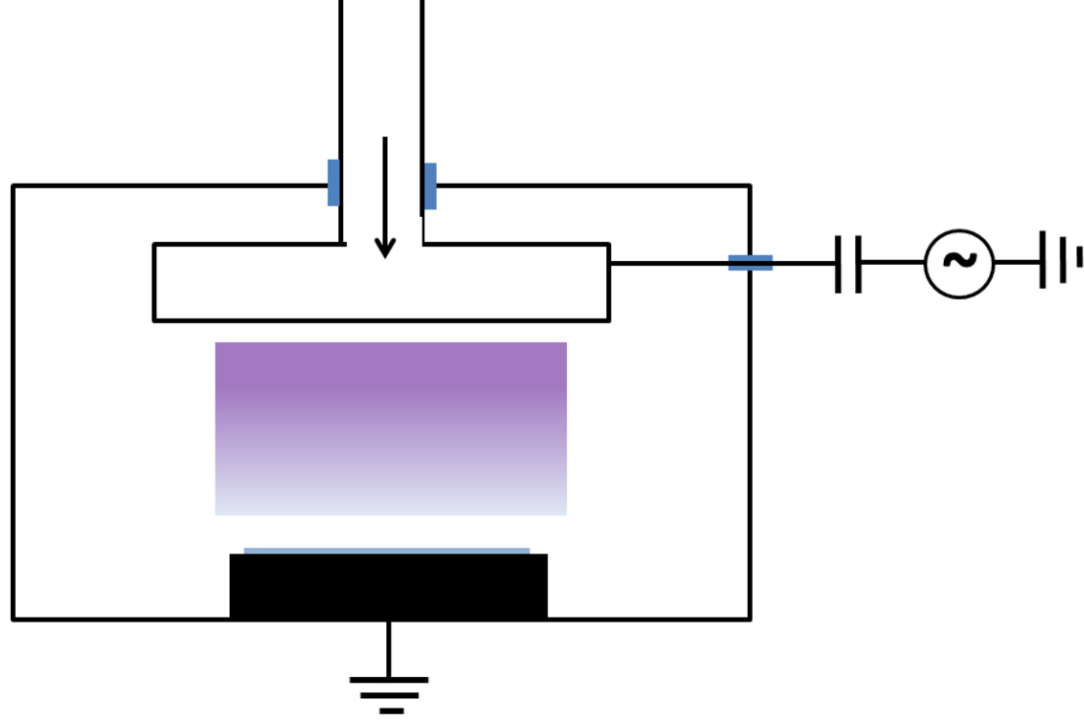
This is the author's peer reviewed, accepted manuscript. However, the online version of record will be different from this version once it has been copyedited and typeset.

PLEASE CITE THIS ARTICLE AS DOI: 10.1063/1.5087759



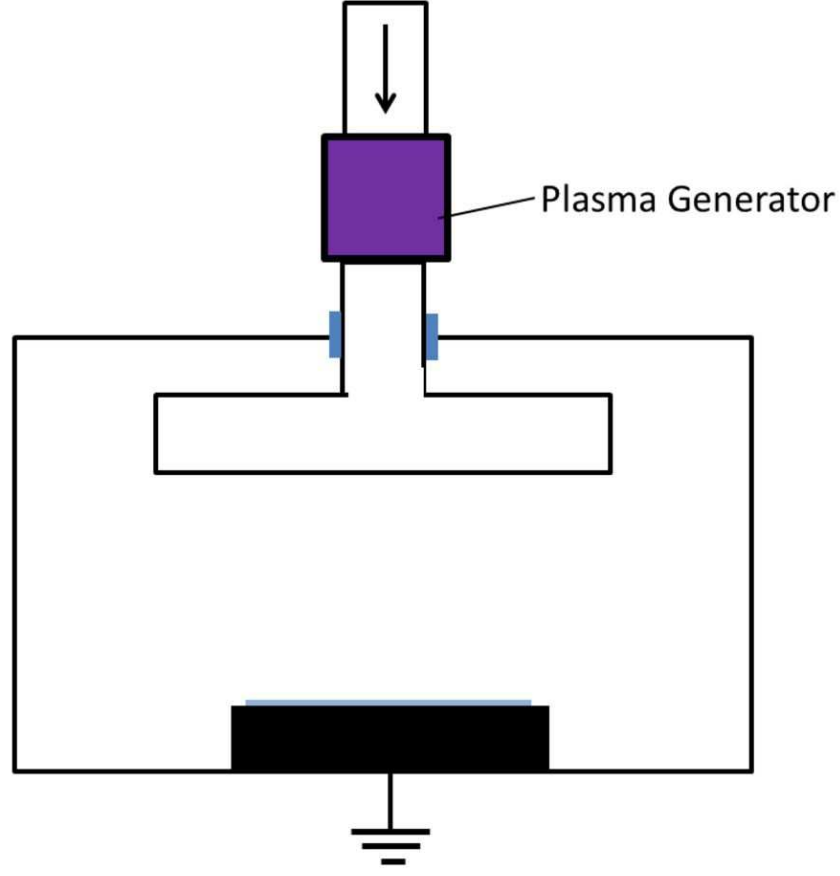
This is the author's peer reviewed, accepted manuscript. However, the online version of record will be different from this version once it has been copyedited and typeset.

PLEASE CITE THIS ARTICLE AS DOI: 10.1063/1.5087759



This is the author's peer reviewed, accepted manuscript. However, the online version of record will be different from this version once it has been copyedited and typeset.

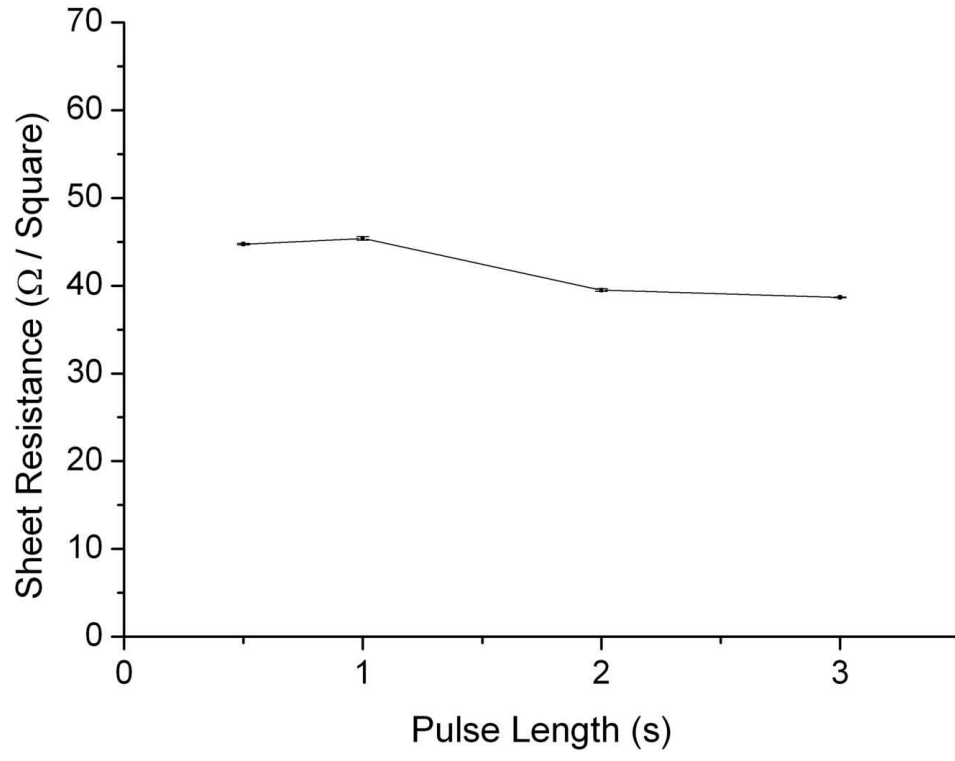
PLEASE CITE THIS ARTICLE AS DOI: 10.1063/1.5087759





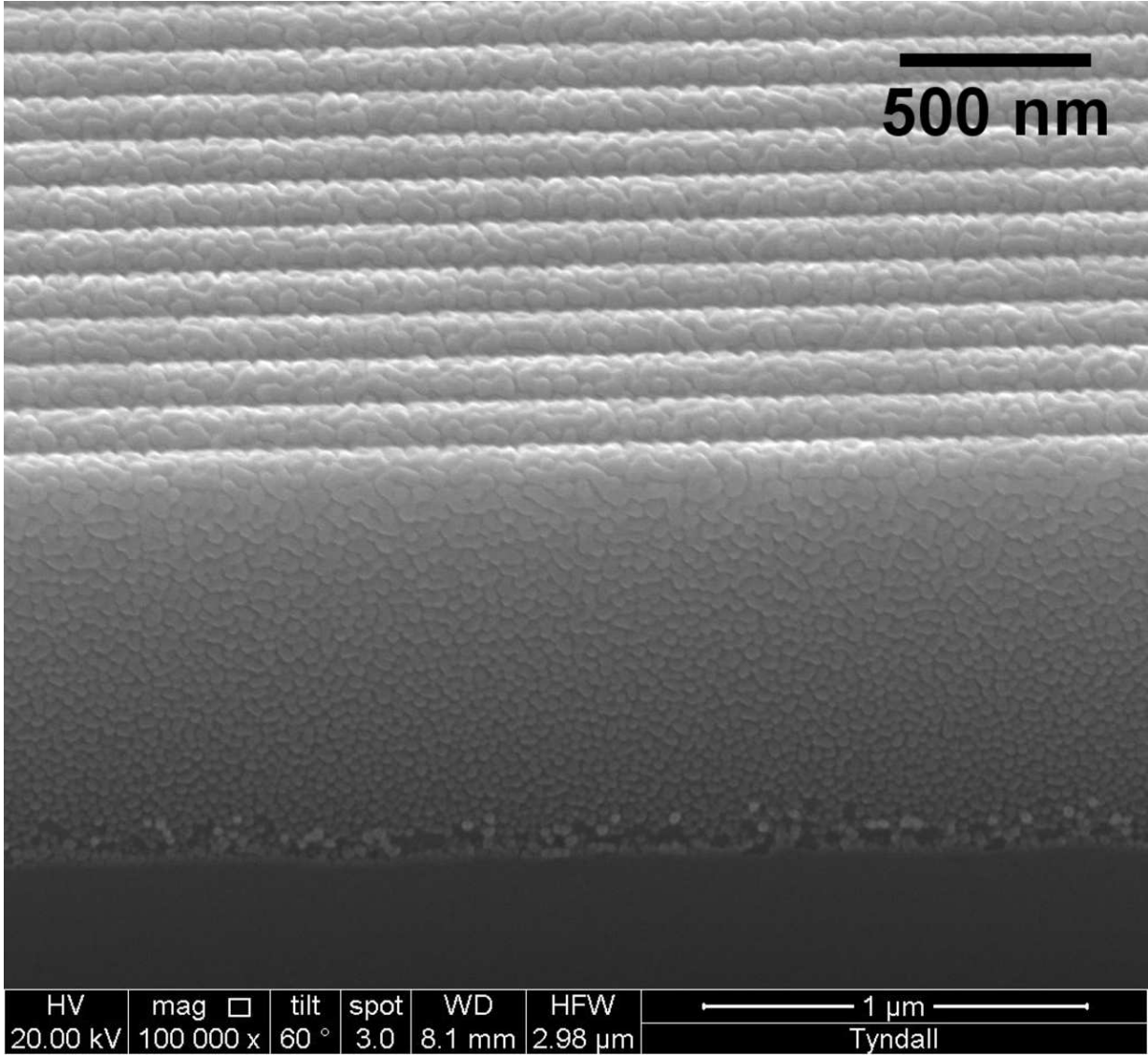
This is the author's peer reviewed, accepted manuscript. However, the online version of record will be different from this version once it has been copyedited and typeset.

PLEASE CITE THIS ARTICLE AS DOI: 10.1063/1.5087759



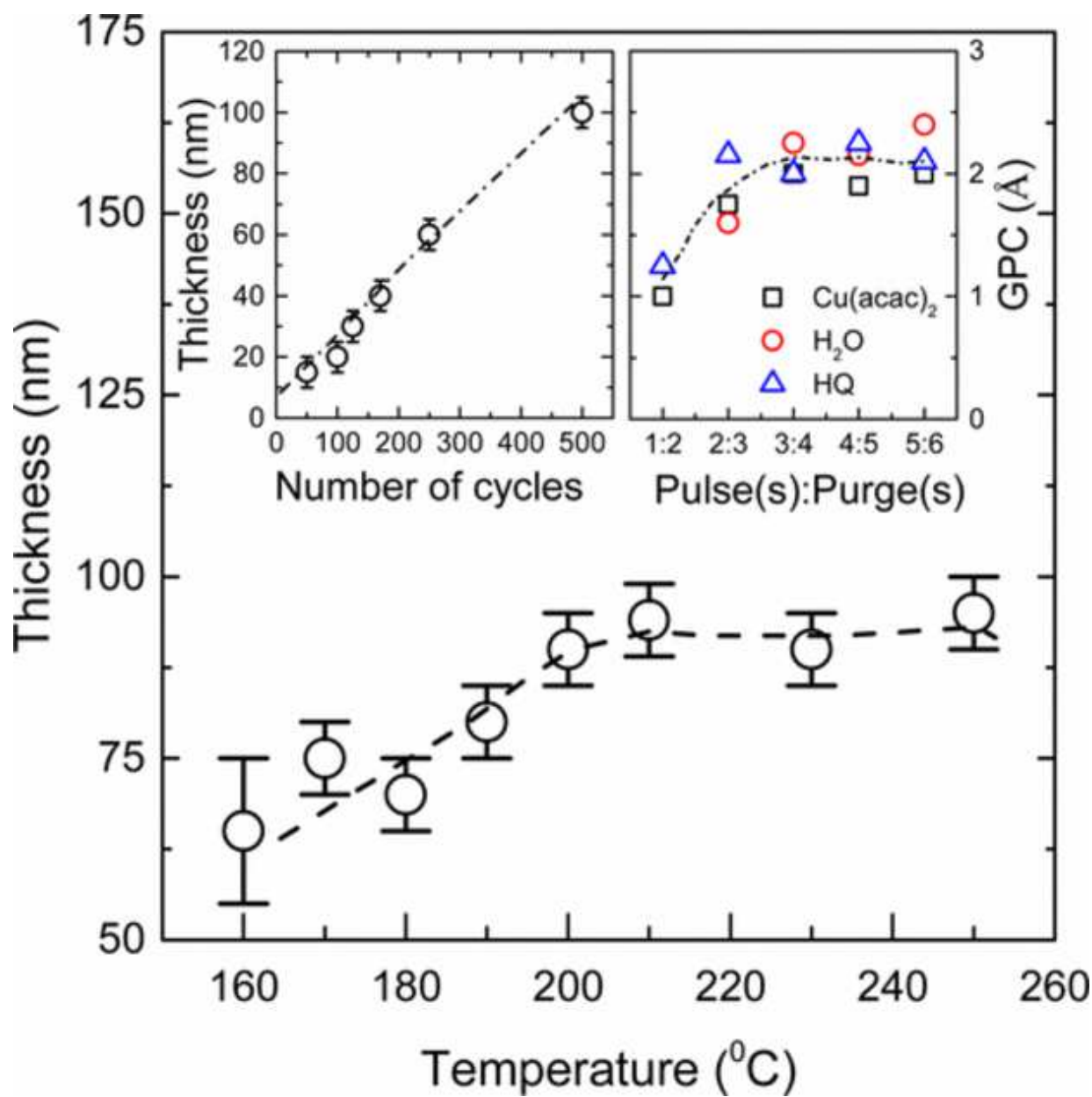
This is the author's peer reviewed, accepted manuscript. However, the online version of record will be different from this version once it has been copyedited and typeset.

PLEASE CITE THIS ARTICLE AS DOI: 10.1063/1.5087759



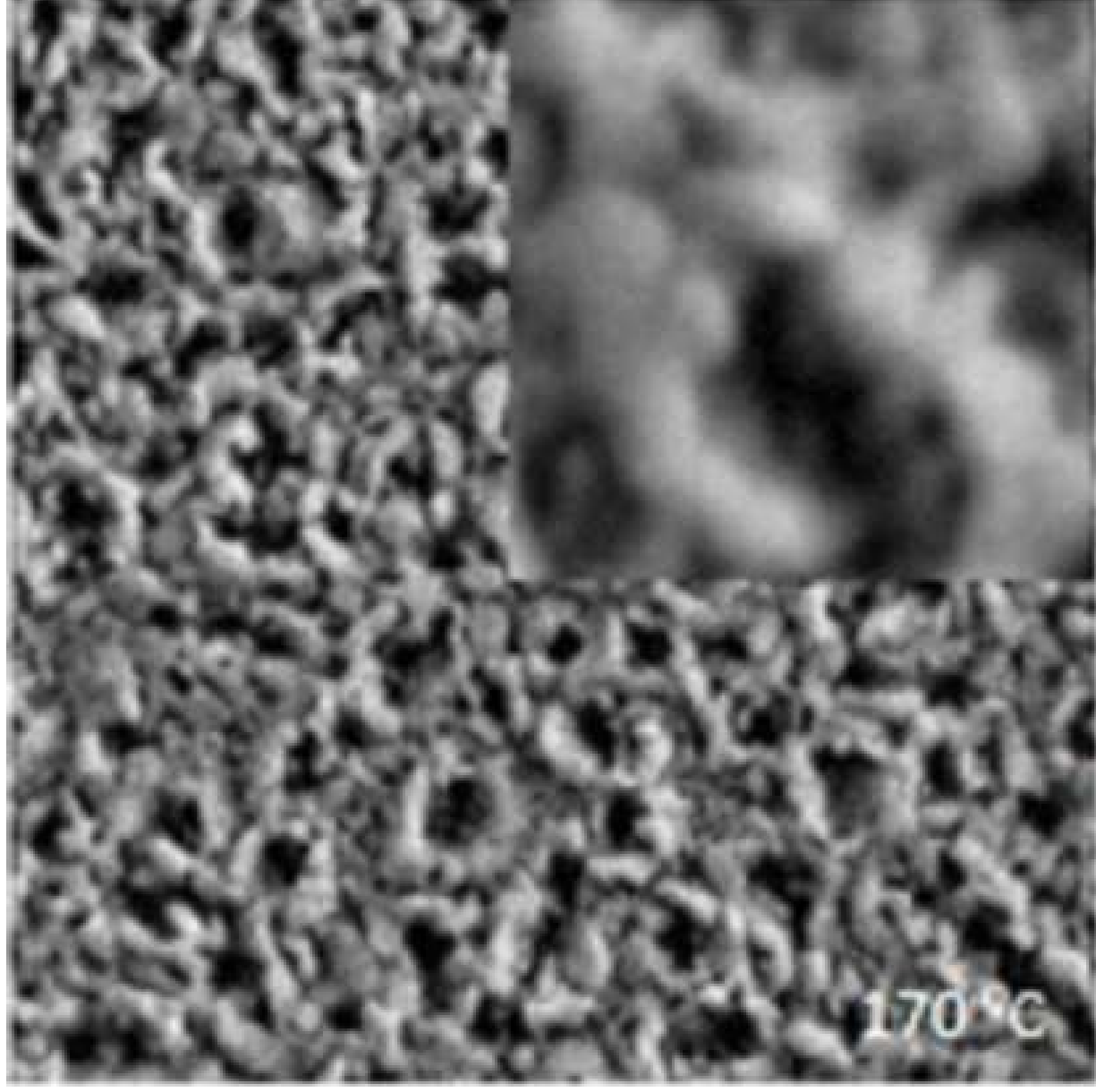
This is the author's peer reviewed, accepted manuscript. However, the online version of record will be different from this version once it has been copyedited and typeset.

PLEASE CITE THIS ARTICLE AS DOI: 10.1063/1.5087759



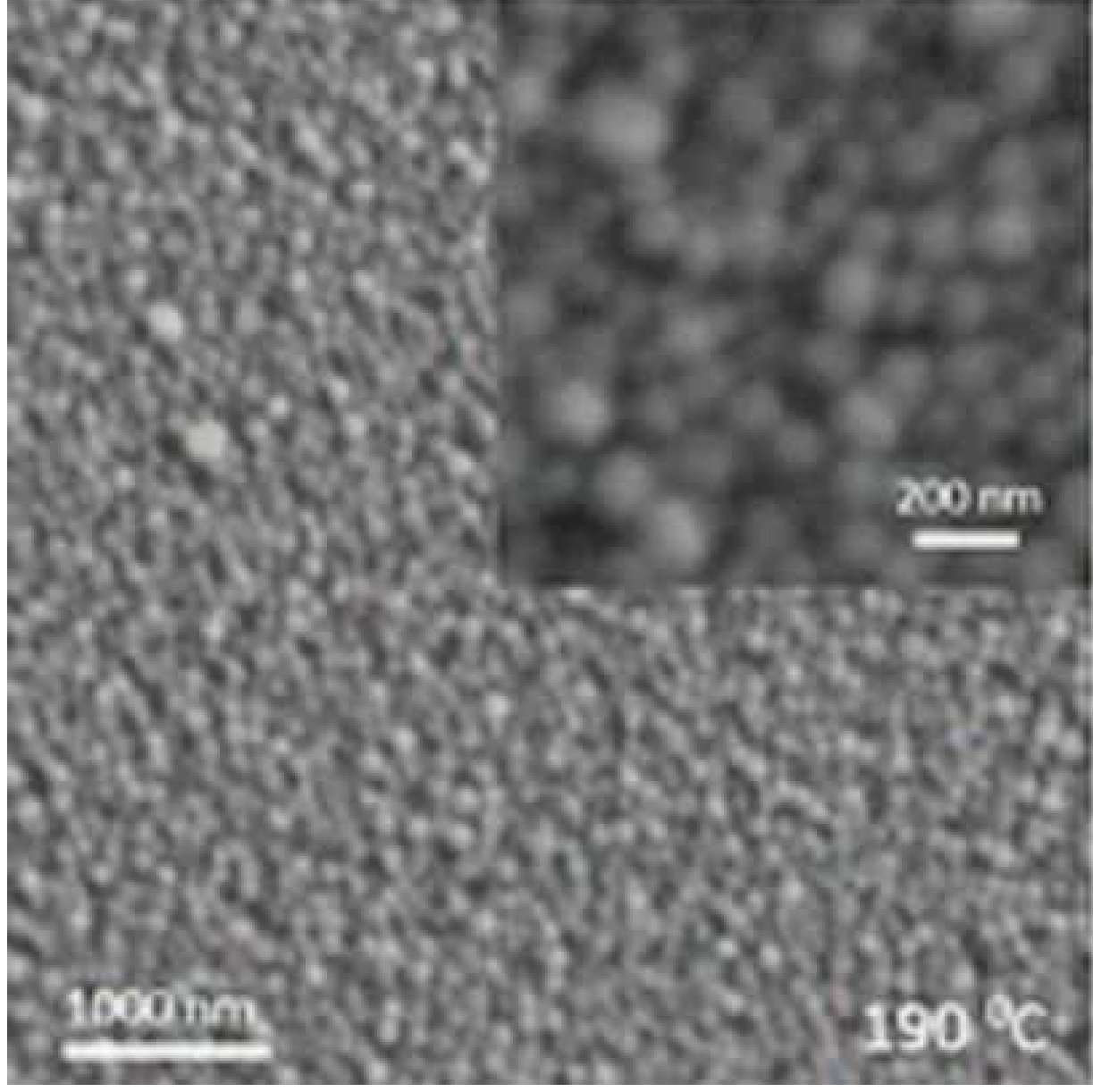
This is the author's peer reviewed, accepted manuscript. However, the online version of record will be different from this version once it has been copyedited and typeset.

PLEASE CITE THIS ARTICLE AS DOI: 10.1063/1.5087759



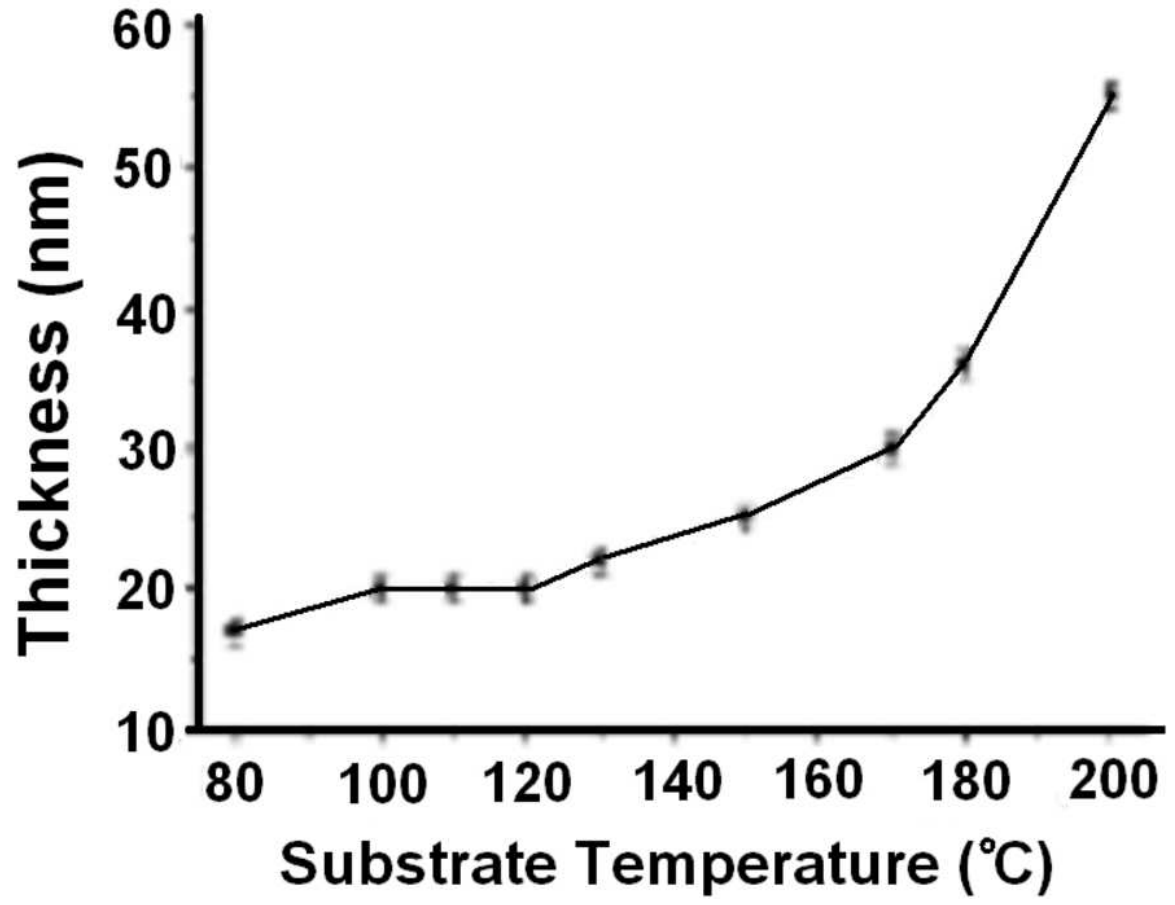
This is the author's peer reviewed, accepted manuscript. However, the online version of record will be different from this version once it has been copyedited and typeset.

PLEASE CITE THIS ARTICLE AS DOI: 10.1063/1.5087759



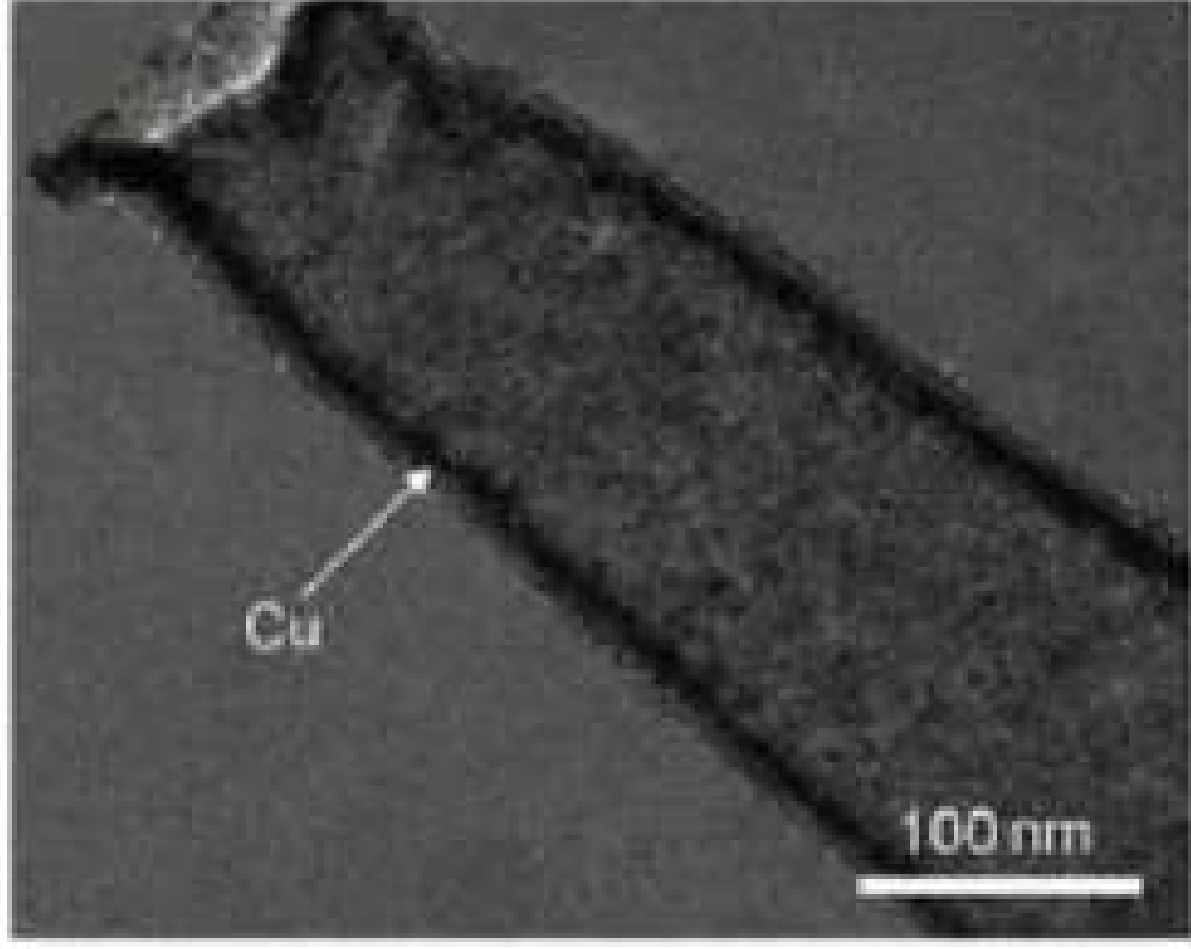
This is the author's peer reviewed, accepted manuscript. However, the online version of record will be different from this version once it has been copyedited and typeset.

PLEASE CITE THIS ARTICLE AS DOI: 10.1063/1.5087759



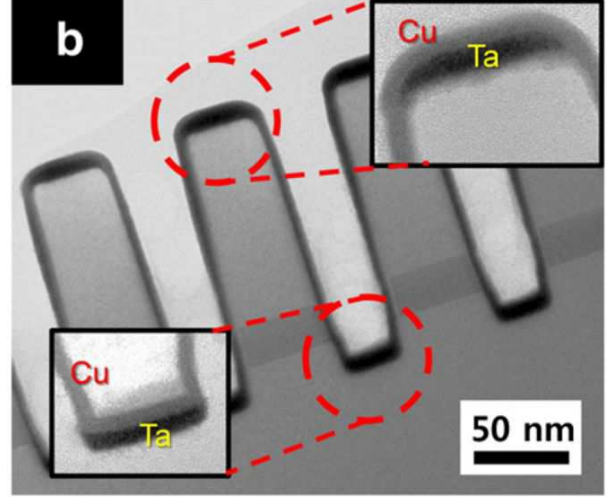
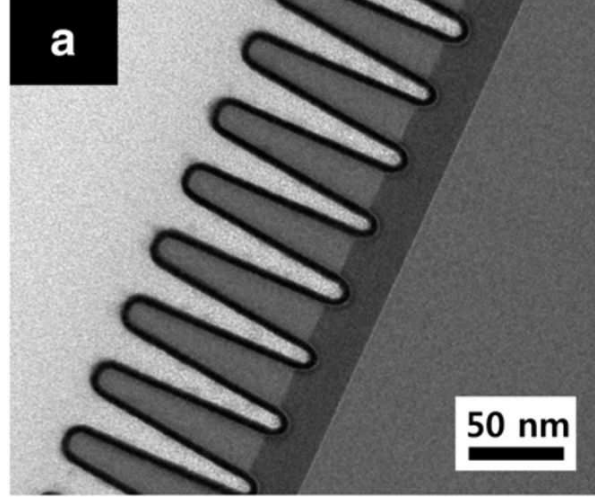
This is the author's peer reviewed, accepted manuscript. However, the online version of record will be different from this version once it has been copyedited and typeset.

PLEASE CITE THIS ARTICLE AS DOI: 10.1063/1.5087759



This is the author's peer reviewed, accepted manuscript. However, the online version of record will be different from this version once it has been copyedited and typeset.

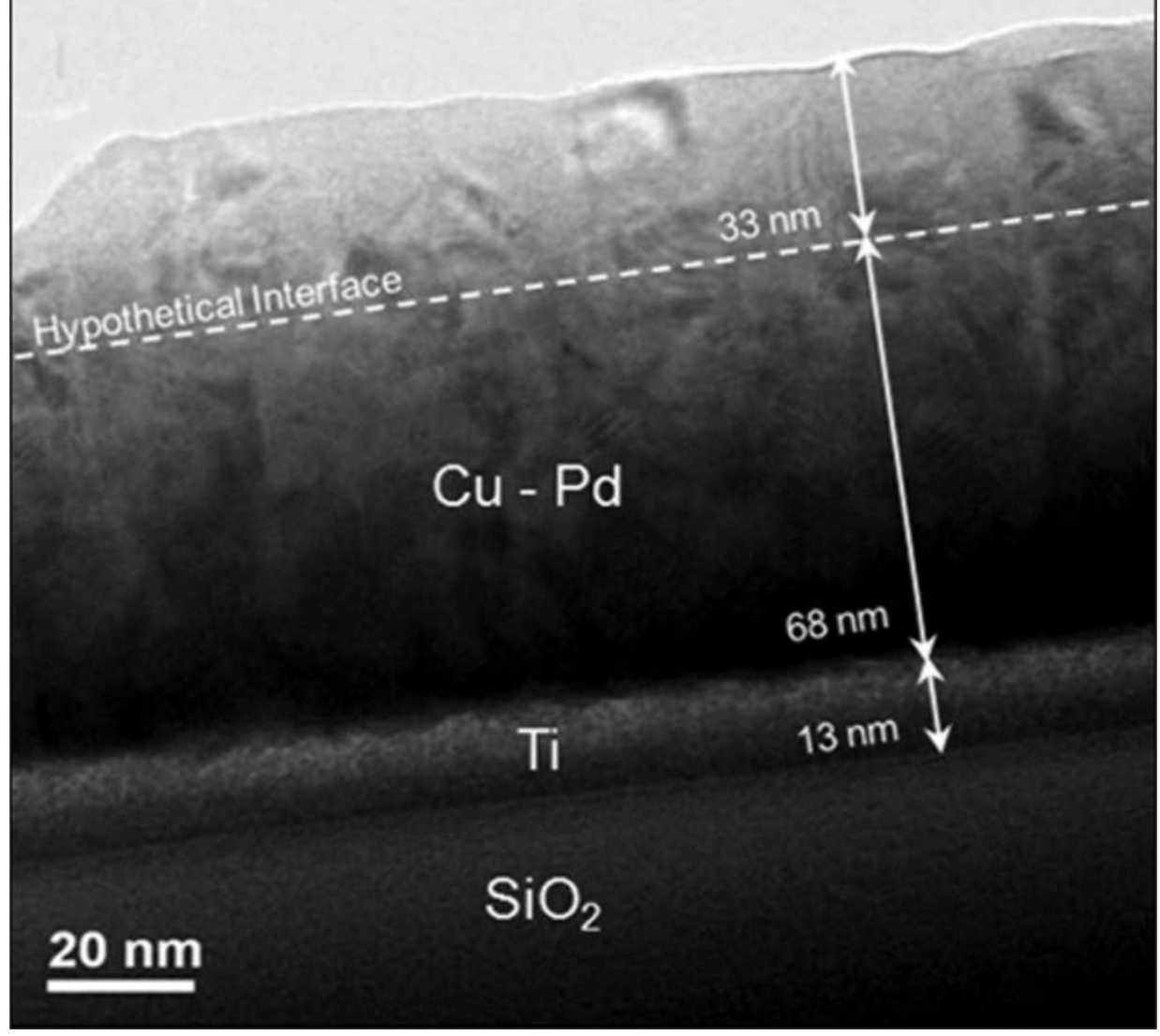
PLEASE CITE THIS ARTICLE AS DOI: 10.1063/1.5087759





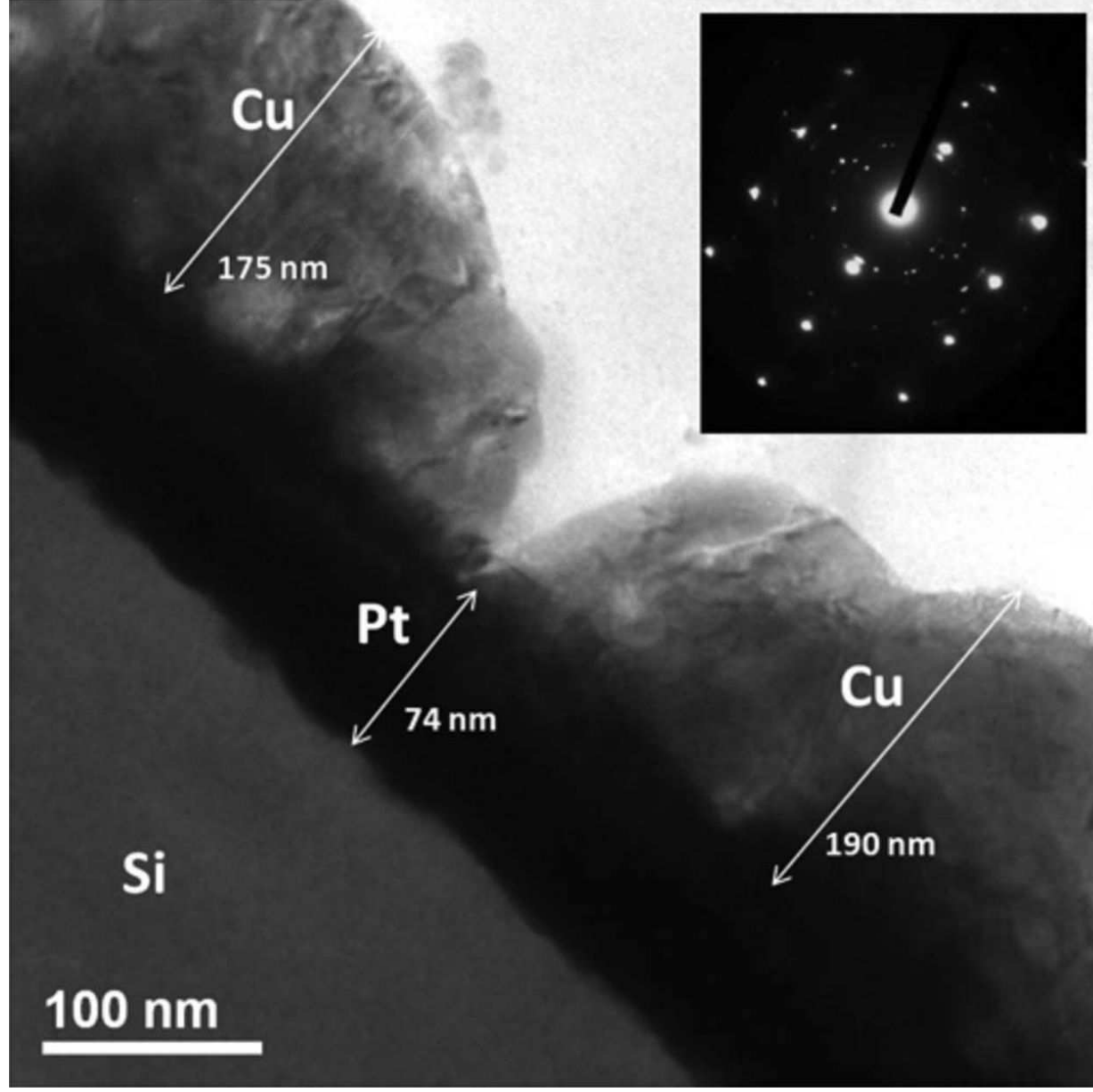
This is the author's peer reviewed, accepted manuscript. However, the online version of record will be different from this version once it has been copyedited and typeset.

PLEASE CITE THIS ARTICLE AS DOI: 10.1063/1.5087759



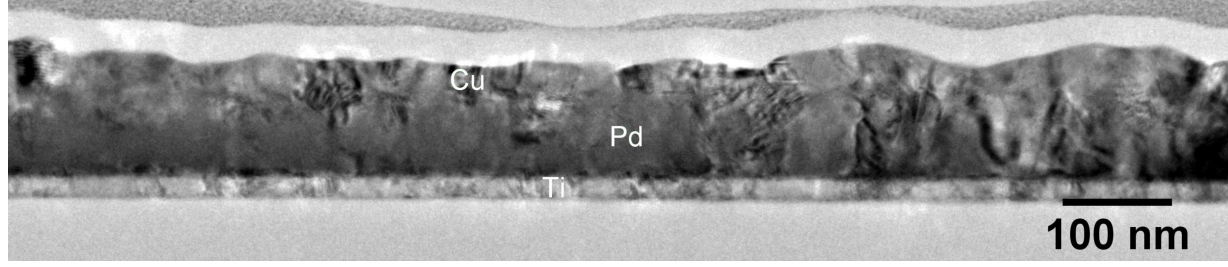
This is the author's peer reviewed, accepted manuscript. However, the online version of record will be different from this version once it has been copyedited and typeset.

PLEASE CITE THIS ARTICLE AS DOI: 10.1063/1.5087759



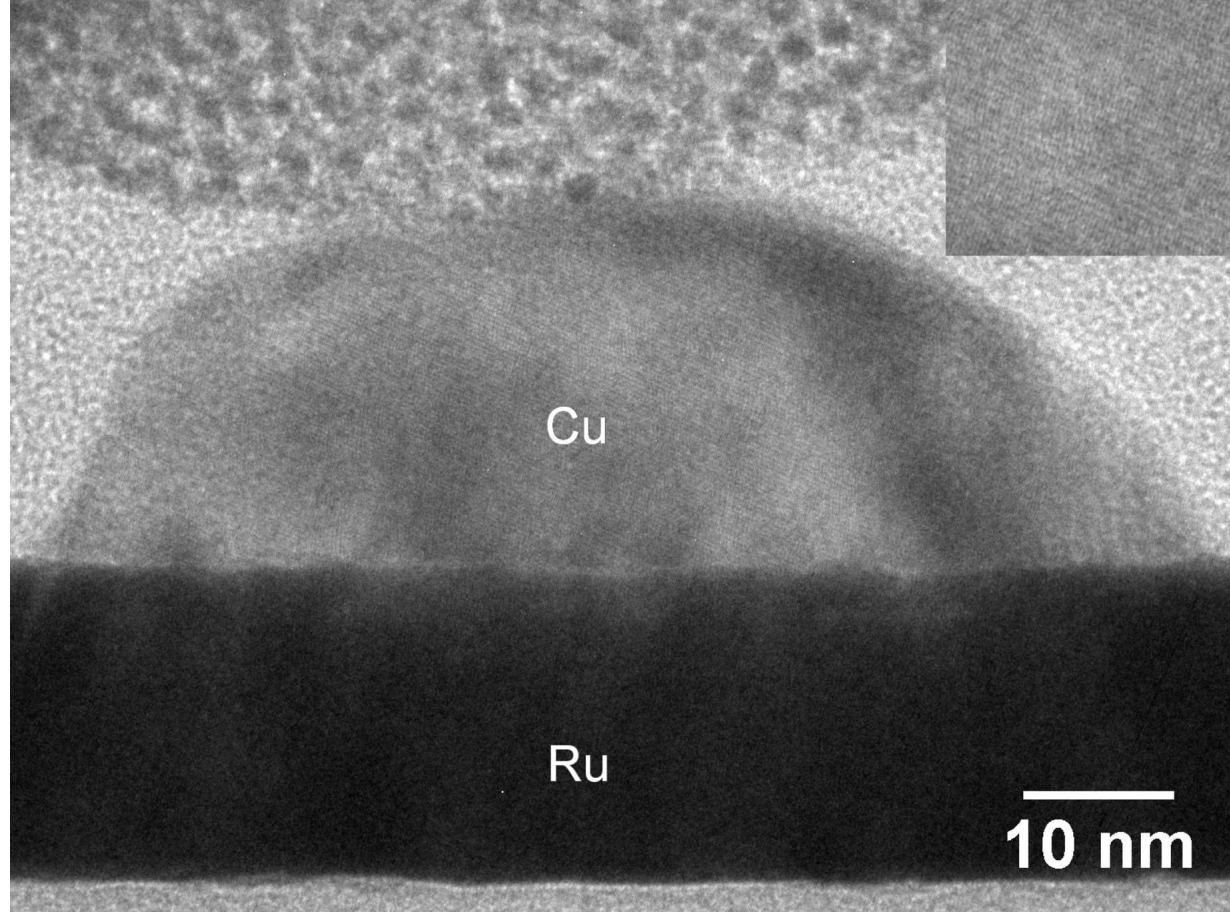
This is the author's peer reviewed, accepted manuscript. However, the online version of record will be different from this version once it has been copyedited and typeset.

PLEASE CITE THIS ARTICLE AS DOI: 10.1063/1.5087759



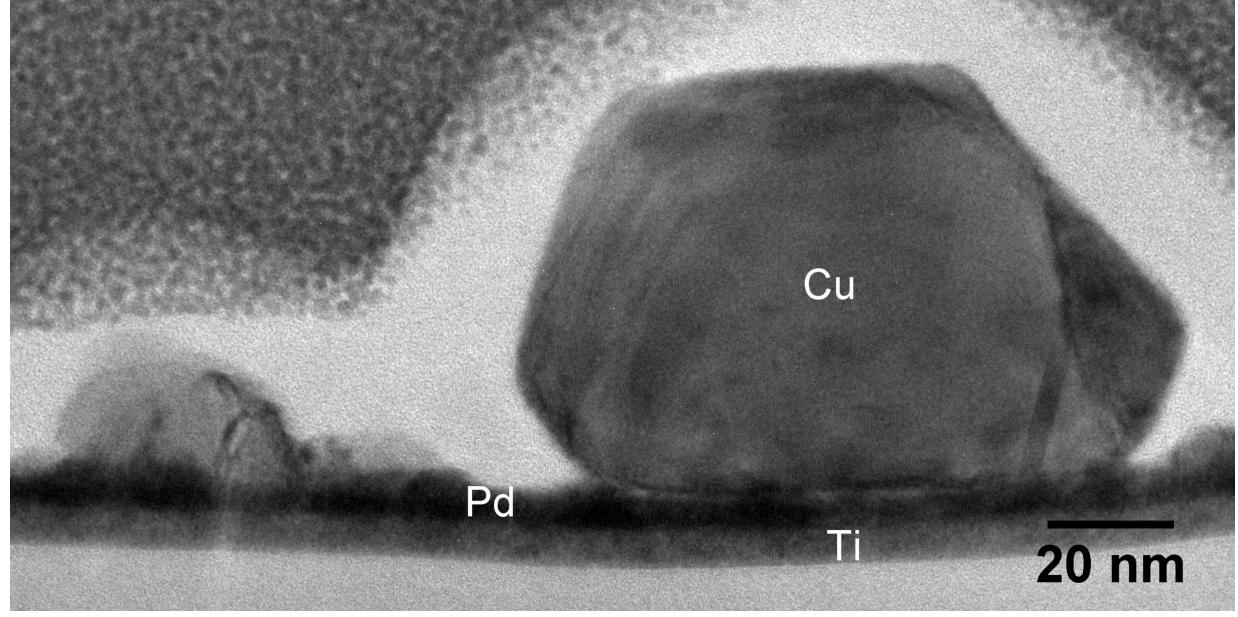
This is the author's peer reviewed, accepted manuscript. However, the online version of record will be different from this version once it has been copyedited and typeset.

PLEASE CITE THIS ARTICLE AS DOI: 10.1063/1.5087759



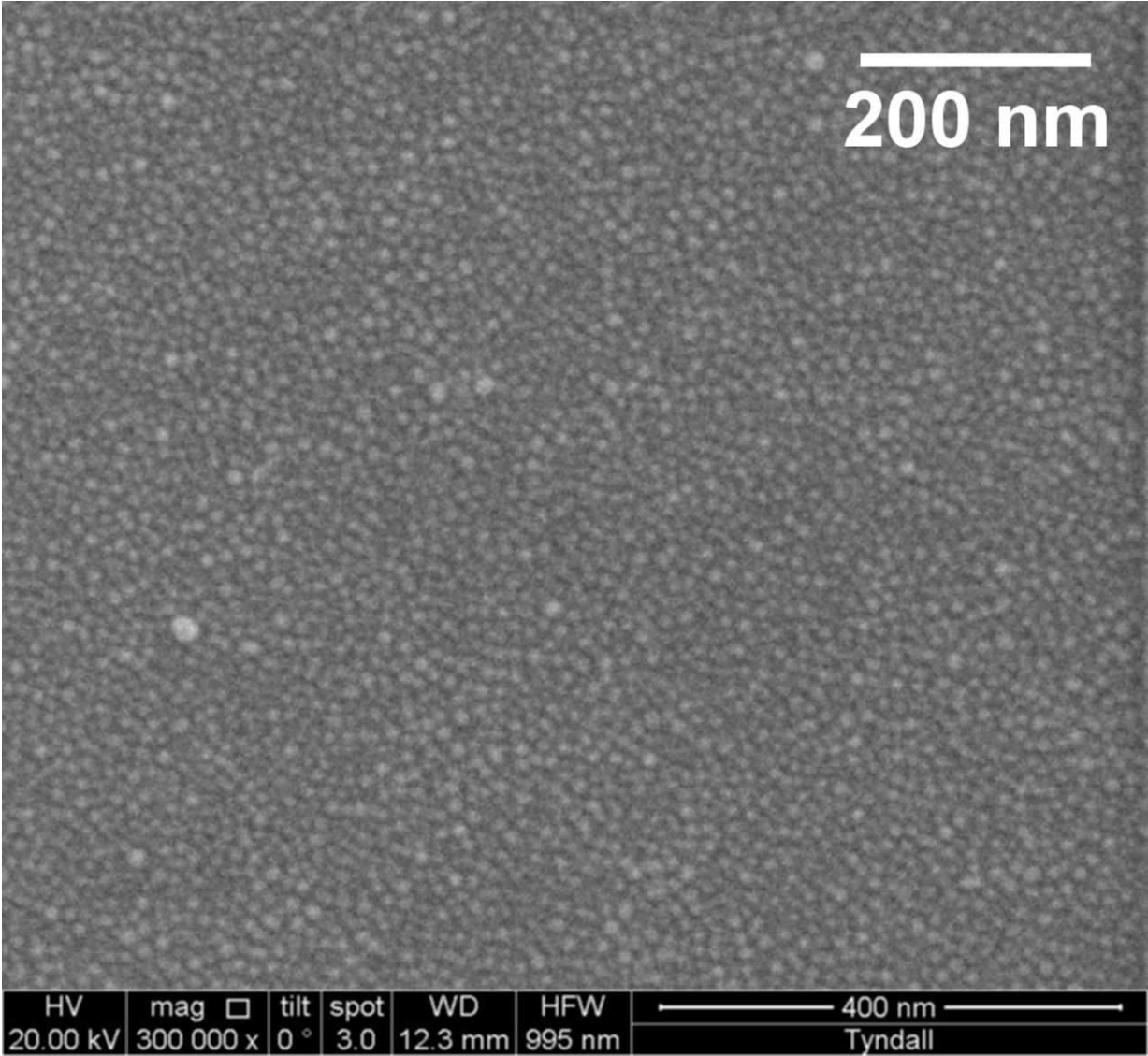
This is the author's peer reviewed, accepted manuscript. However, the online version of record will be different from this version once it has been copyedited and typeset.

PLEASE CITE THIS ARTICLE AS DOI: 10.1063/1.5087759



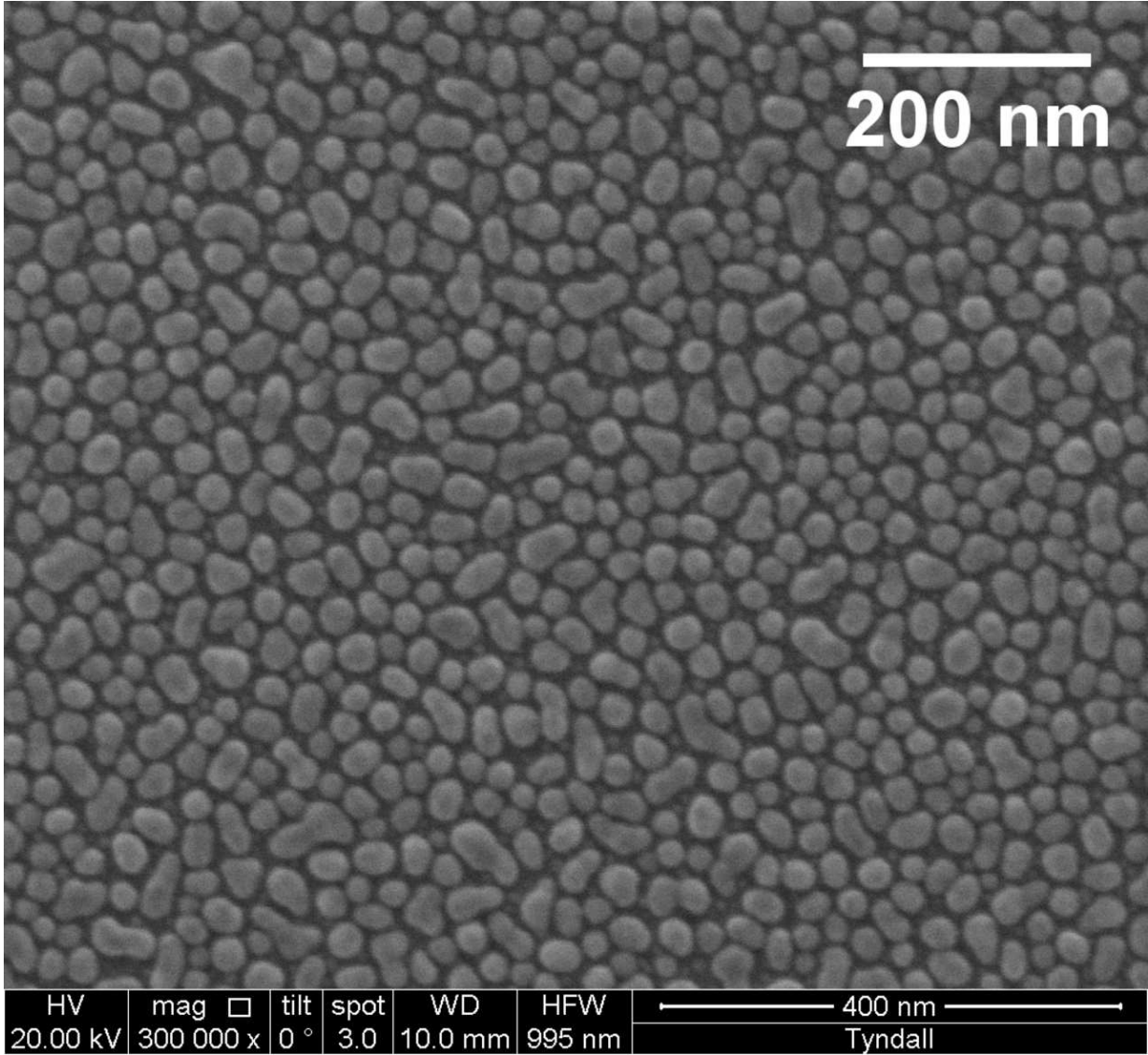
This is the author's peer reviewed, accepted manuscript. However, the online version of record will be different from this version once it has been copyedited and typeset.

PLEASE CITE THIS ARTICLE AS DOI: 10.1063/1.5087759



This is the author's peer reviewed, accepted manuscript. However, the online version of record will be different from this version once it has been copyedited and typeset.

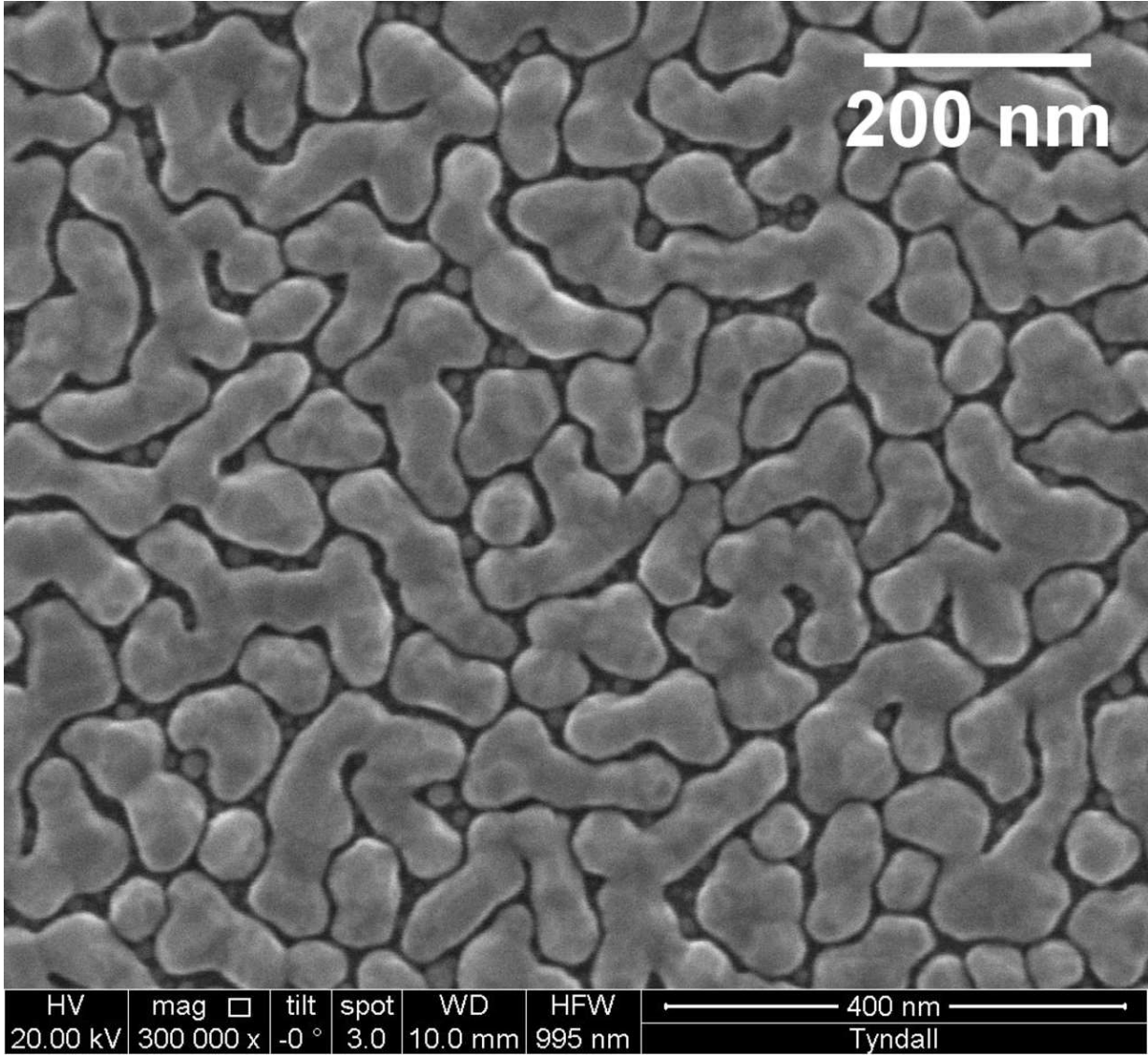
PLEASE CITE THIS ARTICLE AS DOI: 10.1063/1.5087759





This is the author's peer reviewed, accepted manuscript. However, the online version of record will be different from this version once it has been copyedited and typeset.

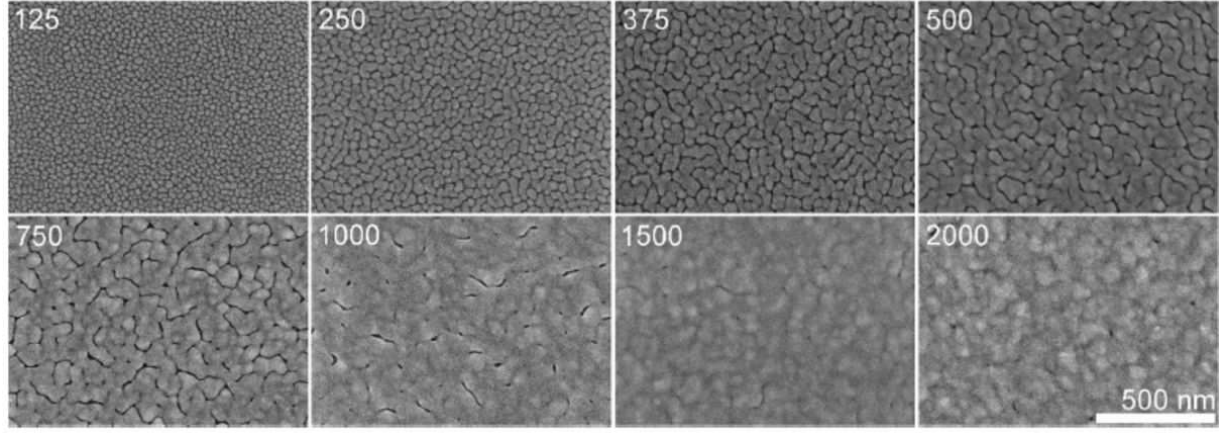
PLEASE CITE THIS ARTICLE AS DOI: 10.1063/1.5087759





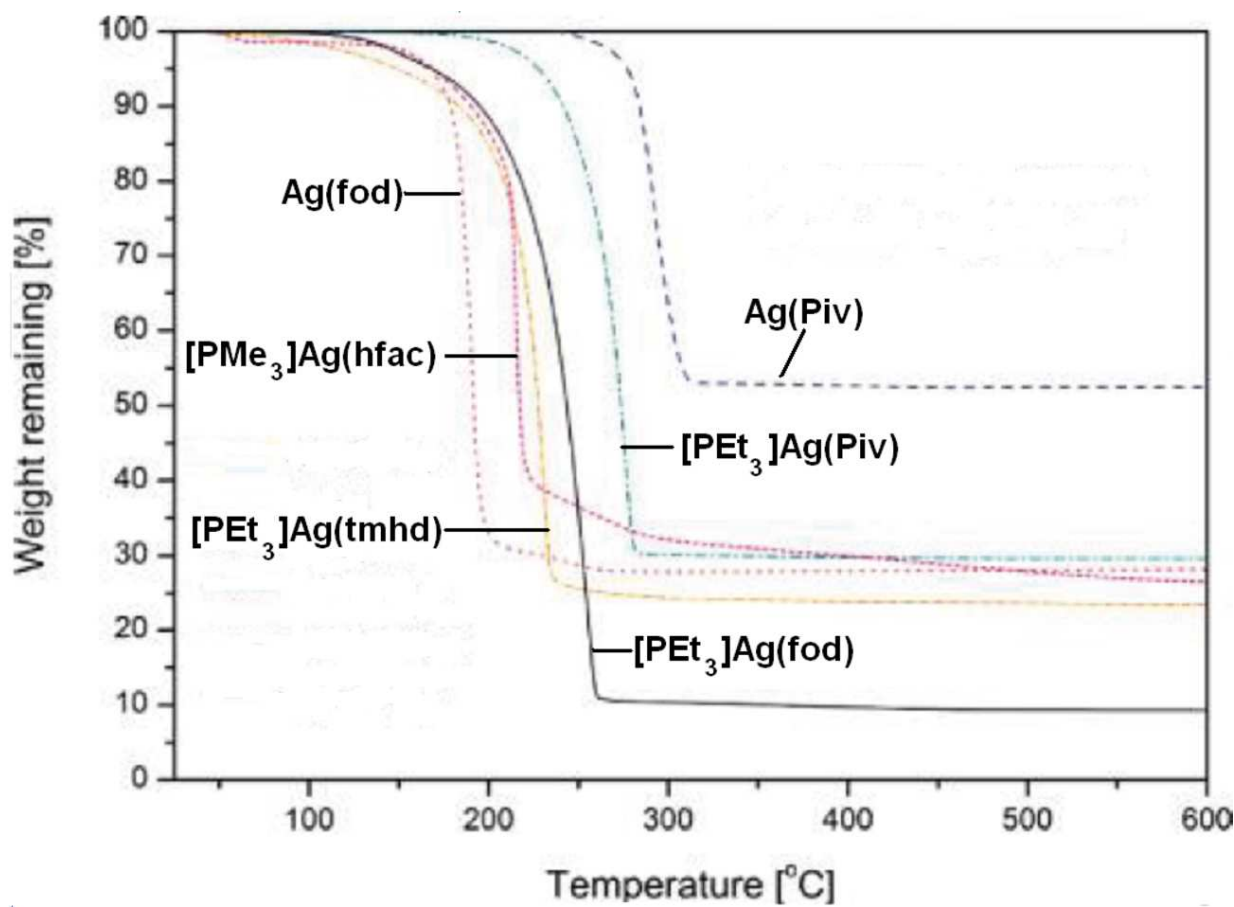
This is the author's peer reviewed, accepted manuscript. However, the online version of record will be different from this version once it has been copyedited and typeset.

PLEASE CITE THIS ARTICLE AS DOI: 10.1063/1.5087759



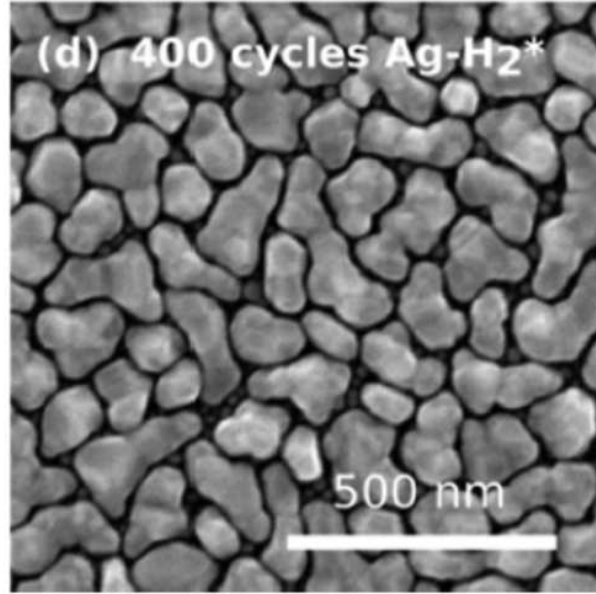
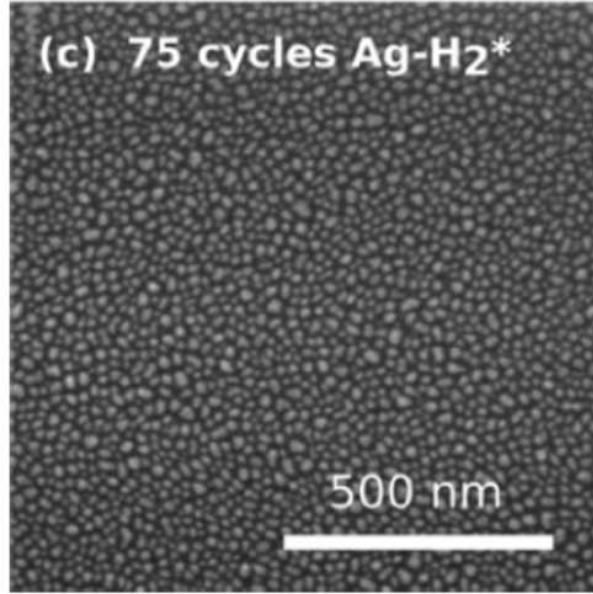
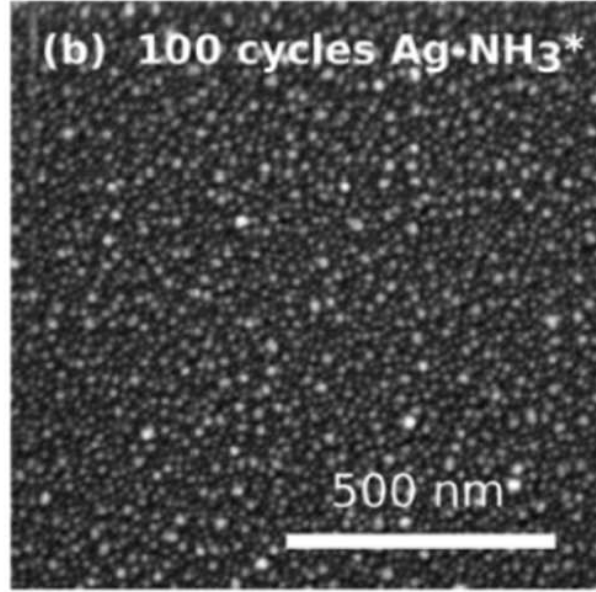
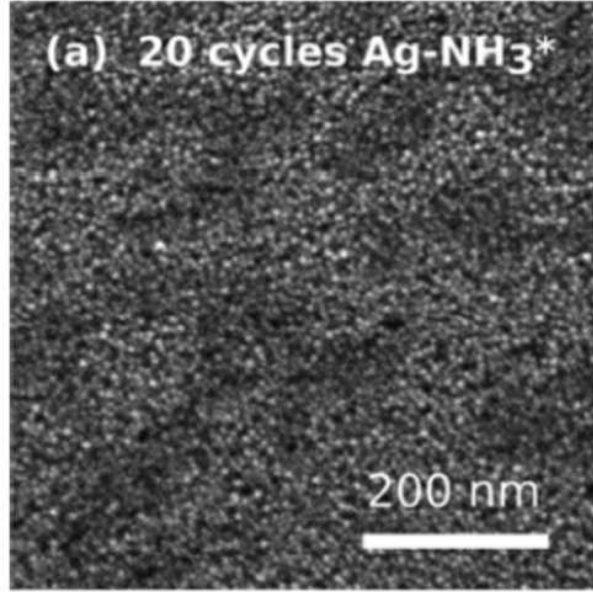
This is the author's peer reviewed, accepted manuscript. However, the online version of record will be different from this version once it has been copyedited and typeset.

PLEASE CITE THIS ARTICLE AS DOI: 10.1063/1.5087759



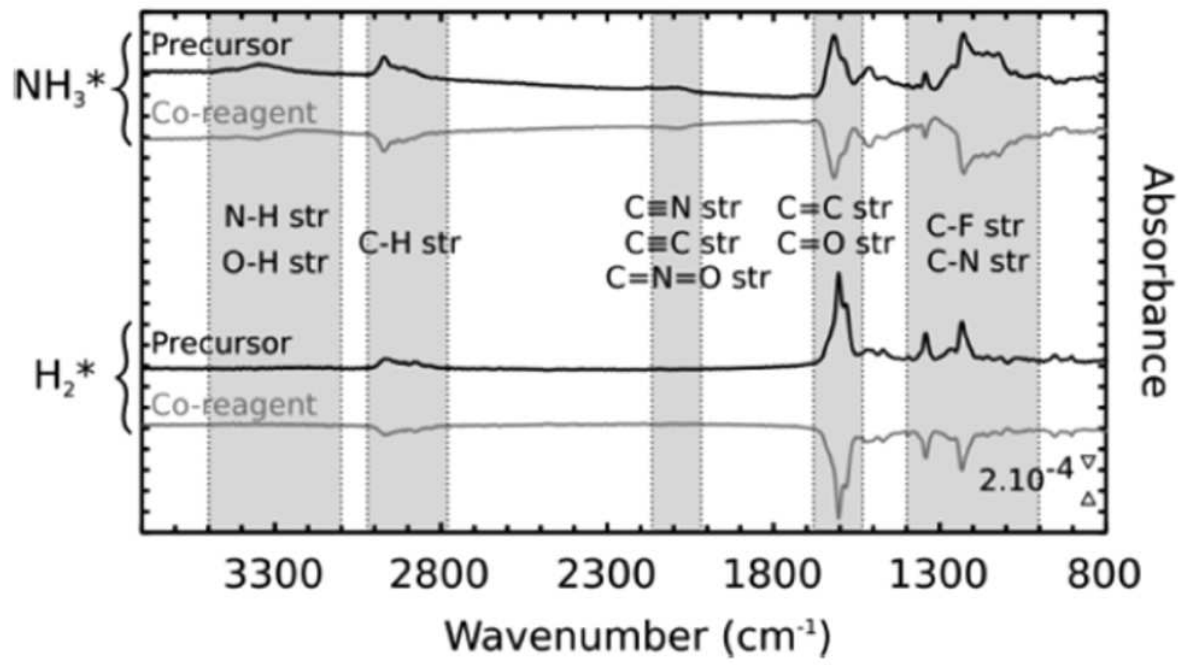
This is the author's peer reviewed, accepted manuscript. However, the online version of record will be different from this version once it has been copyedited and typeset.

PLEASE CITE THIS ARTICLE AS DOI: 10.1063/1.5087759



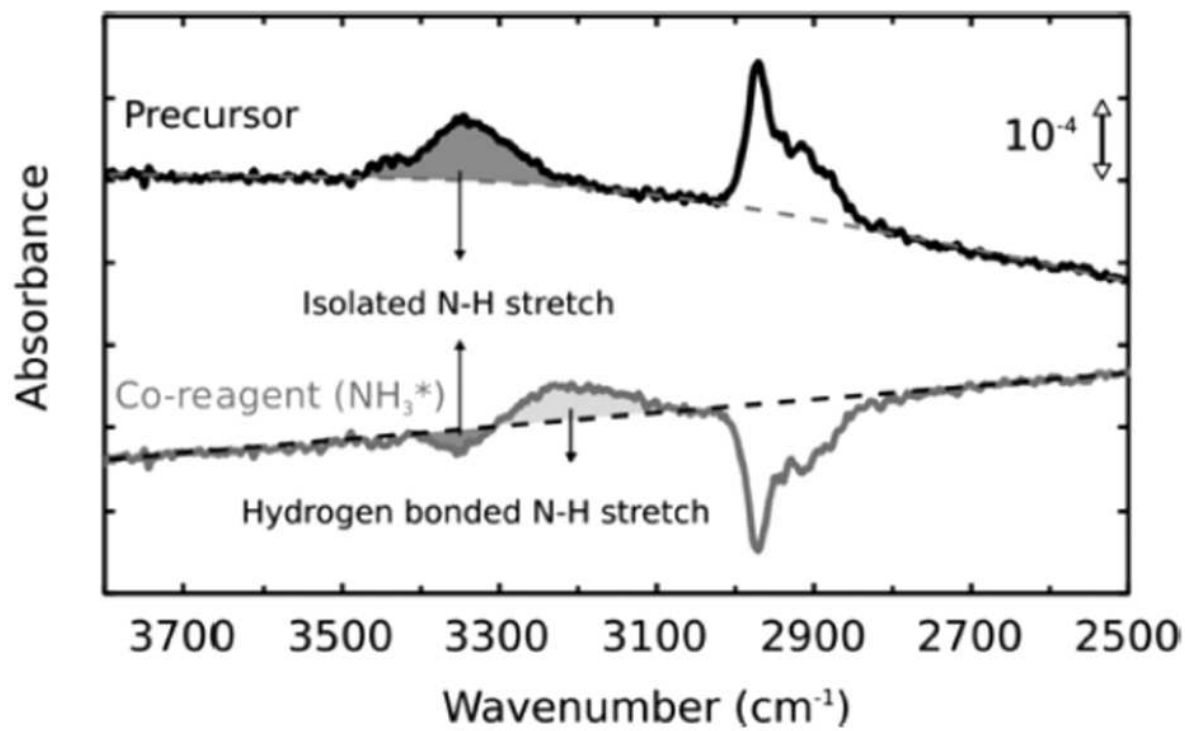
This is the author's peer reviewed, accepted manuscript. However, the online version of record will be different from this version once it has been copyedited and typeset.

PLEASE CITE THIS ARTICLE AS DOI: 10.1063/1.5087759



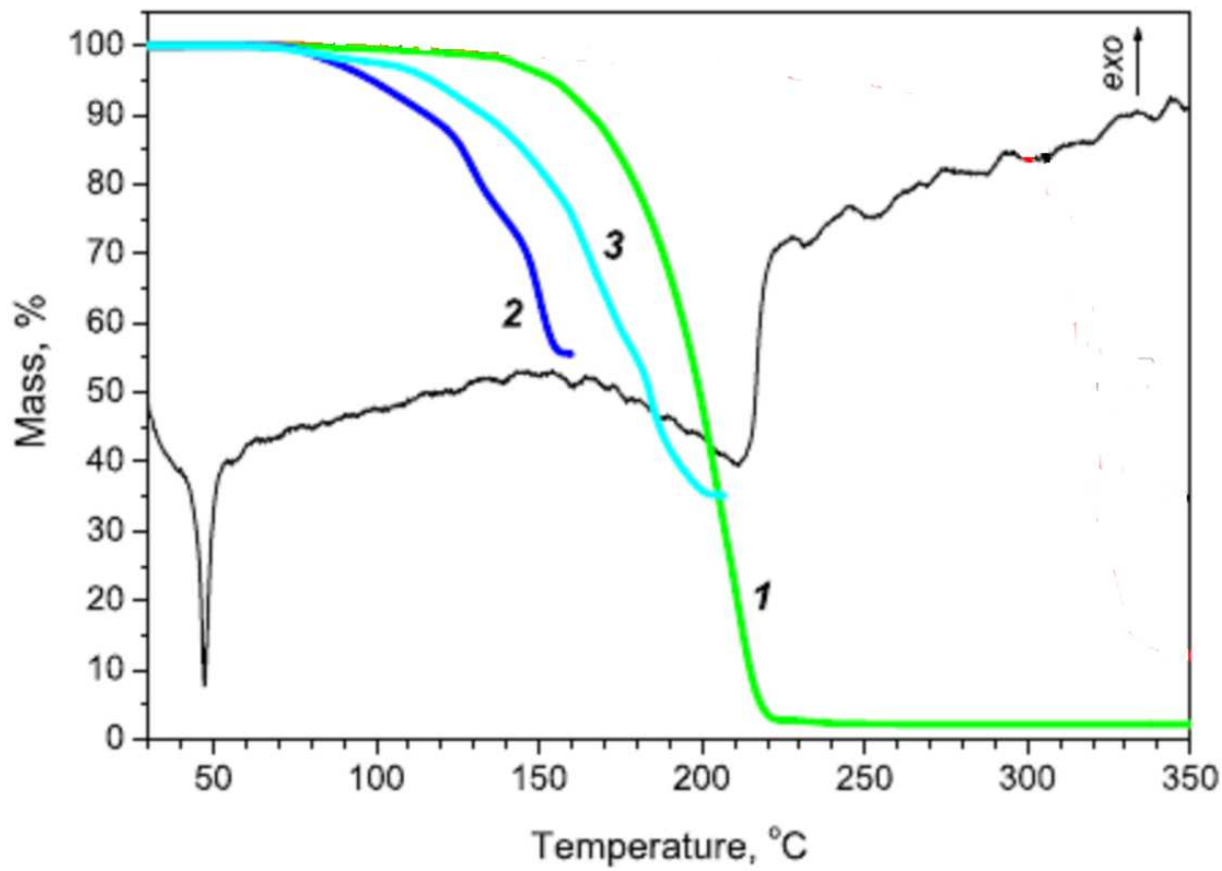
This is the author's peer reviewed, accepted manuscript. However, the online version of record will be different from this version once it has been copyedited and typeset.

PLEASE CITE THIS ARTICLE AS DOI: 10.1063/1.5087759



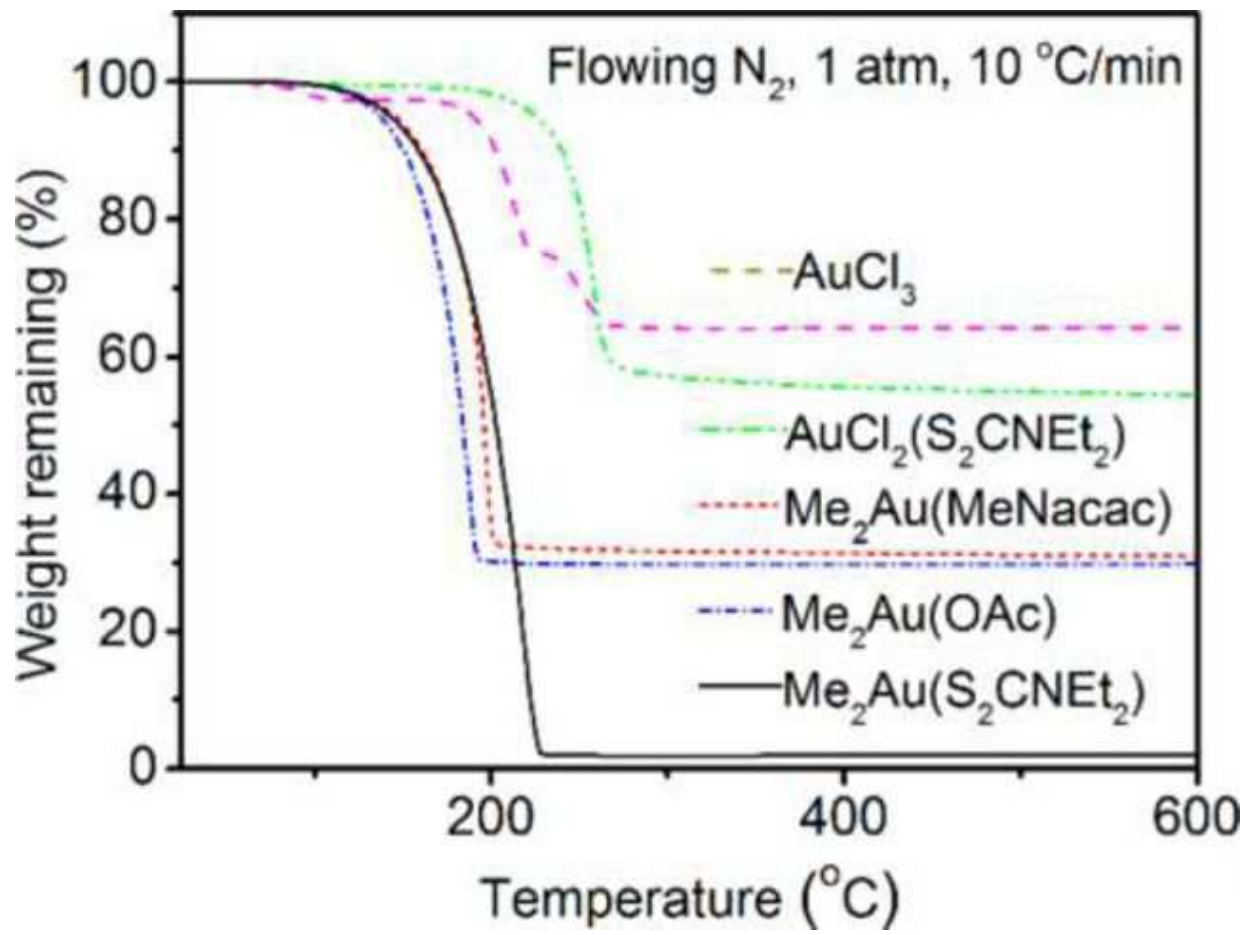
This is the author's peer reviewed, accepted manuscript. However, the online version of record will be different from this version once it has been copyedited and typeset.

PLEASE CITE THIS ARTICLE AS DOI: 10.1063/1.5087759



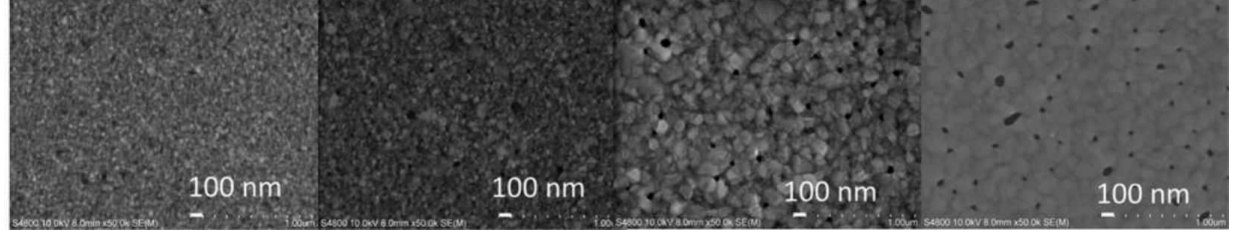
This is the author's peer reviewed, accepted manuscript. However, the online version of record will be different from this version once it has been copyedited and typeset.

PLEASE CITE THIS ARTICLE AS DOI: 10.1063/1.5087759



This is the author's peer reviewed, accepted manuscript. However, the online version of record will be different from this version once it has been copyedited and typeset.

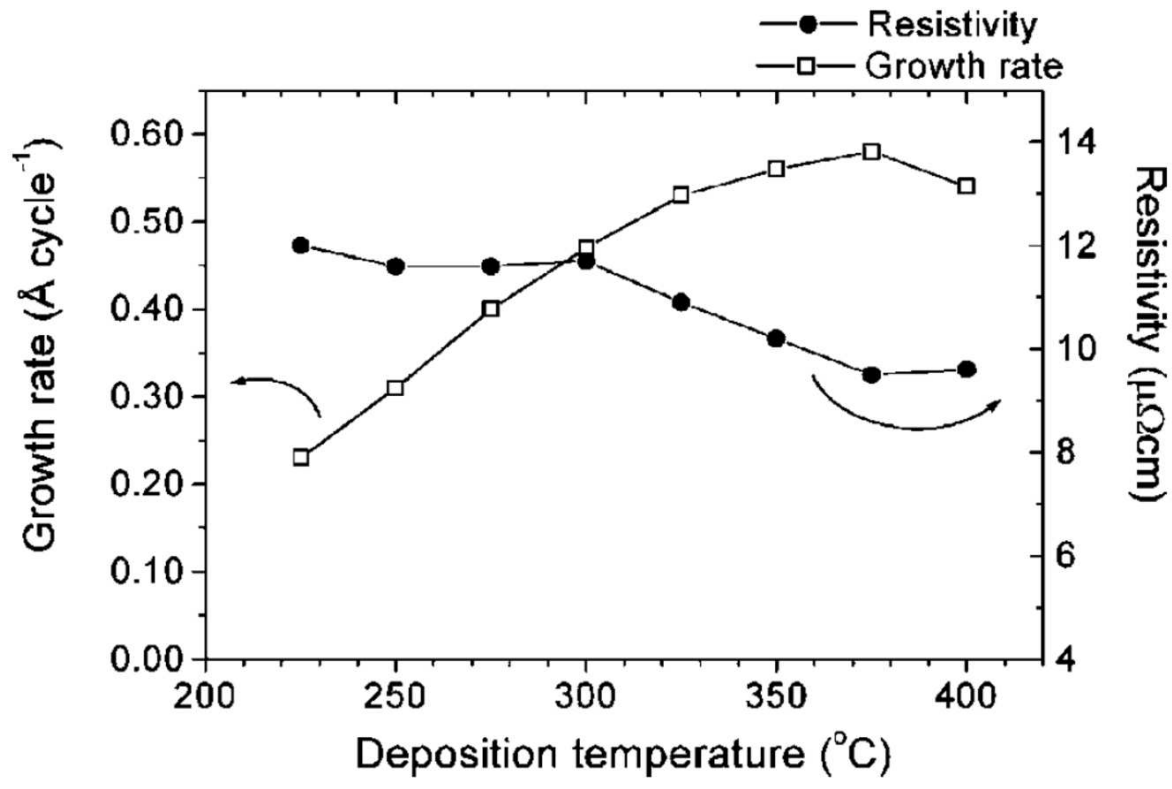
PLEASE CITE THIS ARTICLE AS DOI: 10.1063/1.5087759





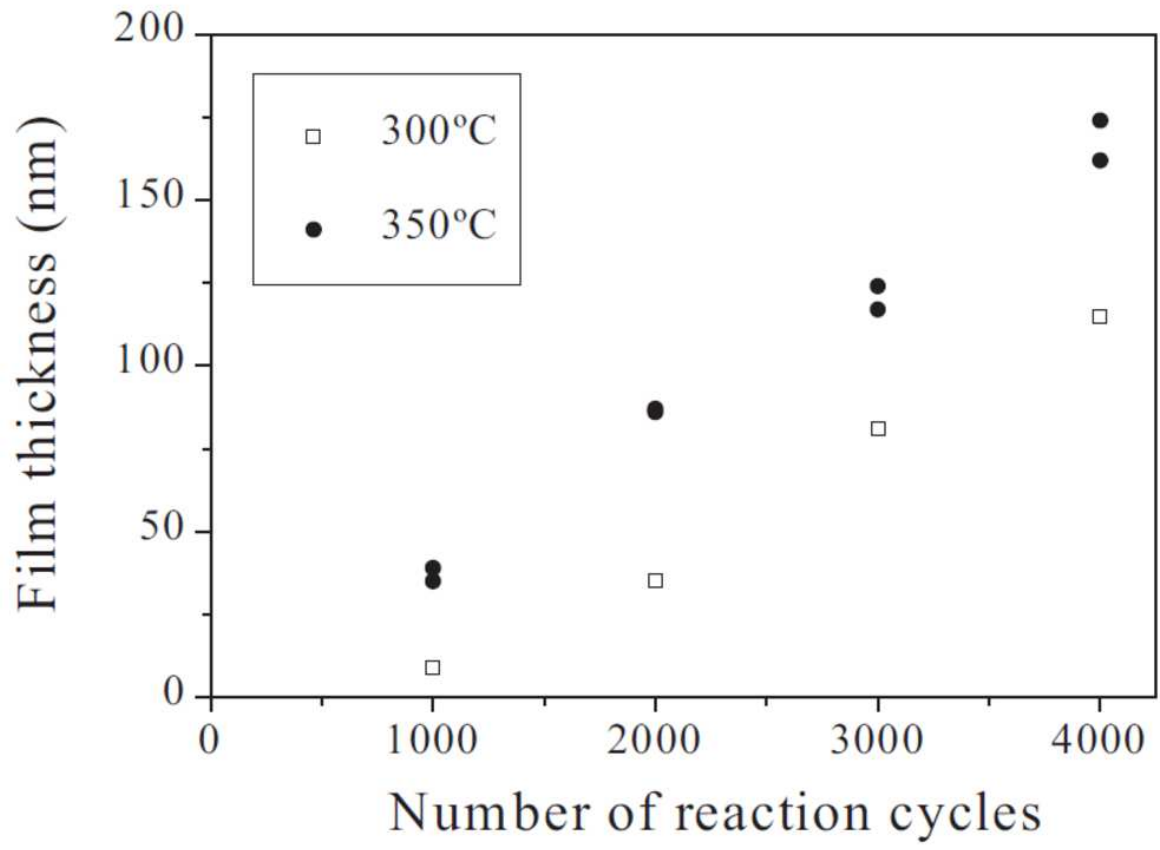
This is the author's peer reviewed, accepted manuscript. However, the online version of record will be different from this version once it has been copyedited and typeset.

PLEASE CITE THIS ARTICLE AS DOI: 10.1063/1.5087759



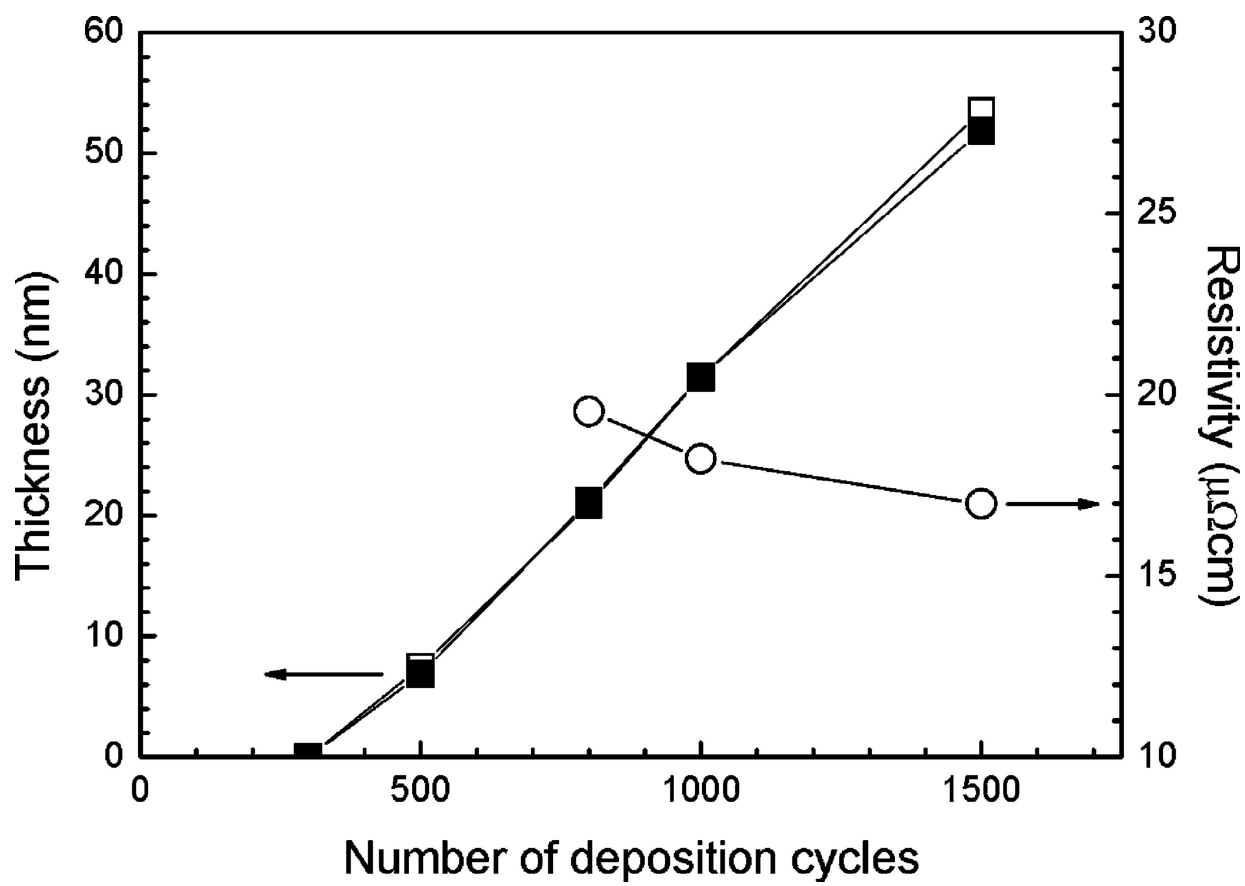
This is the author's peer reviewed, accepted manuscript. However, the online version of record will be different from this version once it has been copyedited and typeset.

PLEASE CITE THIS ARTICLE AS DOI: 10.1063/1.5087759



This is the author's peer reviewed, accepted manuscript. However, the online version of record will be different from this version once it has been copyedited and typeset.

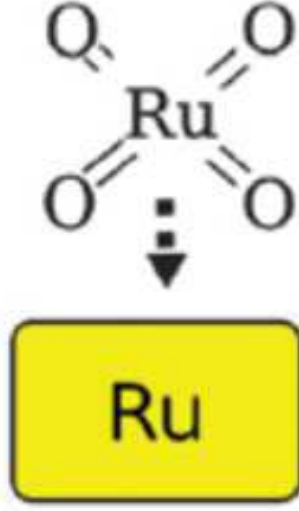
PLEASE CITE THIS ARTICLE AS DOI: 10.1063/1.5087759



This is the author's peer reviewed, accepted manuscript. However, the online version of record will be different from this version once it has been copyedited and typeset.

PLEASE CITE THIS ARTICLE AS DOI: 10.1063/1.5087759

# Halfreaction 1



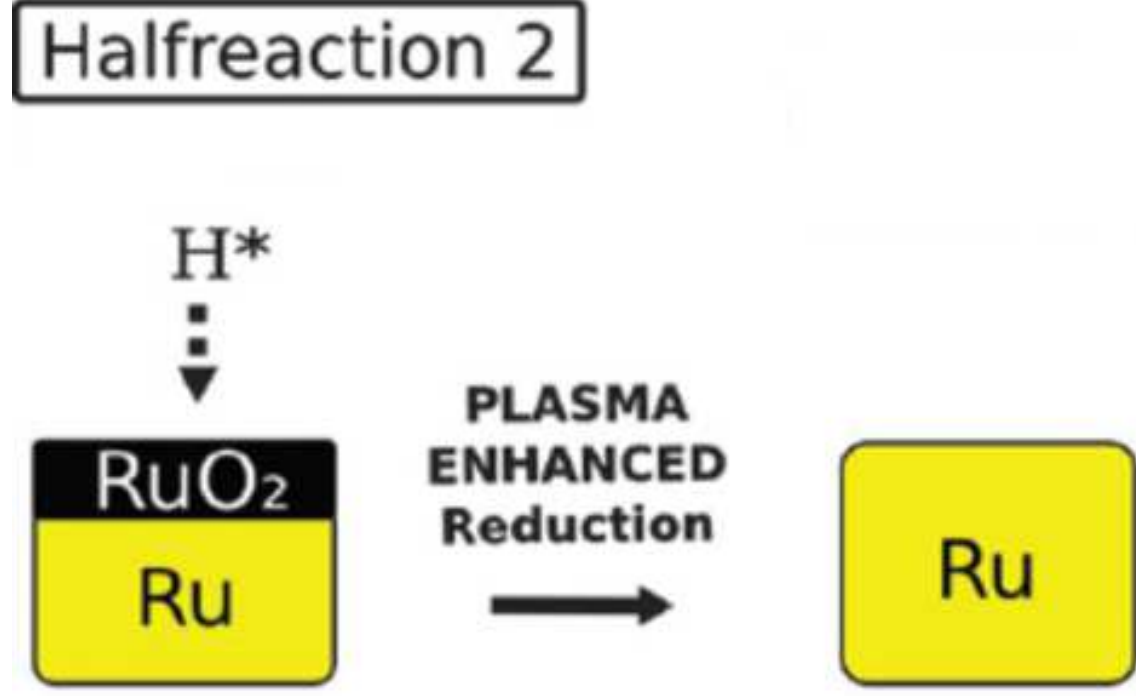
**RuO<sub>4</sub>/Ru  
surface  
reaction**

→



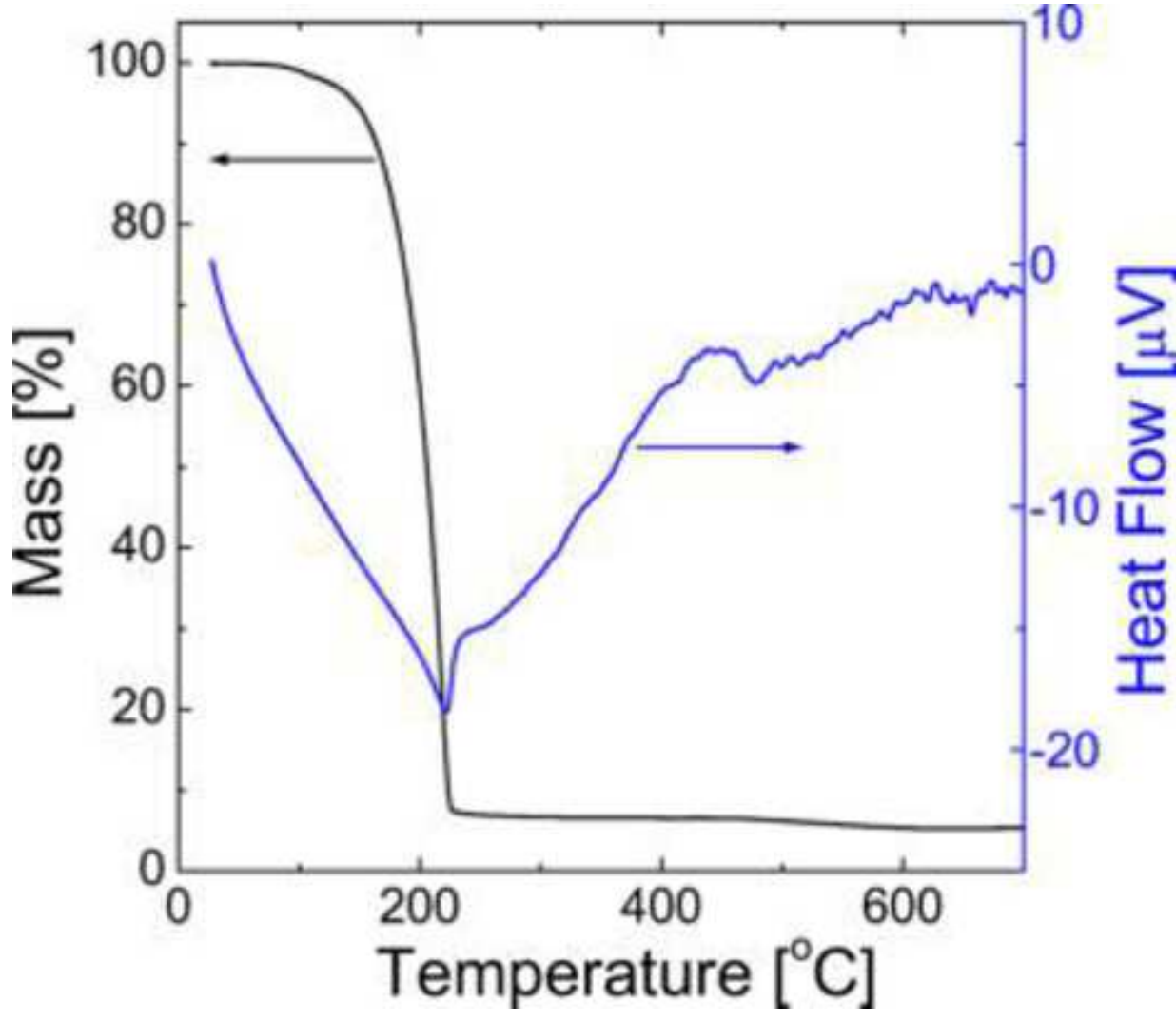
This is the author's peer reviewed, accepted manuscript. However, the online version of record will be different from this version once it has been copyedited and typeset.

PLEASE CITE THIS ARTICLE AS DOI: 10.1063/1.5087759



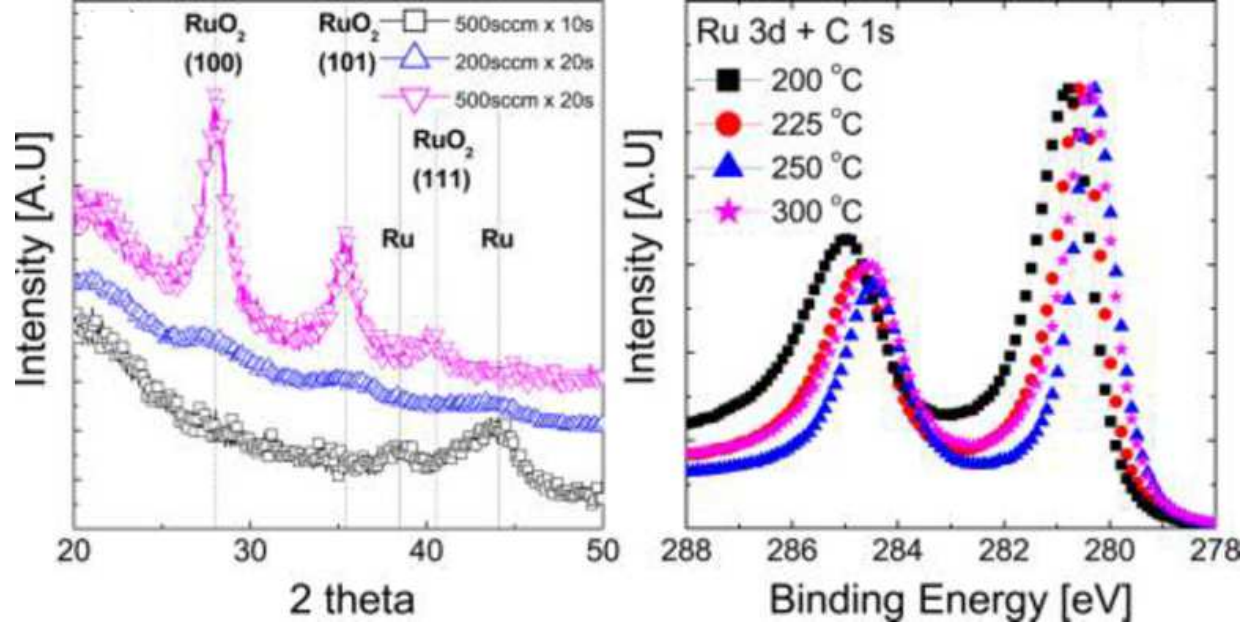
This is the author's peer reviewed, accepted manuscript. However, the online version of record will be different from this version once it has been copyedited and typeset.

PLEASE CITE THIS ARTICLE AS DOI: 10.1063/1.5087759



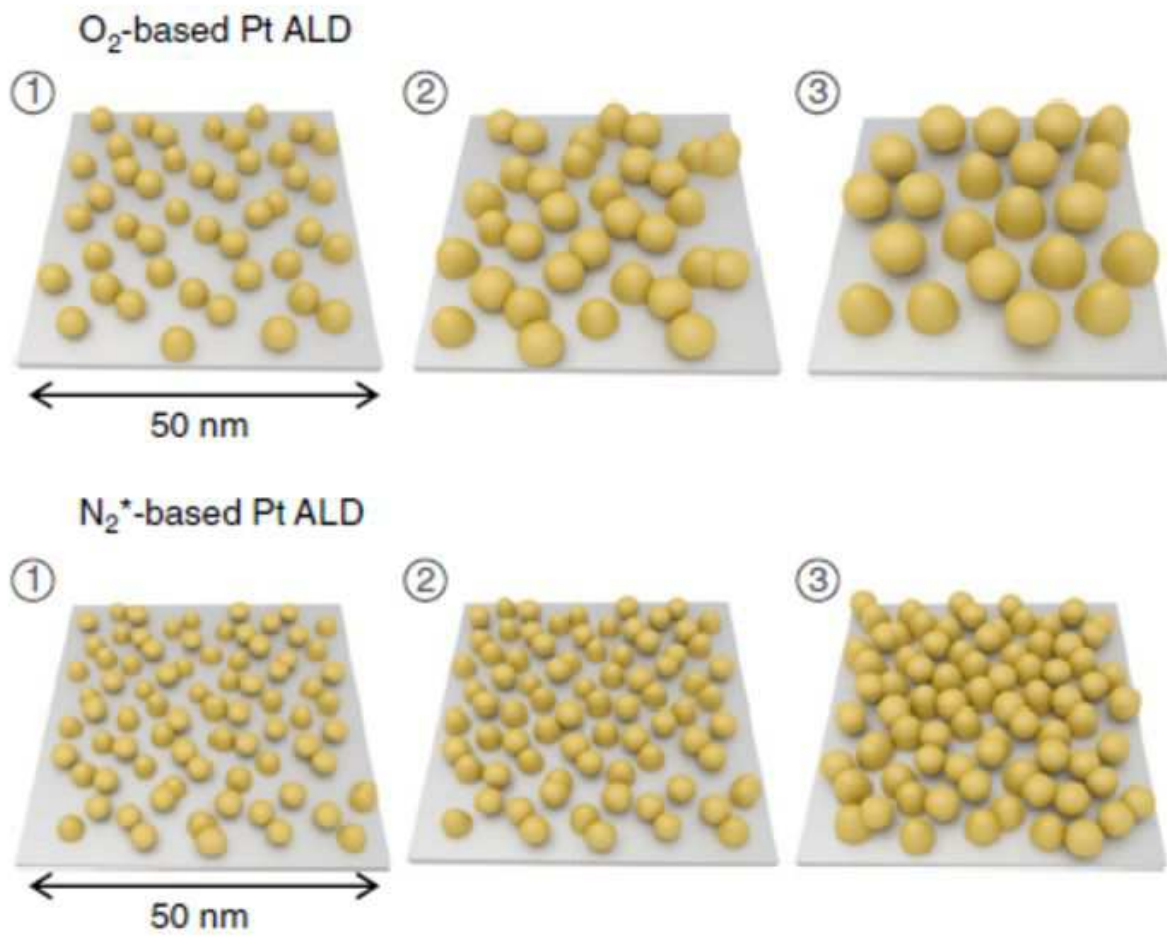
This is the author's peer reviewed, accepted manuscript. However, the online version of record will be different from this version once it has been copyedited and typeset.

PLEASE CITE THIS ARTICLE AS DOI: 10.1063/1.5087759



This is the author's peer reviewed, accepted manuscript. However, the online version of record will be different from this version once it has been copyedited and typeset.

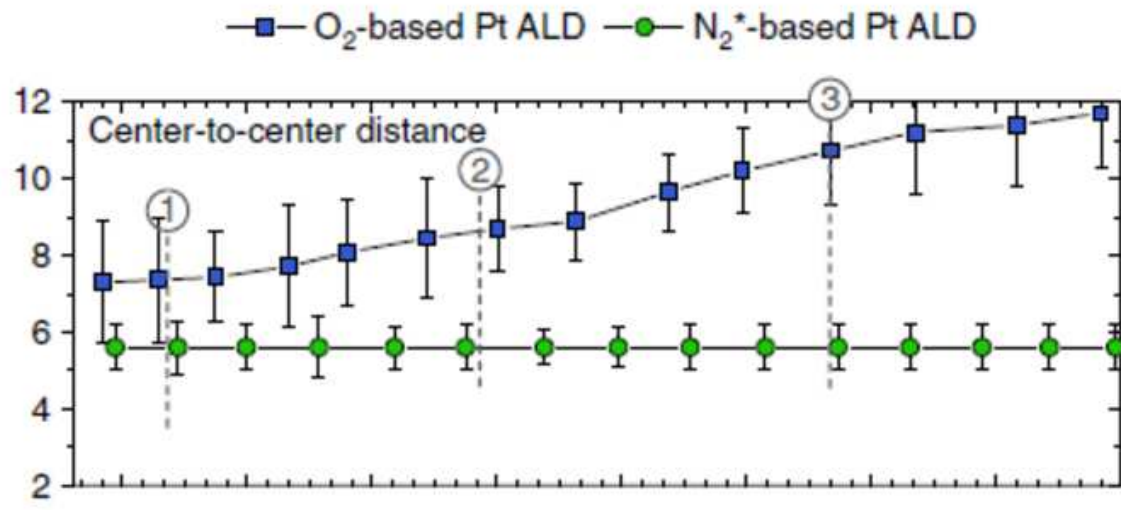
PLEASE CITE THIS ARTICLE AS DOI: 10.1063/1.5087759





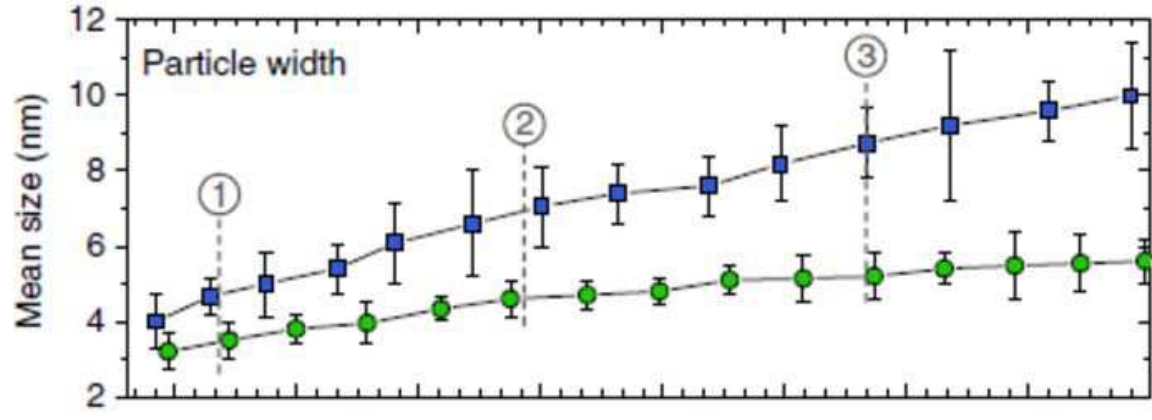
This is the author's peer reviewed, accepted manuscript. However, the online version of record will be different from this version once it has been copyedited and typeset.

PLEASE CITE THIS ARTICLE AS DOI: 10.1063/1.5087759



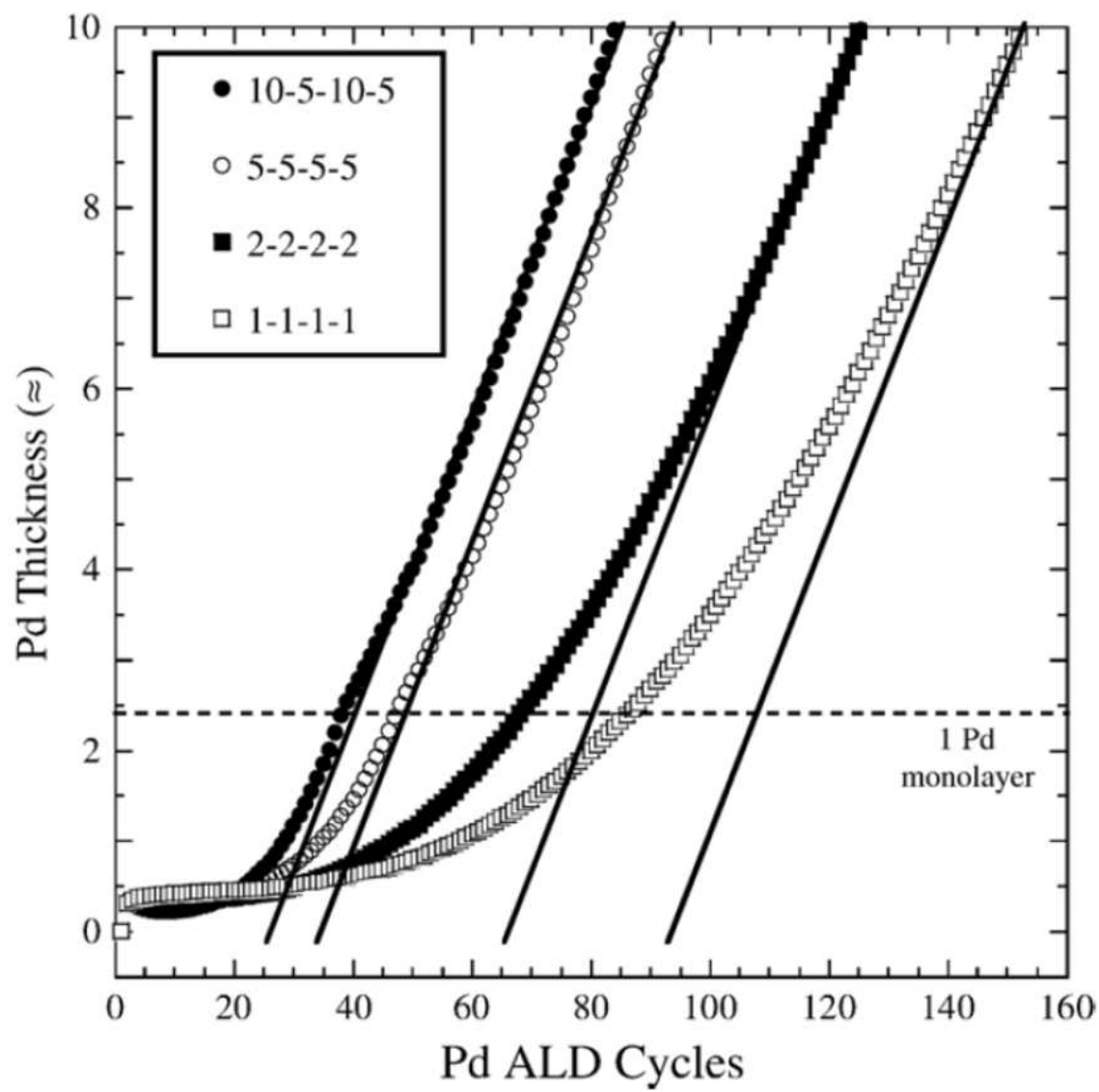
This is the author's peer reviewed, accepted manuscript. However, the online version of record will be different from this version once it has been copyedited and typeset.

PLEASE CITE THIS ARTICLE AS DOI: 10.1063/1.5087759



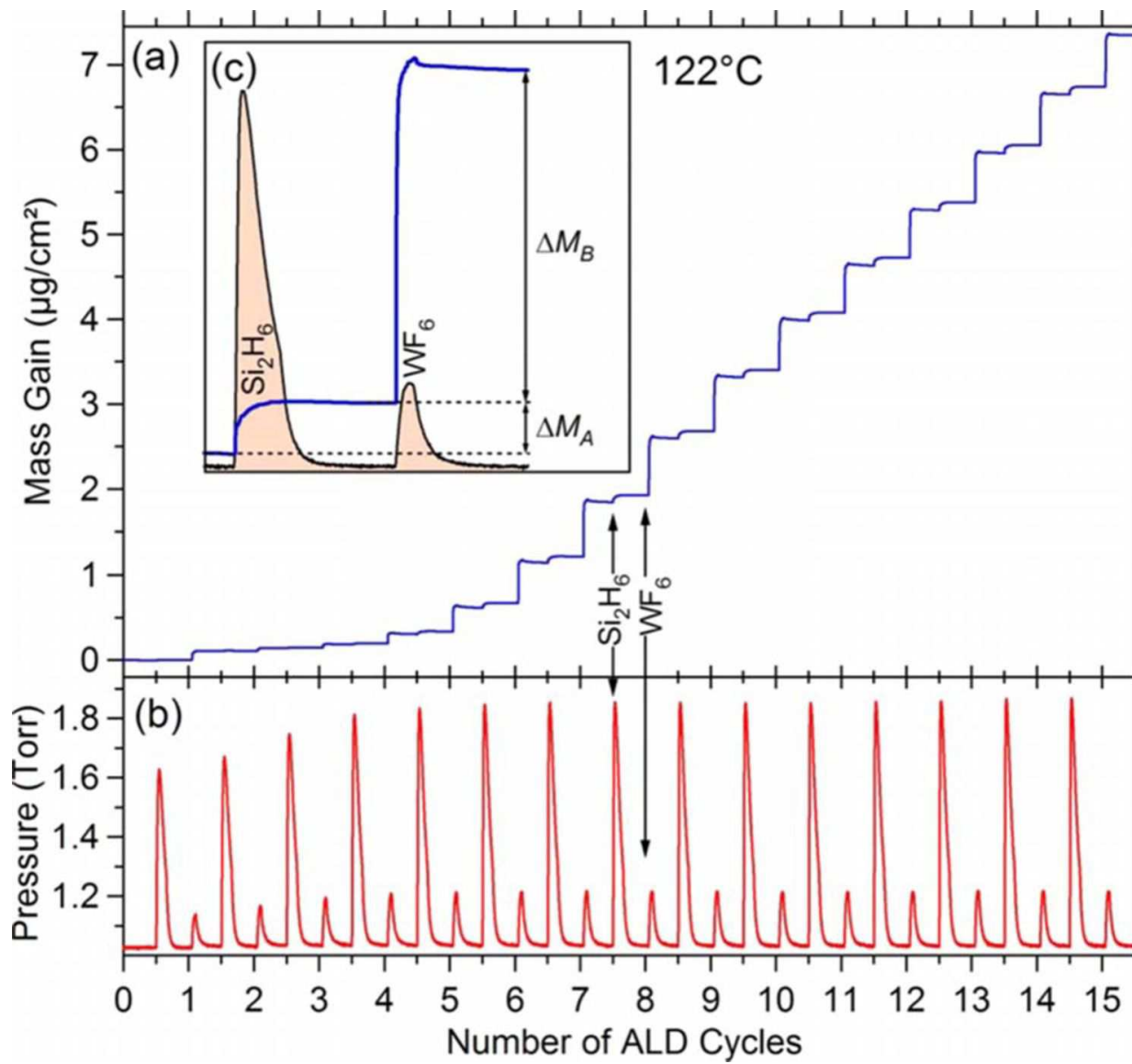
This is the author's peer reviewed, accepted manuscript. However, the online version of record will be different from this version once it has been copyedited and typeset.

PLEASE CITE THIS ARTICLE AS DOI: 10.1063/1.5087759



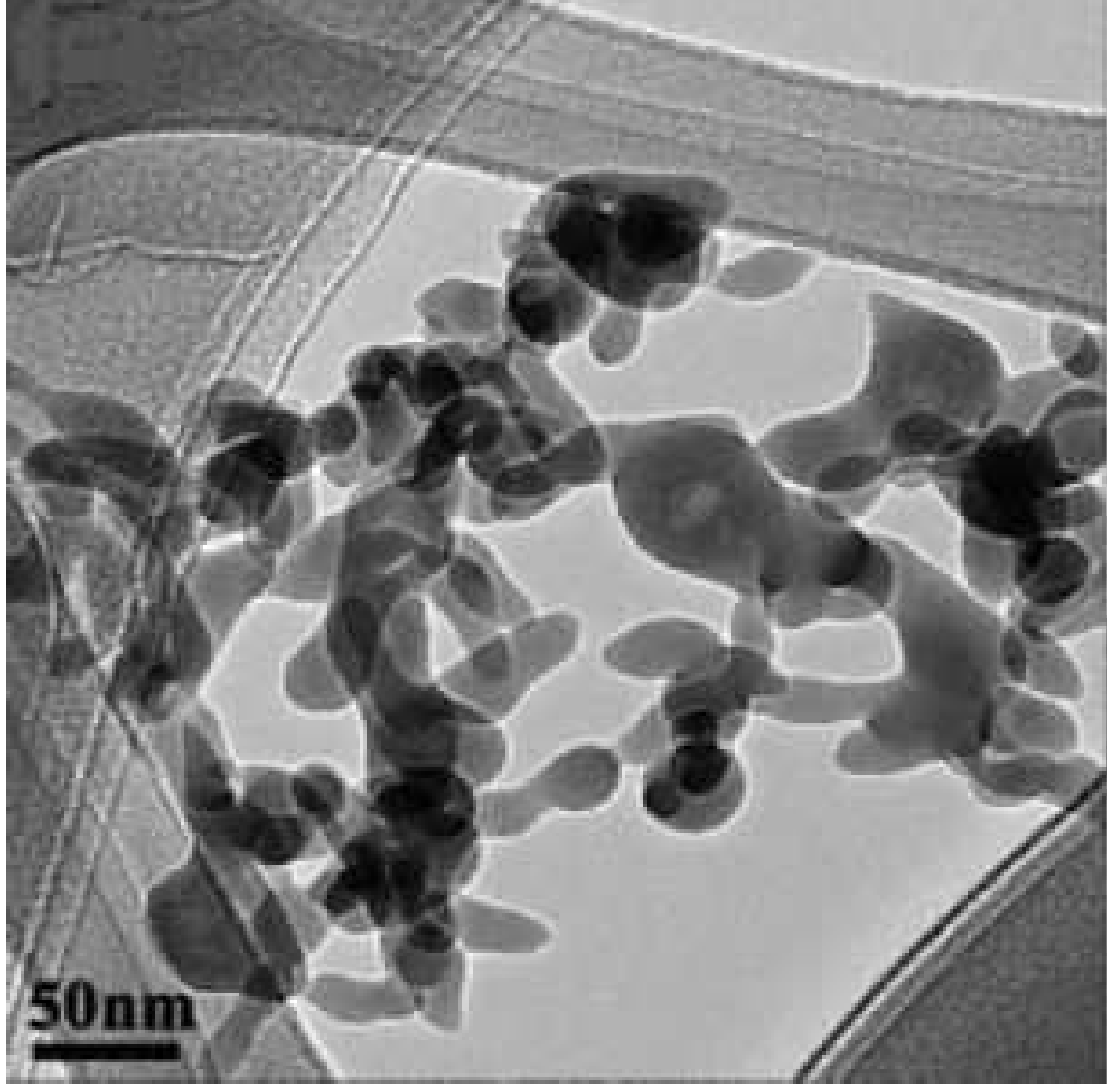
This is the author's peer reviewed, accepted manuscript. However, the online version of record will be different from this version once it has been copyedited and typeset.

PLEASE CITE THIS ARTICLE AS DOI: 10.1063/1.5087759



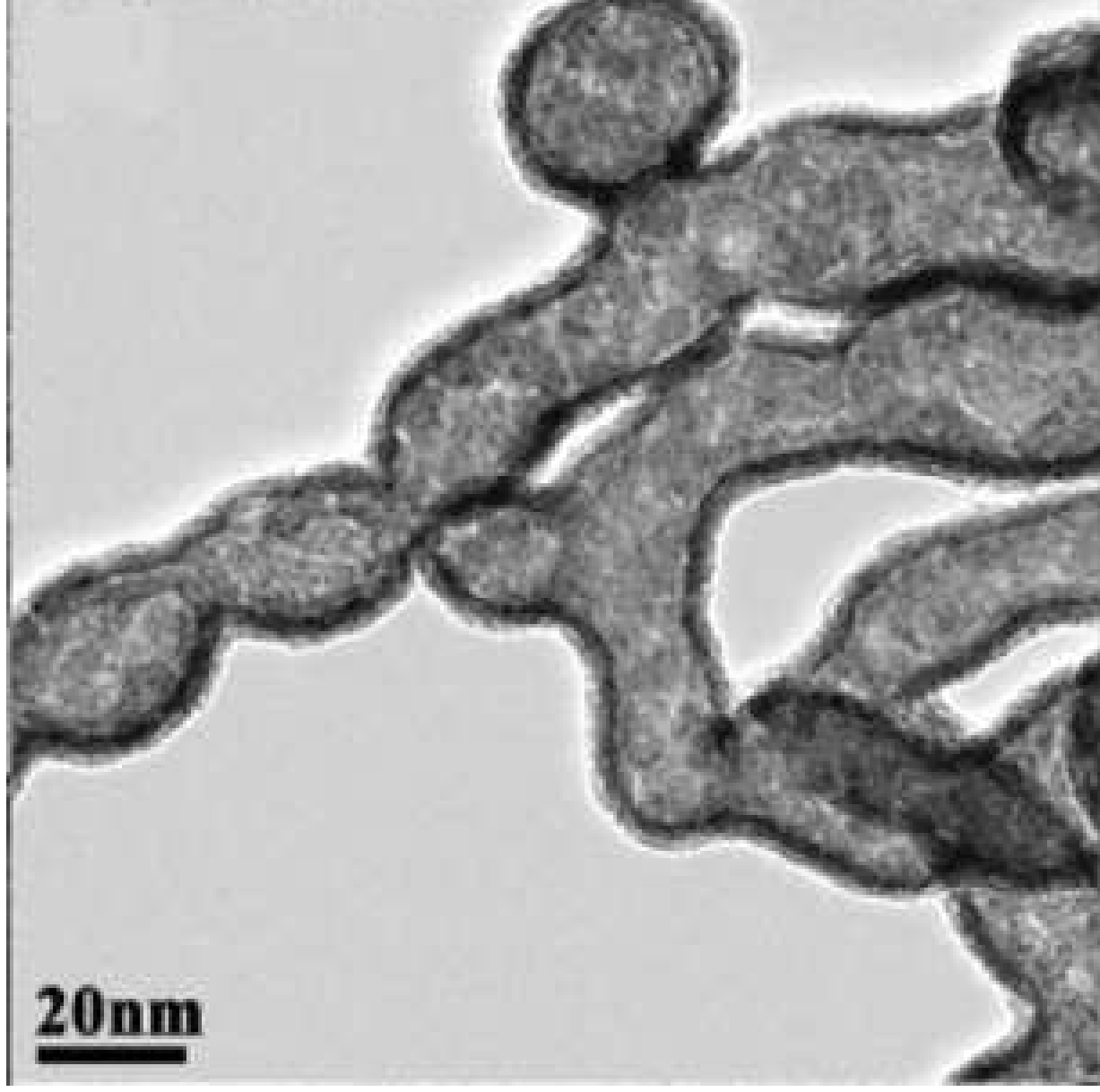
This is the author's peer reviewed, accepted manuscript. However, the online version of record will be different from this version once it has been copyedited and typeset.

PLEASE CITE THIS ARTICLE AS DOI: 10.1063/1.5087759



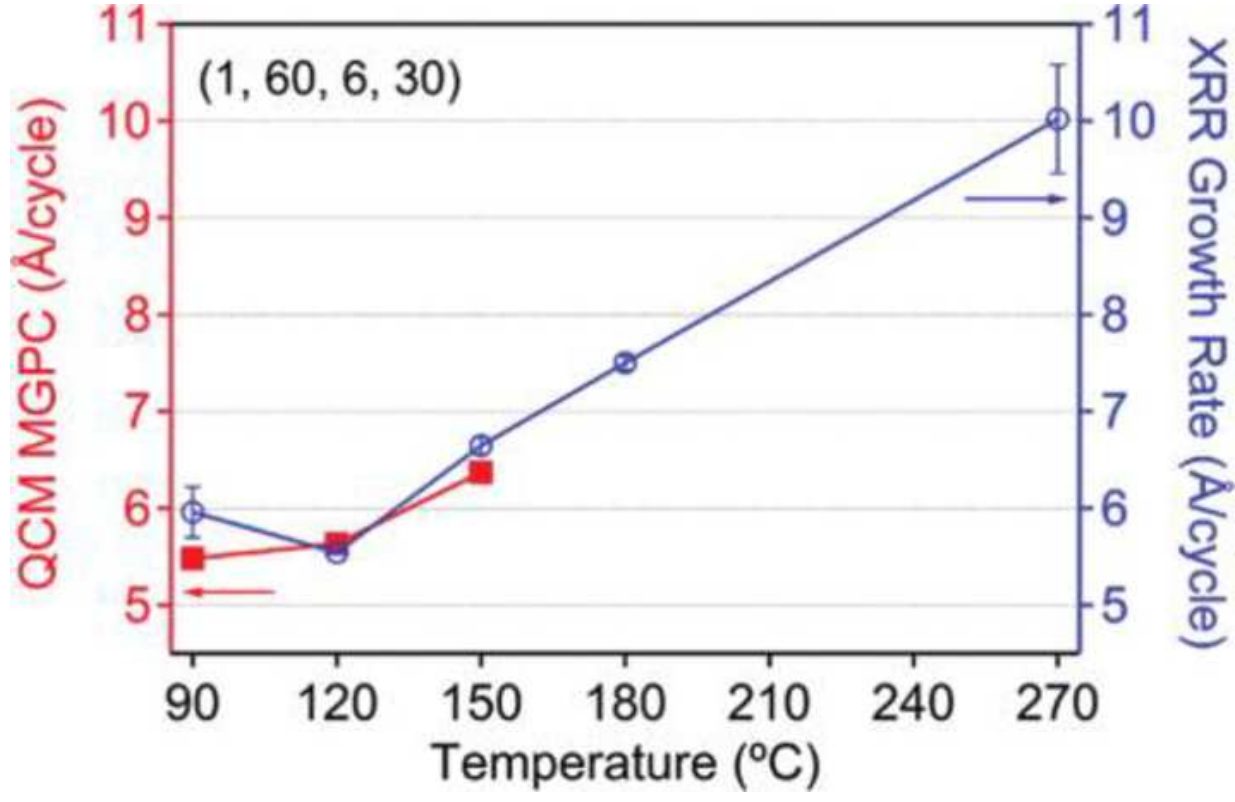
This is the author's peer reviewed, accepted manuscript. However, the online version of record will be different from this version once it has been copyedited and typeset.

PLEASE CITE THIS ARTICLE AS DOI: 10.1063/1.5087759



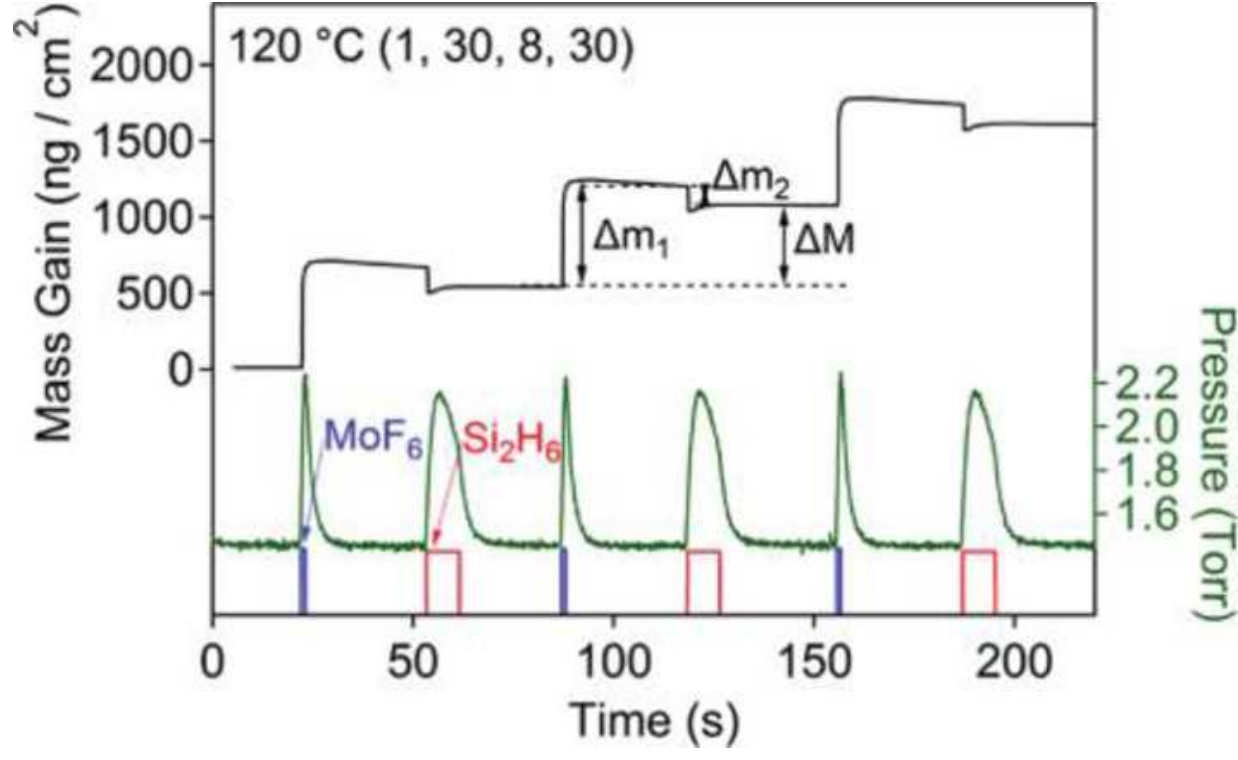
This is the author's peer reviewed, accepted manuscript. However, the online version of record will be different from this version once it has been copyedited and typeset.

PLEASE CITE THIS ARTICLE AS DOI: 10.1063/1.5087759



This is the author's peer reviewed, accepted manuscript. However, the online version of record will be different from this version once it has been copyedited and typeset.

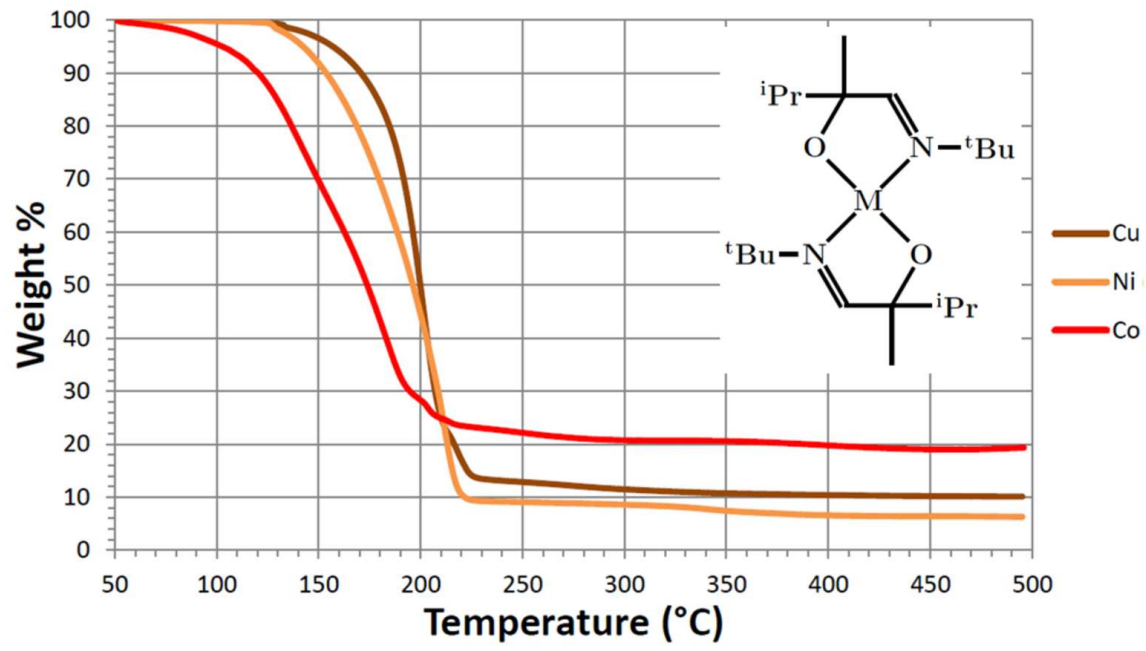
PLEASE CITE THIS ARTICLE AS DOI: 10.1063/1.5087759





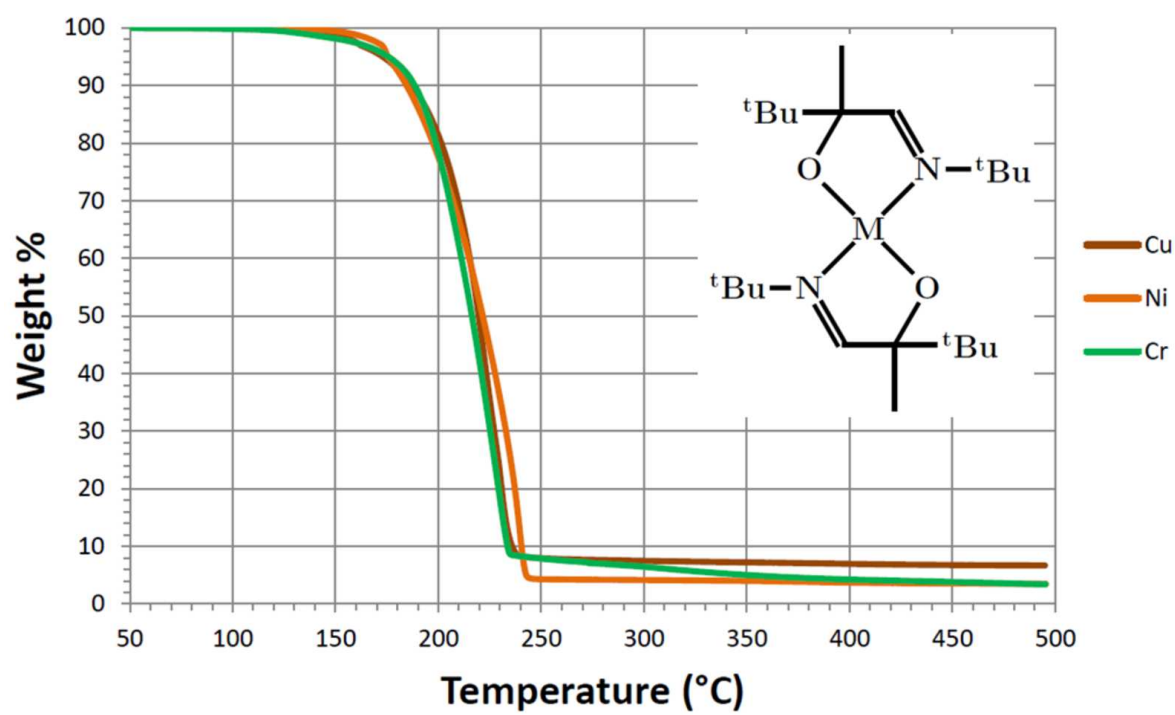
This is the author's peer reviewed, accepted manuscript. However, the online version of record will be different from this version once it has been copyedited and typeset.

PLEASE CITE THIS ARTICLE AS DOI: 10.1063/1.5087759



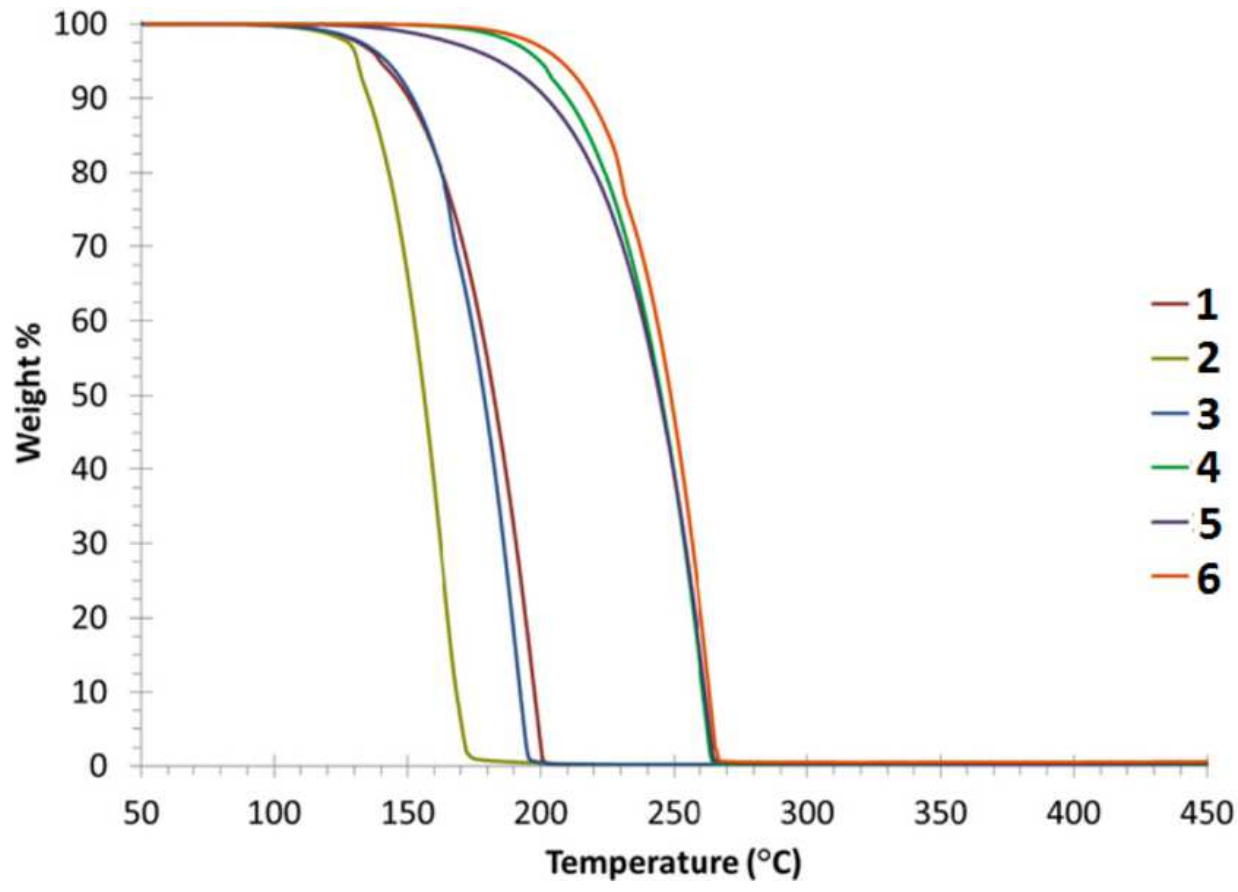
This is the author's peer reviewed, accepted manuscript. However, the online version of record will be different from this version once it has been copyedited and typeset.

PLEASE CITE THIS ARTICLE AS DOI: 10.1063/1.5087759



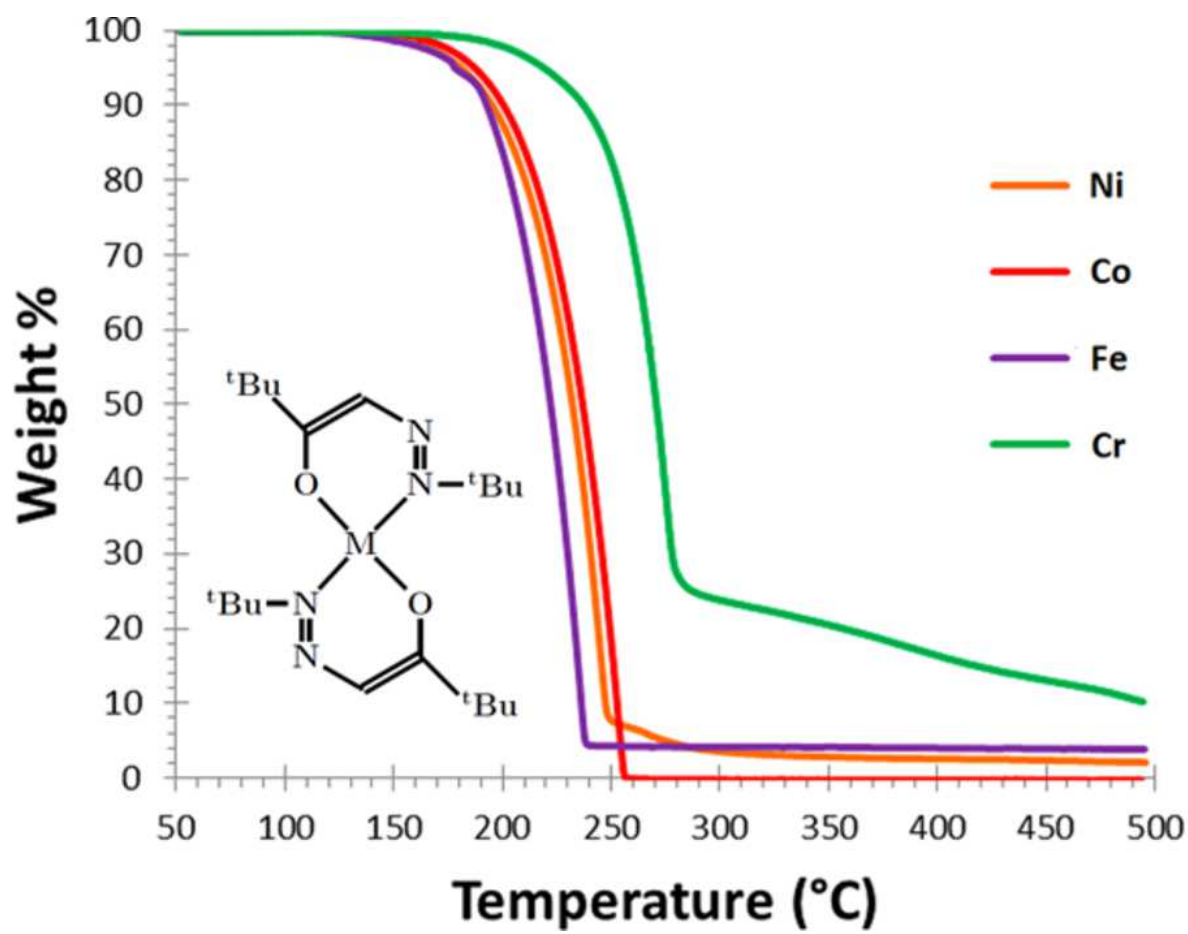
This is the author's peer reviewed, accepted manuscript. However, the online version of record will be different from this version once it has been copyedited and typeset.

PLEASE CITE THIS ARTICLE AS DOI: 10.1063/1.5087759



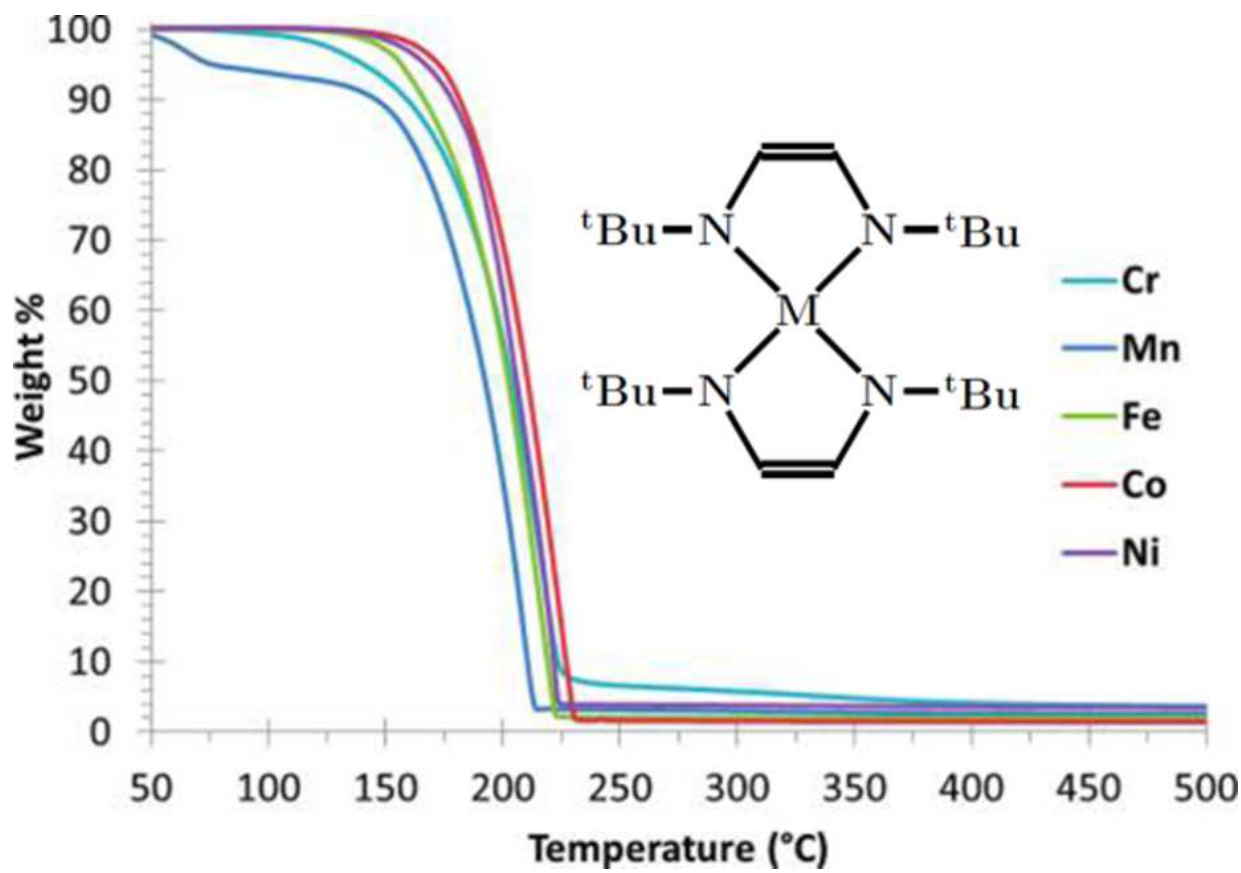
This is the author's peer reviewed, accepted manuscript. However, the online version of record will be different from this version once it has been copyedited and typeset.

PLEASE CITE THIS ARTICLE AS DOI: 10.1063/1.5087759



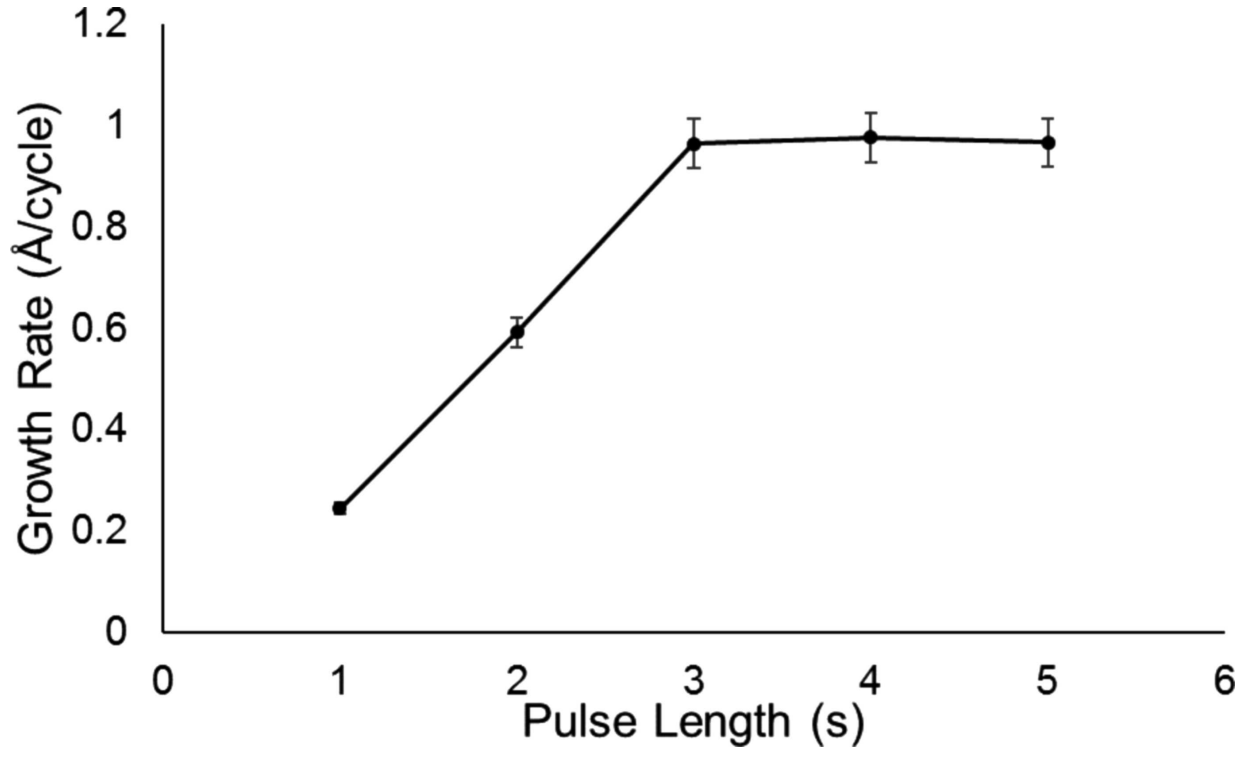
This is the author's peer reviewed, accepted manuscript. However, the online version of record will be different from this version once it has been copyedited and typeset.

PLEASE CITE THIS ARTICLE AS DOI: 10.1063/1.5087759



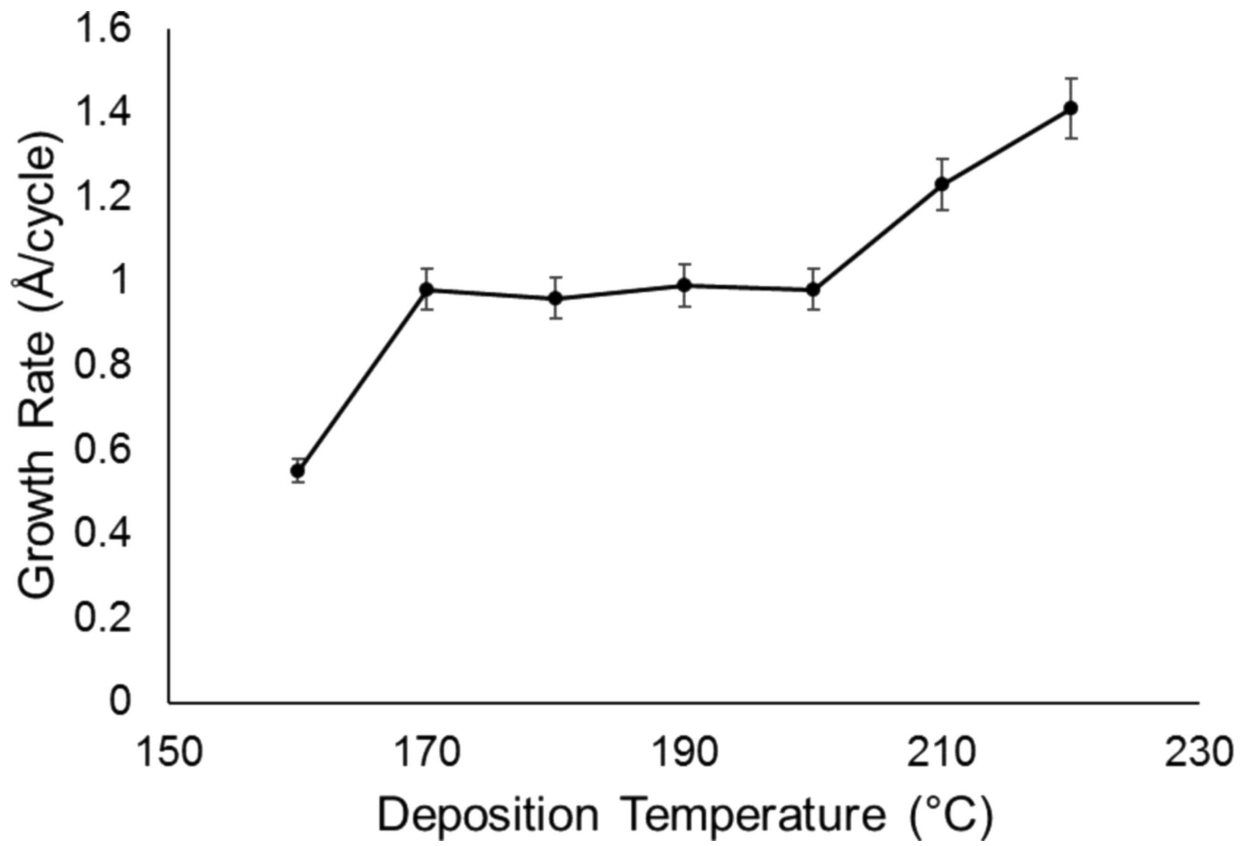
This is the author's peer reviewed, accepted manuscript. However, the online version of record will be different from this version once it has been copyedited and typeset.

PLEASE CITE THIS ARTICLE AS DOI: 10.1063/1.5087759



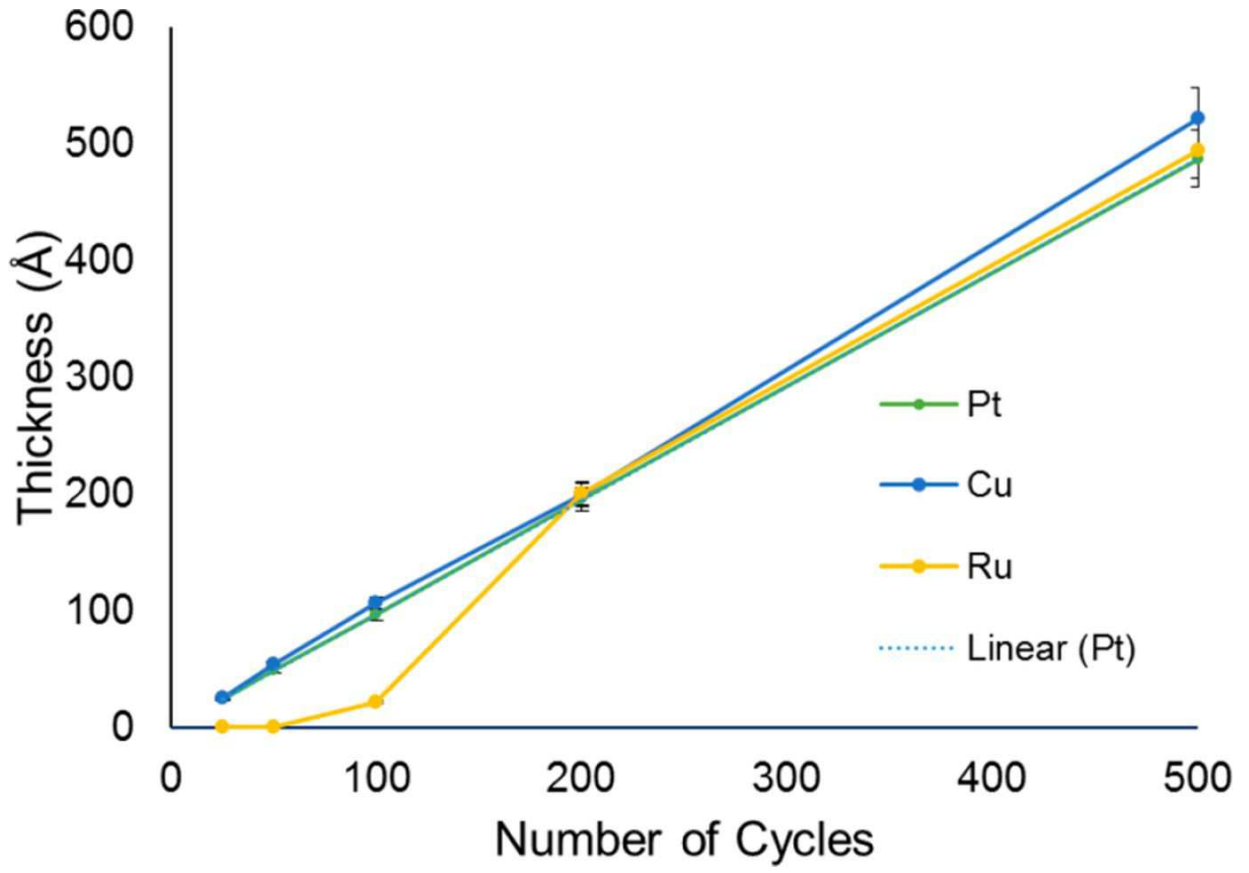
This is the author's peer reviewed, accepted manuscript. However, the online version of record will be different from this version once it has been copyedited and typeset.

PLEASE CITE THIS ARTICLE AS DOI: 10.1063/1.5087759



This is the author's peer reviewed, accepted manuscript. However, the online version of record will be different from this version once it has been copyedited and typeset.

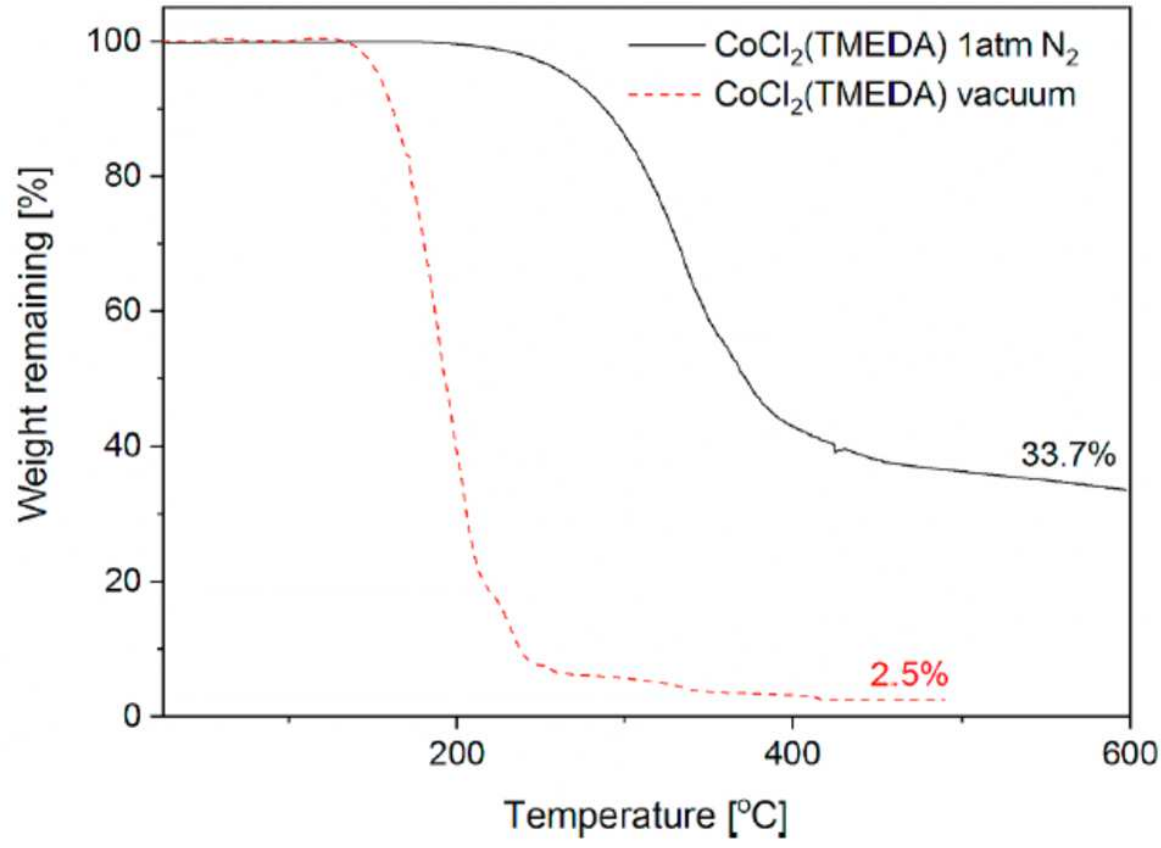
PLEASE CITE THIS ARTICLE AS DOI: 10.1063/1.5087759





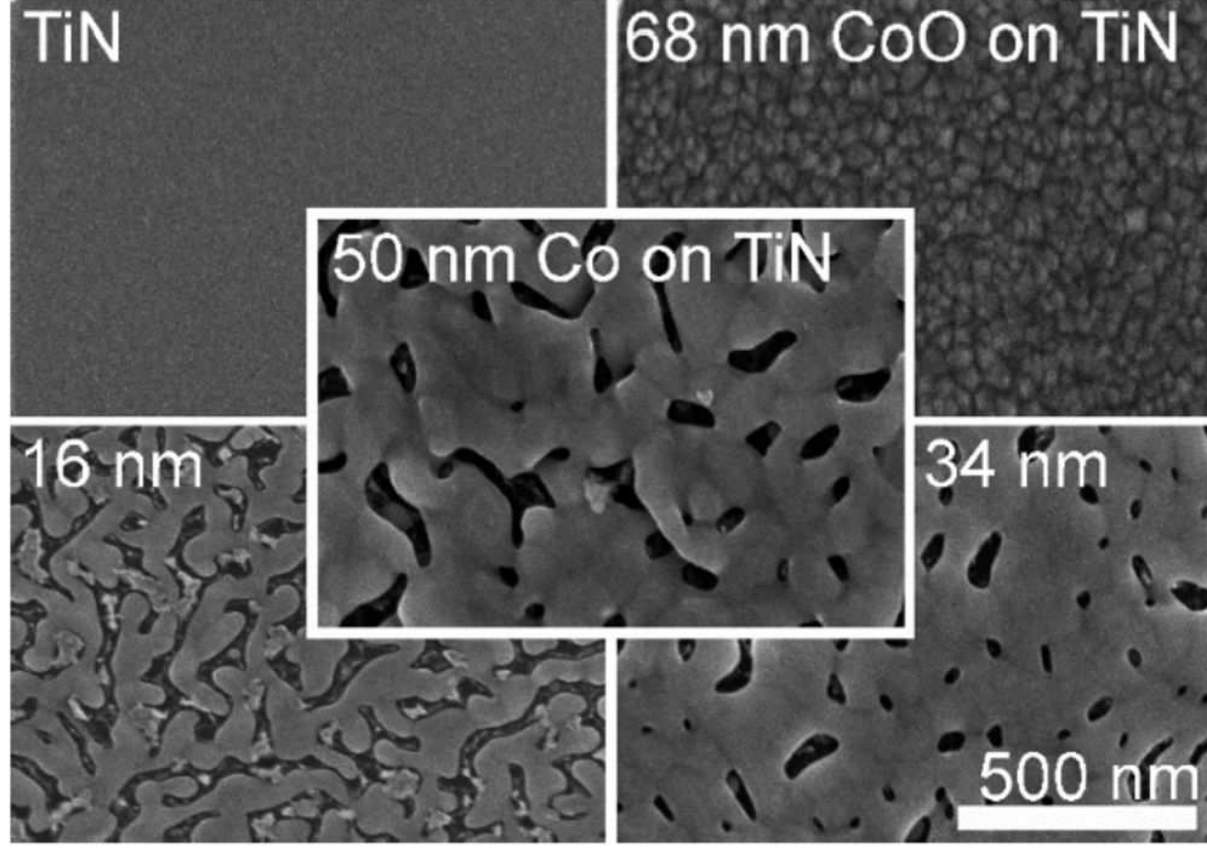
This is the author's peer reviewed, accepted manuscript. However, the online version of record will be different from this version once it has been copyedited and typeset.

PLEASE CITE THIS ARTICLE AS DOI: 10.1063/1.5087759



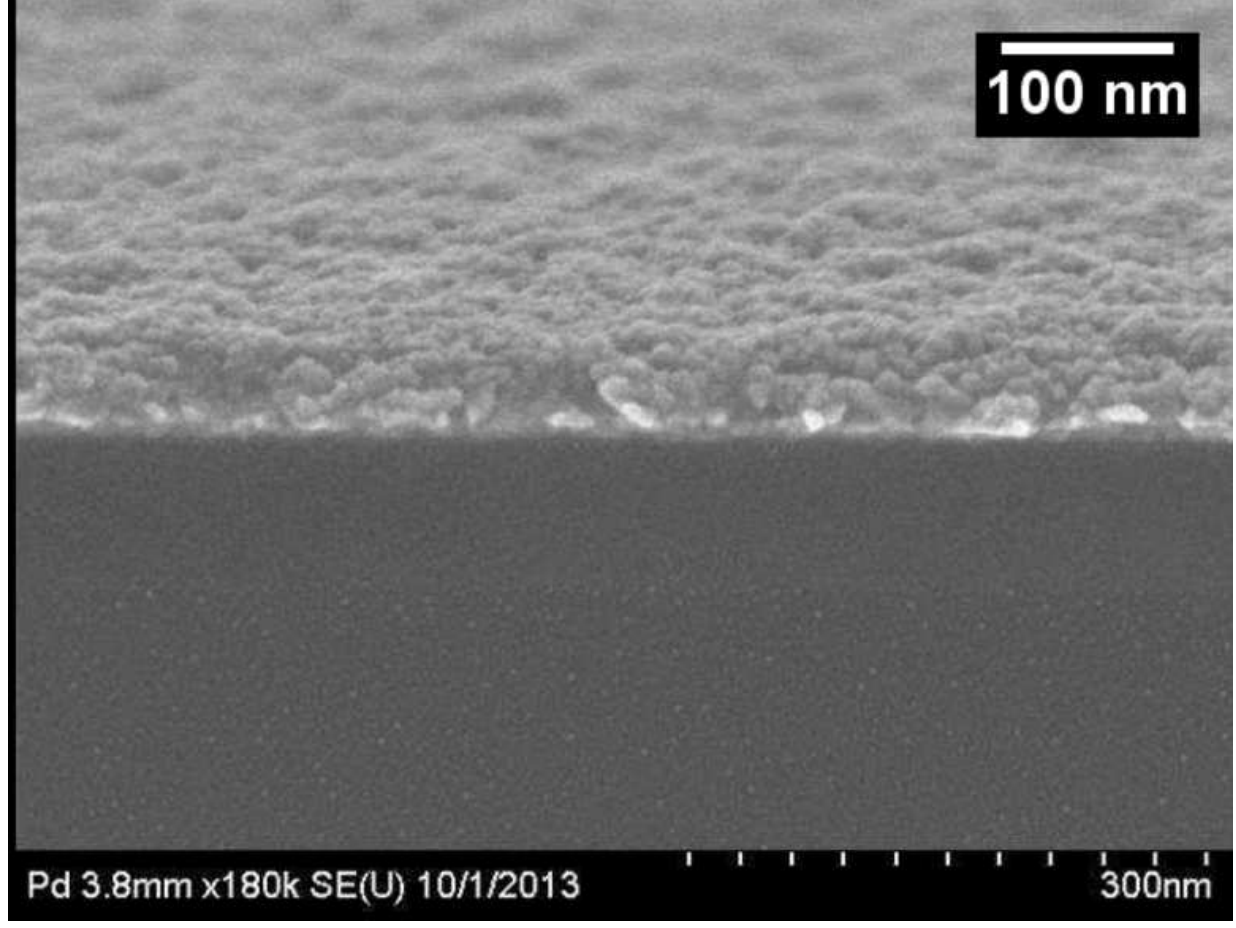
This is the author's peer reviewed, accepted manuscript. However, the online version of record will be different from this version once it has been copyedited and typeset.

PLEASE CITE THIS ARTICLE AS DOI: 10.1063/1.5087759



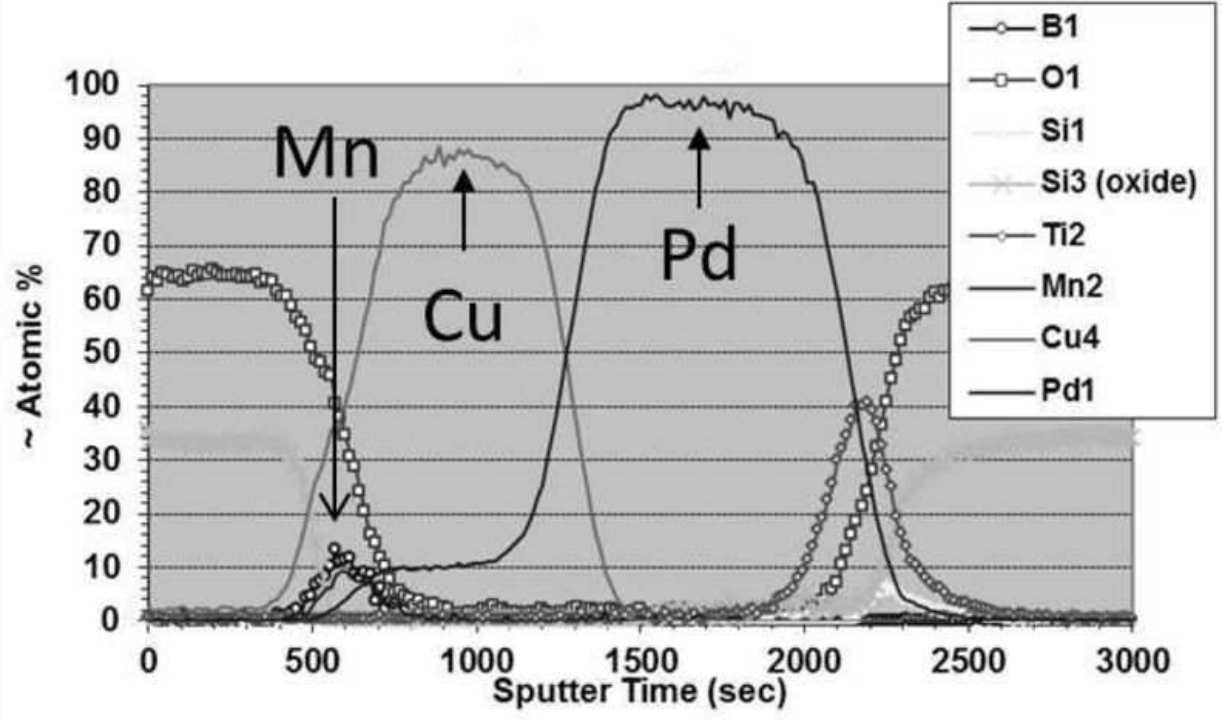
This is the author's peer reviewed, accepted manuscript. However, the online version of record will be different from this version once it has been copyedited and typeset.

PLEASE CITE THIS ARTICLE AS DOI: 10.1063/1.5087759



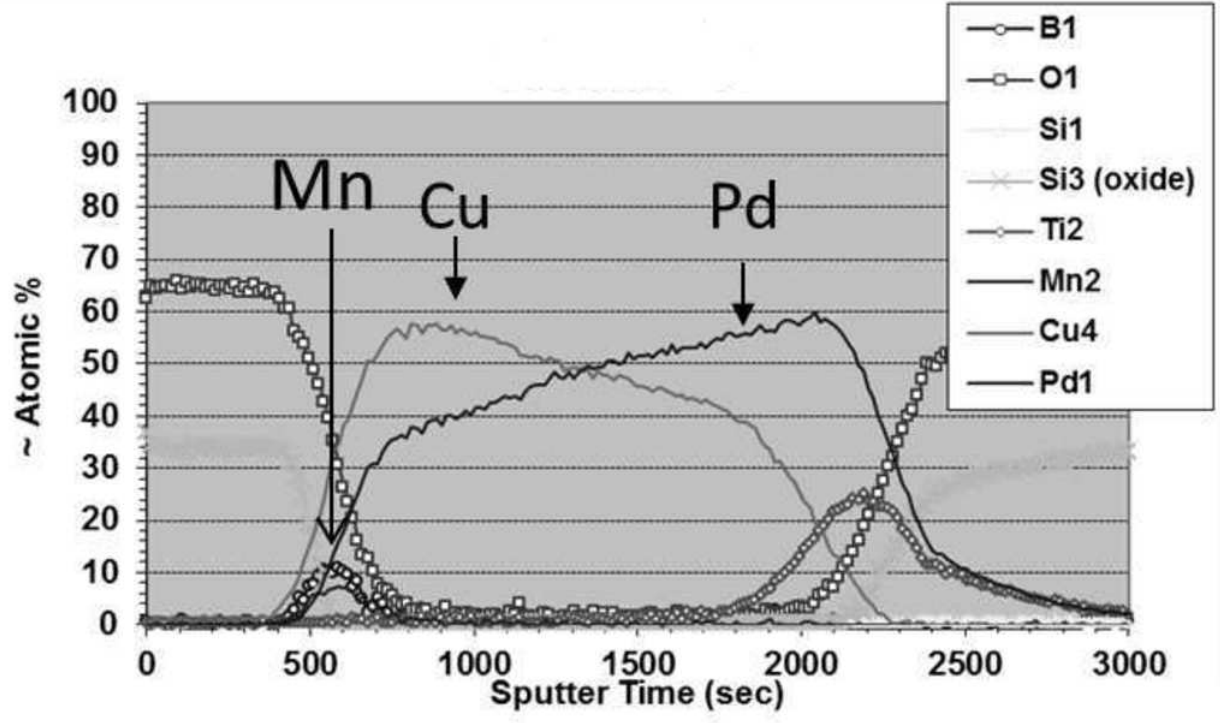
This is the author's peer reviewed, accepted manuscript. However, the online version of record will be different from this version once it has been copyedited and typeset.

PLEASE CITE THIS ARTICLE AS DOI: 10.1063/1.5087759



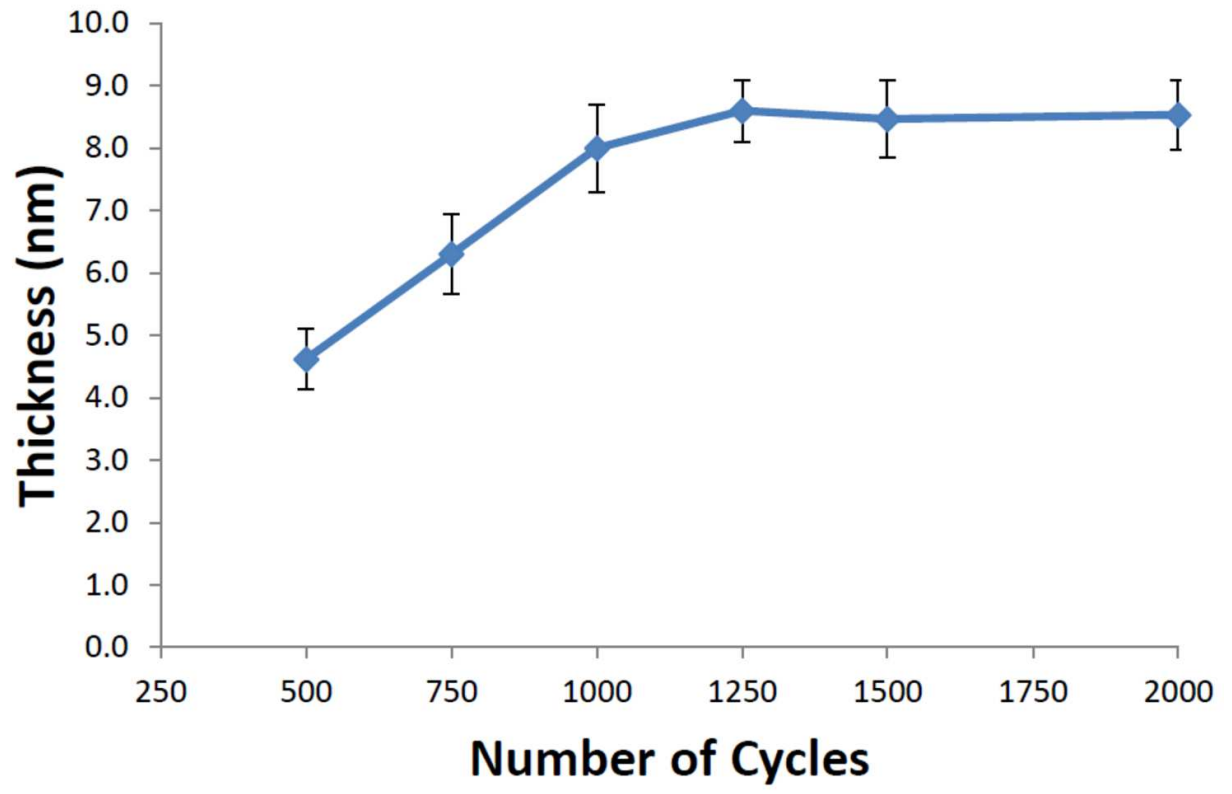
This is the author's peer reviewed, accepted manuscript. However, the online version of record will be different from this version once it has been copyedited and typeset.

PLEASE CITE THIS ARTICLE AS DOI: 10.1063/1.5087759



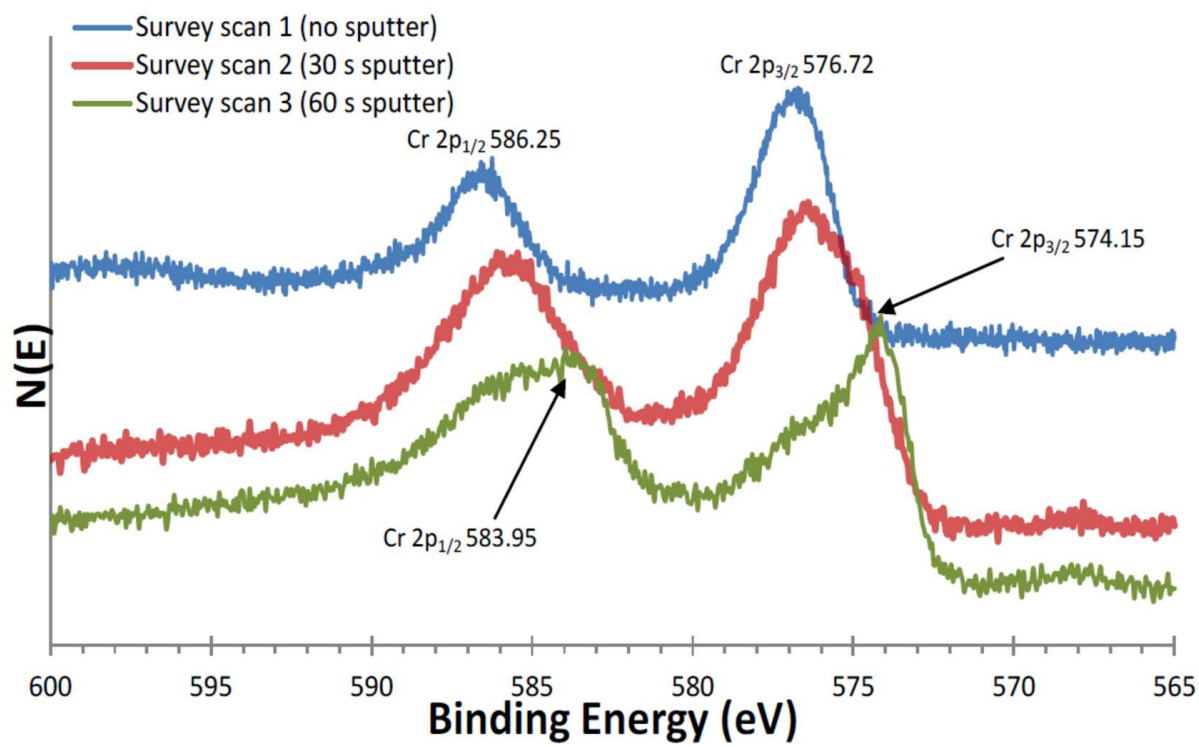
This is the author's peer reviewed, accepted manuscript. However, the online version of record will be different from this version once it has been copyedited and typeset.

PLEASE CITE THIS ARTICLE AS DOI: 10.1063/1.5087759



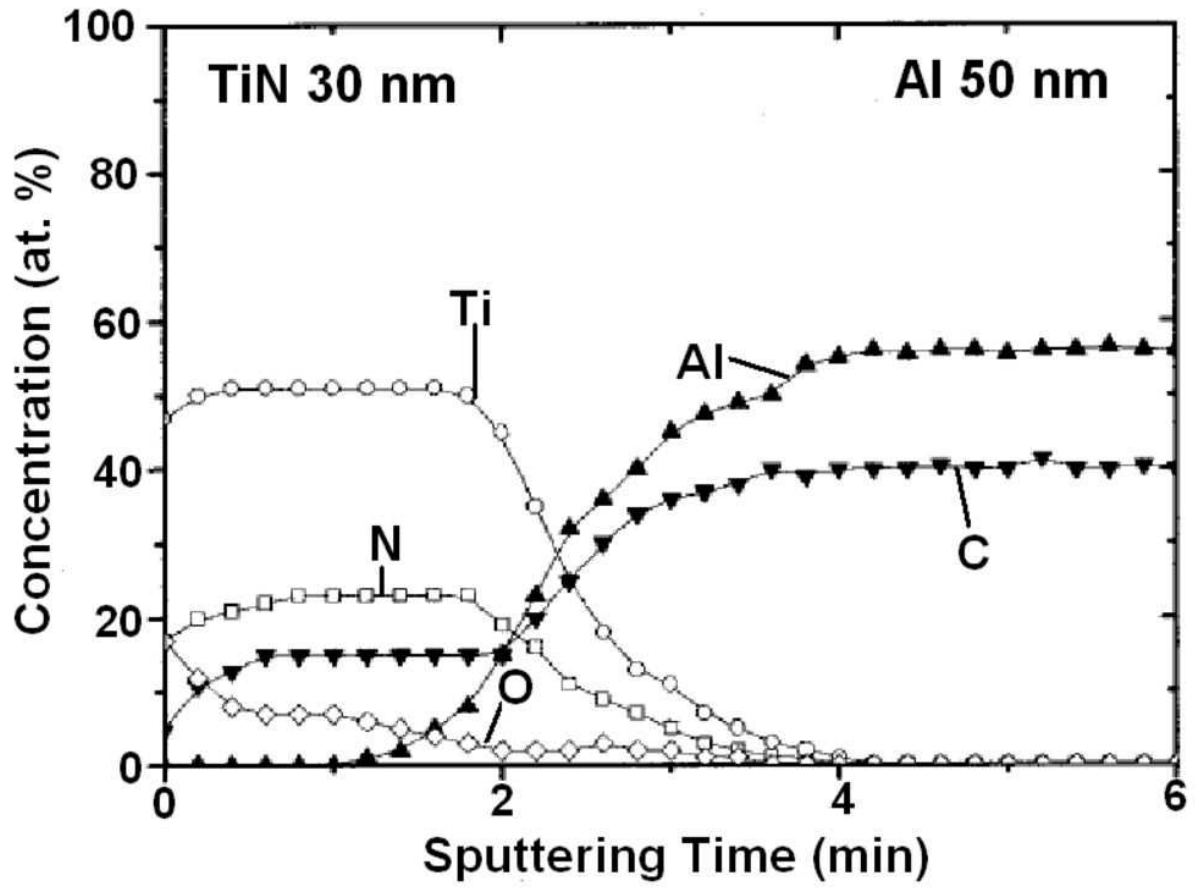
This is the author's peer reviewed, accepted manuscript. However, the online version of record will be different from this version once it has been copyedited and typeset.

PLEASE CITE THIS ARTICLE AS DOI: 10.1063/1.5087759



This is the author's peer reviewed, accepted manuscript. However, the online version of record will be different from this version once it has been copyedited and typeset.

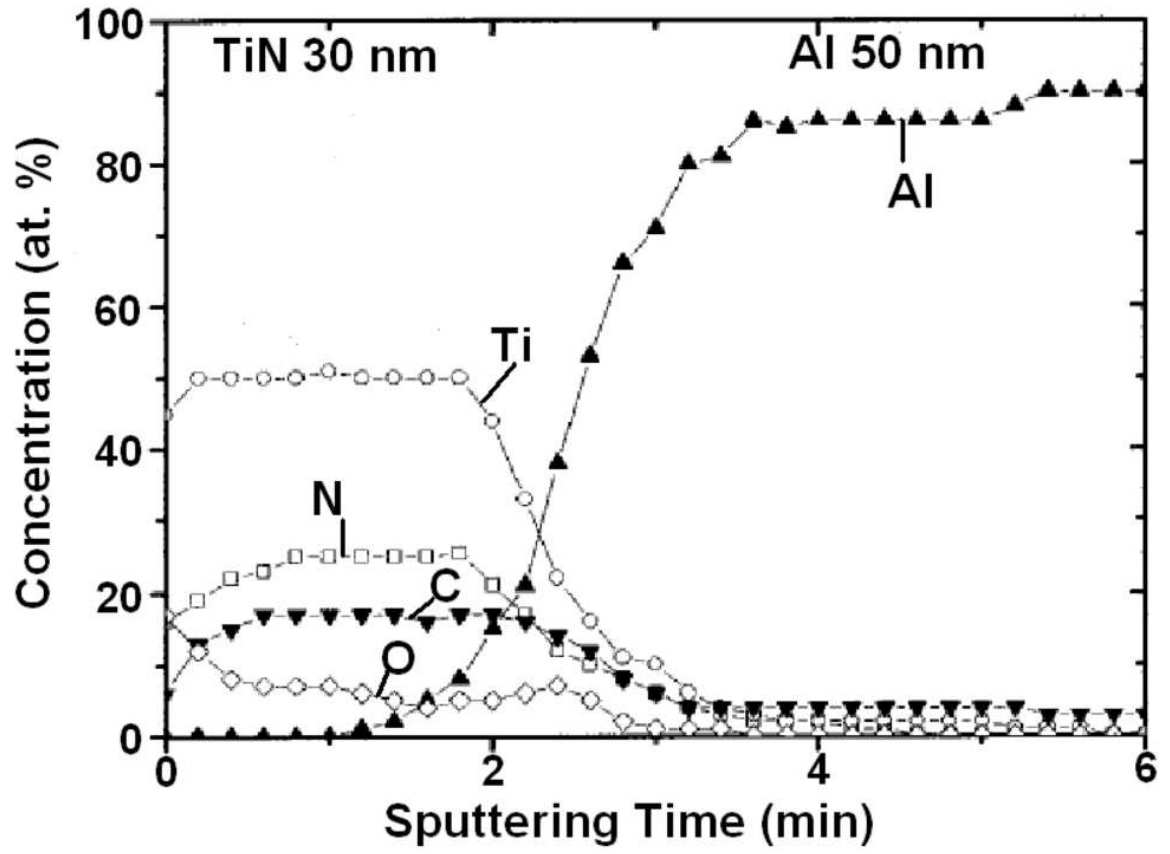
PLEASE CITE THIS ARTICLE AS DOI: 10.1063/1.5087759





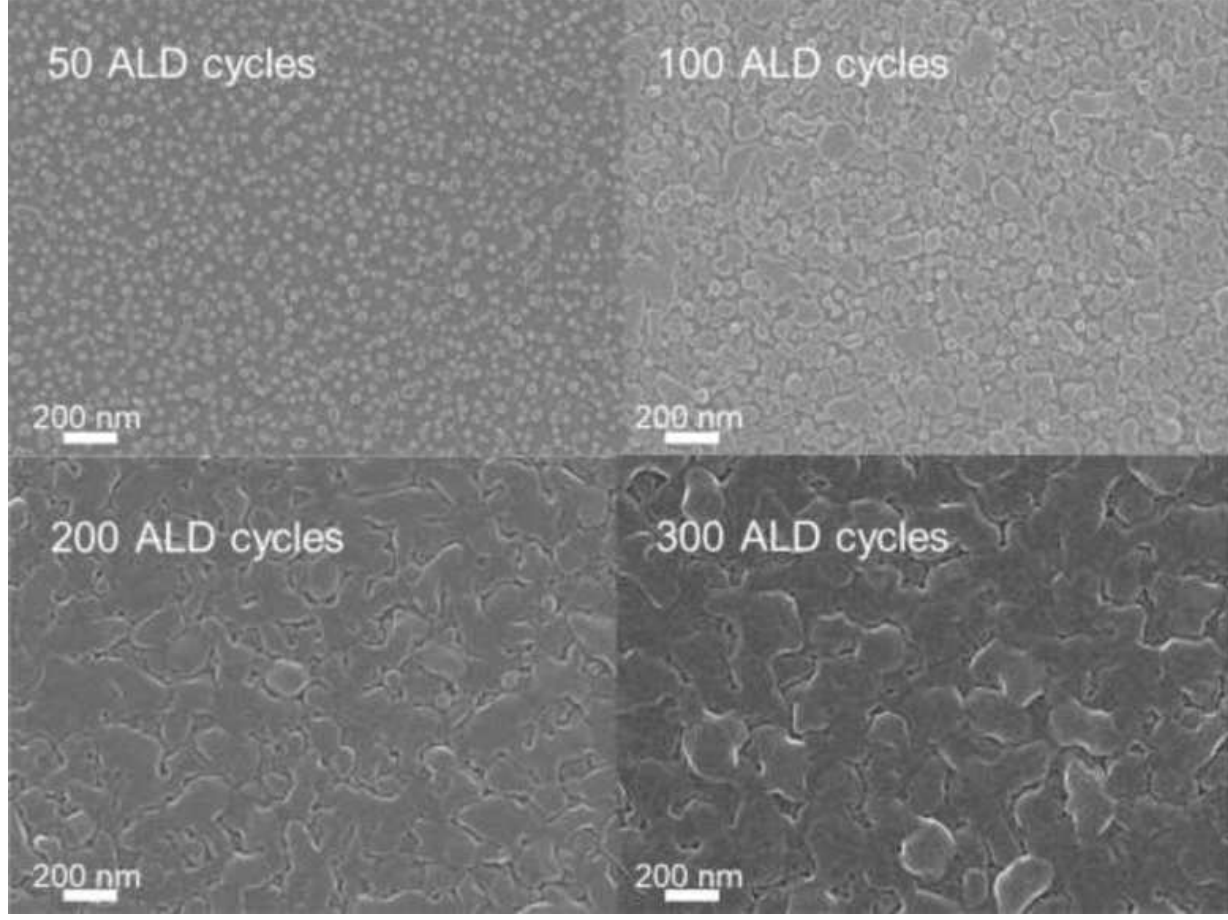
This is the author's peer reviewed, accepted manuscript. However, the online version of record will be different from this version once it has been copyedited and typeset.

PLEASE CITE THIS ARTICLE AS DOI: 10.1063/1.5087759



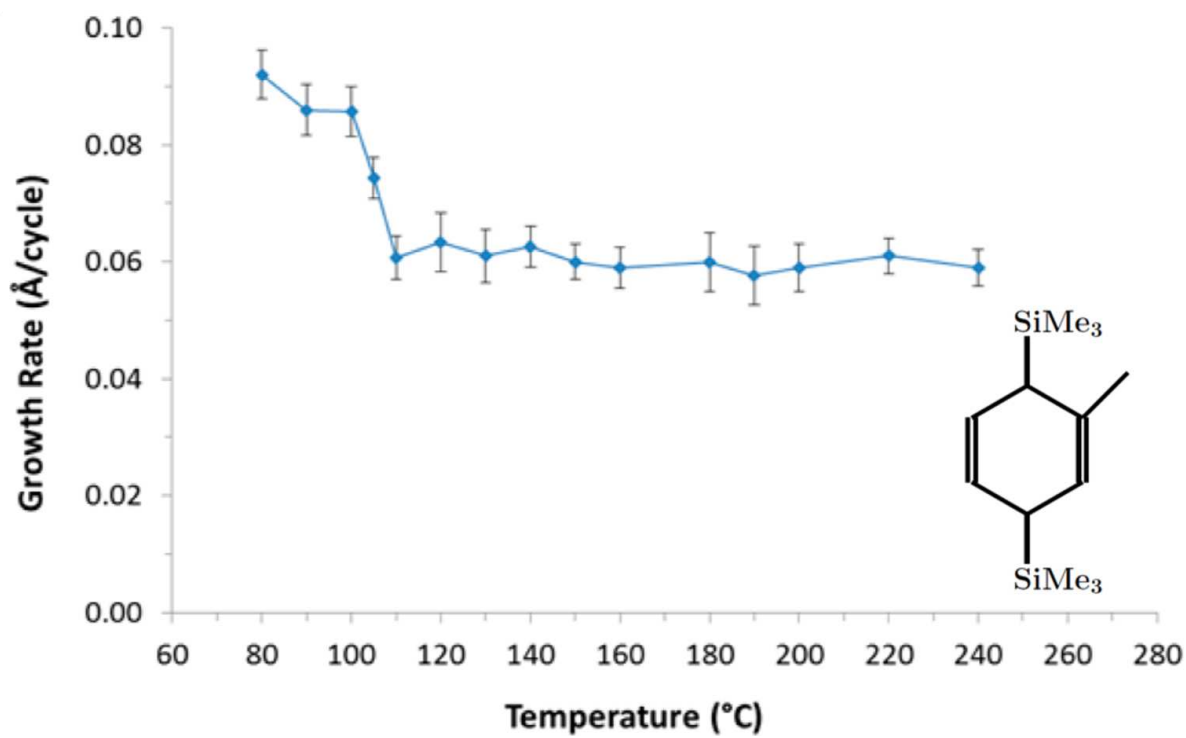
This is the author's peer reviewed, accepted manuscript. However, the online version of record will be different from this version once it has been copyedited and typeset.

PLEASE CITE THIS ARTICLE AS DOI: 10.1063/1.5087759



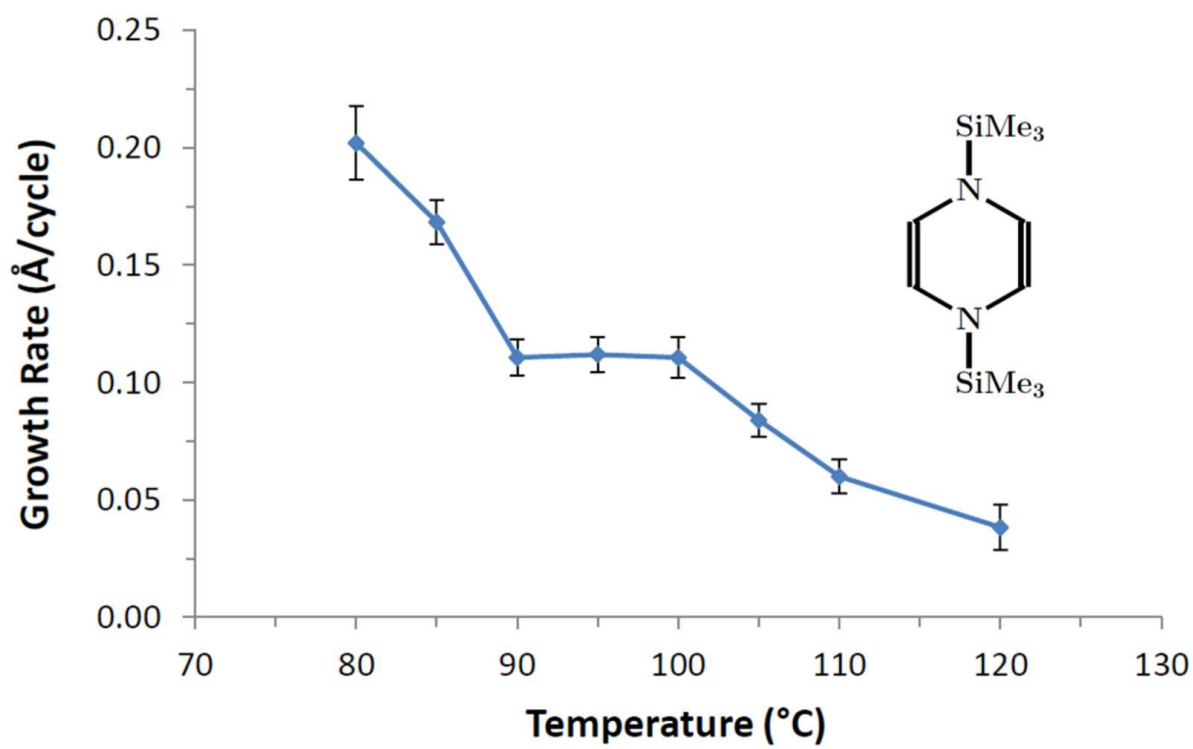
This is the author's peer reviewed, accepted manuscript. However, the online version of record will be different from this version once it has been copyedited and typeset.

PLEASE CITE THIS ARTICLE AS DOI: 10.1063/1.5087759



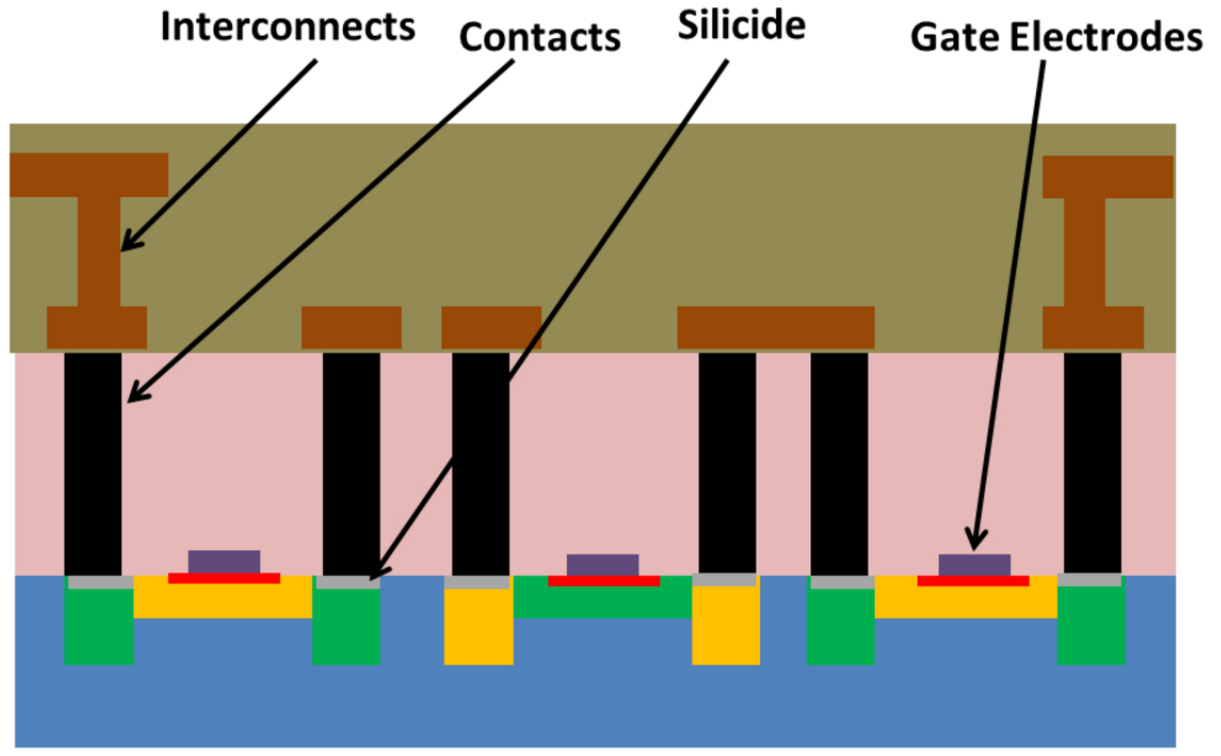
This is the author's peer reviewed, accepted manuscript. However, the online version of record will be different from this version once it has been copyedited and typeset.

PLEASE CITE THIS ARTICLE AS DOI: 10.1063/1.5087759



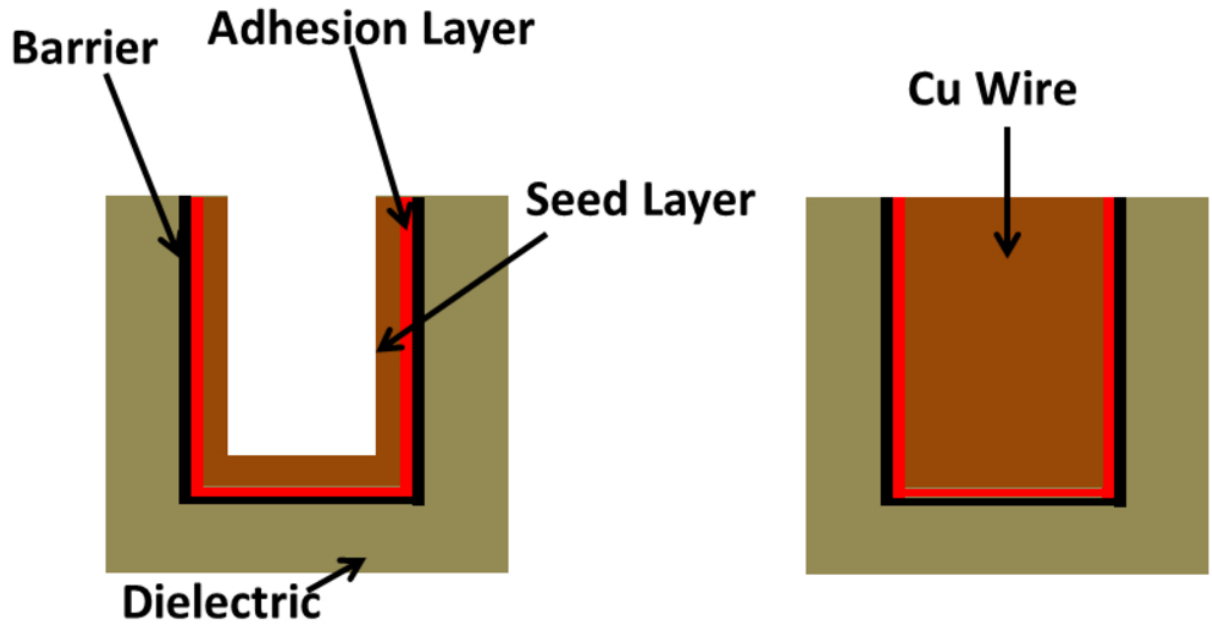
This is the author's peer reviewed, accepted manuscript. However, the online version of record will be different from this version once it has been copyedited and typeset.

PLEASE CITE THIS ARTICLE AS DOI: 10.1063/1.5087759



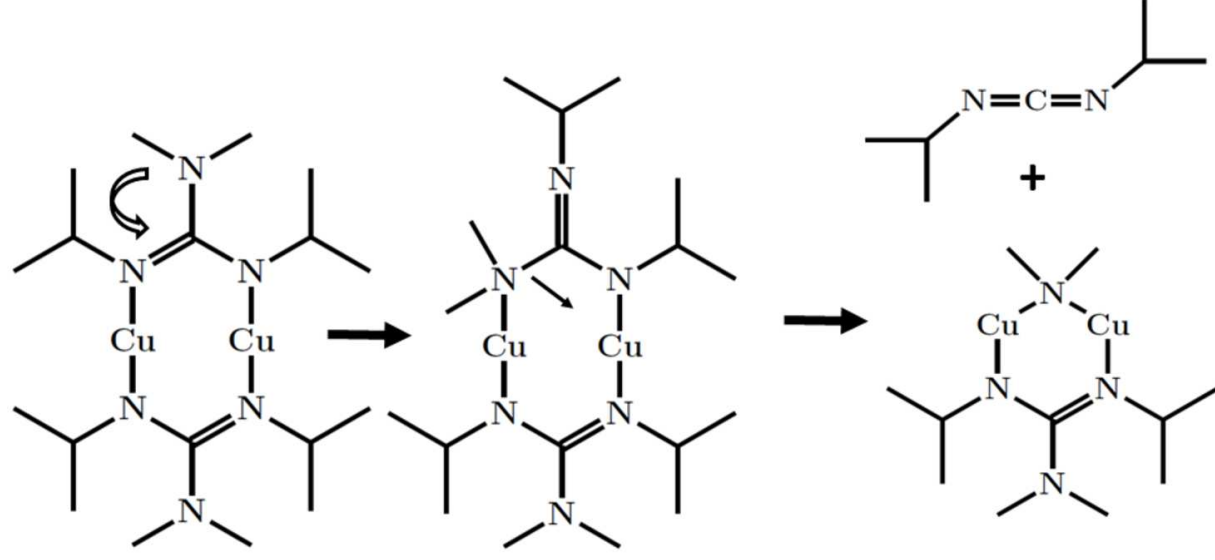
This is the author's peer reviewed, accepted manuscript. However, the online version of record will be different from this version once it has been copyedited and typeset.

PLEASE CITE THIS ARTICLE AS DOI: 10.1063/1.5087759



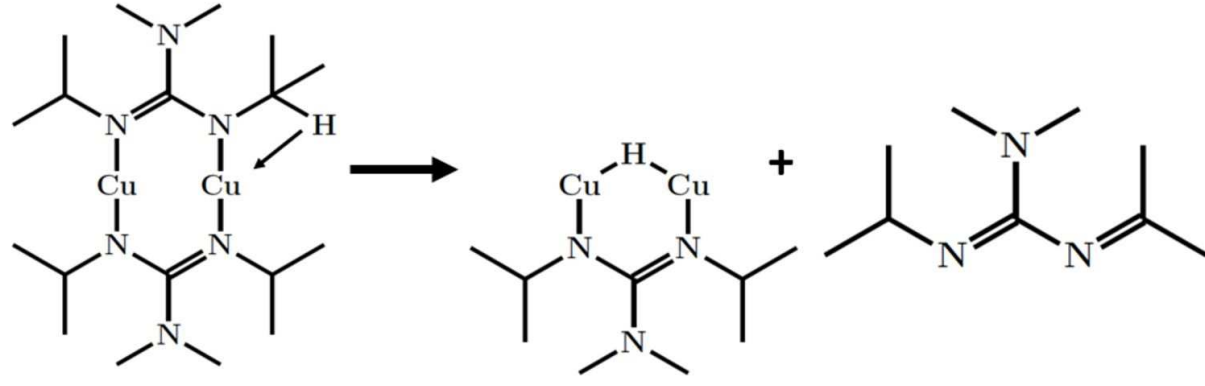
This is the author's peer reviewed, accepted manuscript. However, the online version of record will be different from this version once it has been copyedited and typeset.

PLEASE CITE THIS ARTICLE AS DOI: 10.1063/1.5087759



This is the author's peer reviewed, accepted manuscript. However, the online version of record will be different from this version once it has been copyedited and typeset.

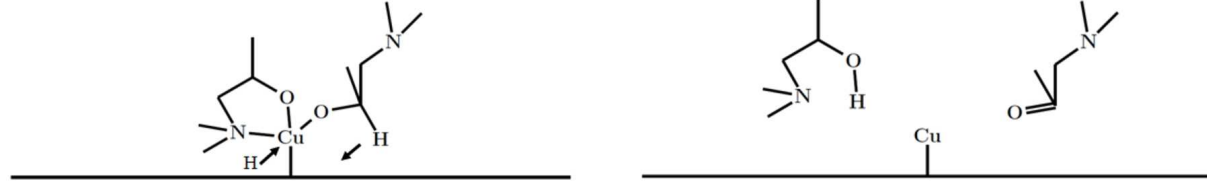
PLEASE CITE THIS ARTICLE AS DOI: 10.1063/1.5087759





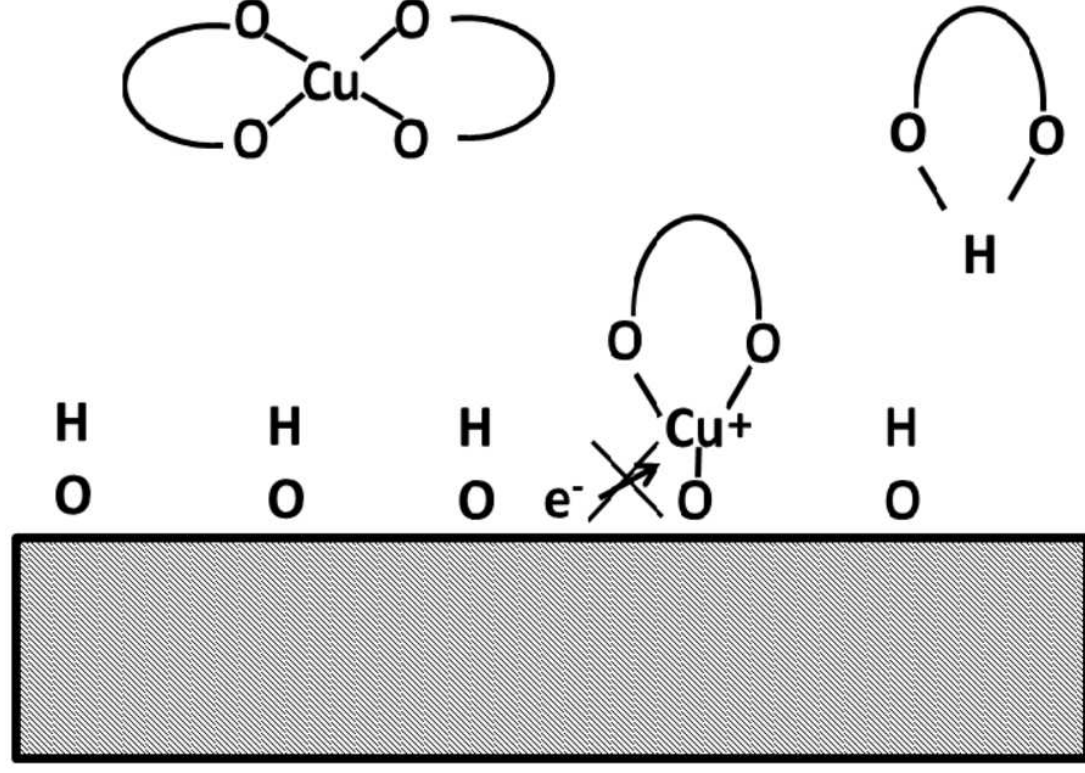
This is the author's peer reviewed, accepted manuscript. However, the online version of record will be different from this version once it has been copyedited and typeset.

PLEASE CITE THIS ARTICLE AS DOI: 10.1063/1.5087759



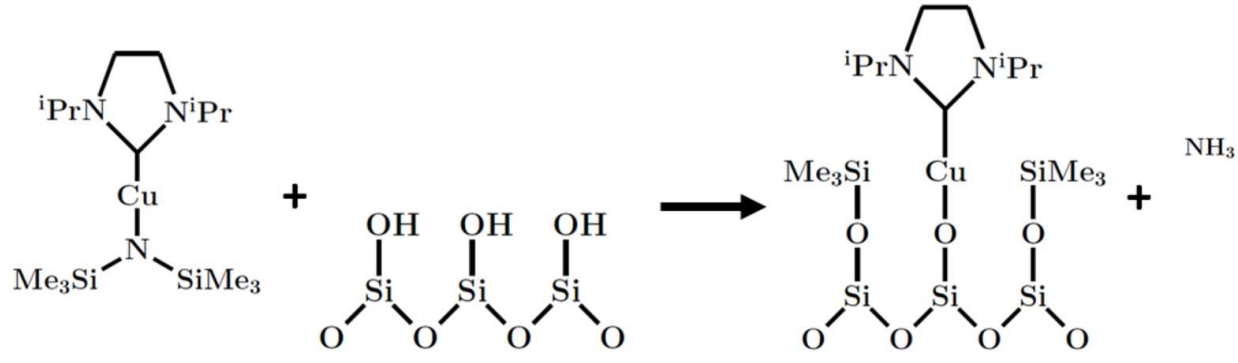
This is the author's peer reviewed, accepted manuscript. However, the online version of record will be different from this version once it has been copyedited and typeset.

PLEASE CITE THIS ARTICLE AS DOI: 10.1063/1.5087759



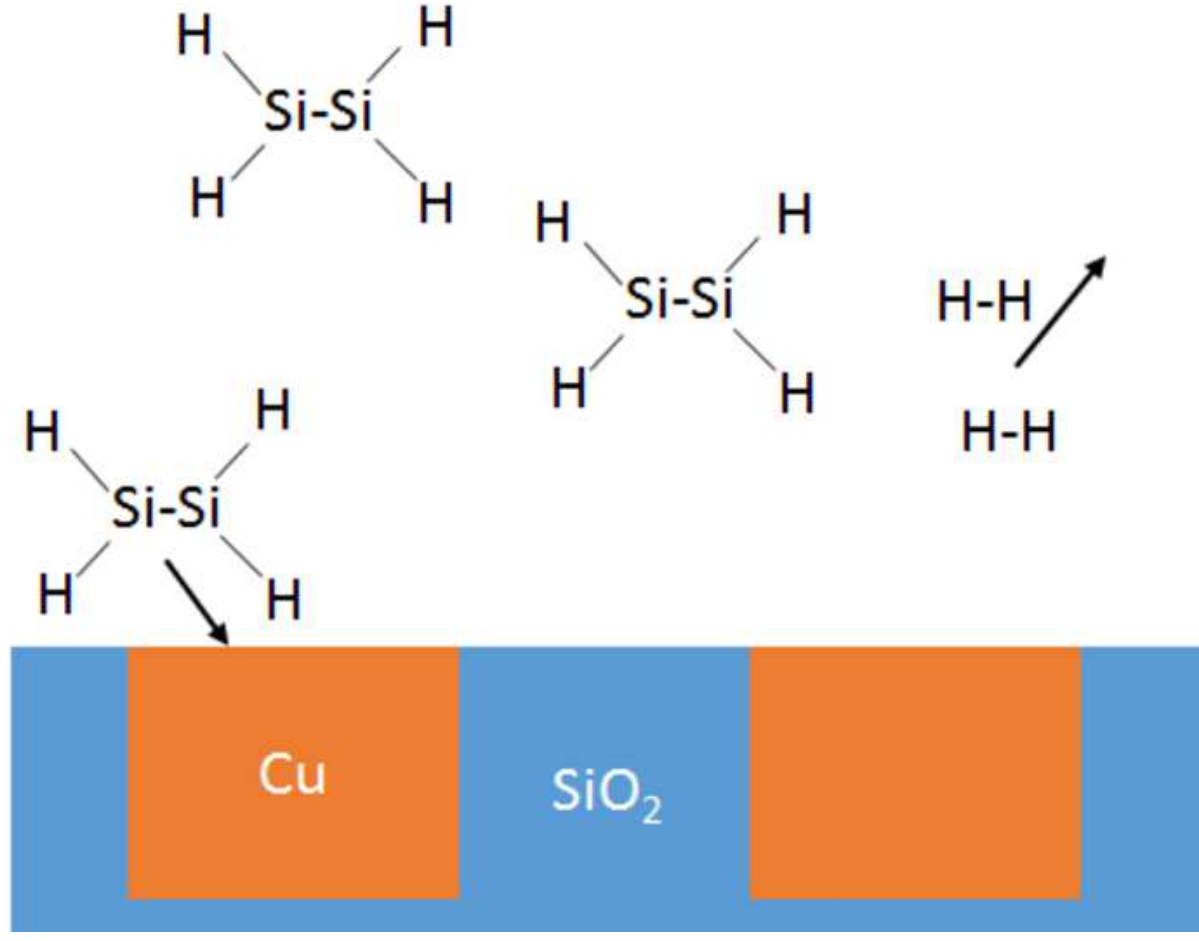
This is the author's peer reviewed, accepted manuscript. However, the online version of record will be different from this version once it has been copyedited and typeset.

PLEASE CITE THIS ARTICLE AS DOI: 10.1063/1.5087759



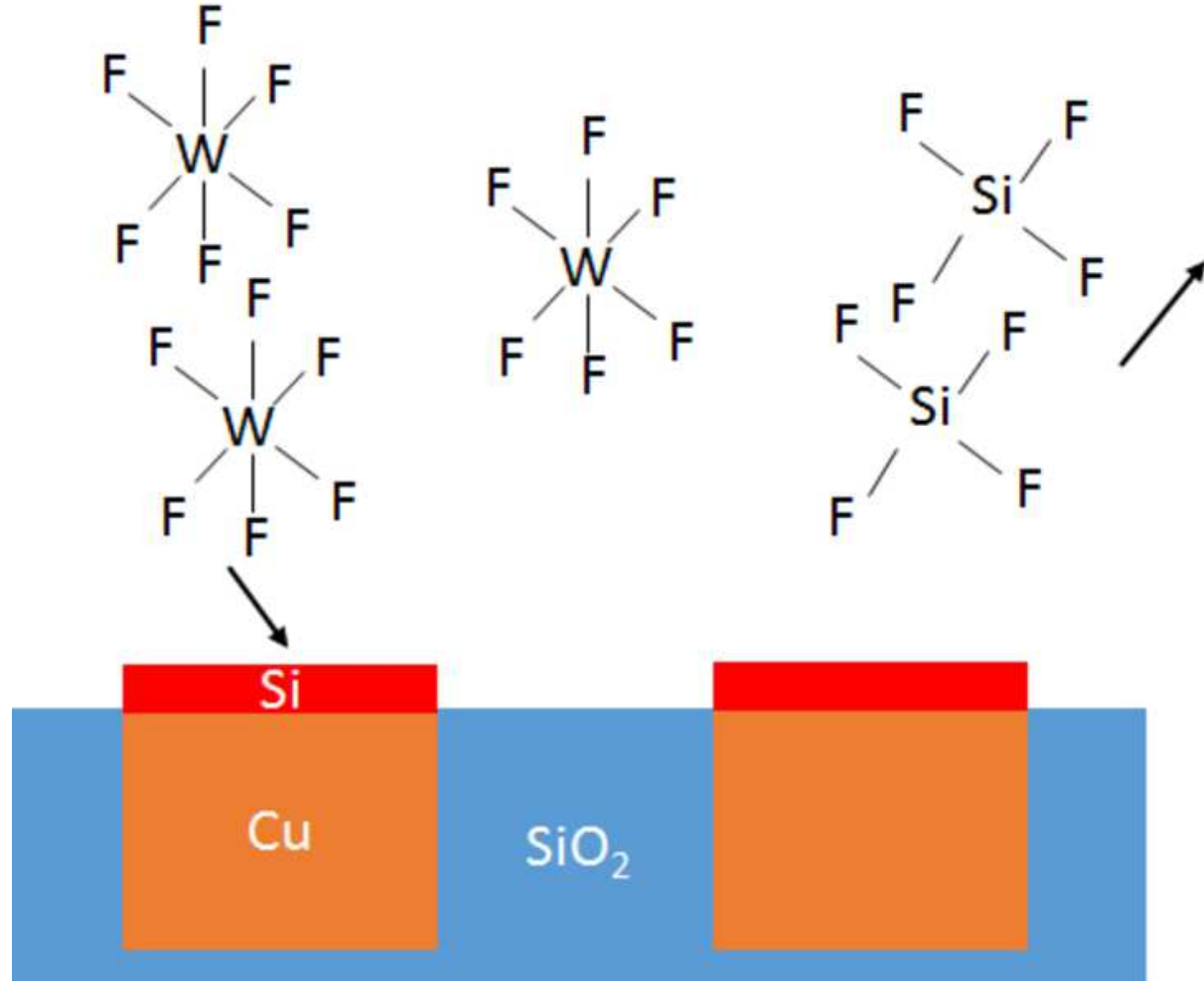
This is the author's peer reviewed, accepted manuscript. However, the online version of record will be different from this version once it has been copyedited and typeset.

PLEASE CITE THIS ARTICLE AS DOI: 10.1063/1.5087759



This is the author's peer reviewed, accepted manuscript. However, the online version of record will be different from this version once it has been copyedited and typeset.

PLEASE CITE THIS ARTICLE AS DOI: 10.1063/1.5087759



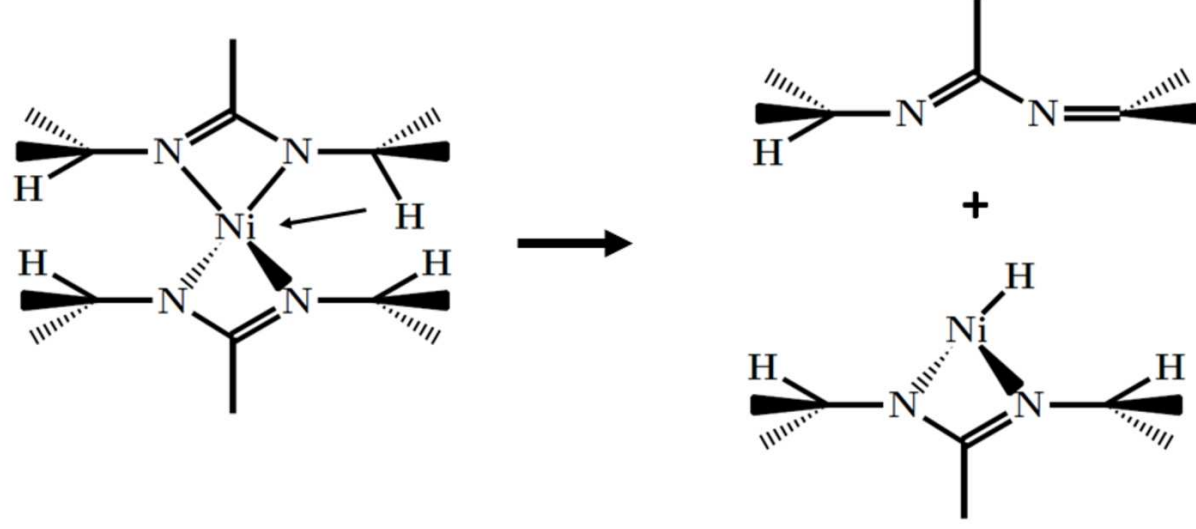
This is the author's peer reviewed, accepted manuscript. However, the online version of record will be different from this version once it has been copyedited and typeset.

PLEASE CITE THIS ARTICLE AS DOI: 10.1063/1.5087759



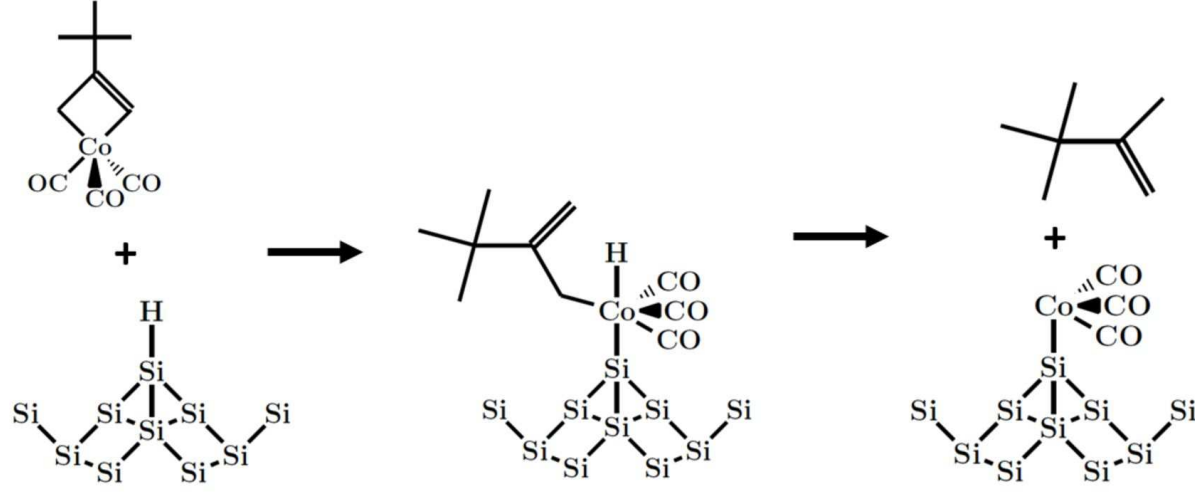
This is the author's peer reviewed, accepted manuscript. However, the online version of record will be different from this version once it has been copyedited and typeset.

PLEASE CITE THIS ARTICLE AS DOI: 10.1063/1.5087759



This is the author's peer reviewed, accepted manuscript. However, the online version of record will be different from this version once it has been copyedited and typeset.

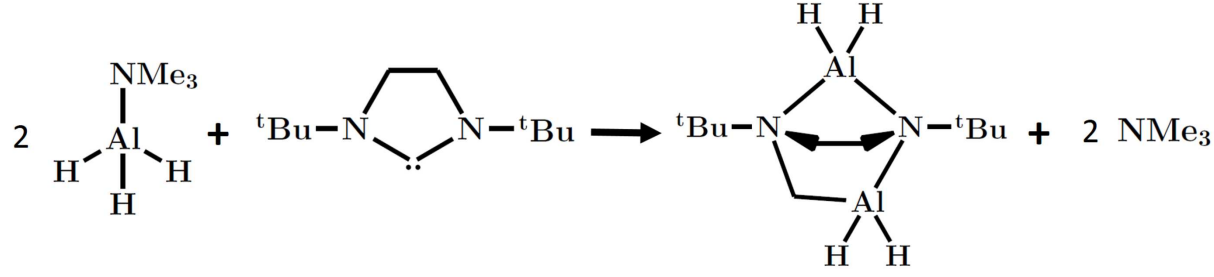
PLEASE CITE THIS ARTICLE AS DOI: 10.1063/1.5087759





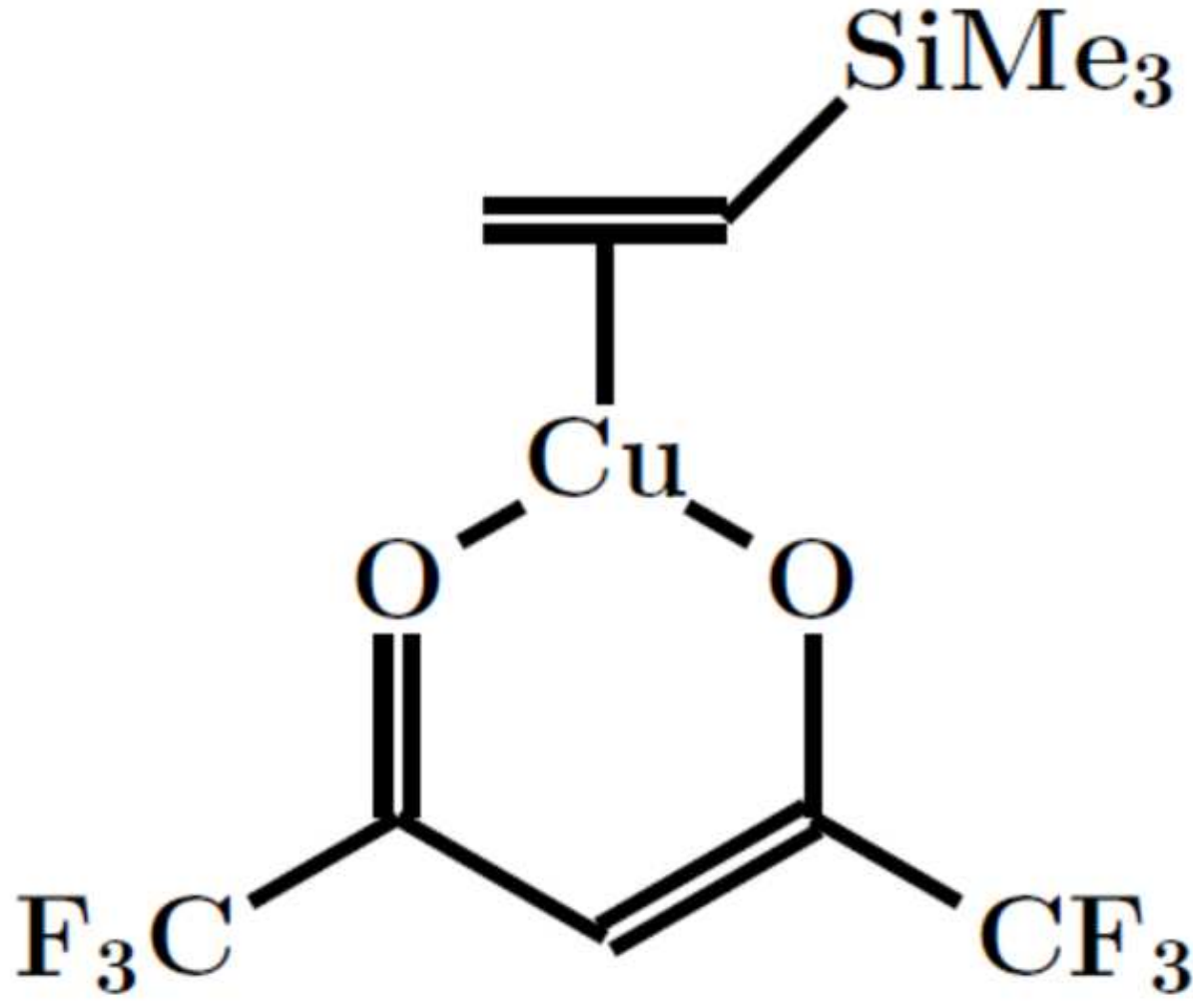
This is the author's peer reviewed, accepted manuscript. However, the online version of record will be different from this version once it has been copyedited and typeset.

PLEASE CITE THIS ARTICLE AS DOI: 10.1063/1.5087759



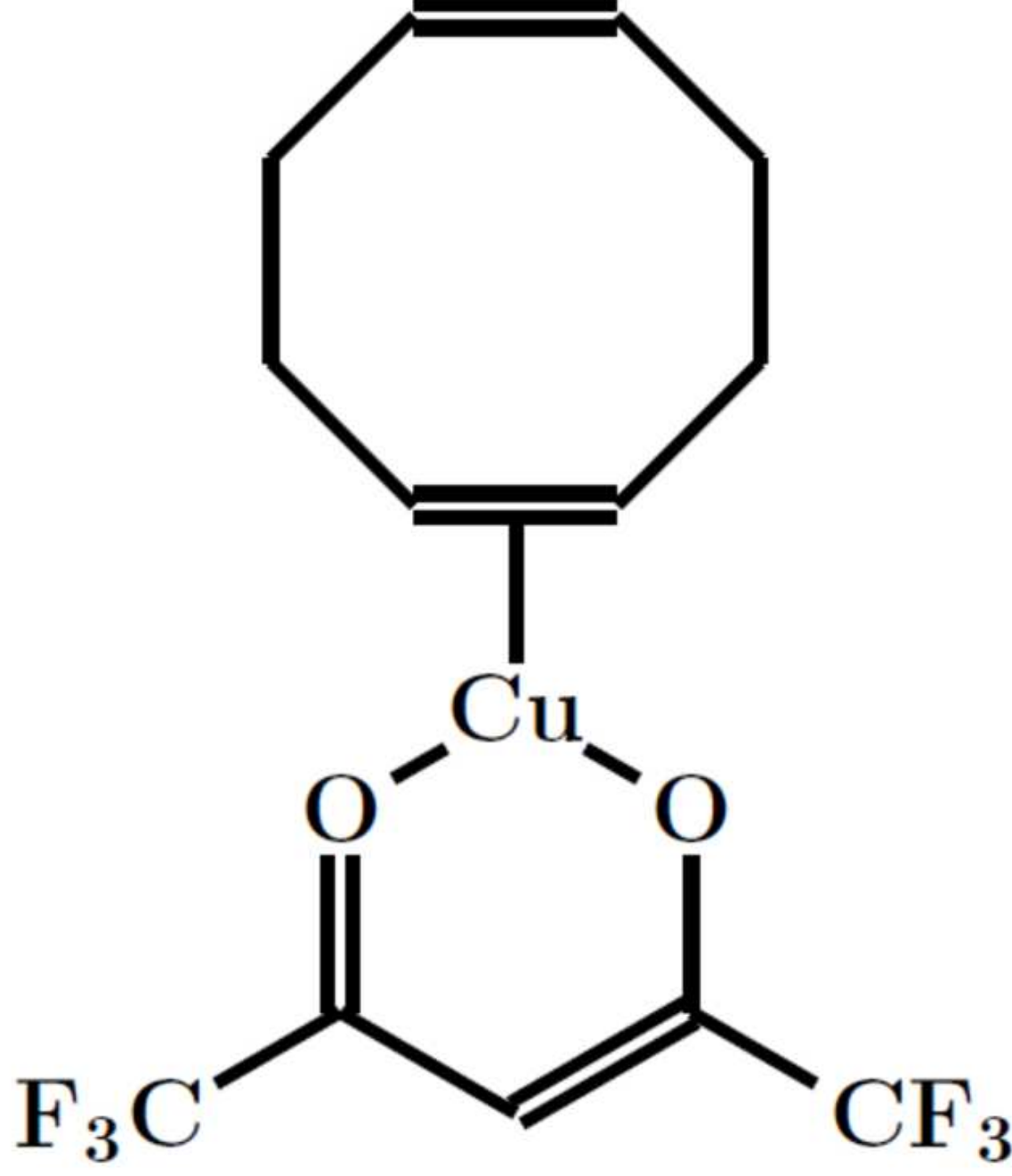
This is the author's peer reviewed, accepted manuscript. However, the online version of record will be different from this version once it has been copyedited and typeset.

PLEASE CITE THIS ARTICLE AS DOI: 10.1063/1.5087759



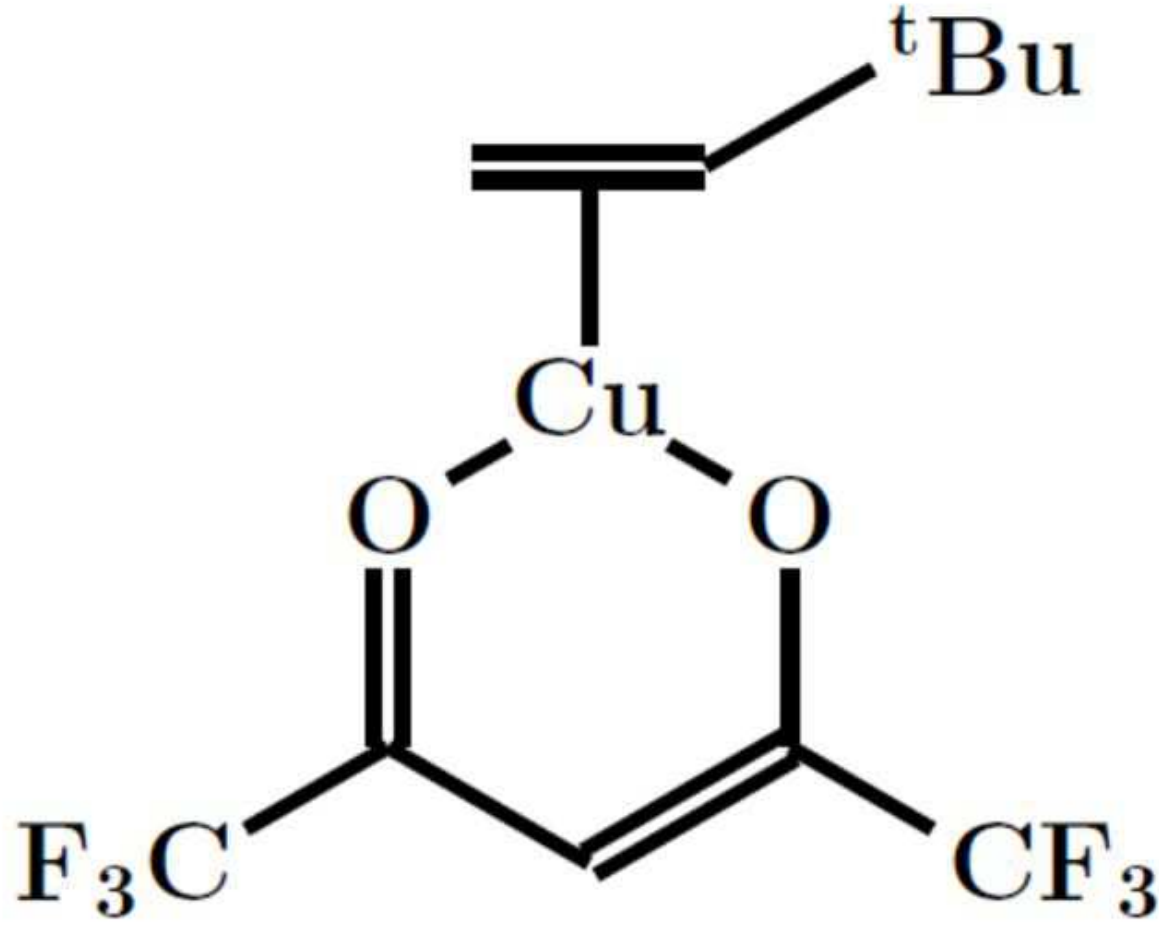
This is the author's peer reviewed, accepted manuscript. However, the online version of record will be different from this version once it has been copyedited and typeset.

PLEASE CITE THIS ARTICLE AS DOI: 10.1063/1.5087759



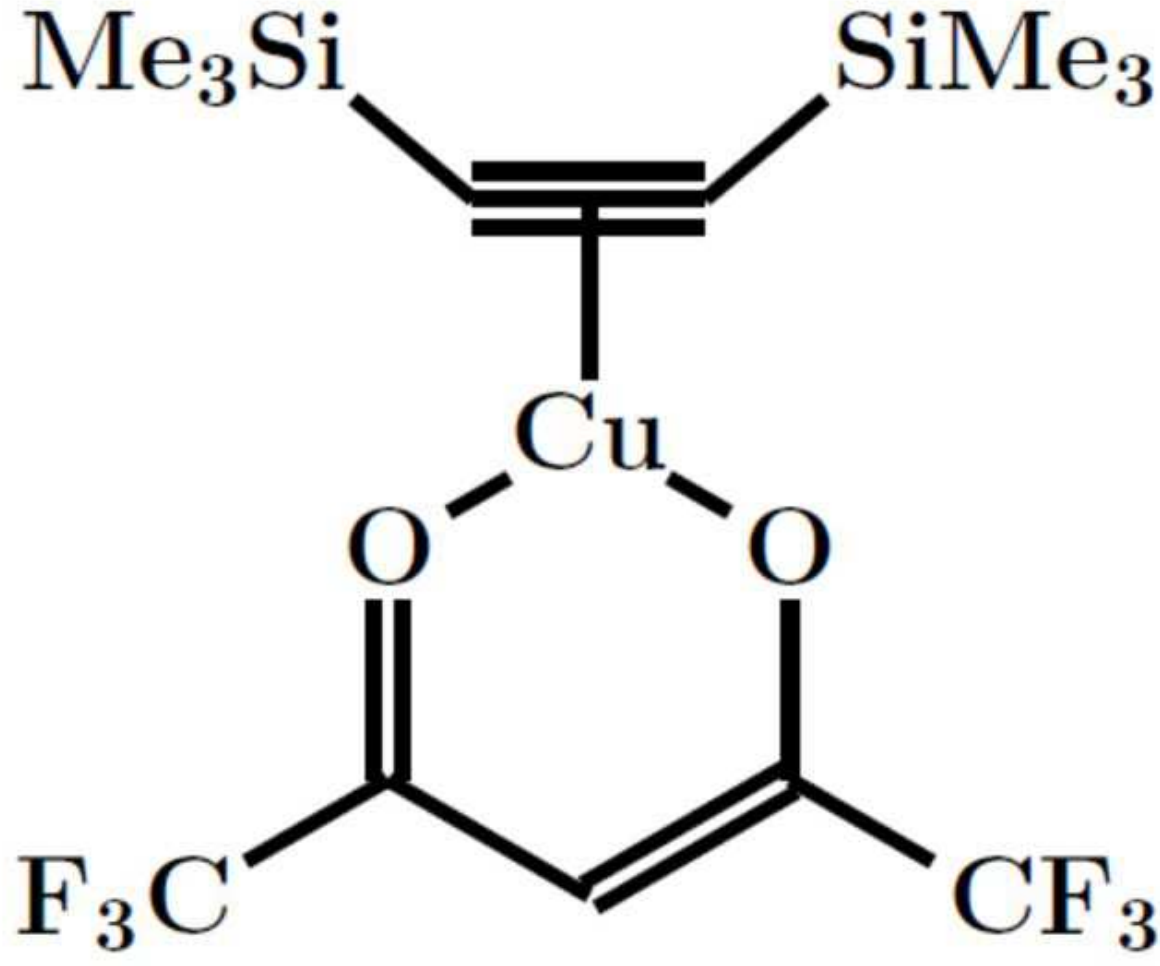
This is the author's peer reviewed, accepted manuscript. However, the online version of record will be different from this version once it has been copyedited and typeset.

PLEASE CITE THIS ARTICLE AS DOI: 10.1063/1.5087759



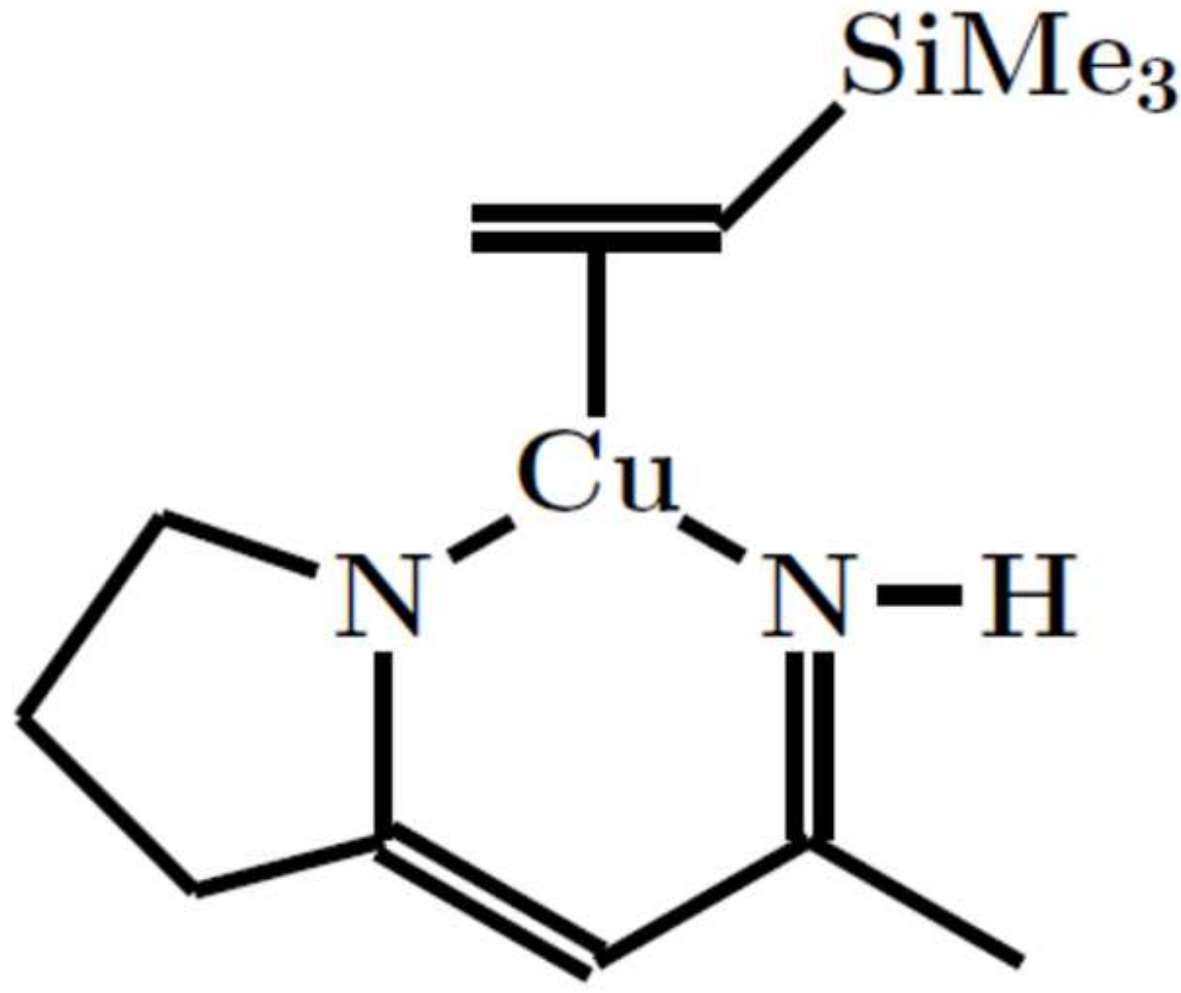
This is the author's peer reviewed, accepted manuscript. However, the online version of record will be different from this version once it has been copyedited and typeset.

PLEASE CITE THIS ARTICLE AS DOI: 10.1063/1.5087759



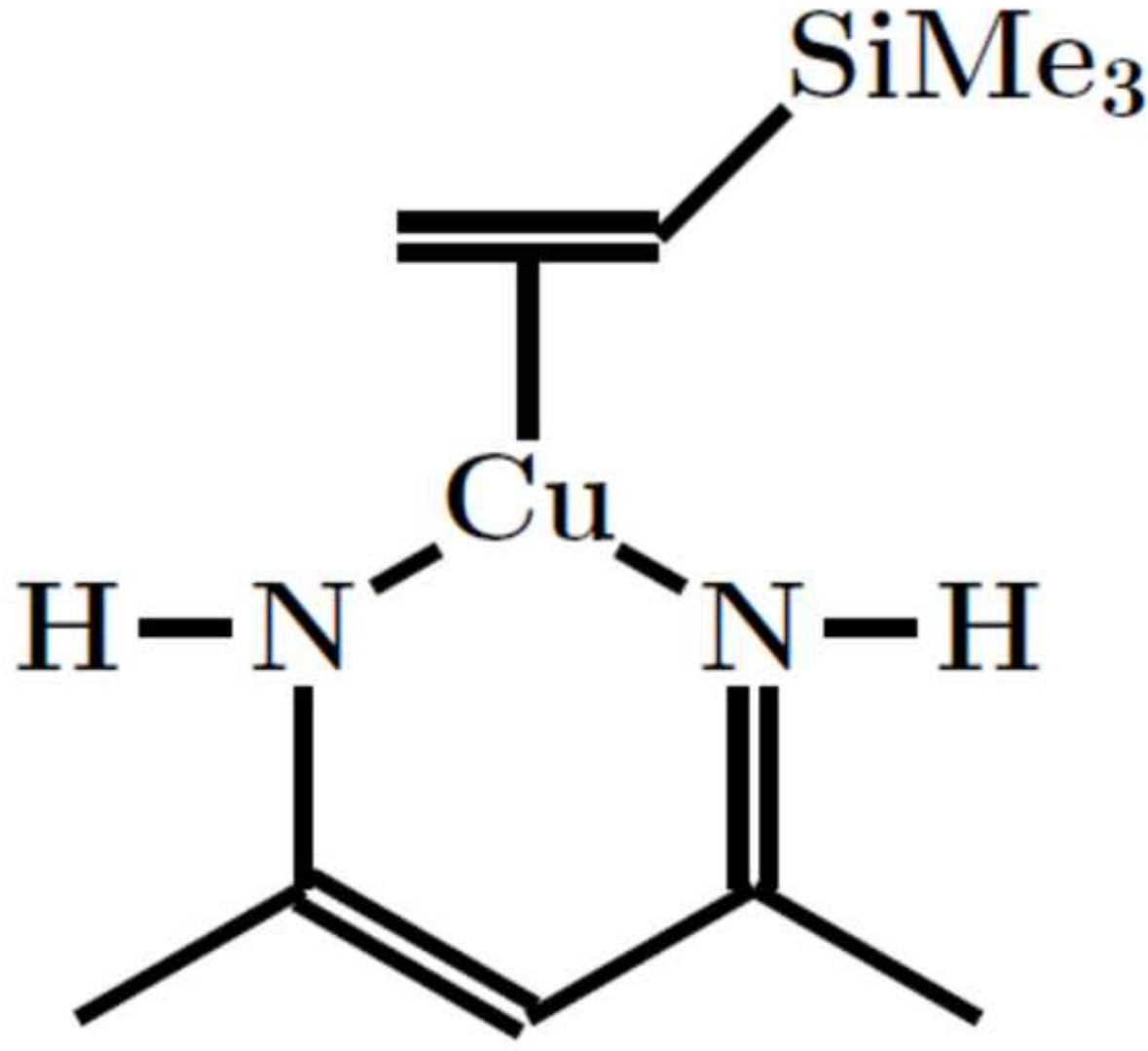
This is the author's peer reviewed, accepted manuscript. However, the online version of record will be different from this version once it has been copyedited and typeset.

PLEASE CITE THIS ARTICLE AS DOI: 10.1063/1.5087759



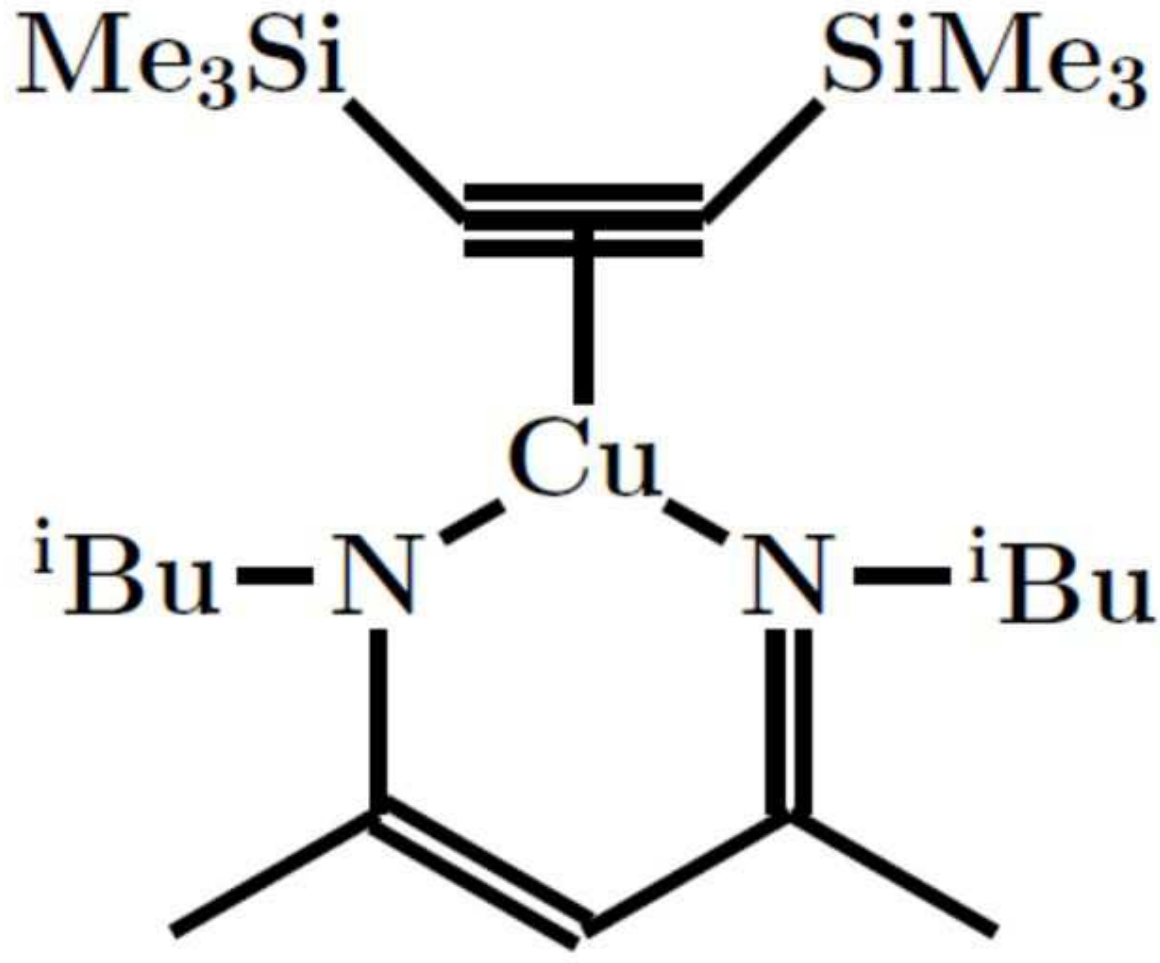
This is the author's peer reviewed, accepted manuscript. However, the online version of record will be different from this version once it has been copyedited and typeset.

PLEASE CITE THIS ARTICLE AS DOI: 10.1063/1.5087759



This is the author's peer reviewed, accepted manuscript. However, the online version of record will be different from this version once it has been copyedited and typeset.

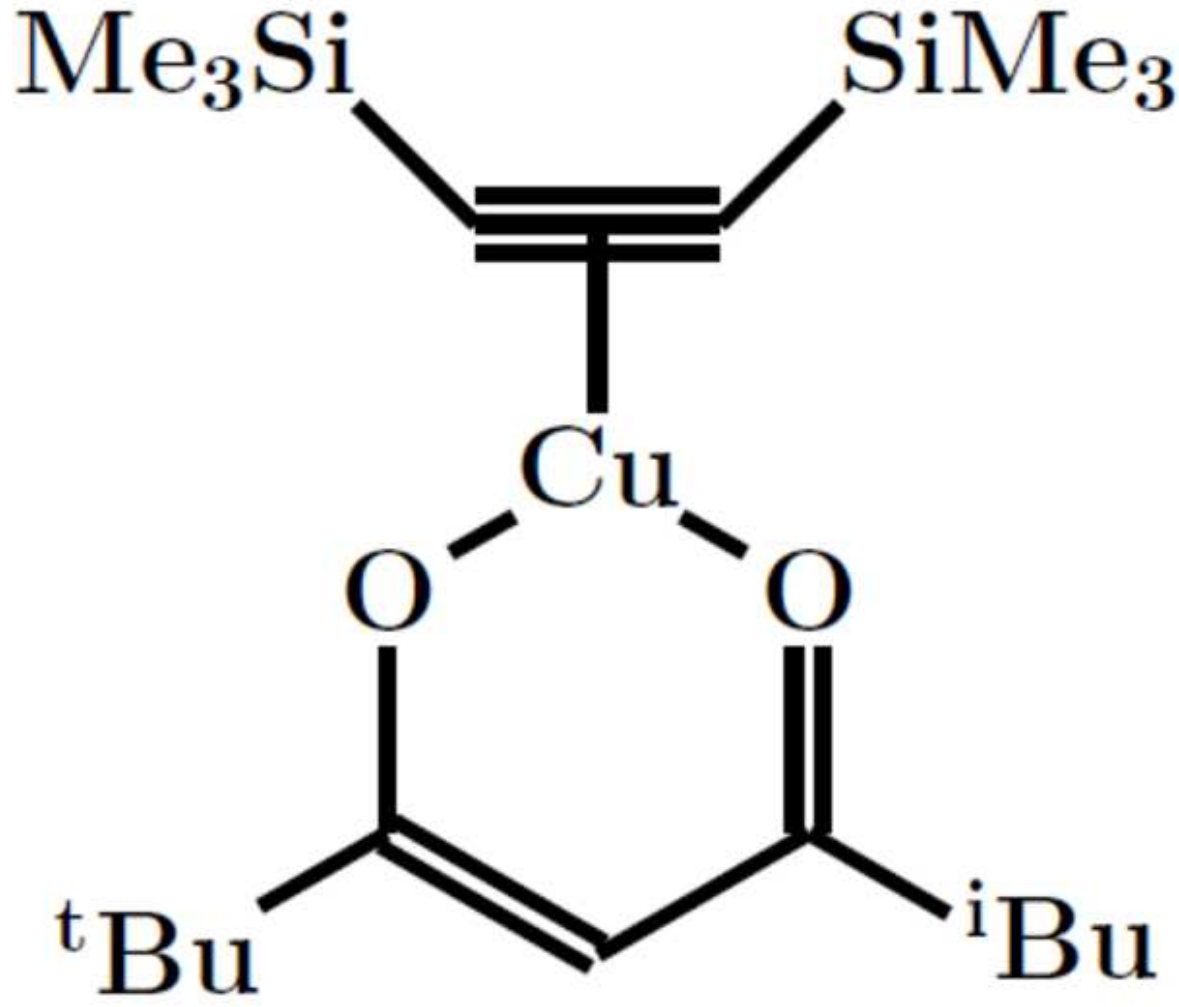
PLEASE CITE THIS ARTICLE AS DOI: 10.1063/1.5087759





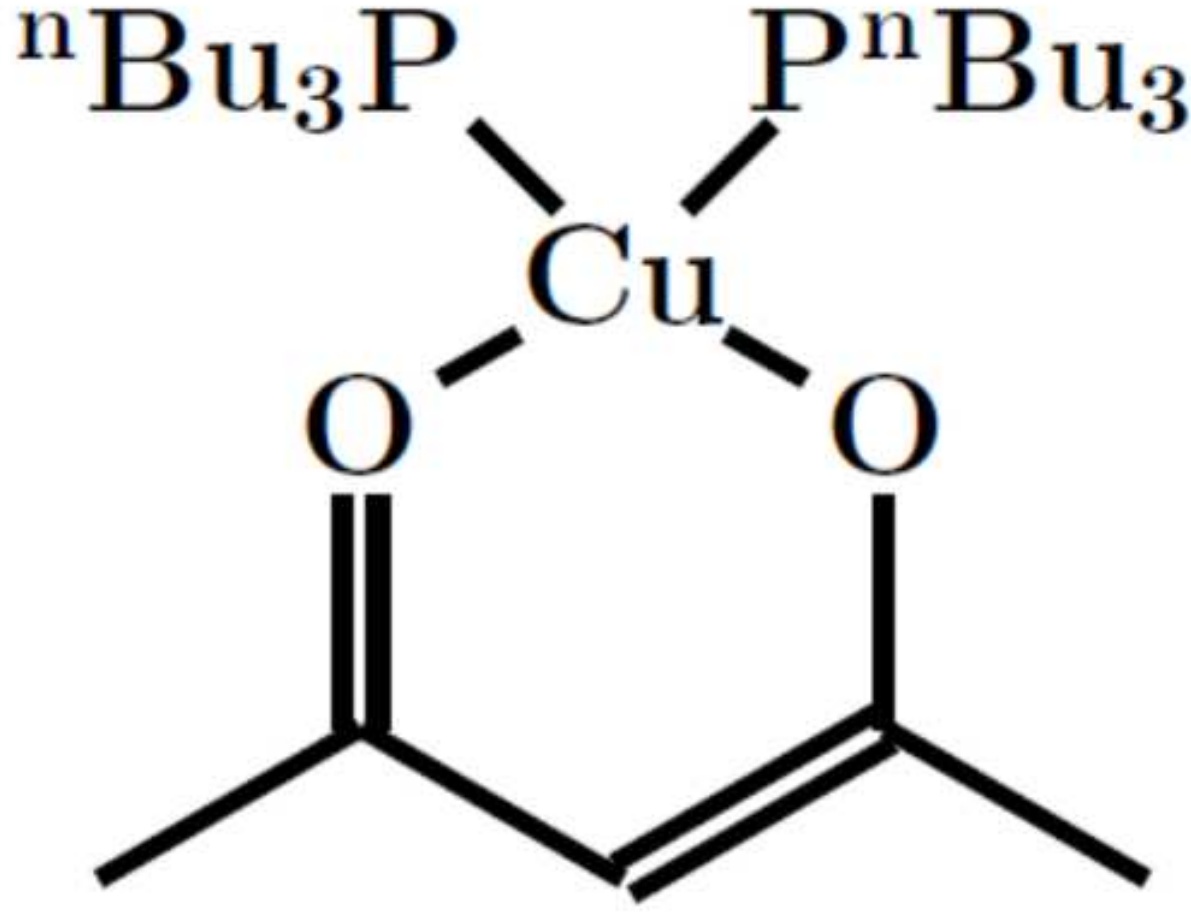
This is the author's peer reviewed, accepted manuscript. However, the online version of record will be different from this version once it has been copyedited and typeset.

PLEASE CITE THIS ARTICLE AS DOI: 10.1063/1.5087759



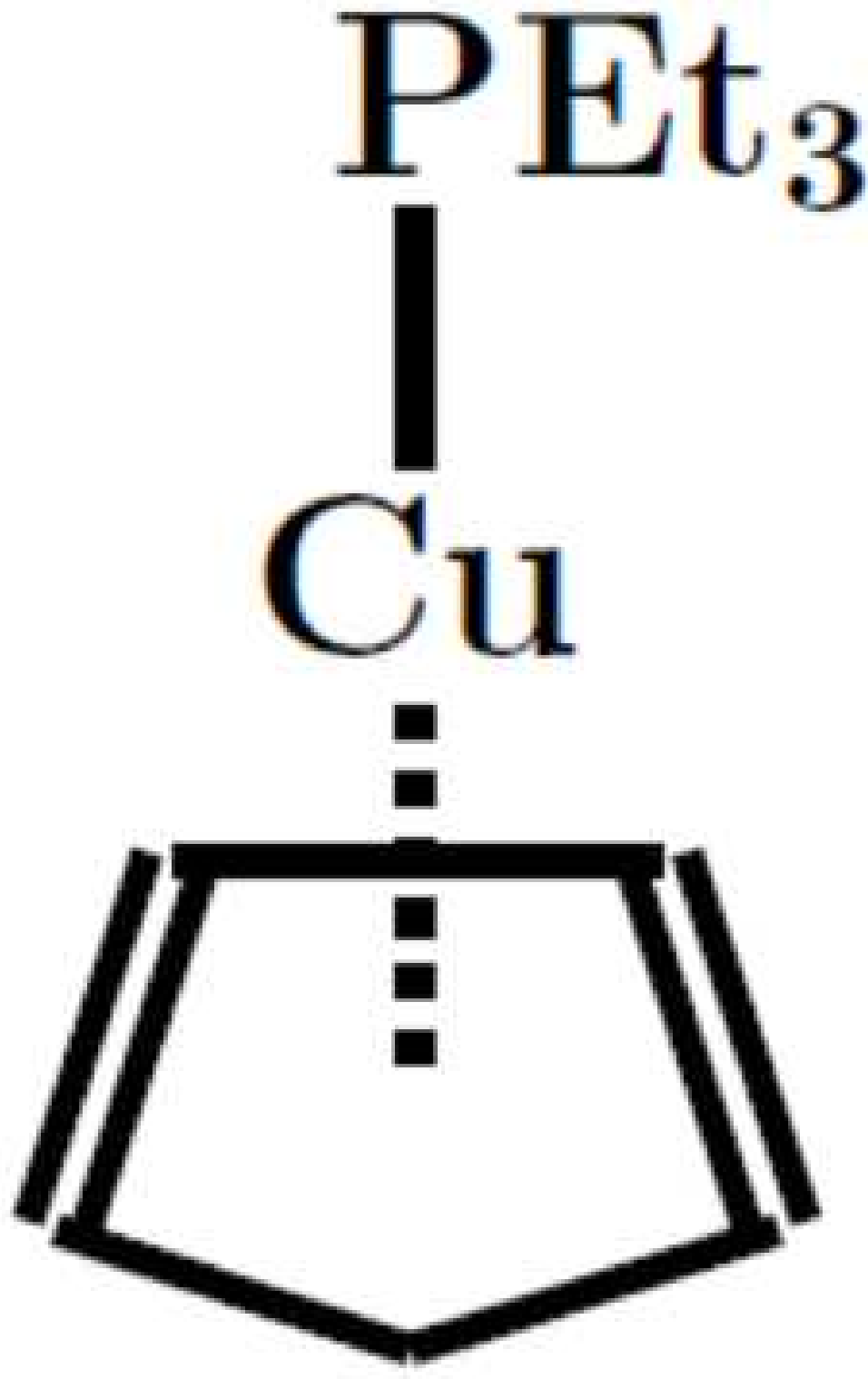
This is the author's peer reviewed, accepted manuscript. However, the online version of record will be different from this version once it has been copyedited and typeset.

PLEASE CITE THIS ARTICLE AS DOI: 10.1063/1.5087759



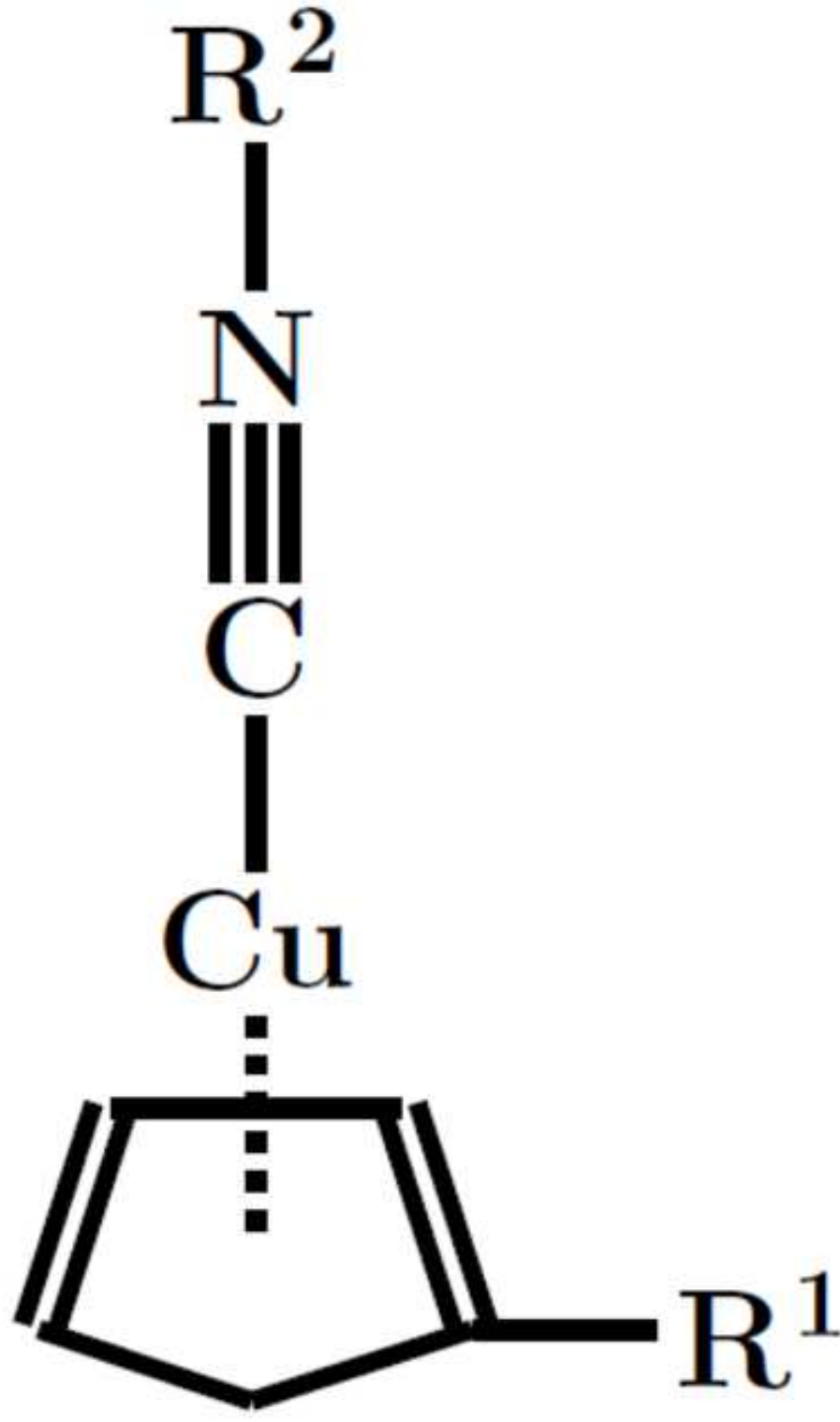
This is the author's peer reviewed, accepted manuscript. However, the online version of record will be different from this version once it has been copyedited and typeset.

PLEASE CITE THIS ARTICLE AS DOI: 10.1063/1.5087759



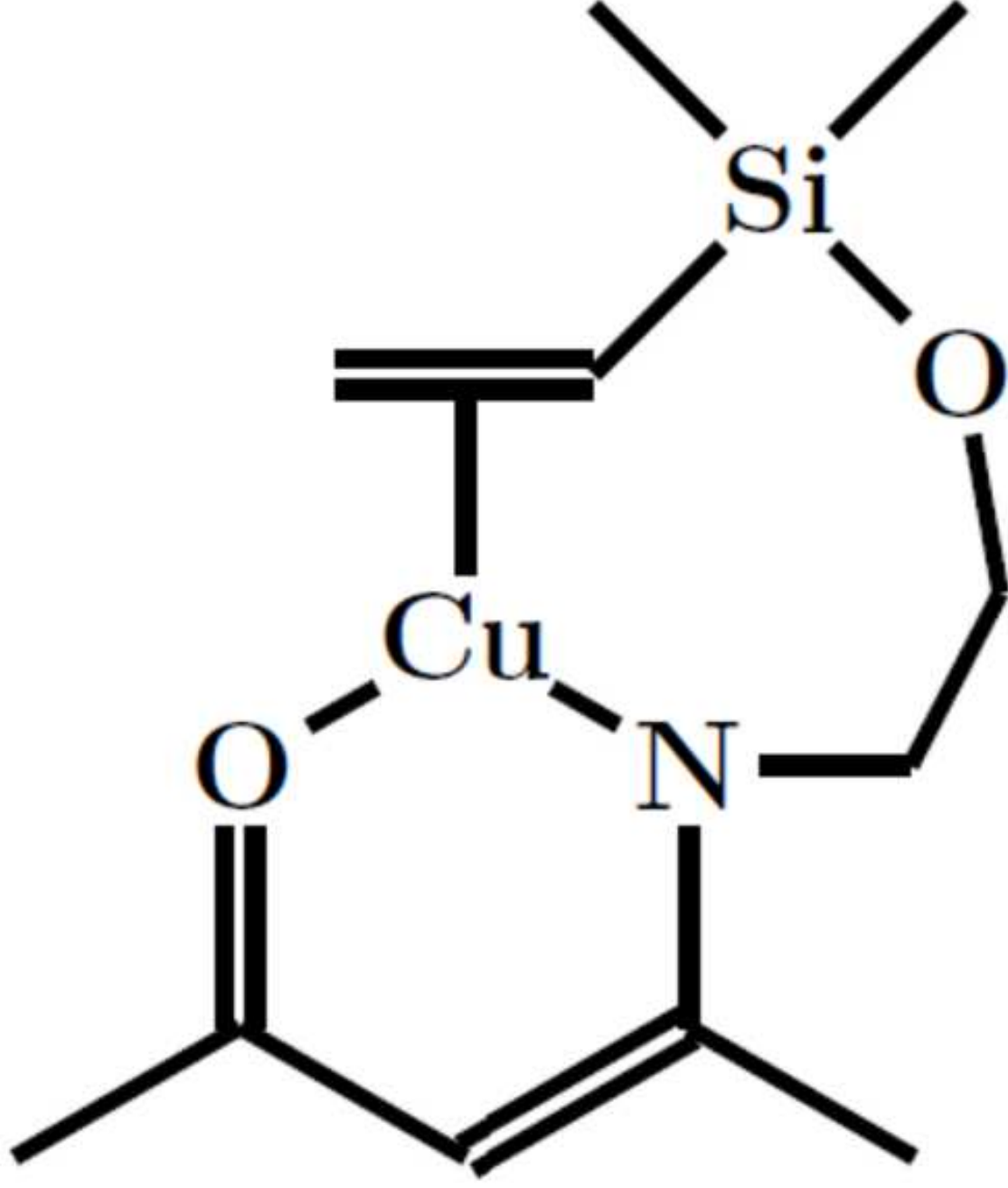
This is the author's peer reviewed, accepted manuscript. However, the online version of record will be different from this version once it has been copyedited and typeset.

PLEASE CITE THIS ARTICLE AS DOI: 10.1063/1.5087759



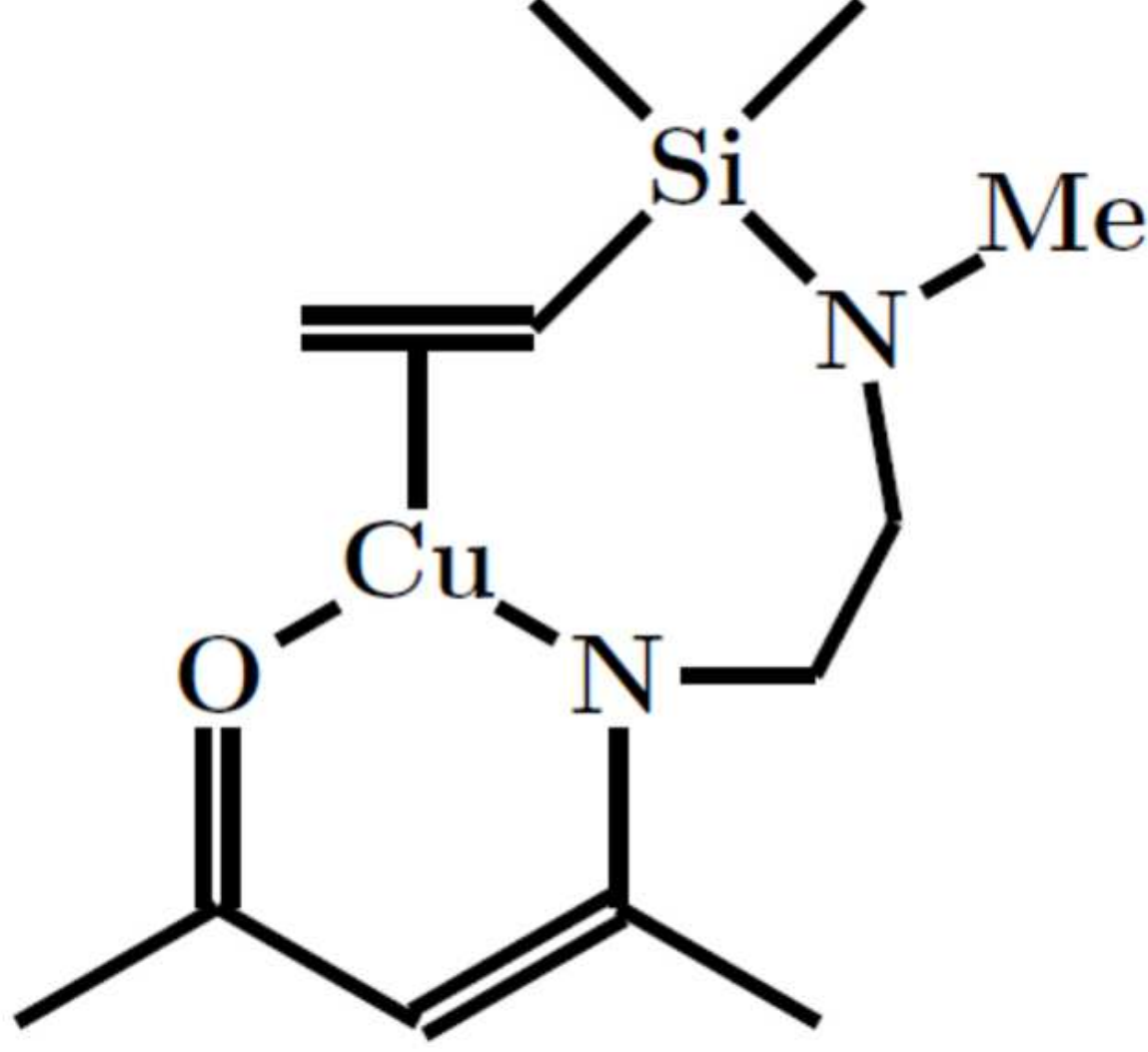
This is the author's peer reviewed, accepted manuscript. However, the online version of record will be different from this version once it has been copyedited and typeset.

PLEASE CITE THIS ARTICLE AS DOI: 10.1063/1.5087759



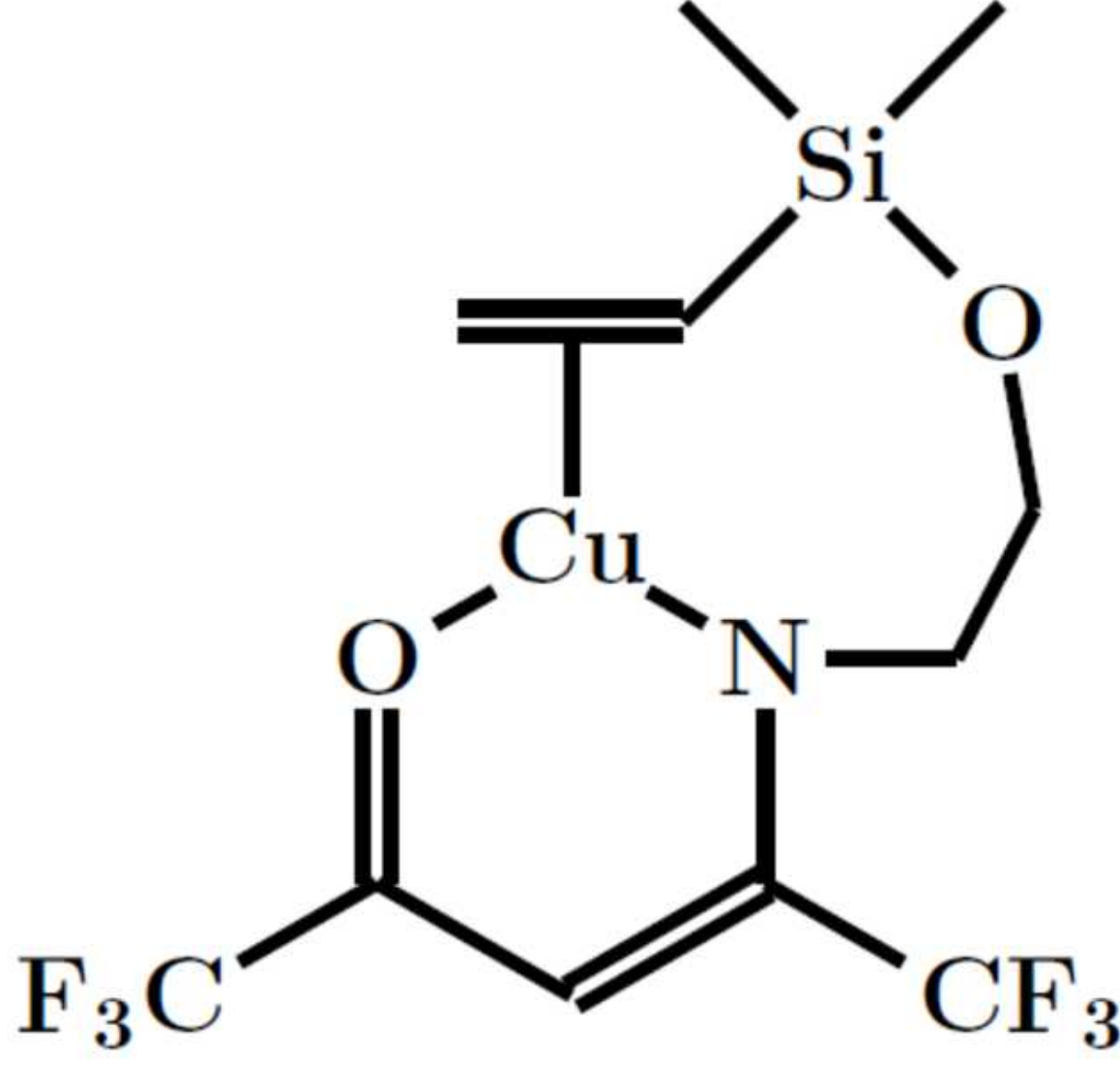
This is the author's peer reviewed, accepted manuscript. However, the online version of record will be different from this version once it has been copyedited and typeset.

PLEASE CITE THIS ARTICLE AS DOI: 10.1063/1.5087759



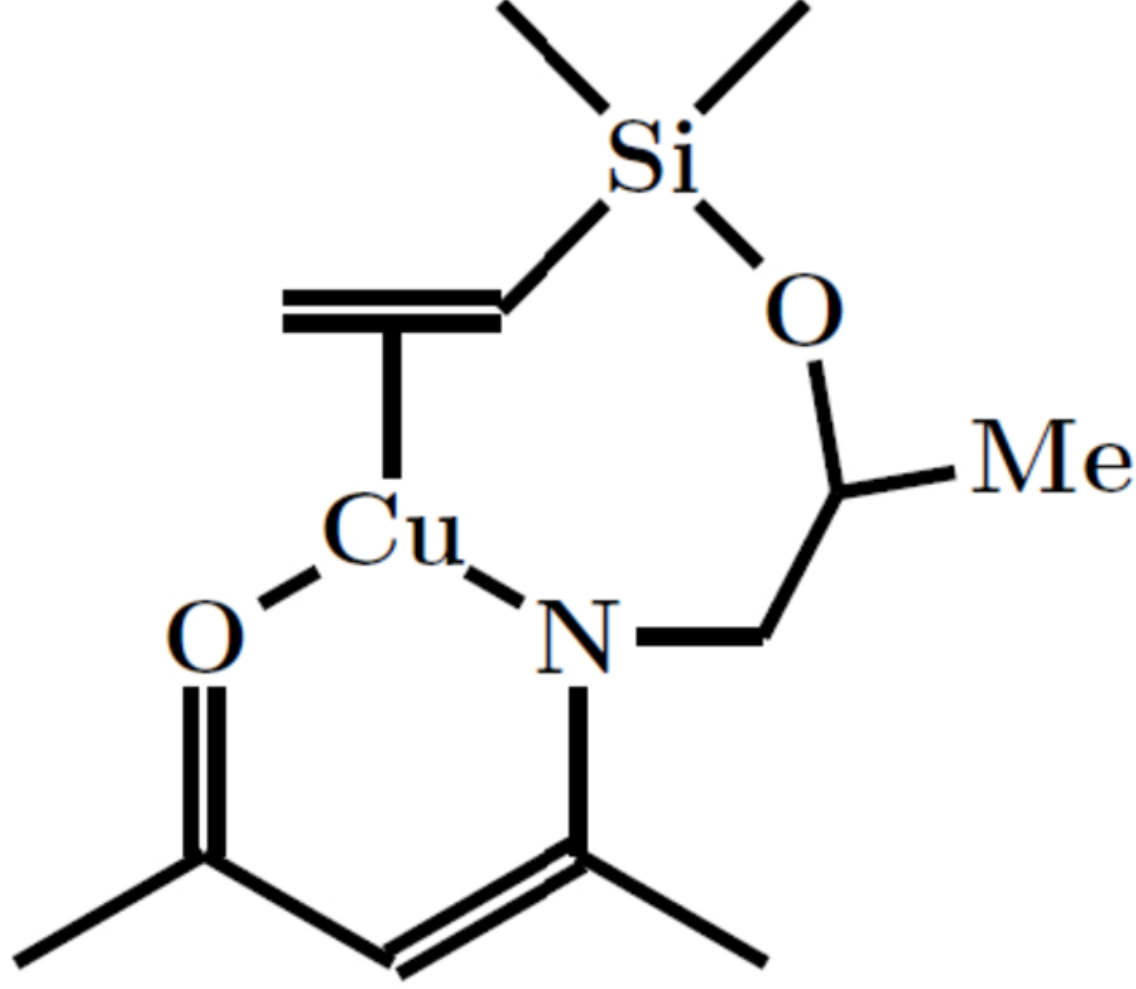
This is the author's peer reviewed, accepted manuscript. However, the online version of record will be different from this version once it has been copyedited and typeset.

PLEASE CITE THIS ARTICLE AS DOI: 10.1063/1.5087759



This is the author's peer reviewed, accepted manuscript. However, the online version of record will be different from this version once it has been copyedited and typeset.

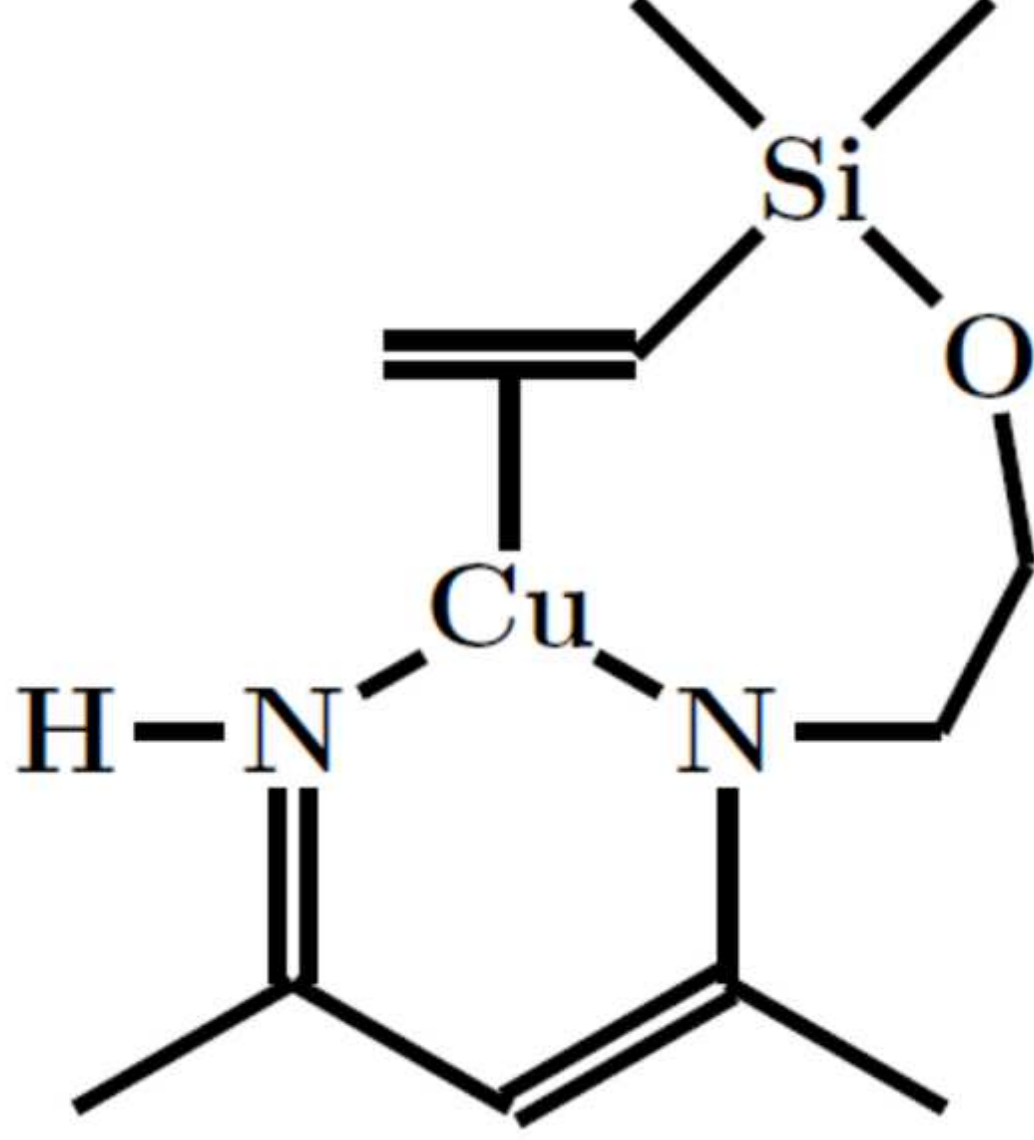
PLEASE CITE THIS ARTICLE AS DOI: 10.1063/1.5087759





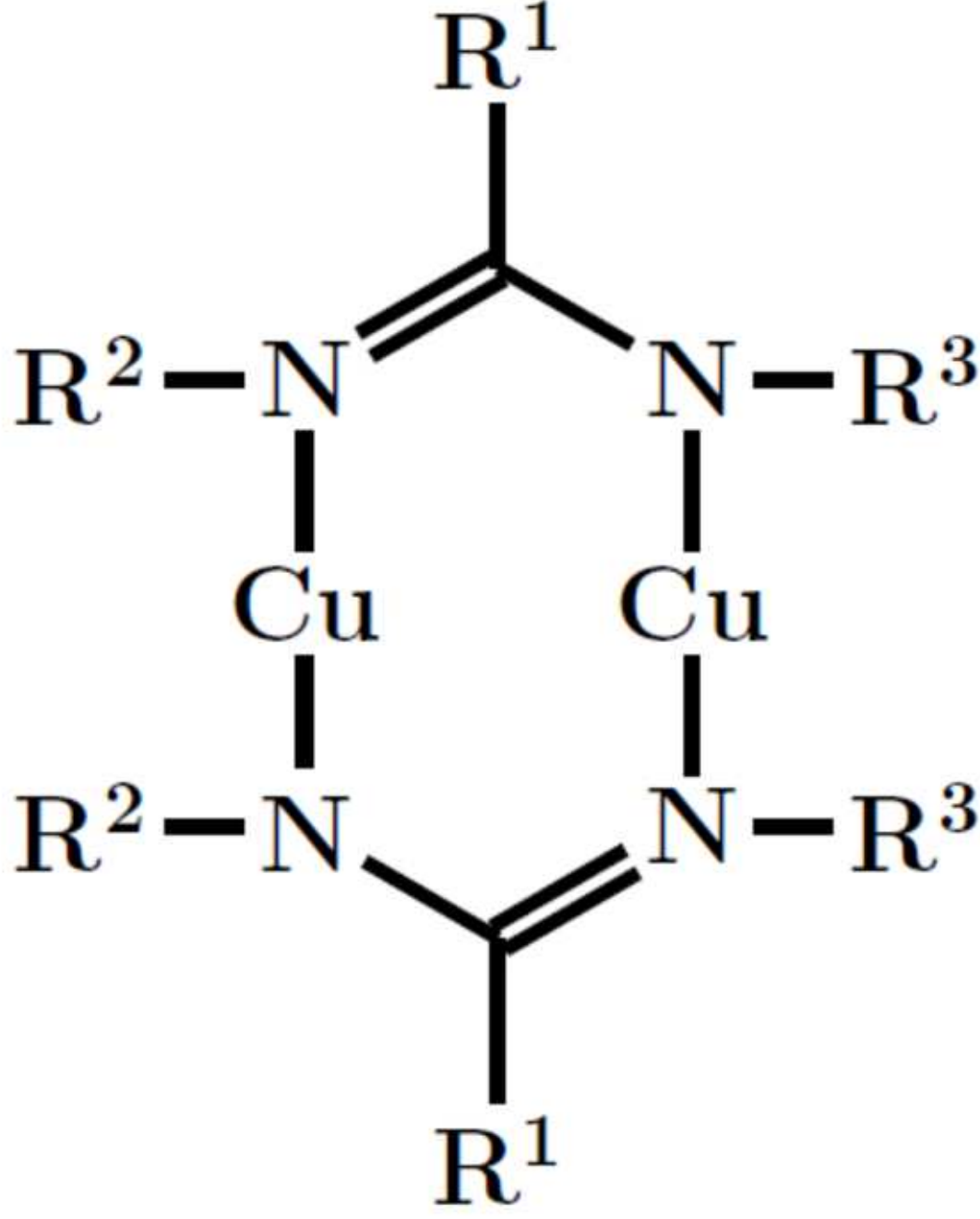
This is the author's peer reviewed, accepted manuscript. However, the online version of record will be different from this version once it has been copyedited and typeset.

PLEASE CITE THIS ARTICLE AS DOI: 10.1063/1.5087759



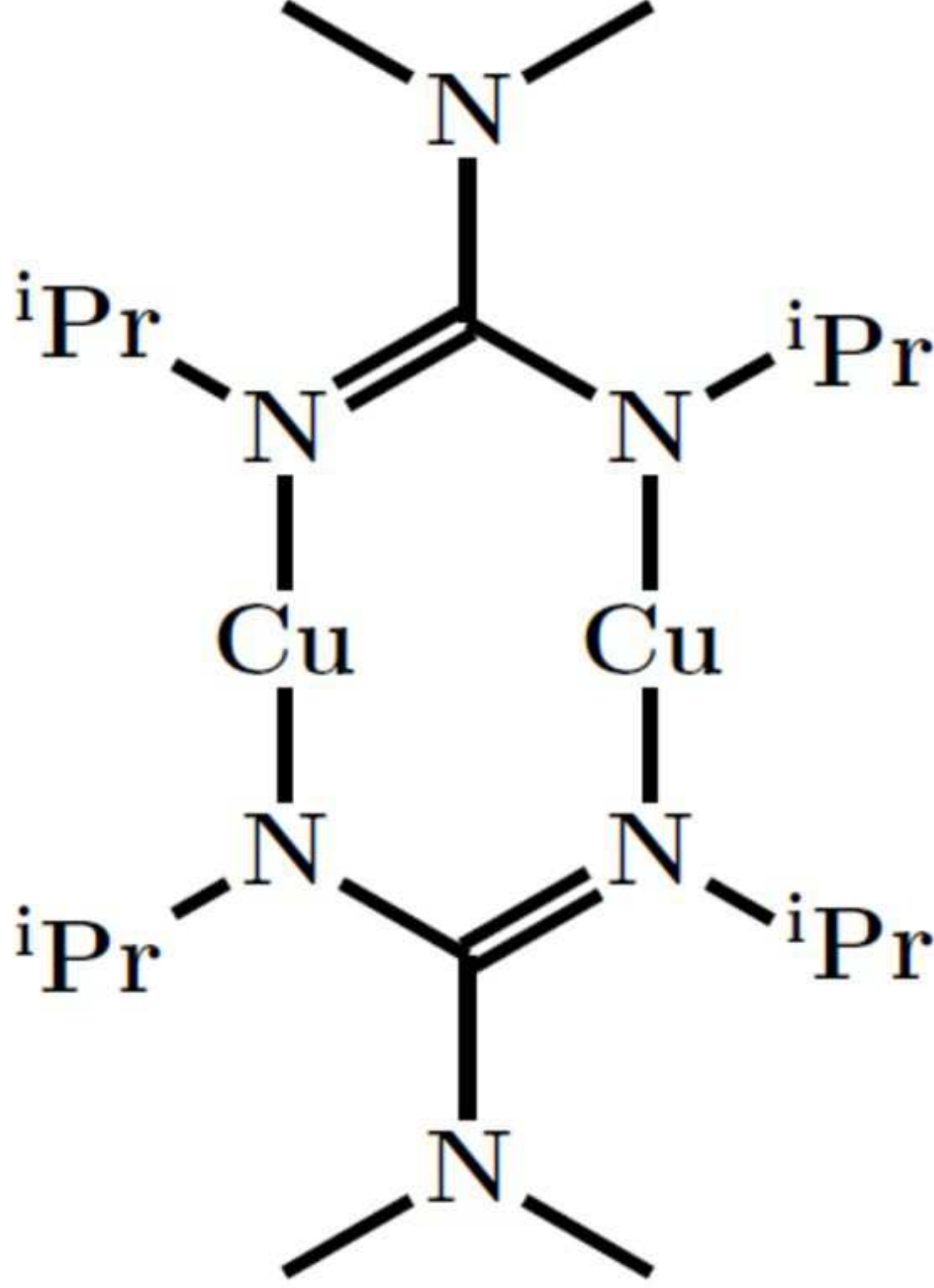
This is the author's peer reviewed, accepted manuscript. However, the online version of record will be different from this version once it has been copyedited and typeset.

PLEASE CITE THIS ARTICLE AS DOI: 10.1063/1.5087759



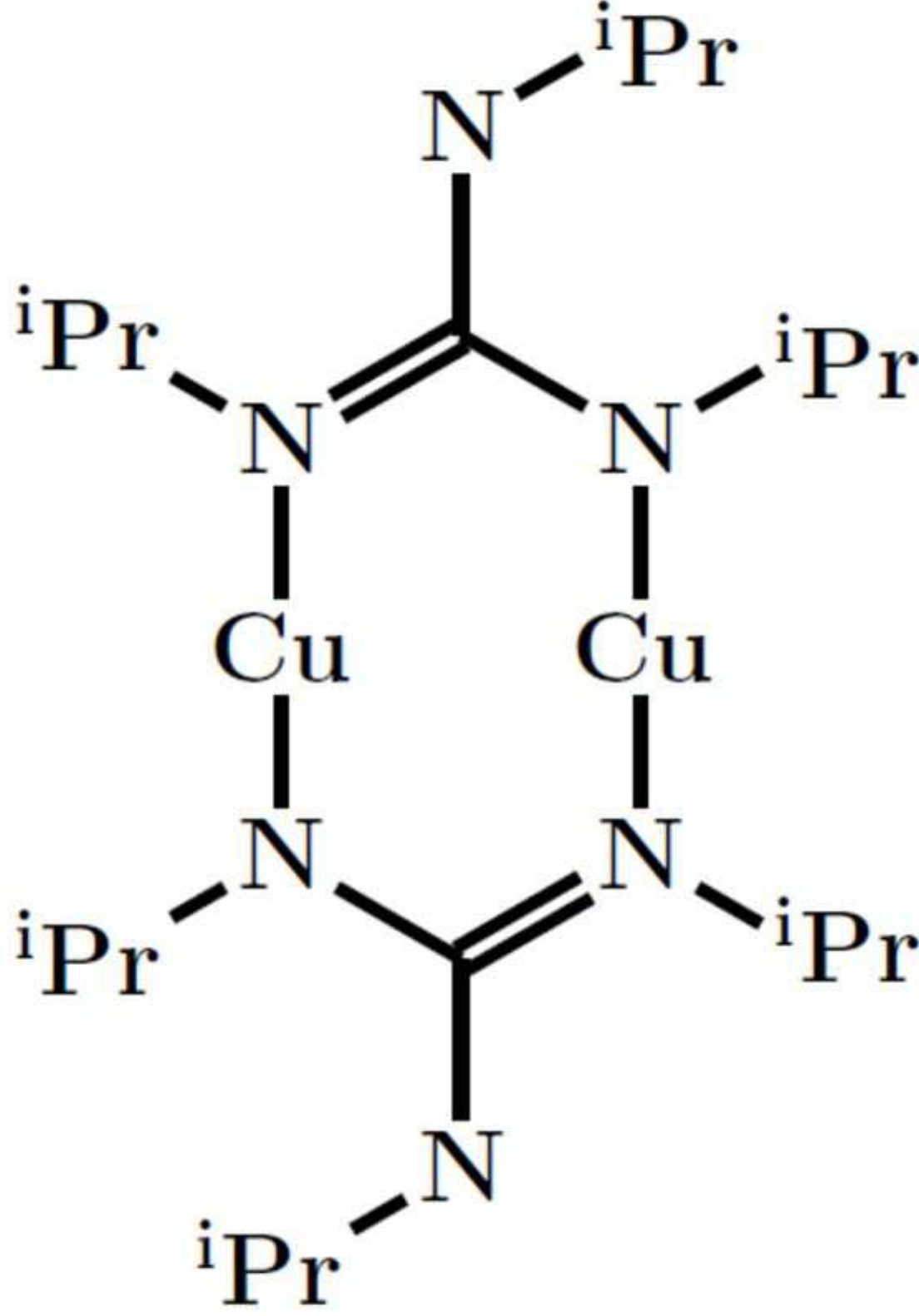
This is the author's peer reviewed, accepted manuscript. However, the online version of record will be different from this version once it has been copyedited and typeset.

PLEASE CITE THIS ARTICLE AS DOI: 10.1063/1.5087759



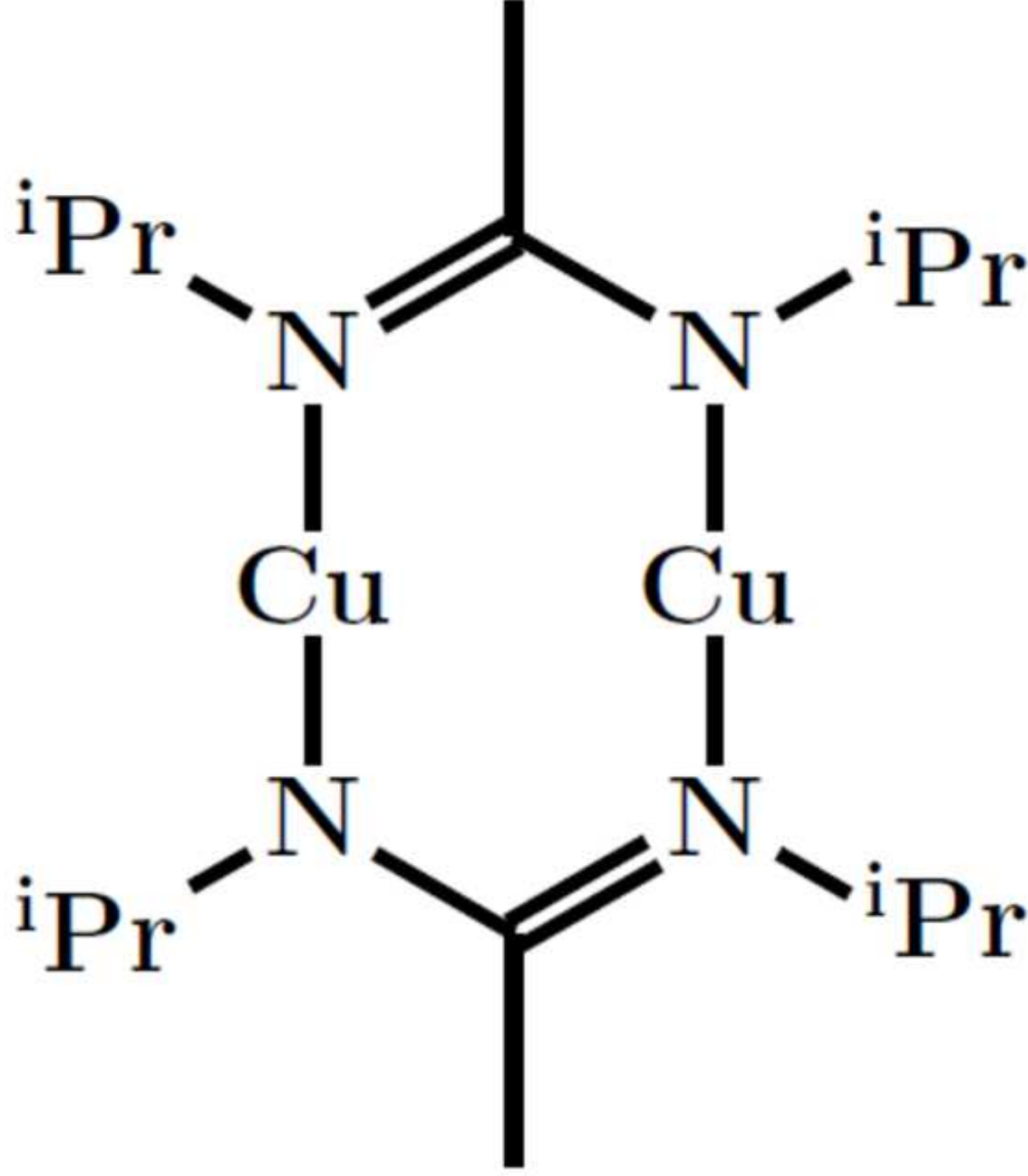
This is the author's peer reviewed, accepted manuscript. However, the online version of record will be different from this version once it has been copyedited and typeset.

PLEASE CITE THIS ARTICLE AS DOI: 10.1063/1.5087759



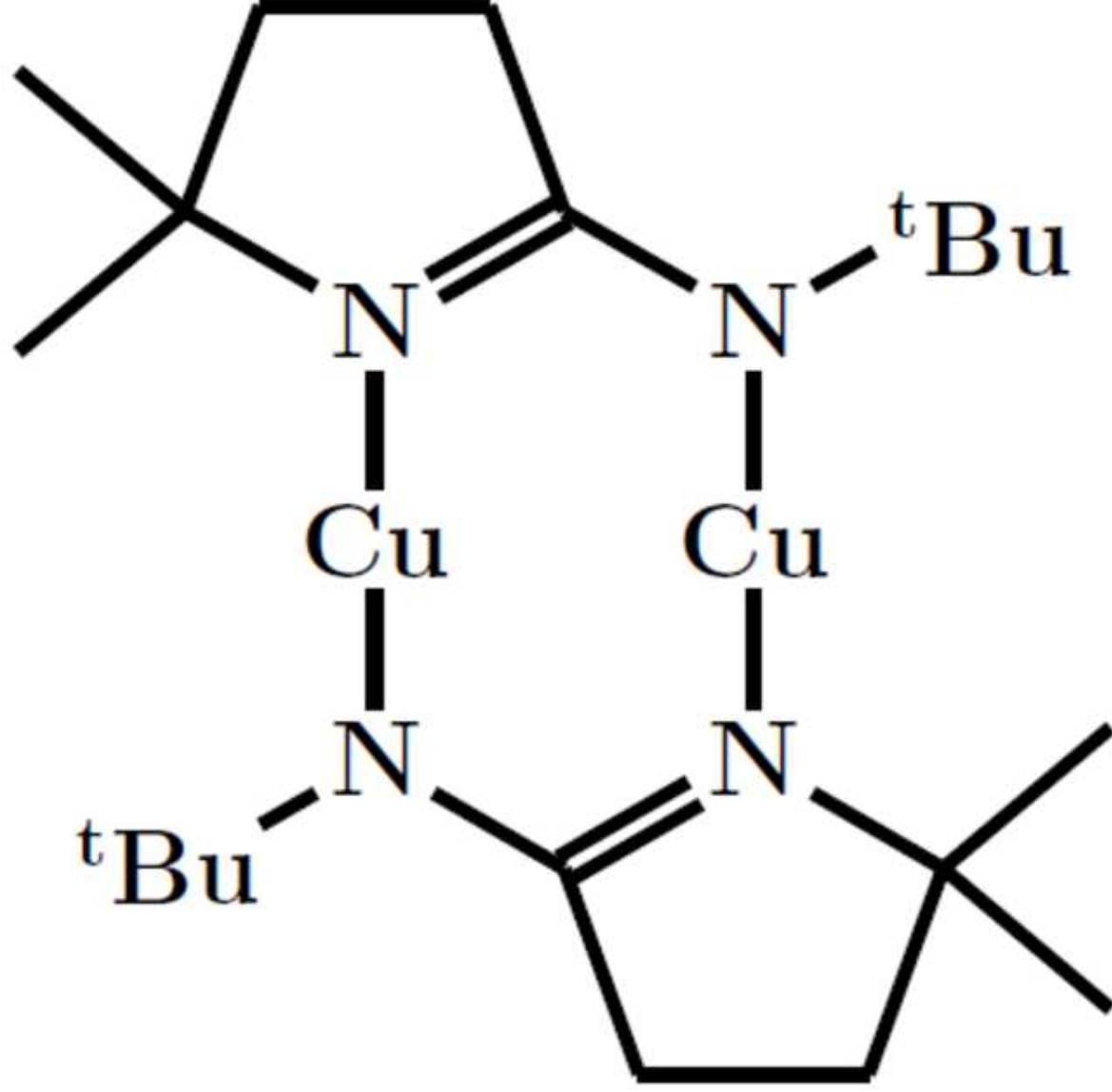
This is the author's peer reviewed, accepted manuscript. However, the online version of record will be different from this version once it has been copyedited and typeset.

PLEASE CITE THIS ARTICLE AS DOI: 10.1063/1.5087759



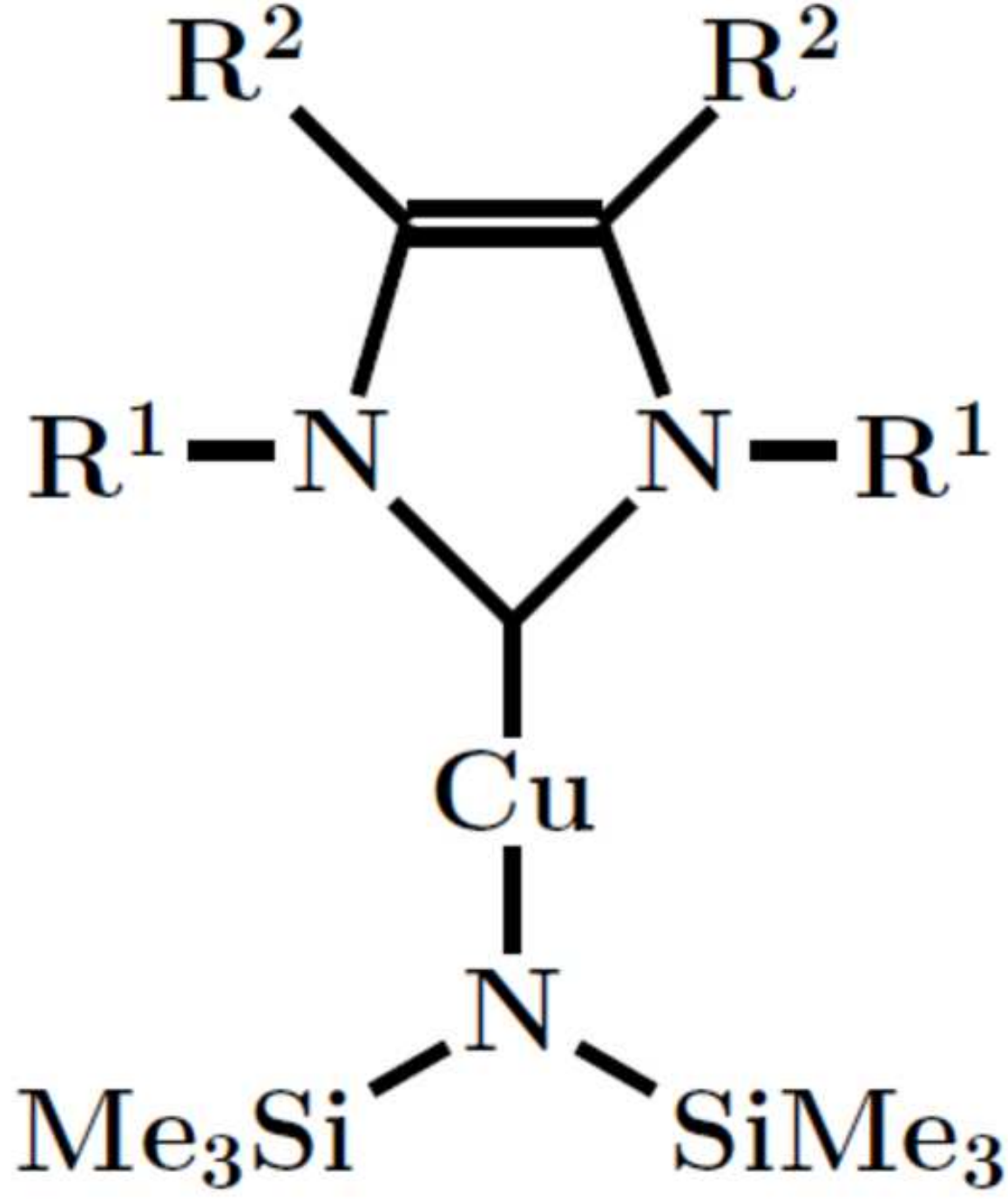
This is the author's peer reviewed, accepted manuscript. However, the online version of record will be different from this version once it has been copyedited and typeset.

PLEASE CITE THIS ARTICLE AS DOI: 10.1063/1.5087759



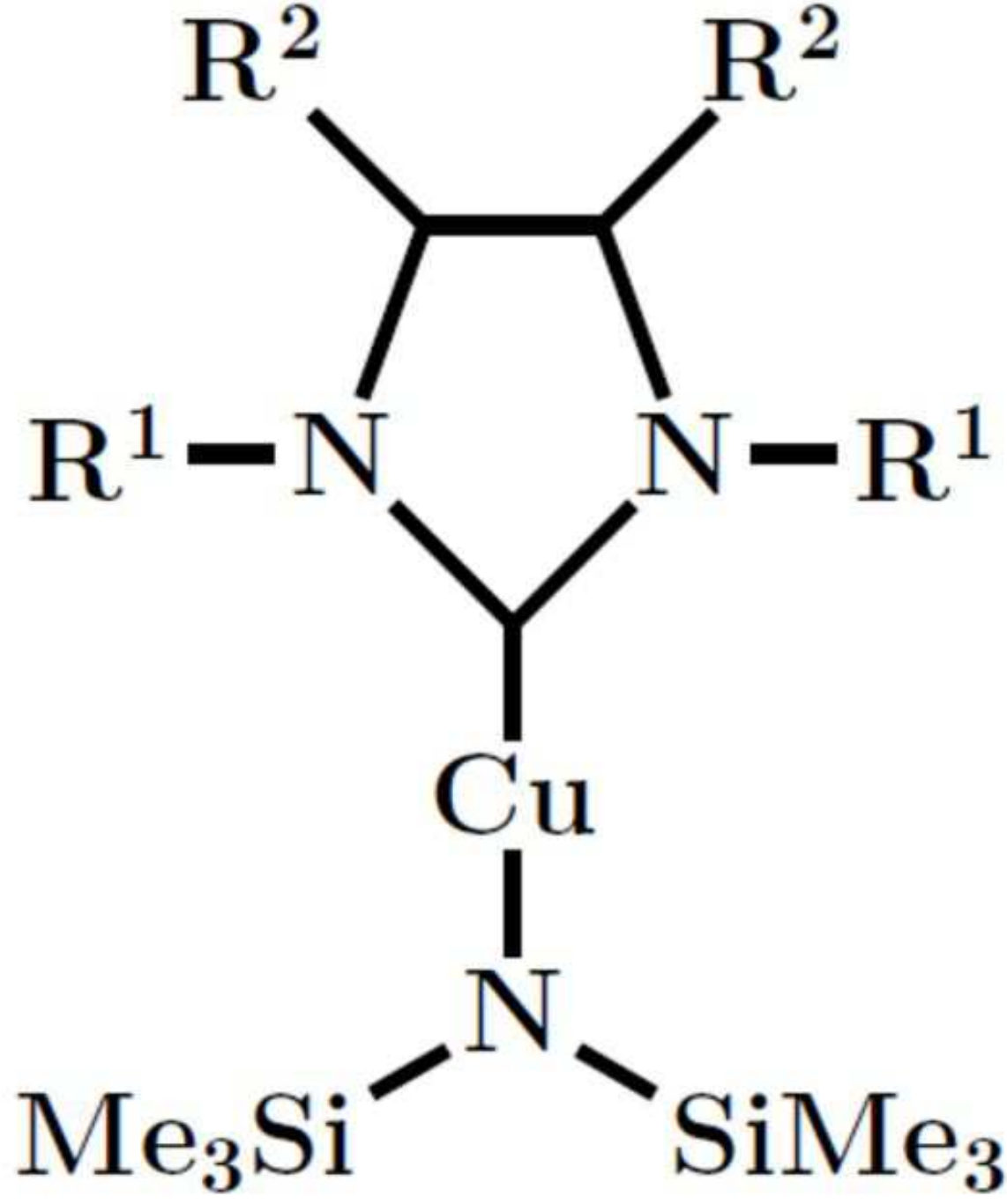
This is the author's peer reviewed, accepted manuscript. However, the online version of record will be different from this version once it has been copyedited and typeset.

PLEASE CITE THIS ARTICLE AS DOI: 10.1063/1.5087759



This is the author's peer reviewed, accepted manuscript. However, the online version of record will be different from this version once it has been copyedited and typeset.

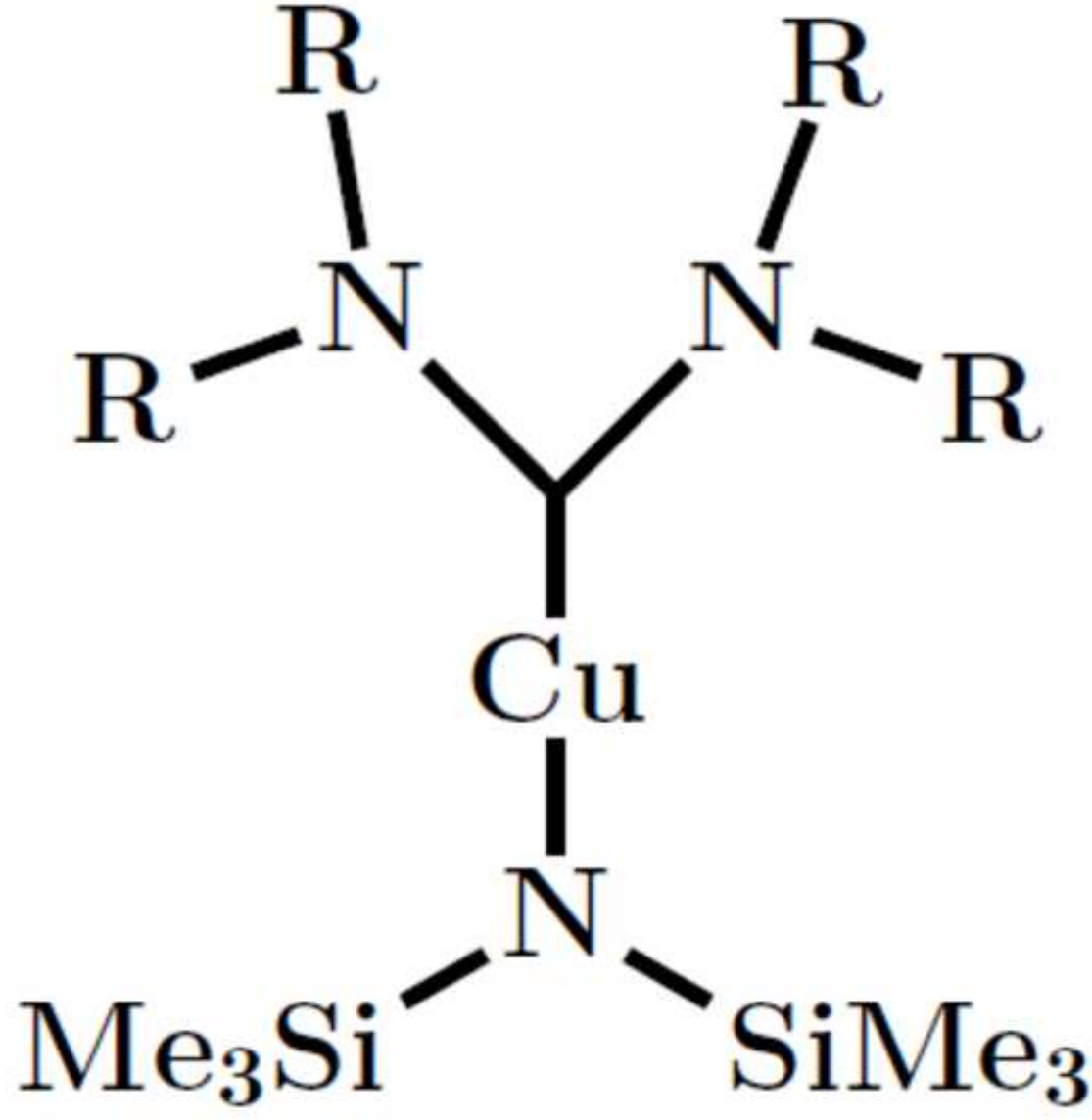
PLEASE CITE THIS ARTICLE AS DOI: 10.1063/1.5087759





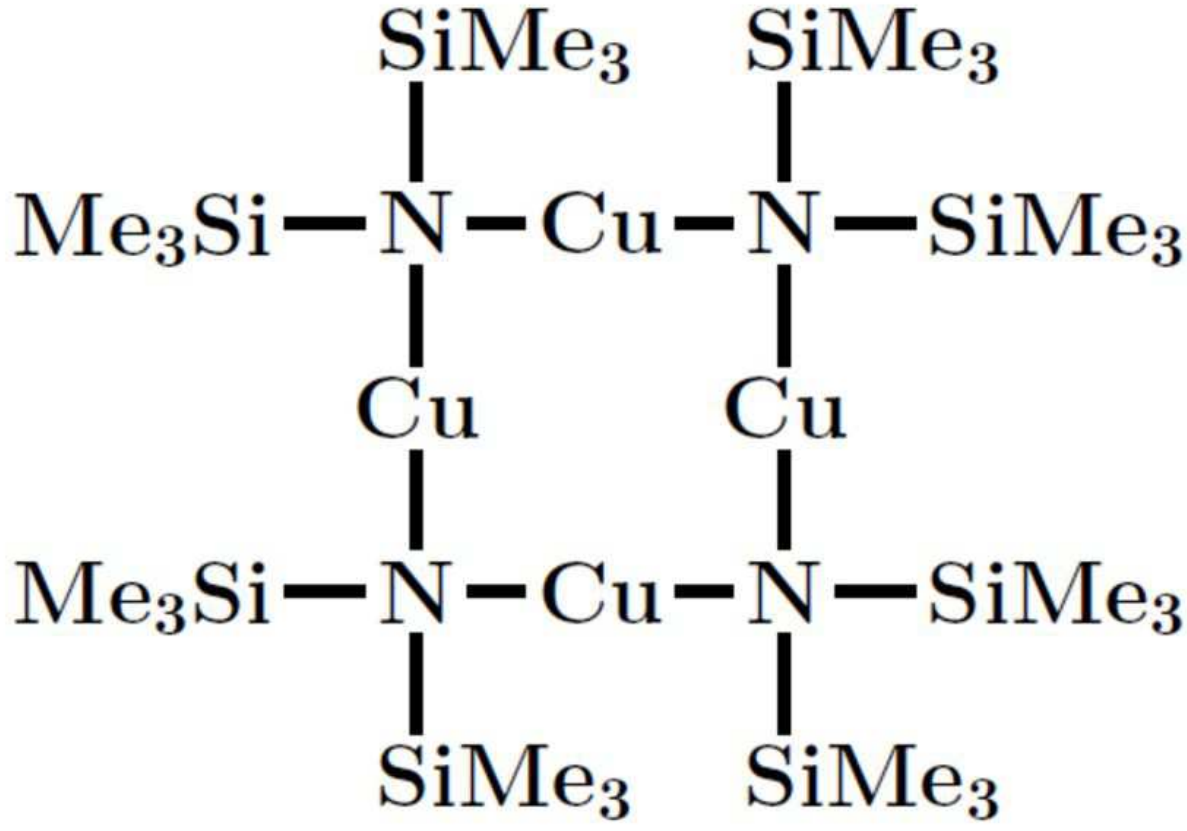
This is the author's peer reviewed, accepted manuscript. However, the online version of record will be different from this version once it has been copyedited and typeset.

PLEASE CITE THIS ARTICLE AS DOI: 10.1063/1.5087759



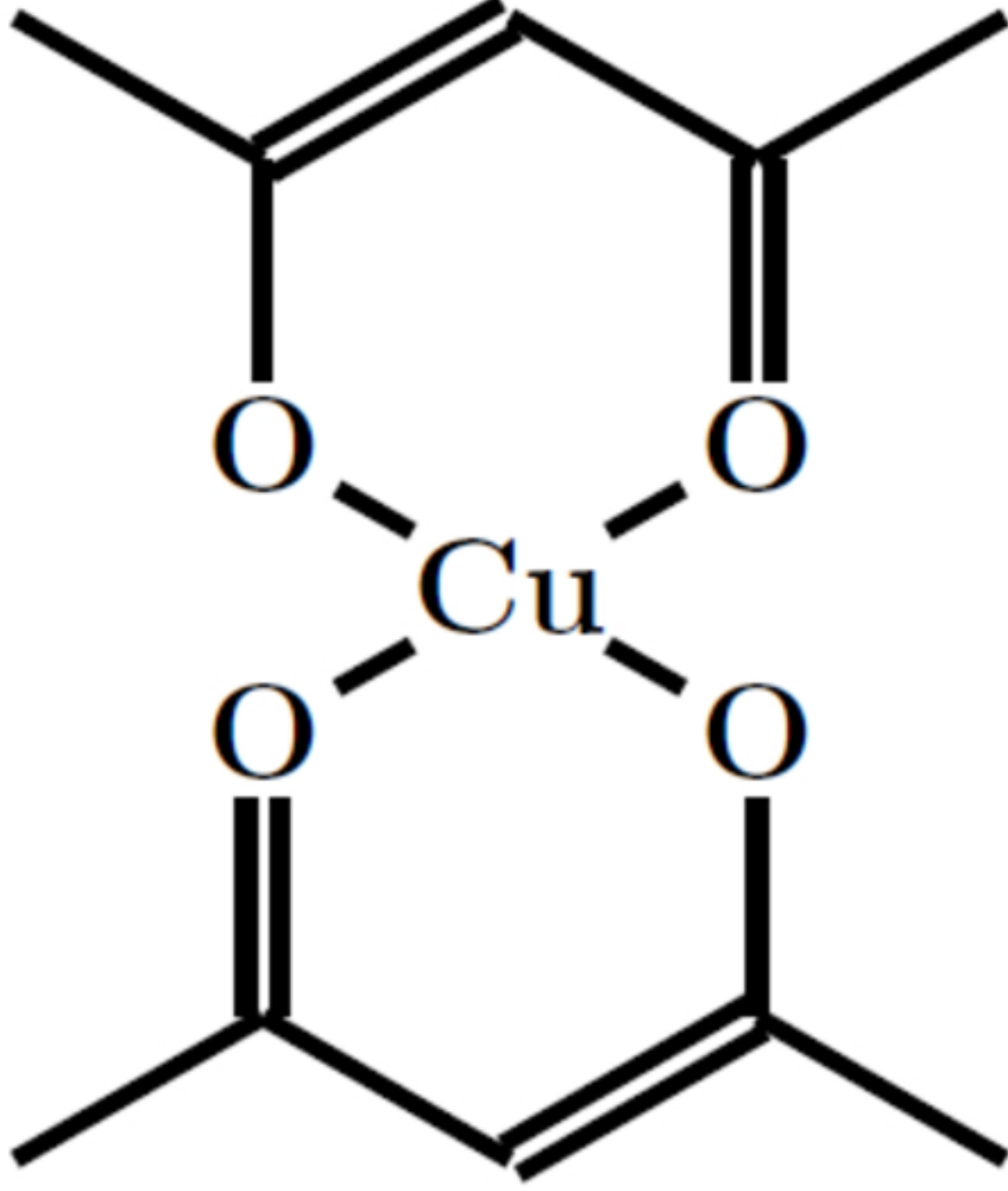
This is the author's peer reviewed, accepted manuscript. However, the online version of record will be different from this version once it has been copyedited and typeset.

PLEASE CITE THIS ARTICLE AS DOI: 10.1063/1.5087759



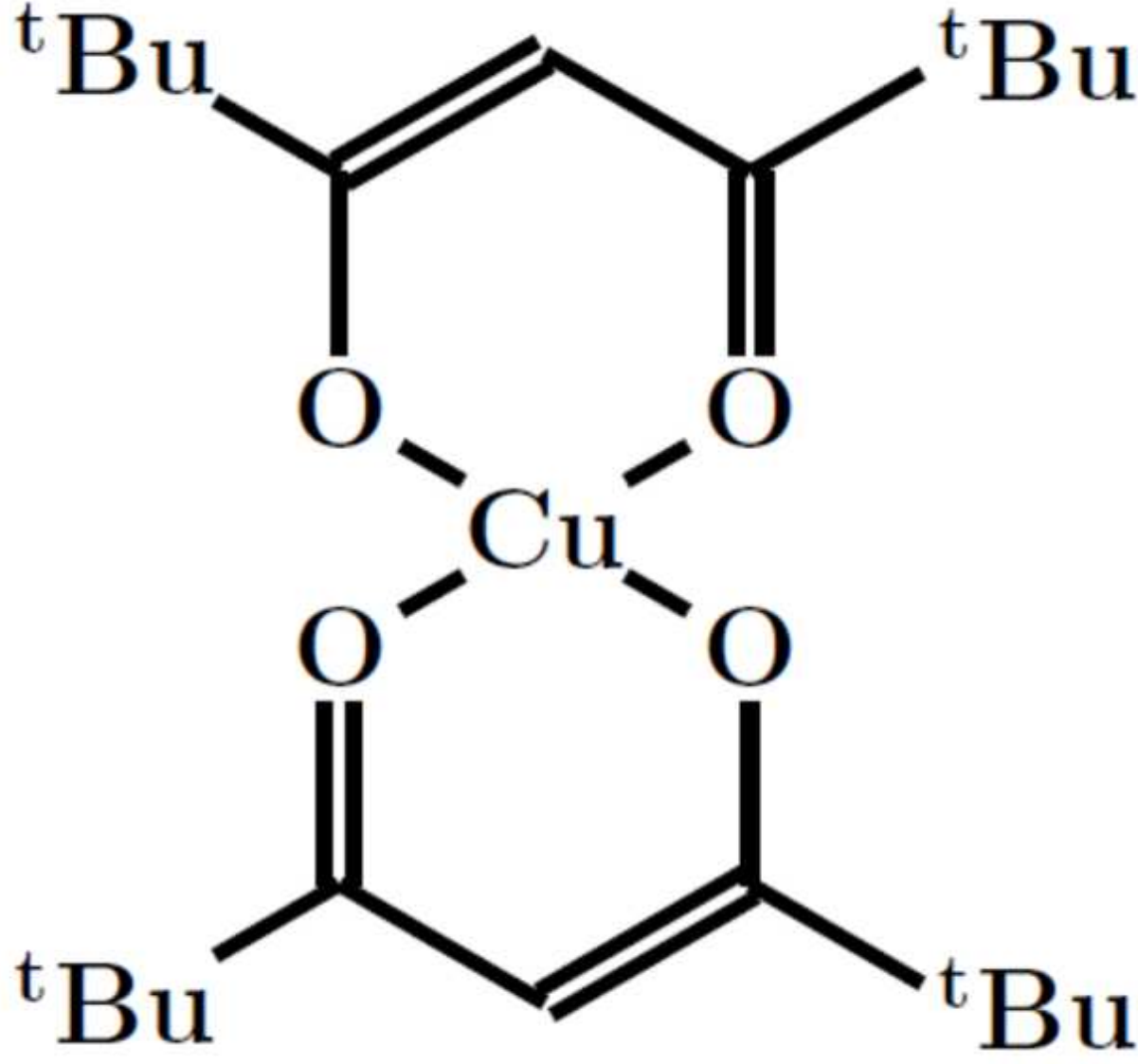
This is the author's peer reviewed, accepted manuscript. However, the online version of record will be different from this version once it has been copyedited and typeset.

PLEASE CITE THIS ARTICLE AS DOI: 10.1063/1.5087759



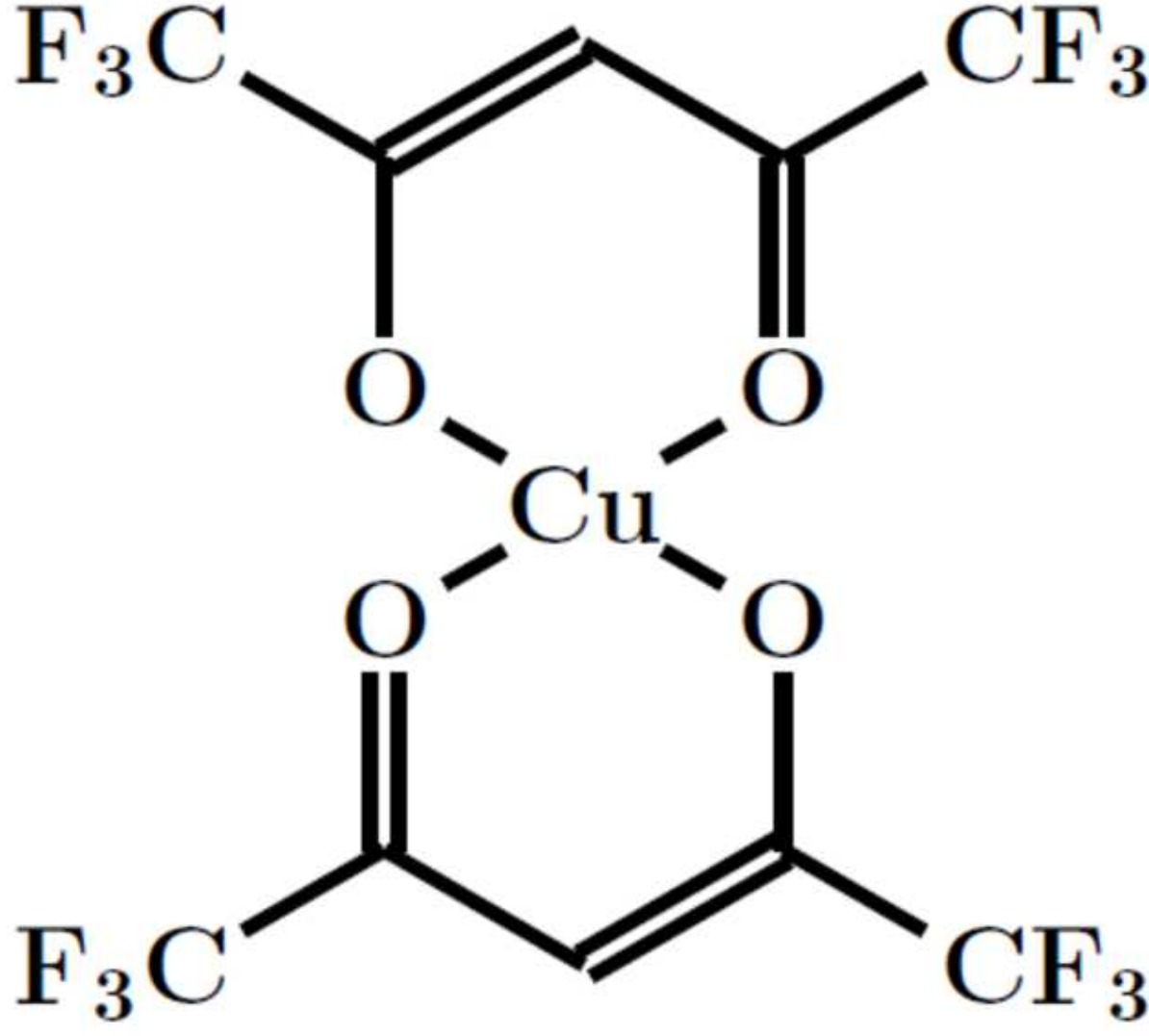
This is the author's peer reviewed, accepted manuscript. However, the online version of record will be different from this version once it has been copyedited and typeset.

PLEASE CITE THIS ARTICLE AS DOI: 10.1063/1.5087759



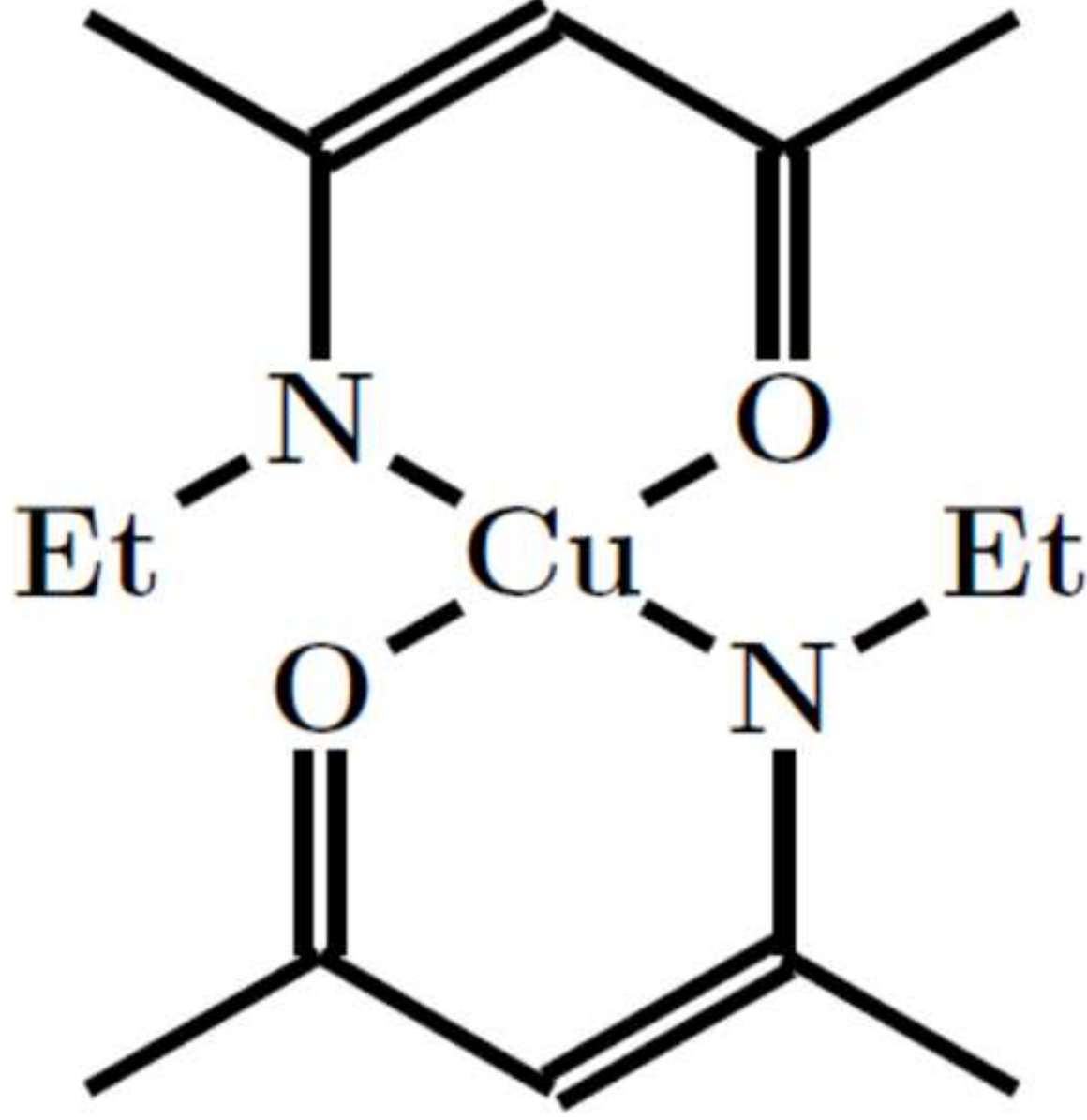
This is the author's peer reviewed, accepted manuscript. However, the online version of record will be different from this version once it has been copyedited and typeset.

PLEASE CITE THIS ARTICLE AS DOI: 10.1063/1.5087759



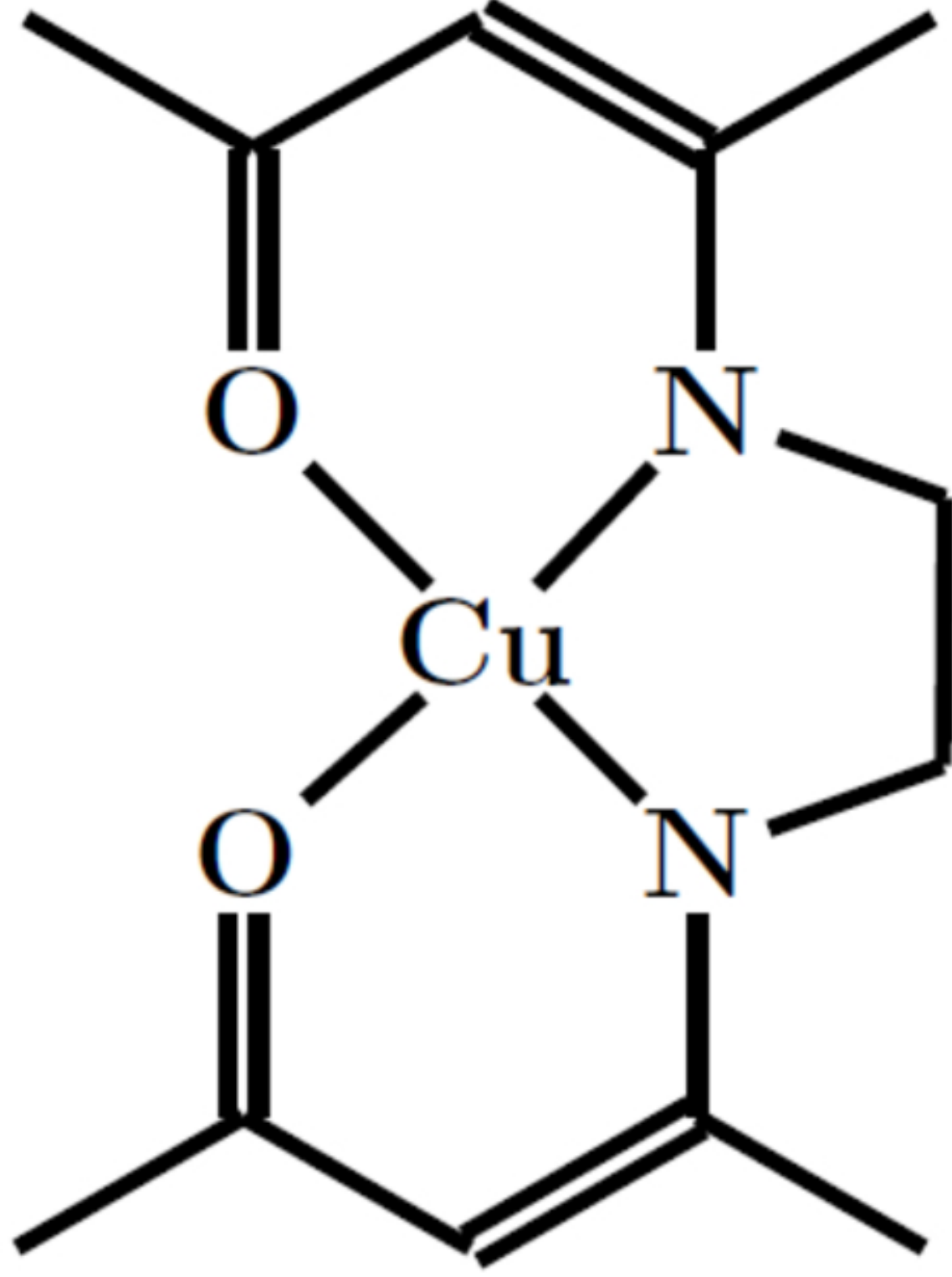
This is the author's peer reviewed, accepted manuscript. However, the online version of record will be different from this version once it has been copyedited and typeset.

PLEASE CITE THIS ARTICLE AS DOI: 10.1063/1.5087759



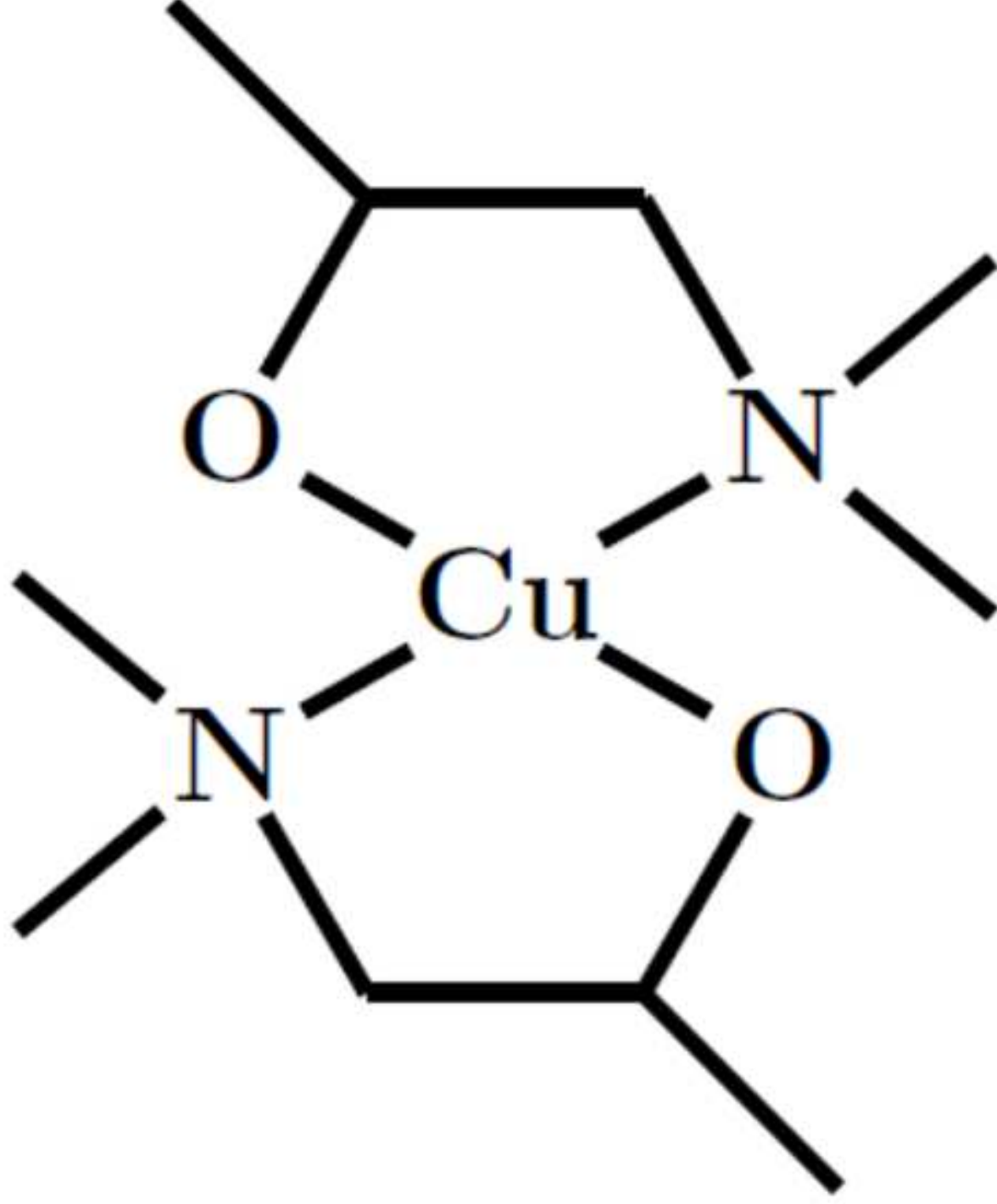
This is the author's peer reviewed, accepted manuscript. However, the online version of record will be different from this version once it has been copyedited and typeset.

PLEASE CITE THIS ARTICLE AS DOI: 10.1063/1.5087759



This is the author's peer reviewed, accepted manuscript. However, the online version of record will be different from this version once it has been copyedited and typeset.

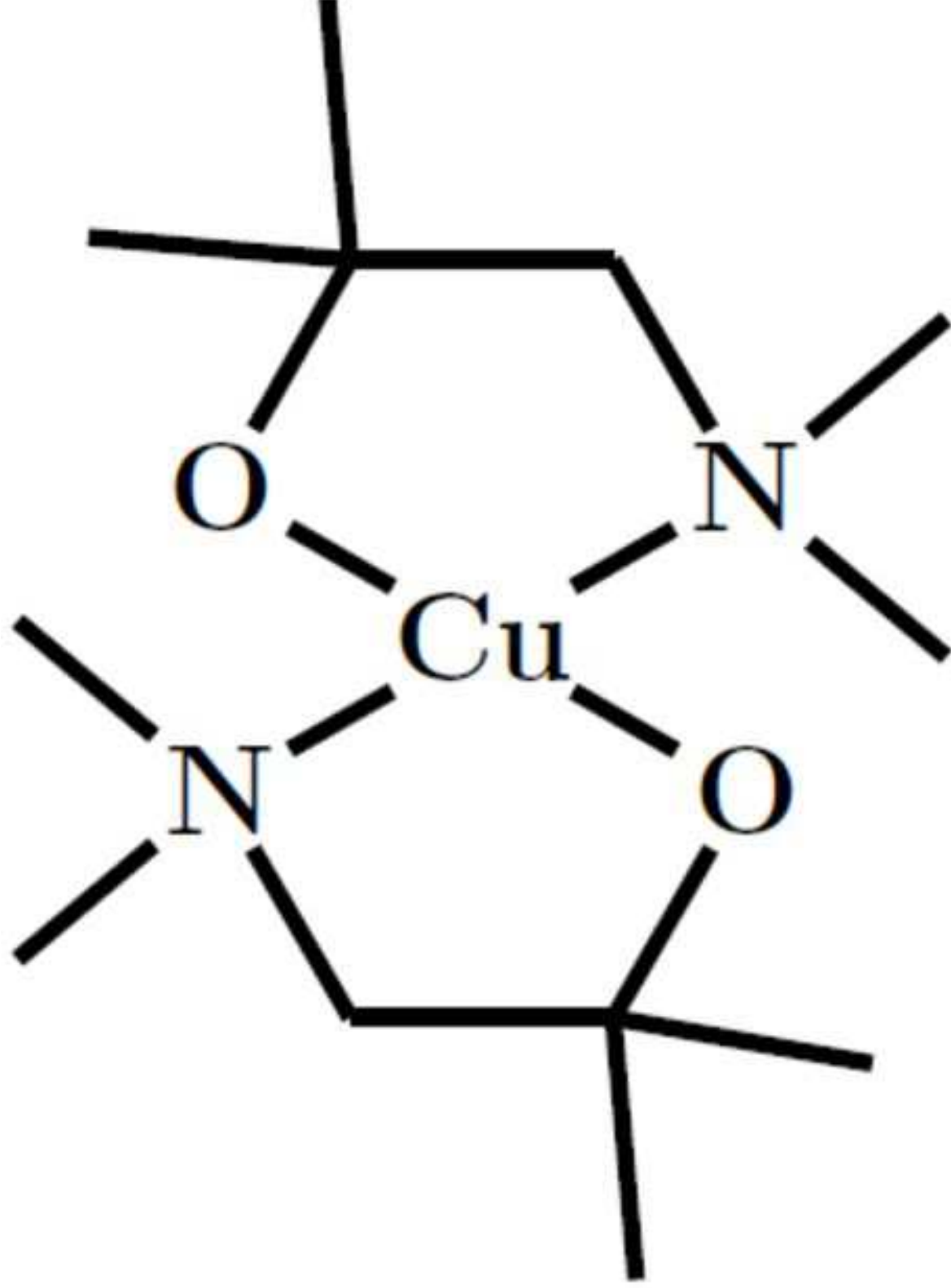
PLEASE CITE THIS ARTICLE AS DOI: 10.1063/1.5087759





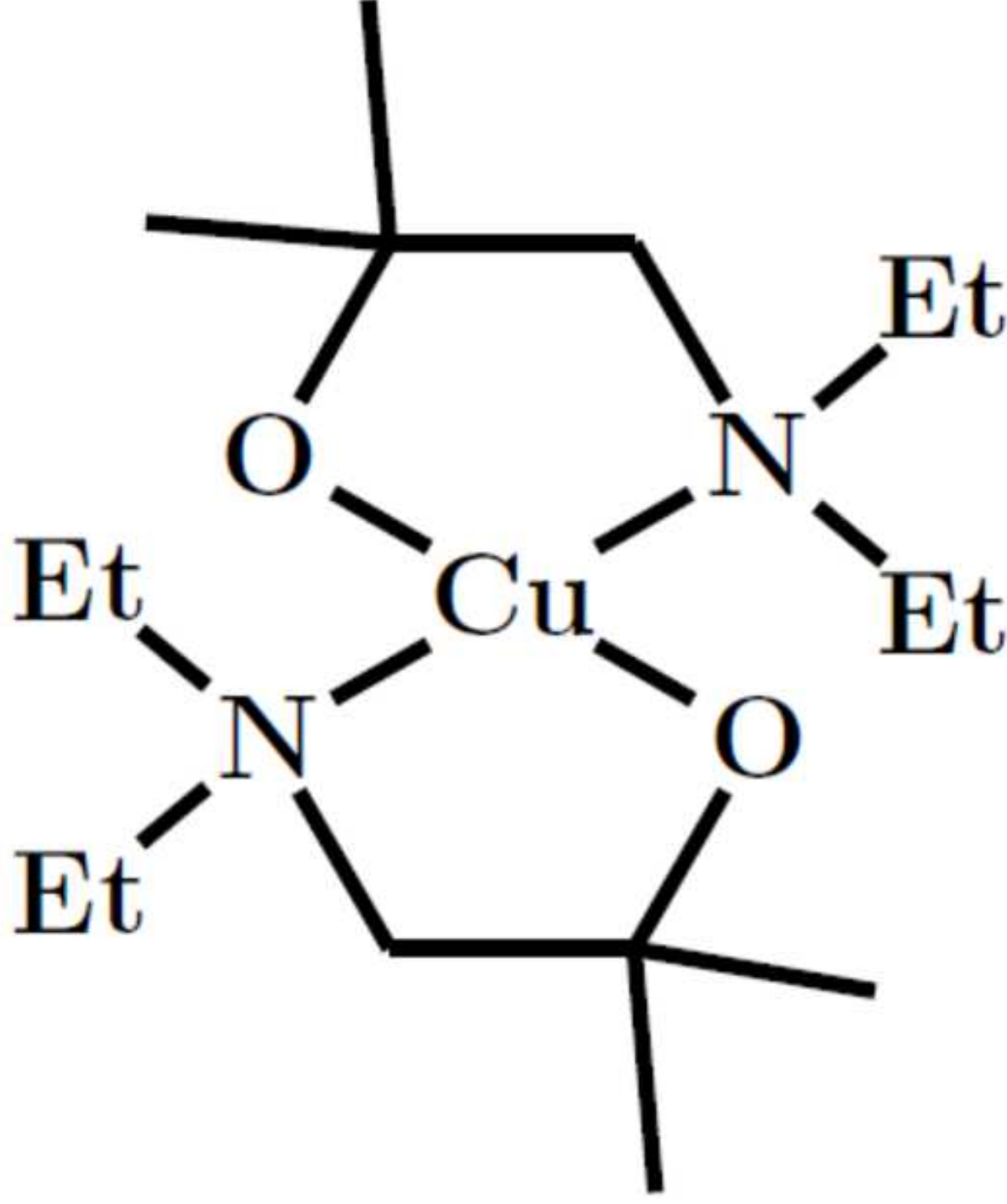
This is the author's peer reviewed, accepted manuscript. However, the online version of record will be different from this version once it has been copyedited and typeset.

PLEASE CITE THIS ARTICLE AS DOI: 10.1063/1.5087759



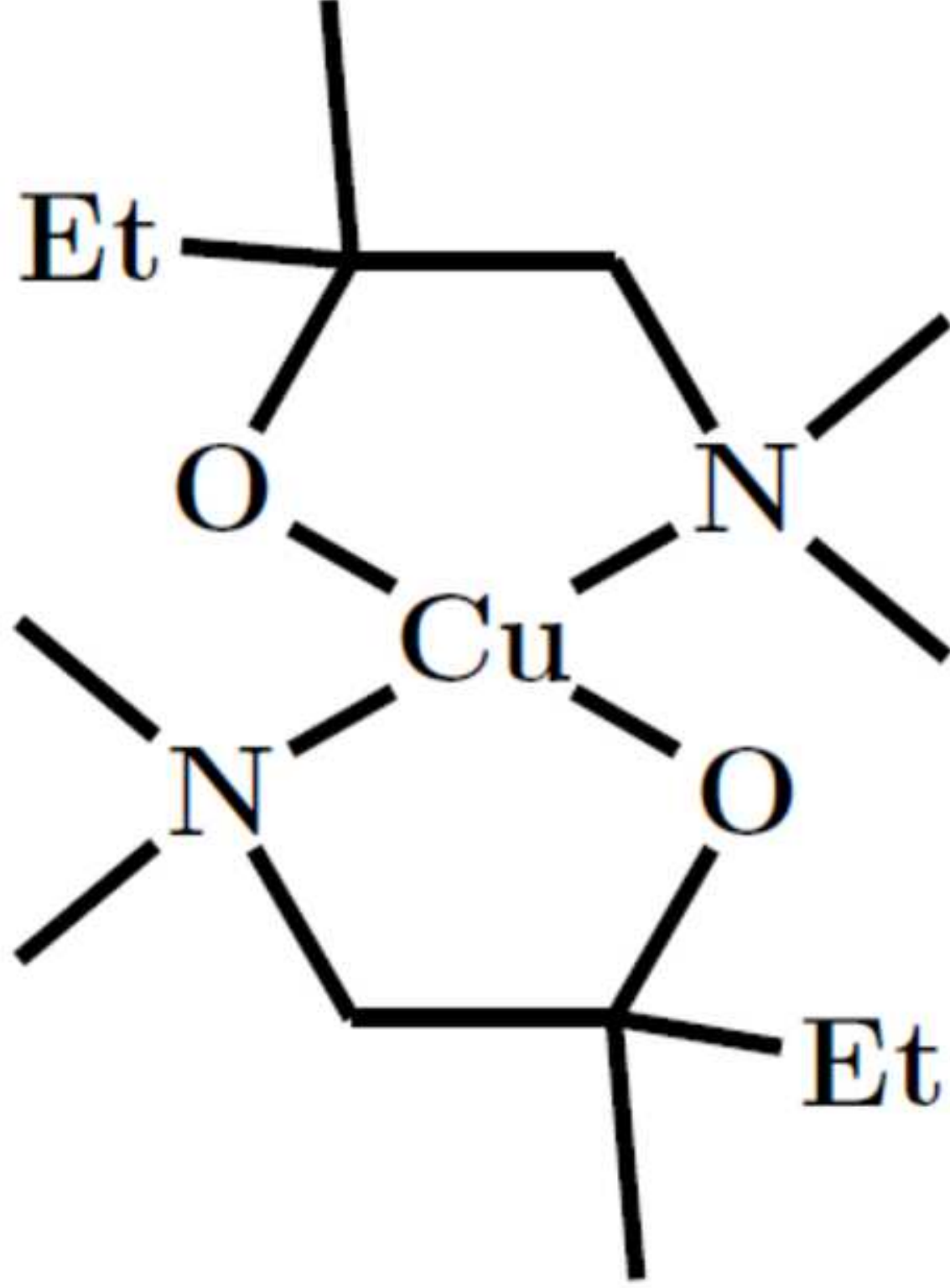
This is the author's peer reviewed, accepted manuscript. However, the online version of record will be different from this version once it has been copyedited and typeset.

PLEASE CITE THIS ARTICLE AS DOI: 10.1063/1.5087759



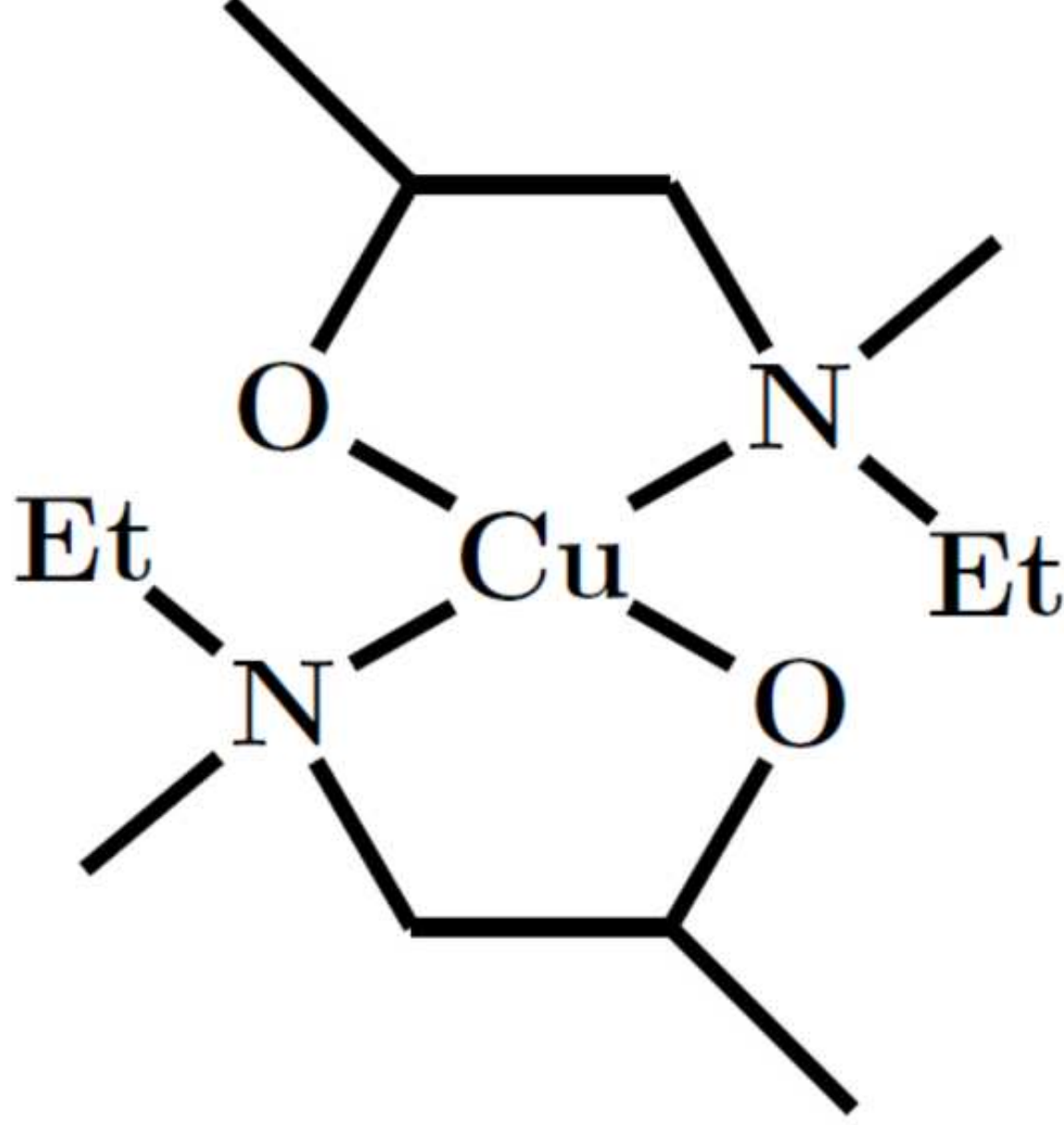
This is the author's peer reviewed, accepted manuscript. However, the online version of record will be different from this version once it has been copyedited and typeset.

PLEASE CITE THIS ARTICLE AS DOI: 10.1063/1.5087759



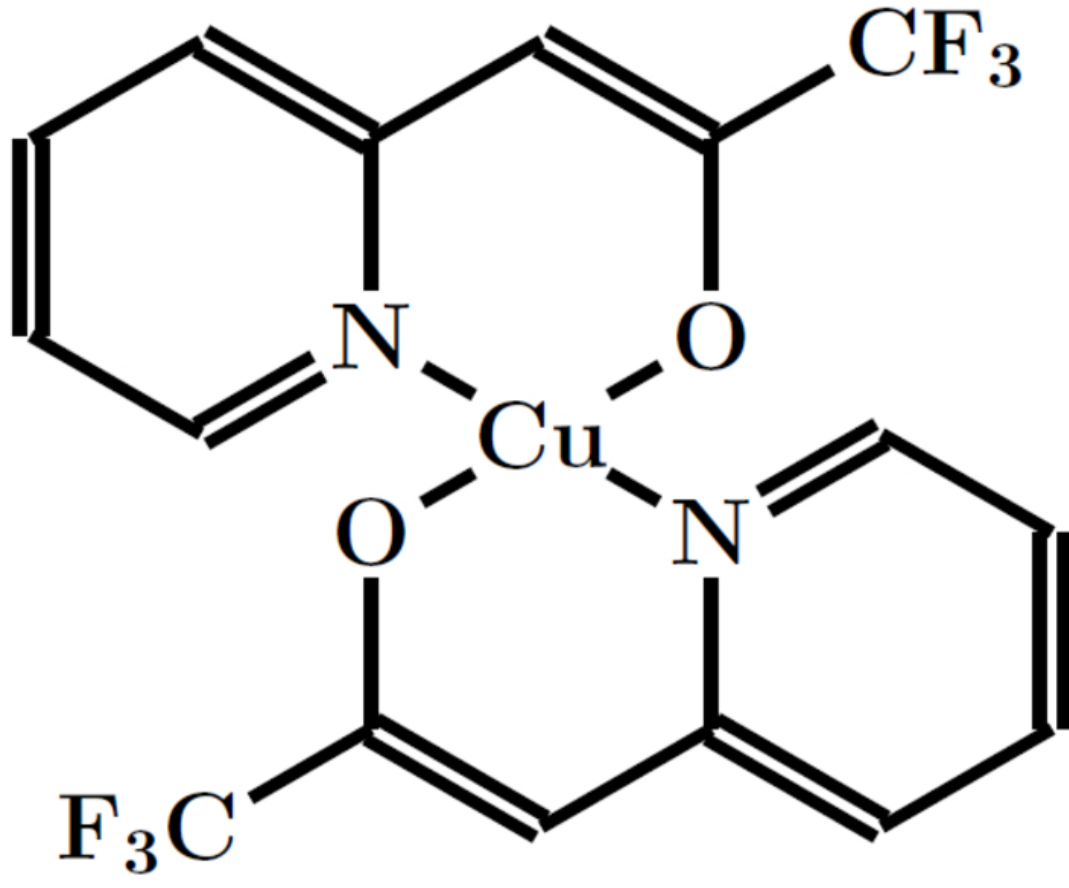
This is the author's peer reviewed, accepted manuscript. However, the online version of record will be different from this version once it has been copyedited and typeset.

PLEASE CITE THIS ARTICLE AS DOI: 10.1063/1.5087759



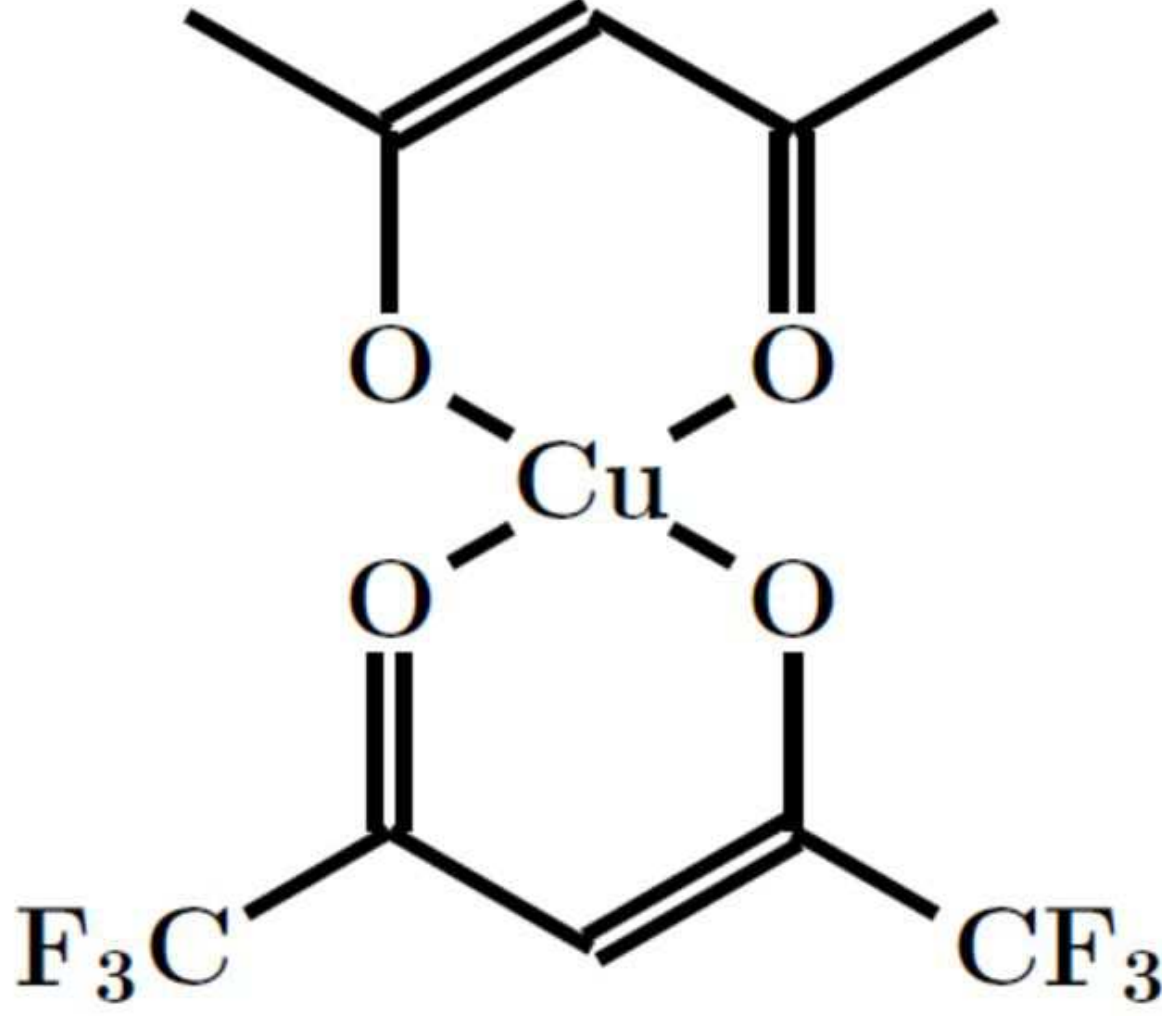
This is the author's peer reviewed, accepted manuscript. However, the online version of record will be different from this version once it has been copyedited and typeset.

PLEASE CITE THIS ARTICLE AS DOI: 10.1063/1.5087759



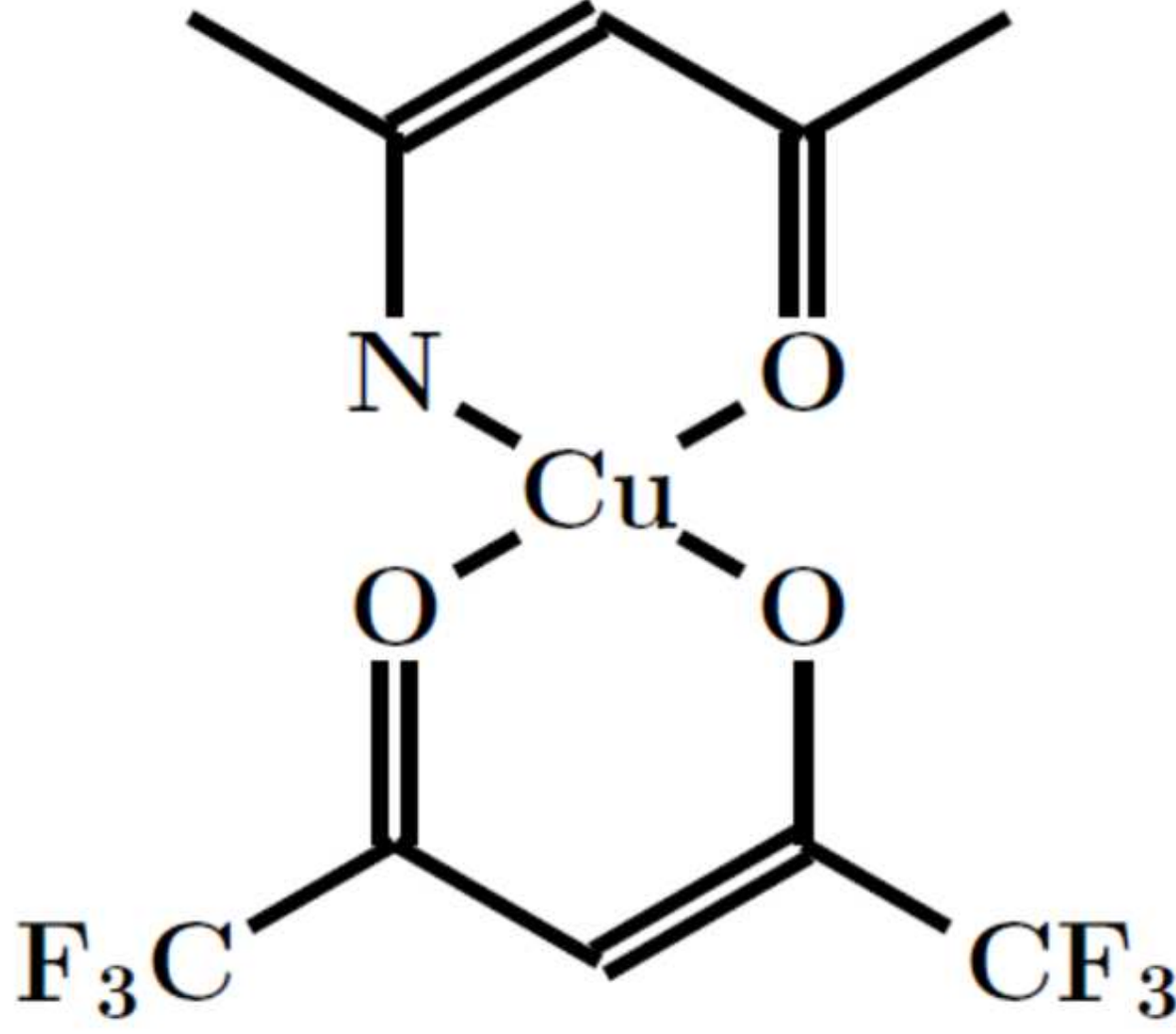
This is the author's peer reviewed, accepted manuscript. However, the online version of record will be different from this version once it has been copyedited and typeset.

PLEASE CITE THIS ARTICLE AS DOI: 10.1063/1.5087759



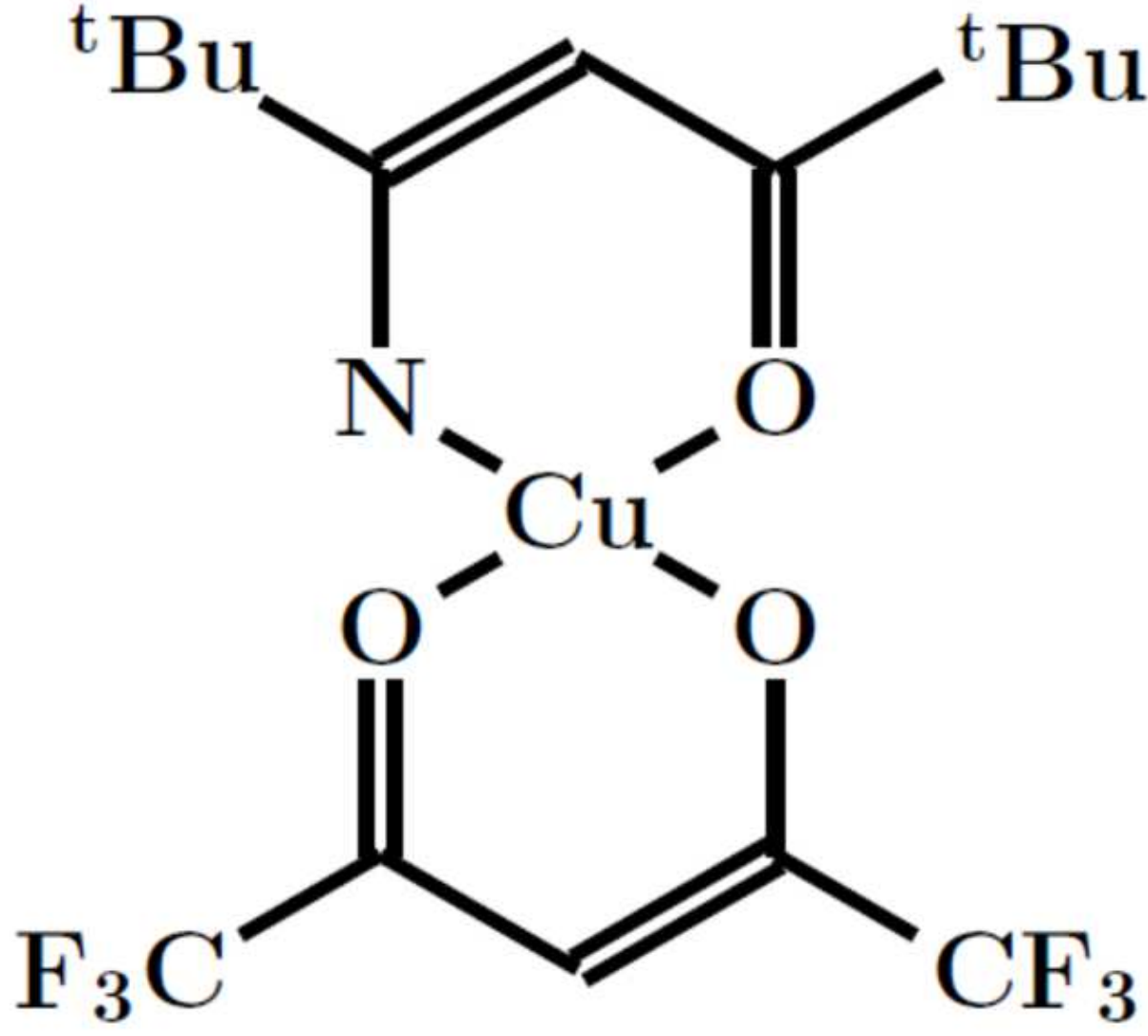
This is the author's peer reviewed, accepted manuscript. However, the online version of record will be different from this version once it has been copyedited and typeset.

PLEASE CITE THIS ARTICLE AS DOI: 10.1063/1.5087759



This is the author's peer reviewed, accepted manuscript. However, the online version of record will be different from this version once it has been copyedited and typeset.

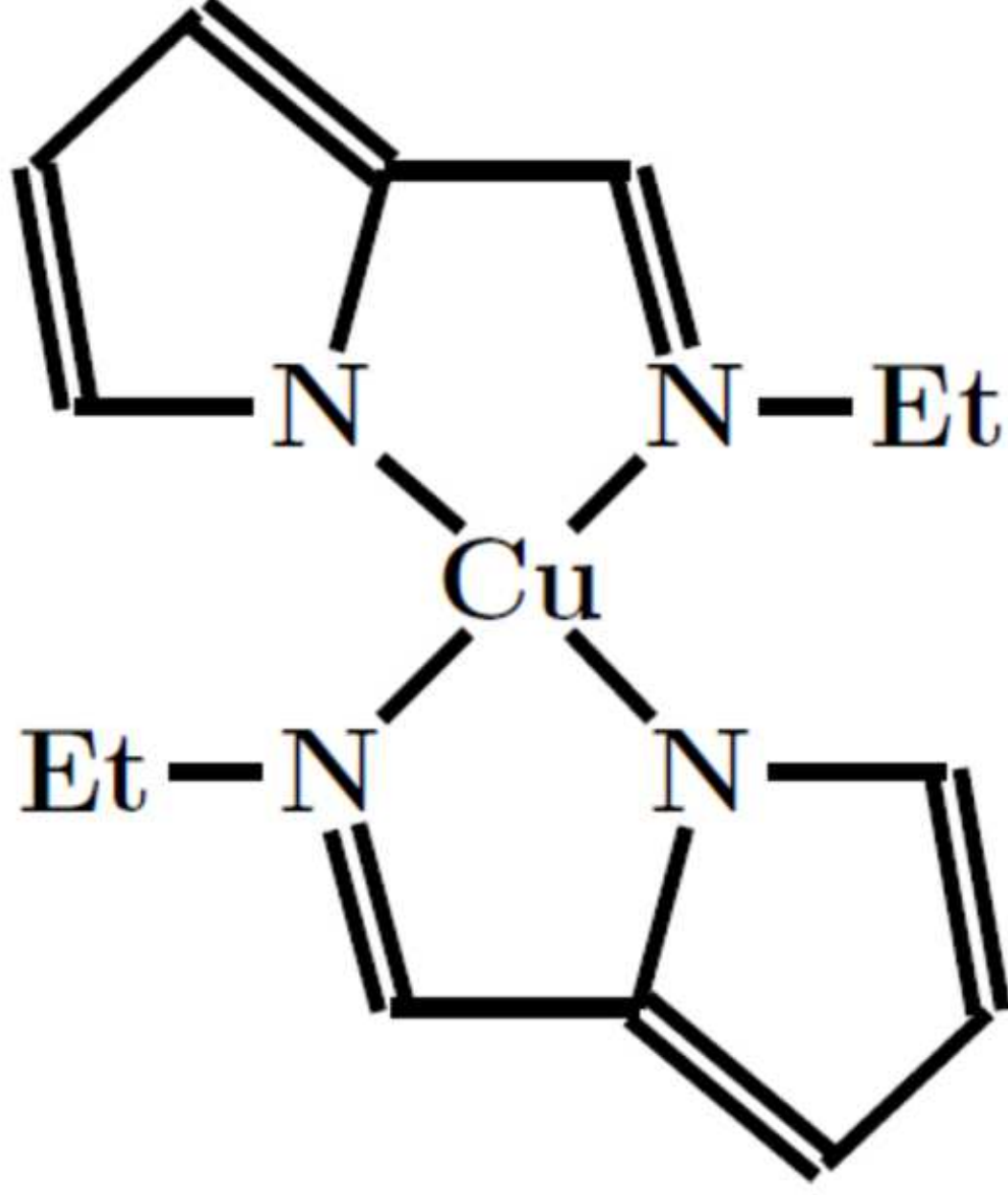
PLEASE CITE THIS ARTICLE AS DOI: 10.1063/1.5087759





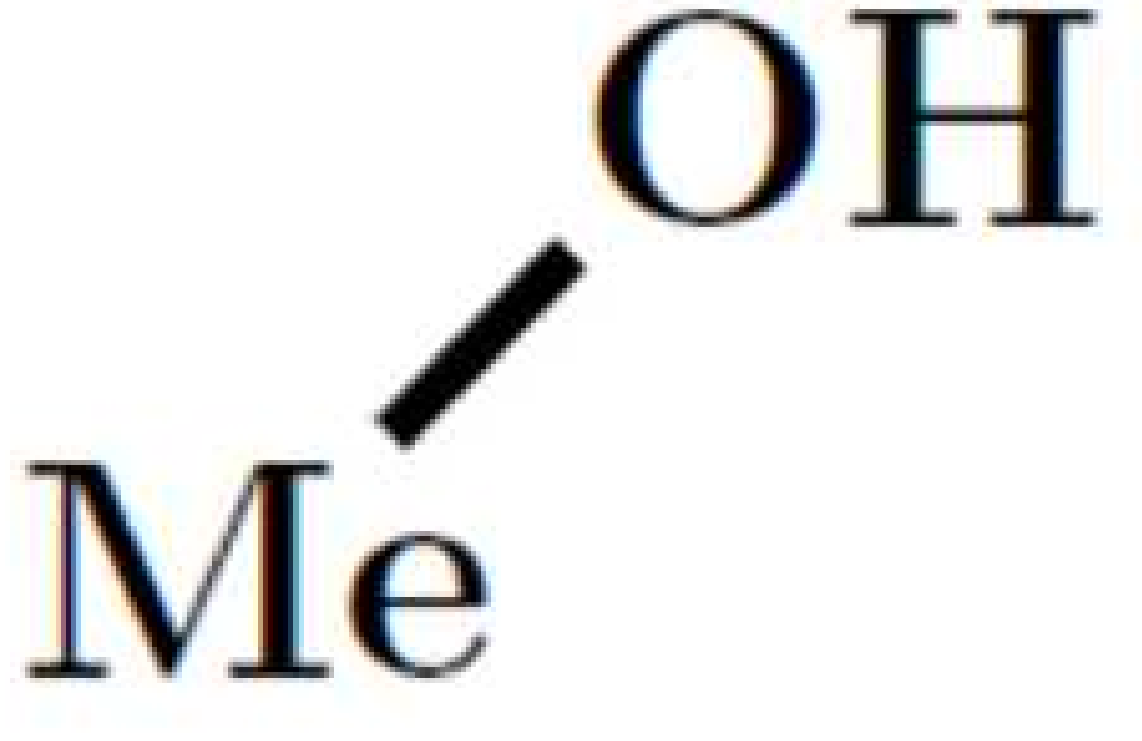
This is the author's peer reviewed, accepted manuscript. However, the online version of record will be different from this version once it has been copyedited and typeset.

PLEASE CITE THIS ARTICLE AS DOI: 10.1063/1.5087759



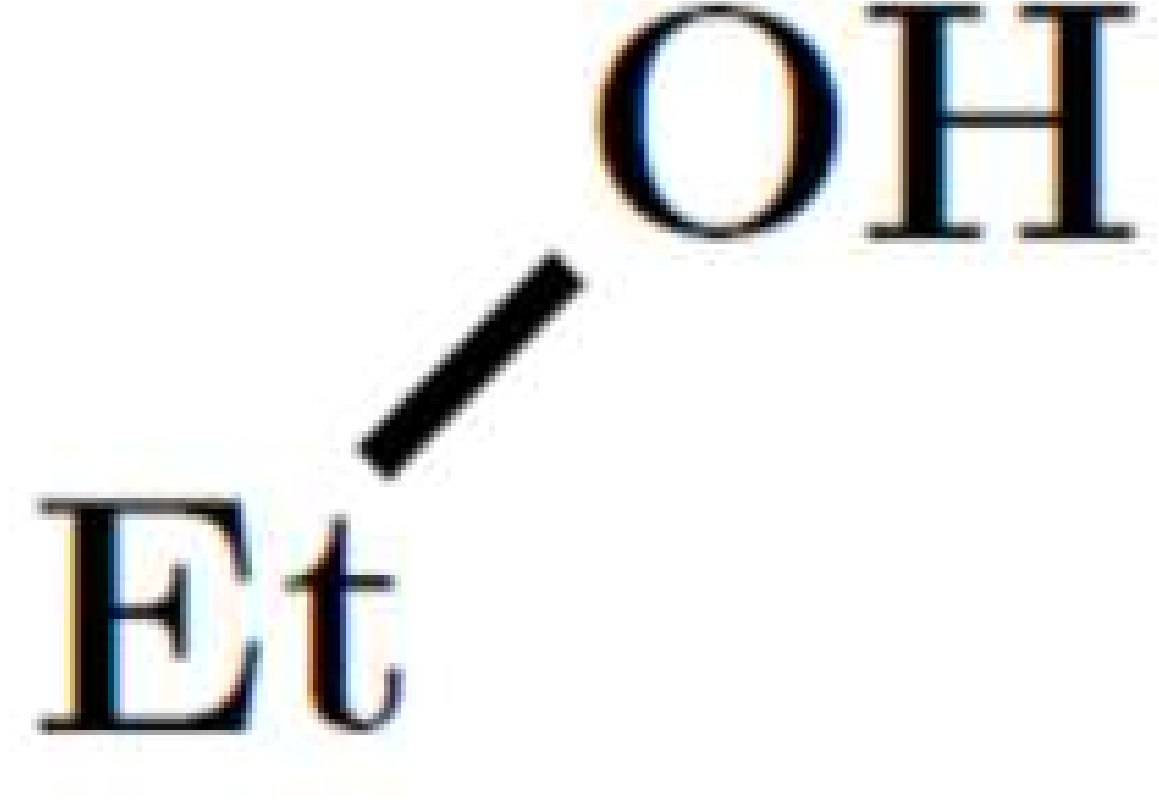
This is the author's peer reviewed, accepted manuscript. However, the online version of record will be different from this version once it has been copyedited and typeset.

PLEASE CITE THIS ARTICLE AS DOI: 10.1063/1.5087759

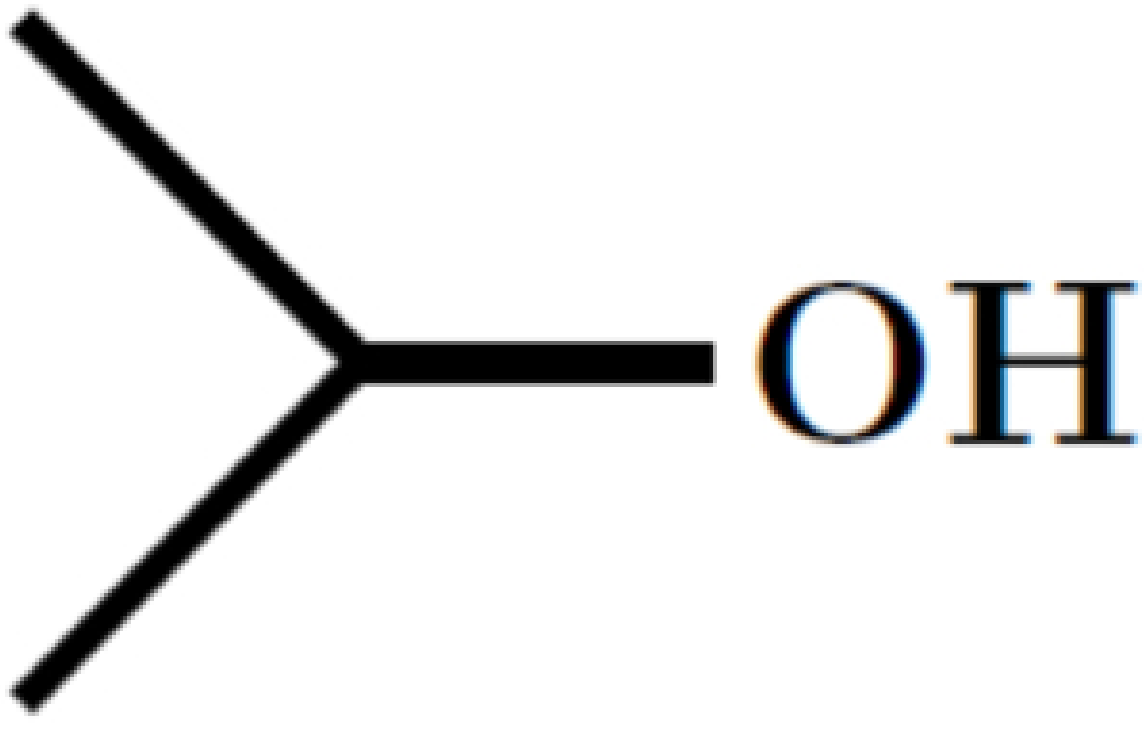


This is the author's peer reviewed, accepted manuscript. However, the online version of record will be different from this version once it has been copyedited and typeset.

PLEASE CITE THIS ARTICLE AS DOI: 10.1063/1.5087759

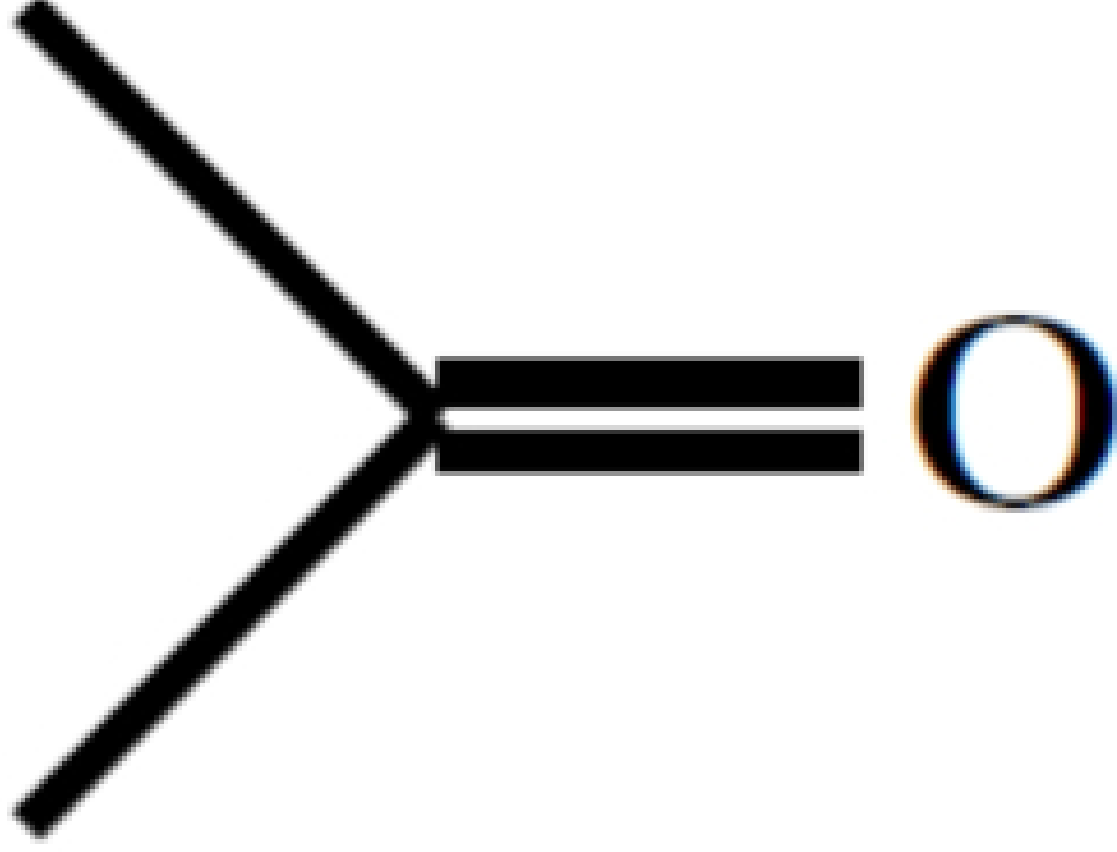


This is the author's peer reviewed, accepted manuscript. However, the online version of record will be different from this version once it has been copyedited and typeset.  
PLEASE CITE THIS ARTICLE AS DOI: 10.1063/1.5087759



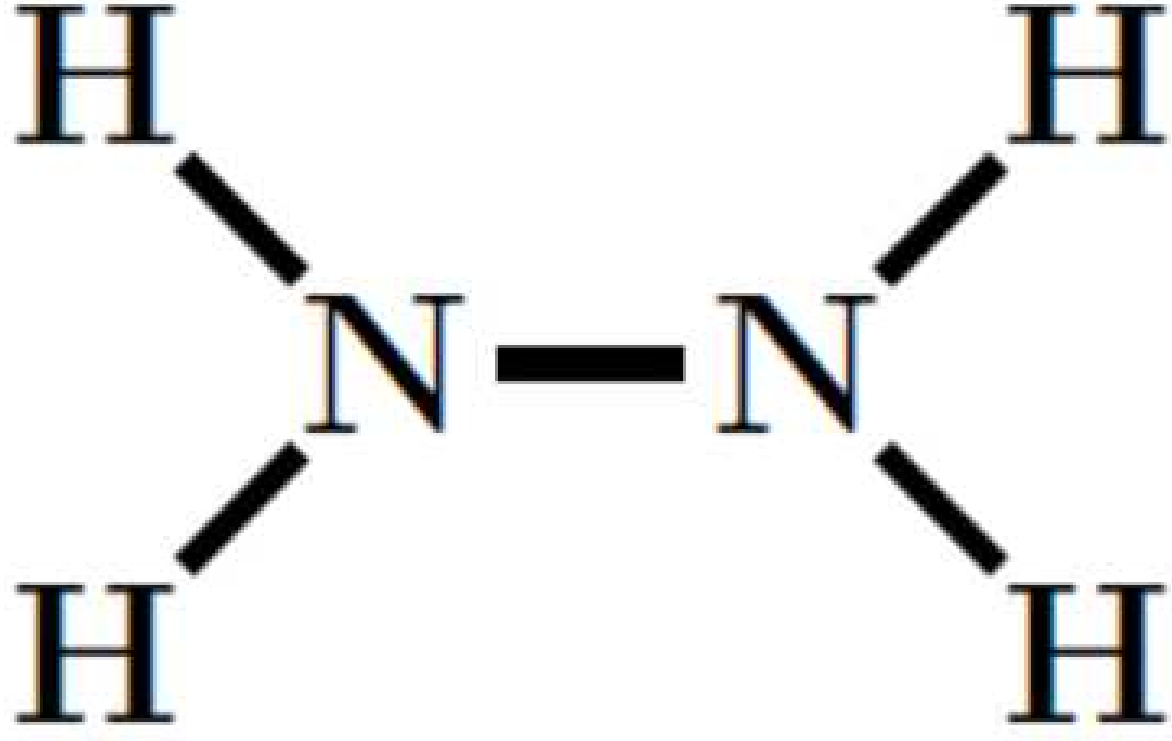
This is the author's peer reviewed, accepted manuscript. However, the online version of record will be different from this version once it has been copyedited and typeset.

PLEASE CITE THIS ARTICLE AS DOI: 10.1063/1.5087759



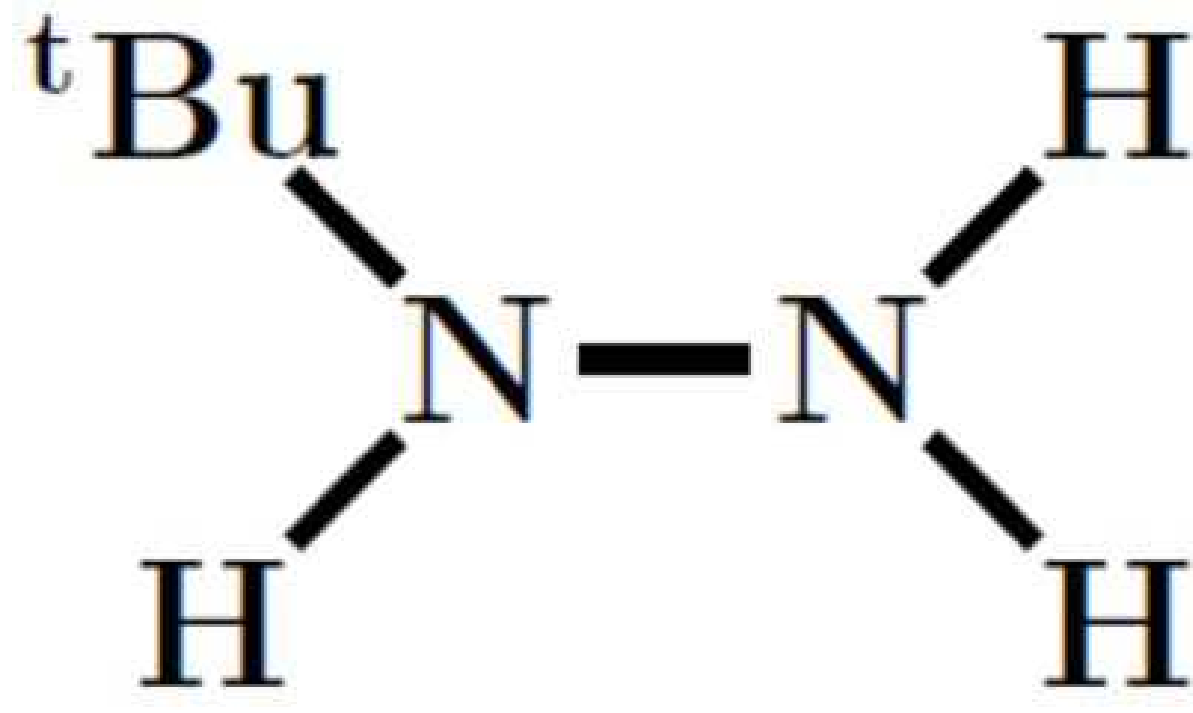
This is the author's peer reviewed, accepted manuscript. However, the online version of record will be different from this version once it has been copyedited and typeset.

PLEASE CITE THIS ARTICLE AS DOI: 10.1063/1.5087759



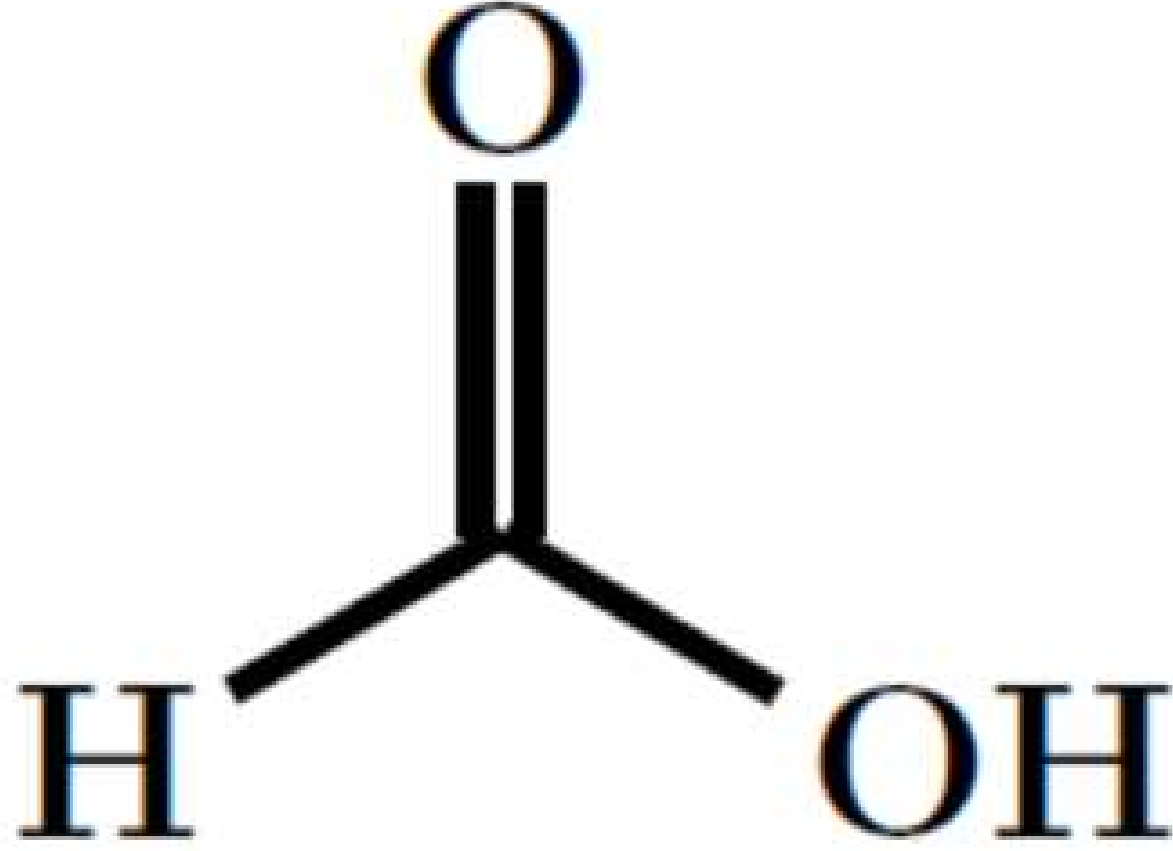
This is the author's peer reviewed, accepted manuscript. However, the online version of record will be different from this version once it has been copyedited and typeset.

PLEASE CITE THIS ARTICLE AS DOI: 10.1063/1.5087759



This is the author's peer reviewed, accepted manuscript. However, the online version of record will be different from this version once it has been copyedited and typeset.

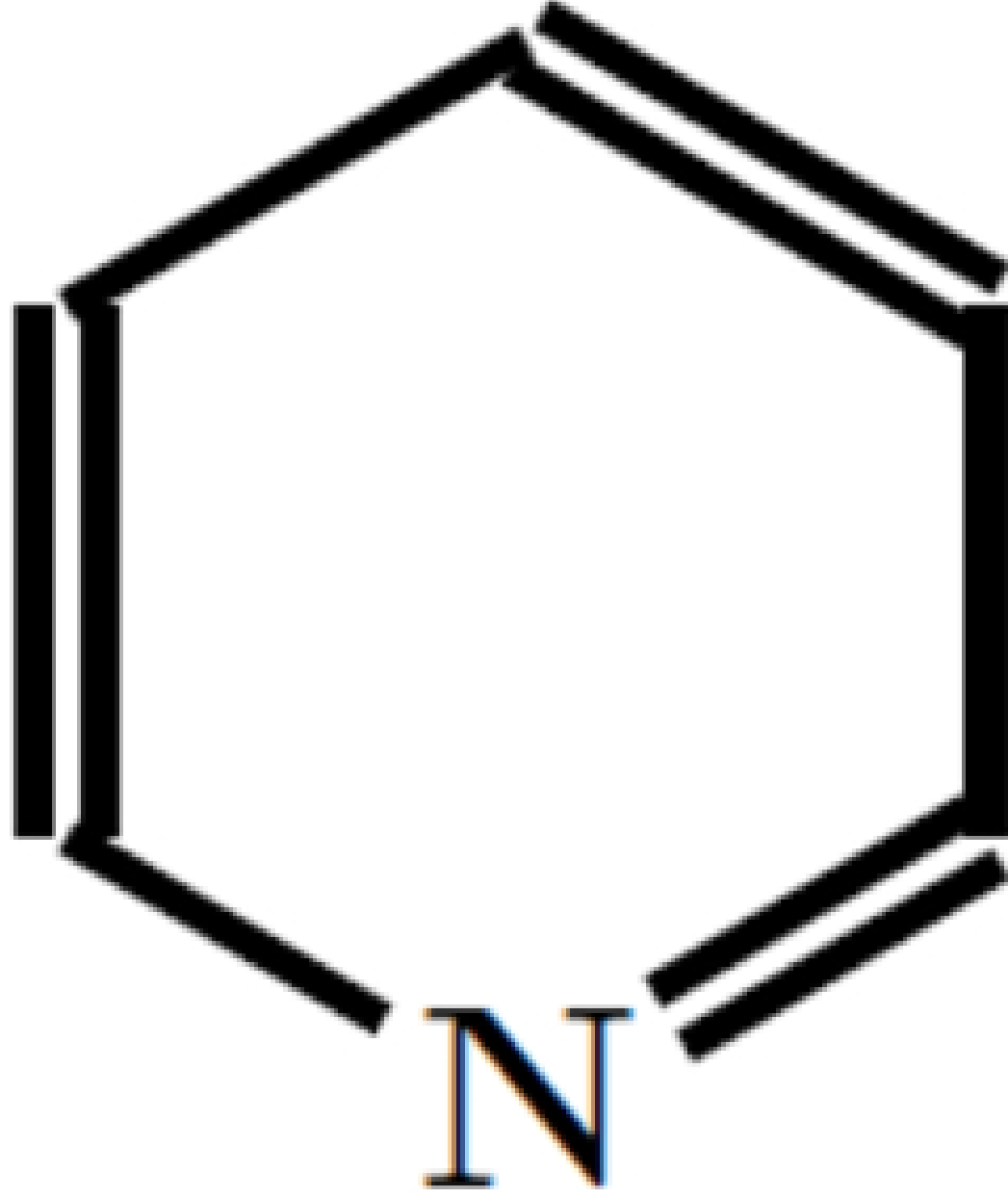
PLEASE CITE THIS ARTICLE AS DOI: 10.1063/1.5087759





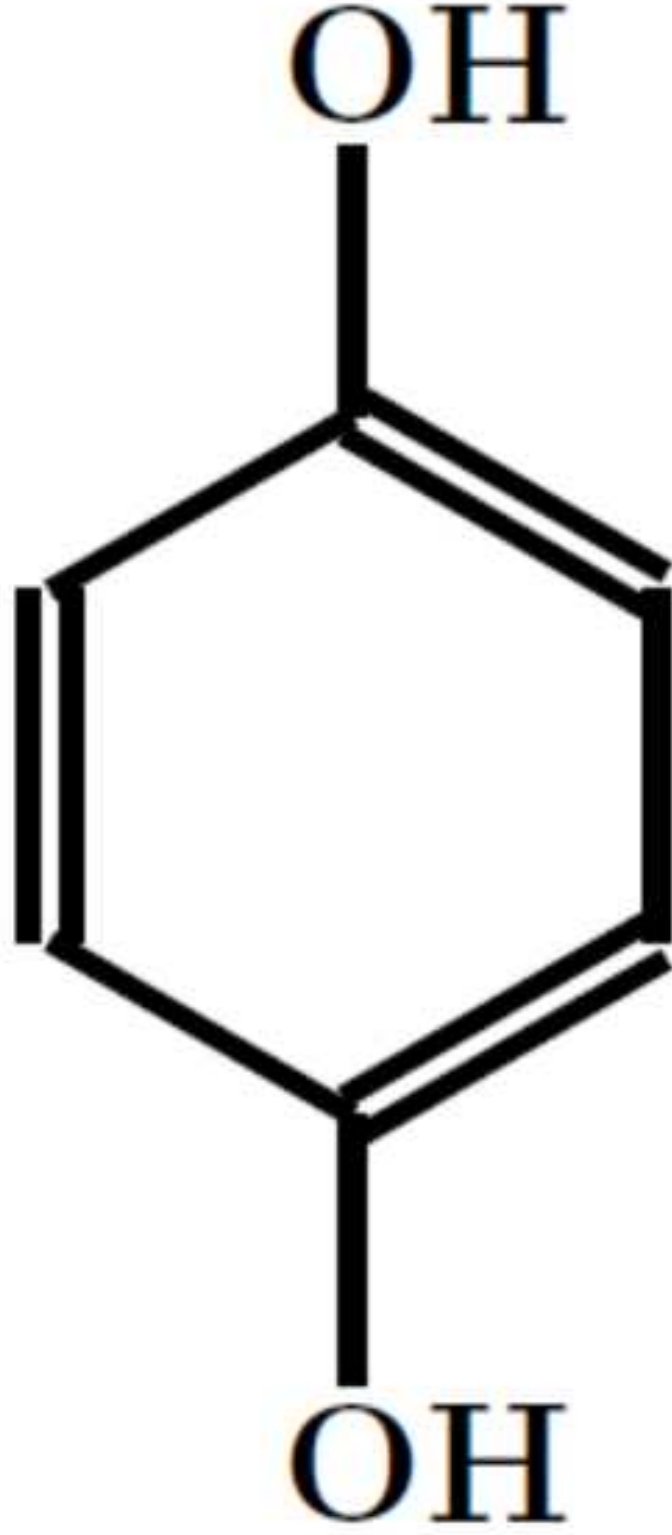
This is the author's peer reviewed, accepted manuscript. However, the online version of record will be different from this version once it has been copyedited and typeset.

PLEASE CITE THIS ARTICLE AS DOI: 10.1063/1.5087759



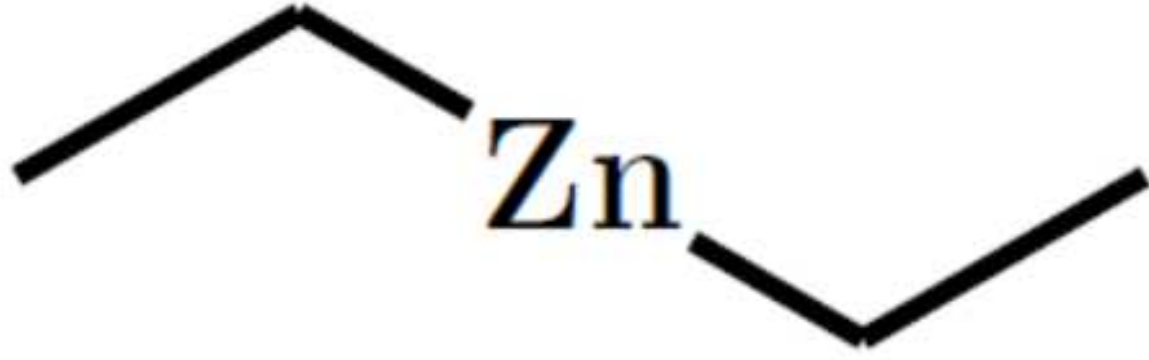
This is the author's peer reviewed, accepted manuscript. However, the online version of record will be different from this version once it has been copyedited and typeset.

PLEASE CITE THIS ARTICLE AS DOI: 10.1063/1.5087759



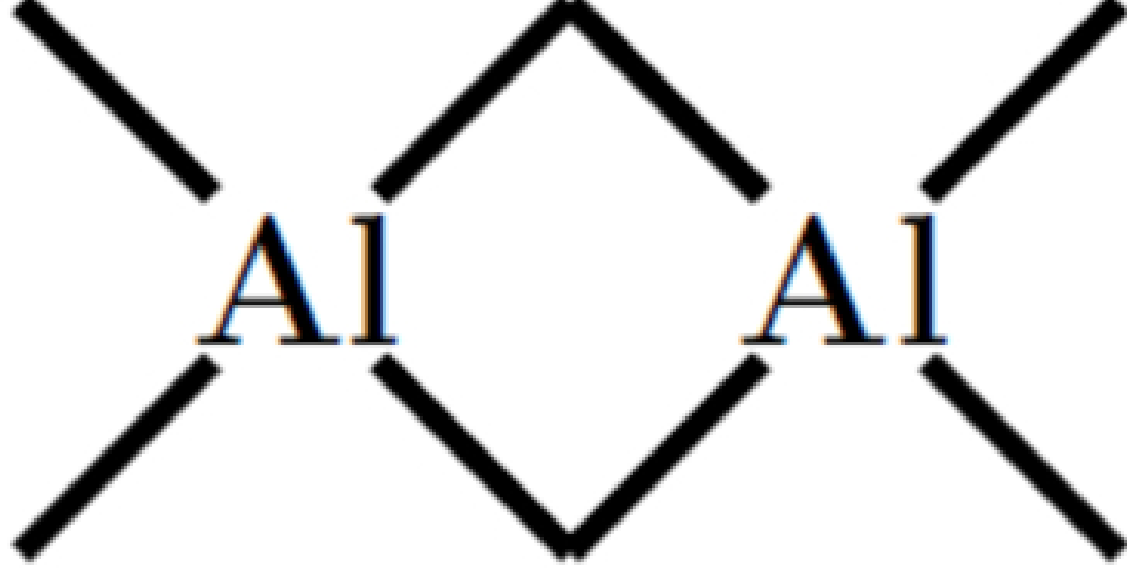
This is the author's peer reviewed, accepted manuscript. However, the online version of record will be different from this version once it has been copyedited and typeset.

PLEASE CITE THIS ARTICLE AS DOI: 10.1063/1.5087759



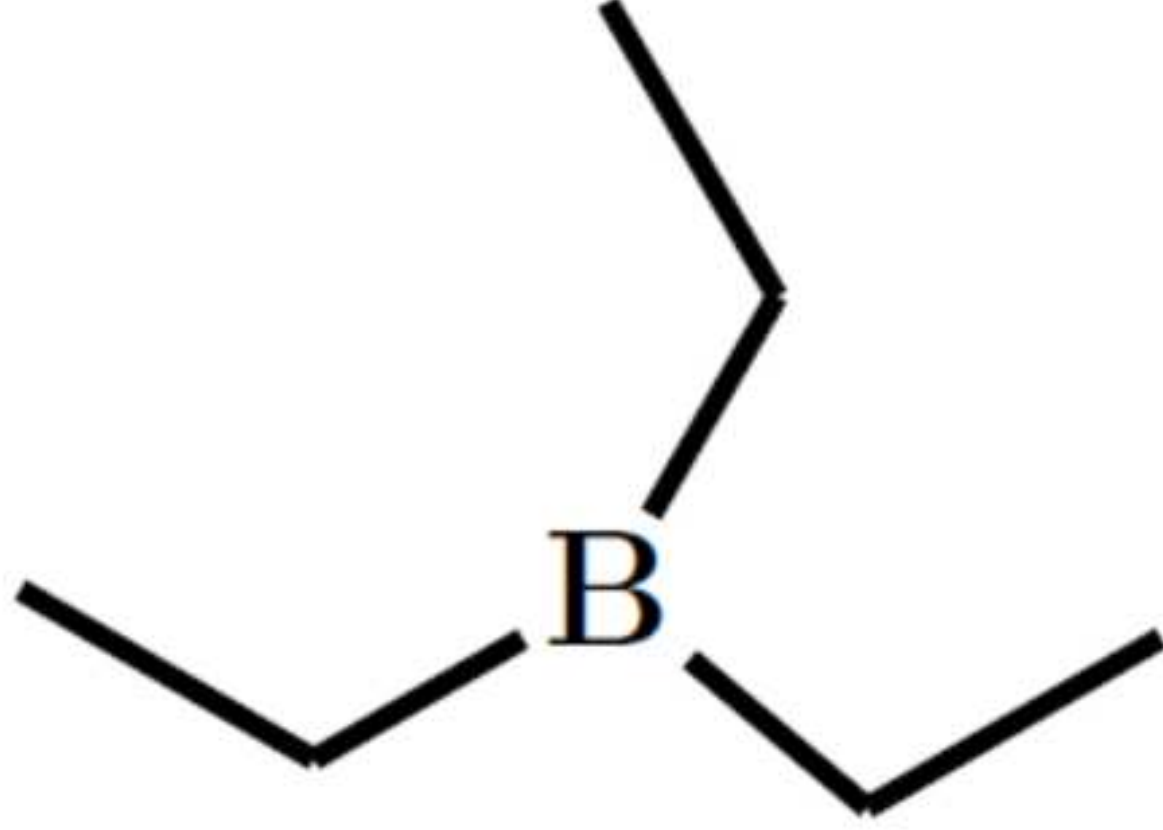
This is the author's peer reviewed, accepted manuscript. However, the online version of record will be different from this version once it has been copyedited and typeset.

PLEASE CITE THIS ARTICLE AS DOI: 10.1063/1.5087759



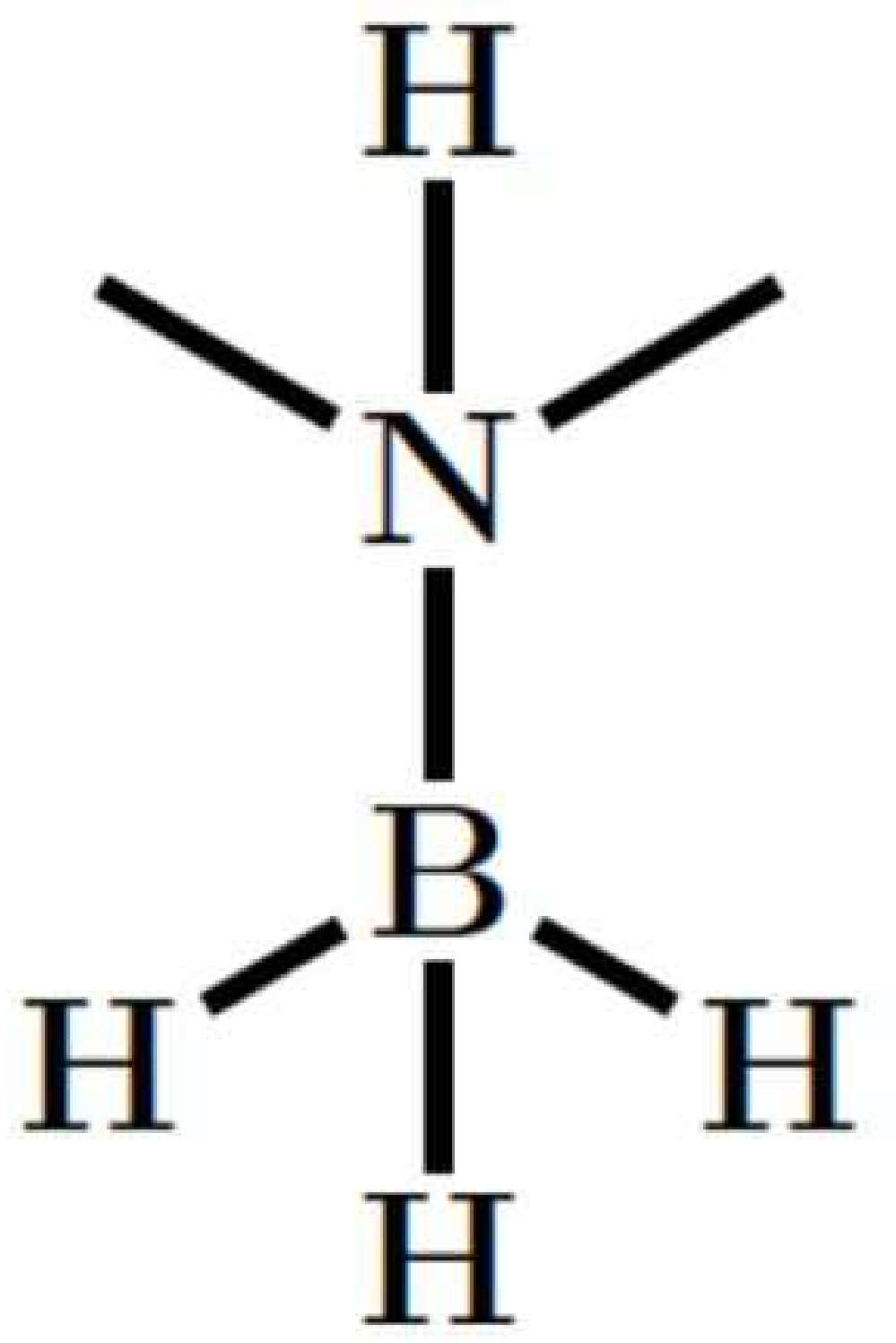
This is the author's peer reviewed, accepted manuscript. However, the online version of record will be different from this version once it has been copyedited and typeset.

PLEASE CITE THIS ARTICLE AS DOI: 10.1063/1.5087759



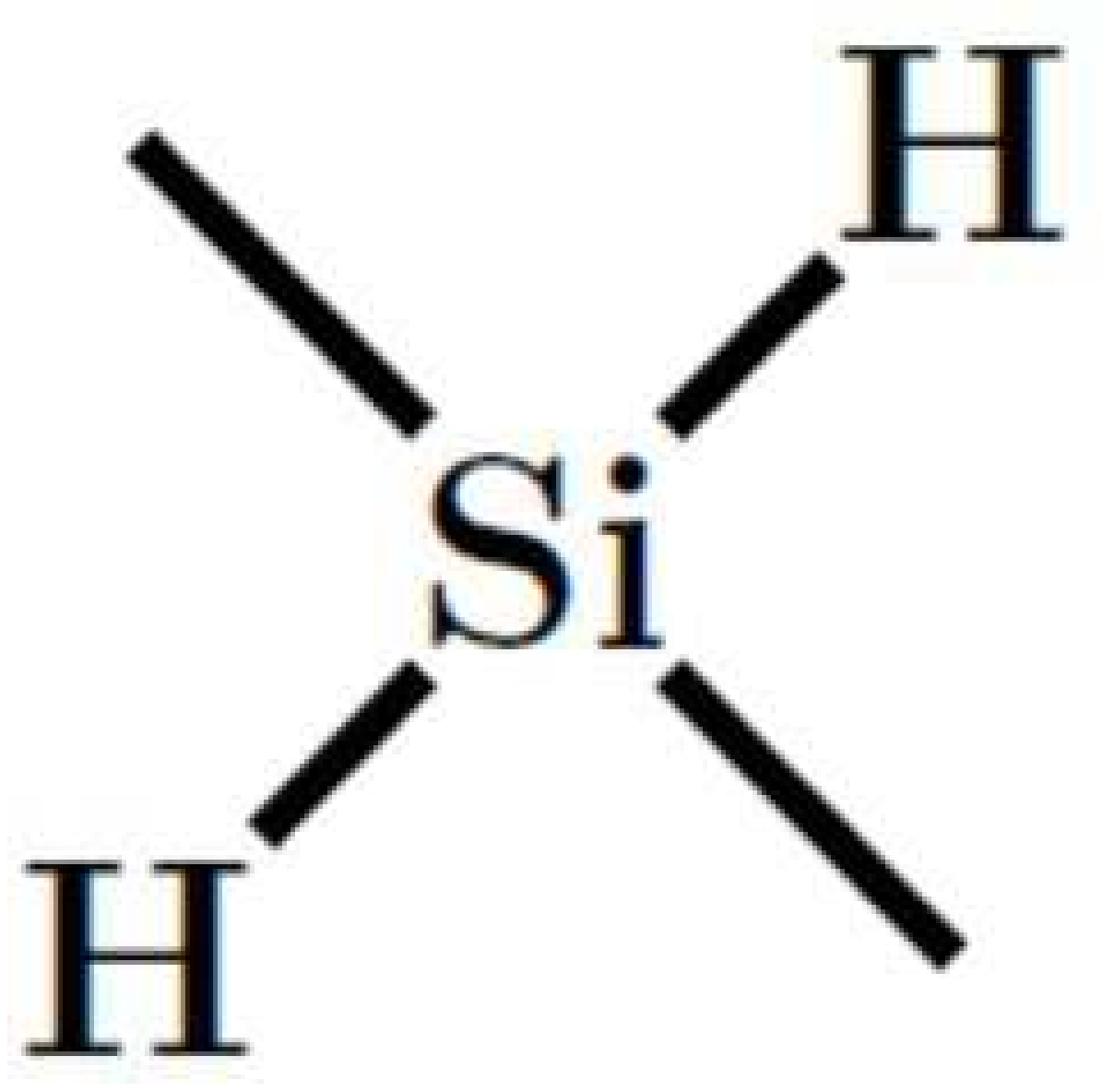
This is the author's peer reviewed, accepted manuscript. However, the online version of record will be different from this version once it has been copyedited and typeset.

PLEASE CITE THIS ARTICLE AS DOI: 10.1063/1.5087759



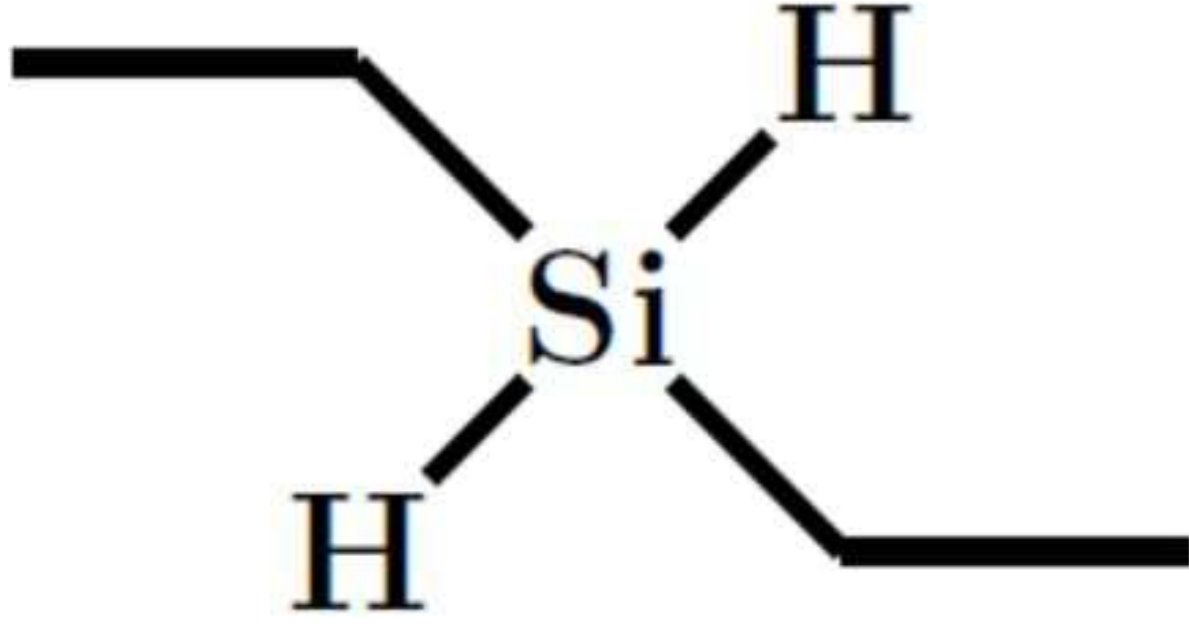
This is the author's peer reviewed, accepted manuscript. However, the online version of record will be different from this version once it has been copyedited and typeset.

PLEASE CITE THIS ARTICLE AS DOI: 10.1063/1.5087759



This is the author's peer reviewed, accepted manuscript. However, the online version of record will be different from this version once it has been copyedited and typeset.

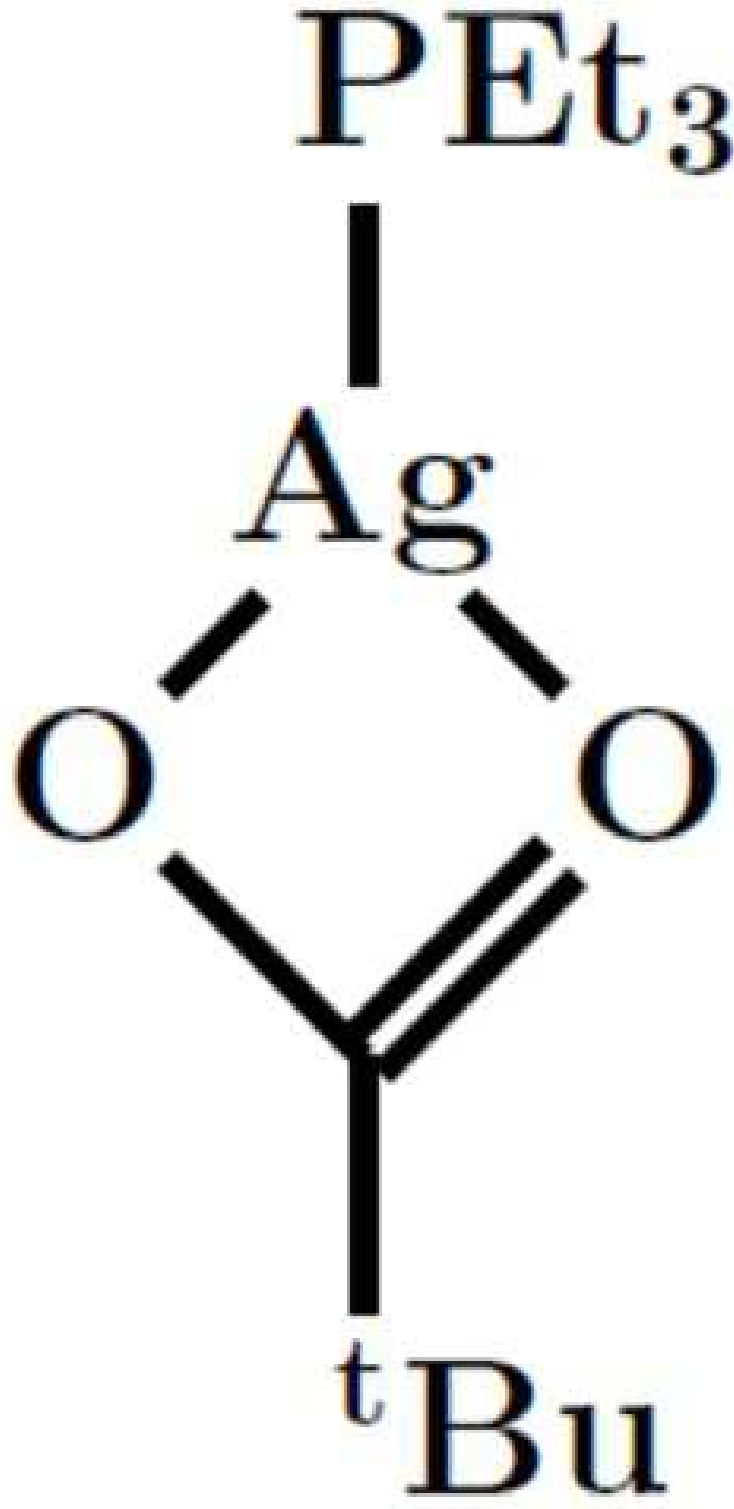
PLEASE CITE THIS ARTICLE AS DOI: 10.1063/1.5087759





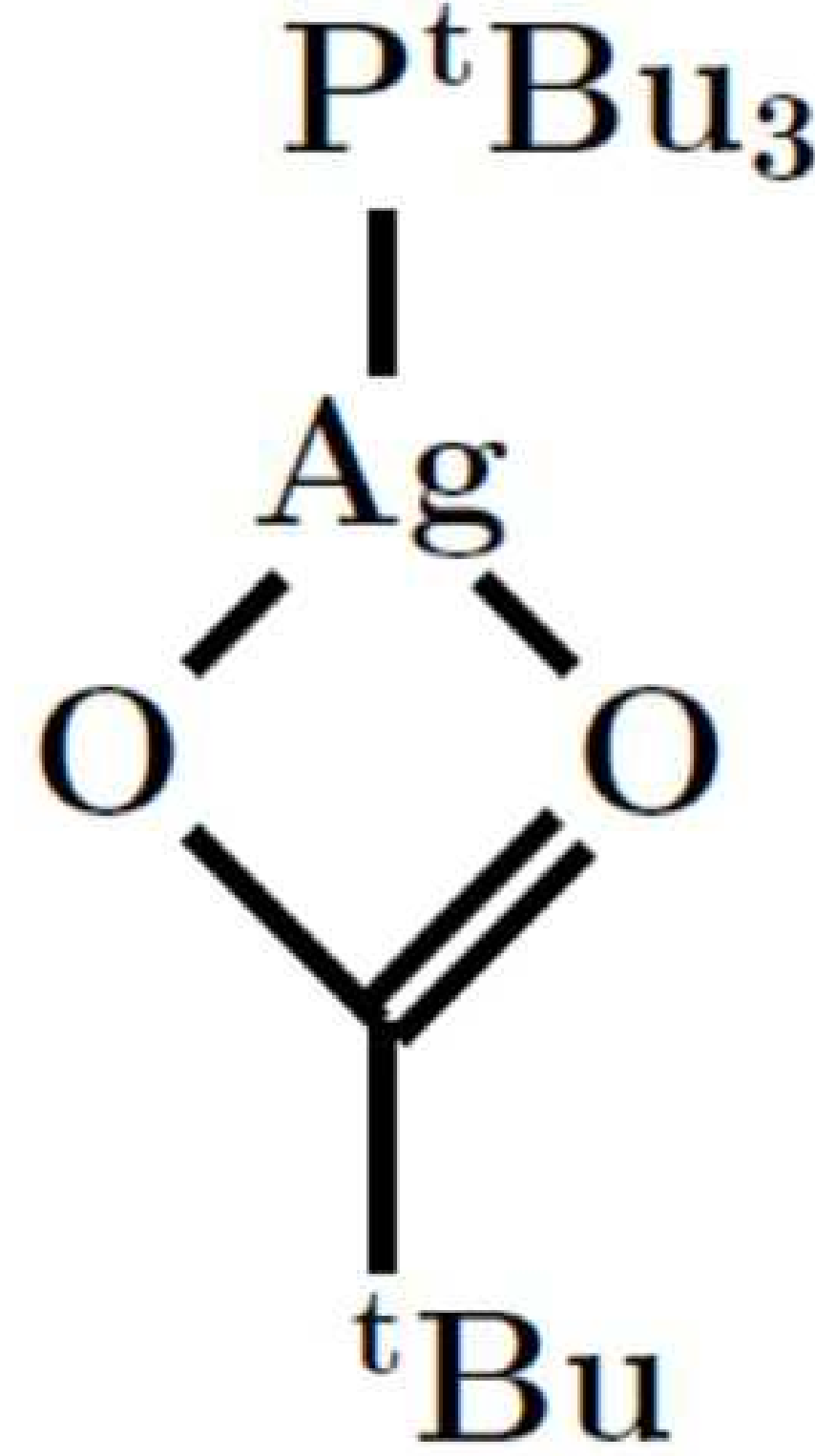
This is the author's peer reviewed, accepted manuscript. However, the online version of record will be different from this version once it has been copyedited and typeset.

PLEASE CITE THIS ARTICLE AS DOI: 10.1063/1.5087759



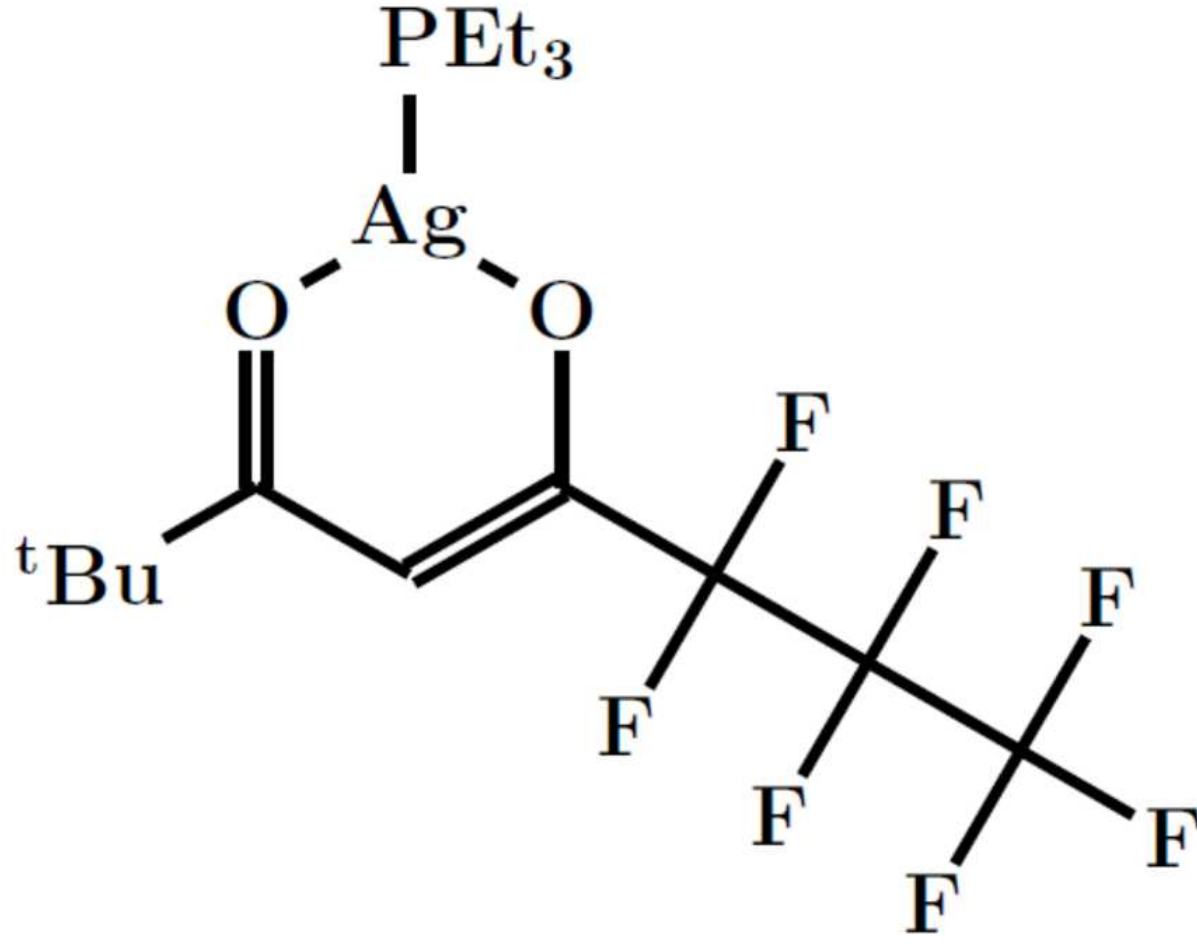
This is the author's peer reviewed, accepted manuscript. However, the online version of record will be different from this version once it has been copyedited and typeset.

PLEASE CITE THIS ARTICLE AS DOI: 10.1063/1.5087759



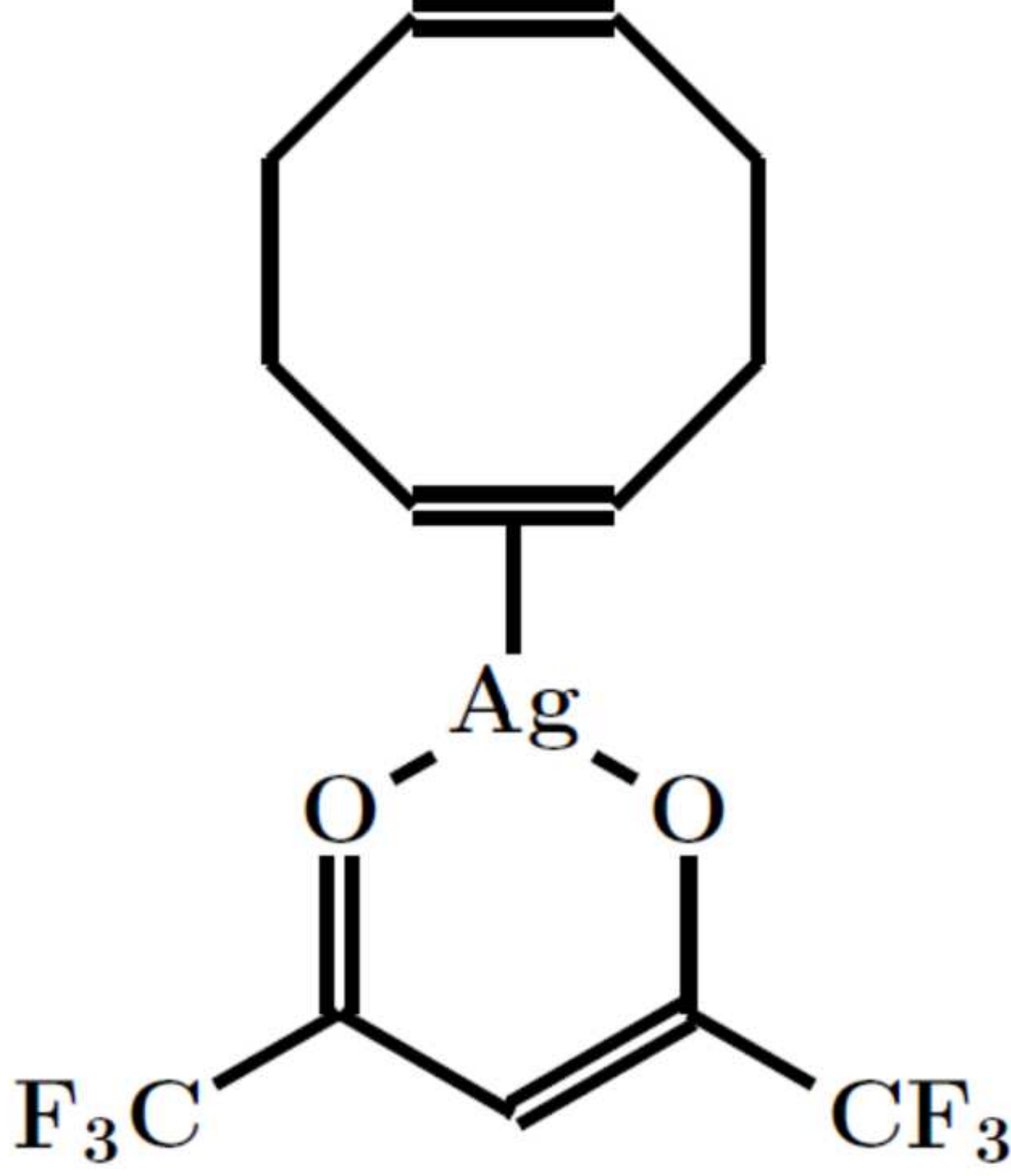
This is the author's peer reviewed, accepted manuscript. However, the online version of record will be different from this version once it has been copyedited and typeset.

PLEASE CITE THIS ARTICLE AS DOI: 10.1063/1.5087759



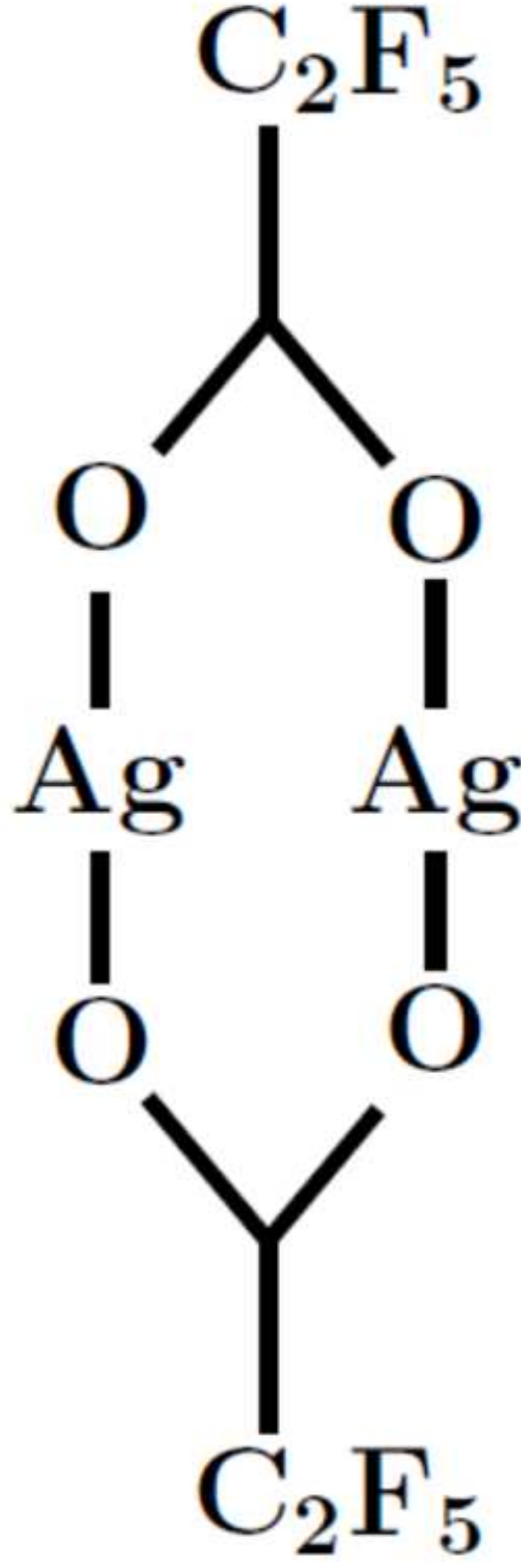
This is the author's peer reviewed, accepted manuscript. However, the online version of record will be different from this version once it has been copyedited and typeset.

PLEASE CITE THIS ARTICLE AS DOI: 10.1063/1.5087759



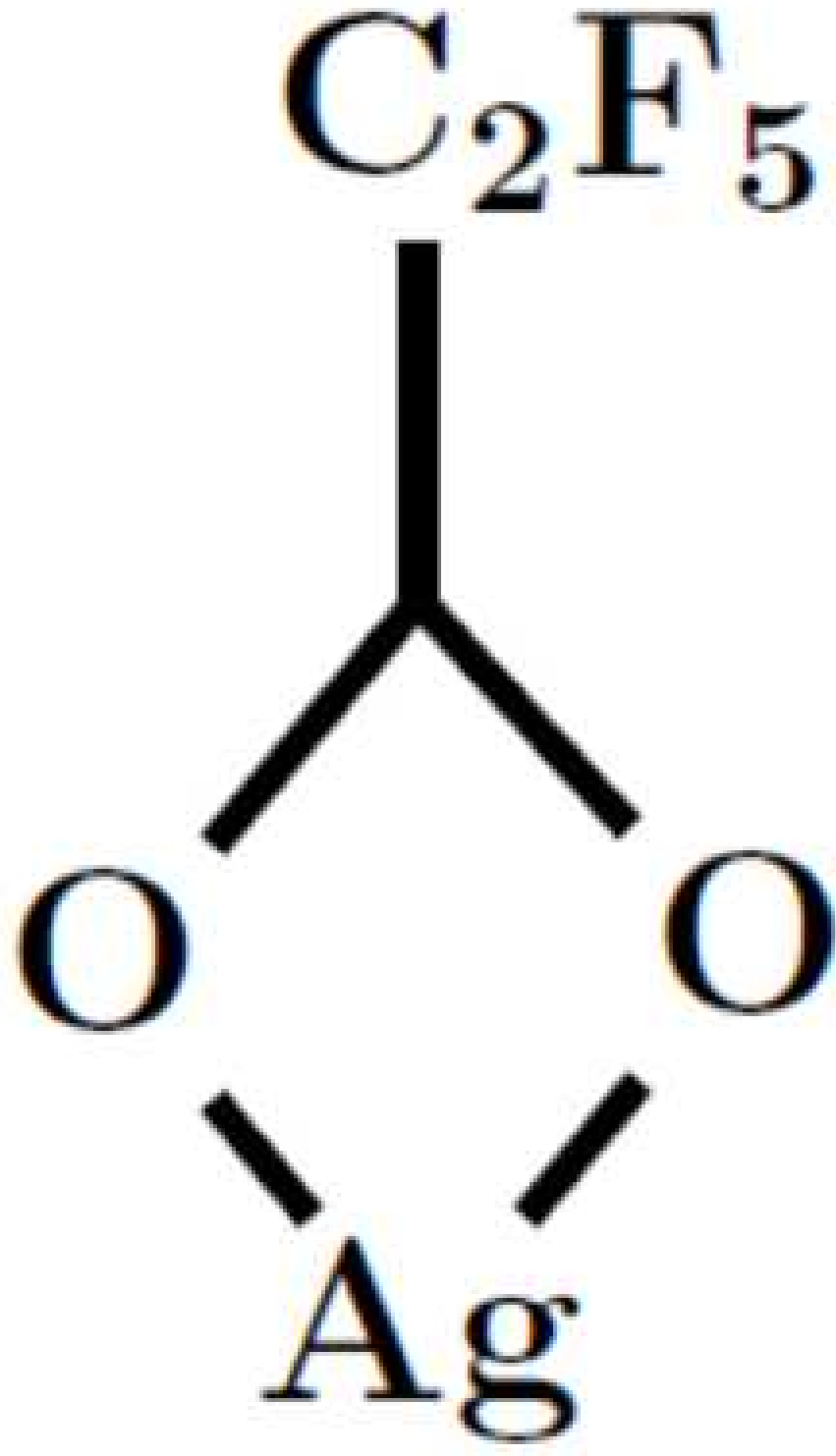
This is the author's peer reviewed, accepted manuscript. However, the online version of record will be different from this version once it has been copyedited and typeset.

PLEASE CITE THIS ARTICLE AS DOI: 10.1063/1.5087759



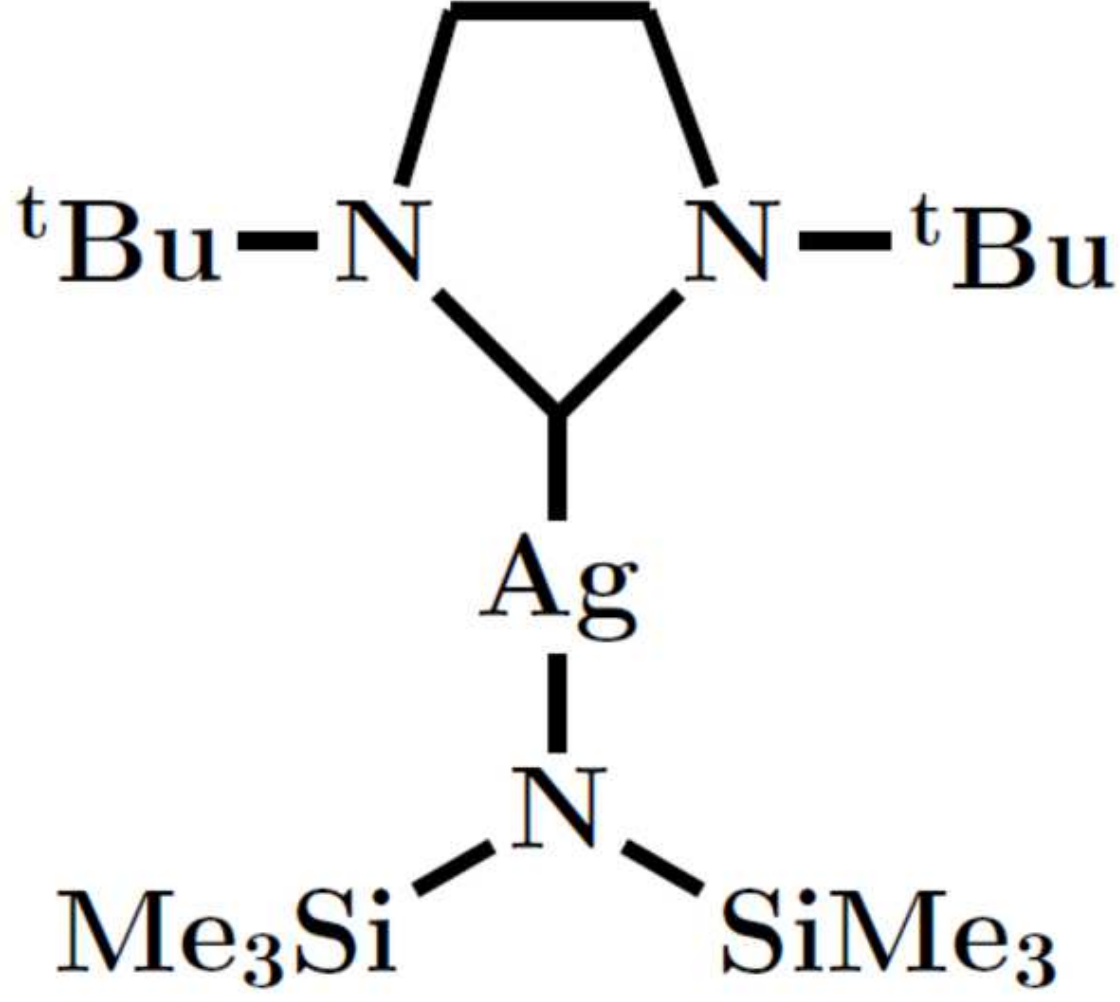
This is the author's peer reviewed, accepted manuscript. However, the online version of record will be different from this version once it has been copyedited and typeset.

PLEASE CITE THIS ARTICLE AS DOI: 10.1063/1.5087759



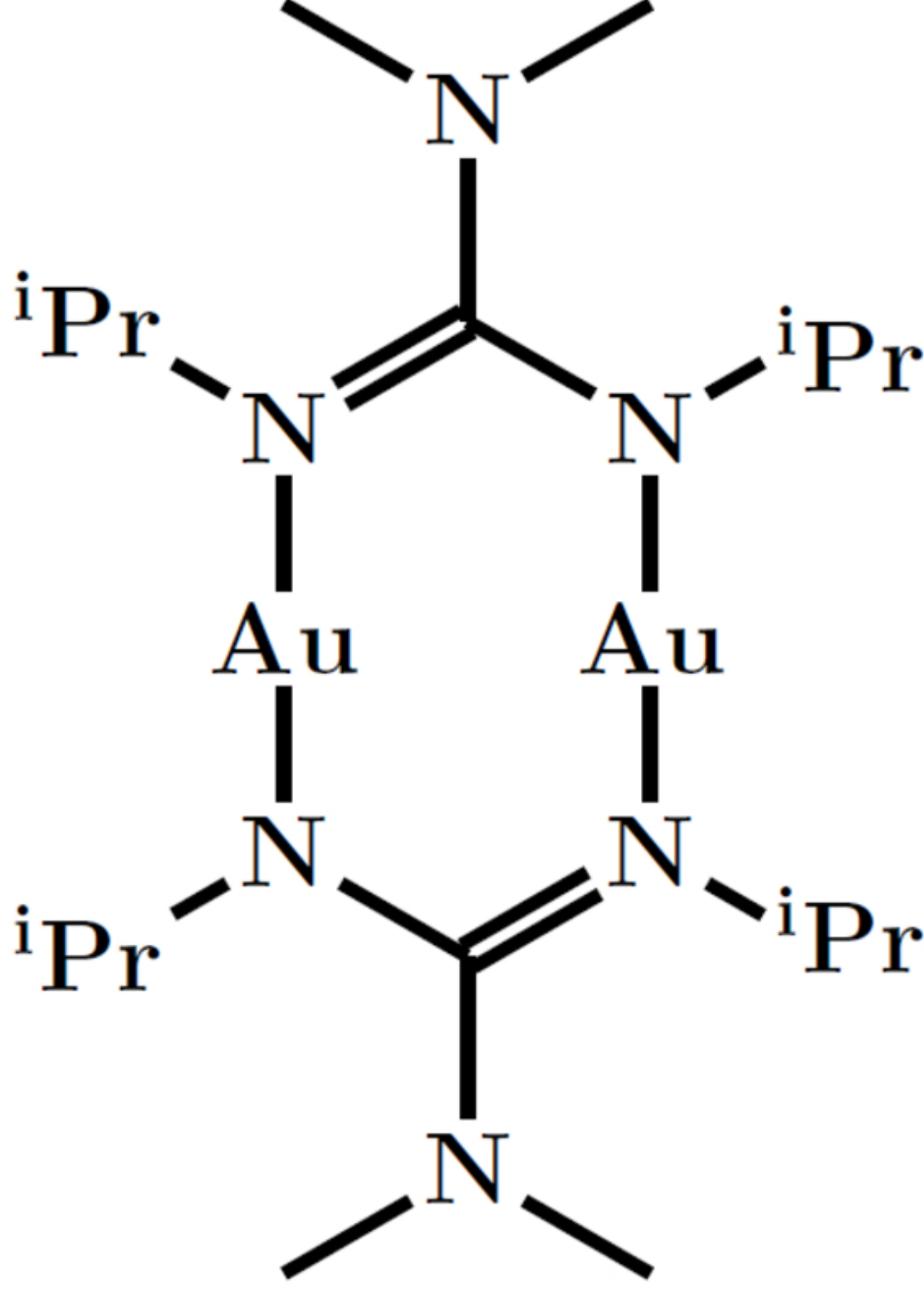
This is the author's peer reviewed, accepted manuscript. However, the online version of record will be different from this version once it has been copyedited and typeset.

PLEASE CITE THIS ARTICLE AS DOI: 10.1063/1.5087759



This is the author's peer reviewed, accepted manuscript. However, the online version of record will be different from this version once it has been copyedited and typeset.

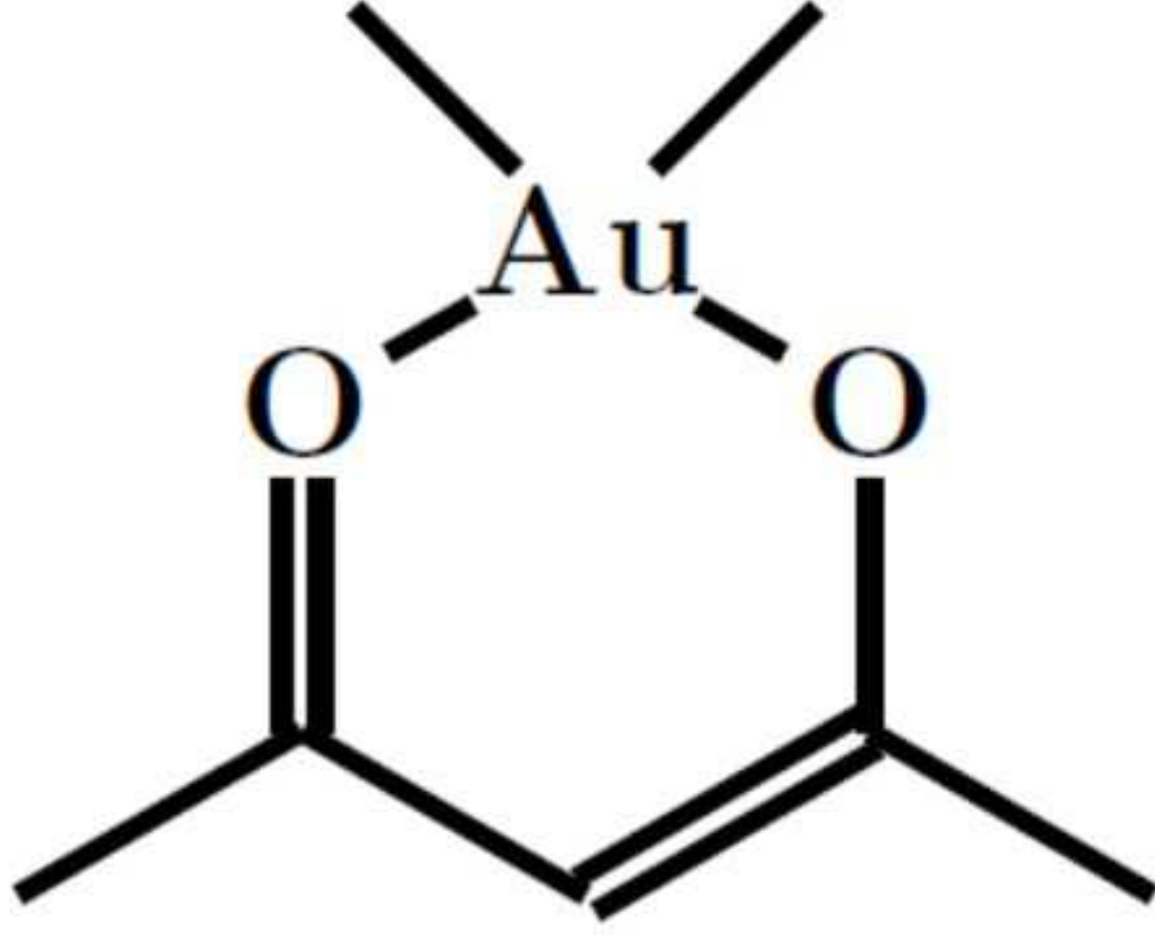
PLEASE CITE THIS ARTICLE AS DOI: 10.1063/1.5087759





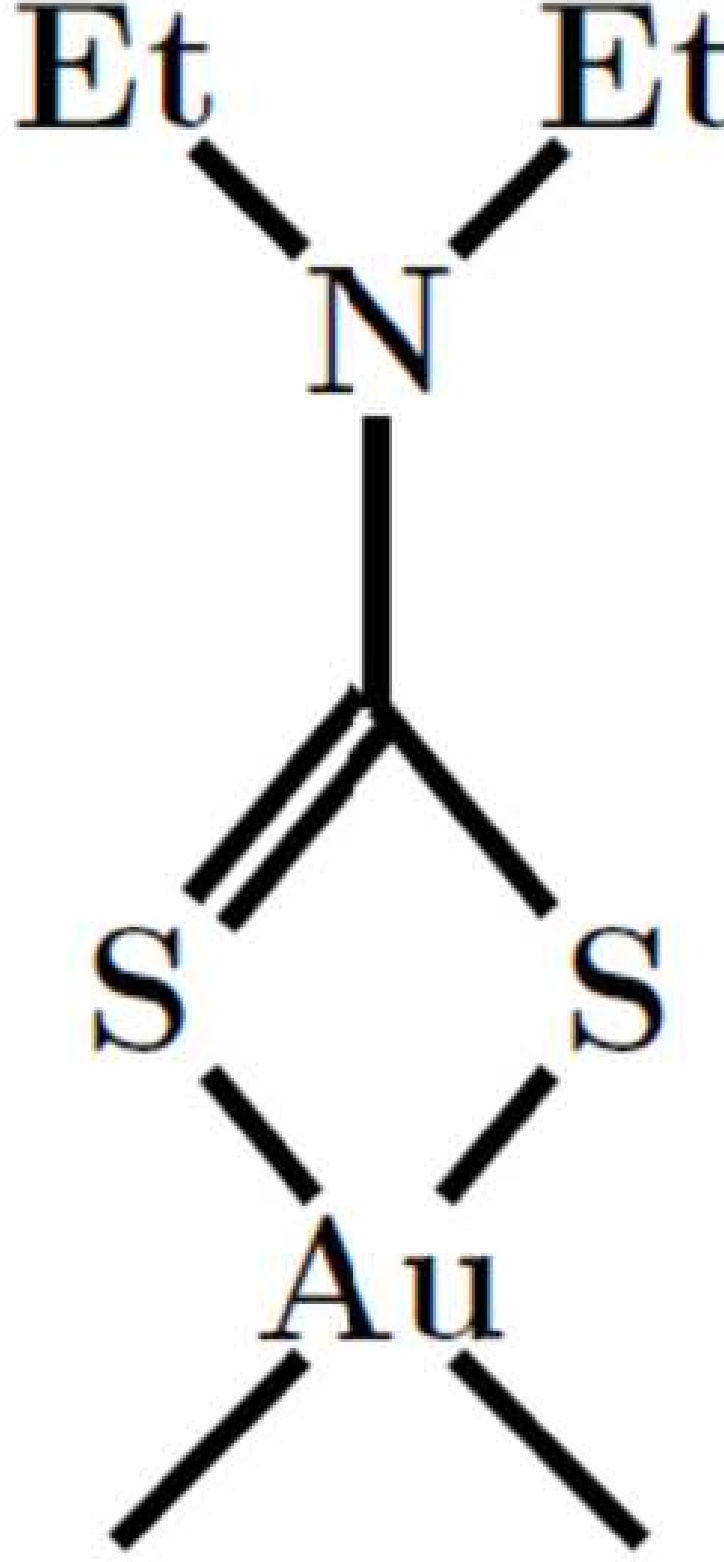
This is the author's peer reviewed, accepted manuscript. However, the online version of record will be different from this version once it has been copyedited and typeset.

PLEASE CITE THIS ARTICLE AS DOI: 10.1063/1.5087759



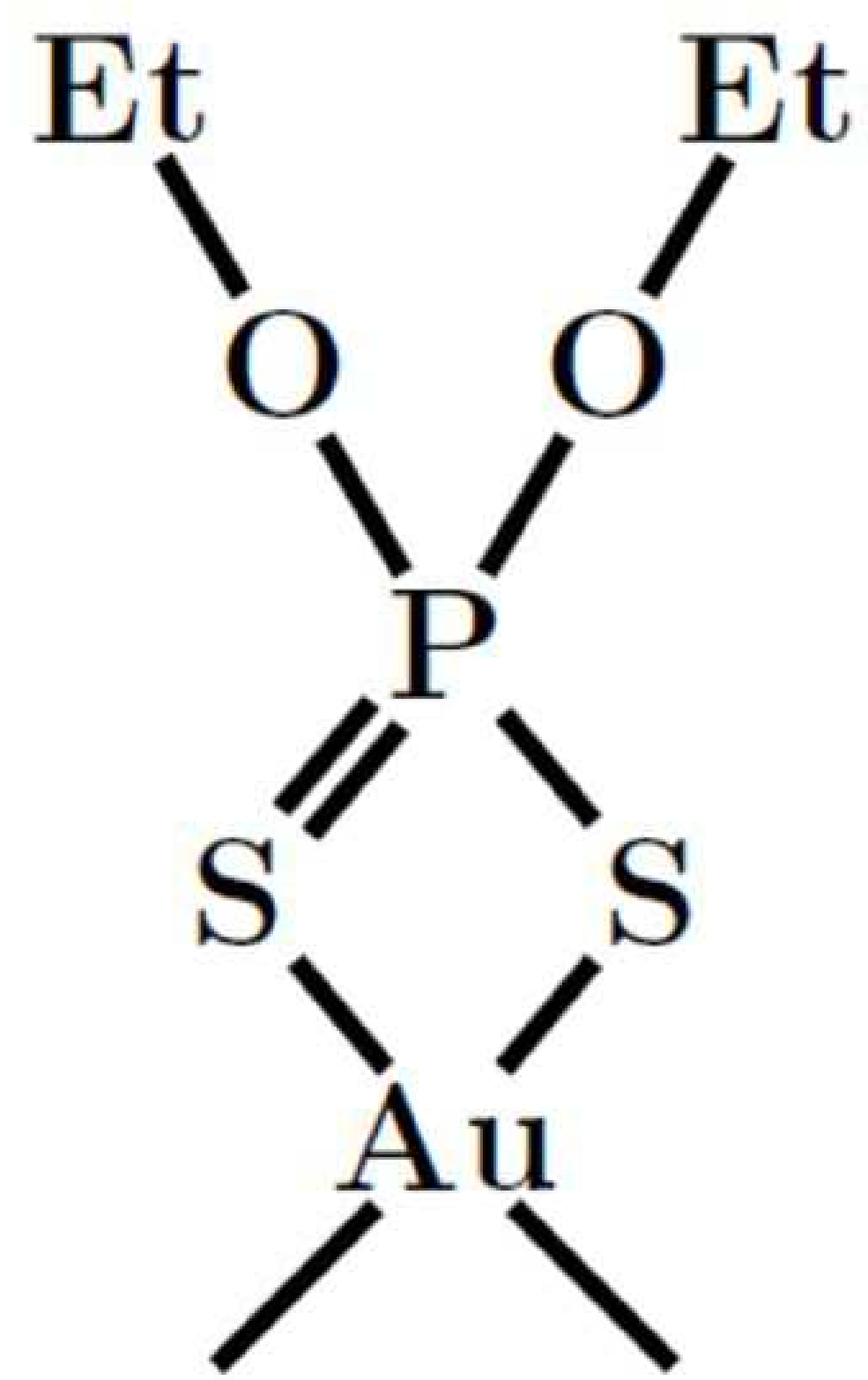
This is the author's peer reviewed, accepted manuscript. However, the online version of record will be different from this version once it has been copyedited and typeset.

PLEASE CITE THIS ARTICLE AS DOI: 10.1063/1.5087759



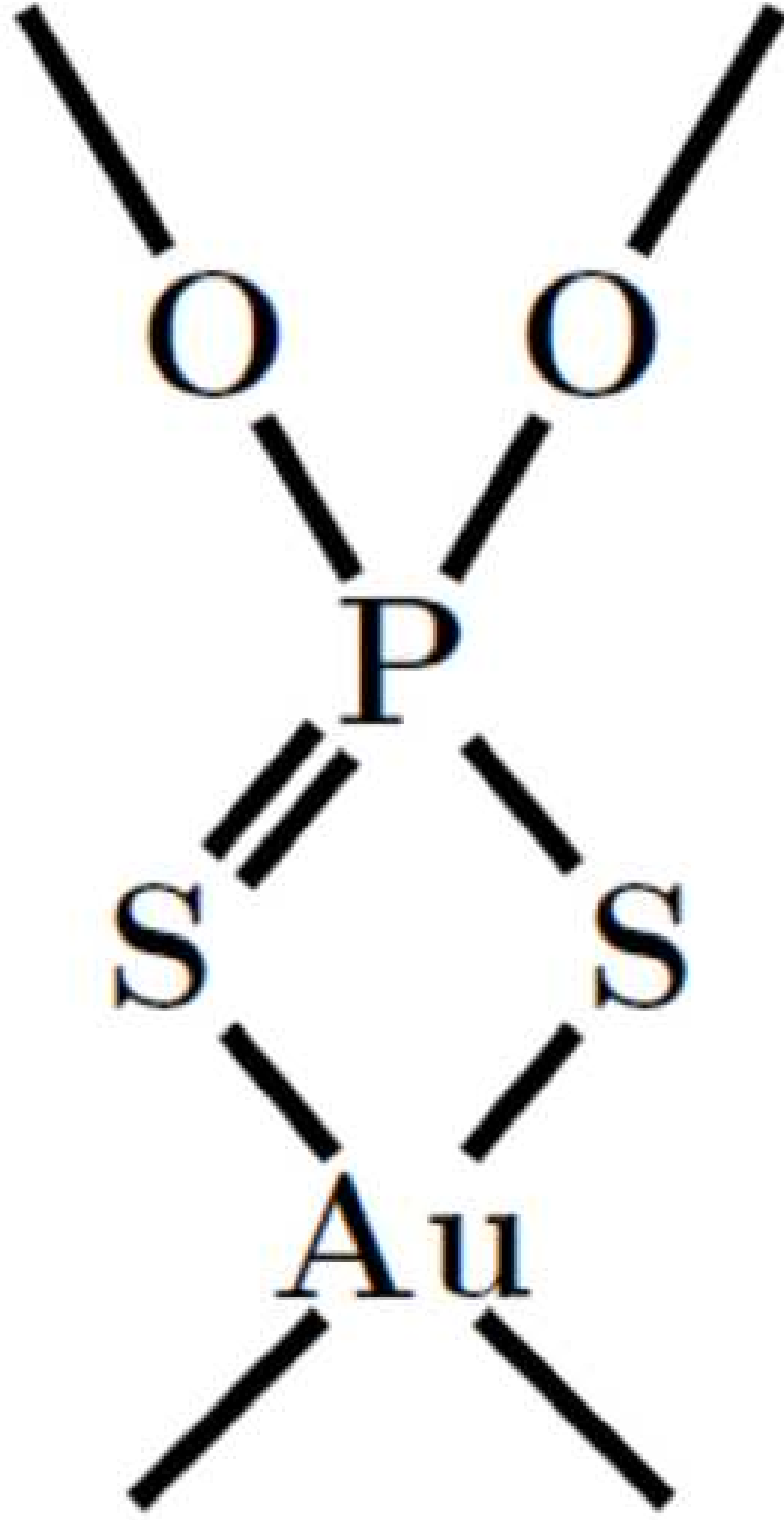
This is the author's peer reviewed, accepted manuscript. However, the online version of record will be different from this version once it has been copyedited and typeset.

PLEASE CITE THIS ARTICLE AS DOI: 10.1063/1.5087759



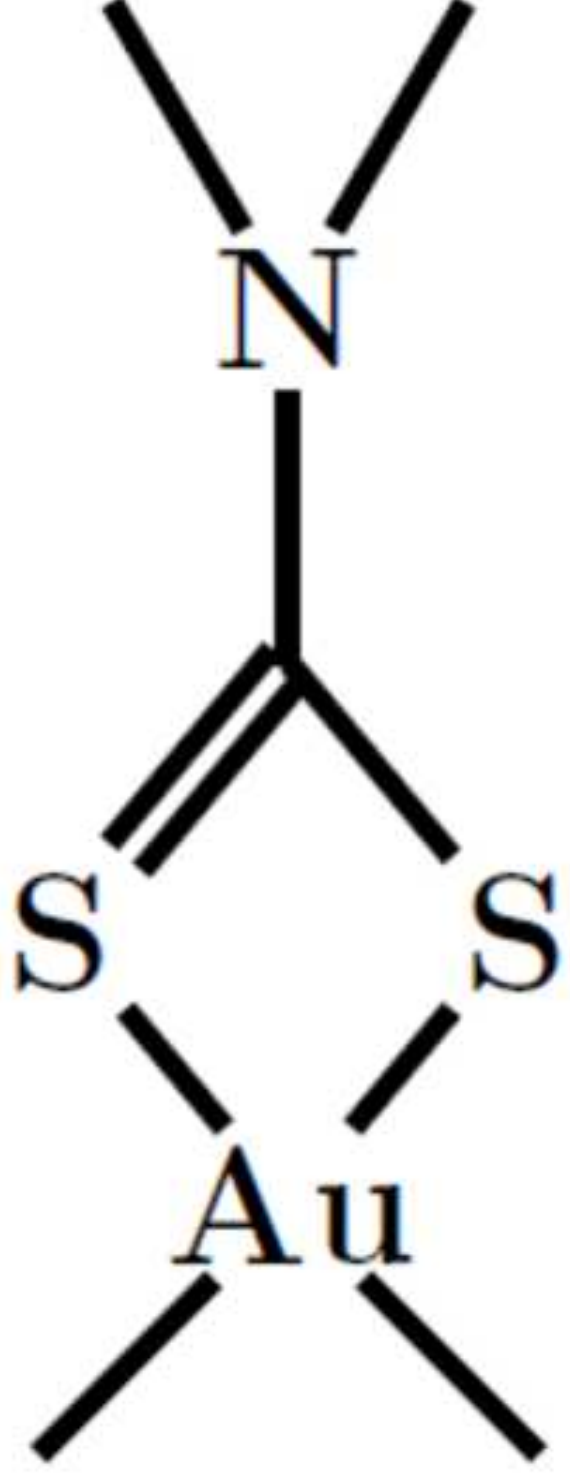
This is the author's peer reviewed, accepted manuscript. However, the online version of record will be different from this version once it has been copyedited and typeset.

PLEASE CITE THIS ARTICLE AS DOI: 10.1063/1.5087759



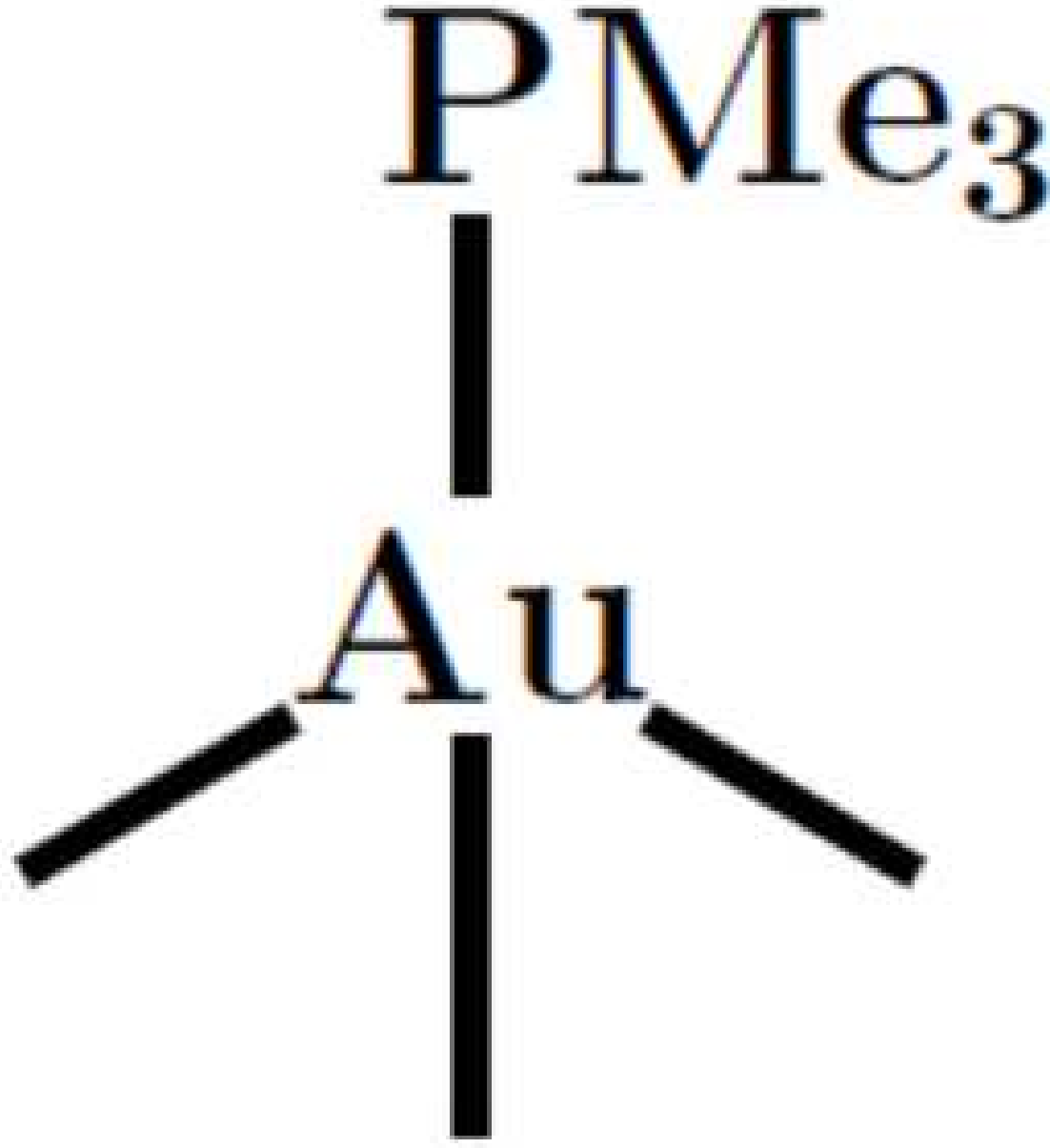
This is the author's peer reviewed, accepted manuscript. However, the online version of record will be different from this version once it has been copyedited and typeset.

PLEASE CITE THIS ARTICLE AS DOI: 10.1063/1.5087759



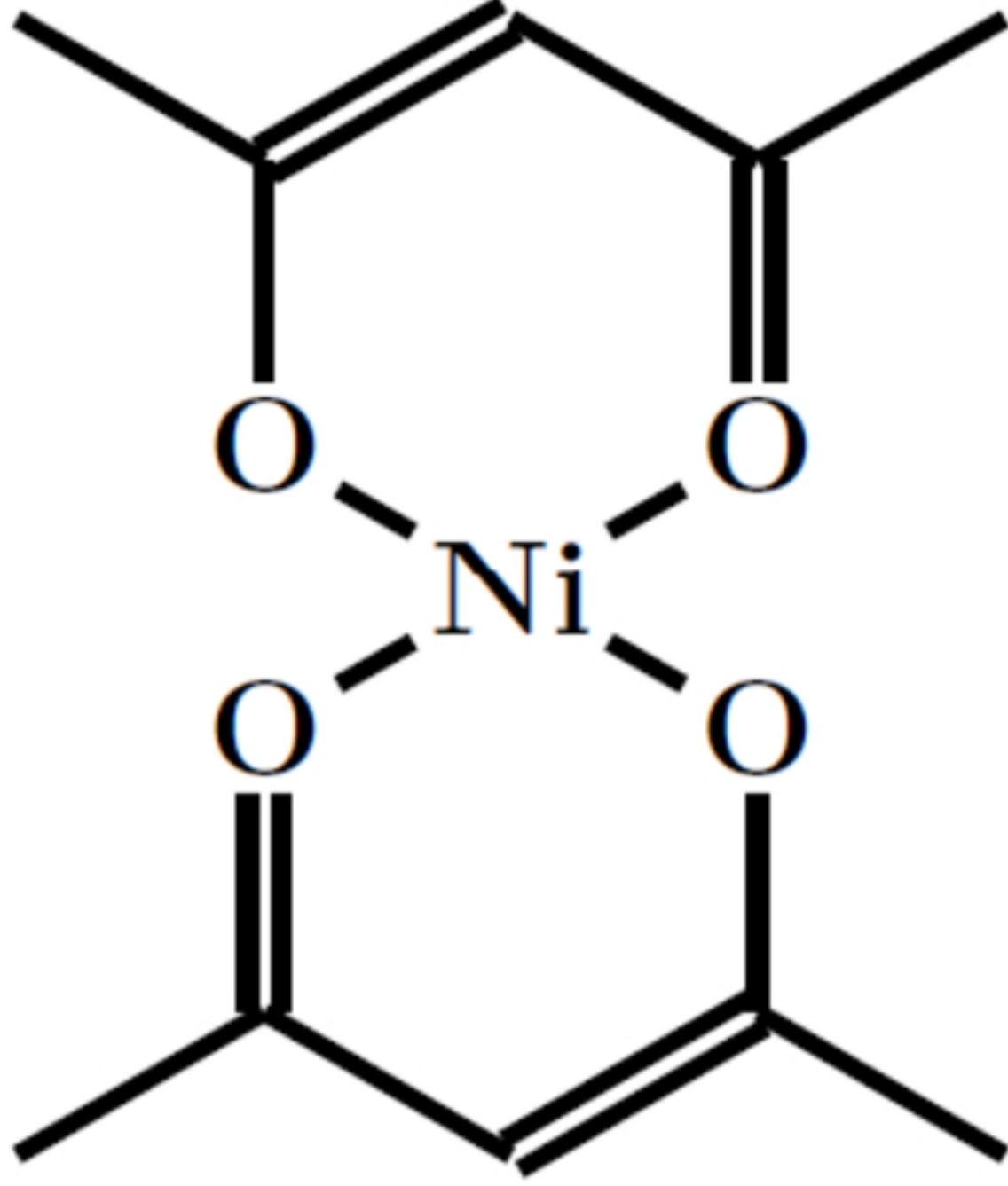
This is the author's peer reviewed, accepted manuscript. However, the online version of record will be different from this version once it has been copyedited and typeset.

PLEASE CITE THIS ARTICLE AS DOI: 10.1063/1.5087759



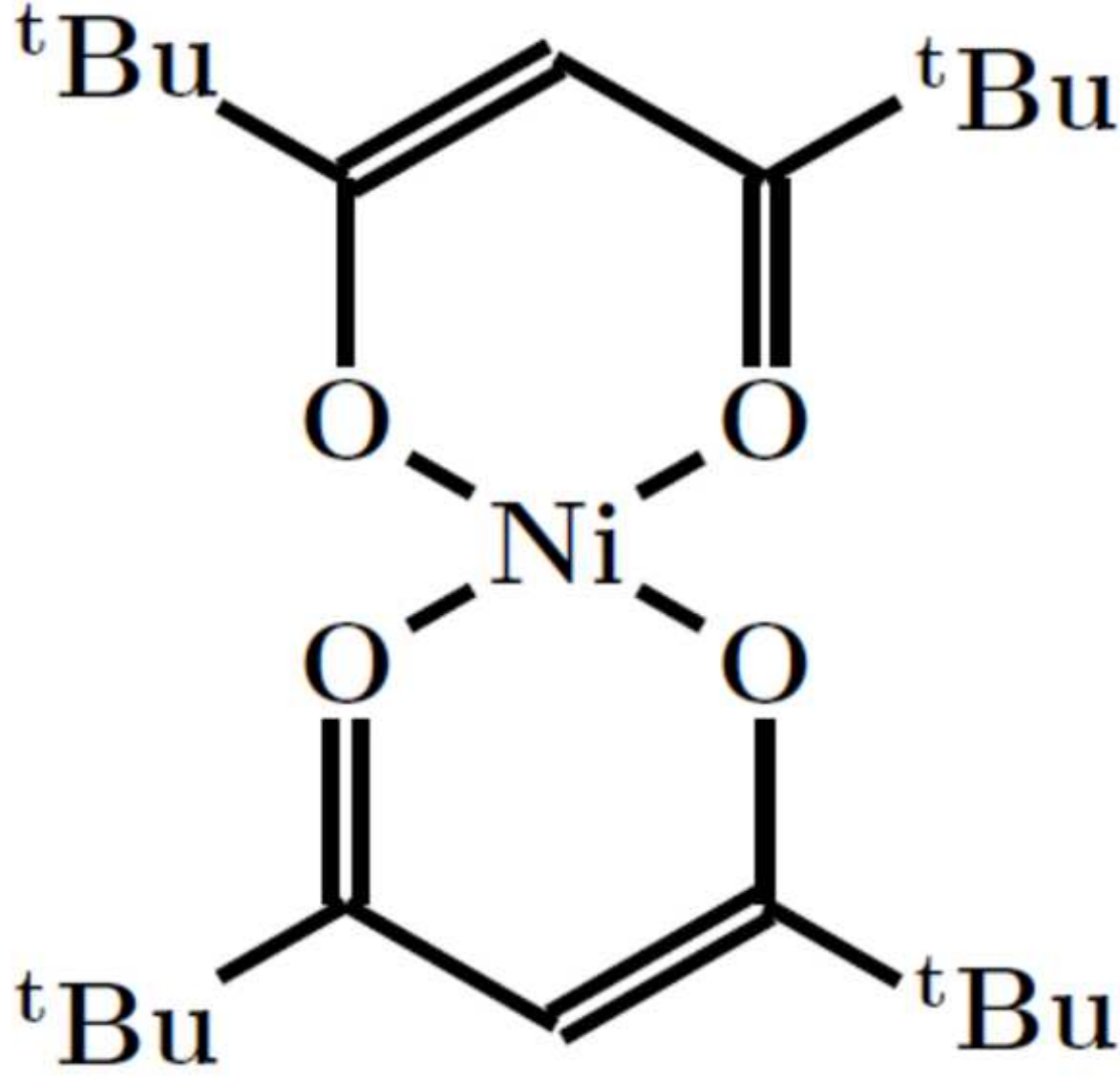
This is the author's peer reviewed, accepted manuscript. However, the online version of record will be different from this version once it has been copyedited and typeset.

PLEASE CITE THIS ARTICLE AS DOI: 10.1063/1.5087759



This is the author's peer reviewed, accepted manuscript. However, the online version of record will be different from this version once it has been copyedited and typeset.

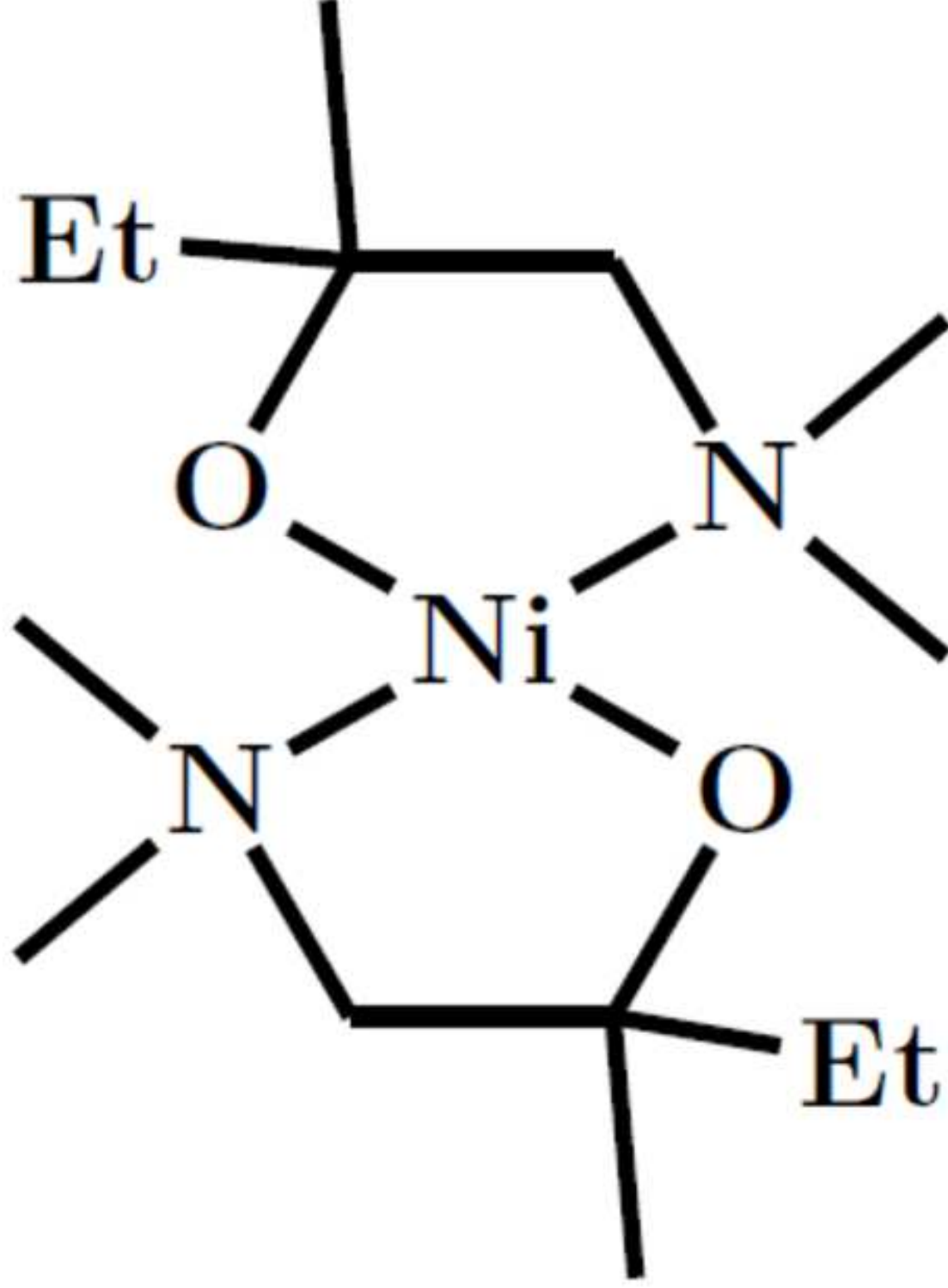
PLEASE CITE THIS ARTICLE AS DOI: 10.1063/1.5087759





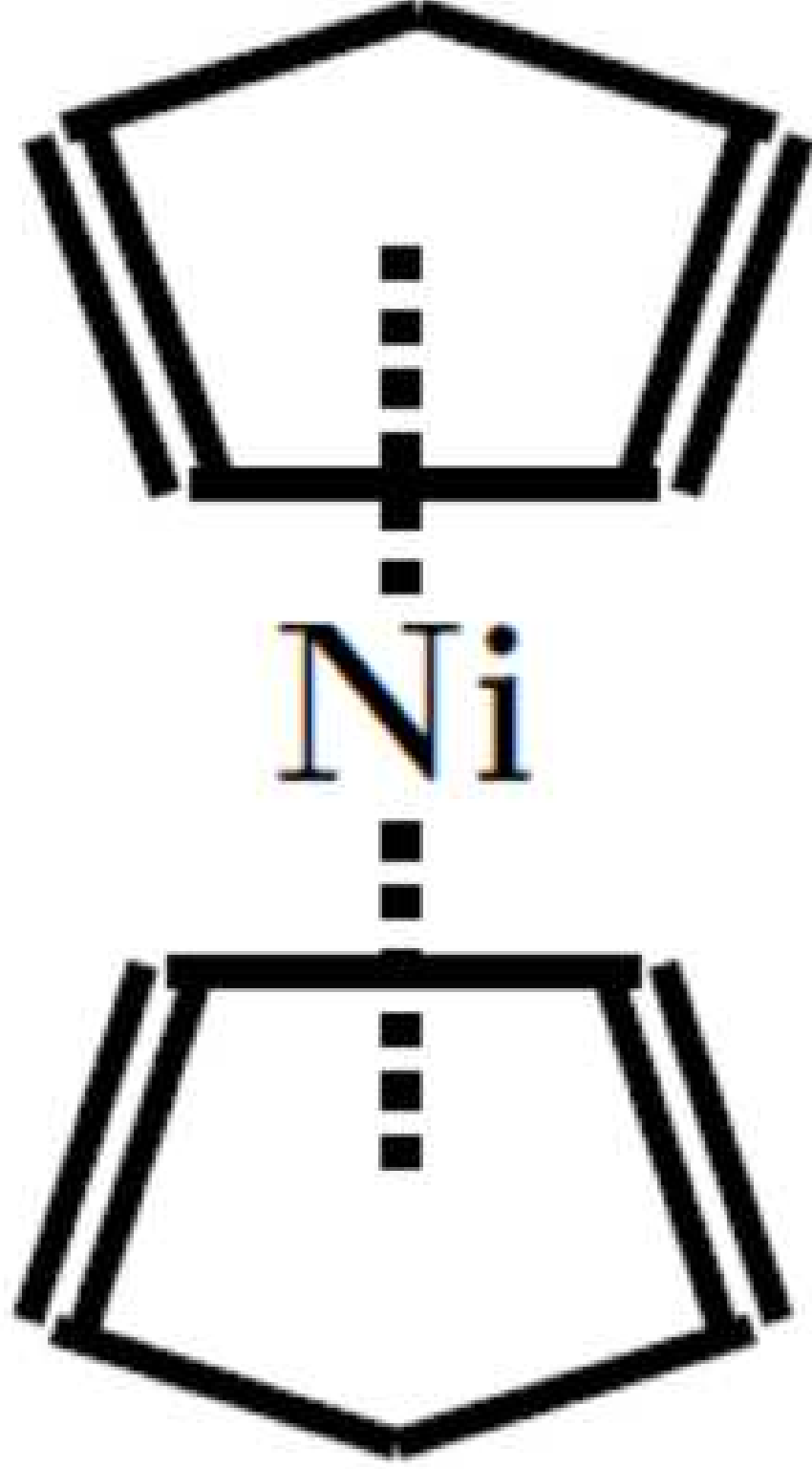
This is the author's peer reviewed, accepted manuscript. However, the online version of record will be different from this version once it has been copyedited and typeset.

PLEASE CITE THIS ARTICLE AS DOI: 10.1063/1.5087759



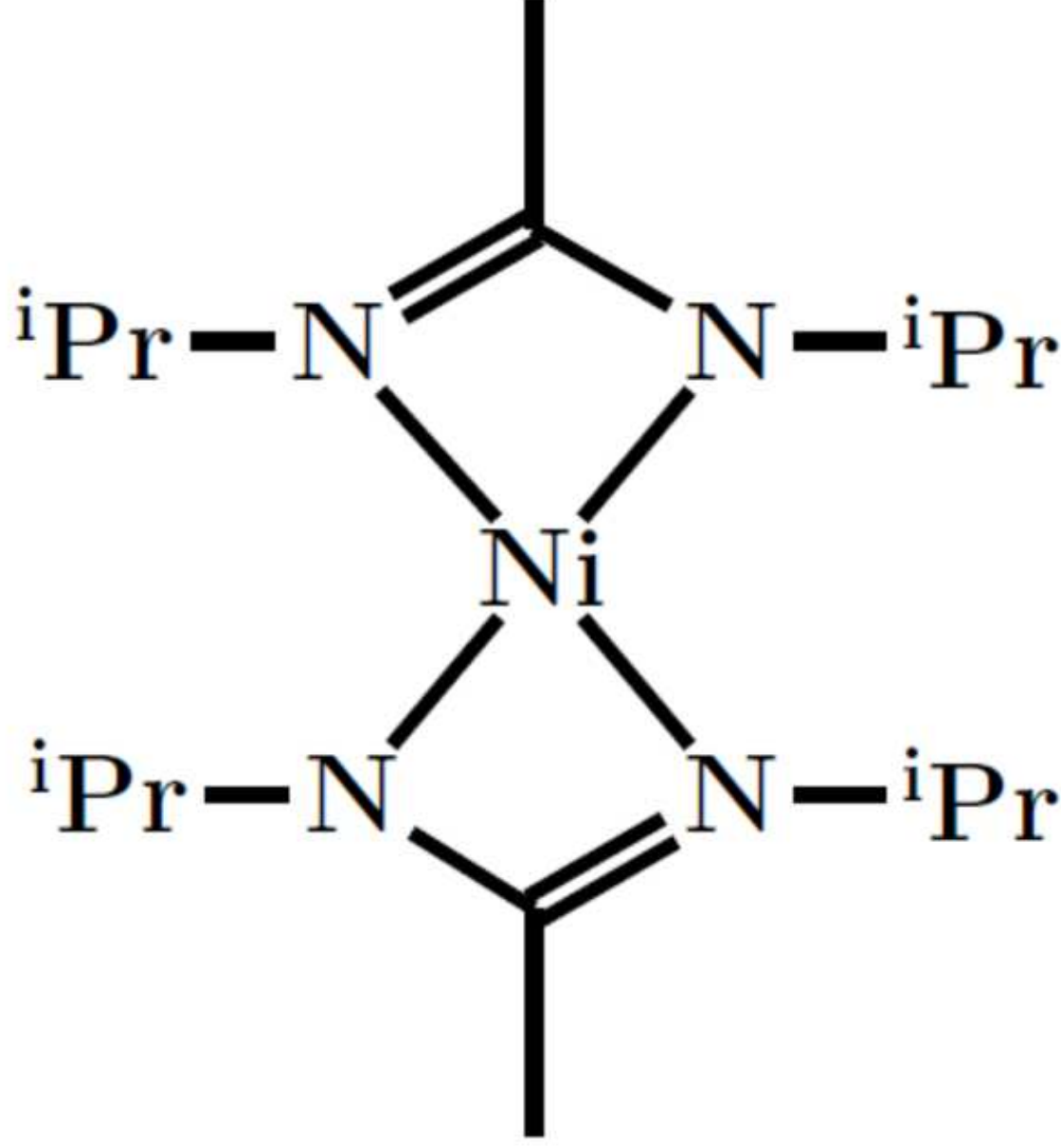
This is the author's peer reviewed, accepted manuscript. However, the online version of record will be different from this version once it has been copyedited and typeset.

PLEASE CITE THIS ARTICLE AS DOI: 10.1063/1.5087759



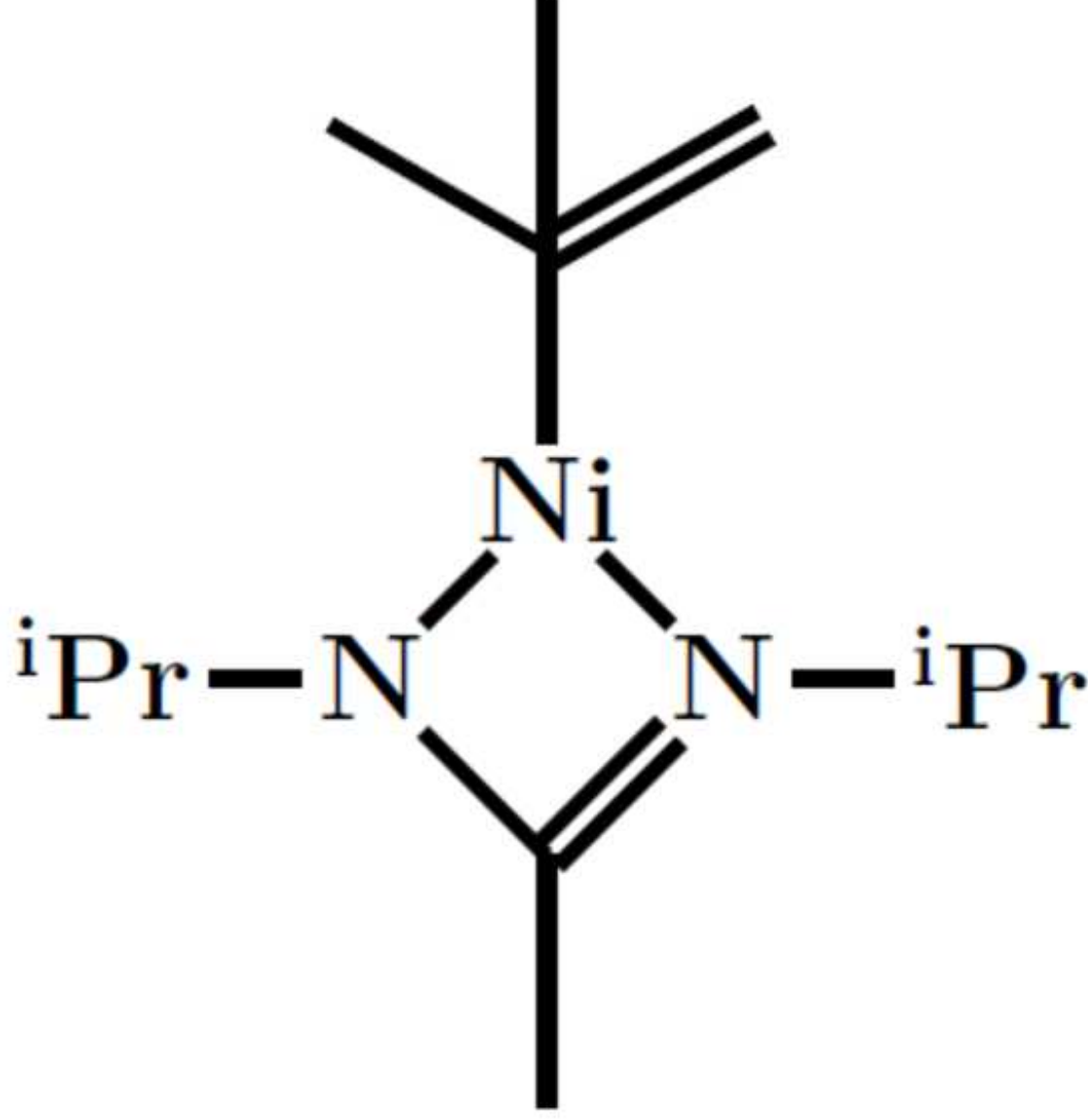
This is the author's peer reviewed, accepted manuscript. However, the online version of record will be different from this version once it has been copyedited and typeset.

PLEASE CITE THIS ARTICLE AS DOI: 10.1063/1.5087759



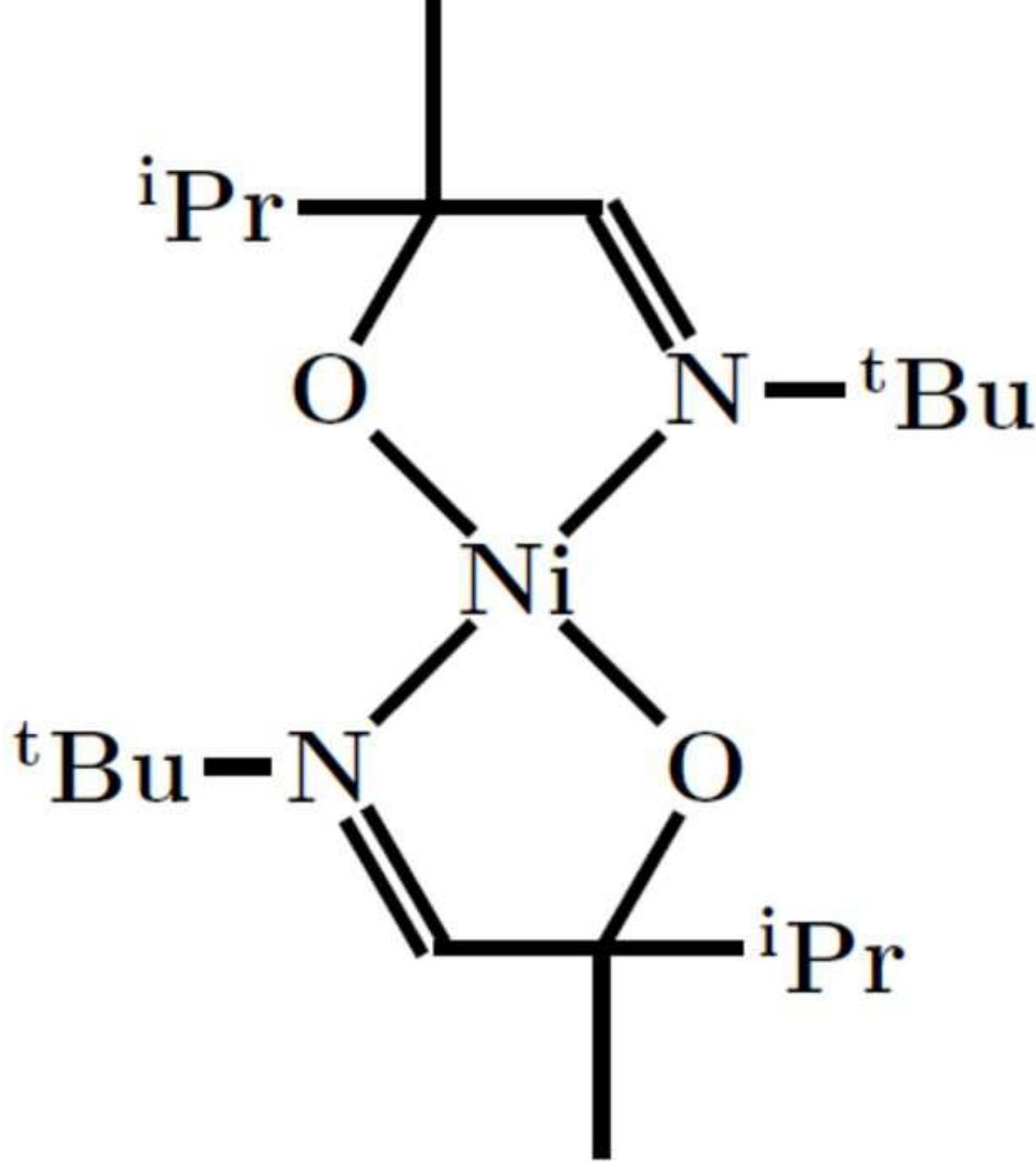
This is the author's peer reviewed, accepted manuscript. However, the online version of record will be different from this version once it has been copyedited and typeset.

PLEASE CITE THIS ARTICLE AS DOI: 10.1063/1.5087759



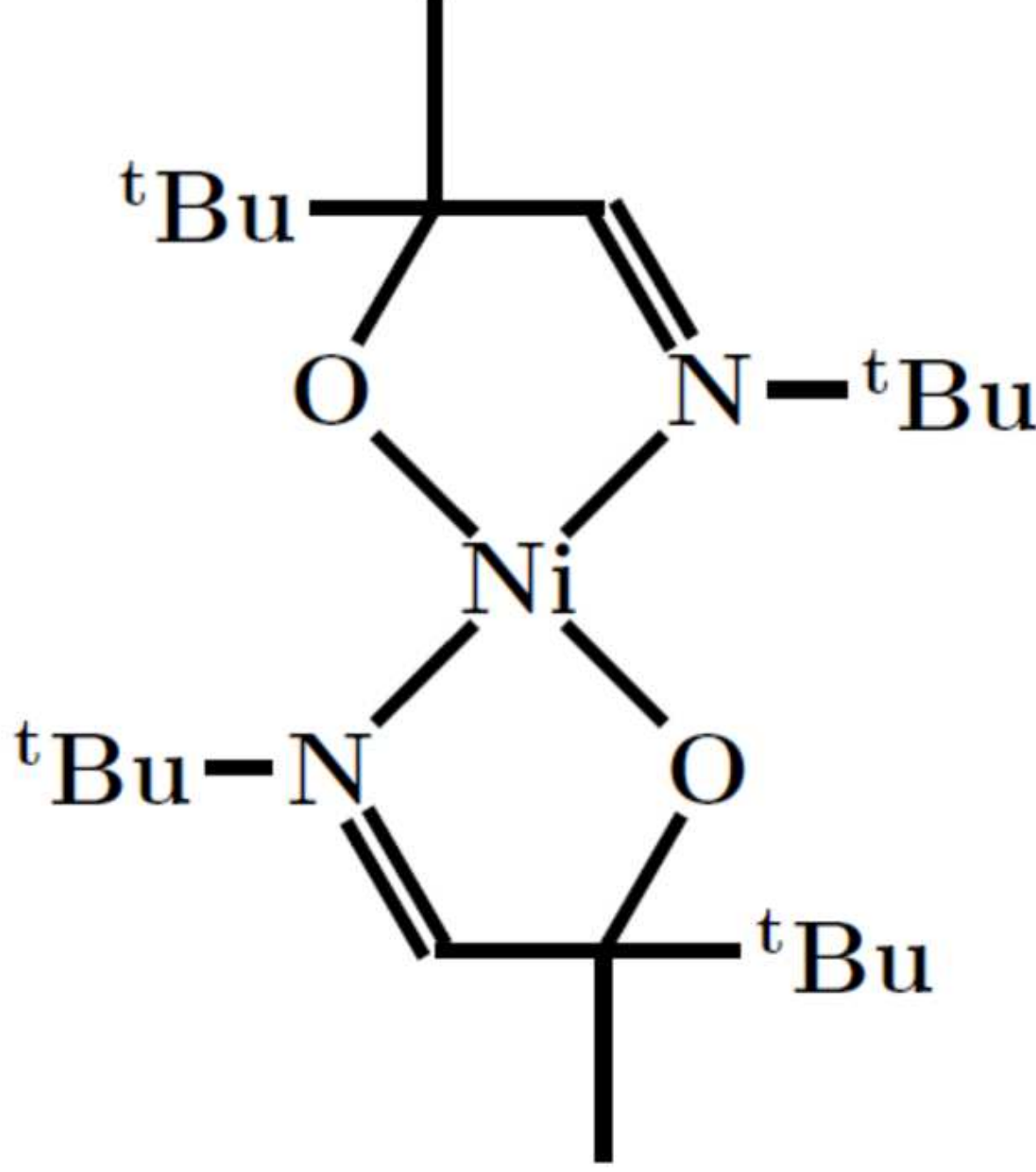
This is the author's peer reviewed, accepted manuscript. However, the online version of record will be different from this version once it has been copyedited and typeset.

PLEASE CITE THIS ARTICLE AS DOI: 10.1063/1.5087759



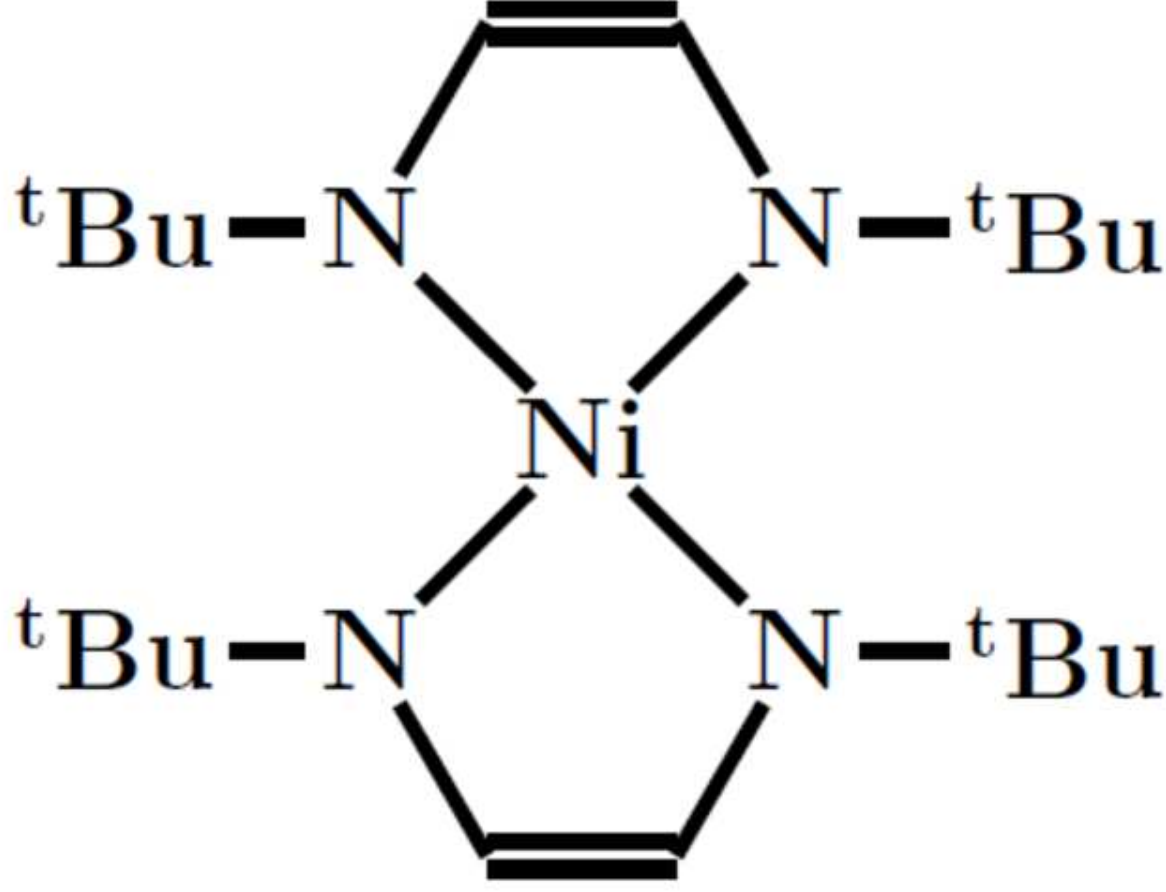
This is the author's peer reviewed, accepted manuscript. However, the online version of record will be different from this version once it has been copyedited and typeset.

PLEASE CITE THIS ARTICLE AS DOI: 10.1063/1.5087759



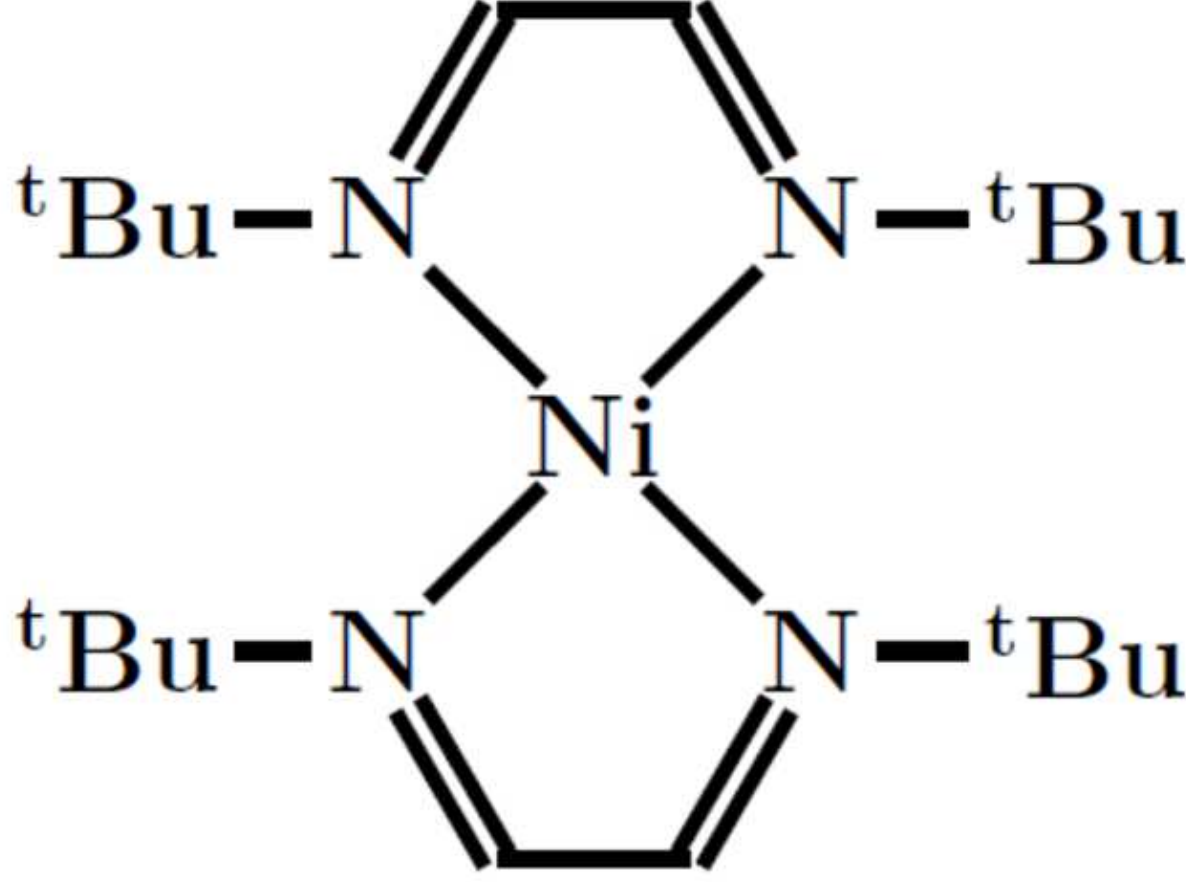
This is the author's peer reviewed, accepted manuscript. However, the online version of record will be different from this version once it has been copyedited and typeset.

PLEASE CITE THIS ARTICLE AS DOI: 10.1063/1.5087759



This is the author's peer reviewed, accepted manuscript. However, the online version of record will be different from this version once it has been copyedited and typeset.

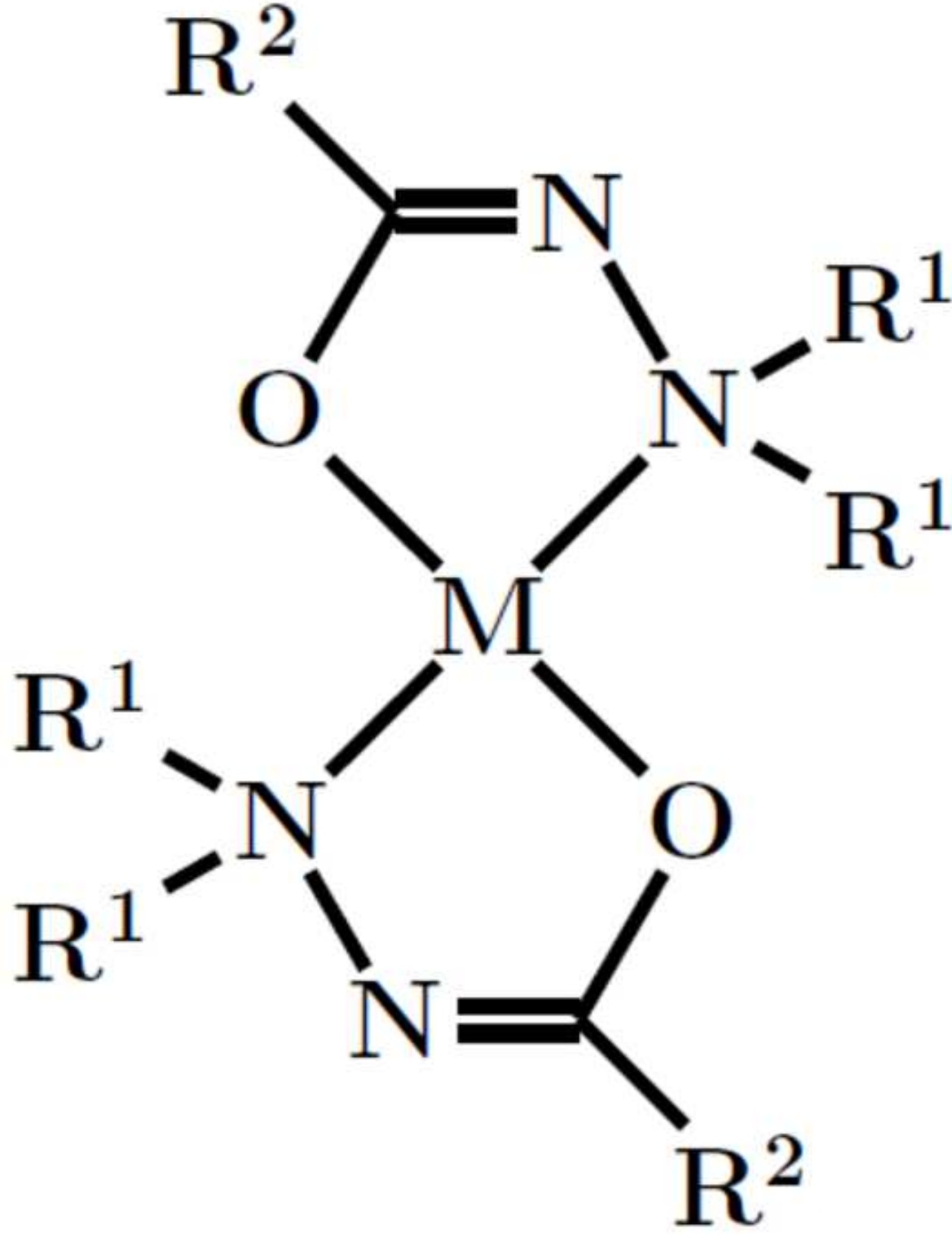
PLEASE CITE THIS ARTICLE AS DOI: 10.1063/1.5087759





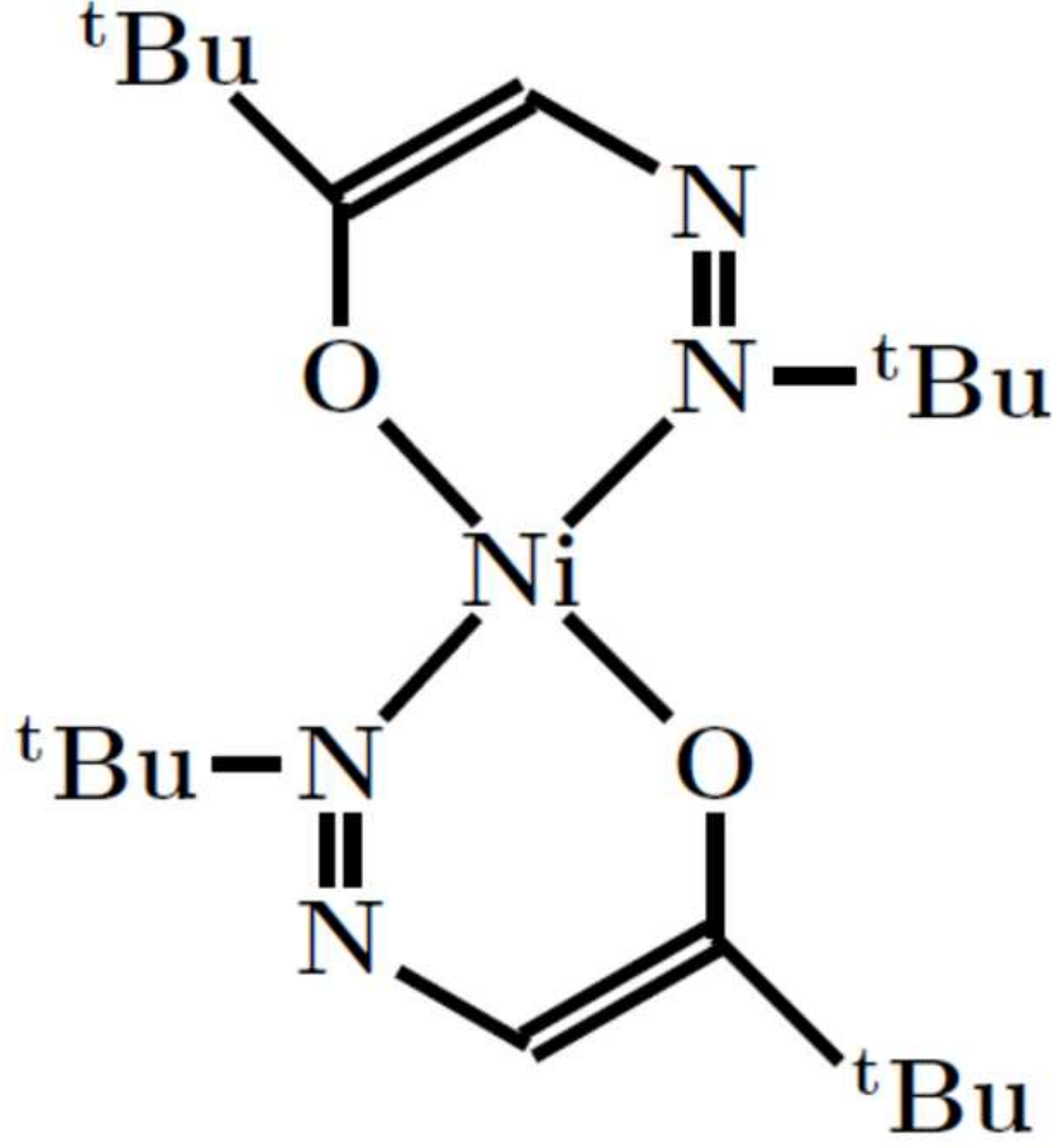
This is the author's peer reviewed, accepted manuscript. However, the online version of record will be different from this version once it has been copyedited and typeset.

PLEASE CITE THIS ARTICLE AS DOI: 10.1063/1.5087759



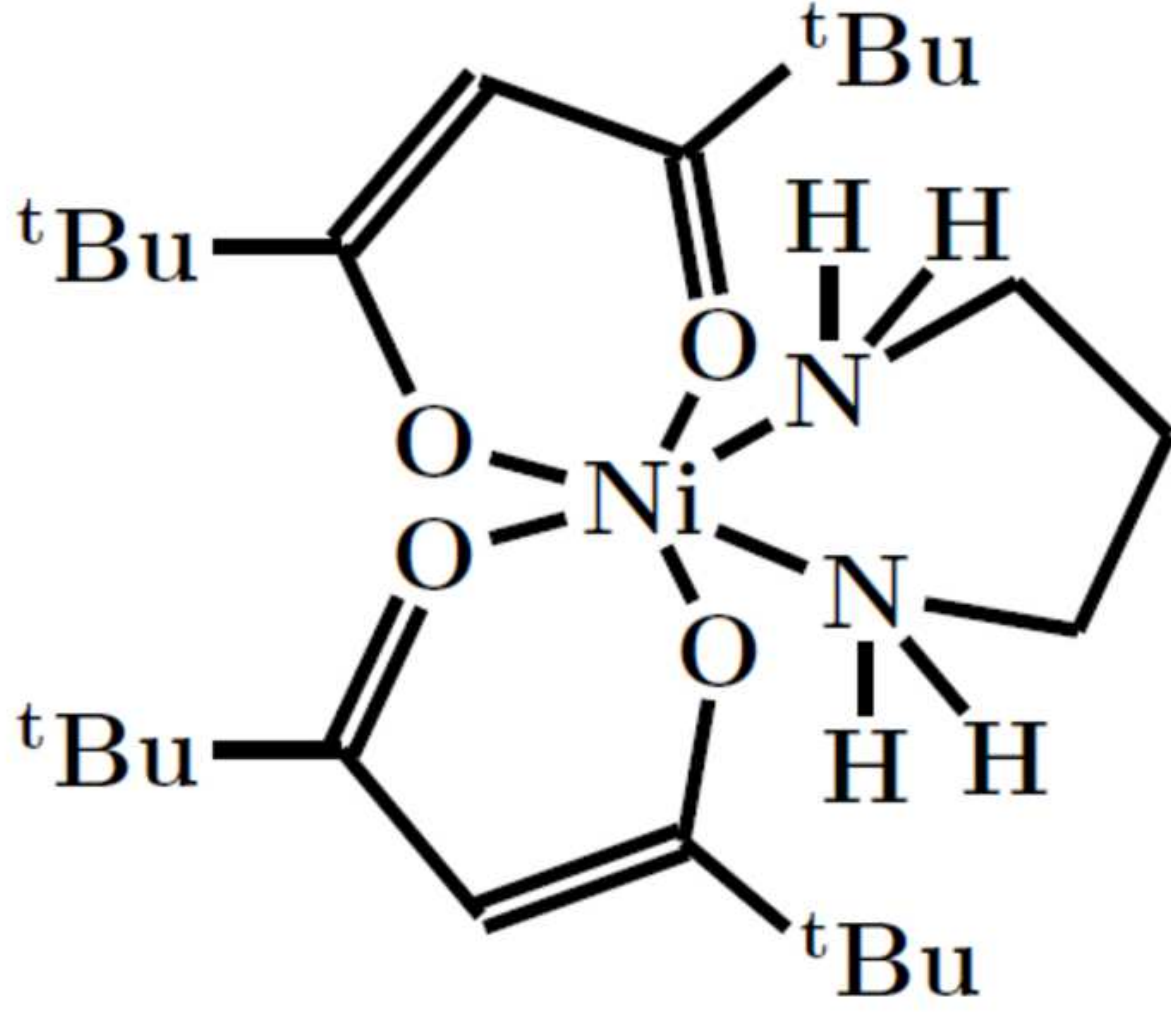
This is the author's peer reviewed, accepted manuscript. However, the online version of record will be different from this version once it has been copyedited and typeset.

PLEASE CITE THIS ARTICLE AS DOI: 10.1063/1.5087759



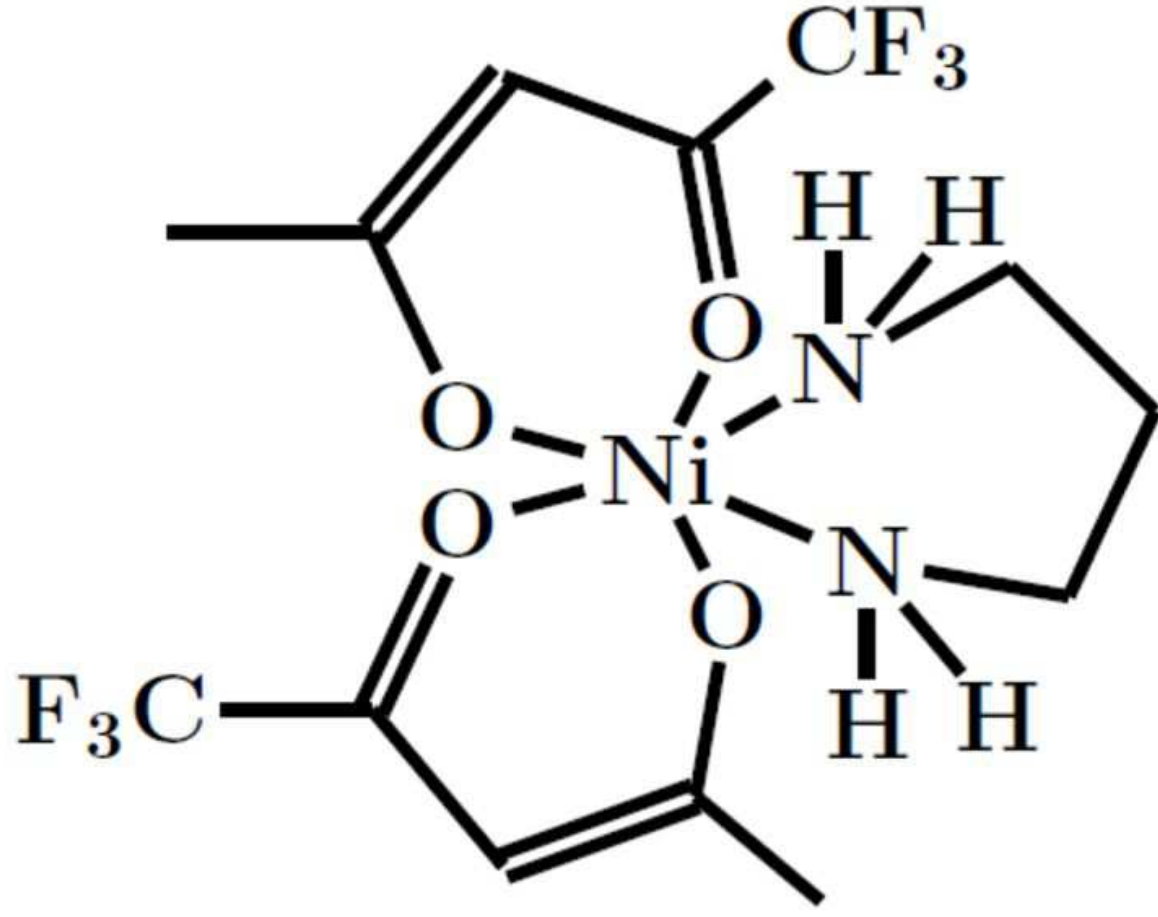
This is the author's peer reviewed, accepted manuscript. However, the online version of record will be different from this version once it has been copyedited and typeset.

PLEASE CITE THIS ARTICLE AS DOI: 10.1063/1.5087759



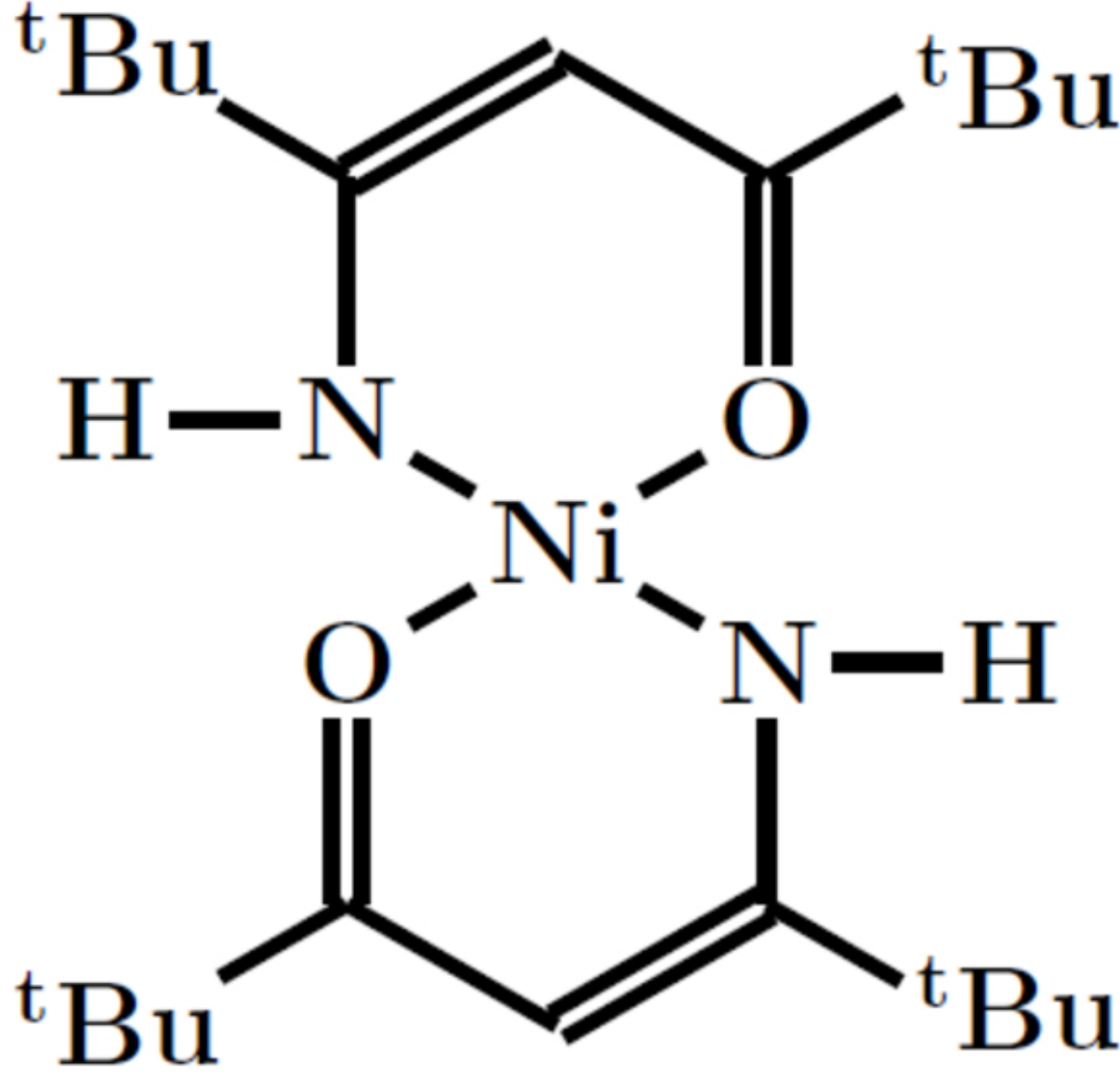
This is the author's peer reviewed, accepted manuscript. However, the online version of record will be different from this version once it has been copyedited and typeset.

PLEASE CITE THIS ARTICLE AS DOI: 10.1063/1.5087759



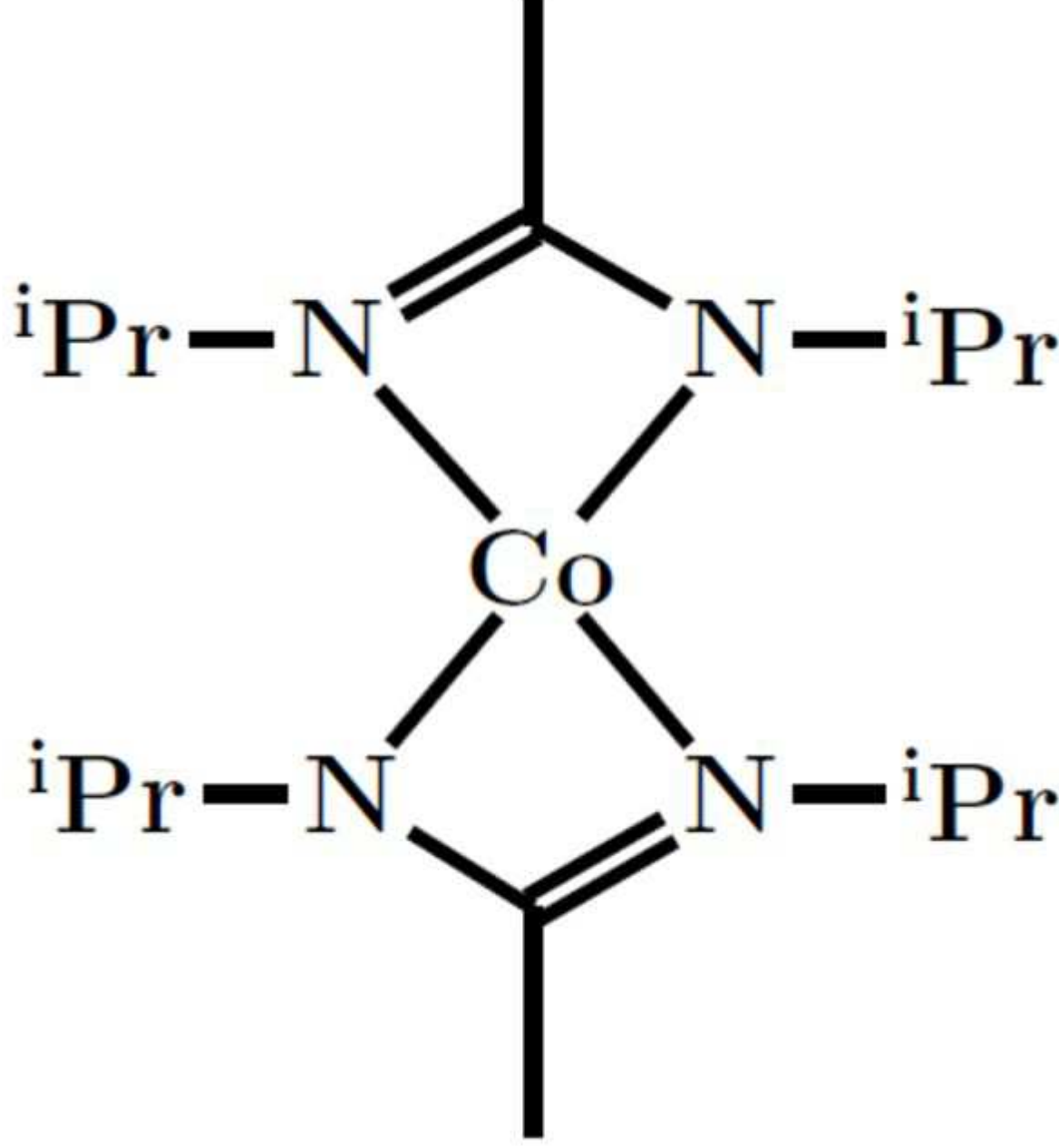
This is the author's peer reviewed, accepted manuscript. However, the online version of record will be different from this version once it has been copyedited and typeset.

PLEASE CITE THIS ARTICLE AS DOI: 10.1063/1.5087759



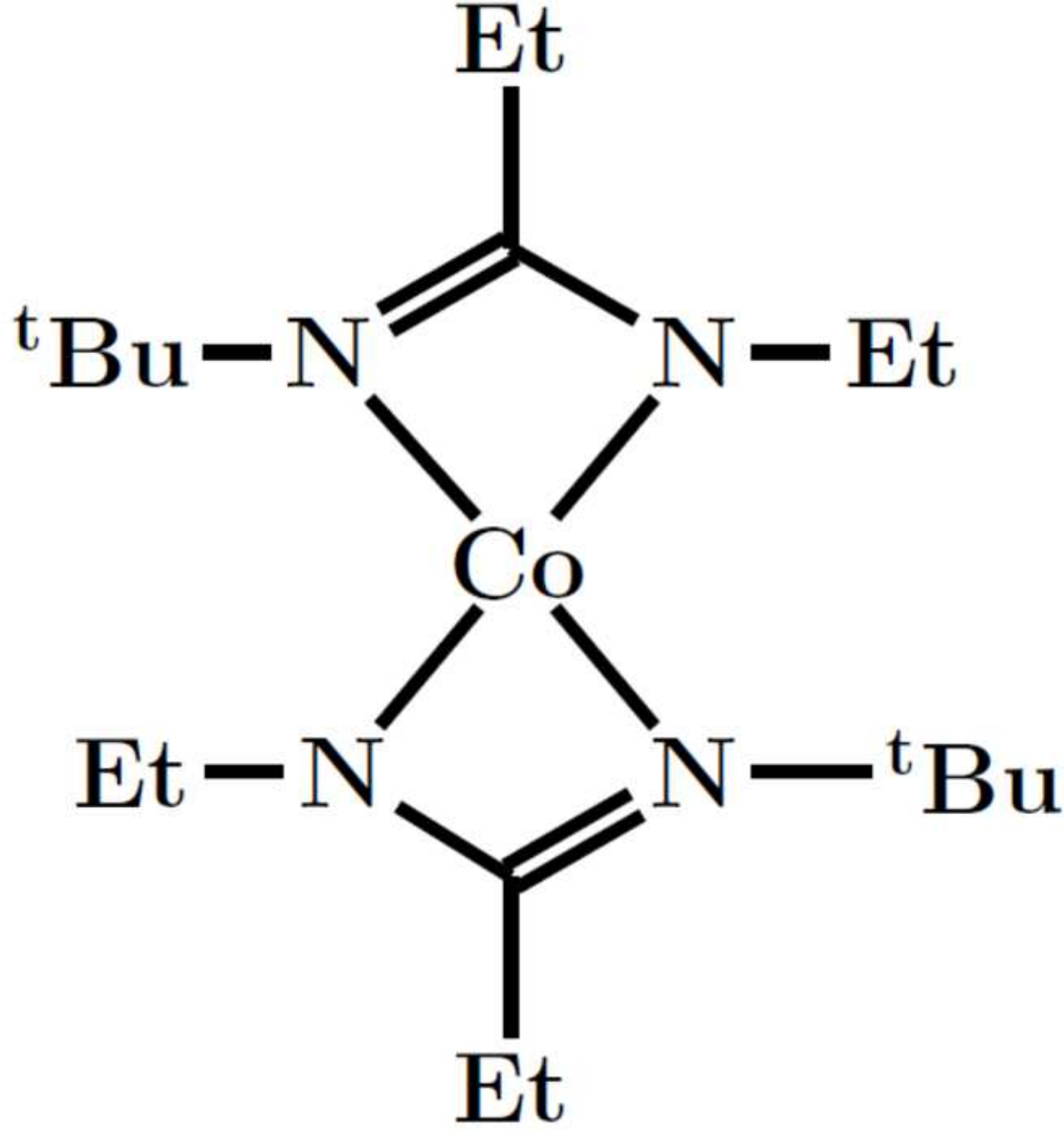
This is the author's peer reviewed, accepted manuscript. However, the online version of record will be different from this version once it has been copyedited and typeset.

PLEASE CITE THIS ARTICLE AS DOI: 10.1063/1.5087759



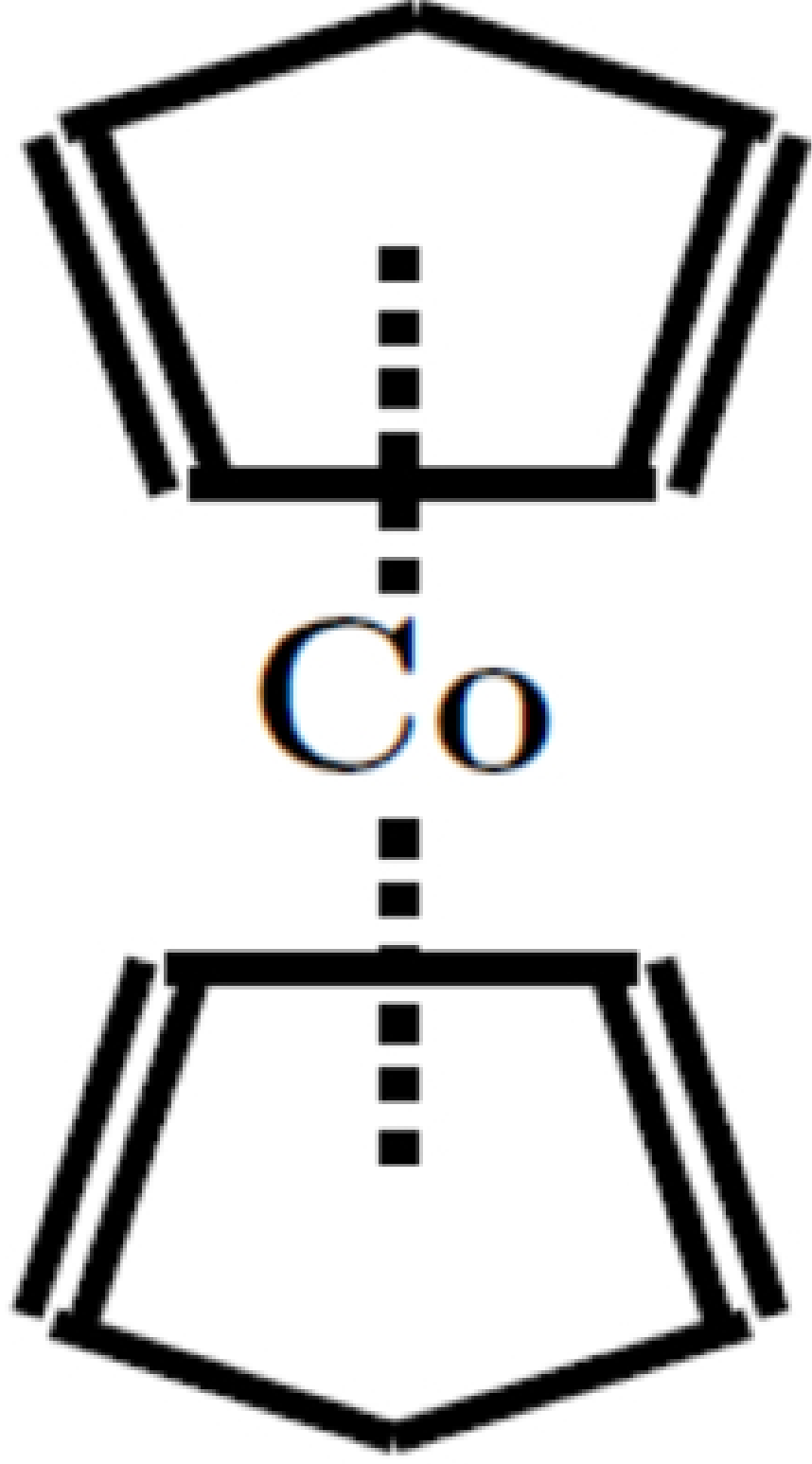
This is the author's peer reviewed, accepted manuscript. However, the online version of record will be different from this version once it has been copyedited and typeset.

PLEASE CITE THIS ARTICLE AS DOI: 10.1063/1.5087759



This is the author's peer reviewed, accepted manuscript. However, the online version of record will be different from this version once it has been copyedited and typeset.

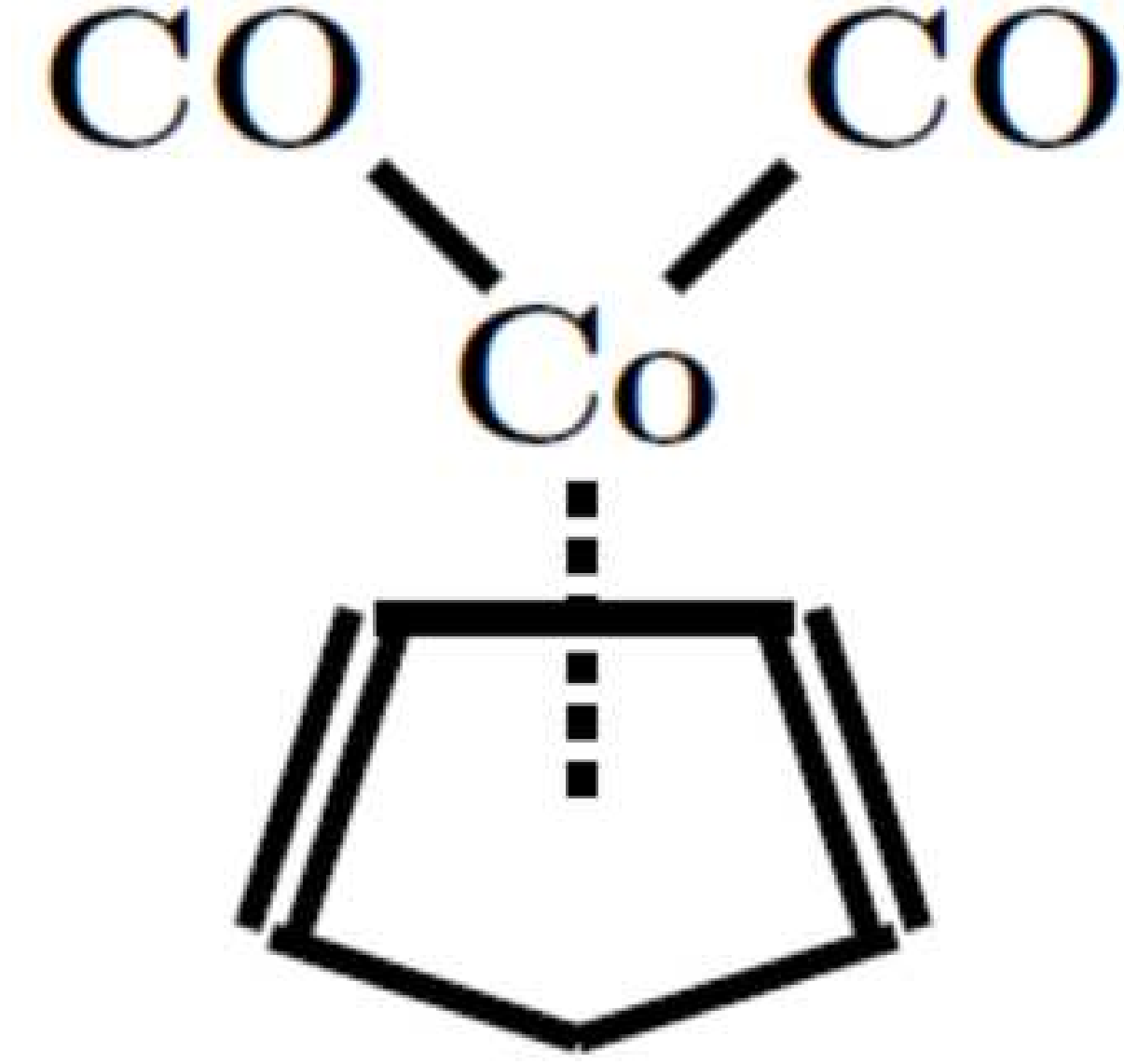
PLEASE CITE THIS ARTICLE AS DOI: 10.1063/1.5087759





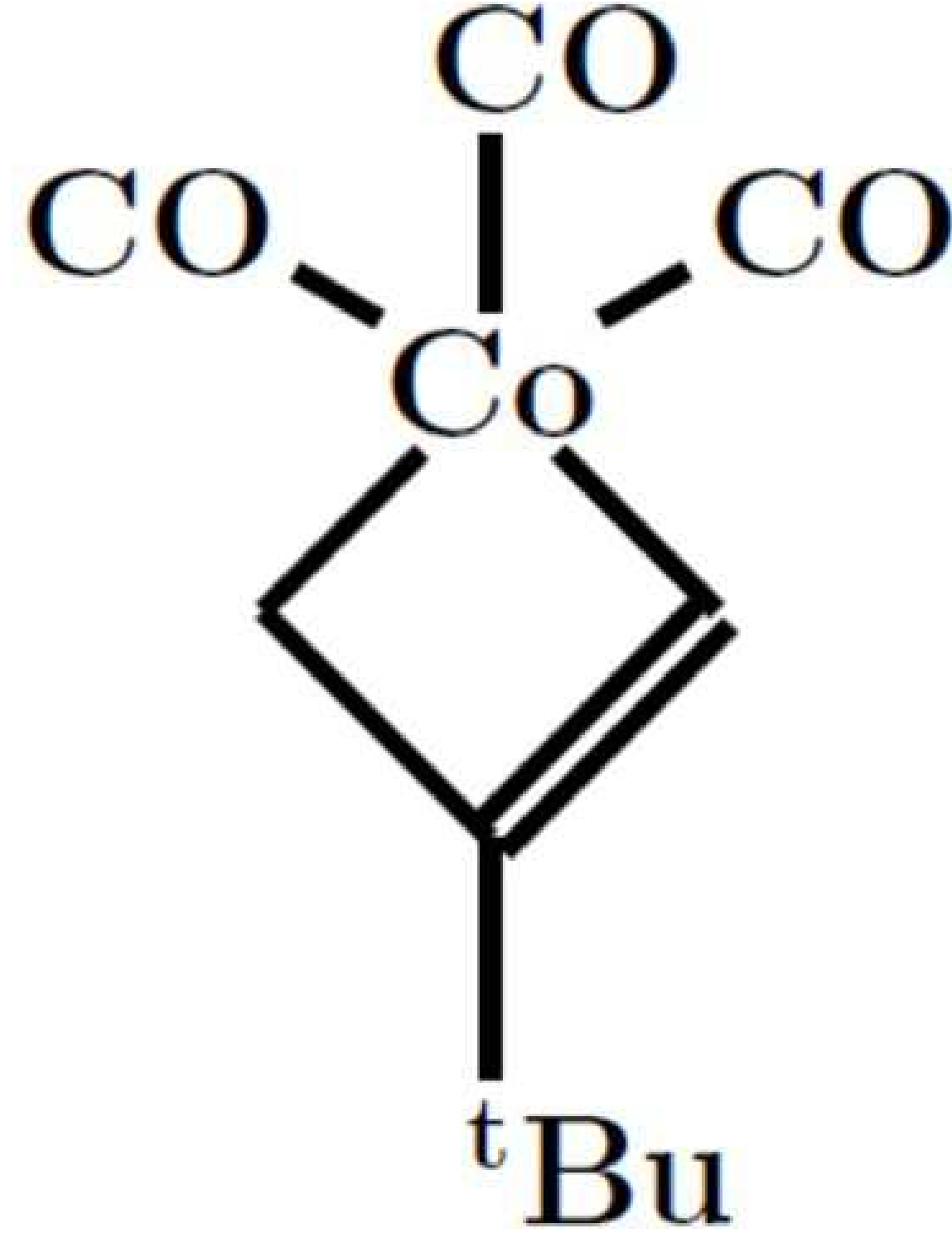
This is the author's peer reviewed, accepted manuscript. However, the online version of record will be different from this version once it has been copyedited and typeset.

PLEASE CITE THIS ARTICLE AS DOI: 10.1063/1.5087759



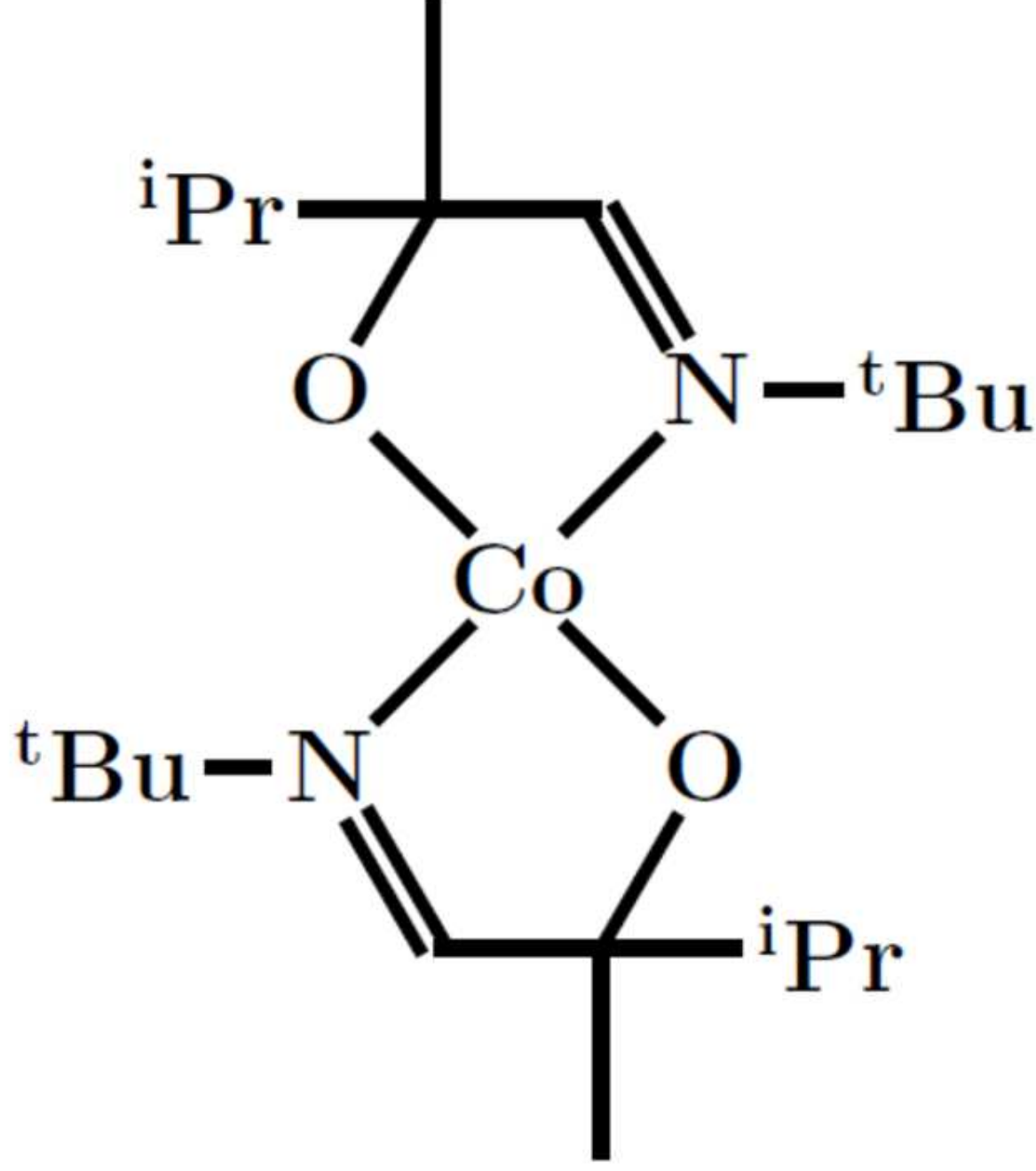
This is the author's peer reviewed, accepted manuscript. However, the online version of record will be different from this version once it has been copyedited and typeset.

PLEASE CITE THIS ARTICLE AS DOI: 10.1063/1.5087759



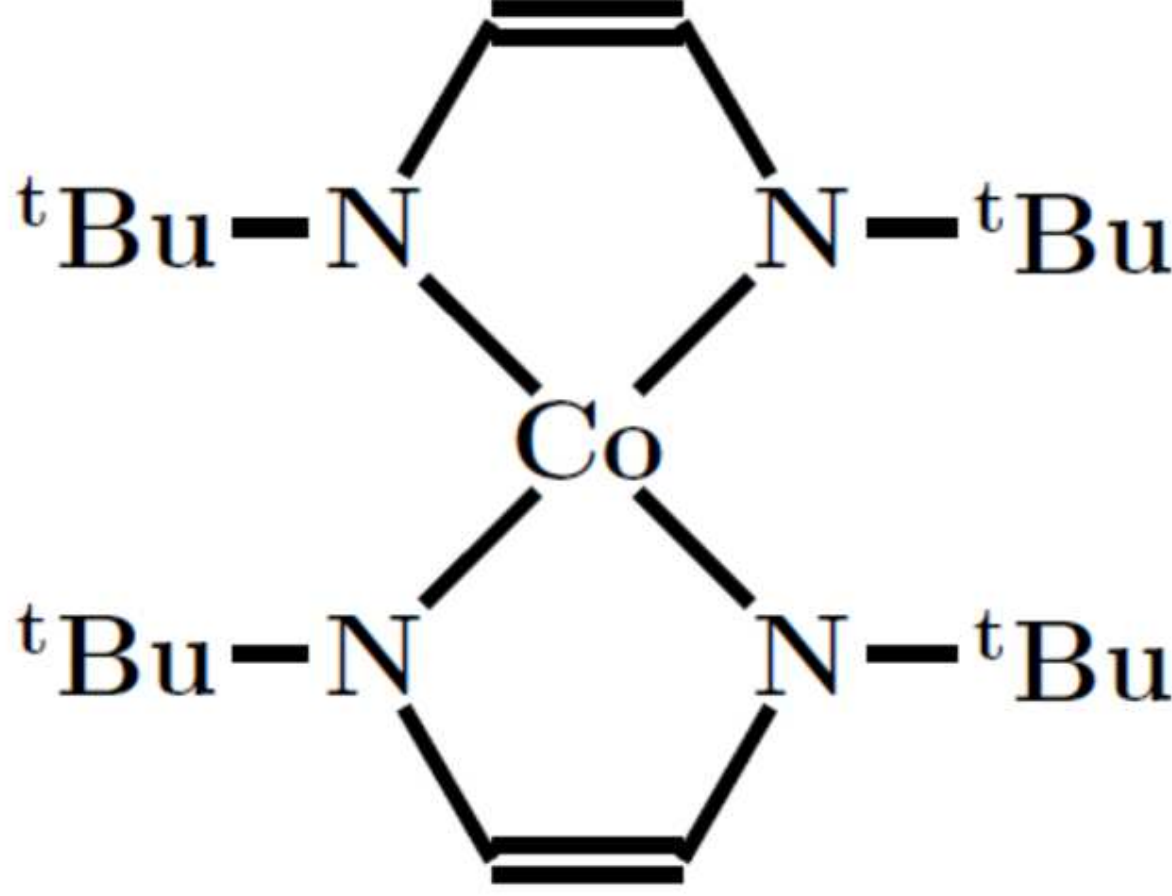
This is the author's peer reviewed, accepted manuscript. However, the online version of record will be different from this version once it has been copyedited and typeset.

PLEASE CITE THIS ARTICLE AS DOI: 10.1063/1.5087759



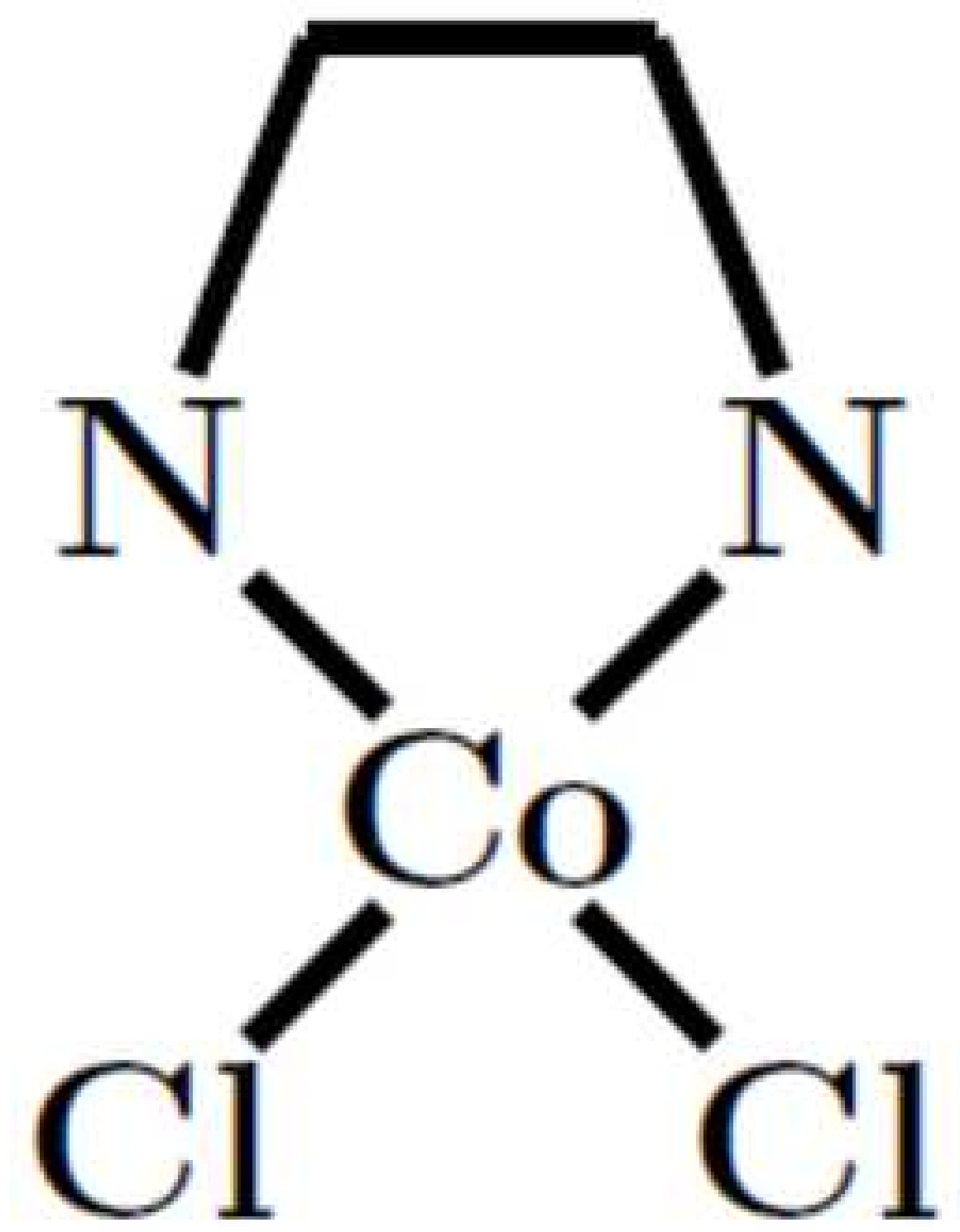
This is the author's peer reviewed, accepted manuscript. However, the online version of record will be different from this version once it has been copyedited and typeset.

PLEASE CITE THIS ARTICLE AS DOI: 10.1063/1.5087759



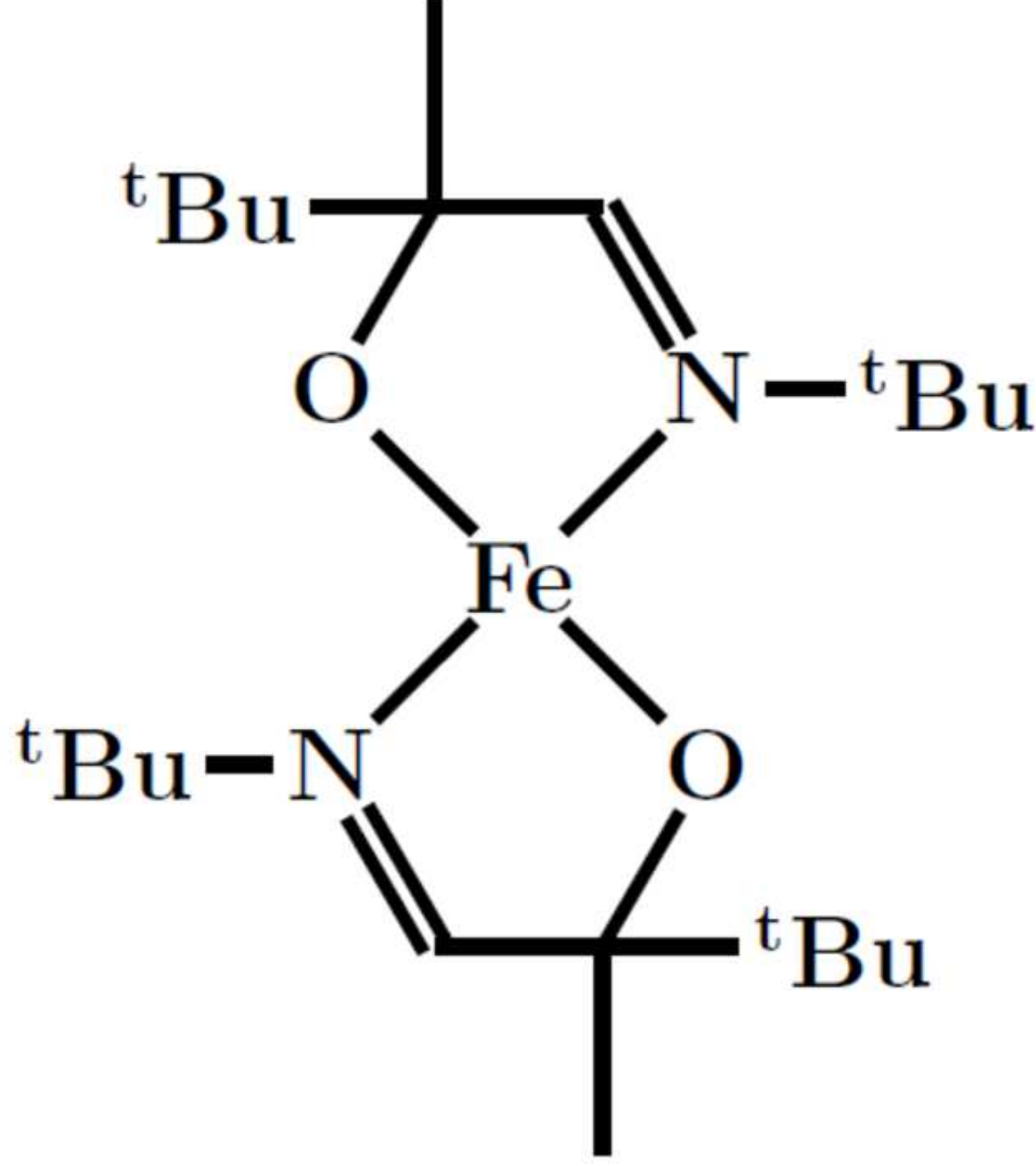
This is the author's peer reviewed, accepted manuscript. However, the online version of record will be different from this version once it has been copyedited and typeset.

PLEASE CITE THIS ARTICLE AS DOI: 10.1063/1.5087759



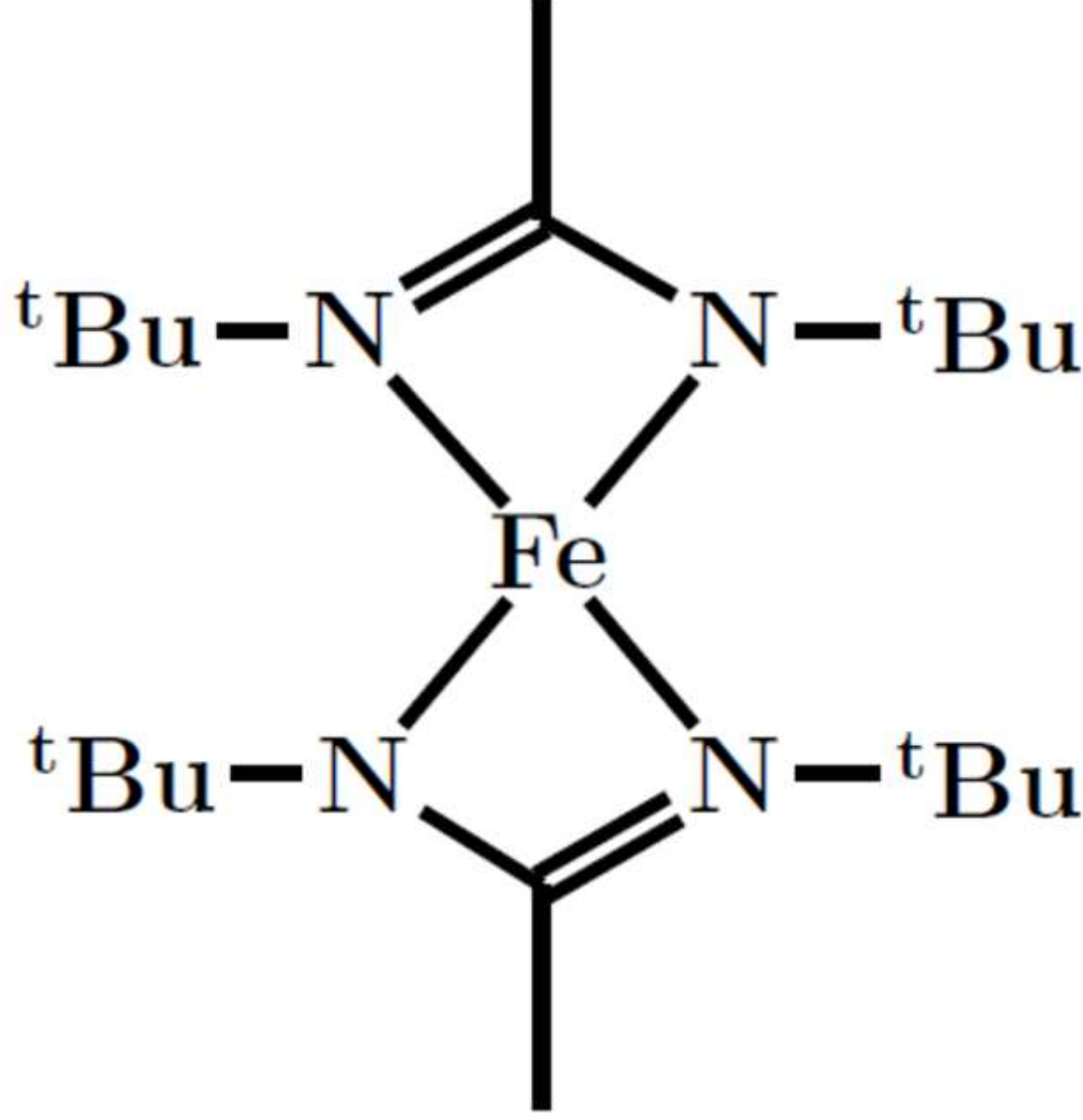
This is the author's peer reviewed, accepted manuscript. However, the online version of record will be different from this version once it has been copyedited and typeset.

PLEASE CITE THIS ARTICLE AS DOI: 10.1063/1.5087759



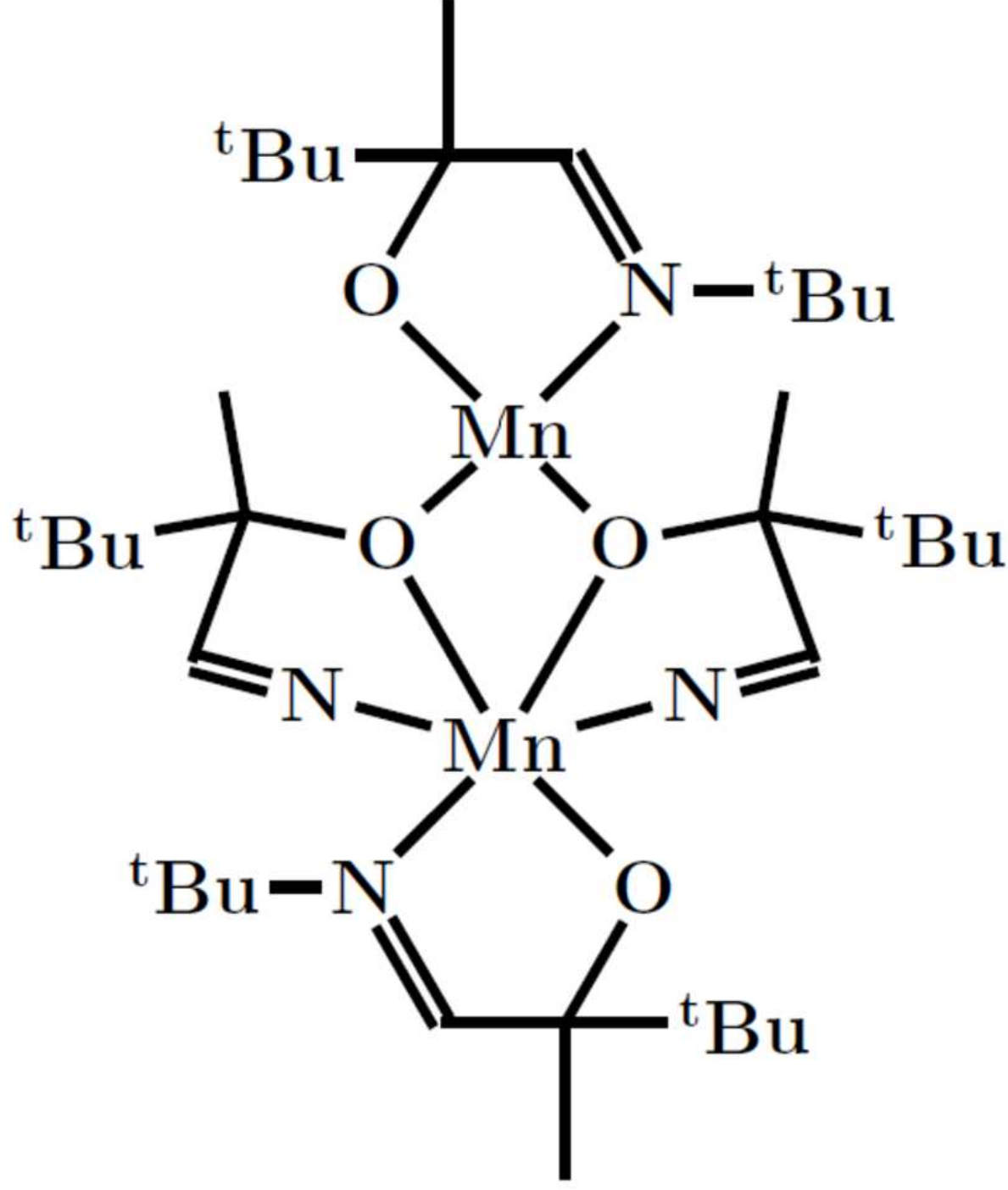
This is the author's peer reviewed, accepted manuscript. However, the online version of record will be different from this version once it has been copyedited and typeset.

PLEASE CITE THIS ARTICLE AS DOI: 10.1063/1.5087759



This is the author's peer reviewed, accepted manuscript. However, the online version of record will be different from this version once it has been copyedited and typeset.

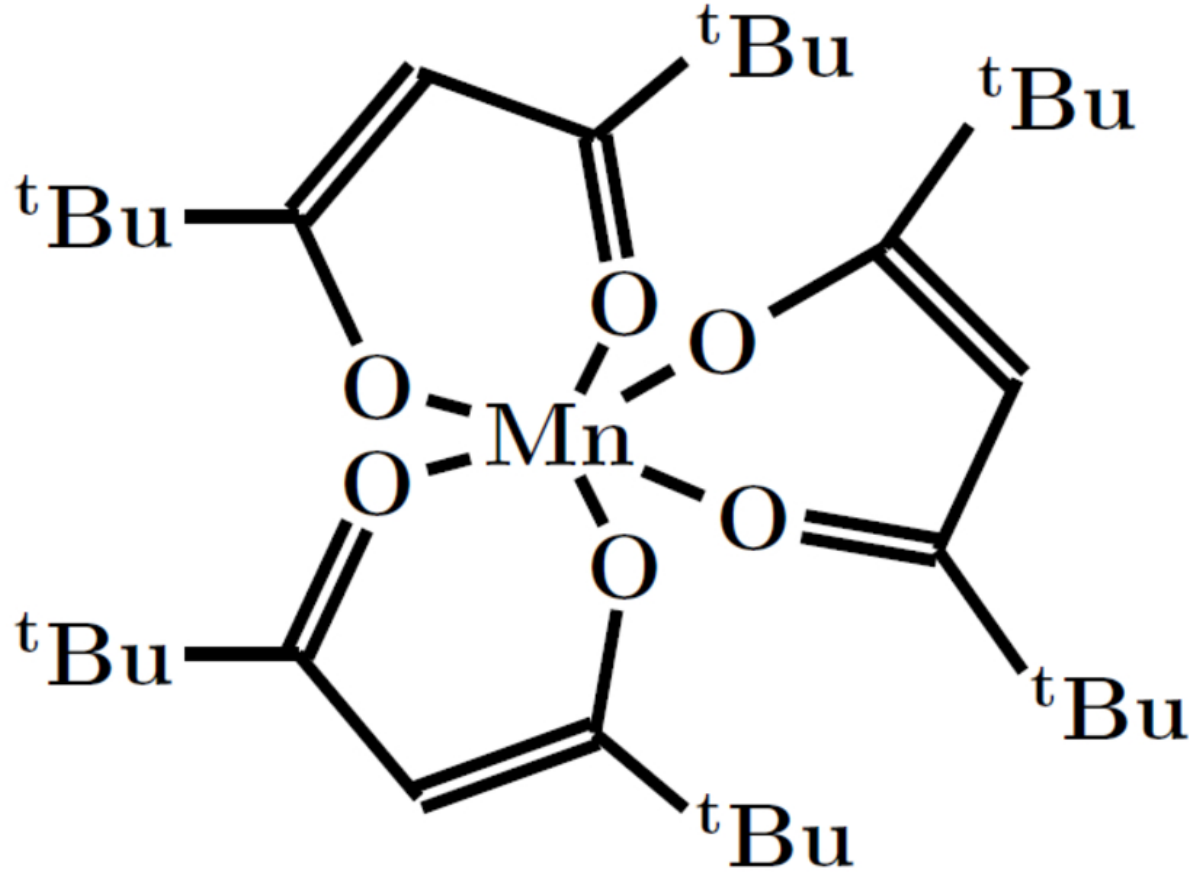
PLEASE CITE THIS ARTICLE AS DOI: 10.1063/1.5087759





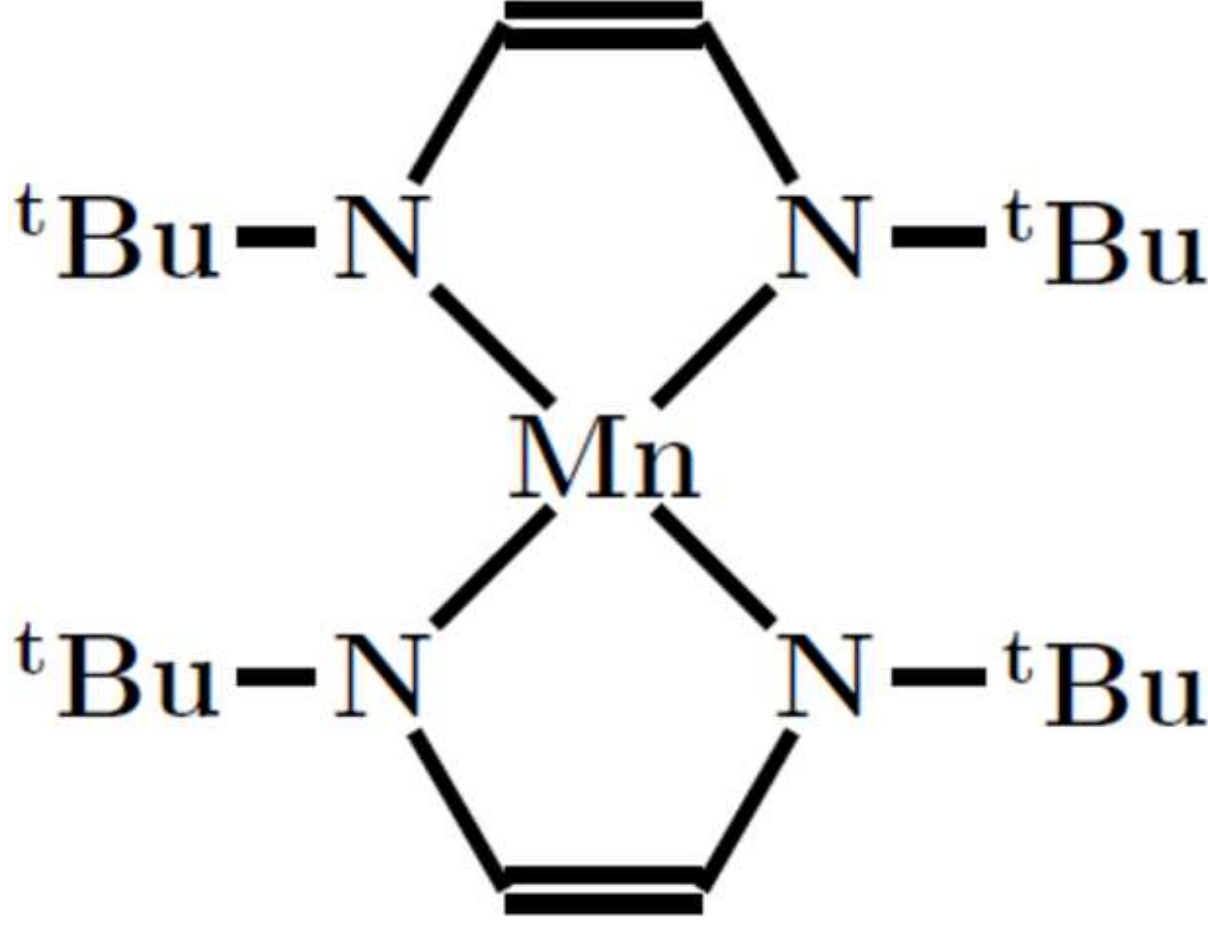
This is the author's peer reviewed, accepted manuscript. However, the online version of record will be different from this version once it has been copyedited and typeset.

PLEASE CITE THIS ARTICLE AS DOI: 10.1063/1.5087759



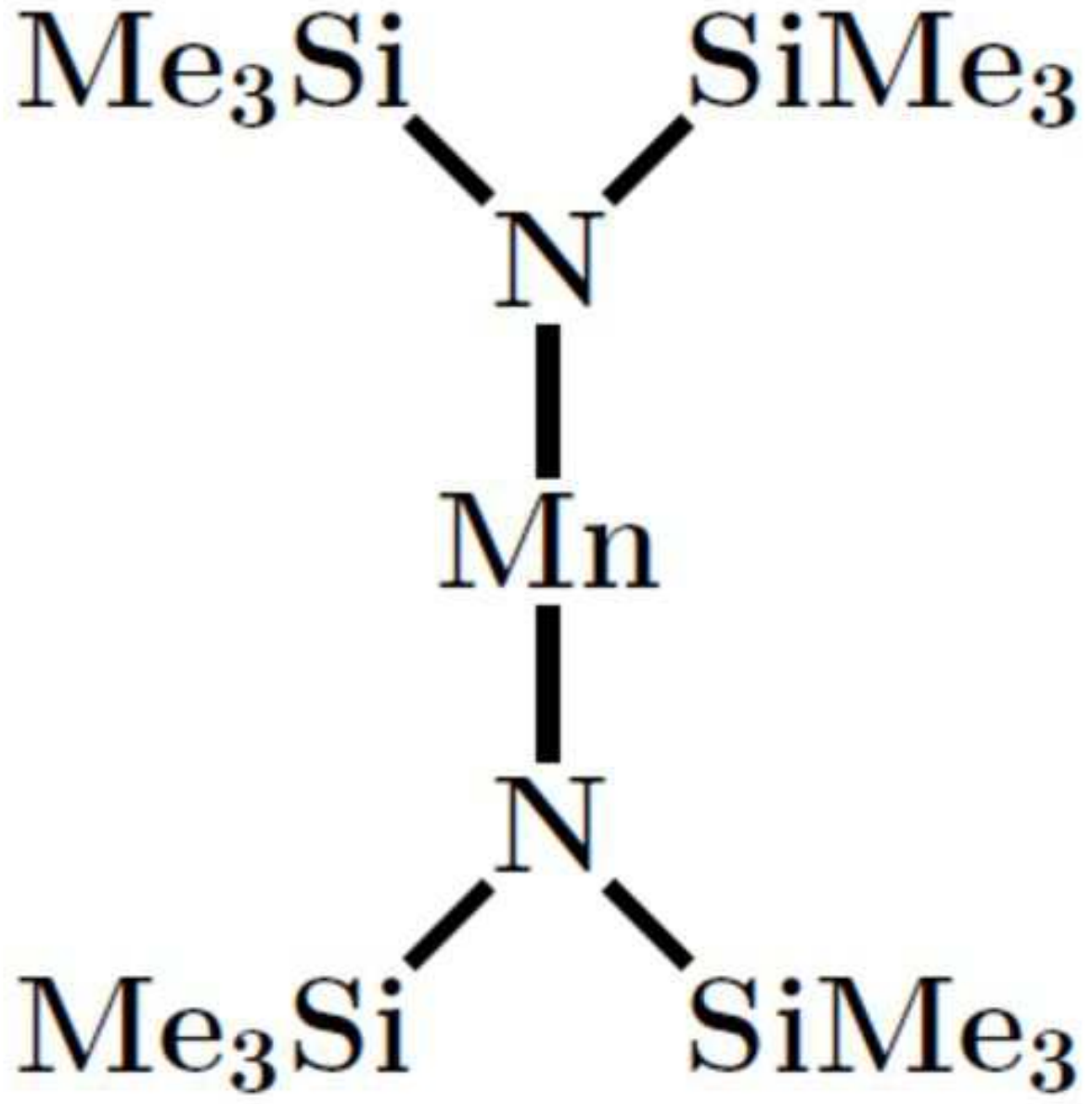
This is the author's peer reviewed, accepted manuscript. However, the online version of record will be different from this version once it has been copyedited and typeset.

PLEASE CITE THIS ARTICLE AS DOI: 10.1063/1.5087759



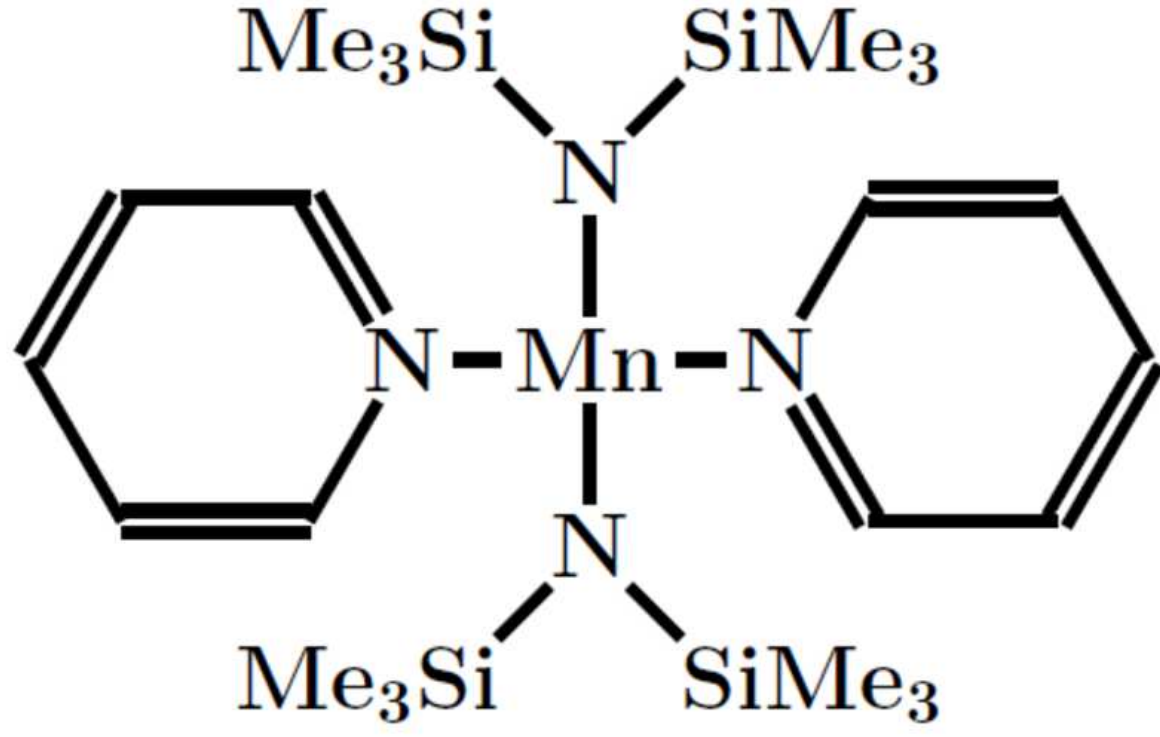
This is the author's peer reviewed, accepted manuscript. However, the online version of record will be different from this version once it has been copyedited and typeset.

PLEASE CITE THIS ARTICLE AS DOI: 10.1063/1.5087759



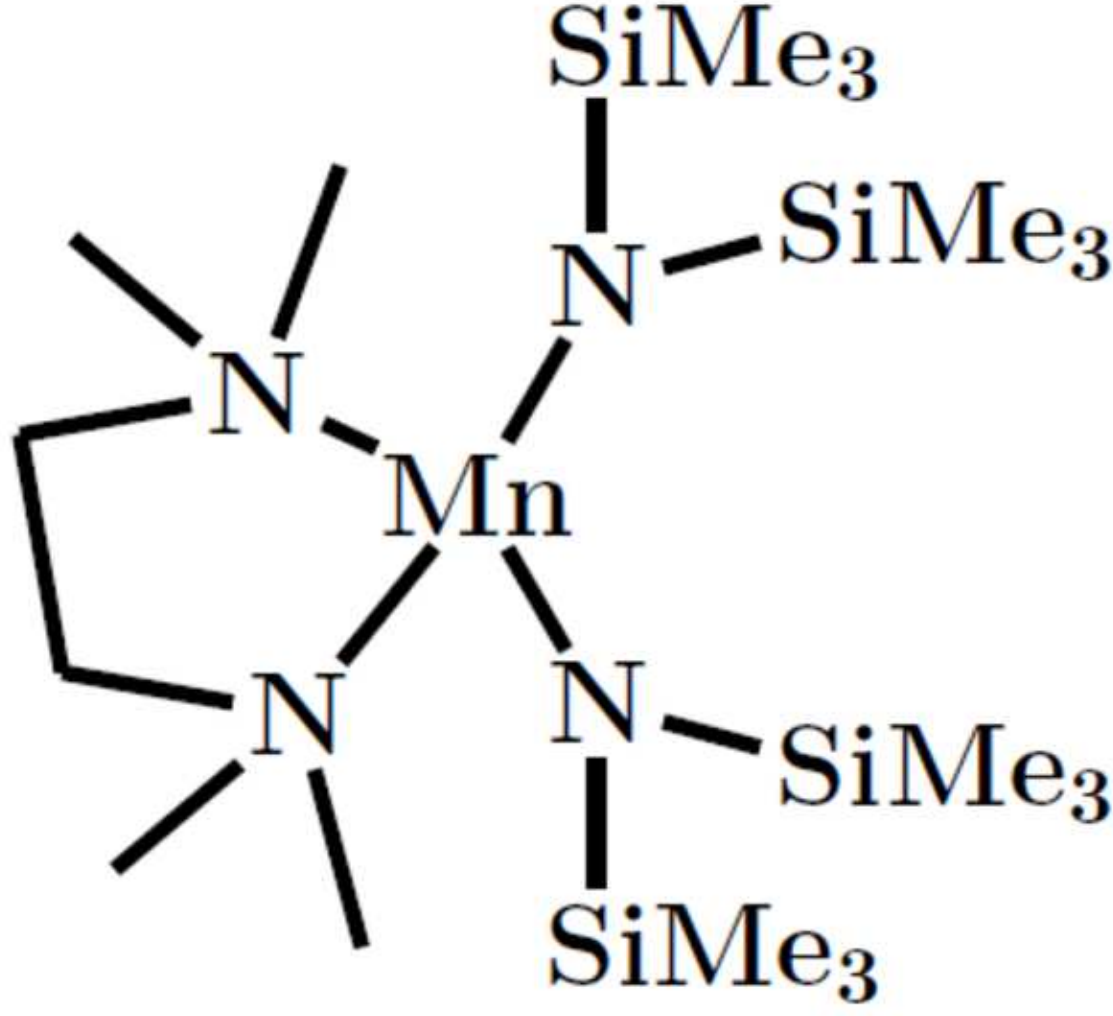
This is the author's peer reviewed, accepted manuscript. However, the online version of record will be different from this version once it has been copyedited and typeset.

PLEASE CITE THIS ARTICLE AS DOI: 10.1063/1.5087759



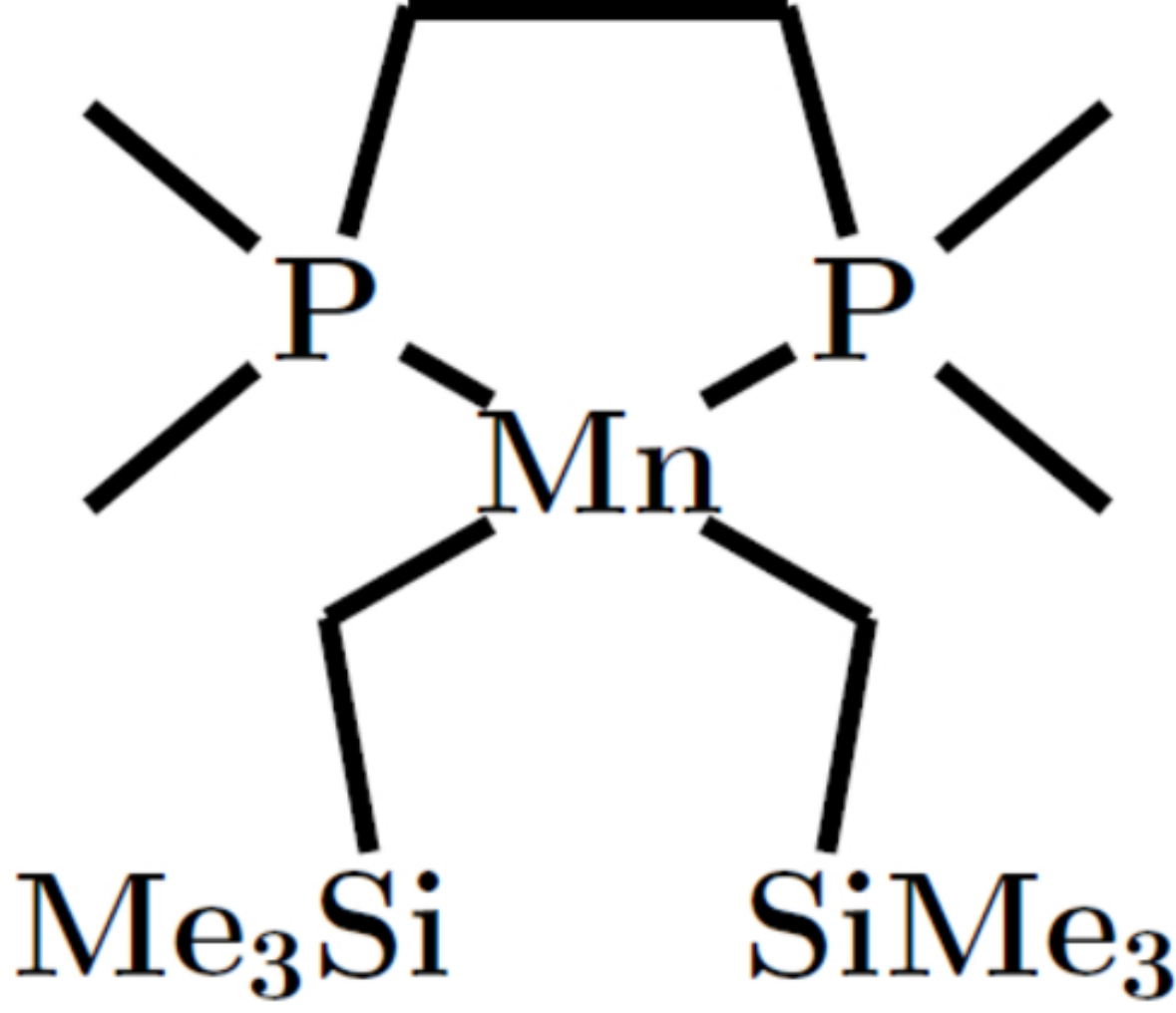
This is the author's peer reviewed, accepted manuscript. However, the online version of record will be different from this version once it has been copyedited and typeset.

PLEASE CITE THIS ARTICLE AS DOI: 10.1063/1.5087759



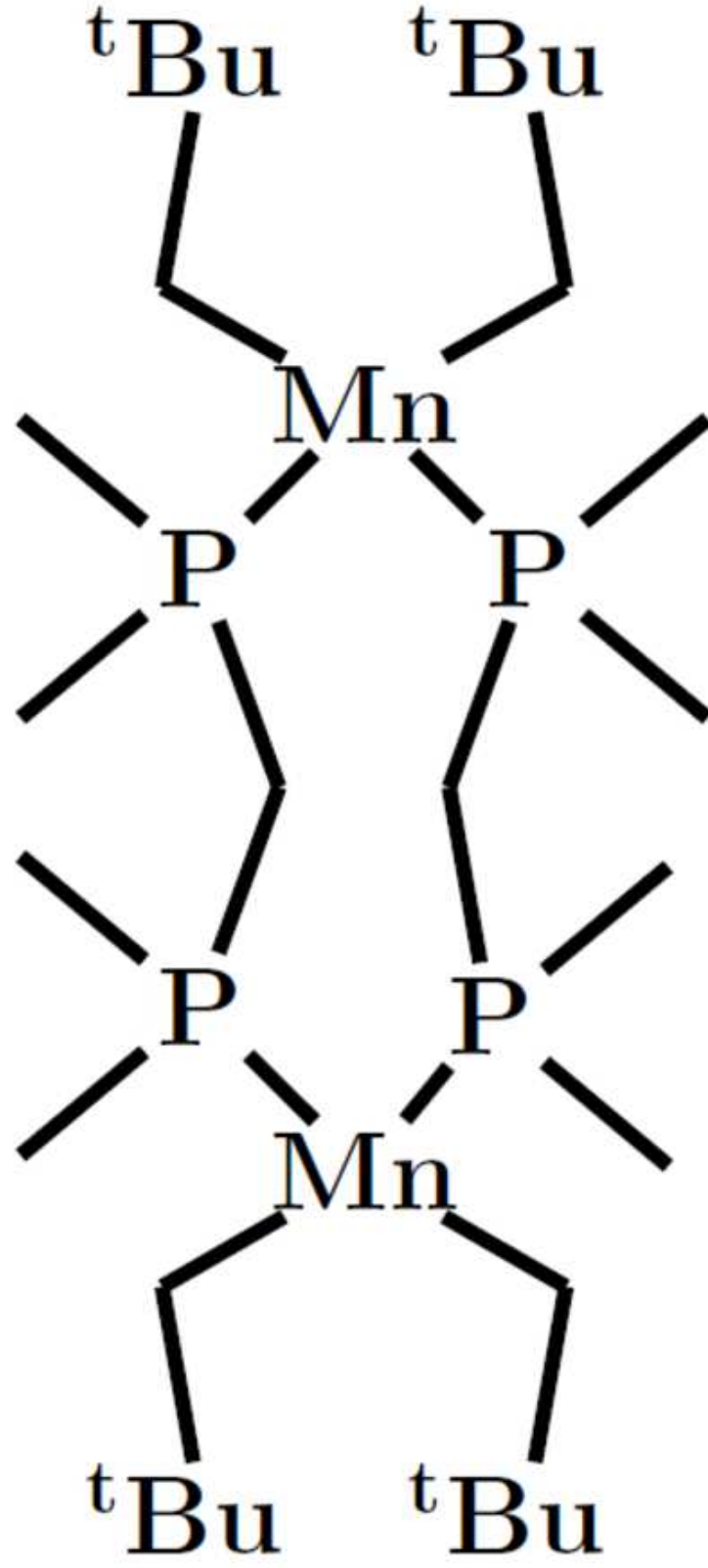
This is the author's peer reviewed, accepted manuscript. However, the online version of record will be different from this version once it has been copyedited and typeset.

PLEASE CITE THIS ARTICLE AS DOI: 10.1063/1.5087759



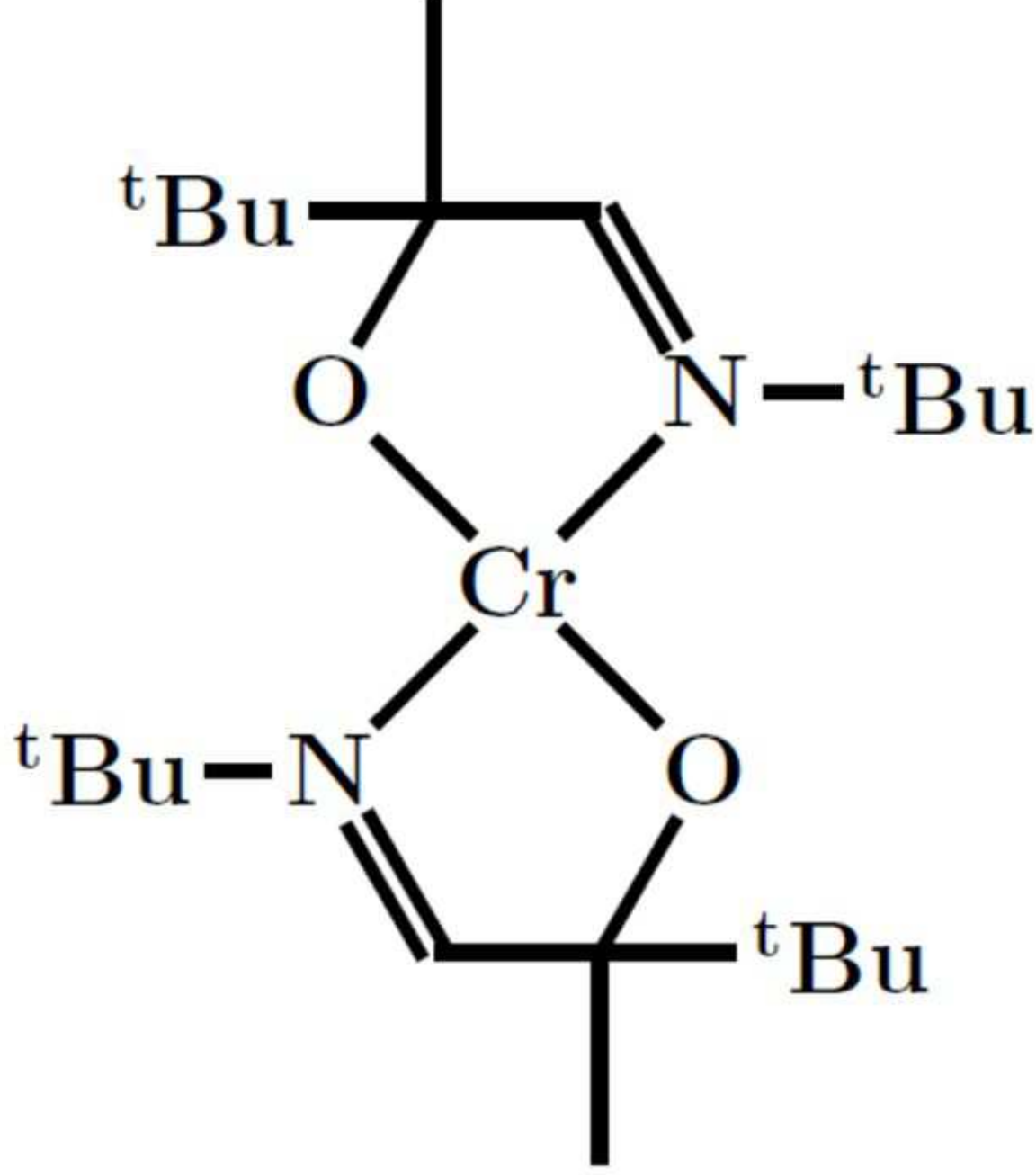
This is the author's peer reviewed, accepted manuscript. However, the online version of record will be different from this version once it has been copyedited and typeset.

PLEASE CITE THIS ARTICLE AS DOI: 10.1063/1.5087759



This is the author's peer reviewed, accepted manuscript. However, the online version of record will be different from this version once it has been copyedited and typeset.

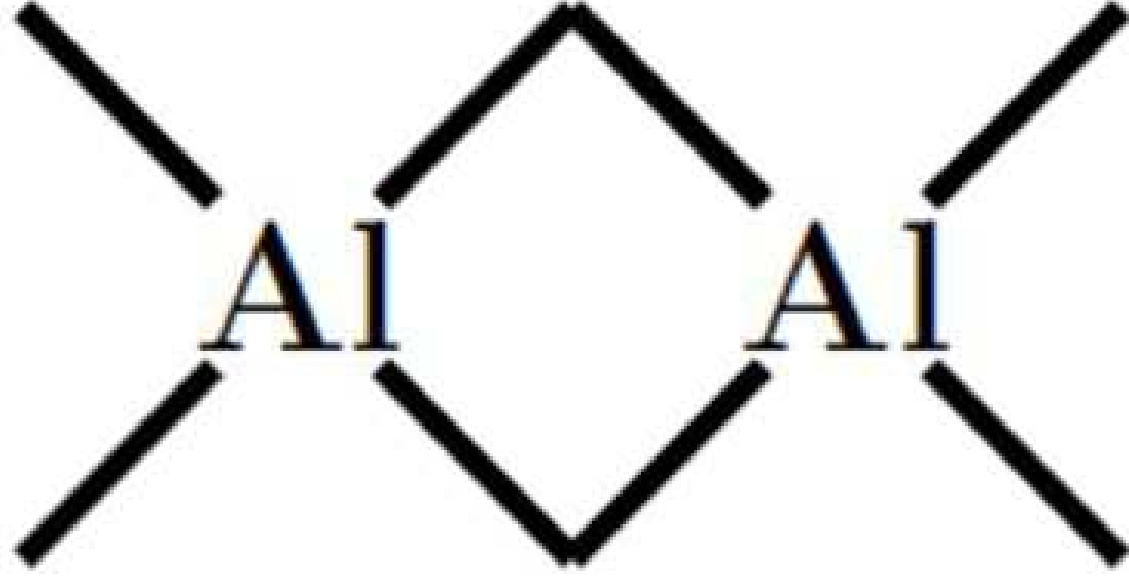
PLEASE CITE THIS ARTICLE AS DOI: 10.1063/1.5087759





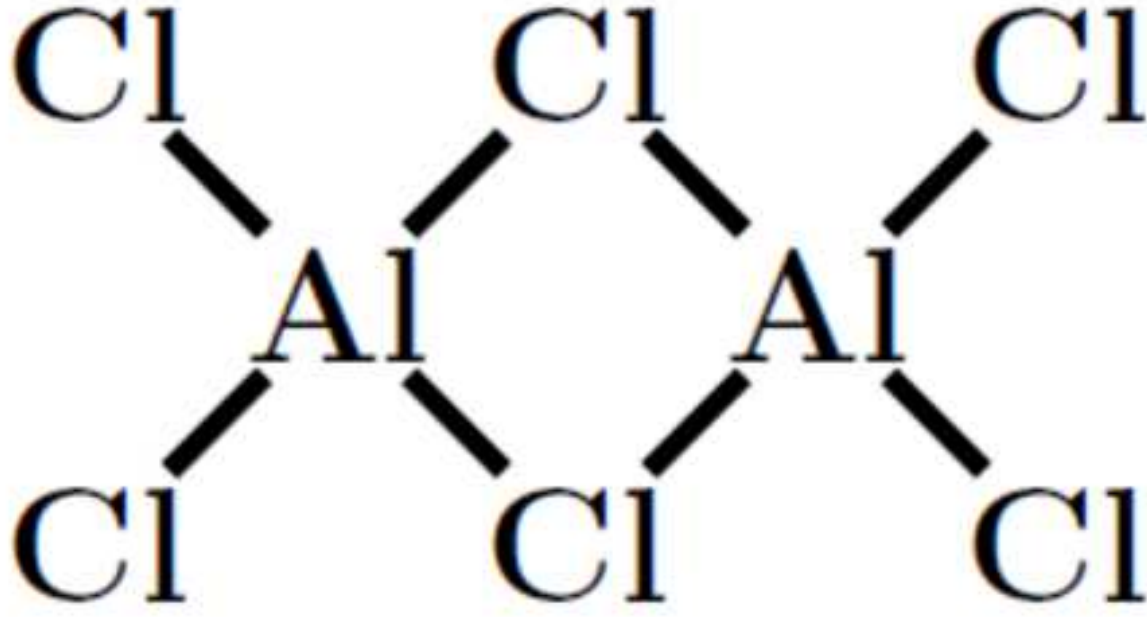
This is the author's peer reviewed, accepted manuscript. However, the online version of record will be different from this version once it has been copyedited and typeset.

PLEASE CITE THIS ARTICLE AS DOI: 10.1063/1.5087759



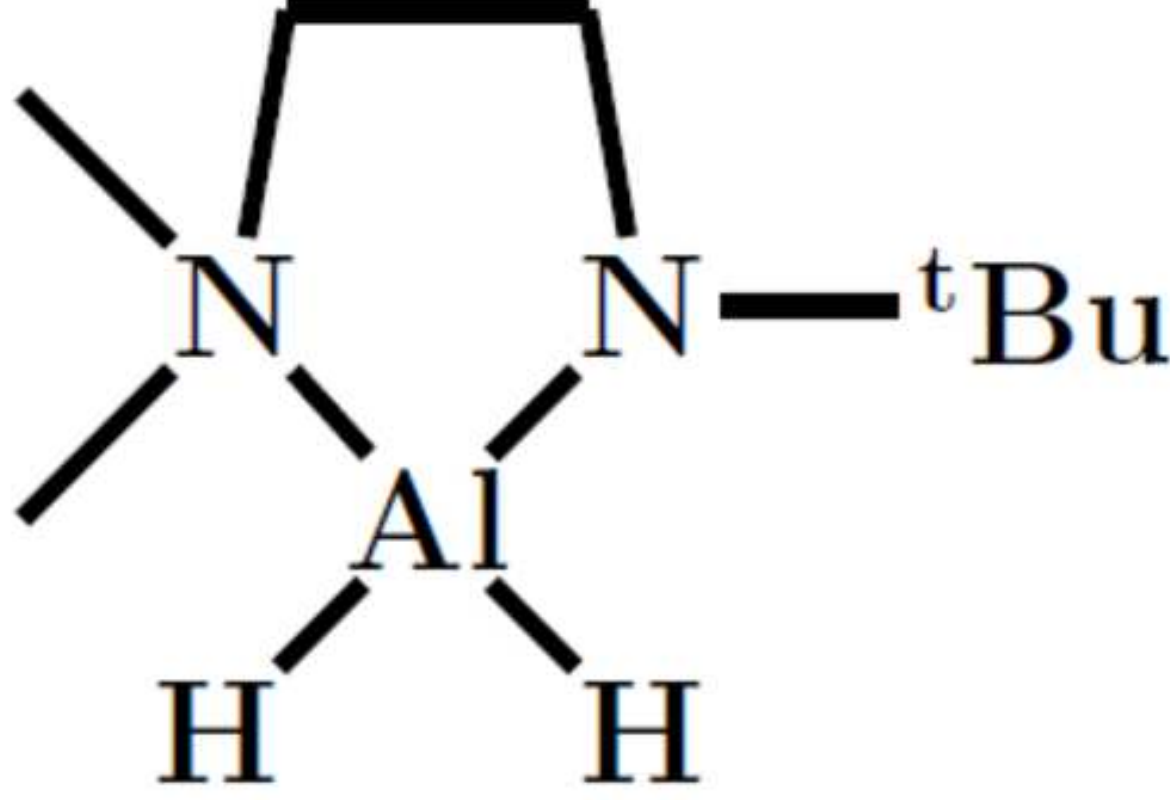
This is the author's peer reviewed, accepted manuscript. However, the online version of record will be different from this version once it has been copyedited and typeset.

PLEASE CITE THIS ARTICLE AS DOI: 10.1063/1.5087759



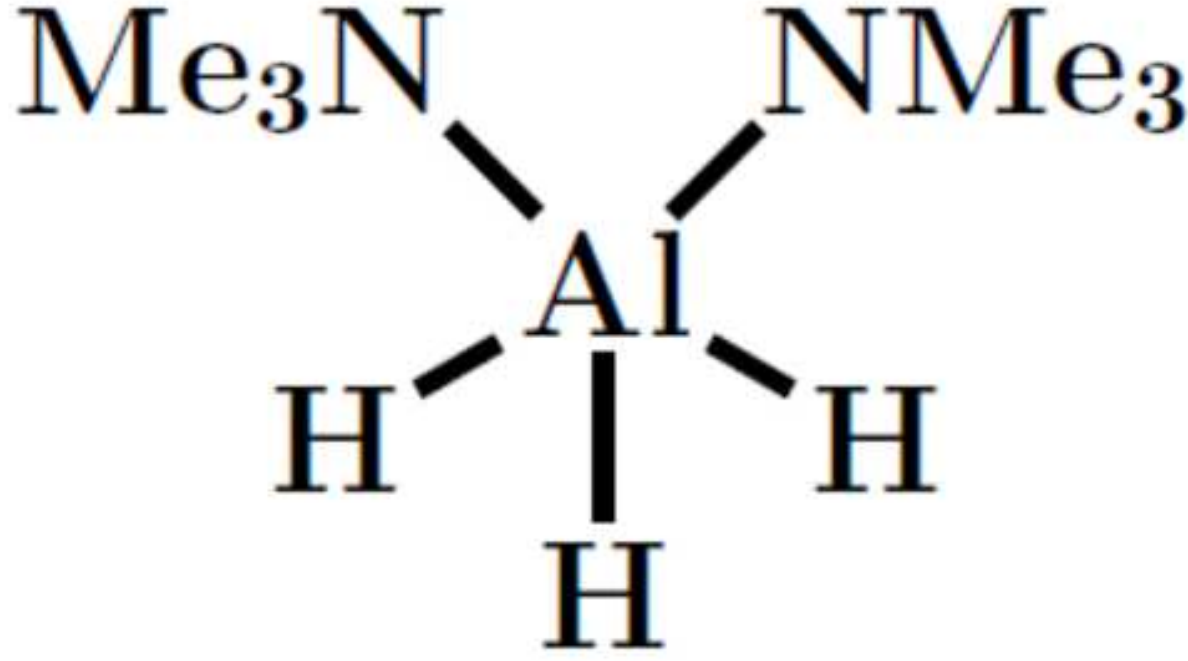
This is the author's peer reviewed, accepted manuscript. However, the online version of record will be different from this version once it has been copyedited and typeset.

PLEASE CITE THIS ARTICLE AS DOI: 10.1063/1.5087759



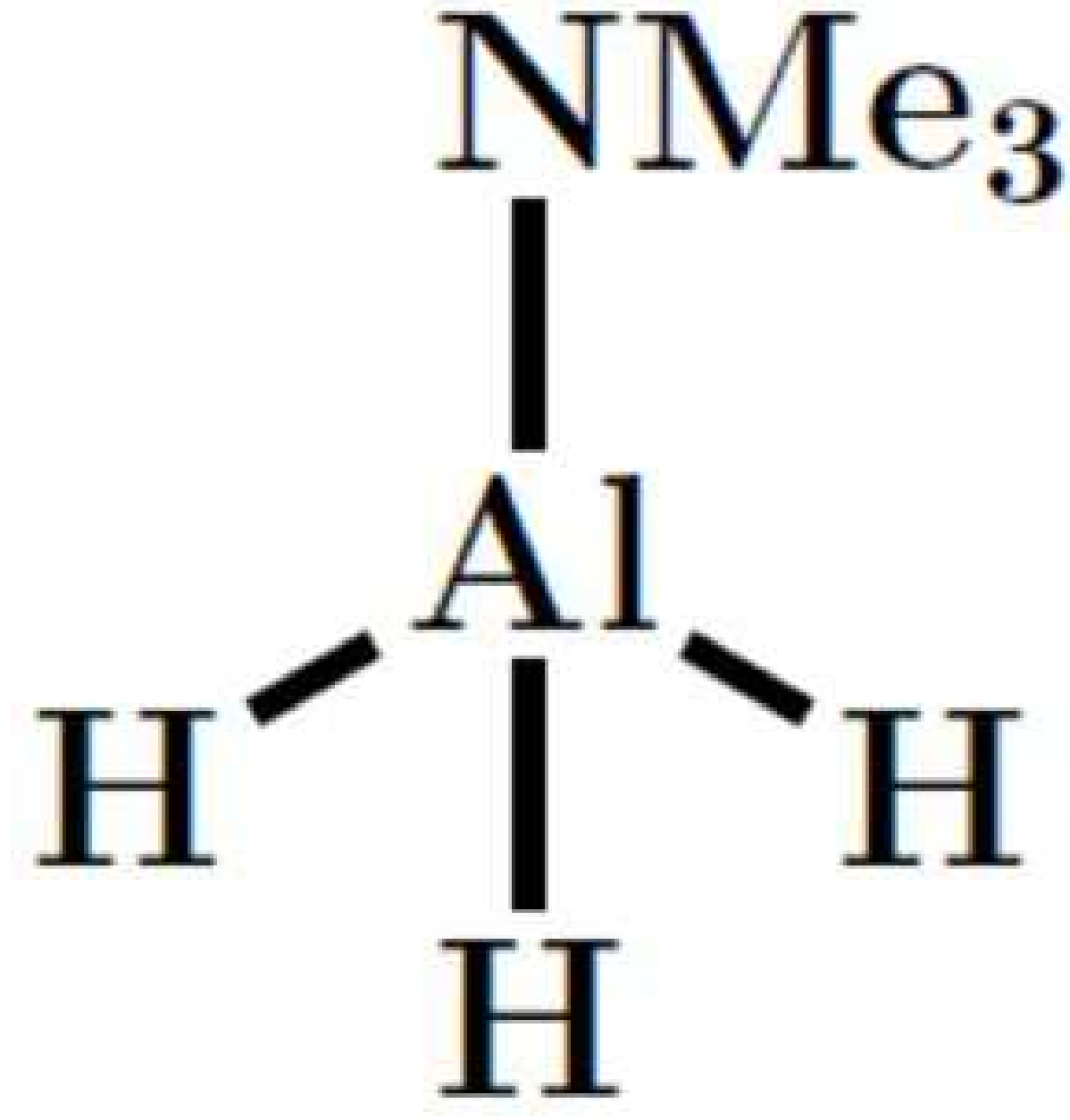
This is the author's peer reviewed, accepted manuscript. However, the online version of record will be different from this version once it has been copyedited and typeset.

PLEASE CITE THIS ARTICLE AS DOI: 10.1063/1.5087759



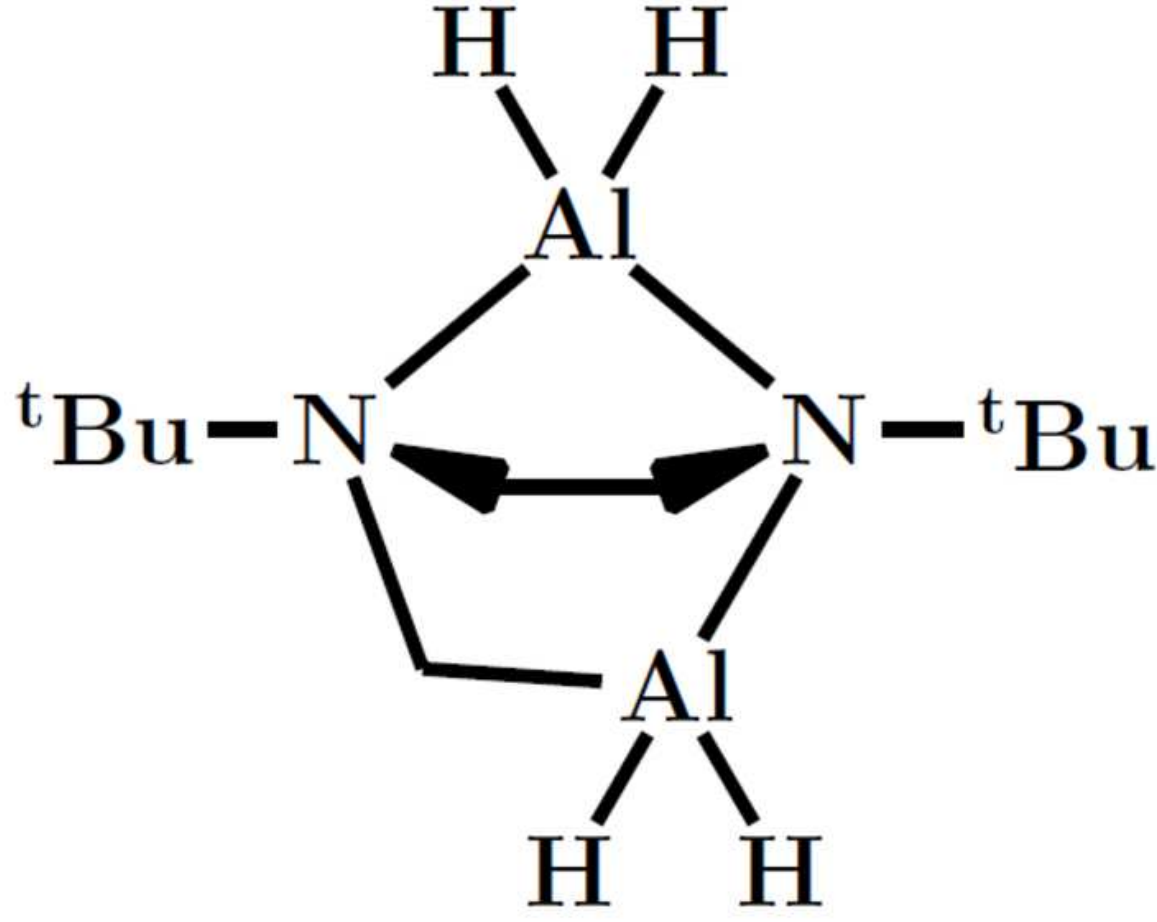
This is the author's peer reviewed, accepted manuscript. However, the online version of record will be different from this version once it has been copyedited and typeset.

PLEASE CITE THIS ARTICLE AS DOI: 10.1063/1.5087759



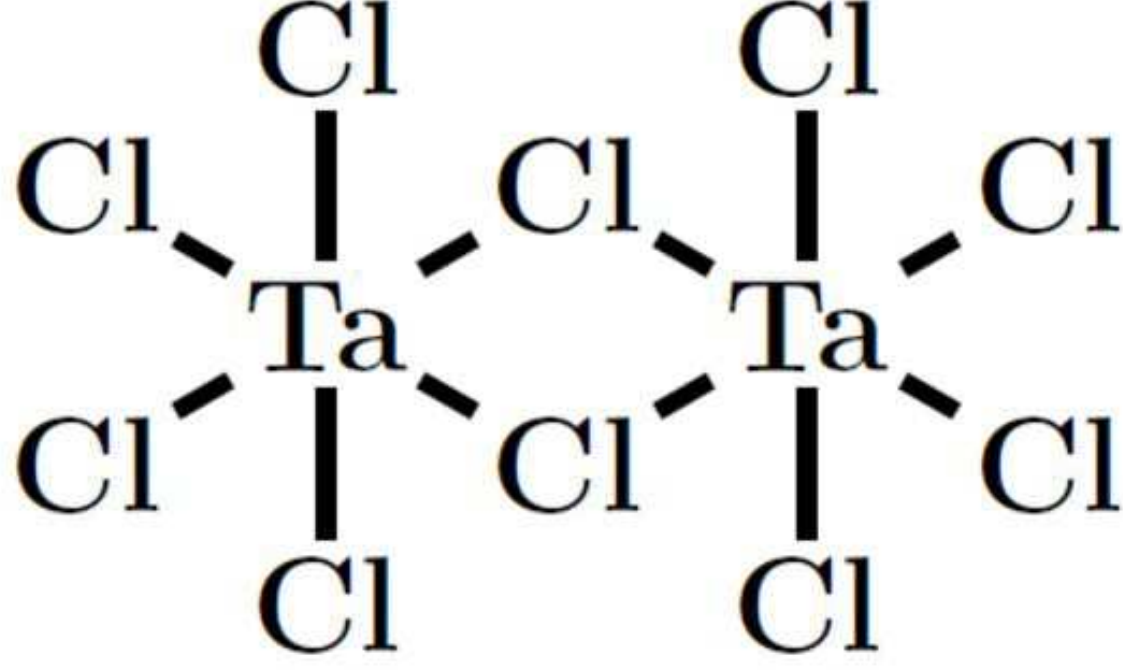
This is the author's peer reviewed, accepted manuscript. However, the online version of record will be different from this version once it has been copyedited and typeset.

PLEASE CITE THIS ARTICLE AS DOI: 10.1063/1.5087759



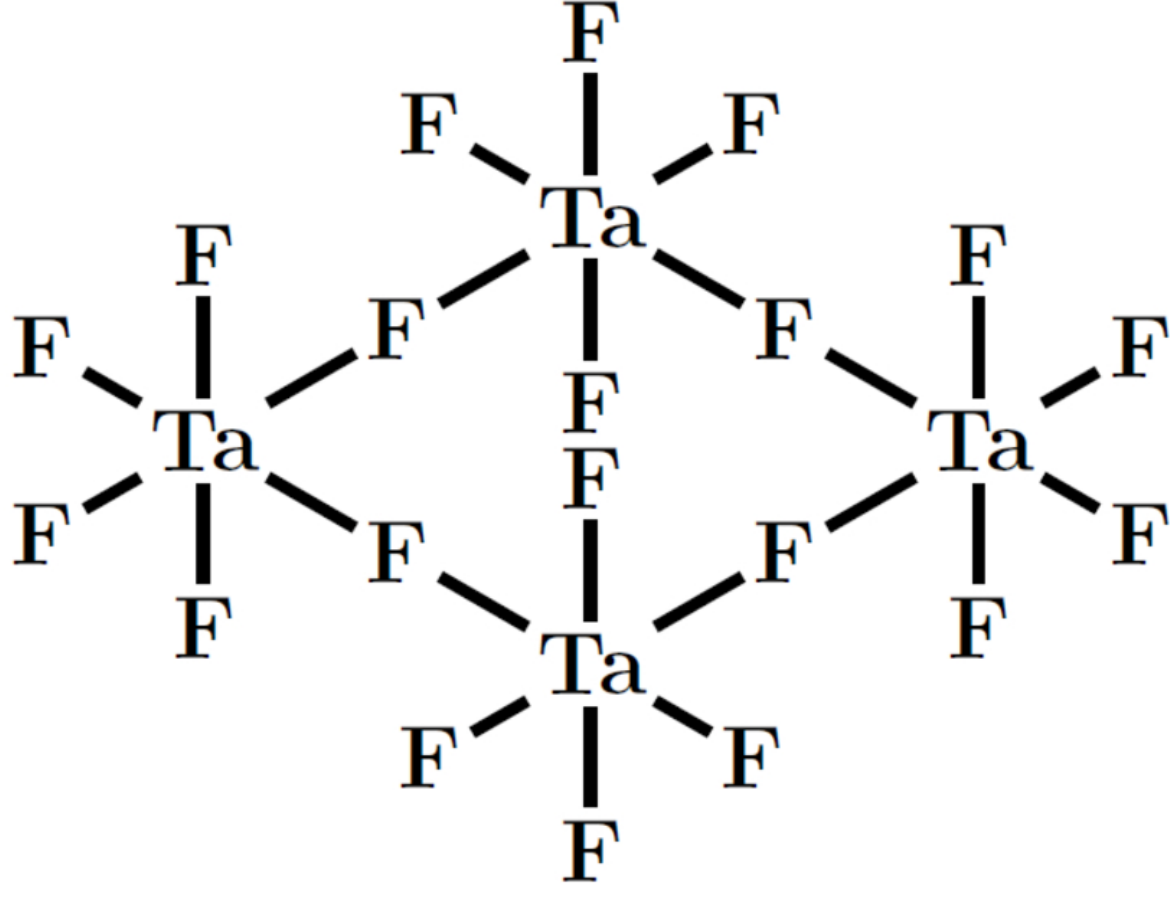
This is the author's peer reviewed, accepted manuscript. However, the online version of record will be different from this version once it has been copyedited and typeset.

PLEASE CITE THIS ARTICLE AS DOI: 10.1063/1.5087759



This is the author's peer reviewed, accepted manuscript. However, the online version of record will be different from this version once it has been copyedited and typeset.

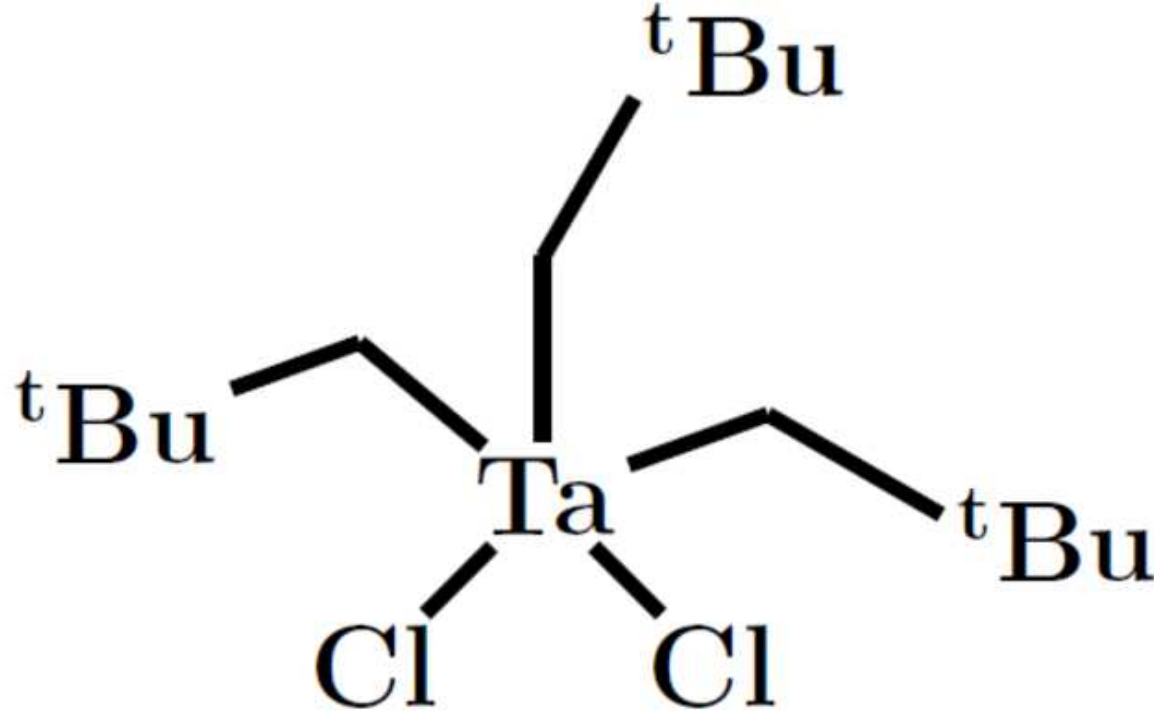
PLEASE CITE THIS ARTICLE AS DOI: 10.1063/1.5087759





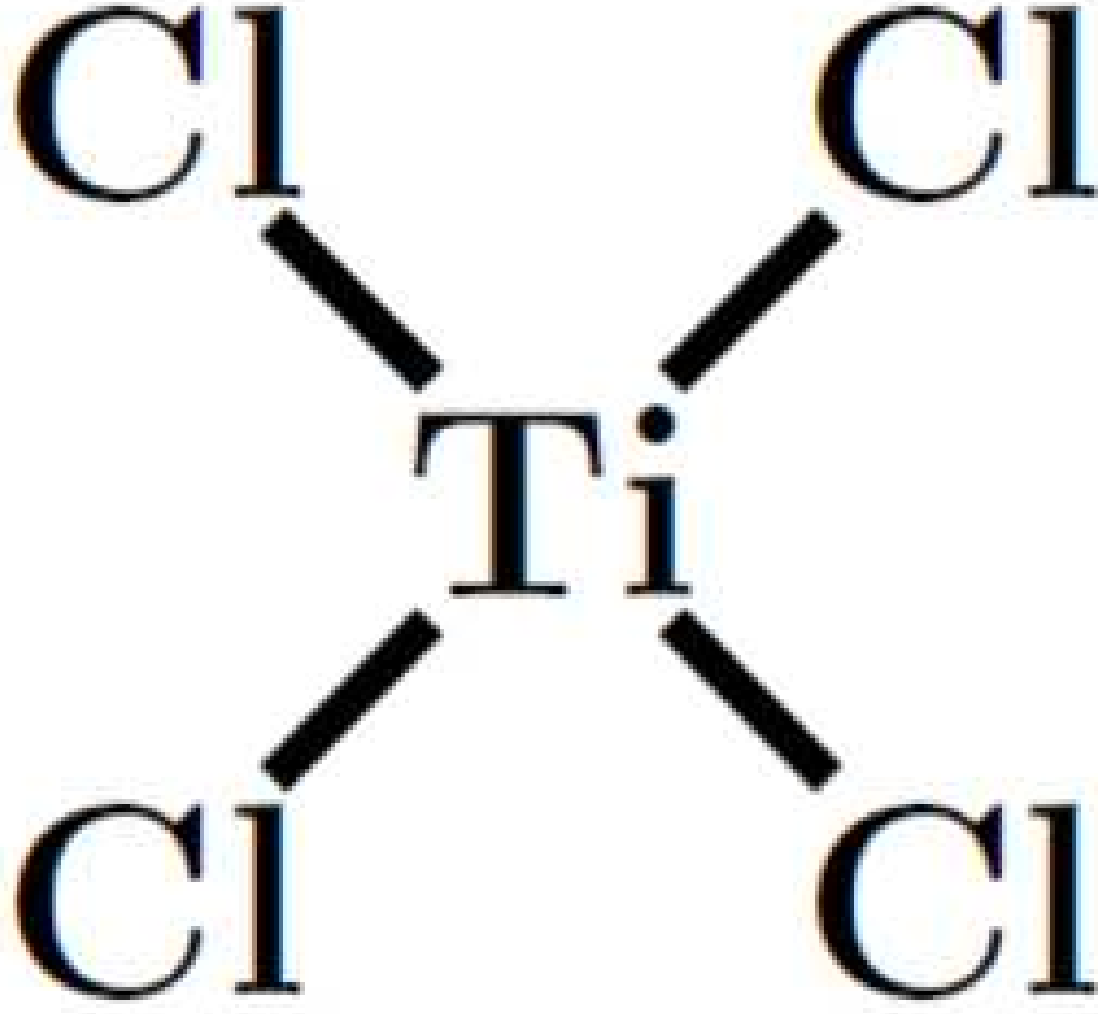
This is the author's peer reviewed, accepted manuscript. However, the online version of record will be different from this version once it has been copyedited and typeset.

PLEASE CITE THIS ARTICLE AS DOI: 10.1063/1.5087759



This is the author's peer reviewed, accepted manuscript. However, the online version of record will be different from this version once it has been copyedited and typeset.

PLEASE CITE THIS ARTICLE AS DOI: 10.1063/1.5087759



This is the author's peer reviewed, accepted manuscript. However, the online version of record will be different from this version once it has been copyedited and typeset.

PLEASE CITE THIS ARTICLE AS DOI: 10.1063/1.5087759

